

THE EFFECTS OF PLIOCENE-PLEISTOCENE CLIMATIC CHANGES ON EVOLUTION OF RIVER SYSTEMS IN SOUTHERN AFRICA: FOCUS ON THE ZAMBEZI AND ORANGE RIVER DRAINAGE BASIN

Report to the
WATER RESEARCH COMMISSION

by

L NCUBE, HJ VAN NIEKERK, B ZHAO, SK RASMENI & AA MKONDE

Department of Environmental Sciences
University of South Africa

&

HM SICHINGABULA, K BANDA, HK MUBANGA & M MUCHANGA

Department of Geography and Environmental Studies
University of Zambia

WRC Report No. 3123/1/23

ISBN 978-0-6392-0600-4

March 2024

Obtainable from

Water Research Commission
Bloukrans Building, Lynnwood Bridge Office Park
4 Daventry Street
Lynnwood Manor
PRETORIA

orders@wrc.org.za or download from www.wrc.org.za

This is the final report of WRC project no. C2019/2020-00019.

DISCLAIMER

This report has been reviewed by the Water Research Commission (WRC) and approved for publication. Approval does not signify that the contents necessarily reflect the views and policies of the WRC, nor does mention of trade names or commercial products constitute endorsement or recommendation for use.

EXECUTIVE SUMMARY

Steep gorges incised by rivers and related fluvial terraces are common geomorphologic features on the margins of orogenic plateaus, such as the Great Escarpment of Southern Africa. Such features are often used to infer the timing and amplitude of surface uplift. However, climatic changes, such as intensified precipitation and increased amplitudes of glacial-interglacial climatic fluctuations, could also potentially enhance fluvial incision. Separating the relative roles of tectonics or climate influences in fluvial incision is a fundamental question in the Earth Sciences, with ramifications for understanding large scale landscape development, the timing and mechanisms of plateau formation, and the collateral effects on global climate change. However, unravelling the complex interplay between processes is challenging. Southern African rivers provide an excellent opportunity to explore the effects of late Cenozoic climatic changes on fluvial erosion and river evolution because tectonic activities in this area were limited to the Pliocene-Pleistocene. More so, rivers such as the Zambezi, and the Orange are primary water supply for both social and economic activities and are shared by several riparian states who have challenges in managing these drainage systems due to lack of transboundary water management policies in the riparian states.

In this study, International Ocean Discovery Program (IODP) drilling cores surrounding the Southern African continent were utilised to capture significant river evolution events, through the establishment of sedimentary accumulation rates and provenance variation records since the Pliocene. Furthermore, provenance and geomorphological studies were performed to extend the state of knowledge on the drainage areas of the Zambezi and the Orange Rivers (and their tributaries) to aid the interpretation of the marine records.

To further extend the state of the knowledge, hydrological characteristics, future climatic conditions, and their implications on water security was also studied. In addition, analysis of projected impacts of sedimentation and bathymetry of selected small reservoirs to water scarcity problems on the priority water-linked sectors was carried out. The study further established aridity evolution in Southern Africa using the evolution of the African savanna which has been traced back to 10-6 million years (Ma) ago.

Finally, developmental perspective for water-linked sectors in a future climate for Africa, the different developmental response models considering socio-economics drivers, and policies were established and proposed.

Based on the study, the following results were obtained:

1. Provenance and geomorphological studies

- i. The Zambezi River is the fourth longest river in Africa. The river has its source in the Ikeleng District North-Western Province, Zambia. To the east of the source, the watershed between Congo and the Zambezi drainage basin is a well-marked belt of

high ground, running nearly east-west and falling abruptly to the north and south. This distinctly cuts off the basin of the Luabala from that of the Zambezi. In the neighbourhood of the source the watershed is not as clearly defined, but the two river systems do not connect. The region drained by the Zambezi is a vast broken-edged plateau 900-1200 m high, composed in the remote interior of metamorphic beds and fringed with the igneous rocks of the Victoria Falls. The river flows across the low-relief Kalahari Plateau, meets Karoo basalt, plunges into Victoria Falls, follows along Karoo rifts, and pierces through Precambrian basement to eventually deliver its load onto the Mozambican passive margin. Reflecting its polyphase evolution, the river is subdivided into segments with different geological and geomorphological character, a subdivision finally fixed by man's construction of large reservoirs and faithfully reflected by sharp changes in sediment composition. Pure quartzose sand recycled from Kalahari Desert dunes in the uppermost tract are next progressively enriched in basaltic rock fragments and clinopyroxene. Sediment load is renewed first downstream Lake Kariba and next downstream Lake Cahora Bassa, documenting a stepwise decrease in quartz and durable heavy minerals until composition becomes quartzo-feldspathic in the lower tract, where most sediment is supplied by high-grade basements rejuvenated by the southward propagation of the East African rift. Feldspar abundance in Lower Zambezi sand has no equivalent among big rivers on Earth and far exceeds that in sediments of the northern delta and shelf, revealing that provenance signals from the upper and middle reaches have ceased to be transmitted across the routing system after closure of the big dams. This high-resolution petrologic study of Zambezi sand allows us to critically reconsider several dogmas, such as the supposed increase of mineralogical "maturity" during long-distance fluvial transport and forges a key to unlock the rich information stored in sedimentary archives, with the goal to accurately reconstruct the evolution of this mighty river and African landscapes since the late Mesozoic.

- ii. Elemental geochemistry, Nd-isotopes, clay minerals, and U-Pb zircon ages integrated by petrographic and heavy-mineral data offer a multi-proxy panorama of mud and sand composition across the Zambezi sediment-routing system into the Indian Ocean. Detrital-zircon geochronology reflects four major episodes of crustal growth in southern Africa: Irumide ages predominate over Pan-African, Eburnean, and Neoproterozoic ages. Smectite, dominant in mud generated from Karoo basalts or in the equatorial/winter-dry climate of Mozambican lowlands, prevails over illite and kaolinite. Elemental geochemistry reflects quartz addition by recycling (Uppermost Zambezi), supply from Karoo basalts (Upper Zambezi), and first-cycle provenance from Precambrian basements (Lower Zambezi). Mildly negative ϵ_{Nd} values for sediments derived from mafic granulites, gabbros, and basalts, ϵ_{Nd} values are most negative for sand derived from cratonic gneisses. Intrasample variability among cohesive mud, frictional silt, and sand fractions reflects concentration of Nd-rich heavy minerals in the fine tail of the size distribution. The settling-equivalence

effect also explains deviations from the theoretical relationship between ϵNd and TNd , DM model ages, suggesting that LREE rich monazite carries a more negative ϵNd signal than heavy minerals with flatter REE patterns. Elemental geochemistry and Nd-isotopes reveal that the Mazowe-Luenha Rivers contribute most of the sediment reaching the Zambezi Delta today, with minor supply by the Shire River. Sediment yields and erosion rates are an-order-of magnitude less on the low-relief Kalahari Plateau than in rugged Precambrian terranes. On the Plateau, mineralogical and geochemical indices testify to extensive breakdown of feldspars and garnet unjustified by the presently dry climate. Detrital kaolinite is produced by incision of Cretaceous-Cenozoic paleosoils even in the wetter lower catchment, where inefficient hydrolysis is testified by abundant fresh feldspars and undepleted Ca and Na. Mud geochemistry and surficial corrosion of ferromagnesian minerals indicate that, at present, weathering increases only slightly downstream the Zambezi.

2. Hydrological characteristics, and future climatic conditions

This report, which forms deliverable 1.0 of the project, is on modelled future climatic conditions and the implication on water security and is written in the framework of the “Effects of Pliocene-Pleistocene climatic changes on evolution of river systems in Southern Africa” research project, focusing on the Zambezi and Orange River basins. The report is divided into three sections, the hydrological characterisation, future climate modelling and impacts on water security. The hydrological character of both the Zambezi and Orange support livelihoods and hosts critical ecosystems that support ecosystem-system services. Climate variability/change is seen as a threat to ensuring a future that is water secure. Climate analysis is therefore a critical element of this analysis besides the hydrological characterisation. Several downscaled, bias corrected regional climate models (RCMs) are available to the science community. RCMs are critical to capturing climate impacts at regional or local scales. One RCM (SMHI-RCA4) driven by seven Coupled Multi-Intercomparison Project Phase 5 (CMIP5) GCMs (CCCma-CanESM2, IPSL-IPSL-CM5A-MR, MIROC-MIROC5, MPI-M-MPI-ESM-LR, NCC-NorESM1-M, MOHC-HadGEM2-ES, NOAA-GFDL-GFDL-ESM2M) and two scenarios (RCP4.5, RCP8.5) were used in this study extracted from the CORDEX Africa domain (AFR-44). The RCM simulation runs at 0.5o spatial resolution of daily precipitation, minimum and maximum temperature covers 1980-2010 (baseline scenario) and 2020-2050 (future climate scenario). The 50 km resolution CORDEX African-domain RCMs was used to generate a seven-member ensemble of climate projections for the Orange and Zambezi River Basins. The Representative Concentration Pathways (RCPs) depicts greenhouse gas concentration trajectory adopted by the Intergovernmental Panel on Climate Change (IPCC) during the fifth Assessment Report (AR5) in 2014 (IPCC, 2014). The RCP4.5 represents intermediate GHG emissions (650 ppm CO₂ eq) while RCP8.5 represents very high GHG emissions (1370 ppm CO₂ eq). Future climate projections indicate an increase in precipitation and temperature for the Orange River whereas, the Zambezi would have reduced precipitation and increased temperature. Water security for the Zambezi would require investments in water infrastructure

such as dams or other water harvesting approaches. In the Orange River, potential for flooding exists and therefore the infrastructure must be flexible enough to capture this variability. Additional studies are required in linking climate scenarios to hydrological modelling to evaluate the impacts on catchment water balance yields.

3. Analysis of projected impacts of sedimentation and bathymetry of selected small reservoirs to water scarcity problems on the priority water-linked sectors

- i. Based on the preliminary findings from secondary and primary information, the study indicated that majority of reservoirs in the Zambezi Basin could be as silted up as those, which were targeted for this study such that their storage capacities may not sustain the current water demands for household and livestock use. Based on assorted bathymetrically surveyed reservoirs in selected parts of the Zambezi Basin and particularly the three surveyed in southern Zambia, the study concludes that small dams are at the highest risks of losing storage capacities. Therefore, catchments where such small reservoirs are located could also be prone to severe water scarcity and stress especially between July and early November. This inspired the conclusion that most communities within the Zambezi basin are water insecure and are subject to high risks of economic scarcity within next 50 years amidst climatic changes. All reservoirs in the Zambezi Basin with similar characteristics as those sampled in the current study are only water-secure between December and April, a situation which affects crop and animal productivity, fishing activities, hydropower generation, among others. Agricultural activities remain the drivers of siltation and loss of storage capacities for most reservoirs. The cost of addressing sedimentation among reservoirs bears a heavy toll on the government planning process, but at the same time, the very propellant of reservoirs' loss of storage capacities could be transformatively be utilised to build profitable business models and be reused for fertilisation of crops. This remains poorly utilised coping strategy and opportunity for most countries within the Zambezi Catchment. The coping strategies such as alternative livelihood, water harvesting, and water shedding recorded in various parts of the catchment suggests a spatially distributed nature of the problem of water scarcity due to siltation and climatic changes. Some sub-catchments within the Zambezi Basin adopted destructive approaches such as conflicts, cultivating within the legally forbidden buffer zones, digging wells right on dry beds of river channels and reservoirs especially during water stressful period, among others, as coping strategies water scarcity problem. Given the systemic and complex nature of water scarcity the study proposed a conceptual model that is inherently proposing integrated and transdisciplinary approaches to address the challenges of reservoirs' storage losses and siltation challenges for sustainable water resources by 2030 and beyond.
- ii. In this research, *Global Mapper* was used to determine the water surface area and the volume of Gariep dam, and to analyse areas and volumes by contours as a way

of determining the dynamics of circumference changes. The occurrence of healthy vegetation during drought period is indicative of the presence of underground water. This was observed through LANDSAT explorer rendered colour infrared- and short-wave infrared images. There is pronounced greening in the area, especially during wet period image, indicatively of a densely vegetated area. This is ascribed to underlying rocks which store water, used to support growth of vegetation. The Kalahari sand cover that is underlying the middle to lower Gariep catchment is associated with high porosity or permeability. Although sandstones only retain small part of intergranular pore space that was present before the rock was consolidated, secondary openings such as joints and fractures along with bedding planes on the other hand are grounds for water movements and transmit most groundwater. Furthermore, the study showed that in the Gariep dam area, dolerite intrusions are dominant, and groundwater is mainly found in joints and fractures on the contact zones, in weathered dolerite zones, weathered and jointed sedimentary rocks and on bedding planes with borehole yields varying from 0.5-2.0 l/s. Lastly, the moisture index rendered satellite images shows the occurrence of moisture content even during the drought period, probably this is from the deep tap rooted trees present in the area which can also be due to the presence of groundwater.

4. Reflect on the smaller dams upstream of Gariep that act as sediment traps

The results obtained indicate that continuous entrapment of sediment by dams, result in reduction of their water storage capacity. However, the Gariep dam has lost 16,8% of its capacity suggesting that the dams are still useful and economical. This is attributable to the rate of sedimentation of the dams in relation to the size, amongst other factors. The results obtained, indicated that it will take 88 years for the dam to reach its half-life, thus, if sedimentation rates remain the same. However, sedimentation is advancing, and the upper reaches of the dam have accumulated large amounts of sediments. This places the Orange-Fish tunnel intake (located at Oviston) at risk of receiving an excessive amount of sediment which reduces its efficiency to transfer water to the Fish and Sundays Rivers and, this may block the intake.

5. Paleoclimatic changes and depositional rates in southern Africa: Impacts of regional groundwater quality

Based on the study the following were observed:

Various studies investigated recharge mechanisms in the Makgadikgadi-Okavango-Zambezi Basin (MOZB), which suggest recharge occurs within the MOZB, but is lost to the vegetation cover; regional studies support this assertion and further confirms that isolation of palaeo and recent recharge is not possible; Sediment ages within the MOZB are generally old (> 300 Ka) compared to groundwater ages, which are Late Pleistocene to Holocene (< 50 Ka). Saline groundwater observed today is not a result of connate lake water preserved in sediments but other processes including evapotranspiration and mineral dissolution processes:

- a. Hydrochemical facies within MOZB are generally a result of redissolution of evaporated minerals, composed of chloride (in the central zone), sulphate (in the fringes) and carbonates typically beyond the boundaries of MOZB or within the Okavango Delta. We suggest sulphate is a result of surface water-groundwater interaction in which evaporation from the surface water formed primary evaporites rapidly exchanged solutes to the groundwater; increased solute accumulated then formed evaporites of sulphates. Precipitation of halite is a result of progressive evaporation loss from the capillary fringe and groundwater discharge at the shoreline margins of the lake system. Carbonate groundwater is due to recent recharge water within the surrounding fresh groundwater input and surface water (particularly in the Okavango Delta Region);
- b. River chemistry water from present day river channels within the PLM (Zambezi, Okavango, Kwando/Linyanti) are carbonate dominated. We demonstrate that under progressive evaporation, the river water under chemical evolution following Hardie-Eugster's model precipitate halite after 50,000 times concentration; and
- c. Sediments within the MOZB have been resolved using geophysics and typically are of resistivities $< 3 \Omega\text{m}$ (saline/clay), $3\text{-}10 \Omega\text{m}$ (brackish, clayey sands), $20\text{-}100 \Omega\text{m}$ (Kalahari sands and Basement rocks) using electrical based methods. Recent works within the Okavango Delta have mapped and resolved a high saline formation below the Okavango Delta probably hosting connate saline-brackish lake water from an earlier stage of the PLM.

6. Aridity evolution in Southern Africa since the Pliocene using wildfire history and savanna expansion across southern Africa since the late Miocene

The origin of the African savanna is one technique that is used for aridity evolution in Southern Africa, and has been traced back to 10-6 million years (Ma) ago, but the forcing mechanisms underlying its evolution is characterised by hot debates, from global atmospheric CO₂, regional fire activities, herbivore competitions to regional hydrological climate, etc. Here, we present the first microcharcoal-based fire activity records over the last ~6 Ma at four International Ocean Discovery Program (IODP) sites near southern Africa. The records show that fire activities in both savanna and non-savanna regions were stable. However, grass vegetation in burnt biomass continued to expand from 6 Ma into the present savanna region, whereas no grass expansion is observed in the non-savanna regions. A compilation of regional data suggests asynchronous C₄ grass expansion since 6 Ma on the African continents. We consider that the CO₂ and wildfire might have caused the origination of C₄ plants at ~10 Ma and ~7-6 Ma, respectively. Then since 6 Ma the regional climate began to drive the C₄ plants, expanding into the today's savanna habitat.

7. Analysis of projected impacts of sedimentation and bathymetry of selected small reservoirs to water scarcity problems on the priority water-linked sectors

- i. The study presented a vulnerability assessment of the Zambezi and Orange-Senqu River Basins and provides measures that will increase the resilience of the water-linked sectors considering a changing climate that negatively affects the Zambezi and Orange River Basins. Furthermore, alternative development options aimed at improving riparian communities and the water sector's adaptive capacity are evaluated. Climate change remains a contentious topic and international scientific research hotspot, which is extensively discussed amongst various disciplines and policymakers. Detecting future changes in the climate enables development sectors to make informed decisions regarding climate change responses. In addition, early detection approaches to climate change provide a resilient approach for tackling the challenges to sustainable economic growth. The study explores adaptation strategies aimed at maintaining the balance between the projected water demand against the available supply for the benefit of riparian countries and communities, and to a certain extent the entire Southern African Development Countries. In addition to the threats associated with extreme weather variability, the Basins' water resource is further strained by heavy reliance on the shared water resource and lack of coordinated efforts in managing and conserving water and maintaining balance in water utilisation by various sectors. Therefore, the threats render the Zambezi River and Orange-Senqu River Basin vulnerable, and hence the adoption of effective strategies is required.

The Zambezi and Orange-Senqu River Basin vulnerability emanate from these main environmental issues:

- a. Water quality degradation – the water pollution from various activities such as the radioactive minerals used as fertilisers in commercial and subsistence agriculture, mining and processing, water transport systems such as fishing vessels that discharge tons of human waste directly to the lakes, disposal of domestic and solid waste from small towns and communities, and litter and garbage adversely reduces the quality of the water resources. The degraded water quality has widespread economic and environmental impacts and often poses a direct threat to human and animal health if not properly managed.
- b. Water quantity reduction – the increasing demand for shared water resources and increased occurrence of extreme climatic events such as prolonged drought periods strain the resource.

Apart from environmental issues, the shared water resource is strained by challenges posed by conflicting interests and difficulty in managing the resource. While riparian states have established water commissions to jointly manage these resources it remains vulnerable due to the following reasons:

- a. Multiple riparian countries are involved in the utilisation of Zambezi and Orange-Senqu water resources;
- b. Inadequate basin-level institutional structures;
- c. Competing interests and prioritisation of certain sectors over another;
- d. Prioritisation of other urgent and competing issues that requires member state's urgent attention and budget to fulfil;
- e. Resources constraints within each member state. Such resources include institutional, legal, economic, and human resource requires a budget that in many cases is not readily available;
- f. Poor data collection on the water resource hydrology and environmental monitoring within the borders of most riparian countries;
- g. Poor stakeholder engagements and communication on pertinent issues affecting the shared water resource; and
- h. Inadequate training on pertinent issues such as water conservation and utilisation, and educational awareness on the impact of climate change and mitigation measures.

The water quality degradation and reduction of water resources in Zambezi and Orange Senqu basins often lead to social and economic vulnerability of the riparian countries and communities, as key sectors of such as energy, health, food production, cannot function at maximum capacity. The recent effects of climate change, cyclones Kenneth and Idai in the lower Zambezi River Basin in Mozambique affected the economy of the Southern African Development Community and resulted in people's displacement and loss of lives, amongst others. It is accepted that climate change is the main cause of water resources, hence the riparian countries' vulnerabilities. Therefore, adaptive response strategies must include conservation-based farming (irrigation and fishing) techniques, soil conservation, water-harvesting techniques, and reforestation. Furthermore, effective public education awareness training on the importance of maintaining a clean environment and water resources and demystification of climate change must be undertaken across various segments of people. More collaboration between riparian countries and knowledge exchange on various issues affecting the precious resource is deemed one of the best strategies to respond to climate change:

- a. With regards to climate change and water security: developmental perspectives for water-linked sectors in a future climate for Africa, the study indicates that the increasing demand for electricity throughout the SADC region can be met if these issues are addressed:
- b. Any planned projects on renewable energy and energy efficiency strategies should be based on extensively researched information on paleo-climate change patterns to predict future impacts.
- c. Studies on paleo-climate changes should be based on scientific evidence and must be aimed at modelling the changes in the river morphologies, flow and flood patterns, aridity evolution, and sediment deposit rates and frequencies.
- d. Despite hydropower and other renewable energy sources having the potential of providing a reliable, greenhouse gas emission-free energy source, the main barrier to HEP is the impact of climate change. The energy strategies and government policies do not acknowledge the impact of climate change, with no impacts modelled.

8. Paleoclimatic evolution and deposition rates in Southern Africa: Recommendations for policy

This report on deliverable 10, a report on paleoclimatic evolution and deposition rates in Southern Africa: recommendations for policy, is written in the framework of the ‘effects of pliocene-pleistocene climatic changes on evolution of river systems in Southern Africa’ research project, focusing on the Zambezi and Orange River basins. The report outlines three important issues with regards to policy recommendations, viz increasing electricity demand, adaptive strategy policy recommendation and sedimentation policy recommendation. Regarding increasing demand for electricity throughout the SADC region:

- a. Any planned projects on renewable energy and energy efficiency strategies should be based on extensively researched information on paleo-climate change patterns to predict future impacts.
- b. Studies on paleo-climate changes should be based on scientific evidence and must be aimed at modelling the changes in the river morphologies, flow and flood patterns, aridity evolution, and sediment deposit rates and frequencies.
- c. Despite hydropower and other renewable energy sources having the potential of providing a reliable, greenhouse gas emission-free energy source, the main barrier to HEP is the impact of climate change. The energy strategies and government policies do not acknowledge the impact of climate change, with no impacts modelled.

Hydropower is one of the major resources, not only to riparian states of the Orange and Zambezi River Basin but other major rivers in the SADC region such as the Congo River in DRC. The total developed capacity in the main Zambezi River and along its major tributaries is currently 5 862 MW and confirmed potential projects have an additional capacity of 13 126 MW. The SADC countries that do not have a share in the Orange and the Zambezi River waters derive indirect benefits through regional power exchanges managed through various organisations interconnection. It is therefore imperative that the development of hydropower within the Orange and the Zambezi River Basin include both riparian states and members of the organisations. Furthermore, energy laws and policies should be developed in line with the following SADC Protocols:

- The SADC Protocol on Energy of 1996 commits member states to develop and use energy to support economic growth and development, poverty alleviation, and improvement of the standard and quality of life throughout the sub-region

Policy: All riparian states should develop and use energy to support economic growth and development, poverty alleviation, and improvement of the standard and quality of life for their communities

- SADC Energy Sector Action Plan of 1997 recommends that the SADC energy program concentrates on priority activities that could be implemented efficiently on a regional basis for the benefit of the entire region.

Policy: All riparian states should concentrate on priority activities that could be implemented efficiently on a regional basis for the benefits of the entire region.

Adaptive strategy policy is based on the vulnerability study which was conducted earlier and provides measures that will increase the resilience of the water-linked sectors considering a changing climate that negatively affects the Zambezi and Orange River Basins. Furthermore, alternative developmental options aimed at improving riparian communities and the water sector's adaptive capacity were evaluated. Climate change remains a contentious topic and international scientific research hotspot, which is extensive, discussed amongst various disciplines and policymakers. Detecting future changes in the climate will enable development sectors to make informed decisions regarding climate change responses and enable a resilient approach for tackling the challenges to sustain economic growth to be adopted. Strategies aimed at maintaining the balance between water demands for various uses against the available supply and provide adaptation strategies for water resources and affected riparian states and communities were outlined. Apart from the already low levels of water resources due to shared utilisation of the water resource, the impact of climate change on the Zambezi River and Orange-Senqu River requires the adoption of effective strategies aimed at addressing the extreme weather variability. The Zambezi and Orange-Senqu River Basin vulnerability emanate from these main environmental issues:

- a. Water quality degradation – subsistence agricultural activities, mining and processing activities, water pollution that arises from water transport systems such as fishing vessels that discharge tons of human waste directly to the lakes, disposal of domestic and solid waste from small towns and communities, and litter and garbage along with the water bodies impact on water resources. The degraded water quality has widespread economic and environmental impacts and often poses a direct threat to human and animal health if not managed.
- b. Water quantity reduction – the increasing demand for shared water resources and increased occurrence of extreme climatic events such as prolonged drought periods strain the resource.

Apart from environmental issues, the shared water resource is strained by ineffective management. While riparian states have established water commissions to jointly manage these resources remains vulnerable due to the following reasons:

- a. Difficulty in water management due to the involvement of multiple riparian countries;
- b. Inadequate basin-level institutional structures;
- c. Competing interests and prioritisation of certain sectors over another;
- d. Competing issues other than water that demand time, attention, and money;

- e. Institutional, legal, economic, and human resource constraints within each country;
- f. Poor data collection in some riparian countries;
- g. Poor stakeholder engagements and communication;
- h. Inadequate training on pertinent issues such as water conservation and educational awareness on the impact of climate change and mitigation measures.

The water quality degradation and reduction of water resources in these basins lead to social and economic vulnerability of the riparian countries and communities, as key sectors of such as energy, health, food production, cannot function at maximum capacity. It is accepted that climate change is the main cause of water resources and hence the riparian countries' vulnerabilities. Therefore, adaptive response strategy policies must include conservation-based farming (irrigation and fishing) techniques, soil conservation, water-harvesting techniques, and reforestation. Furthermore, effective public education awareness training on the importance of maintaining a clean environment and water resources and demystification of climate change must be undertaken across various segments of people. More collaboration between riparian countries knowledge exchange on various issues affecting the precious resource is deemed one of the best strategies to respond to climate change.

With regards to sedimentation policy, most reservoirs in the Orange and Zambezi Basin could be as silted up and their storage capacities may not sustain the current water demands for household and livestock use. Small dams are at the highest risks of losing storage capacities. This implies that most communities within the Orange and Zambezi basin are water insecure and are subject to high risks of economic scarcity within next 50 years amidst climatic changes. Agricultural activities remain the drivers of siltation and loss of storage capacities for most reservoirs. The cost of addressing sedimentation among reservoirs bears a heavy toll on the government planning process, but at the same time, the very propellant of reservoirs' loss of storage capacities could be transformatively be utilised to build profitable business models and be reused for fertilisation of crops. This remains poorly utilised coping strategy and opportunity for most countries within the catchments. The coping strategies such as alternative livelihood, water harvesting, and water shedding recorded in various parts of the catchment suggests a spatially distributed nature of the problem of water scarcity due to siltation and climatic changes. Some sub-catchments within the Orange and Zambezi Basin, adopted destructive approaches such as conflicts, cultivating within the legally forbidden buffer zones, digging wells right on dry beds of river channels and reservoirs especially during water stressful period, among others as coping strategies water scarcity problem. Given the systemic and complex nature of water scarcity study proposed a conceptual model that is inherently proposing integrated and transdisciplinary approaches to address the challenges of reservoirs' storage losses and siltation challenges for sustainable water resources by 2030 and beyond.

Based on the finding that reservoirs' storage capacities of earth dams are low and are losing storage capacities due to siltation, it is recommended that the drivers of siltation be addressed through policies.

- a. The water scarcity risk within the Orange and Zambezi Basin are spatially distributed across all countries that share the basins, hence, policy should advocate for dredging more medium to large reservoirs to cushion water deficits especially during water-stressful period between July and early November.
- b. High sedimentation remains a major threat to the water security within the catchments, it is recommended that business models should be explored around it to address it in a profitable way as this remains quite unexplored option.
- c. Policy which enforces both local and international laws around water protection.
- d. Given the high rates of siltation and being the major threat to the sustainability of water resources amidst climatic changes, a dedicated policy on research bathymetric surveying and siltation monitoring is recommended to determine and keep checks on the full extent of the problem and how it is punctuating waters scarcity.
- e. Given that the water challenges within the Orange and Zambezi are largely human induced, there is also need for deliberate policies on educational programmes that bring about behavioural changes for sustainable small basin management.

The results obtained, improved our understanding of the ability of geological processes, tectonic movements, and climatic changes to control fluvial erosion, which informs existing evolution theories.

ACKNOWLEDGEMENTS

First and foremost, we would like to acknowledge the efforts of the many people who have contributed to this work, and the development of this report. Specifically, we would like to thank the following scientists for actively participating in research, their hard work, tenacity and perseverance and transforming all the data into this report, *viz*:

Professor Eduardo Garzanti	Bayon Germain	Pedro Dinis
Pieter Vermeesch	Guido Pastore	Alberto Resentini
Marta Barbarano	Gwenael Jouet	Massimo Dall'Asta
Jing Yang	Junsheng Nie	Haobo Zhang
Xiaofei Hu	Yunfa Miao	Taian Chen
Zheng Wan	Yongtao Zhao	

We received all the assistance that we required from them, and we particularly value their resolute and insightful guidance of our work. We were indeed under proper guidance and in safe hands.

We are also indebted to the College of Agriculture and Environmental Sciences of the University of South Africa for providing guidance and leadership, i.e. Professor Solomon R. Magano. We also express our sincere gratitude to the UNISA research office: Mr Harry M. Bopape and Prof. Thenjiwe C. Meyiwa for their tireless efforts in assisting us, and for being great understanding people who always stood by us.

Special thanks to this project's reference group members for their valuable time, comments, and guidance. Last, but not least, we are grateful to Dr B Petja the WRC Research Manager, who awarded us an opportunity to do this research, enabled us to grow as scientists, and to learn from our mistakes, and guided us throughout the project.

REFERENCE GROUP

Dr BM Petja	Research Manager: Climate Change: Water Research Commission (Chair)
Prof. A Green	University of KwaZulu-Natal
Dr F Mphephu	Cort and Fred Consulting Engineers
Prof. M Humphries	University of Witwatersrand
Dr Grant Baybes	Witwatersrand University
Dr M Mgquba	Department of Water and Sanitation

This page was intentionally left blank

TABLE OF CONTENTS

EXECUTIVE SUMMARY	iii
ACKNOWLEDGEMENTS	xv
REFERENCE GROUP	xv
TABLE OF CONTENTS	xvii
LIST OF TABLES	xxvii
LIST OF FIGURES.....	xxix
CHAPTER 1	1
BACKGROUND INFORMATION.....	1
1.1 Introduction	1
1.2 Project Relevance.....	1
1.3 Overview, background, and rationale.....	2
1.4 Aims and objectives	6
1.5 Methodology.....	7
1.6 Deliverables.....	7
CHAPTER 2	9
PROVENANCE OF DEVELOPMENTAL RIVER SYSTEMS OF SOUTHERN AFRICA: USING THE ZAMBEZI RIVER AS A CASE STUDY	9
2.1 Introduction	9
2.2 Geology	11
2.2.1 The Precambrian.....	11
2.2.2 The break-up of Gondwana.....	13
2.3 The Zambezi River.....	13
2.3.1 Drainage evolution through time	16
2.4 Methodology.....	16
2.4.1 Petrography	17
2.4.2 Heavy minerals	17
2.4.3 River morphometry	18
2.5 Results and discussion	19
2.5.1 The Uppermost Zambezi.....	21
2.5.2 The Upper Zambezi.....	24
2.5.3 The Middle Zambezi	24
2.5.4 The Lower Zambezi.....	24
2.5.5 The northern coast, the shelf, and the slope	25
2.5.6 Sand generation in the Zambezi catchment.....	26

2.5.7 The Upper Zambezi: mixing with detritus from Karoo basalts	27
2.5.8 The Middle Zambezi: first cycle and recycled detritus from Zambia	28
2.5.9 The Lower Zambezi: feldspar-rich sand from Precambrian basements	29
2.5.10 The Zambezi passive margin.....	31
2.5.11 How does Zambezi sand fit with classical sedimentary-petrology theories?.....	31
2.5.12 Provenance models	32
2.5.13 The final signature of Zambezi sand	33
2.5.14 Do minerals “mature” during fluvial transport?.....	34
2.5.15 Broken transmission of provenance signals: the anthropic effect.....	36
2.5.16 Weathering effects inherited from the past.....	37
2.6 Conclusions	38
CHAPTER 3	39
INPUTS OF SOUTHERN AFRICAN TERRESTRIAL SYSTEMS INTO THE ATLANTIC-INDIAN OCEAN	39
3.1 Introduction	39
3.2 Study area	41
3.2.1 Geology	41
3.2.2 Geomorphology and River Drainage	44
3.3 Methodology.....	48
3.3.1 Silt and Clay Mineralogy	48
3.3.2 Sand and mud geochemistry	49
3.3.3 Isotope Geochemistry.....	50
3.3.4 Detrital-Zircon Geochronology	51
3.4 Results and discussion	52
3.4.1 The Uppermost Zambezi.....	52
3.4.2 The Upper Zambezi.....	57
3.4.3 The Middle Zambezi.....	58
3.4.4 The Lower Zambezi.....	58
3.4.5 The Northern Zambezi Delta.....	59
3.4.6 Provenance Insights from Clay Mineralogy and Sediment Geochemistry.....	59
3.5 Conclusions	76
CHAPTER 4	78
MODELLER FUTURE CLIMATIC CONDITIONS AND THE IMPLICATION ON WATER SECURITY: ORANGE & ZAMBEZI RIVER BASINS	78
4.1 Introduction	78
4.1.1 Background.....	78
4.2 Hydrological features of the basins.....	81

4.2.1 Rivers.....	81
4.2.2 Reservoirs.....	86
4.2.3 Rapids and waterfalls.....	87
4.2.4 Wetlands.....	88
4.3 Hydrological Modelling.....	90
4.4 Climate Modelling of the Zambezi and Orange Basin.....	92
4.4.1 Sources of data	93
4.4.2 Regional Climate Models Data.....	94
4.4.3 Climate Data Operators	95
4.4.4 Observations.....	95
4.4.5 Climate scenarios.....	96
4.5 Validation of the model data	96
4.6 Computation of climate indices	96
4.7 Projected changes in temperature and precipitation.....	98
4.7.1 Zambezi River Basin	98
4.7.2 Orange River Basin.....	99
4.8 Water Security implications.....	101
CHAPTER 5	102
ANALYSIS OF PROJECTED IMPACTS OF SEDIMENTATION AND BATHYMETRY OF SELECTED SMALL RESERVOIRS TO WATER SCARCITY PROBLEMS ON THE PRIORITY WATER-LINKED SECTORS IN THE ZAMBEZI RIVER BASIN OF ZAMBIA	102
5.1 Introduction	102
5.2 Aims and objectives	106
5.3 Description of the study area.....	107
5.4 Methodology.....	109
5.5 Storage capacities of selected reservoirs.....	109
5.6 Water scarcity risks based on the hydrological regimes of the reservoirs	113
5.7 Estimation of quantity of sediment accumulated in selected reservoirs	113
5.8 Main drivers of sedimentation in the reservoirs	115
5.9 Impact of the status of water availability and sedimentation on livestock, crop farming, fishing, and other water dependent socio-economic activities.....	115
5.10 Cost-benefit analysis of reservoir siltation on government planning process	115
5.11 Community-initiated coping strategies to water stresses and scarcity.....	115
5.12 Sediment control conceptual model and sustainable water resources management in reservoirs	116
5.13 Results.....	116

5.13.1 Storage capacities of selected reservoirs	116
5.13.2 Hydrological regimes of the reservoirs based on Bathymetric assessment and remote sensing	128
5.13.3 Estimation of quantity of sediment accumulated in selected reservoirs.....	129
5.13.4 Main drivers of sedimentation in the reservoirs	135
5.13.5 Community-initiated coping strategies to water stresses and scarcity.....	137
5.13.6 Sediment control measures and sustainable water resources management in reservoirs	141
5.14 Discussion.....	141
5.14.1 Impact of the status of water availability and sedimentation on livestock, crop farming, fishing, and other water dependent socio-economic activities	145
5.15 Policy implications	148
5.16 Conclusion.....	149
5.17 Recommendations	150
CHAPTER 6	151
ANALYSIS OF PROJECTED IMPACTS OF SEDIMENTATION AND BATHYMETRY ON THE GARIEP DAM TO WATER SCARCITY PROBLEMS ON THE PRIORITY WATER-LINKED SECTORS IN THE ORANGE RIVER BASIN OF SOUTH AFRICA.....	151
6.1 Introduction	151
6.2 Work planning and task description	152
6.3 Projects	153
6.3.1 Water management and allocation of the Gariep dam water	153
6.4 Research Problem Statement	156
6.5 Aims and Objectives.....	156
6.6 Methodology.....	156
6.7 Results and discussion	159
6.8 Conclusion.....	163
6.9 Water Resources management: Making use of the Department of Water and Sanitation’s water information to reflect on future water needs	164
6.9.1 Introduction.....	164
6.9.2 Study area	164
6.9.3 Water planning and future needs.....	164
6.9.4 Aim and Objectives.....	165
6.9.5 Methodology	166
6.9.6 Results.....	167
6.9.7 Conclusion.....	169
6.10 Using the DWS survey information to reflect on lost volume through siltation	170

6.10.1 Introduction	170
6.10.2 Methodology	172
6.10.3 Results.....	173
6.11 DWS planning information and water loss through evapotranspiration	177
6.11.1 Introduction	177
6.11.2 Results.....	179
6.12 Geology, engineering, siltation and groundwater	180
6.12.1 Introduction	180
6.12.2 An objective summary of the DWS reports pertaining to geology and the environment in the Upper Orange River.....	182
6.12.3 Results.....	184
6.12.4 Conclusions.....	188
6.12.5 The Statement and Motivation of the need for sedimentation dams outside of the Gariep dam	189
6.12.6 Study of the geology of the Gariep dam region and find evidence that Gariep contributes to groundwater. Estimate deep drainage losses. Motivate your estimates from literature.....	191
6.12.7 Conclusion	195
6.13 The engineering process of dam siltation evaluation in South Africa using GIS and satellite information, with a focus on the Vanderkloof dam	196
6.13.1 Introduction	196
6.13.2 Aims and objectives.....	195
6.13.3 Methodology	197
6.13.4 Monitoring of the dam volume and dam siltation.....	197
6.13.5 Results and discussion	199
6.13.6 Conclusion	202
6.14 A geological reflection on signs of water loss.....	203
6.14.1 Materials and Methods	203
6.14.2 Results.....	205
6.15 Measurement of dam circumference and the dynamics of circumference change as a function of Google Earth.....	210
6.15.1 Introduction	210
6.15.2 Aims and objectives.....	210
6.15.3 Study Area.....	211
6.15.4 Methodology	211
6.15.5 Production of perimeter maps of the dam using satellite imagery for various stages of dam fullness	217

6.15.6 Correlation analysis between water body surface area and depth values	220
6.15.7 Area best suited for continuous measurement whereby remote means can be focused	222
6.15.8 Automated procedure for the recording of dam water body surface area using . satellite imagery; how this can replace the level recordings done by the DWA	223
6.15.9 Novelty of research.....	223
6.16 Mapping of the topography before the dam was built	225
6.16.1 Methodology	225
6.16.2 Results and discussion	225
6.17 Setting up a database relating dam depth and dam perimeter change.....	227
6.17.1 Introduction and methodology	227
6.17.2 Results.....	228
6.18 Dam volume calculations, using GIS and the old dam floor information	230
6.18.1 Introduction and methodology	230
6.18.2 Results.....	231
6.19 A reflection on sedimentation in the Gariep based on evidence found in upstream dams.....	234
6.19.1 Introduction	234
6.19.2 Methodology	236
6.19.3 Results.....	237
6.19.4 Conclusion	243
6.20 Sediment origin tracing by reflecting on evidence and sampling procedures	243
6.20.1 Introduction and methodology	243
6.20.2 Limitations	248
6.21 Reflect on the smaller dams upstream of Gariep that act as sediment traps	248
6.21.1 Introduction and methodology	248
6.21.2 Results.....	249
6.22 The contributions remote sensing does or don't contribute to the Gariep situation	254
6.22.1 Introduction.....	254
6.22.2 Field methodology.....	258
6.22.3 Results.....	258
6.22.4 Conclusion	260
6.23 Discussion and conclusion	258
6.24 Measurement of dam circumference and the dynamics of circumference change	260
CHAPTER 7	261
PALAEO-CLIMATIC CHANGES AND DEPOSITION RATES IN SOUTHERN AFRICA: IMPACTS OF REGIONAL GROUNDWATER QUALITY	261

7.1 Introduction	261
7.2 Aims and objectives	263
7.3 Regional setting and basin development.....	263
7.4 Methodology.....	265
7.5 Results.....	265
7.5.1 Geology and geochronology.....	265
7.5.2 Recharge and stable isotopes.....	272
7.5.3 Groundwater ages	274
7.5.4 Groundwater chemistry.....	274
7.5.5 Hydrochemistry	279
7.6 Discussion.....	281
7.6.1 River water chemistry and formation of evaporites	281
7.6.2 Conceptual lake stage development and groundwater salinity.....	286
7.7 Conclusions	289
CHAPTER 8	290
ARIDITY EVOLUTION IN SOUTHERN AFRICA SINCE THE PLIOCENE USING WILDFIRE HISTORY AND SAVANNA EXPANSION ACROSS SOUTHERN AFRICA SINCE THE LATE MIOCENE	290
8.1 Introduction	290
8.2 Geographical and Geological Setting.....	291
8.3 Methodology.....	292
8.4 Results.....	293
8.5 Discussion.....	294
8.5.1 Wildfire evolution and C4 plant expansion routes in southern Africa	294
8.5.2 The driving mechanism of C4 expansion across Africa.....	297
8.6 Conclusion.....	300
CHAPTER 9	301
CLIMATE CHANGE AND WATER SECURITY: DEVELOPMENTAL PERSPECTIVES FOR WATER-LINKED SECTORS IN A FUTURE CLIMATE FOR AFRICA (BI-NATIONAL ASSESSMENT)	301
9.1 Introduction	301
9.2 Study aims and objectives.....	301
9.3 Project locality	302
9.3.1 Upper Zambezi Section (UZS)	302
9.3.2 Middle Zambezi Section (MZS).....	303
9.3.3 Lower Zambezi Section (LZS)	303
9.3.4 Rainfall patterns.....	304
9.4 Zambezi River Basin: hydropower resource assessment.....	305

9.4.1 Introduction	305
9.4.2 Existing Hydropower Stations.....	306
9.4.2.1 Major Hydropower Station.....	306
9.5 New and planned hydropower projects	309
9.5.1 Mozambique hydropower potential	309
9.6 Zambia hydropower potential	310
9.6.1 Devil’s Gorge Project	310
9.6.2 Batoka Gorge	310
9.6.3 Mupata Gorge.....	311
9.6.4 The Kafue Gorge Lower	311
9.7 Tanzania hydropower potential.....	311
9.7.1 Rumakali Hydropower Scheme	311
9.7.2 Songwe hydropower scheme	311
9.8 Malawi hydropower potential	312
9.8.1 Tedzani IV.....	312
9.8.2 Songwe	312
9.8.3 Kholombidzo hydro.....	312
9.8.4 Mpatamanga Hydropower Project	312
9.8.5 Lower Fufu hydro-power project.....	312
9.8.6 Kapichira III	313
9.9 Southern African power generation overview.....	313
9.9.1 Establishment of the Southern African Power Pool	313
9.9.2 The SAPP energy generation capacity	314
9.9.3 Energy generation mix.....	316
9.9.4 The role of Zambezi River in Mozambique energy mix	317
9.9.5 The role of Zambezi River in Zambia energy mix.....	318
9.9.6 The role of Zambezi River in Tanzania energy mix	319
9.9.7 The role of the Zambezi River in the Angolan energy mix.....	319
9.9.8 The role of the Zambezi River in the Namibian energy mix	319
9.9.9 The role of the Zambezi River in the Zimbabwean energy mix.....	319
9.9.10 The role of the Zambezi River in the Malawian energy mix	320
9.9.11 The role of the Zambezi River in the DRC energy mix	320
9.9.12 The role of the Zambezi River in the Botswanan energy mix.....	320
9.9.13 The role of the Zambezi River in the Lesotho energy mix	321
9.9.14 The role of the Zambezi River in the South African energy mix.....	321

9.9.15 Advantages of hydropower	323
9.10 Effects of climate change on hydropower	324
9.10.1 Droughts	324
9.10.2 Catastrophic natural disasters	325
9.11 Electricity supply threats and challenges.....	326
9.11.1 The Role of South Africa in the SADC region	326
9.11.2 Impact of Load Shedding on the economy	326
9.12 Energy policy framework, laws, and regulations	326
9.12.1 South Africa	327
9.12.2 Mozambique.....	329
9.12.3 Zambia	330
9.12.4 Angola	330
9.13 Discussion.....	330
9.14 Conclusion.....	331
9.15 Recommendations	331
CHAPTER 10	333
CLIMATE CHANGE AND WATER SECURITY: DEVELOPMENTAL PERSPECTIVES FOR WATER-LINKED SECTORS IN A FUTURE CLIMATE FOR AFRICA (BI-NATIONAL ASSESSMENT): DIFFERENT DEVELOPMENTAL RESPONSE MODELS CONSIDERING SOCIO-ECONOMIC DRIVERS.....	333
10.1 Introduction	333
10.2 Aims and objectives	334
10.3 Study area	334
10.3.1 The Orange River Basin.....	334
10.3.2 The Orange-Senqu River Basin.....	340
10.4 Zambezi and Orange-Senqu river water management.....	344
10.4.1 Zambezi River Authority	344
10.4.2 Zambezi Watercourse Commission	344
10.4.3 The Orange-Senqu River Commission	344
10.5 Water resources utilisation.....	345
10.5.1 Non-consumptive uses	345
10.5.2 Consumptive uses.....	348
10.6 Inter-basin transfer	349
10.6.1 Mining.....	350
10.7 Vulnerability assessment	350
10.7.1 Basin’s water resource vulnerability	350
10.8 Peoples’ vulnerability.....	353

10.8.1 Economic vulnerability	353
10.8.2 Social vulnerability.....	355
10.9 Adaptive response strategies.....	355
10.9.1 Strategies on drought vulnerabilities	356
10.9.2 Strategies on improve flood management.....	356
10.9.3 Improved water management and collaboration	357
10.9.4 Public educational awareness programme	358
10.10 Discussion.....	359
10.11 Conclusions and recommendations.....	359
CHAPTER 11	360
RECOMMENDATIONS FOR POLICY	360
11.1 Introduction	360
11.2 Aims and objectives	361
11.3 Provision of water services	361
11.4 Study areas.....	362
11.5 Energy policy framework	362
11.5.1 South Africa	362
11.5.2 Mozambique.....	364
11.5.3 Zambia	365
11.5.4 Angola	365
11.5.5 Discussion	366
11.6 Adaptive response strategies policy framework	366
11.6.1 Strategies on drought vulnerabilities	366
11.6.2 Strategies on improve flood management.....	367
11.6.3 Improved water management and collaboration	367
11.6.4 Public Educational Awareness Programme Policies	368
11.6.5 Discussion	369
11.7 Sedimentation policy framework.....	369
11.7.1 Discussion	372
11.8 Conclusion and recommendations	373
11.8.1 Conclusion	373
11.8.2 Recommendations.....	374
REFERENCES	375

LIST OF TABLES

Table 1.1: Deliverables	7
Table 2.1: Key compositional parameters	20
Table 3.1: Silt and clay mineralogy in the Zambezi catchment, determined by X-ray powder-diffraction.....	47
Table 3.2: Sand and mud geochemistry in the Zambezi catchment	48
Table 3.3: Neodymium isotope values and Sm-Nd model ages for cohesive mud	50
Table 4.1: Orange basin: areas and rainfall by country	80
Table 4.2: Estimates of flow contributed by the main tributaries of the Zambezi River	82
Table 4.3: Total use values of the Zambezi wetlands.....	89
Table 4.4: Summary of the modelling statistics of the main subbasins of the ZRB based on CRU rainfall	90
Table 4.5: SMHI-RCA4 Africa CORDEX 50 km matrix	94
Table 4.6: Core ET-SCI indices.....	96
Table 4.7: Non-core ET-SCI indices	97
Table 5.1: Criteria for determination of Water Scarcity.....	112
Table 5.2: Water Depth, Surface area and Volume data for Musokotwane Reservoir.....	117
Table 5.3: Water depth, Surface, and volume relationship for Mulabalaba Reservoir.....	122
Table 5.4: Water depth, Water surface are and Volume for Sianankanga Reservoir	125
Table 5.5: Estimated Total Sediment Loaded in the Reservoirs	129
Table 5.6a: Water availability and Sedimentation records for selected reservoirs in the Magoye sub-catchment of the Kafue Catchment in the Zambezi Basin.....	130
Table 5.6b: Sedimentation status among selected reservoirs in Kalomo, Zimba and Kazungula District in the Zambezi River Basin	133
Table 5.7: Summary of factors influencing reservoir sedimentation, water flows and water quality	134
Table 5.8: Some coping Strategies adopted by communities to water stresses induced by siltation and climate change	137
Table 5.9: Livestock and human population in the selected districts	144
Table 5.10: Summary of the Impact of sedimentation and poor water supply	146
Table 6.1: Gariep dam water allocations.....	157
Table 6.2: Gariep dam depths at different sampling points.....	173
Table 6.3: Gariep dam depths at different sampling points.....	184
Table 6.4: Area capacity relationship of Gariep dam	226
Table 6.5: Table of the perimeter change of the Gariep dam from March 1975-June 2022.....	227

Table 6.6: A table showing area capacity relationship of the Gariep dam.....	230
Table 6.7: Sediment survey data (DWA, 2006).....	237
Table 6.8: Rain survey data (DWA, 2012).....	237
Table 6.9: Sediment survey data (DWA, 2006).....	238
Table 6.10: Showing the rain survey data (DWA, 2012).....	238
Table 6.11: Showing the rain survey data (DWA, 2012).....	239
Table 6.12: Summary of the properties of the rendering options	246
Table 6.13: Surveyed sedimentation statistics of the Bethulie Dam (WRC, 1992)	249
Table 6.14: The annual total discharge/overspill volumes at Bethulie Dam for periods when there was an overspill (DWS website, 2022).....	250
Table 6.15: Sedimentation statistics of the Vanderkloof dam (DWS, 2006; DWS website, 2022).....	251
Table 6.16: Gariep dam object visibility	258
Table 7.1: A synthesis tabular matrix of sediment and groundwater ages within MOZB.....	267
Table 7.2: Synthesis tabular matrix of regional resistivities, methods and hydrogeological interpretations in the MOZB.....	275
Table 7.3: The river water chemistry of major rivers	251
Table 9.1: Current hydropower generation in the Zambezi River Basin	307
Table 9.2: Committed planned generation capacity (by country) from 2020 to 2023	319
Table 10.1: Percent of the River Basin in each country and population	334
Table 10.2: Geographic coverage of the Orange River Basin per country	339
Table 10.3: Summary of Basin Characteristics per country.....	340
Table 10.4: The current hydropower generation in the Zambezi River Basin.....	344
Table 10.5: The hydrological data from the two major hydropower plants in the Zambezi River major tributaries – 27 July 2021.....	353

LIST OF FIGURES

Figure 2.1: The Zambezi drainage basin	9
Figure 2.2: Geological domains and time structure map of the Zambezi catchment and adjacent regions.....	12
Figure 2.3: Southern African map showing Zambezi River and associated geomorphological features	15
Figure 2.4: River morphometry	19
Figure 2.5: Petrographic changes along the Zambezi sediment-routing system from source to sink .	21
Figure 2.6: Sand composition in major Zambezi tributaries.....	23
Figure 2.7: Downstream quartz decrease along the segmented Zambezi sediment-routing system..	26
Figure 2.8: Changes in transparent-heavy-mineral suites downstream the segmented Zambezi sediment-routing system	27
Figure 2.9: Stepwise changes in mineralogical signatures along the Zambezi sediment-routing system	29
Figure 2.10: Zambezi River sands compared with coastal and offshore sediments	35
Figure 3.1: The Zambezi drainage basin (base map from Google Earth™)	40
Figure 3.2: Geology and geomorphology of Southern Africa	43
Figure 3.3: Composition of the Zambezi river sands	53
Figure 3.4: Sand and mud geochemistry	54
Figure 3.5: Rare Earth Element geochemistry	55
Figure 3.6: Relationship between $\epsilon Nd(0)$ values and depleted mantle model ages (TNd,DM) for the Zambezi mainstem and tributaries	56
Figure 3.7: U-Pb age spectra of detrital zircons	57
Figure 3.8: Relationships among chemical elements in Zambezi sand and cohesive mud	62
Figure 3.9: Multiple controls on $^{143/144}Nd$ isotope values.....	63
Figure 3.10: Multidimensional scaling map based on U-Pb zircon-age spectra.....	66
Figure 3.11: Discriminating the effects of weathering, recycling, and grain size from geochemical data of Zambezi sands, levee silty sands, and muds	73
Figure 4.1: The Orange and Zambezi River Basins.....	78
Figure 4.2: The Zambezi River basin and its 13 subbasins.....	79
Figure 4.3: Mean monthly flow hydrograph of the 13 subbasins of the ZRB and flow hydrograph of the 1991-1992 drought.....	86
Figure 4.4: Major dams of the ZRB	87
Figure 4.5: ZRB maps of hydrological features: dams, waterfalls, rapids, islands, springs, rivers, lakes	88

Figure 4.6: Baseflow index of tributaries of the ZRB	92
Figure 4.7: CORDEX African domain	94
Figure 4.8: Projected changes in minimum and maximum temperature and precipitation 2020-2050/1970-2000 in the Zambezi River Basin	99
Figure 4.9: Projected changes in minimum and maximum temperature and precipitation 2020-2050/1970-2000 in the Orange River Basin.....	100
Figure 5.1: Density of human population.....	104
Figure 5.2: Conceptual Framework of the study	105
Figure 5.3a: General location of Kazungula and Zimba District in Southern Zambia	107
Figure 5.3b: Distribution of some dams in the Kazungula, Livingstone, Zimba and Kalomo	108
Figure 5.4: Process of setting up the equipment before deployment for bathymetric survey adapted from Muchanga (2020:59)	110
Figure 5.5: Visual impression of the window interface during Bathymetric Survey	112
Figure 5.6a: Satellite image overlaid with survey transects.....	116
Figure 5.6b: Bathymetric Map of the Musokotwane Reservoir	117
Figure 5.7: Water (a) depth-volume relationship and, (b) surface area-volume relationship for Musokotwane dam	119
Figure 5.8: Delineated Catchment of the Musokotwane Reservoir in Kazungula District, Southern Zambia (April 2022).....	120
Figure 5.9: (a) Satellite image overlaid with survey transects and (b) Bathymetric Map of Mulabalaba reservoir (Field data, April 2022)	121
Figure 5.10: (a) Water depth-volume relationship and (b) Water surface area-volume relationship for Mulabalaba Reservoir (April 2022)	122
Figure 5.11: Delineated catchment of Mulabalaba Reservoir in Kazungula District, Southern Zambia (April 2022)	124
Figure 5.12: Satellite image overlaid with survey (a) pathways; and (b) Bathymetric Map of Siankanga Reservoir	125
Figure 5.13: Water surface area-Volume (a) and Water depth-volume (b) relationships for Siankanga reservoir.....	127
Figure 5.14: Delineated catchment of Siankanga Reservoir in Kalomo District, Southern Zambia (April 2022)	128
Figure 5.15: Hydrological regimes of (a) Musokotwane, (b) Mulabalaba and, (c) Siankanga Reservoirs, 2017-2022 (computed based on remote sensed water surface areas at different times from Sentinel A and B, 2022)	129
Figure 5.16: Drivers of Sedimentation in the Musokotwane, Mulabalaba and Siankanga Catchments (Field data, 2022)	137
Figure 5.17: Signature of aggregate water use relative to available discharge along two major river corridors under normal and 30-year drought conditions.....	140

Figure 5.18: Conceptual Model for sustainable management of water resources and siltation control in reservoirs in the Zambezi River Basin	144
Figure 6.1: Gariep dam and the surrounding geology.....	155
Figure 6.2: Demarcation of the Gariep dam.....	155
Figure 6.3: Major water transfer schemes from the Gariep and Vanderkloof dams	160
Figure 6.4: Gariep dam hydrology data	162
Figure 6.5: a. Picture and, b. map of Gariep the dam	164
Figure 6.6: Graph showing capacity, inflow, and outflow of the Gariep dam.....	168
Figure 6.7: Remaining Water Capacities of Gariep dam after sedimentation.....	177
Figure 6.8: Map of the Gariep dam	181
Figure 6.9: Water capacity of the Gariep dam after sedimentation from 1971 to 2022	189
Figure 6.10: Sedimentation in the Gariep dam	190
Figure 6.11: Geology of the Upper Orange WMA	192
Figure 6.12: Geohydrology of the Upper Orange WMA.....	193
Figure 6.13: Drainage State of the Gariep dam on 16 May 2022.....	195
Figure 6.14: The Gariep dam	197
Figure 6.15: The Vanderkloof dam	198
Figure 6.16: The hydrological state of the Gariep dam	199
Figure 6.17: The Gariep dam in December 1994 captured on Google Earth	199
Figure 6.18: The Gariep dam in December 2012 captured on Google Earth	200
Figure 6.19: The Gariep dam in May 2022 captured on Google Earth.....	200
Figure 6.20: The hydrological state of the Vanderkloof dam	201
Figure 6.21: The Vanderkloof dam captured in December 1990 on Google Earth	201
Figure 6.22: The Vanderkloof dam captured in December 2002 on Google Earth	202
Figure 6.23: The Vanderkloof dam captured in December 2020 on Google Earth	202
Figure 6.24: Colour Infrared (5, 4, 3)	203
Figure 6.25: Short-Wave Infrared (7, 6, 4).....	204
Figure 6.26: Geology (7, 6, 2).....	204
Figure 6.27: Moisture Indexes	204
Figure 6.28: LANDSAT explorer rendering colour infrared image: November 2016.....	205

Figure 6.29: LANDSAT explorer rendering colour infrared image: December 2021	206
Figure 6.30: LANDSAT explorer rendering a short-wave infrared image: November 2016	207
Figure 6.31: LANDSAT explorer rendering a short-wave infrared image; December 2021.....	207
Figure 6.32: LANDSAT explorer rendering a geological image: November 2016	208
Figure 6.33: LANDSAT explorer rendering a geological image: December 2021	208
Figure 6.34: LANDSAT explorer rendering a geological image: 28 November 2016	209
Figure 6.35: LANDSAT explorer rendering a geological image: 12 December 2021	209
Figure 6.36: Image of the Gariep dam	211
Figure 6.37: Digitized contour lines of the Gariep dam area showing dam floor topography.....	214
Figure 6.38: Digitized extract of the extracted contour lines from raster data 3025DA-1994b	215
Figure 6.39: Map of digitized contours of the Gariep dam	216
Figure 6.40: The digitized extent of the Gariep dam from the extent provided in Google Earth	216
Figure 6.41: Gariep dam water levels in 1993	218
Figure 6.42: Gariep dam water levels in 1994	218
Figure 6.43: Image of the change in dam water levels in 2020.....	219
Figure 6.44: Capacity comparisons of the Gariep dam.....	219
Figure 6.45: Capacity of Gariep dam	220
Figure 6.46: Dam water level changes in 2019.....	221
Figure 6.47: Dam water level changes in 2022.....	221
Figure 6.48: The georeferenced 1:50k maps draped over Google Earth in QGis with the digitized contours in red.....	226
Figure 6.49: The georeferenced 1:50k maps draped over Google Earth in QGis with the digitized contours converted to points	226
Figure 6.50: The new depth elevation model for the Gariep dam, generated from the old contour maps.....	227
Figure 6.51: Bar graph and line graph showing the relationship between elevation and perimeter values	229
Figure 6.52: Line graph showing the change in perimeter of the Gariep dam from March 1975 to June 2022	229
Figure 6.53: Field elevation (m) and surface area (km ²) appear highly correlated	232
Figure 6.54: Field depth and surface area (km ²) appear highly correlated.....	232

Figure 6.55: Field storage (million m ³) and surface area (km ²) appear highly correlated.....	233
Figure 6.56: Sedimentation of reservoirs in South Africa.....	235
Figure 6.57: Sediment colours near the mouth of the Zambezi River as it empties into the sea	237
Figure 6.58: The observed loss in storage capacity due to sedimentation in Welbedacht dam.....	240
Figure 6.59: Satellite image of the Gariep dam/Orange River	241
Figure 6.60: Satellite image showing the deposited sediments in Gariep dam	241
Figure 6.61: Deposited sediment in the Vanderkloof dam	242
Figure 6.62: Sediments in the Welbedacht dam	243
Figure 6.63: Natural colour image of the Gariep dam as well as the Caledon River and Orange River confluence.....	244
Figure 6.64: Caledon River and Orange River Confluence and the Gariep dam reservoir over time.	246
Figure 6.65: Temporal change in sedimentation and storage capacity of the Gariep dam	252
Figure 6.66: True colour imagery of the Gariep dam – 5 January 2022	253
Figure 6.67: False colour (colour infrared) imagery showing the Gariep dam (bottom right) and the Vanderkloof dam (upper left)	254
Figure 6.68: Bethulie dam (top) and a portion of the Gariep dam (bottom), captured in May 2022. a) True colour, b) False colour	254
Figure 7.1: Outline of the Palaeo-Lake Deception (995 m amsl) and Palaeo-Lake Makgadikgadi (945 m amsl), extracted from the digital elevation model (Shuttle Radar Topographic Mission – SRTM) within the Kalahari Group Formation	262
Figure 7.2: Digital elevation model (Shuttle Radar Topographic Mission – SRTM) exhibiting structural depressions of the northern and central Kalahari with geographic references.....	265
Figure 7.3: Surficial geology over the Makgadikgadi-Okavango-Zambezi Basin and the main structural fault systems	267
Figure 7.4: Synthesis of stable isotope of Oxygen-18 and Deuterium	273
Figure 7.5: A synthesis of the regional resistivity profiles within MOZB conducted using both ground and air based on geophysics	278
Figure 7.6: Water quality sampled points over the MOZB with a background of lake stages at 995 and 945 m amsl, with corresponding ages of 3-2.5 and 1.4 Ma, respectively	280
Figure 7.7: PHREEQC 3 simulation of evolving lake chemistry in the closed lake filled with fresh water (Zambezi water) with evaporation and precipitation of minerals.....	284
Figure 7.8: Evaporation path of closed lake system of solutes with progressive evapo-concentration	266

Figure 7.9: Summarised conceptual model of the evolution stages from the formation of the PLD to formation of evaporations that were partially flushed resulting in salinity	288
Figure 8.1: Study sites used to evaluate savanna evolution.....	291
Figure 8.2: Summary of a. Major lithological characteristics of sediment cores and b. Age-depth relationships of Sites U1475, U1476, U1478, and U1479 in Expedition IODP 361.....	292
Figure 8.3: Fire evolution and savanna expansion across southern Africa	294
Figure 8.4: Evolution of Savanna across Africa over the last 10 Ma basing on microcharcoals, isotope records, and correlations with the wildfire and atmospheric CO ₂	296
Figure 8.5: Correlations between grass-based climate and C4 plants changes during two different periods at the Limpopo drainage, south-eastern Africa	294
Figure 9.1: Southern African map showing the Zambezi River and associated geomorphological features	304
Figure 9.2: The average rainfall of the Zambezi River Basin based on various literature	305
Figure 9.3: SAPP energy mix and electricity (installed vs operating vs maximum demand vs peak demand + reserves) generation capacity.....	315
Figure 9.4: The SAPP 2019 generation energy mix from operating members	317
Figure 9.5: Ratio of installed capacity in the Central & Northern region, and southern area	318
Figure 9.6: South African installed Generation capacity from Eskom-owned power stations (A) and IPPs based on operating stations.....	322
Figure 9.7: South African electricity exports to SADC countries	323
Figure 9.8: Lifecycle (median estimates) of greenhouse gas (GHG) emissions of selected energy sources	324
Figure 10.1: Generalised Geological map of the Zambezi River basin	337
Figure 10.2: Zambezi River Basin average temperature.....	338
Figure 10.3: The average rainfall of the Zambezi River Basin.....	339
Figure 10.4: The Orange Basin.....	343
Figure 11.1: Conceptual Model for sustainable management of water resources and siltation control in reservoirs in the Orange and Zambezi River Basin	371

CHAPTER 1

BACKGROUND INFORMATION

1.1 Introduction

Southern Africa's surface water resources are under increasing stress due to modifications of river flow regimes influenced by climatic changes and geological processes. For example, the Orange and Zambezi rivers have altered their patterns and extent over geological time. The rivers are used by riparian states for economic benefits. The observed changes of the river channels are speculatively attributed to tectonic, geological, and climatic processes. However, the effects of climatic change and geological processes on the evolution of the Orange and Zambezi River drainage basins are not well understood, since unravelling the complex interplay between the different processes is a challenging issue. In this study, integrated provenance analysis to reconstruct paleo-climatic changes, fluvial incision, aridity evolution and sedimentation were conducted. The knowledge obtained on climatic effects and the aridity trends will enable better planning and management of Southern African water resources and assist in the modelling of future flood and drought patterns.

1.2. Project Relevance

There is currently scanty scientific information on the effects of climatic evolution and geological processes on the evolution of the Orange and Zambezi rivers. These two rivers are sources of water for domestic, agricultural, industrial, fisheries, and tourism purposes, as well as for the generation of hydroelectricity by the riparian states. The uses and demands for water are set to increase in the next decade due to increased migrations, urbanization, industrialization, and agricultural activities. The reliance of the riparian states on the two rivers for their economic benefits and citizen's well-being emphasizes the importance of the rivers, and therefore, the need to understand their evolution as influenced by geological processes and climatic evolution through time. Conducting the research project will result in a better understanding of the effects of late Cenozoic climatic changes on fluvial erosion and river evolution in Southern Africa during the Pliocene-Pleistocene. Furthermore, records on sedimentary accumulation rates and provenance variation since the Pliocene, as well as climatic evolution for Southern Africa will be generated. As mentioned earlier, the developed records will enable scientists, private companies, and governments to develop new policies on climate change and support further scientific studies and applications. In addition, the resultant knowledge obtained regarding climatic effects and the aridity trends will aid better planning and management of Southern African water resources and assist in the modelling of the flood and drought patterns. This will potentially save lives and ensure better health and well-being of communities in riparian states. In summary the consequences of the project will be scientific collaborations (University of Zambia, University of South Africa, and the University of Fort Hare), knowledge generation and dissemination, human capacity development, influencing

public policy services and regulation, societal and international engagement, and safeguarding the well-being and health of riparian communities.

1.3 Overview, background, and rationale

Southern Africa's freshwater resources such as rivers, lakes, and groundwater, are under increasing stress due to natural modifications of river flow regimes, changing land use or land cover patterns influenced by climatic changes (Tooth *et al.*, 2004). The long-term evolution of climatic conditions is associated with tectonic and geological processes. These processes had a significant impact on the global surface landscape. According to Zhang *et al.* (2001) an increase in sedimentation rates of 4-2 Ma in many parts of the world are the result of increased climatic fluctuations associated with tectonic and geological processes. However, the geographic location of an area affects the interpretation of palaeoclimatological events, for example, the study of Quaternary Sea level changes (Craddock *et al.*, 2010; Kong *et al.*, 2014; Li, 1991; Wang *et al.*, 2002).

Both alluvial and bedrock river channels are found in Southern Africa, with alluvial channels being mainly shaped by flow and sediment transport processes, and bedrock channels shaped mainly by lithological and structural controls (Baker and Pickup, 1987; Ashley *et al.*, 1988). However, mixed bedrock-alluvial river channels are common in the sub-humid to semi-arid interior of Southern Africa, specifically where the local geology is composed of late Carboniferous to mid-Jurassic Karoo sequence. During the breakup of the Gondwana supercontinent, the Karoo sequence was intruded extensively by dolerite sills and dykes, coupled with intensive deformation of the flood basalts (Elburg and Goldberg, 2000). With reference to tectonic activities after the Gondwana breakup, late Mesozoic and Cenozoic landscape development encompassed downcutting by rivers, coupled with down wearing or back wearing of slopes. As a result, substantial thicknesses (1-2 km) of basalt and weaker rocks were removed (Gilchrist *et al.*, 1994), which lead to widespread river superimposition onto the underlying resistant dolerite sills and dykes. The sills and dykes now outcrop sporadically over an area covering nearly two-thirds of South Africa (Chevallier and Woodford, 1999) and continue to exert strong, but variable controls on river behaviour, not only in the immediate area of the outcrop but also in upstream reaches underlain by weaker sedimentary rocks.

Southern Africa's rivers have a long history of formation, with the formation of the modern river framework related to the uplift of the three crustal deformation belts of the Escarpment Axis, Okavango-Kalahari-Zimbabwe (O-K-Z) Axis, and Etosha-Griqualand-Transvaal (E-G-T) Axis. These axes were caused by the tectonic movement in Southern Africa and form the main watersheds of modern rivers (Moore and Blenkinsop, 2002). The Escarpment Axis is parallel to southern South Africa's coastline, and its upliftment is closely related to the collapse of the late Jurassic-Early Cretaceous Gondwana. The E-G-T Axis is the watershed of the Orange River, which formed during the Late Cretaceous. Although small scale tectonic activities took place thereafter, further evolution of the river system was mainly affected by the Cenozoic climatic changes and river erosion.

The modern-day Orange River has its catchment area in the Maluti Mountains (Drakensberg Mountains) of Lesotho, receives inflows from several important tributaries while flowing through central and western South Africa before it flows along the border between Namibia and South Africa and empties into the Atlantic Ocean (Kistin & Ashton, 2008). The Orange River is divided into the Upper Orange above its confluence with the Vaal, the Middle Orange between this confluence and the Augrabies Falls situated just over 100 km downstream from Upington, and the Lower Orange from the Augrabies Falls to the sea.

Since the Cretaceous, the Orange River drainage basin system has altered its pattern and extent (Dollar, 1998; Jacob *et al.*, 1999). Studies on offshore sediments indicates that the upper Orange River entered the South Atlantic through the Cape Canyon, presently located 300-500 km south of the present mouth at Oranjemund. The river diverted to its present course during the end of Miocene after it's capture by the Koa River system. Before the capture, thus during the middle Miocene, the Koa River drainage basin system was characterized by a north-flowing perennial system. Diversion of the Orange River from its initial course was further aggravated by aridification and tectonic activities, leading to the abandonment of the flow through the Koa River drainage system (Dingle and Hendey, 1984).

It is speculated that the Orange River drained large parts of the Kalahari, being fed by the Trans-Tswana River (McCarthy, 1983), with the Molopo, Morokweng and Harts comprising the major northern bank tributaries (Bootsman, 1997; Bootsman *et al.*, 1999). However, tectonic activities along the Griqualand-Transvaal Axis, which initiated the development of the Kalahari Basin caused the expiration of the mentioned palaeotributaries (Moore, 1999).

McCarthy (1983) suggest that the Orange River drainage basin 's catchment area included the tropical Central Africa, and the Kafue (presently one of the main tributaries of the Zambezi River in Zambia), Upper Zambezi and possibly the Kwando and Okavango rivers. However, De Wit (2000) indicated that some of the catchment areas were drained by the palaeo-Limpopo River. Evidence of biogeographic studies (Barber-James, 2003) points to two main rivers draining the interior of southern Africa during the middle of the Cretaceous (De Wit, 1999). The northerly river, referred to as the Kalahari River drained Namibia and southern Botswana and emptied into the Atlantic Ocean through the lower Orange River. The southern river, referred to as the Karoo River had its catchment in the present Orange/Vaal basin and its mouth at the present Olifants river mouth.

During the early Cenozoic, the lower Kalahari River had captured the upper part of the Karoo River. This capture was prompted by an accelerated uplift of the southern and eastern subcontinental margins (ca. 100 to 80 million years). However, the postulated position of the Atlantic outlet of the Kalahari River is disputed, with Stevenson and McMillan (2004) suggesting its location during the Late Cretaceous, offshore of the present-day Groen to Buffels rivers.

In Southern Africa, the drainage pattern was affected by doming over large mantle plumes after the continental breakup in the Cretaceous. In the west, there was the Parana plume and in the east the Karoo plume (Moore and Blenkinsop, 2002). To some extent, and in some parts of the catchment, drainage radiated away from the centre of the plumes (Cox, 1989). However, the precise location and number of the plumes is unknown. Some of the drainages radiating from the Parana plume include the Fish and Molopo rivers, the Okavango, Cubango and upper Zambezi rivers as well as the headwaters of the Congo River. This phenomenon explains the absence of major westward draining systems between the modern Orange and Congo rivers.

Further, during the Cenozoic, interior basins subsided to accommodate sediments bounded by uplifting sub-swells, i.e. the Transvaal-Griqualand axis and the Okavango-Kalahari-Zimbabwe axis (Moore and Larkin, 2001). The uplift of the sub-swells caused drainage dismemberment (Gumbrecht *et al.*, 2001) severing the links between the Limpopo and the Okavango, Cubango and Zambezi-Luangwa drainage systems (Moore and Larkin, 2001).

During the early Cretaceous period, the Zambezi River was much smaller than the Limpopo River. The formation of the modern Zambezi River is thought to have occurred in the early Pleistocene, through the gradual migration of the lower reaches of the river (Moore and Larkin, 2001). According to this model, the geochemical signals, and inputs of the material to the oceans from the Zambezi River may have changed significantly during the early Pleistocene.

Sinha *et al.* (2012) suggested that the upper and middle parts of the Zambezi River evolved separately but were later joined together through several stages of river capture and tectonic activities (Shaw and Thomas, 1988, 1992; Goudie, 2005) probably during the Pliocene or mid-Pleistocene. The middle Zambezi was linked to the Shire system while the upper Zambezi was captured by the middle Zambezi because of down warping and tectonically triggered headward erosion, possibly during the lower Pleistocene. Following this capture, complex drainage reorganization took place in this area. The enhanced down warping along the Gwembe trough caused rejuvenation of the Zambezi River, leading to the development of the Victoria Falls and the deeply incised middle Zambezi gorge. Unfortunately, very little stratigraphic information is available on the Quaternary sediments in the Zambezi basin although extensive alluvium and lacustrine deposits have been reported between the Kafue Flats and the Machili Basin (Dixey, 1944).

These alluvial deposits provide evidence for a former major inland lake, Paleo-Lake Makgadikgadi, into which the Zambezi River was diverted (Thomas and Shaw, 1991). It has been suggested that the limit of the older alluvium reflects the approximate extent of this lake that comprised of two subsidiary basins linked via a narrow neck along the Boteti River valley in modern day Botswana (Thomas and Shaw, 1991). Timing of the high lake level and thus the diversion of the Zambezi River into northern Botswana is not well constrained but based on Acheulian artifacts from the floor of Lake Makgadikgadi, is during the mid-Pleistocene (minimum age of 500 ka) (McBrearty and Brooks, 2000; McFarlane and Sagadika, 2001,

Mcfarlane and Eckardt, 2006). The early to middle Pleistocene history is still speculative and the age of the lake system is still uncertain.

Even though many sources have suggestions regarding the present evolution of the Zambezi-Limpopo systems, none have adequately explained the strange right-angle change of directions from south-westerly to east and south-easterly directions of the present Kafue, Zambezi, and Cubando/Chobe rivers, previously suggested as indicative of river capture (Bond, 1975).

The explanations fail to account for apparent capture taking place at predictable intersection points on a common axis. Sichingabula (2000) contended that the eastward turning of the Kafue, Zambezi and Chobe/Cuando rivers across a common axis could not have occurred prior to the crustal tectonic dislocation and downward slip along the Mwembeshi Dislocation Zone described by Swardt *et al.* (1965a; 1965b). According to Sichingabula (2000) the downward slip of the crustal rocks on the eastern and south-eastern sides of the dislocation zone, was the determining factor controlling the changed directions of the three rivers and hence paved the way for the formation of the Kafue Flats and the Victoria Falls on the Zambezi River.

Additionally, limited evidence recently emerged from the Lusaka area indicating the possible existence of another paleo-lake, smaller than Lake Makgadikgadi. Based on discovered lacustrine deposits at Twin Rivers farm southwest of Lusaka, Simms (2000) postulated that an ancient lake (Palaeo-Lake Patrick) once covered part of the Kafue Flats. Coincidentally and independently, Sichingabula (2000) asserted that the Kafue Flats formed during a period of tectonic quiescence after the Kafue River at Itezhi-Tezhi changed flow direction from southwest to the east which led to pondage of its waters from the immediate area up to the Kafue Gorge-Munali Hills area as there was no outlet for the river flow. Sichingabula (2000) named this much larger ancient body of water 'Namwaze Lake'. The features of the Kafue Flats suggest that it is a relic of the Namwaze Lake, which requires confirmation by empirical evidence partly supported by Simms (2000). Research on the sedimentary architecture of the Kafue Flats will unravel the mystery of this 'lost' ancient lake. Additionally, based on formative processes, Sichingabula (2000) classified the Kafue Flats as an anastomosed fluvial system, currently the only one known to exist in this part of the world.

So far, the research done using ocean boreholes, indicates that the global climatic conditions were mainly dominated by the 40,000-year period in the Early Pliocene and Early Quaternary periods, and late in Quaternary it changed to the 100,000-year cycle (Imbrie *et al.*, 1993). During the Quaternary climatic changes are consistent with the ice volume, which controlled climate in North Africa. The results of drilling in East Africa and West Africa yielded results like this basic framework. In addition, the East African records indicate that the area was more arid before the Pleistocene and that the climate and wet winds fluctuated significantly and are driven by eccentricity (Lyons *et al.*, 2015). However, these records cover only sediments deposited since 1.5 Ma, and the research sites are in the tropics and cannot represent the Southern African climate controlled by the tributary of the Hadley circulation cell in the southern hemisphere.

Southern Africa has no continuous record of observable orbital scale climate changes, and existing records are mostly focused on tectonic-scale climate changes. For example, a study by van Zinderen Bakker (1984) on carbon and leaf wax stable isotopic data indicated that the wide spread of C₄ vegetation since 9 Ma is related to persistent drought and fire enhancement, however it lacks data since 2.5 Ma.

Indeed, according to Sinha *et al.* (2012), more studies are needed on the African river systems especially the Orange and Zambezi Rivers, and their tributaries. More so, understanding the impact of the Pliocene-Quaternary climate changes on the Southern African landforms requires the generation of a reliable Southern African climatic change record.

Therefore, this study will focus on the Orange and Zambezi Rivers to carry out meticulous provenance research work, comprehensive analysis of paleoclimatic changes and deposition rate changes. Provenance determination will be based on the study of provenance of the continental origin and the evolution of the basin geomorphology, and the influence of the Late Cenozoic climatic changes on the Orange and Zambezi River evolution, to understand the impacts of climatic changes on landform evolution.

Both the Orange and the Zambezi rivers serve several riparian countries. The Orange River serves Lesotho, South Africa, Botswana, and Namibia. The Zambezi River serves Zambia, Democratic Republic of Congo, Angola, Namibia, Botswana, Zimbabwe, Malawi, and Mozambique. These riparian countries benefit in terms of agriculture, fisheries, tourism, as well as water for domestic and industrial use. The Zambezi River provides electricity to many countries in Southern Africa of which South Africa utilizes the largest share (~ 55%) of the interconnected electrical power system managed through the Southern African Power Pool. This dominance is expected to continue until 2022 (SAPP, 2018).

1.4 Aims and objectives

The aim of the study was to determine the effects of Epeirogenic processes and Pliocene-Pleistocene climatic changes on the evolution of the Orange and Zambezi River drainage systems in Southern Africa. The objectives of the study were:

- a. determine the development of Southern African river systems using integrated provenance, stratigraphic and sedimentological analyses;
- b. determine the development of the Zambezi River system in Zambia using topographic and hydrological analyses;
- c. determine the aridity evolution since the Pliocene in Southern Africa;
- d. determine the role and impact of sedimentation and bathymetry of small reservoirs to water scarcity problems in South Africa and Zambia;
- e. recommend policy for the transboundary management of the studied drainage systems.

1.5 Methodology

- a. The following methodologies were applied by are discussed in detail under each chapter:
- b. Stratigraphic and sedimentological analyses;
- c. Topographic and hydrological analyses
- d. Detrital Zircon U-Pb geochronology
- e. Heavy minerals analysis
- f. Nd isotopic analysis
- g. Petrography
- h. Mineralogy
- i. Whole rock geochemistry
- j. Bathymetric and Sedimentation Survey of Small Reservoirs

1.6 Deliverables

The following deliverables were obtained:

Table 1.1: Deliverables

No.	Deliverable Title	Description	Target Date
0	Nonapplicable	Start-up finance	03/Feb/2020
1	Report on modelled future climatic conditions and the implication on water security.	Deliverable 1 will be accounted for by aim 1 and will encompass the topographic analysis and hydrological analysis. Geographic visual display of the study areas will be constructed.	15/Mar/2020
2	Report on provenance of developmental river systems of Southern Africa.	Will be accounted for by aim 2. Under this deliverable, provenance of the Zambezi and Orange rivers will be inferred using detrital zircon U-Pb geochronology, Nb isotopes, heavy mineral separation, stratigraphic and sedimentological analysis.	31/Dec/2020
3	Report on options for developmental response considering socio-economic drivers.	Different developmental response models will be formulated and presented as a report (see attached for details).	01/Feb/2021
4	Report on the strategies for adaptive response and to address reduction of impacts.	Different strategies directed at communities relying on the two rivers for their livelihoods, industries such as mining, fisheries and government organizations will be formulated.	30/Jul/2021

No.	Deliverable Title	Description	Target Date
5	Workshop	Present deliverable 4 to selected communities.	30/Aug/2021
6	A report on the comparative analysis of projected impacts on the priority water-linked sectors.	Deliverable 6 will be accounted for by aim 3, which addresses the role and impact of sedimentation and bathymetry of small reservoirs to water scarcity problems (see attached).	31/Dec/2021
7	A report outlining the inputs of Southern African terrestrial drainage systems into the Atlantic and Indian Oceans.	Deliverable 7 will be accounted for by aim 4, which seeks to establish the inputs of Southern African terrestrial drainage systems into the Atlantic and Indian oceans.	01/Feb/2022
8	A report on aridity evolution in Southern Africa since the Pliocene.	Deliverable 8 will be accounted for by aim 5, which seeks to determine the aridity evolution from the Pliocene in Southern Africa.	30/Jul/2022
9	A report on paleo-climatic evolution and deposition rates in Southern Africa.	Deliverable 9 will be accounted for by aim 6. Paleomagnetic information and sporopollen analysis will be used to reconstruct paleoclimatic changes and deposition rate changes.	30/Oct/2022
10	A report on paleoclimatic evolution and deposition rates in Southern Africa. Recommendations for policy.	During the research project, researchers will work together with government officials from South Africa and Zambia to help formulate policies that will favour economic growth.	30/Dec/2022
11	Workshop	Project closing workshop	01/Feb/2023
12	Final report	A final report will be written and presented to the Water Research Commission. The report will include all the aspects of the research project.	28/Feb/2023

The projected deliverables have been formulated to satisfy the “*Climate Change and Water Security: Developmental Perspectives for Water-Linked Sectors in a Future Climate for Africa (Bi-National Assessment)*” call.

CHAPTER 2

PROVENANCE OF DEVELOPMENTAL RIVER SYSTEMS OF SOUTHERN AFRICA: USING THE ZAMBEZI RIVER AS A CASE STUDY

2.1 Introduction

The Zambezi River flows across wild landscapes from the Ikeleng District of Zambia, plunges to deep gorges carved in basalt in Victoria Falls plunging, and empties into the Indian Ocean (Figure 2.1; Main, 1990; Moore *et al.*, 2007).

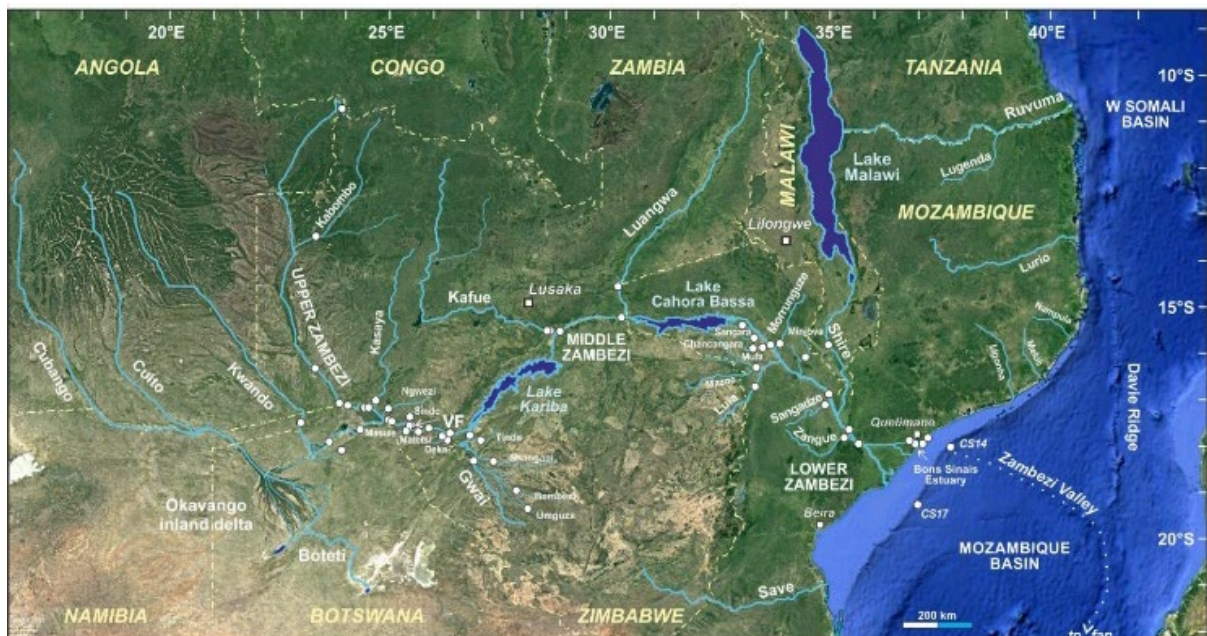


Figure 2.1: The Zambezi drainage basin. White circles indicate sampling locations. VF = Victoria Falls

The Zambezi River is Southern Africa's largest drainage basin flowing across eight countries namely: north of Zambia to the west towards Angola, then to south towards Namibia, Botswana and Zimbabwe and finally, to the east towards Mozambique, Malawi and Tanzania before it empties into the Indian Ocean (Matondo and Tumbare, 1998; Tumbare, 2004). Out of these countries, only five have the largest share of the watershed and the catchment area varies in each state. Zambia has the largest share of about 40.7%, followed by Angola with approximately 18.3%, Zimbabwe with about 15.9%, Mozambique and Malawi contributing about 11.4% and 7.7% respectively (Shela, 2000) while the remaining countries constitute 6% of the catchment area.

As mentioned earlier on, the water resource of the Zambezi River is continuously strained by various factors that include mining, agriculture, floods and droughts, water pollution, deforestation, socio-economic factors and recently by climate change. The Zambezi Basin has undergone a series of evolution and flow regime changes since the Cretaceous period. Sinha *et al.*, 2012 suggested that the upper and middle parts of the river having evolved separately and then joined together through several stages of river capture and tectonic activities (Shaw and Thomas, 1988; Goudie, 2005) perhaps in Pliocene or mid-Pleistocene (Thomas and Shaw, 1991). The middle Zambezi was linked to the Shire system while the upper Zambezi was captured by the middle Zambezi because of down warping and tectonically triggered headward erosion, possibly in the lower Pleistocene. Following this capture, complex drainage reorganization took place in this area.

The enhanced down warping along the Gwembe trough caused rejuvenation leading to the development of the Victoria Falls and the incised middle Zambezi gorge. Unfortunately, very little stratigraphic information is available on the Quaternary sediments in the Zambezi basin although extensive alluvium and lacustrine deposits have been reported between the Kafue Flats and the Machili Basin (Dixey, 1945; Thomas and Shaw, 1991). During the early Cretaceous period (145-100 Ma) the Zambezi River was much smaller than the Limpopo River and until the Pleistocene era (2.6 Ma) was flowing through Makgadikgadi depressions in Botswana into the Limpopo River (Goudie, 2005). Spaliviero *et al.* (2014) presented an overview of the geomorphological evolution of Limpopo and Zambezi Rivers.

So far, the IODP research done using ocean boreholes indicates that the global climatic conditions were mainly dominated by the 40,000 years in the Early Pliocene and the Early Quaternary period, and late in Quaternary changed to the 100,000 cycles (Imbrie *et al.*, 1993; Lisiecki and Raymo, 2007). The Quaternary climatic changes are consistent with the ice volume, which controlled the climate in North Africa. The results of drilling in East Africa and West Africa yielded similar results. For example, Africa's equatorial temperatures changed over 600,000 years, and these results agree with variations in ultraviolet radiation and ice volume in the northern hemisphere (Tierney *et al.*, 2008).

Records from the East African drilling program show that the area was more arid before Pleistocene and that the climate and wet winds fluctuate significantly and are significantly driven by eccentricity (Lyons *et al.*, 2015). However, these records cover only sediments deposited since 1.5 Ma, and the research sites are in the tropics and cannot represent the Southern African climate controlled by the tributary of the Hadley circulation in the southern hemisphere. Furthermore, the results showed that climatic changes occurred in three stages. The main stages occurred at 2.7-2.5, 1.9-1.7 and 1.0-0.7 Ma. The outcrop profile has a track scale of climatic changes with a record of 5 Ma, which shows that a 400,000 eccentricity drives climate change, but its resolution may not be as continuous as the continent's drilling record, therefore, its effectiveness remains to be further studied.

This study focusses specifically on:

- a) the relative effects on sand mineralogy of source-rock lithology and chemical weathering in subequatorial climate;
- b) the transmission of compositional signals along the sediment-routing system from source to sink;
- c) the use and misuse of current petrologic models to infer sediment provenance and of mineralogical parameters to infer climatic conditions. Our ultimate purpose is to build up a solid knowledge of the modern river system that can be applied to trace sediment transport from the land to the deep sea and, eventually, to investigate provenance changes documented by sedimentary succession accumulated in marine sedimentary basins through time and thus unravel the complex evolution of the Zambezi River system from the late Mesozoic to the present time.

2.2 Geology

2.2.1 The Precambrian

The Archean core of southern Africa includes the Zimbabwe Craton, Limpopo Mobile Belt, Kaapvaal Craton in the south and bounded by the mid-Paleoproterozoic Magondi Belt in the west (Fig. 2). The Zimbabwe Craton comprises a central terrane flanked by greenstone belts. Gneisses of the central terrane are non-conformably overlain by volcanic rocks and conglomerates or by a SE-ward thickening sedimentary succession. The craton was stabilized in the mid-Neoproterozoic and finally sealed by the Great Dyke swarm at 2575 Ma (Jelsma and Dirks, 2002; Söderlund *et al.*, 2010).

The composite Archean core grew progressively along its NW side during the Paleoproterozoic and Mesoproterozoic. The Proto-Kalahari Craton was established by the late Paleoproterozoic and affected by widespread intraplate magmatism at 1.1 Ga (Hanson *et al.*, 2006), not long before the Kalahari Craton was formed during the orogenic event when Rodinia was assembled (Jacobs *et al.*, 2008).

Orogens developed in the Paleoproterozoic and reworked in the Neoproterozoic at the southern margin of the Tanzania Craton include the NW/SE trending Ubendian metamorphic belt, bounding the Bangweulu Block to the north (Boniface and Appel, 2018) and the SW/NE striking Usagaran Belt to the east (Collins *et al.*, 2004). In northern Zimbabwe, the Orosirian Magondi Belt contains arc-related volcano-sedimentary and plutonic rocks metamorphosed up to amphibolite facies (Majaule *et al.*, 2001; Master *et al.*, 2010).

Orogens generated in the Mesoproterozoic include the Kibaran Belt in the north (Kokonyangi *et al.*, 2006; Debruyne *et al.*, 2015) and the Irumide Belt, which stretches from central Zambia in the SW to northern Malawi in the NE, is delimited by the largely undeformed basement of the Bangweulu block in the NW and was largely affected by the Neoproterozoic orogeny in the west and southwest (Fig. 2). The Irumide Belt includes a Paleoproterozoic gneissic

basement overlain by siliciclastics and minor carbonates deposited during the late Orosirian (Muva Supergroup), as well as granitoid suites emplaced in the earliest, middle, and latest Mesoproterozoic. During the ~1 Ga orogeny, metamorphic grade increased from greenschist facies in the NW to upper amphibolite facies in the SE (De Waele *et al.*, 2006, 2009). The Choma-Kalomo block in southern Zambia is a distinct Mesoproterozoic domain also including amphibolite-facies metasediments and granitoid intrusions affected by the latest Mesoproterozoic thermal event (Glynn *et al.*, 2017).

The Kalahari Craton of southern Africa was finally welded to the Congo Craton during the major Neoproterozoic Pan-African orogeny, testified by the Damara-Lufilian-Zambezi belt stretching from coastal Namibia in the west and across Botswana and southern Zambia to finally connect with the Mozambique Belt in the east (Frimmel *et al.*, 2011; Fritz *et al.*, 2013; Goscombe *et al.*, 2020). The Lufilian Arc, located between the Congo and Kalahari Cratons, consists of Neoproterozoic low- to high-grade metasedimentary and metaigneous rocks hosting Cu-Co-U and Pb-Zn mineralization (Kampunzu and Cailteux, 1999; John *et al.*, 2004; Eglinger *et al.*, 2016). The Zambezi Belt contains a volcano-sedimentary succession deformed under amphibolite-facies conditions at in the early Neoproterozoica (Hanson, 2003), whereas eclogite-facies metamorphism constrains the timing of subduction and basin closure as latest Neoproterozoic (Hargrove *et al.*, 2003; John *et al.*, 2003).

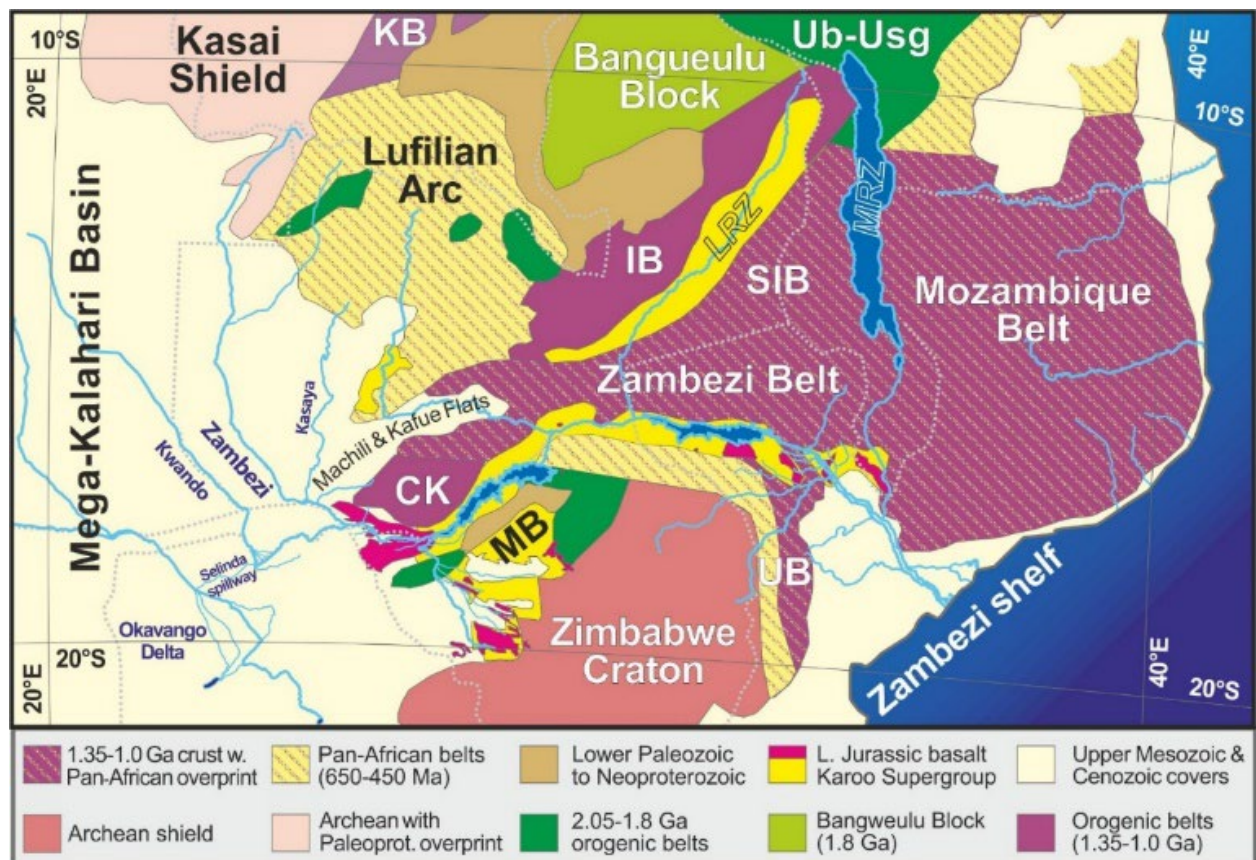


Figure 2.2: Geological domains and time structure map of the Zambezi catchment and adjacent regions (after Hanson, 2003, and CGMW-BRGM, 2016).

Where: CK = Choma-Kalomo block; IB = Irumide Belt; KB = Kibaran Belt; LRZ = Luangwa Rift Zone, activated in the Permian and reactivated in the Neogene; MB = Magondi Belt; MRZ = Malawi Rift Zone; SIB = South Irumide Belt, deeply affected by the Pan-African orogeny; UB = Umkondo Belt; Ub-Usg = Ubendian-USagaran Belts

2.2.2 The break-up of Gondwana

A major tectono-magmatic event straddling the Paleozoic/Mesozoic boundary is widely documented across southern Africa (Jourdan *et al.*, 2005; Manninen *et al.*, 2008), when the several km-thick Upper Carboniferous to Lower Jurassic Karoo Supergroup was deposited, including glacial sediments, shale and volcanoclastic sandstone followed by quartzofeldspathic-lithic fluvial sediments (Johnson *et al.*, 1996). Sedimentation was influenced by changing climate, from initially cold to warmer since the mid-Permian, to finally hot with fluctuating precipitation in the Triassic, when braidplain sandstone and floodplain mudstone were capped by aeolian sandstone (Catuneanu *et al.*, 2005). Karoo-type basins formed in intra- and inter-cratonic settings by rift-related extension. In the Tuli and Mid-Zambezi basins of Zimbabwe, glacial deposits are overlain by Permian sandstones and coal-bearing mudrocks, followed by ~0.5 km-thick Triassic redbeds and pebbly sandstones (Bicca *et al.*, 2017). Karoo sedimentation was terminated by flood-basalt eruptions recorded throughout southern Africa in the Early Jurassic (Svensen *et al.*, 2012). Finally, rifting and break-up of Gondwana in the mid-Jurassic was followed by opening of the Indian Ocean in the Early Cretaceous, an event associated with formation of sedimentary basins (Salman and Abdula, 1995; Walford *et al.*, 2005), strike-slip deformation (Klimke *et al.*, 2016), and extensive volcanism in the Mozambique Channel (Vallier *et al.*, 1974; König and Jokat, 2010). In the Cenozoic, fluvial and lacustrine sediments were deposited inland in the Mega-Kalahari rim basin (from Tswana language Kgalagadi, “waterless place”), which comprises the largest continuous sand sea on Earth extending for over 235 106 km² on the southern Africa plateau (Haddon and McCarthy, 2005). Repeated phases of aeolian deposition took place during Quaternary dry stages, separated by depositional hiatuses corresponding to more humid stages (Stokes *et al.*, 1998; Thomas and Shaw, 2002). The East African rift developed throughout the Neogene (Ebinger and Scholz, 2012; Roberts *et al.*, 2012; Maselli *et al.*, 2019), until along-axis propagation reached the Kalahari region in the Quaternary, through a network of unconnected basins extending south-west Lake Tanganyika (Kinabo *et al.*, 2007). Since the late Pleistocene, faulting and subsidence in the incipient Okavango rift zone has exerted a major control on drainage reorganization.

2.3 The Zambezi River

The river's geographic location from the source extends for about 50 km northward, towards the Democratic Republic of Congo into the Kalene Hills before the river changes its course towards the south-west, a direction that is maintained for a distance of approximately 270 km into Angola. From Angola, the river flow changes direction to the south back to Namibia and

finally flows in an eastward direction towards the border of Namibia and Botswana, border of Zambia and Zimbabwe pass through to Mozambique into the Indian Ocean (Figure 2. 3).

The total drainage area is approximately 1,300,000 km² and covers about 2600 km in length (Shela, 2000 and Long *et al.*, 2014). The most striking physical features are floodplains, waterfalls, lakes, and human made hydroelectric dams. The notable tributaries of the Zambezi River are Luena in Angola; Lungue Bungo flowing within Angola and Zambia; the Luangwa, Kafue, and Kabompo Rivers in Zambia; the Cuando flowing through Angola and the Caprivi Strip of Namibia before it enters Botswana as Chobe River and finally the Shire River flowing through Malawi and Mozambique.

The Zambezi River basin is subdivided into three distinctive geomorphological sections from the west to east: the Upper, Middle and Lower Sections (Wellington, 1955 and Moore *et al.*, 2007).

Upper Zambezi Section (UZS)

The UZS covers an area of approximately 515,008 km² (Beilfuss, 2012) and comprises of the north-western and western territories of Zambia, parts of the eastern regions of Angola and borders north of Namibia, Botswana, and Zimbabwe. The UZS section represents the highest elevation of the river, with a maximum elevation of 1500 m above sea level (asl) in the north and has a maximum elevation of 900 m asl in the south, closer to the Victoria Falls (Figure 2.3). The UZS section also hosts headwaters from the north of Zambia, and the watercourse stretches to Angola, and then back to the Zambian territory before it ends towards the Victoria Falls of Zimbabwe. In the segment where the river re-enters Zambia, there is a drastic drop in elevation, and this resulted in the development of the Chavuma Falls. Further, downstream, one of the largest tributaries, the Kabompo River, joins the main Zambezi River. At this juncture, the river widens into one of the most extensive wetlands in Africa, the Barotse Floodplain, measuring about 230 km in length and 35 km in width. Further, downstream, the river flows into Ngoye/Sioma Falls (1000 m asl). From this juncture, the river flows slightly in a south-east direction and briefly borders Namibia's Caprivi Strip where the course changes in an eastward's direction, towards the Victoria Falls, where the elevation is about 950 m (Figure 2.3).

Middle Zambezi Section (MZS)

The MZS covers an area of approximately 511,430 km² (Beilfuss, 2012). The MZS section is mainly composed of the Copperbelt, Central, Southern, and Lusaka territories together with small areas of the north-western and eastern provinces of Zambia. The section also covers Matabeleland North, the Midlands, and western Mashonaland areas of Zimbabwe. The Victoria waterfalls in Zimbabwe are considered a boundary that separates upper and middle sections of Zambezi River. Downstream from Victoria Falls, the River continues to flow to the east through a deep incision, the Batoka Gorge at an elevation of 650 m asl.

Further downstream, thus after 100 km the river flows into Devil's Gorge, which has an elevation of approximately 600-450 m asl. Further downstream, at about 10 km from the Devil's Gorge the River drains into Lake Kariba (one of the most prominent structures measuring approximately 240 km in length and 10-20 km in width). At about 70 km downstream another tributary, the Kafue River that flows from the Copperbelt region of northern Zambia is encountered. From this point, the river flows for about 100 km and is joined by the Luangwa tributary in the north. This point marks the beginning of the western end of Cahora Bassa Reservoir and the international boundary between Zambia and Mozambique.

Lower Zambezi Section (LZS)

The LZS section covers an area of approximately 340,000 km² stretching below the eastern end of the 200 km long Cahora Bassa Dam to the Indian Ocean (Beilfuss, 2012). The drainage area covers the whole of Malawi, a small strip of southern Tanzania along the eastern coast of the Malawi River, north-eastern and central areas of Mozambique, and some areas in northeast Zimbabwe. The Shire River, which originates as an outflow from Lake Malawi/Niassa/Nyasa is the largest tributary in the LZS section, flowing through southern Tanzania, Malawi, and Mozambique north of the Zambezi.

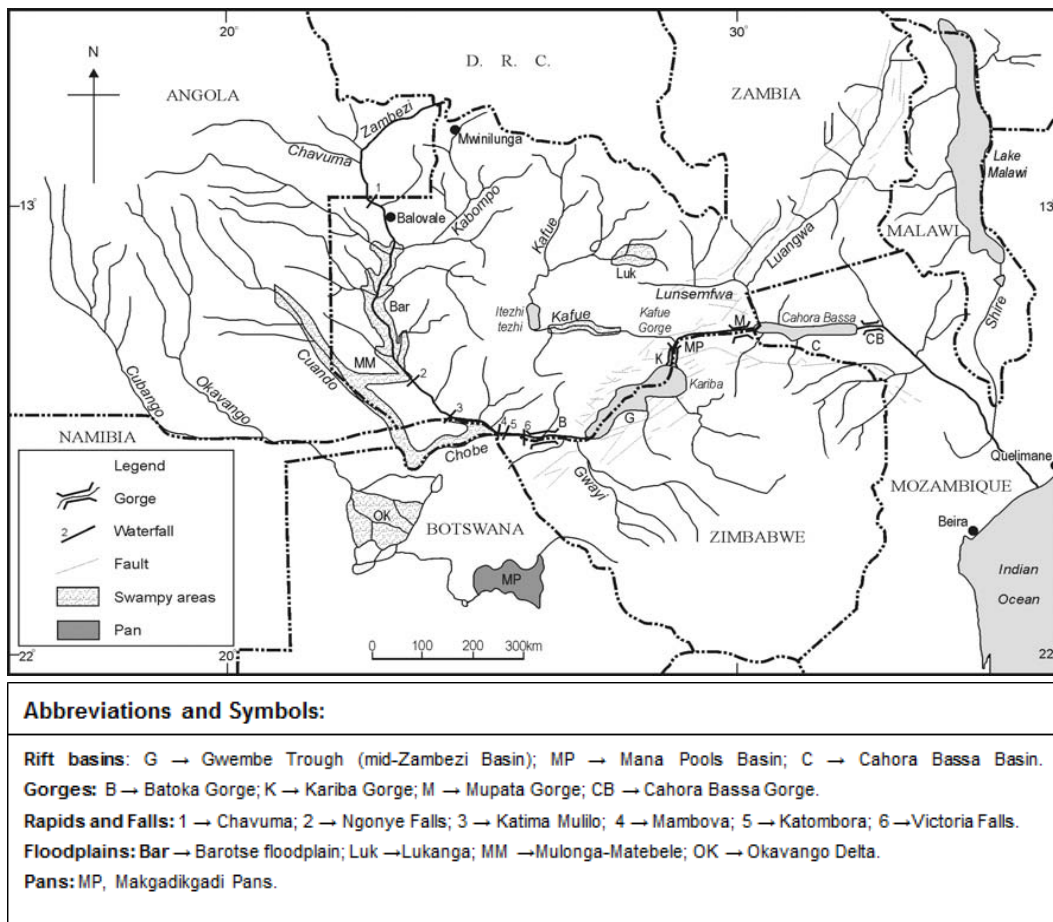


Figure 2.3: Southern African map showing Zambezi River and associated geomorphological features. Source modified: Adapted from Nugent (initial) (1990) cited in Moore et al. (2007)

2.3.1 Drainage evolution through time

The history of the Zambezi River reflects the multistep changes of African landscape caused by the progressive break-up of Gondwana (Key *et al.*, 2015). Extensional phases in eastern southern Africa started from the Permian (MacGregor, 2018), possibly linked with initial opening of Neotethys in the northeast (Sciunnach and Garzanti, 1992). The entire Middle Zambezi, as its major tributary the Luangwa River, flow along Permo-Triassic rift zones (Fig. 2). The eastward slope, instead, originated in the Early Cretaceous by domal uplift related to incipient rifting of the South Atlantic and emplacement of the Paranà-Etendeka large igneous province in the west (Cox, 1989; Moore and Blenkinsop, 2002). Superposed onto Precambrian mobile belts and Permo-Triassic rifts, or intersecting them, the southward propagation of the East African Rift during the Neogene has created further tectonic depressions, including those occupied by Lake Malawi in the east and by the Okavango inland delta in the west (Ebinger and Scholz, 2012). The modern Zambezi drainage is thus the result of inheritance from multiple Permo-Mesozoic extensional events on both sides of Africa combined with rifting inside Africa that is still ongoing.

Successive events of river capture and drainage reversal, indicated by sharp changes in direction of its major Kwando, Kafue, and Luangwa tributaries, and the genetic similarities of fish populations between the Kafue and Upper Zambezi, and between the Middle Zambezi and the Limpopo, have long suggested that the Zambezi, Okavango and Limpopo originally formed a single transcontinental river following Cretaceous uplift associated with rifting of the South Atlantic (Thomas and Shaw, 1988; Moore *et al.*, 2007). In the Paleogene, uplift of the Ovamboland-Kalahari-Zimbabwe axis resulted in endorheic drainage of the Okavango and upper Zambezi (Moore and Larkin, 2001). The then isolated Lower Zambezi initiated headward erosion, leading to the sequential capture of its middle- and upper-course tributaries. Both Kafue and Luangwa Rivers once drained south-westward, the former joining the Upper Zambezi in the Machili Flats and the latter flowing across the Gwembe trough presently occupied by Lake Kariba (Thomas and Shaw, 1991). Linking with the upper course in the Plio-Pleistocene was followed by the capture of the Kwando River, and by the presently occurring capture of the Okavango as well (Wellington, 1955; Moore *et al.*, 2007). In NW Zimbabwe, drainage is largely controlled by an old pre-Karoo surface, tilted westward during domal uplift in the Early Jurassic (Moore *et al.*, 2009a). The present east-bank tributaries of the Gwai River all drained westwards toward Botswana, until they were captured progressively by headward erosion of the Gwai River after establishment of the modern Zambezi River course (Thomas and Shaw, 1988).

2.4 Methodology

A total of 31 sediment samples were collected from the Zambezi River and of its major tributaries in Zambia and Mozambique ranging in size from very fine to coarse sand. An additional 25 samples were collected in the Zambezi, Kwando, and Gwai catchments in

Zambia, Caprivi Strip, Botswana, and Zimbabwe. To cover the entire Zambezi system from source to sink, 4 fine sands from the Bons Sinais Estuary and adjacent beaches in the Quelimane area of the northern Zambezi delta, and 5 sandy silts collected offshore of Quelimane (Site CS14, 330 m bsl) and of the Zambezi delta (Site CS17; 570 m bsl) were collected during the PAMELA-MOZ04 Ifremer-Total survey (Jouet and Deville, 2015). Offshore samples, collected by piston corer within 2.5 m below the sea floor, were deposited either during glacial lowstands (MOZ 4-CS14-162-167 cm, MOZ 4-CS17-702-707 cm, and MOZ 4-CS17-2402-2407 cm) or the Holocene high stand (MOZ4-CS14-21-26 cm and MOZ4-CS17-52-57 cm). Full information on sampling sites is provided in Table 2.1 and Google Earth™ file Zambezi.kmz.

2.4.1 Petrography

A quartered fraction of each sample was saturated with Araldite, cut into a standard thin section, and analysed by counting between 400 to 450 points using the Gazzi-Dickinson method (Ingersoll *et al.*, 1984). Sand is classified according to the three main groups of framework components (Q= quartz; F= feldspars; L= lithic fragments), considered where exceeding 10%QFL and listed in order of abundance (classification scheme after Garzanti, 2019). Feldspatho-quartzose sand is thus defined as $Q > F > 10\%QFL > L$, formally distinguishing between feldspar-rich ($Q/F < 2$; plagioclase-rich if plagioclase/K-feldspar > 2 , K-feldspar-rich if K-feldspar/plagioclase > 2) and quartz-rich ($Q/F > 4$) compositions. Quartzose sand is defined as $Q/QFL > 90\%$, and pure quartzose sand as $Q/QFL > 95\%$. These distinctions proved to be essential to discriminate among lithic-poor siliciclastic sediments generated from cratonic blocks and deposited along passive continental margins in different geomorphological settings (Garzanti *et al.*, 2018a). Microcline with crosshatch twinning is called for brevity “microcline” through the text. Median grain size was determined in thin section by ranking and visual comparison with standards of $f/4$ classes prepared by sieving in our laboratory.

2.4.2 Heavy minerals

From a split aliquot of the widest convenient size-window obtained by wet sieving (mainly 15-500 μm), heavy minerals were separated by centrifuging in Na-polytungstate (2.90 g/cm^3) and recovered by partial freezing with liquid nitrogen. In grain mounts, ≥ 200 transparent heavy minerals for each sample were either grain-counted by the area method or point-counted at appropriate regular spacing to obtain correct volume percentages (Garzanti and Andò, 2019). Mineralogical analyses were carried out by routinely coupling observations under the microscope and the Raman spectroscope. Transparent heavy-mineral assemblages, called for brevity “tHM suites” throughout the text, are defined as the spectrum of detrital extrabasinal minerals with density $> 2.90 \text{ g/cm}^3$ identifiable under a transmitted-light microscope. According to the transparent-heavy-mineral concentration in the sample (tHMC), tHM suites are defined as extremely poor (tHMC < 0.1), very poor ($0.1 \leq \text{tHMC} < 0.5$), poor ($0.5 \leq \text{tHMC}$

<1), moderately poor ($1 \leq \text{tHMC} < 2$), moderately rich ($2 \leq \text{tHMC} < 5$), rich ($5 \leq \text{tHMC} < 10$), very rich ($10 \leq \text{tHMC} < 20$), or extremely rich ($\text{tHMC} > 20$).

The sum of zircon, tourmaline, and rutile over total transparent heavy minerals (ZTR index of Hubert, 1962) expresses the chemical durability of the tHM suite. The “Amphibole Colour Index” ACI, varying from 0 in detritus from greenschist-facies and blueschist facies to lowermost amphibolite-facies rocks yielding exclusively blue or blue/green amphibole to 100 in detritus from granulite-facies or volcanic rocks yielding exclusively brown amphibole or oxy-hornblende is introduced here to discriminate the source rocks of amphibole grains. The “Metasedimentary Minerals Index” MMI, used to estimate the average grade of metasedimentary source rocks, varies from 0 in detritus from greenschist-facies to lowermost amphibolite-facies rocks yielding chloritoid, to 50 in detritus from amphibolite facies rocks yielding staurolite, andalusite and/or kyanite, and 100 in detritus from granulite-facies rocks yielding sillimanite. The “Sillimanite Index” SI, defined as the ratio between prismatic sillimanite and total (prismatic + fibrolitic) sillimanite grains, varies from 0 in detritus from upper amphibolite-facies metasediments to 100 in detritus from granulite-facies metasediments (Andò *et al.*, 2014). Significant minerals are listed in order of abundance (high to low) throughout the text.

2.4.3 River morphometry

The geomorphological properties of the Zambezi River and its major tributaries were quantified using TopoToolbox, a set of MATLAB functions for the analysis of relief and flow pathways in digital elevation models (DEM; Schwanghart and Scherler, 2014). The analysis of the longitudinal profile of bedrock channels was carried out on a 90 m-resolution DEM provided by Shuttle Radar Topography Mission Global (SRTM GL3; <https://opentopography.org>) to identify major knickpoints, defined as sites where the channel gradient changes abruptly owing to sharp local changes in bedrock strength and/or uplift rate. Channel concavity θ and normalized channel-steepness k_{sn} (referenced to a fixed concavity 0.45 to facilitate comparison among channel slopes with widely varying drainage areas and concavities) are defined by the power-law relationship $S = k_s A^{-\theta}$ between the local channel slope S and the contributing drainage area A used as a proxy for discharge (Flint, 1974; Whipple, 2004).

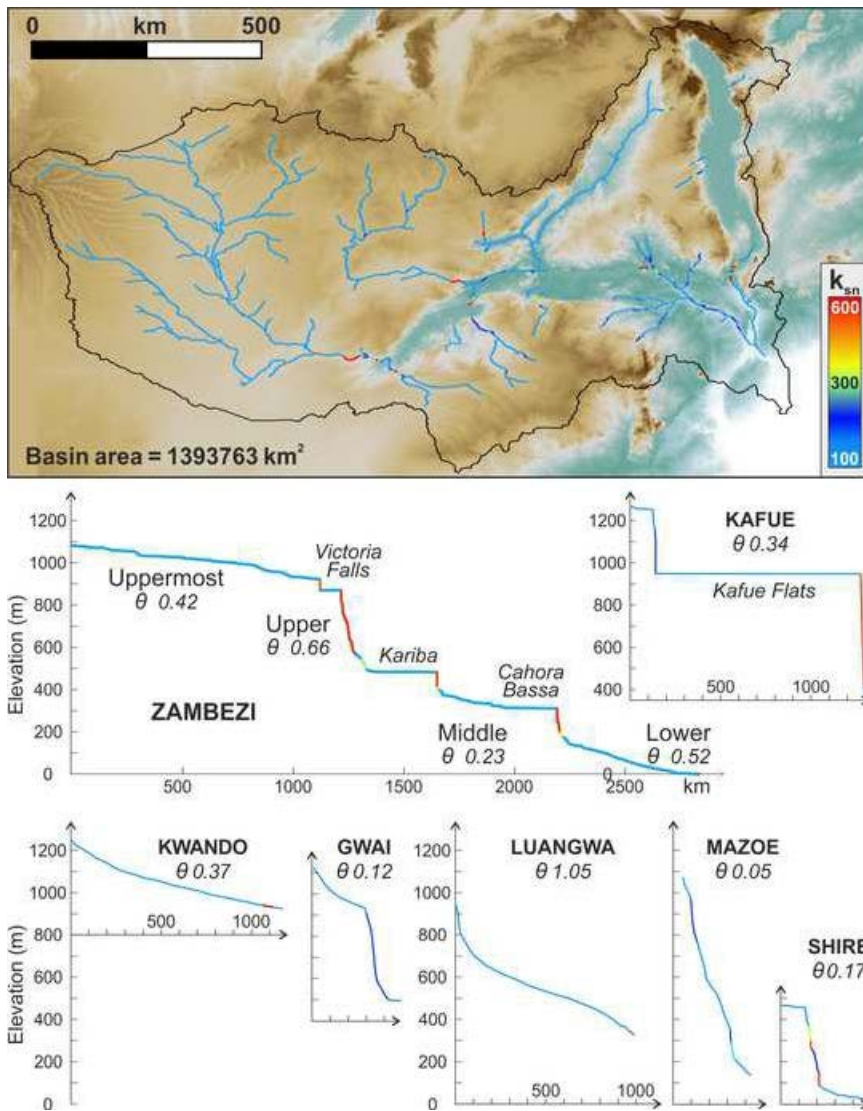


Figure 2.4: River morphometry (same vertical scale for all profiles; same horizontal scale for tributaries).

Besides the concave equilibrium profile of the Kwando, longitudinal channels are highly irregular, as highlighted by extreme variation in both steepness and concavity indices k_{sn} and ϑ . As most rivers in southern Africa, the Zambezi and several tributaries (e.g. Gwai, Kafue, Shire) display youthful, staircase profiles with long flat segments separated by very steep tracts, reflecting the presence of stepped planation surfaces separated by escarpments, a 754 characteristic feature of southern African landscape (Knight and Grab, 2018).

2.5 Results and discussion

In the partitioned Zambezi sediment-routing system, sand compositional signatures are radically different upstream and downstream of both Lake Kariba and Lake Cahora Bassa (Table 1), indicating that no sand can pass across each reservoir. In the Uppermost Zambezi mainstem, as in some of its major tributaries including the Kwando and the Kafue, another factor hampering the continuity of downstream sediment transport is the occurrence of densely

vegetated flat lowland occupied by numerous pans commonly aligned with shallow grassy valleys (dambos) acting as natural sediment traps (Moore *et al.*, 2007).

Table 2.1: Key compositional parameters

RIVER Kwando	Ttn	Ep	Grt	St	Ky	Sil	Amp	Cpx	Hy	&tH		AC
Kwando river	0.3	3	0	16	16	0	2	0	0	1	100.0	39
& U st Z.	1	38	2	5	6	1	7	5	2	2	100.0	2
Uppermost	0.4	5	0.3	7	18	0	2	4	0	2	100.0	0
U.Z. tributaries	0	0.4	0	1	0	0	0.4	92	0	0	100.0	n.d
Upper Zambezi	0	8	0.2	3	23	0.5	3	27	0.3	1	100.0	18
U.Z. tributaries	0	3	0	0	0	0	0	97	0.2	0	100.0	n.d
Upper Zambezi	0	2	0.2	2	6	0	1	84	0.3	1	100.0	n.d
Gwai River	0	18	7	0.3	1	1	35	30	0.2	1	100.0	24
Gwai tributaries	2	27	2	1	0.2	0	12	43	0	0.4	100.0	23
Kafue	3	10	2	1	4	1	67	1	0	1	100.0	12
Middle Zambezi	4	14	2	0	6	0.2	51	6	1	2	100.0	13
Luangwa	4	18	6	4	11	7	35	1	0	2	100.0	46
Sangara-	0.2	4	3	0	1	0	20	41	21	4	100.0	18
Morrunguze	3	12	4	0	0	0	30	36	12	0	100.0	41
Minjova	1	7	25	0	0	0.5	26	24	9	0.5	100.0	91
Mufa	3	2	2	0	0.5	0	71	9	8	1	100.0	48
Mazoe-Luia	4	12	3	0	2	1	73	1	0.5	0	100.0	34
Lower Zambezi	1	9	25	0	0.2	0.5	43	7	5	2	100.0	39
Shire	0.4	6	4	0	1	0	76	2	2	0	100.0	41
Sangadze-	1	5	58	7	4	3	18	1	0.2	0.5	100.0	54
Lower Zambezi	4	21	3	2	1	0.2	58	3	3	0	100.0	32
Zambezi upper	4	23	3	0.2	1	3	46	11	2	1	100.0	5
Quelimane	4	17	4	0.5	1	2	53	8	3	0.2	100.0	8
Quelimane outer shelf	2	24	0.2	0	0.2	4	47	14	1	1	100.0	6

2.5.1 The Uppermost Zambezi

Near the source, close to the political boundary between Zambia, Congo and Angola, sand is pure quartzose with K-feldspar \gg plagioclase and a very poor tHM suite dominated by zircon with tourmaline, minor rutile, and staurolite (Fig. 5-4A). Kyanite increases downstream and clinopyroxene is significant upstream of the Kwando.

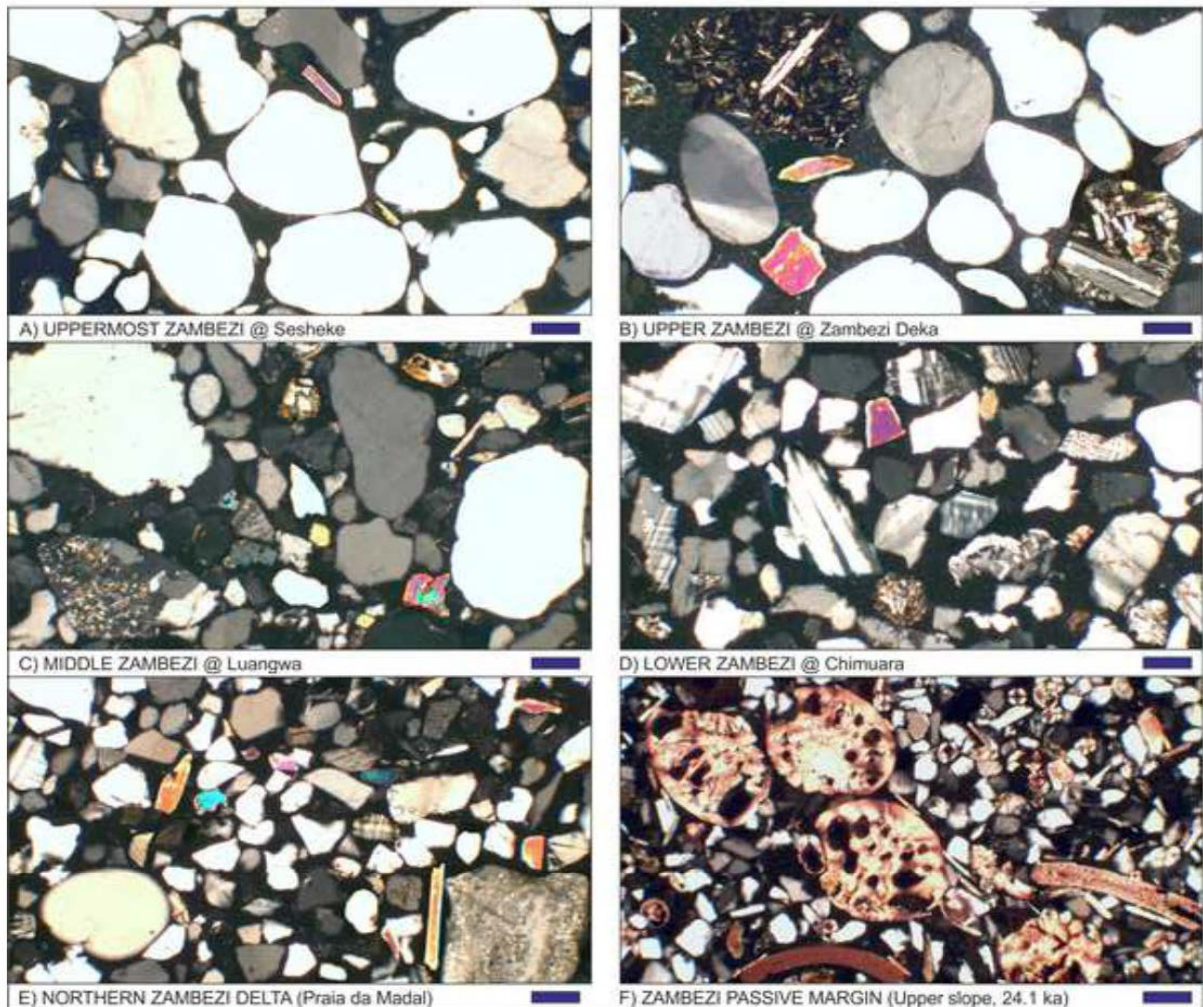


Figure 2.5: Petrographic changes along the Zambezi sediment-routing system from source to sink.

Where: A) Pure quartzose sand recycled from the Mega-Kalahari Desert. B) Marked enrichment in basaltic rock fragments and clinopyroxene in quartzose sand downstream of Victoria Falls. C) Reconstituted feldspathoid-quartzose metamorphiclastic bedload downstream of Lake Kariba. D) Sharp increase in feldspars in reconstituted bedload downstream of Lake Cahora Bassa. (E) Feldspathoid-quartzose beach sand of the Quelimane area. F) Very fine-grained feldspar-rich feldspathoid-quartzose sand, containing benthic foraminifera (stained by alizarine red) and deposited during the last glacial low stand on the

upper slope offshore of the Zambezi mouth. All photos with crossed polarizers; blue bar for scale = 100 μ m.

The Kwando River from Angola contributes pure quartzose sand with a very poor tHM suite including zircon, tourmaline, kyanite, and staurolite (Fig. 5-5A). Sand of left tributaries from Zambia range from quartz-rich feldspathoid-quartzose with K-feldspar > plagioclase (Kabombo, Ngwezi) to pure quartzose with K-feldspar >> plagioclase (Kasaya). Muscovite occurs. The tHM suites vary from poor with tourmaline, rutile, epidote and kyanite (Kabombo) to very poor and including epidote, zircon, tourmaline, staurolite and green augite (Kasaya), or epidote-dominated with amphibole and minor garnet (Ngwezi).



Figure 2.6: Sand composition in major Zambezi tributaries

Where: A) Up to well-rounded monocrystalline quartz grains recycled from Mega-Kalahari dunes. B) High-rank metamorphic rock fragments and microcline derived first-cycle from the Magondi Belt. C) Biotite-rich metamorphic detritus from the Lufilian Arc and Zambezi Belt mixed with rounded recycled quartz. D) Deeply corroded quartz and feldspar grains derived from the Irumide Belt or recycled from Karoo strata. E) Abundant microcline with high-rank metamorphic rock fragments from the Archean Zimbabwe Craton and Proterozoic gneisses. F) Microcline and gabbroic rock fragments from the southern Irumide Belt and Tete gabbro

anortosite complex. G) Dominant feldspar derived from orthogneisses and granulites of the Blantyre domain. H) Skeletal quartz and deeply weathered K-feldspar grains in Mozambican lowlands. All photos with crossed polarizers; blue bar for scale = 100 μm .

2.5.2 The Upper Zambezi

Basaltic detritus from Karoo lavas mixes with quartz as the river approaches Victoria Falls, and in steadily increasing proportions across the gorges downstream of the Falls. Upstream of Lake Kariba, bedload sand and levee silty sand include mafic volcanic rock fragments and are, respectively, quartzose with plagioclase = K-feldspar and litho-feldspatho-quartzose with plagioclase \gg K-feldspar (Figure 2.5B). The moderately rich tHM suite consists almost entirely of green augite with a few olivine grains. Upstream of Victoria Falls, the Sinde tributary from Zambia carries quartzose sand with mafic volcanic grains and a poor tHM suite dominated by brown and green augite. Basaltic detritus increases in abundance in tributary sand downstream of the Falls. Masuie and Matetsi sands are, respectively, lithic-rich litho-quartzose and quartzo-lithic basalticlastic, with rich and very rich tHM suites consisting almost exclusively of augite and augite-bearing rock fragments. River bars and levees of the Gwai River from Zimbabwe consist of feldspatho-quartzose sand with plagioclase $>$ K-feldspar (Figure 2.6B). Mostly biotitic mica is concentrated in levee silty sand. The moderately rich tHM suite consists of amphibole with subordinate epidote, garnet, and clinopyroxene. The Deka River carries quartz-rich litho-quartzose basalticlastic 298 sand with a very rich tHM suite dominated by clinopyroxene with some epidote.

2.5.3 The Middle Zambezi

Downstream of Lake Kariba, Zambezi sand has the same feldspar-rich feldspatho-quartzose composition as Kafue River sand, with K-feldspar \gg plagioclase, some metamorphic rock fragments, and micas (biotite \geq muscovite) (Fig. 5C; Fig. 6C). The rich tHM suite includes amphibole (blue-green to green-brown hornblende and actinolite) and subordinate epidote, kyanite, and clinopyroxene. Amphibole decreases and zircon increases slightly downstream the mainstem. The Luangwa River carries feldspatho-quartzose sand with K-feldspar \gg plagioclase and granitoid to gneissic rock fragments, with a moderately rich tHM suite including mainly amphibole (green-brown to blue-green hornblende), kyanite, zircon, and prismatic or fibrolitic sillimanite (Fig. 6D).

2.5.4 The Lower Zambezi

In Mozambique, Zambezi sand ranges from quartzo-feldspathic to feldspar rich feldspatho-quartzose with K-feldspar \geq plagioclase (Fig. 5D). Mica (mostly biotite) is common in very fine sand. The rich tHM suite includes mostly amphibole (blue green to green-brown hornblende and actinolite), subordinate epidote, locally strongly enriched garnet, and minor

titanite, zircon, clinopyroxene, and hypersthene. Most tributaries contribute quartzofeldspathic sand with K-feldspar \geq plagioclase and rich tHM suite (Fig. 6E, F, G). An exception is represented by the Minjova and Zangue tributaries, which carry feldspatho-quartzose and quartz-rich feldspathoid-quartzose sand with poor tHM suite (Fig. 6H). Feldspars (mostly plagioclase) are twice as abundant as quartz in Shire sand from Malawi. Metabasite grains are significant in Morrunguze sand (Fig. 6E). Chacangara sand includes gabbroic, quartzose sandstone/metasandstone, and shale/slate rock fragments. The tHM suites are diverse. Amphibole (mainly green-brown and blue-green hornblende) is dominant in Mufa, Mazoe, Luia, and Shire sand (ACI 31-50), and common in most other tributaries (ACI 13-27 in Sangara, Chacangara, Zangue sand, but up to 80-91 in Sangadze and Minjova sand). Clinopyroxene and hypersthene are most abundant in Chacangara sand and characterize Sangara, Morrunguze, Minjova and, to a lesser extent, Mufa sand (Table 1). Epidote is invariably present in moderate amounts. Garnet is dominant in Sangadze sand and common in Zangue and Minjova sand. Staurolite is associated with kyanite and prismatic or fibrolitic sillimanite in Zangue sand. Kyanite and sillimanite also occur in Luia sand. Zircon and other durable minerals, as well as titanite and apatite, are minor (ZTR up to 8 in Sangara sand). Rare olivine was detected in Sangara, Chacangara, and Mufa sand.

2.5.5 The northern coast, the shelf, and the slope

Sand in the Bons Sinais estuary near Quelimane and adjacent beaches, located between 100 and 130 km north of the Zambezi mouth, is feldspatho quartzose with plagioclase \geq K-feldspar and a rich tHM suite including mainly blue-green amphibole, subordinate epidote, clinopyroxene, and minor titanite, garnet, hypersthene, and mostly prismatic sillimanite (Fig. 5E). Very fine-grained sand to coarse silt, cored on the upper continental slope ~85 km offshore of the Zambezi Delta and close to the shelfbreak ~80 km to the ENE of the Bons Sinais mouth, is feldspar rich feldspatho-quartzose with K-feldspar \approx plagioclase and a moderately rich tHM suite including blue-green amphibole, epidote, clinopyroxene, and minor prismatic sillimanite, titanite, tourmaline, apatite, hypersthene, and garnet. Benthic foraminifera are abundant (Fig. 5F). No major mineralogical difference is observed either between samples cored offshore of the Zambezi mouth and Quelimane area or between sediments deposited during the last glacial low stand, the post-glacial sea-level transition, and the Holocene high stand in both areas.

2.5.6 Sand generation in the Zambezi catchment

The Uppermost Zambezi: polycyclic sand from the Kalahari.

Sand generated in south-eastern Angola and westernmost Zambia and carried by the Uppermost Zambezi and its Kwando tributary consists almost entirely of monocrystalline quartz with very poor, ZTR-dominated tHM suite including staurolite and kyanite, a mineralogical signature that reflects extensive recycling of Kalahari Desert sand (Fig. 2.7, 2.8). The sedimentary succession of this vast rim basin, formed on the 351 low-relief central southern Africa plateau confined between the rejuvenated shoulders of Indian and Atlantic Oceans rifts, is largely of fluvial origin with secondary aeolian imprint (Moore and Dingle, 1998). Kalahari dunes are generally best developed west of river channels, suggesting deflation of fluvial sediments by easterly winds during drier periods (Shaw and Goudie, 2002).

Conversely, rivers have inundated interdune areas and incised their course across dune ridges during wetter periods (Thomas *et al.*, 2000). Between a fourth and half of quartz grains are well rounded in both dune and river sediments, indicating that climate-controlled cycling of quartzose sand has taken place repeatedly from the fluvial to the aeolian environment and back (Thomas and Shaw, 2002).

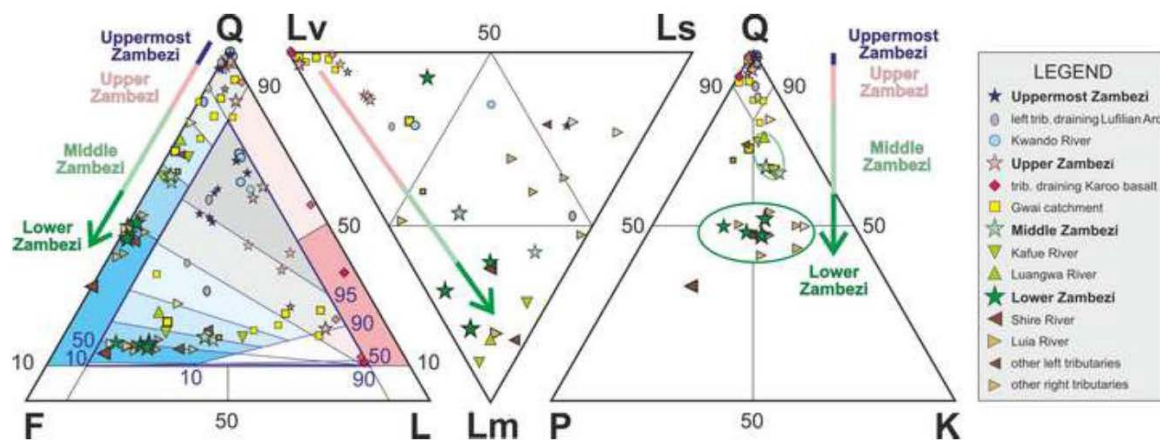


Figure 2.7: Downstream quartz decrease along the segmented Zambezi sediment-routing system.

Composition changes stepwise from pure quartzose (Uppermost Zambezi) to quartzose volcaniclastic (Upper Zambezi), feldspar-rich feldspathoid-quartzose (Middle Zambezi), and finally quartzo-feldspathic metamorphiclastic (Lower Zambezi). Symbol size is roughly proportional to tributary size and increases downstream along the mainstem. Smaller symbols with thicker outline for the Upper Zambezi and Gwaii River are levee samples representing deep suspended load. Q = quartz; F = feldspars (P = plagioclase; K = K-feldspar); L= lithics (Lm = metamorphic; Lv = volcanic; Ls = sedimentary). Fields in the QFL diagram after Garzanti (2019); in the nested blue version of the same QFL plot, data are centred to allow better visualization of quartz-rich samples (von Eynatten *et al.*, 2002).

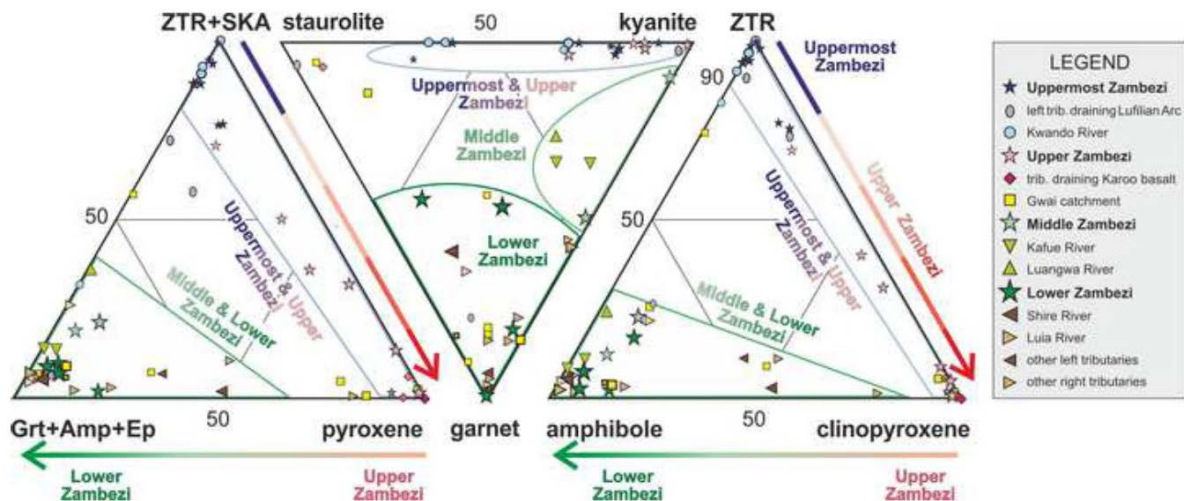


Figure 2.8: Changes in transparent-heavy-mineral suites downstream the segmented Zambezi sediment-routing system

Note: 1) dominance of durable ZTR (zircon, tourmaline, and rutile) and SKA minerals (staurolite, kyanite, sillimanite, and andalusite) in the Uppermost Zambezi; 2) progressive increase in clinopyroxene along the Upper Zambezi; 3) sharp increase in basement derived garnet (Grt), amphibole (Amp) and epidote (Ep) in the Middle and Lower Zambezi. Scarcity of garnet in Uppermost and Upper Zambezi sand is ascribed to high weatherability inherited from past hot-humid subequatorial climate. Symbol size is roughly proportional to tributary size and increases downstream along the mainstem. Smaller symbols with thicker outline for the Upper Zambezi and Gwai River are levee samples representing deep suspended load.

2.5.7 The Upper Zambezi: mixing with detritus from Karoo basalts

The Zambezi first meets Karoo basalt at Ngonye Falls in SW Zambia and from there on the river flows along Karoo rift basins as far as the Mozambican lowlands. Pure quartzose sand recycled from the Kalahari mixes downstream with detritus derived locally from Lower Jurassic Karoo basalt in increasing proportions, which are determined accurately with forward mixing models based on integrated petrographic and heavy mineral data (Garzanti *et al.*, 2012; Resentini *et al.*, 2017). Although the sand generation potential of mafic lava is notably less than that of sandstone or granite (e.g. Garzanti *et al.*, 2019a, 2021a, 2021b), basalt contains and sheds much more clinopyroxene than the few heavy minerals that quartzose sandstone contains and can thus supply. Therefore, wherever basaltic detritus mixes with recycled quartz, as in the Upper Zambezi, quartz still dominates among main framework grains but the tHM suite rapidly becomes clinopyroxene-dominated (Figure 2.7 and 2.8). From upstream of Victoria Falls to the Batoka Gorge, basaltic detritus accounts for < 3% of total sediment only and Upper Zambezi sand remains pure quartzose although clinopyroxene steadily increases from 14% to 86% of the very poor to poor tHM suite. Basaltic detritus increases to ~12% in sediment

entering Lake Kariba, with composition changed to quartzose with 9% basaltic rocks fragments in bedload sand and to litho-feldspatho-quartzose in levee silty sand. Clinopyroxene represents 95% and 90% of the moderately rich and rich tHM suite, respectively. Among Upper Zambezi tributaries, basaltic detritus represents ~10% of Sinde sand in Zambia, and ~15% of Shangani sand, 50% of Masuie sand, and up to 70% of Matetsi sand in Zimbabwe, the rest being mostly represented by quartz recycled from Kalahari dunes. Clinopyroxene invariably represents > 90% of the tHM suite in these rivers. Such estimates are corroborated by clay-mineral and geochemical data, displaying an increase in smectite and in the concentration of Fe, Mg, Ca, Na, Sr, Ti, Eu, V, Cr, Mn, Co, Ni, Cu and P downstream of the Upper Zambezi, while the $^{87}\text{Sr}/^{86}\text{Sr}$ and weathering indices decrease, $\epsilon\text{Nd}(0)$ becomes only moderately negative, and tDM model ages younger (Garzanti *et al.*, 2014b). Forward mixing calculations based on the integrated geochemical dataset indicate that volcanic detritus increases from ~1% for sand and ~14% for cohesive (< 32 μm) mud upstream of Victoria Falls up to 17-18% for sand, 19-20% for sandy silt, and ~41% for cohesive mud upstream of Lake Kariba. These estimates imply that up to ~27% of the sand and ~45% of the mud that the Upper Zambezi delivers to Lake Kariba is generated downstream of Victoria Falls, from basaltic rocks of the Batoka Gorge and supplied by tributaries draining Karoo lavas and overlying Kalahari dunes.

2.5.8 The Middle Zambezi: first cycle and recycled detritus from Zambia

The Middle Zambezi flows along Karoo extensional troughs (Figure 2.2). These formed on top of the Kuunga suture zone, marking the boundary between the Zimbabwe-Kalahari and Congo cratonic blocks and sealed during the final stages of the Neoproterozoic Pan-African orogeny (Goscombe *et al.*, 2020).

The first major tributary joining the Zambezi ~70 km downstream of Lake Kariba is the Kafue River, which largely drains mid-Neoproterozoic volcano-sedimentary rocks and upper Tonian granites of the Lufilian Arc in the upper course. In the lowermost course, the Kafue cuts across the West Zambezi Belt, including polymetamorphic basement of the Congo Craton deformed at upper-amphibolite facies conditions around 675 Ma (Figure 2.6 in Goscombe *et al.*, 2020).

Because sand cannot pass Lake Kariba, Middle Zambezi sand downstream of the Kafue confluence acquires the same feldspar-rich feldspatho-quartzose metamorphic signature of Kafue sand- with a little more siltstone/sandstone rock fragments and clinopyroxene derived locally from the Karoo Supergroup – which is maintained as far as the confluence with the Luangwa River near the entry point into Lake Cahora Bassa (Figure 2.9). The Luangwa River, sourced in Paleoproterozoic gneisses of the Ubendian Belt, follows for most of its course another arm of the Karoo rift network. The Luangwa rift is bordered to the north by the external nappes of the Irumide Belt, including Paleoproterozoic granitoid gneiss overlain by quartzite and schist of the Muva Supergroup deformed at greenschist to amphibolite facies at 1.02-1.05 Ga (De Waele *et al.*, 2009). Exposed to the south is the high-grade internal zone of the Southern Irumide Province (fig. 7 in Goscombe *et al.*, 2020). Luangwa sand is thus a mixture of detritus derived from up to high-grade metamorphic rocks and recycled from Carboniferous to Jurassic

siliciclastic strata, as indicated by relatively high quartz and ZTR index coexisting with blue-green to brown hornblende and mainly prismatic sillimanite.

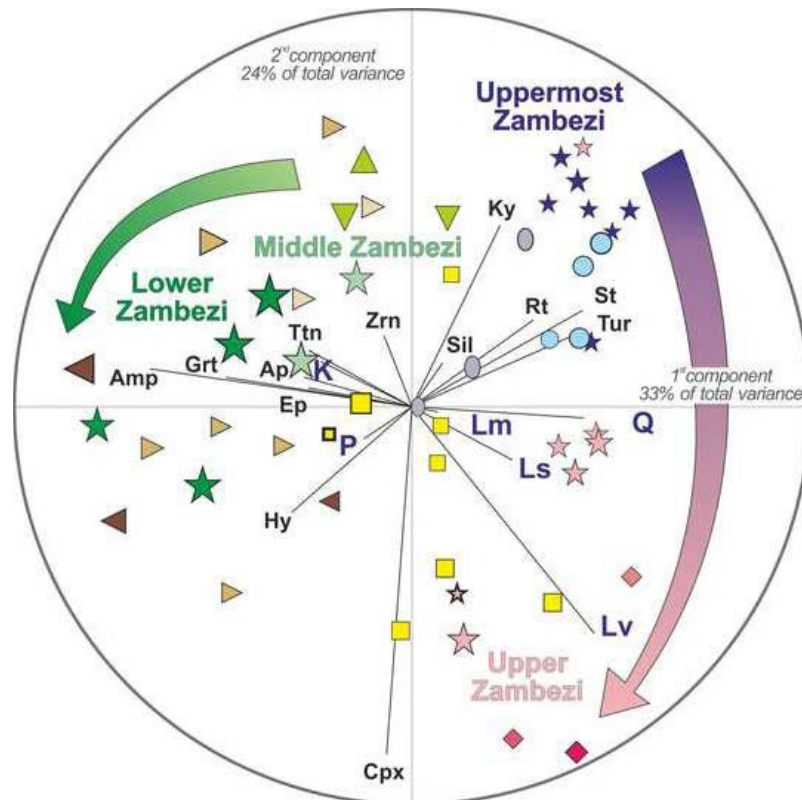


Figure 2.9: Stepwise changes in mineralogical signatures along the Zambezi sediment-routing system

Note: Pure quartzose sand in the Uppermost Zambezi and Kwando River is progressively enriched in clinopyroxene and basaltic rock fragments downstream the Upper Zambezi. Middle Zambezi sand chiefly reflects contribution from the Kafue River. Lower Zambezi sand is markedly enriched in feldspars, amphibole, and garnet largely derived from Irumide Belts strongly affected by the Pan-African orogeny. The biplot (Gabriel, 1971) displays multivariate observations (points) and variables (rays). The length of each ray is proportional to the variance of the corresponding variable; if the angle between two rays is 0°, 90°, or 180°, then the corresponding variables are perfectly correlated, uncorrelated, or anticorrelated, respectively. Symbols as in Figures 2.7 and 2.8.

2.5.9 The Lower Zambezi: feldspar-rich sand from Precambrian basements

As Upper Zambezi sand is dumped into Lake Kariba, Middle Zambezi sand is stored in Lake Cahora Bassa. Composition changes therefore again in the Lower Zambezi, where sand contributed by tributaries largely draining felsic to mafic igneous and up to high-grade metamorphic rocks acquires a quartzo-feldspathic signature unique among the Earth's big rivers (Garzanti, 2019). Most Lower Zambezi tributaries carry sand with Q/F ratio ≤ 1 (Figure 2.7), reflecting mostly first-cycle provenance from mid-crustal crystalline basements. Detritus

recycled from the sedimentary fill of Karoo, Cretaceous, or Cenozoic extensional basins is widespread, although subordinate. This is revealed by sandstone and shale rock fragments in Chacangara sand and by higher Q/F ratio and poor tHM suite in sand of the Zangue River draining the northern edge of the Urema Graben and of the Minjova River draining the Karoo Moatize-Minjova Basin (Fernandes *et al.*, 2015). The Sangara, Chacangara, and Mufa right (west) tributaries and the Morrunguze and Minjova left (east) tributaries drain high-grade rocks of the internal zone of the Southern Irumide Province including the Tete gabbro-anorthosite complex (fig. 1 in Goscombe *et al.*, 2020). This is reflected by the occurrence of gabbroic or metabasite rock fragments and by up to very rich tHM suites including hypersthene and clinopyroxene, brown hornblende, and rare olivine. The Luia-Mazoe river system drains well into the Archean Zimbabwe Craton in the upper course and cuts downstream across the polymetamorphic Mudzi migmatitic gneisses remobilized during the Pan-African orogeny, and next across the Neoproterozoic Marginal Gneiss. The mostly first-cycle origin of their quartzofeldspathic sand is reflected by the rich amphibole-dominated tHM suite, as in Mufa sand to the north (Fig. 8). The lowest Q/F ratio is recorded in Shire sand, also including a very rich, amphibole-dominated tHM suite derived from granitic orthogneisses and granulitic gneisses of the Blantyre domain (southern Malawi-Unango Complex), where Stenian-age crust was extensively recrystallized at granulite facies during the Pan-African orogeny (Goscombe *et al.*, 2020). The Sangadze and Zangue lowermost-course tributaries are sourced in the Pan-African Umkondo Belt including greenschist- to lower-amphibolite-facies schists thrust onto the margin of the Zimbabwe Craton and upper amphibolite-facies migmatitic gneisses in the core, whereas the lower course cuts across the Cretaceous to Cenozoic sediment fill of the Lower Zambezi graben. Recycling is manifested in Zangue sand by the highest Q/F ratio of all Lower Zambezi tributaries. Poor to moderately poor, garnet-dominated (Sangadze) or garnet-staurolite (Zangue) tHM suites reflect both first-cycle provenance from amphibolite-facies metasediments of the Umkondo Belt and recycling of Cretaceous sandstones derived from them (e.g. Sena Formation; Salman and Abdula, 1995). The occurrence of brown amphibole and prismatic sillimanite, instead, reveals minor but significant contribution from upper amphibolite- to granulite-facies gneisses of the orogen's core (e.g. Stenian Barue complex; Fig. 1 in Goscombe *et al.*, 2020).

Forward mixing models based on integrated petrographic and heavy-mineral data suggest that most Lower Zambezi sand (60-80%) is generated in subequal proportions in the Luia-Mazoe river system sourced in the Zimbabwe Craton and in the trunk-river catchment upstream of the Luia confluence, including the Zambezi Belt and the Southern Irumide Province. Additional contributions from the Umkondo Belt and recycled from the Karoo, Cretaceous, or Cenozoic extensional basins drained by the Minjova, Sangadze, and Zangue tributaries are significant (~20%), whereas supply from the Tete gabbro-anorthosite complex and Blantyre Domain, drained respectively by the Morrunguze and Shire northern tributaries, appears to be subordinate (~10%).

2.5.10 The Zambezi passive margin

Detrital modes of Lower Zambezi sand match neither those of the Bons Sinais estuary and beaches in the northern delta near Quelimane nor sediments cored offshore both Zambezi mouth and Quelimane area and deposited during either the Holocene highstand or the previous post-glacial and glacial relative lowstands (Table 1). The Q/F ratio is 1.0 ± 0.1 in Lower Zambezi sand but 2.5 ± 0.5 in sand of the Quelimane area and 1.6 ± 0.3 in offshore samples. The homogeneous composition of offshore sediments generated before the mid-Holocene (older than 4463 ka) suggests that this could represent the original, pre-Anthropocene signature of Zambezi sediment.

Subsequent closure of the Kariba and Cahora Bassa dam – with consequent reduction of the catchment area effectively contributing sediment to the Zambezi delta – explains the peculiar mineralogical signatures characterizing Lower Zambezi sand today. Besides the abundance of feldspars unusual for a big river, these include the high heavy-mineral concentration and ACI index, reflecting provenance dominantly from middle crustal igneous and high-grade metamorphic rocks. The abundance of mica in offshore sediments, instead, is the effect of preferential winnowing of slow settling platy phyllosilicates by waves, a phenomenon observed on continental shelves worldwide (e.g. Doyle *et al.*, 1968; Garzanti *et al.*, 2015, 2019b)

The mineralogy of estuary and beach sand in the Quelimane area is not the same as either Lower Zambezi or offshore sediment (Table 1). This is more difficult to explain, because predominantly northward littoral drift would be expected to entrain sand from the Zambezi delta, leading to homogeneous composition along the coast. Reasons of such discrepancy may include local reworking of floodplain sediments, whereas littoral drift from the north is unsupported by prevailing longshore current patterns (Fig. 4 in Schulz *et al.*, 2011; van der Lubbe *et al.*, 2014).

2.5.11 How does Zambezi sand fit with classical sedimentary-petrology theories?

The petrographic and mineralogical changes documented along the Zambezi sediment-routing system allow some considerations of consequence. They demonstrate how the knowledge acquired studying present landscapes rings a bell against the uncritical use of simplistic concepts in geological research (Garzanti and Sternai, 2020). In the lack of direct observations, we often try to unravel the past by using ungrounded simplifications and naïve analogies (e.g. sediment that “matures” in time like fruit), unable to constrain or even imagine the complexities of past sediment routing systems including the effects of inheritance and multiple recycling. In the lack of clear evidence, we tend to implicitly assume that the information contained in the compositional signatures of sandstone refers to the targeted sedimentary basin only, but it may as well, and commonly do, largely reflect tectonic or climatic conditions that existed, there or somewhere else, at earlier times. The present may well provide one key to the past, but how many are the doors and locks that this key is unable to open? Are prêt-à-porter models a help

or a hindrance to the understanding of the complex 4D evolution of geological bodies through space and time? There are several specific questions that the present case study helps to investigate. The first one, tackled below, is: “To what extent are classical provenance models adequate?”

2.5.12 Provenance models

The first model linking sand mineralogy with the tectonic setting of source areas was developed by Krynine (1948), who inherited from his Moscow teacher Shvetsov (1934) the belief that sediment composition reflects systematic interactions among lithogenic processes that can be unravelled and understood. The basic assumption is that the continental crust can be envisaged as consisting of sedimentary layers non-conformably overlying deformed metamorphic rocks intruded at depth by plutonic rocks. The progressive top-down erosion of such a rocky layer-cake would generate quartz-rich recycled sediments first, lithic-rich metamorphiclastic detritus next, and finally feldspar-rich plutoniclastic detritus. During a tectonically quiescent stage, recycling of cover strata would go on for a long time, eventually producing a wide sheet of quartzose sand (named “quartzite”). Conversely, tectonic uplift would lead to rapid unroofing of deep-seated plutonic rocks feeding fault-bounded basins with feldspar-rich sand (named “arkose”). These concepts were elaborated further by Krynine’s student at Pennsylvania State College Folk (1980 p.108-144), who pointed out the insufficient attention dedicated by his teacher’s theory to sources of complexities such as geological inheritance, volcanism, and diversity of geodynamic settings. Furthermore, Folk acknowledged the major role of chemical weathering, and thus distinguished “climatic arkose”, generated from basement rocks in dry climate even during stages of tectonic quiescence, from Krynine’s “tectonic arkose”. The essence of such lines of reasoning passed largely unaltered from the pre-plate-tectonic to the post-plate-tectonic era. The same three stages identified in Krynine’s and Folk’s models are recognized in Dickinson’s model (1985), where sediments produced in anorogenic (i.e. subduction-unrelated) settings are designated as “continental block” provenance, distinguished as “craton interior” (the quartz-rich sand produced during tectonically quiescent stages), “transitional”, and “basement uplift” (the feldspar-rich sand shed from rapidly uplifted granitoid crustal blocks).

Differently from Krynine’s scheme, lithic-rich sediments were considered as diagnostic of orogenic (i.e. subduction-related) settings. Heavy minerals were not organically considered in provenance models until later (Nechaev and Isphording, 1993; Garzanti and Andò, 2007). One reason is that they are of limited use in ancient sediments wherever the tHM suite has been strongly depleted and modified by selective intrastratal dissolution of less durable species during diagenesis (Garzanti *et al.*, 2018b). Moreover, the information carried by tHM suites may be profoundly distorted by hydrodynamic processes or fertility effects (Garzanti *et al.*, 2009; Malusà *et al.*, 2016). Heavy-mineral-rich sources such as mafic igneous and high-temperature or high-pressure metamorphic rocks have an overwhelming effect on the detrital tHM suite, heavy-mineral-poor sedimentary rocks or granite being conversely strongly

underrepresented (Fig. 1 in Garzanti and Andò, 2019). Because of the fertility effect, the tHM suite may reflect a radically different provenance than framework petrography, as in the Upper Zambezi where pure quartzose sand contains a clinopyroxene-dominated tHM suite. Combining framework composition and heavy minerals represents a necessary requirement to tackle the complexities of geological landscapes and achieve a refined provenance characterization. Anorogenic provenances could thus be subdivided into volcanic and non-volcanic and the latter, in turn, into undissected (craton interior), transitional, and dissected (basement uplift) continental block subprovenances (Garzanti *et al.*, 2001). Anorogenic volcanic provenance is typified by feldspathic lithic to quartzo-feldspathic-lithic sand with clinopyroxene-dominated tHM suite, undissected continental block subprovenance by quartzose sand with ZTR-dominated tHM suite and dissected continental block subprovenance by quartzo-feldspathic sand with hornblende-dominated tHM suite (Garzanti, 2016). Supply from continental flood basalts such as the Karoo (anorogenic volcanic provenance) is not contemplated in Dickinson's (1985) model. In a hypothetical analogous ancient case study, the uncritical use of that model would erroneously ascribe the compositional trend observed downstream the Upper Zambezi to mixing with arc-derived detritus. Are models right or wrong? Obviously neither. As any tool, they apply well to some circumstances and badly to others. Because they are derived from one setting and extrapolated to another, and because different settings are not the same, models are bound to be partly misleading even in the luckiest case. Their uncritical use is therefore discouraged.

2.5.13 The final signature of Zambezi sand

The Zambezi River carries to the Indian Ocean quartz feldspathic sand, a fingerprint that has hardly an equivalent among the world's big rivers (Potter, 1978). Such a composition compares with that of granitoid-derived sand generated in dry southern California (table 3 in Dickinson, 1985) and represents the typical mark of dissected continental block sub provenance. Shire sand is the richest in feldspars and thus a good example of "ideal arkose" (Dickinson, 1985). Big river catchments typically embrace a very wide range of rocks produced in different geodynamic settings at different times. Their sediments are thus mixtures of different provenances including a considerable fraction of recycled grains. Lower Zambezi sand, characterized by feldspar \geq quartz, very few aphanitic lithics, and a rich hornblende-dominated tHM suite largely shed first-cycle from plutonic and high-grade metamorphic rocks, represents an anomaly in this respect. One main reason, discussed further below, is that quartz-dominated sand recycled in the upper reaches is not transferred to the lower course. Detritus reaching the Indian Ocean is thus generated entirely in the highlands of Zimbabwe and Malawi, where the roots of Archean cratons and Proterozoic orogens have been uplifted and progressively eroded during the southward propagation of the East African rift (Fernandes *et al.*, 2015). Consequently, sand composition is the same as detritus shed from mid-crustal basement rocks exposed along actively uplifted and deeply dissected rift shoulders, such as those flanking the Red Sea (Garzanti *et al.*, 2001, 2013a), rather than that expected for a mature passive margin.

2.5.14 Do minerals “mature” during fluvial transport?

A widely held belief in sedimentary petrology – persistent although long demonstrated untrue (e.g. Russell, 1937; Shukri, 1950) – is that chemically and mechanically durable minerals must increase at the expense of unstable and less resistant minerals during long-distance fluvial transport. Uppermost Zambezi sand consists almost entirely of quartz associated with the most durable heavy minerals zircon, tourmaline, and rutile, thus representing a good example of “highly mature” sediment (Folk, 1951; Hubert, 1962). In the Upper Zambezi downstream, however, mafic volcanic rock fragments increase and clinopyroxene becomes first a significant, then the main, and finally the nearly exclusive transparent heavy mineral. The progressive downstream increase of detritus derived from Karoo lavas, locally including unstable olivine, results in decreasing degree of “maturation” downstream. Decreasing “maturity” with transport distance – which sounds paradoxical because maturation is intended to progress irreversibly with the passing of time – is not unusual in modern river systems wherever less durable detrital components are added downstream, as observed for instance along the Kagera River in equatorial Africa (Garzanti *et al.*, 2013b).

In the Middle Zambezi, sand is notably enriched in feldspars and diverse types of rock fragments supplied by the Kafue and other tributaries draining both Precambrian orogenic belts and Permo-Triassic rift-basin fills. Composition thus becomes even less “mature”. In the Lower Zambezi, owing to prominent supply from local tributaries draining mid-crustal Precambrian basements, quartz content decreases further, becoming equally or even less abundant than feldspars. The Zambezi is thus an exemplary case of sediment-routing system along which the ratio between stable and unstable minerals (too often inappropriately portrayed as degree of “maturity”; (Garzanti, 2017) decreases steadily with transport distance. Although enhanced by the artificial segmentation of the river course after the closure of Kariba and Cahora Bassa dams, preventing the continuity of sand transport across the reservoirs, such a trend towards less durable mineralogical assemblages downstream is primarily a natural phenomenon reflecting the multistep evolution of the river and location of erosional foci (Figure 2.10).

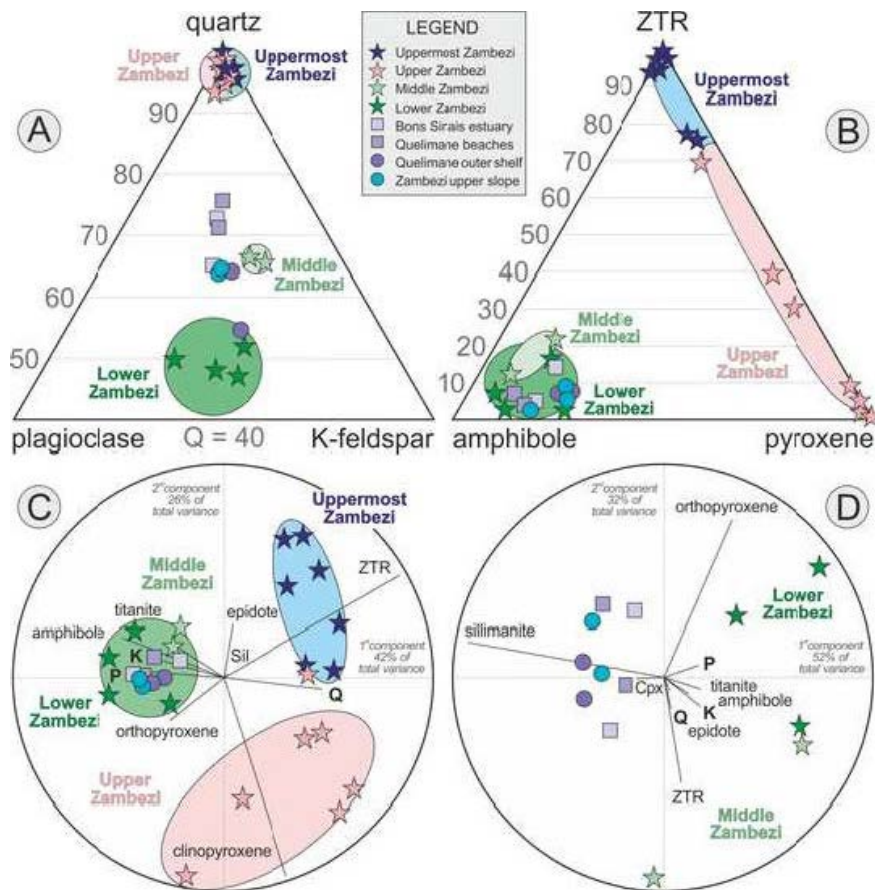


Figure 2.10: Zambezi River sands compared with coastal and offshore sediments

Where: A, B, and C= Uppermost and Upper Zambezi detritus is clearly distinct from any downstream sample. Sediment fed into the Indian Ocean was thus mostly derived from the middle-lower catchment even before closure of the Kariba and Cahora Bassa dams. D) Passive margin sediments, however, do not closely match either Middle or Lower Zambezi sand, indicating significant additional contribution from both the upper catchment and Mozambican lowlands in pre-Anthropocene times. Biplots C and D (Gabriel, 1971) drawn with CoDaPack software by Comas-Cufí and Thió-Henestrosa (2011). Q = quartz; P = plagioclase; K = K-feldspar; ZTR = zircon + tourmaline + rutile; Cpx = clinopyroxene. Sil = sillimanite.

The Zambezi progressively connected stepwise the broad central African plateau underlain by thick cratonic crust and sustained by dynamic uplift since mid-Cenozoic times (Lithgow-Bertelloni and Silver, 1998; Moore et al., 2009b; Flügel et al., 2018) with the middle and lower reaches, entrenched in Karoo rifts and cutting across Precambrian mobile belts rejuvenated by the southward propagation of the East African rift in the late Neogene (Roberts et al., 2012; Hopper et al., 2020). If we just looked at the compositional signature of Lower Zambezi sand and uncritically applied traditional ideas of “maturity” disregarding the character and history of the catchment, then we would falsely infer a scenario like Red Sea shoulders, involving short

fluvial transport from locally uplifted rift highlands. The largest river sourced in the heart of cratonic southern Africa would be left unseen.

2.5.15 Broken transmission of provenance signals: the anthropic effect

One main reason why traditional petrological models apply so badly to the Zambezi is the pronounced segmentation of the fluvial system, which reflects its multistep Neogene evolution finally fixed by man's construction of Kariba and Cahora Bassa dams. Development of the Zambezi River is held to have started by headward erosion operated by a coastal river that captured first the Luangwa and next the Kafue after re-incision of the Cahora Bassa and Gwembe troughs upstream. Only sometime around the early Pleistocene was the gentle-gradient Upper Zambezi captured as well, finally linking the Kalahari Plateau with the Indian Ocean via Victoria Falls (Moore *et al.*, 2007). Rim basins such as the Mega-Kalahari represent huge reservoirs of quartz-rich polycyclic sand stored in continental interiors. Such reservoirs may be tapped by headward-eroding coastal rivers that progressively enhance their discharge as larger segments of endorheic drainage are captured, a process continuing today with incipient piracy of the entire Okavango (Moore and Larkin, 2001).

The undissected continental block (craton interior) sub provenance signal carried by the Upper Zambezi, however, fails to be transmitted beyond Lake Kariba. In the same way, the transitional continental block sub provenance signal carried by the Middle Zambezi fails to be transmitted downstream of Lake Cahora Bassa. The Lower Zambezi thus carries a pure dissected continental block (basement uplift) sub provenance signal to the Indian Ocean, the same that the coastal proto-Zambezi would have had before starting its inland expansion punctuated by the progressive capture of interior drainage. River segmentation was far less pronounced before man's intervention, as indicated by the poor compositional match between the present Lower Zambezi sand and upper Quaternary outer shelf and upper slope sediments, which have notably higher Q/F ratio and a little more clinopyroxene. Such differences cannot be dismissed as a grain-size effect, because the Q/F ratio typically increases with increasing grain size (e.g. Garzanti *et al.*, 2021c) and our river samples are very fine to fine sands whereas offshore samples are sandy silts. Rather than additional contribution by longshore-drifting sediment from outside the Zambezi delta, the plausible explanation is that a larger amount of detritus generated in the upper and middle catchment reached the ocean before closure of Kariba and Cahora Bassa dams. Forward-mixing calculations allow us to estimate that, before the Anthropocene, as much as 40% of detritus transferred to the coast was generated by erosion of Phanerozoic covers (~35% recycled from pure quartzose sandstone and ~5% from basalt). Quartz-rich sandstones and Karoo lavas are widespread in the Zambezi catchment, from Ngonye Falls in the Uppermost Zambezi to the lowermost course, and the pre-Anthropocene contributions from the Upper or Middle Zambezi are therefore hard to accurately quantify. However, the sharp mineralogical contrast between Upper Zambezi and offshore sediments indicates that most detritus was derived from the middle-lower reaches even in pre-Anthropocene times (Figure 2.10A, B, C).

2.5.16 Weathering effects inherited from the past

The last question dealt with Here concerns the possibility to infer climate from mineralogical composition of sand. Spurred by optimism, researchers have widely used chemical indices (e.g. CIA= $[Al_2O_3 / (Al_2O_3 + K_2O + Na_2O + CaO^*)] \cdot 100$; Nesbitt and Young, 1982) or even mineralogical indices (e.g. MIA= $Q/(Q+F) \cdot 100$; Rieu *et al.*, 2007) to infer climatic conditions in strata as old as the Proterozoic. Studies of modern sedimentary systems, however, recommend caution (Garzanti and Resentini, 2016). If we interpret compositional data uncritically using simplistic concepts, then we are bound to make severe mistakes. Because feldspars are scarce in the Uppermost Zambezi ($Q/(Q+F) \geq 95\%$) and abundant in the Lower Zambezi ($Q/(Q+F) \approx 50\%$), an inconsiderate use of the MIA would suggest very humid climate in the upper reaches and very dry climate in the lower reaches. Which is patently wrong? Besides being subject to marked grain-size control (Garzanti *et al.*, 2021c and references therein), the $Q/(Q+F)$ ratio reaches 100% in sand of both hyper-humid equatorial Congo and hyper-arid tropical Arabian or Sahara sand seas (Garzanti *et al.*, 2019c; Pastore *et al.*, 2021), making it evident that climatic conditions cannot be naïvely inferred by mineralogical parameters such as the MIA. The Uppermost Zambezi and its Kwando tributary carry pure quartzose sand mostly recycled from aeolian dunes that grew across the Mega-Kalahari Desert during arid stages of the Quaternary (Thomas and Shaw, 2002). In a desert climate, generation of pure quartzose sand cannot occur in a single sedimentary cycle but requires widespread recycling of older sandstones affected by extensive chemical weathering in very different climatic conditions. Pure quartzose composition of sand, as well as abundant kaolinite in mud (Garzanti *et al.*, 2014b), thus represent the echo of a time when sediments were produced in a chemically aggressive hot-humid climate. Sediments were produced in a chemically aggressive hot-humid climate.

In heavy-mineral suites, this is reflected by the scarcity of garnet relative to staurolite, kyanite, andalusite, and sillimanite ($Gr_t/(Gr_t+SKA) < 5\%$). These minerals characterize amphibolite-facies metasedimentary rocks and unweathered detritus derived from them, where garnet is almost invariably dominant ($Gr_t/(Gr_t+SKA) = 70 \pm 20\%$; Garzanti *et al.*, 2006, 2010). This is the case for sand of the Lower Zambezi and its major tributaries (Fig. 8 middle panel). In the Upper Zambezi, instead, staurolite and kyanite are common but garnet very scarce, which cannot be explained by either provenance or hydraulic factors (garnet being only slightly denser) and is most plausibly ascribed to the low stability of garnet in a humid subequatorial climate (Garzanti *et al.*, 2013b). Dominance of quartz, abundance of kaolinite, and scarcity of garnet in Upper Zambezi sediment as well as in Kalahari dunes (Garzanti *et al.*, 2014a, 2014b) thus consistently reflect humid subequatorial conditions that reigned in the past, dating back to the Cenozoic or Mesozoic well before the arid Quaternary when Kalahari dunes invaded the landscape (Guillocheau *et al.*, 2015, 2018). Today, climate is arid enough to induce only limited weathering in most of southern Africa, where detrital modes largely reflect the dominant parent lithologies exposed in source areas. In Mozambique, where climate ranges from hot semiarid in the interior to tropical savanna downstream the Zambezi Valley (Bsh to Aw classes of the Köppen climate classification; Figure 2.3D), feldspars are more abundant than in any other big

river on Earth. Olivine, which is a most unstable detrital mineral, occurs in small amounts both in the mainstem upstream of Lake Kariba and in western tributaries joining the Zambezi shortly downstream of Cahora Bassa. Sand mineralogy thus fails to reflect a notable effect of weathering occurring at present across most of the Zambezi catchment.

2.6 Conclusions

Sand in the Uppermost Zambezi is pure quartzose and almost entirely recycled from desert dunes across the Kalahari Plateau, thus matching the theoretical sediment produced in cratonic interiors (undissected continental block subprovenance). At the opposite end of both the drainage basin and the petrologic spectrum of sediment shed from continental blocks, sand of the Lower Zambezi and many of its major tributaries is quartzo-feldspathic, even reaching an “ideal arkose” composition (dissected continental block subprovenance). Sand of the Middle Zambezi and its major tributaries has an intermediate feldspatho-quartzose composition (transitional continental block subprovenance). The relative abundance of durable quartz and ZTR minerals thus decreases steadily along the sediment-routing system, a trend that denies the naïve but still popular idea that sediment “matures” with transport distance.

Although enhanced by the artificial segmentation of the river course after the closure of the Kariba and Cahora Bassa dams that prevented the continuity of sand transport across the reservoirs, such a downstream trend towards less durable mineralogical assemblages is primarily a natural phenomenon reflecting dynamic uplift of the low-relief cratonic plateau of central southern Africa and polyphase, ongoing rift-related rejuvenation of Precambrian mobile belts in the middle and lower reaches. The thorough investigation of each part of the river catchment and the precise definition of the mineralogical correspondence between parent rocks and daughter sediments is indispensable to forge a key able to unlock the sedimentary archives represented by the thick stratigraphic successions accumulated through the late Mesozoic and Cenozoic in onshore and offshore basins, and thus reconstruct with improved robustness the complex history of the Zambezi River.

CHAPTER 3

INPUTS OF SOUTHERN AFRICAN TERRESTRIAL SYSTEMS INTO THE ATLANTIC-INDIAN OCEAN

3.1 Introduction

The Zambezi, the fourth longest river in Africa and the largest draining into the Indian Ocean (Figure. 3.1; Moore *et al.*, 2007), underwent a still incompletely understood multistep evolution through time, influenced by all rifting events that punctuated the ~280-Ma-long break-up history of Gondwana (Moore and Larkin, 2001; Key *et al.*, 2015). For large tracts the river flows along Permian-Triassic rift troughs and its general eastward slope originated from domal uplift associated with the Early Cretaceous rifting of the South Atlantic in the west (Cox, 1989; Moore and Blenkinsop, 2002).

The modern drainage developed through the Neogene because of dynamic uplift of the broad Kalahari Plateau and south-westward propagation of the East African Rift, which created the tectonic depressions occupied by Lake Malawi in the east and by the Okavango inland delta in the west (Ebinger and Scholz, 2012). After diverse events of river capture and drainage reversal, a youthful lower course in Mozambique eroded backwards to eventually connect with the upper course on the Kalahari Plateau, forcing it to plunge deeply into Victoria Falls and the basaltic gorges downstream. The drainage basin has continued to expand in the Quaternary, with the capture of the Angolan Kwando tributary and the presently incipient capture of the large Okavango River as well (Wellington, 1955; Gumbrecht *et al.*, 2001).

In the Anthropocene, however, the course of the Zambezi has ceased to be natural and was rigidly segmented by the construction of the great dams that created Lake Kariba and Lake Cahora Bassa. Because the sediment-routing system is strictly partitioned by these two major reservoirs, it is convenient to distinguish here four reaches, the Uppermost Zambezi headwater tract as far as the Kwando confluence, the Upper Zambezi that includes Victoria Falls and the gorges as far as Lake Kariba, the Middle Zambezi between the two reservoirs, and the Lower Zambezi downstream of Lake Cahora Bassa (Figure 3.1).



Figure 3.1: The Zambezi drainage basin (base map from Google Earth™)

Where: white circles indicate sampling locations. VF = Victoria falls; Nyami Nyami is the folkloric snake spirit of the Zambezi River

This study integrates the petrographic and heavy-mineral datasets obtained from the same sample set and discussed in the companion paper (Garzanti et al., 2021a) with original elemental geochemistry, isotope geochemistry, clay mineralogy, and detrital-zircon geochronology data. The two articles combined provide a multi-proxy characterization of the composition of sediments generated in the diverse tracts of the large Zambezi catchment from the Zambian headwaters to the Mozambican coast.

Main aims:

- a. refine provenance diagnoses based on diverse compositional parameters from both sand and mud fractions of the sediment flux;
- b. unravel the relative effects of source-rock lithology, recycling, hydraulic sorting, and chemical weathering on the mineralogical and chemical composition of sand and mud generated in humid subequatorial to dry tropical climate;
- c. make some inferences on sediment yields and erosion patterns in diverse parts of the large basin;
- d. discuss the origin of weathering based on integrated mineralogical, geochemical, and textural evidence

3.2 Study area

3.2.1 Geology

The Zimbabwe Craton represents the northern part of Archean southern Africa (Fig. 3. 2B). A central terrane flanked by two distinct 2.7 Ga greenstone belts includes 3.5-2.95 Ga gneisses non conformably overlain by 2.9-2.8 Ga volcanic rocks and conglomerates or by a SE-ward thickening 3.0-2.7 Ga sedimentary succession. The craton was stabilized between 2.7 and 2.6 Ga and eventually sealed by the Great Dyke swarm at 2575 Ma (Kusky, 1998; Jelsma and Dirks, 2002; Söderlund *et al.*, 2010).

Tectonic activity continued through the Paleoproterozoic, when the Proto-Kalahari Craton formed by the close of the major Orosirian episode of crustal growth, and into the Mesoproterozoic, at the end of which the Kalahari Craton was eventually assembled (Hanson *et al.*, 2006; Jacobs *et al.*, 2008). Orosirian orogens include the Ubendian-Usagaran Belts along the southern margin of the Tanzania Craton, and the Magondi Belt, exposing arc-related volcano-sedimentary and plutonic rocks metamorphosed up to amphibolite facies along the NW margin of the Zimbabwe Craton (Majaule *et al.*, 2001; Master *et al.*, 2010).

The Angola Block far to the west represents instead the southern part of the Congo Craton. It comprises a Central Zone in the east, a Central Eburnean Zone, and the Lubango Zone extending southwards into Namibia, which recorded peak magmatic events at 2.0-1.96, 1.88-1.83 Ga, and 1.80-1.77 Ga (De Carvalho *et al.*, 2000; McCourt *et al.*, 2013; Jelsma *et al.*, 2018).

The next major episode of crustal growth was documented by the formation of the Irumide Belt from Malawi to southern Zambia. The external nappes exposed to the north of the Luangwa Rift include a 2.0-1.9 Ga gneissic basement overlain by quartzite, schist, and minor carbonate deposited around 1.85 Ga (Muva Supergroup). Granitoid suites were emplaced at 1.65-1.55 Ga, 1.36-1.33 Ga, and 1.05-0.95 Ga. Regional metamorphism increasing south-eastwards from greenschist facies to upper amphibolite facies took place at 1.05-1.02 Ga (De Waele *et al.*, 2006, 2009). The high-grade internal zone is exposed north of the Lower Zambezi Valley between the Luangwa and Shire Rivers (Southern Irumide Province; Alessio *et al.*, 2019) and includes the Tete gabbro-anorthosite complex (~1.05 Ga; Westerhof *et al.*, 2008).

The Choma-Kalomo Block in southwestern Zambia is a terrane of uncertain paleogeographic significance. It consists of crystalline basement covered by amphibolite-facies paragneiss and schist yielding zircon grains of Paleoproterozoic age, intruded by two generations of Mesoproterozoic granitoid plutons (1.37 and 1.18 Ga; Bulambo *et al.*, 2006) and documenting a thermal event between 1.02 and 0.98 Ma (Glynn *et al.*, 2017).

The Kalahari Craton of southern Africa was eventually welded to the Congo Craton during the major Neoproterozoic Pan-African orogeny, testified by the Damara-Lufilian-Zambezi Belt

stretching from coastal Namibia and across Botswana and southern Zambia to connect with the Mozambique Belt in the east (Frimmel *et al.*, 2011; Fritz *et al.*, 2013; Goscombe *et al.*, 2020).

The Lufilian Arc consists of Neoproterozoic low- to high-grade metasedimentary and metaigneous rocks hosting Cu-Co-U and Pb-Zn mineralizations (Kampunzu and Cailteux, 1999; John *et al.*, 2004; Eglinger *et al.*, 2016). The Zambezi Belt contains a volcano-sedimentary succession deformed under amphibolite-facies conditions at 0.9-0.8 Ga (Hanson, 2003), whereas eclogite-facies metamorphism dated at 592 Ma constrains the timing of subduction and basin closure (John *et al.*, 2003) with thrust emplacement dated as 550-530 Ma (Hargrove *et al.*, 2003).

The Gondwana supercontinent, assembled during the Pan-African Orogeny, started to be disrupted towards the close of the Paleozoic, when Karoo sediments began to accumulate in several distinct depocenters across southern Africa. Karoo basins include the elongated Gwembe and Luangwa troughs that control the drainage of the Middle Zambezi and Luangwa Rivers (Nugent, 1990). The several km-thick Karoo Supergroup begins with Upper Carboniferous to lowermost Permian diamictite, followed by Permian to Middle Triassic turbidite and coal-bearing fluvio-deltaic strata. Permian sandstones contain andesitic-dacitic volcanic detritus (Johnson, 1991) and interlayered tuffs yielding ages mainly between 270 and 260 Ma (Lanci *et al.*, 2013; McKay *et al.*, 2016). Basin subsidence in the southern retroarc basin was induced by subduction of paleo-Pacific lithosphere, while transtensional stress propagated southwards from the Neotethyan rift in the north (Catuneanu *et al.*, 2005). The upper part of the succession consists of Upper Triassic to Lower Jurassic braidplain sandstone, mudrock, and aeolian sandstone (Johnson *et al.*, 1996). Karoo sedimentation was terminated by flood-basalt eruptions recorded throughout southern Africa around 183 Ma (Svensen *et al.*, 2012; Greber *et al.*, 2020).

In the Early Cretaceous, opening of the Indian Ocean was associated with formation of sedimentary basins (Salman and Abdula, 1995; Ponte *et al.*, 2019) and extensive volcanism in the Mozambique Channel (König and Jokat, 2010). In the Cenozoic, fluvial and lacustrine sediments including basal gravel and mud rock sandstone with calcrete were deposited inland in the Kalahari basin, hosting the largest continuous sand sea on Earth where repeated phases of aeolian deposition took place through the Quaternary (Haddon and McCarthy, 2005; Burrough and Thomas, 2016).

South-westward propagation of the Neogene East African rift (Daly *et al.*, 2019) eventually reached the Kalahari region, where fault-related subsidence in the Okavango Rift is exerting a major control on drainage patterns (McCarthy *et al.*, 2002; Vainer *et al.*, 2021).

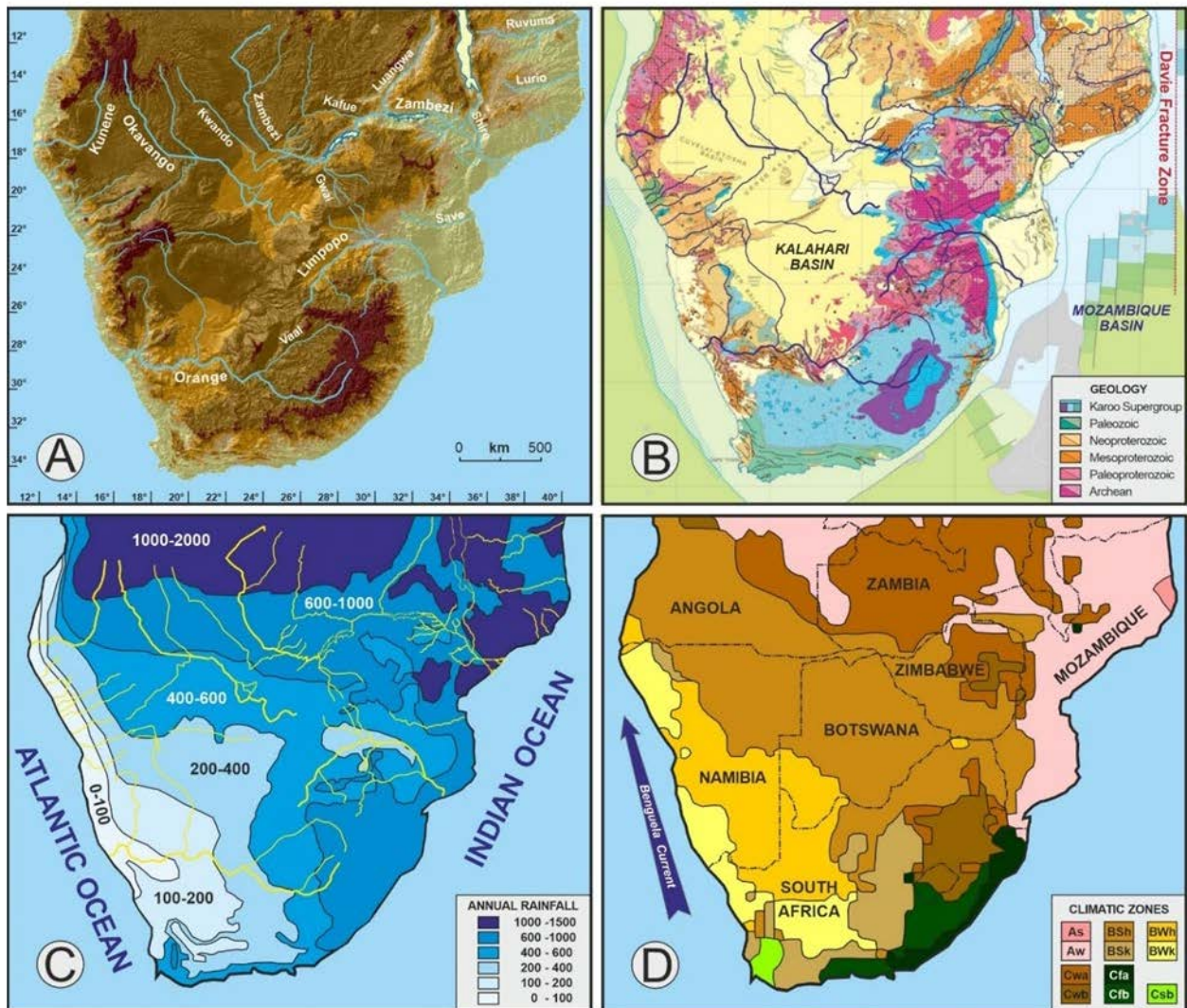


Figure 3.2: Geology and geomorphology of Southern Africa

Where: A) Elevated topography, associated with mantle dynamics and Neogene rifting (Kendall and Lithgow-Bertelloni, 2016). B) Geological map (Thiéblemont et al., 2016). C) Marked precipitation gradients, from the warm Indian Ocean in the east to the cool Atlantic Ocean in the west at subtropical latitudes, and from the dry Kalahari in the south to the humid Congo in the north at subequatorial latitudes. D) Distribution of climatic zones (Köppen-Geiger classification; Kottek et al., 2006): A = equatorial; B = arid; C = warm temperate. Precipitation: W = desert; S = steppe; f = fully humid; s = summer dry; w = winter dry. Temperature: h = hot arid; k = cold arid; a = hot summer; and b = warm summer.

3.2.2 Geomorphology and River Drainage

Climate

Southern Africa, with its largely rural population dependent on rain-fed subsistence agriculture, is particularly vulnerable to climate variability and extreme events. These include severe droughts affecting much of Zambia, Malawi, Zimbabwe, or northern South Africa, alternating with devastating floods such as those periodically striking in Mozambique. Cyclones occur in the wet season, and for the first time in 2019 two cyclones caused floods and destruction in the same year (Siwedza *et al.*, 2021).

Climate variability has a multitude of forcing factors that interact with each other and wax and wane in their importance through time (Reason *et al.*, 2006; Howard and Washington, 2019). Overall, rainfall increases from west to east at subtropical latitudes and from south to north at subequatorial latitudes, the principal sources of humidity being the Indian Ocean in the east and the Atlantic Ocean in the northwest (Figure 3.2).

The African continent divides the tropical high-pressure zone into the Indian Ocean and South Atlantic anticyclones, particularly during the austral summer when heating of the landmass reaches maximum. Moisture derived primarily from air masses moving inland from the warm Indian Ocean is reduced by orographic effects along the eastern escarpment and declines progressively westward resulting in increasing aridity. Descending, divergent air masses occur throughout the year along the west coast, where the temperature inversion is reinforced by the northward-flowing Benguela current and upwelling of cold Antarctic waters offshore. Dominant south-westerly winds are dry, and thus contribute to the marked westward decrease in rainfall across the subcontinent.

A sharp contrast thus exists between humid coastal Mozambique (maximum annual rainfall 1.5 m) and the Kalahari Plateau inland, where quasi-stationary anticyclonic conditions prevail (Figure 3.2C). Mozambique is characterized by tropical climate with a wet season from October to March and a dry season from April to September (average annual rainfall ~0.65 m at Tete).

In subequatorial southern Africa, atmospheric circulation is complex. Moist South Atlantic air moved inland by westerly winds converges with Indian Ocean air along the Congo Air Boundary, frequently associated with development of pressure lows and widespread rains across the Kalahari. Annual rainfall, chiefly associated with the southward shift of the Intertropical Convergence Zone, reaches 1.4 m in Angola during summer (Jury, 2010). In winter, when the Intertropical Convergence Zone and Congo Air Boundary migrate northward, interior southern Africa remains generally dry under the influence of the Indian Ocean anticyclone.

The river system

The Zambezi (length 2575 km, basin area $\sim 1.4 \cdot 10^6 \text{ km}^2$) is the largest river of southern Africa. Sourced in northwesternmost Zambia among low ridges of the Kasai Shield (part of the Congo Craton), the river traverses unconsolidated Kalahari sands in the Barotse floodplain, a 30-50 km-wide wetland flooded for several months by Zambezi waters after the rainy season (peak discharge in April).

The Uppermost Zambezi starts to flow more swiftly as it first encounters basaltic bedrock at Ngonye Falls, and it is next joined by the Kwando River draining the Kalahari Basin in humid Angola. While entering the Okavango Rift, the Kwando (here named Linyanti and next Chobe) deviates sharply eastward along the tectonic depression hosting large swamps and once large paleolakes (Burrough *et al.*, 2009; Moore *et al.*, 2012). The graben continues eastward into the Machili Flats drained by the low-gradient Kasaya and Ngwezi Rivers, eastern Zambezi tributaries draining the Lufilian arc and the Choma-Kalomo Block, respectively.

Downstream of the Kwando confluence, the Upper Zambezi, and its local tributaries – including the Sinde River sourced in the Choma-Kalomo Block – incise into Karoo basaltic lavas and the gradient steepens forming minor rapids upstream of Victoria Falls. Next, after plunging some 100 m into the falls, turbulent Upper Zambezi waters design an astonishing zigzag into steep gorges of black basalt, the result of progressive retreat of the waterfalls during the Quaternary (Derricourt, 1976).

After receiving tributaries draining Karoo lavas overlain by thin Kalahari dune sand (e.g. Masuie and Matetsi), the Zambezi reaches Lake Kariba shortly downstream of the confluence with the Gwai River. Sourced in the Zimbabwe Craton, the low-gradient senile upper course of the Gwai River is incised – as its east-bank tributaries Umguza and Shangani – in Karoo basalt and sedimentary rocks surrounded by Kalahari dune sand (Thomas and Shaw, 1988; Moore *et al.*, 2009). In the youthful lower tract, the Gwai cuts steeply across the Dete-Kamativi Inlier of the Paleoproterozoic Magondi Belt (Glynn *et al.*, 2020) and receives the eastern Tinde tributary mainly draining Pan-African molasse (Goscombe *et al.*, 2020).

The Middle Zambezi between Lakes Kariba and Cahora Bassa flows along a Karoo rift trough formed along the Pan-African (Kuunga) suture zone (Goscombe *et al.*, 2020) and hosting a thick infill of basalt-capped Permian-Triassic sedimentary rocks overlying Ordovician to Devonian siliciclastic strata (Nyambe, 1999). The major tributaries in this tract are the Kafue and the Luangwa, both from Zambia. The Kafue, the longest Zambezi tributary (length 1576 km, basin area $154,200 \text{ km}^2$), is sourced in the Lufilian arc, flows across a 240 km-long swampy flat floodplain, and next drops 550 m into a 60-km-long gorge carved in gneiss and metasedimentary rocks of the West Zambezi Belt to join the Zambezi $\sim 75 \text{ km}$ downstream of Lake Kariba.

The Luangwa (length 770 km, basin area 151,400 km²) is sourced in the Ubendian Belt and flows for most of its course along a Karoo rift trough filled with an 8 km-thick Permian-Triassic sedimentary succession (Banks *et al.*, 1995), separating the external nappes of the Irumide Belt in the north from the high-grade Southern Irumide Province in the south. After cutting across Southern Irumide granulites, the Luangwa joins the Zambezi just upstream of Lake Cahora Bassa.

The Lower Zambezi in Mozambique first receives tributaries from the west (Sangara, Mufa) and north (Luia, Morrunguze) that largely drain high-grade Southern Irumide rocks. The largest tributary is the Shire (chiri = steep banks), the outlet of Lake Malawi, which drains largely garnet-free mafic granulites of the Blantyre domain (southern Malawi-Unango Complex) where middle-lower crust at the southern margin of the Congo Craton underwent high-grade metamorphism at ~920 Ma (Goscombe *et al.*, 2020). From the west, the Mazowe-Luenha River system drains well into the Archean Zimbabwe Craton in the headwaters. Downstream, the two rivers cut across the polymetamorphic Mudzi migmatitic gneisses remobilized during the Pan-African orogeny, and next across the Neoproterozoic Marginal Gneiss. Lowermost-course tributaries include the Sangadze and Zangue Rivers sourced in the Pan-African Umkondo Belt, comprising greenschist facies to lower-amphibolite-facies schists thrust onto the margin of the Zimbabwe Craton and upper-amphibolite-facies to granulite-facies gneisses in the core (Stenian Barue Complex). The northern Minjova tributary largely drains the Moatize-Minjova Basin filled by coal-bearing Permian-Triassic Karoo clastic rocks (Fernandes *et al.*, 2015).

In the lowermost tract, the Zambezi River flows along the Lower Zambezi graben, originated as a failed arm of the Middle Jurassic Mozambique Basin rift (Figure 3.2B; Butt and Gould, 2018). Zambezi sediments have built through time the largest continental shelf along the Indian Ocean coast of Africa (Walford *et al.*, 2005), reaching more than 100 km in width and contributing to a tidal range up to 6.4 m. Large sediment volumes, however, are not deposited in front of the Zambezi mouth but dragged north-eastward by longshore currents (Schulz *et al.*, 2011; van der Lubbe *et al.*, 2014), forming wide beaches as far as Quelimane and beyond (e.g. Praia da Madal; Fig 3.1).

The Zambezi in the Anthropocene

The course of the Zambezi, as that of most big rivers on Earth, has been profoundly modified by man in the last decades. The Kariba and Cahora Bassa Dams built on the mainstem, as well as others built on major tributaries, have substantially altered the hydrological regime of the Zambezi River and its delta, and disrupted the natural sediment-routing system by trapping much if not all the detritus generated upstream (Davies *et al.*, 2000; Beilfuss and dos Santos D., 2001; Calamita *et al.*, 2019). Lake Kariba (length 223 km, area 5200 km², storage capacity 185 km³, completed in 1958) is the world's largest artificial reservoir, whereas Lake Cahora Bassa (length 292 km, area 2700 km², storage capacity 73 km³, completed in 1974) is Africa's fourth largest (Vörösmarty and Moore, 1991).

Since Zambia's independence in 1964, two big dams have been built also on the Kafue River, at Itezhi-Tezhi (“slippery rock”) and in the Kafue Gorge. The Itezhi-Tezhi Dam (reservoir area 370 km², storage capacity 6 km³, completed in 1977) closes the gap through a ridge of ~100-m-high hills where the paleo-Kafue, once flowing southwards towards Lake Makgadikgadi and the Limpopo River, was captured and started to flow eastward as part of the Zambezi drainage (Thomas and Shaw, 1991; Moore and Larkin, 2001). Downstream, the river flows sluggishly in the maze of swampy channels and lagoons of the Kafue Flats and next plunges into the Kafue Gorge, where other dams have been constructed (Upper Kafue Gorge hydropower station: reservoir area 809 km², storage capacity 0.8 km³, operational since 1973) or are under construction (Lower Kafue Gorge hydropower station). Other dams were built (e.g. Nkhula, Tedzani, Kapichira), or are planned, on the Shire River in southern Malawi.

Besides human intervention, the Zambezi sediment-routing system is segmented by natural processes as well, much sediment being retained in large wetlands such as the Barotse floodplain and Chobe swamps on the Uppermost Zambezi, the Kafue Flats, or the Elephant Marsh on the Shire River (Bolton, 1984; Moore *et al.*, 2007).

Sediment Fluxes

Information on sediment loads transported both before and after the closure of the big dams is largely missing throughout the Zambezi drainage basin. In the lack of accurately gauged sediment fluxes, compiled estimates on annual solid transport range widely between 20 and 100 million tons (Hay, 1998), with a median value around 50 million tons (Milliman and Meade, 1983; ESIA, 2011; Milliman and Farnsworth, 2011). These figures correspond to an average annual sediment yield and erosion rate between 6- and 70-tons km⁻² and between 0.003 and 0.03 mm (median values ~ 35 tons km⁻² and ~0.01 mm). Because of low topographic gradient and presence of vast wetlands on the Kalahari Plateau, the annual sediment volume at Victoria Falls was estimated to be only 100,000 m³, whereas nearly half of the sediment flux (22 out of 51 million m³) was generated in the Lower Zambezi catchment (FFEM, 2005; von der Lubbe *et al.*, 2016). After closure of the Kariba and Cahora Bassa Dams, annual sediment supply to the Zambezi Delta may have been reduced to as low as 0.8 million m³, between 1% and 7% of which represented by bedload (Ronco *et al.*, 2010 p.52; ESIA, 2011).

Uncertain by an order of magnitude are also the estimates on sediment accumulation in Lake Kariba (between 7 and 70 million tons according to Bolton, 1984, but only ~4 million tons according to Kunz *et al.*, 2011) and Lake Cahora Bassa (between 20 and 200 million tons according to Bolton, 1984 and ~28.6 million m³ according to Ronco *et al.*, 2010 p.47). In mountain areas, based on sparse data on sediment concentration, annual sediment yields of 40- and 200-tons km⁻² were estimated for the Gwai and Luangwa catchments, corresponding to average erosion rates of 0.016 and 0.08 mm (Bolton, 1984). Similar values were evaluated for minor tributaries in Zambia and Mozambique (200 tons km⁻²) and for the Luangwa and the rest of the Middle Zambezi (170-250 tons km⁻², from sediment volumes of 14.0 and 14.6

million m³ respectively; Ronco *et al.*, 2010 p.47). Very high annual rates of soil loss (up to 2900 tons km⁻²) are reported from the Shire catchment in southern Malawi (Mzuza *et al.*, 2019).

3.3 Methodology

Between 2011 and 2019, seventy-one sediment samples were collected from active sand bars (57), levees (2) and freshly deposited muds (12) of the Zambezi River and its major tributaries from the source in NW Zambia to the delta in Mozambique. Full information on sampling sites is provided in Table 3.A1 and Google Earth™ file Zambezi².kmz.

Table 3.1: Silt and clay mineralogy in the Zambezi catchment, determined by X-ray powder-diffraction

River	BULK SAMPLE (< 32 µm class, wet sieved)								CLAY MINERALS (< 2 µm)				Kao / (Ill+Chl)	
	Qz	KF	Pl	Carb	Amp	Hem	Phyll	total	Sme	Ill	Chl	Kao		total
Uppermost Zambezi	49	15	1	0	0	0	35	100.0	43	21	0	36	100.0	1.7
Ngwezi	33	11	6	0	0	0	50	100.0	76	6	0	18	100.0	3.0
Kwando	89	0	0	4	0	0	7	100.0	70	13	0	17	100.0	1.3
Sinde	14	6	17	0	0	10	53	100.0	87	0	0	13	100.0	∞
Zambezi@Vic.Falls	75	8	2	0	0	0	15	100.0	78	15	0	7	100.0	0.5
Matetsi	7	20	15	4	0	9	45	100.0	93	0	0	7	100.0	∞
Upper Zambezi	41	12	15	0	0	5	27	100.0	54	31	0	15	100.0	0.5
Upper Zambezi	43	11	19	0	0	4	23	100.0	50	33	0	17	100.0	0.5
Unguza	26	8	7	3	0	0	56	100.0	87	4	5	4	100.0	0.4
Upper Gwai	20	4	4	3	0	0	69	100.0	77	5	5	13	100.0	1.3
Tinde	34	24	5	0	0	0	37	100.0	25	40	9	26	100.0	0.5
Kafue	9	7	11	2	2	1	69	100.0	27	54	0.5	19	100.0	0.3
Middle Zambezi	10	7	11	6	1	0.2	64	100.0	60	27	0	12	100.0	0.4
Zambezi@Tete	19	5	19	0	2	0	54	100.0	25	37	0	38	100.0	1.0
Sangadze	12	8	10	3	0.1	0	67	100.0	96	3	0	1	100.0	0.4
Shire	14	7	16	0	2	0	61	100.0	9	49	0	42	100.0	0.9
Lower Zambezi	17	14	20	0	0	0	49	100.0	52	35	0	12	100.0	0.4

Where: Qz = quartz; KF = K-feldspar; Pl = plagioclase; Carb = carbonate; Amp = amphibole; Hem= hematite; Phyll = phyllosilicate; Sme = smectite; Ill= mica/illite; Chl = chlorite (including vermiculite); Kao = kaolinite.

3.3.1 Silt and Clay Mineralogy

The mineralogy of six mud samples from the Middle and Lower Zambezi mainstem and some of its tributaries (Kafue, Sangadze, Shire) was determined on both < 32 µm and < 2 µm fractions by X-ray powder-diffraction (XRD) using an AERIS equipment (PanAlytical) with a Cu tube, at 15 kV, 40 mA. The < 32 µm fraction was separated by wet sieving and diffractograms were performed on randomly oriented powder in the range 2-60° (2θ). The < 2 µm fraction, separated by centrifuging according to Stokes' law, was analysed on oriented aggregates after air-drying (2-30°2θ) and solvation with ethylene-glycol and heating at 550°C (2-15°2θ). Mineral proportions were evaluated semi-quantitatively using diagnostic XRD peak areas (Moore and Reynolds, 1997; Kahle *et al.*, 2002). Further technical information is provided in Dinis *et al.*

(2020). XRD data previously obtained on the < 32 µm fraction of mud samples collected from the upper Zambezi catchment and main tributaries including the Kwando and the Gwai (Garzanti *et al.*, 2014a; Setti *et al.*, 2014) were also considered. The mineralogical dataset is provided in Table 3.2.

Table 3.2: Sand and mud geochemistry in the Zambezi catchment

River	SiO ₂	Al ₂ O ₃	Fe ₂ O ₃	MgO	CaO	Na ₂ O	K ₂ O	TiO ₂	P ₂ O ₅	MnO	LOI	Rb	Sr	Ba	Sc	Y	Th	Zr	Hf	V	Nb	Cr	Ni	CIA*	α ^{Mg}	α ^{Ca}	α ^{Na}	α ^K	α ^{Rb}	α ^{Sr}	α ^{Ba}
WEATHERING INDICES																															
SAND (63-2000 µm)	wt%	wt%	wt%	wt%	wt%	wt%	wt%	wt%	wt%	wt%	wt%	ppm	ppm	ppm	ppm	ppm	ppm	ppm	ppm	ppm	ppm	ppm	ppm	ppm	ppm	ppm	ppm	ppm	ppm	ppm	
Uppermost Zambezi	98.5	0.4	0.2	0.0	0.0	0.0	0.1	0.1	0.02	<0.01	0.8	2	3	29	<1	2	0.8	81	2	14	1	<14	<20	77	1.8	3.0	4.1	1.2	1.0	3.1	0.5
Kasaya	99.2	0.9	0.1	0.0	0.1	0.1	0.4	0.1	<0.01	<0.01	0.9	11	18	124	<1	4	2	128	3	<8	2	<14	<20	55	4.5	2.5	2.1	0.4	0.5	1.1	0.3
Ngwezi	93.4	3.2	0.4	0.0	0.5	0.4	1.7	0.0	<0.01	0.03	0.5	47	50	419	<1	5	1	38	1	11	2	14	<20	49	12.3	1.8	1.9	0.4	0.4	1.4	0.3
Kwando	99.3	0.2	<0.04	<0.01	<0.01	<0.01	<0.01	0.0	0.01	<0.01	0.5	1	2	21	<1	1	0.4	62	2	<8	2	<14	<20	>89	>2.3	>4.4	>4.1	>3.6	1.4	2.1	0.3
Chobe	98.0	0.3	0.9	0.0	0.0	<0.01	0.0	0.1	<0.01	<0.01	0.7	2	4	29	<1	2	1	114	3	15	2	<14	<20	78	2.1	3.4	n.d.	1.4	0.9	1.6	0.4
Upper Zambezi	98.9	0.3	0.1	0.0	0.0	0.0	0.1	0.1	<0.01	<0.01	0.9	2	4	31	<1	2	1	232	6	<8	2	<14	<20	75	2.5	4.2	3.9	1.1	1.1	1.9	0.4
Sinde	94.8	1.3	1.6	0.3	0.5	0.2	0.2	0.4	0.02	0.02	0.9	3	51	58	2	4	1	68	2	57	2	27	<20	47	0.7	0.6	1.5	1.6	2.5	0.5	0.8
Zambezi up. Vic. Falls	98.0	0.6	0.4	0.1	0.1	0.1	0.1	0.2	0.03	<0.01	0.6	3	11	52	<1	2	1	73	2	21	3	14	<20	63	1.7	1.4	2.1	1.0	1.2	1.1	0.4
Zambezi rapid #9	99.2	0.8	0.3	0.1	0.1	0.1	0.2	0.2	<0.01	<0.01	0.8	5	18	81	<1	2	1	62	2	14	3	<14	<20	58	1.9	1.6	2.0	0.8	1.0	1.1	0.4
Zambezi rapid #10	99.4	0.3	0.3	0.1	0.1	0.1	0.1	0.1	<0.01	<0.01	1.0	2	7	157	<1	1	1	31	1	11	2	21	<20	50	0.7	0.7	1.5	1.3	1.2	1.0	0.1
Maswie	61.8	8.3	12.9	3.1	4.9	1.5	0.9	2.8	0.19	0.15	2.4	18	268	295	22	23	2	168	4	414	10	96	78	41	0.4	0.4	1.3	1.9	2.9	0.7	1.1
Upper Zambezi	99.7	0.4	0.4	0.1	0.2	0.1	0.1	0.1	<0.01	<0.01	0.8	1	13	25	<1	2	0	37	1	16	1	<14	<20	47	0.6	0.6	1.4	1.5	1.8	0.6	0.6
Matetsi	63.1	8.4	11.7	3.1	5.0	1.7	0.8	2.8	0.23	0.14	2.9	16	365	296	20	22	2	182	5	356	13	109	70	41	0.4	0.4	1.2	2.0	3.4	0.5	1.1
Zambezi up. Kariba	89.7	3.9	2.0	0.6	1.1	0.8	0.9	0.5	0.05	0.02	0.5	24	85	235	4	7	3	65	2	57	2	27	<20	49	1.1	0.9	1.2	0.9	1.0	1.0	0.6
Umguza	85.4	5.4	2.0	0.4	3.2	1.1	1.6	0.2	0.03	0.07	3.2	52	186	476	3	12	2	57	2	51	3	48	24	37	1.9	0.4	1.2	0.7	0.7	0.6	0.4
Lower Gwai	88.3	7.1	0.9	0.2	0.6	1.3	2.6	0.1	0.05	0.02	0.9	69	87	484	2	11	4	72	2	15	2	27	<20	54	6.2	2.9	1.4	0.6	0.7	1.8	0.5
Kafue (FS)	83.0	6.2	3.5	1.0	1.2	1.0	1.7	0.9	0.10	0.04	1.1	58	80	325	7	18	10	334	9	61	16	68	<20	53	0.9	1.5	1.5	0.8	0.7	1.8	0.7
Kafue (VFS)	81.1	6.5	4.4	1.0	1.5	1.2	1.6	1.3	0.13	0.05	1.0	52	92	316	8	28	16	596	16	84	24	68	<20	52	1.0	1.2	1.4	0.9	0.9	1.6	0.7
Middle Zambezi	80.6	8.0	3.3	1.1	1.3	1.5	2.3	0.8	0.11	0.04	0.9	74	122	415	7	18	8	294	8	58	15	55	<20	53	1.1	1.7	1.4	0.8	0.7	1.5	0.7
Luangwa	89.9	4.7	1.2	0.1	0.3	0.6	2.4	0.2	0.05	0.02	0.3	59	107	620	1	7	3	63	2	18	5	14	<20	54	0.7	3.9	1.9	0.4	0.5	1.0	0.3
Mufa	71.3	11.8	3.9	1.8	3.7	2.4	2.9	0.8	0.18	0.06	0.9	76	315	626	10	18	9	459	12	78	11	109	27	47	0.9	0.9	1.3	0.9	1.0	0.9	0.7
L.Zambezi @ Tete	68.2	14.0	2.1	0.9	3.2	3.2	2.8	0.5	0.16	0.04	4.8	70	313	695	6	15	4	125	3	39	5	68	23	50	2.2	1.2	1.1	1.1	1.4	1.0	0.7
Morunguze	52.4	12.5	15.1	3.9	5.5	2.4	1.5	5.5	0.08	0.17	0.7	27	285	424	26	15	2	181	4	471	7	281	50	45	0.5	0.6	1.4	1.8	3.2	1.0	1.1
Luenha	74.5	10.7	5.1	0.8	2.2	2.4	2.8	1.4	0.08	0.08	-0.3	74	168	552	8	21	32	348	9	89	25	55	<20	50	1.9	1.3	1.1	0.9	1.0	1.5	0.7
Mazowe	78.7	10.2	2.2	0.6	1.7	2.2	3.3	0.4	0.07	0.04	0.5	76	143	560	5	10	4	130	3	39	9	51	<20	50	2.7	1.7	1.2	0.7	0.9	1.6	0.7
Sangadze	82.1	8.5	1.5	0.2	0.9	1.3	4.2	0.5	0.07	0.04	0.6	103	237	1093	3	10	6	212	5	24	10	27	<20	51	8.2	2.7	1.7	0.4	0.6	0.8	0.3
Shire	68.3	14.7	3.8	1.3	3.9	3.7	2.1	0.8	0.20	0.06	0.9	35	585	995	10	14	2	268	7	78	11	55	21	50	1.6	1.0	1.0	1.5	2.9	0.6	0.5
Lower Zambezi (FS)	80.2	9.3	2.1	0.6	1.8	2.0	2.6	0.5	0.10	0.03	0.7	67	199	621	5	10	4	165	5	40	8	55	<20	51	2.3	1.4	1.2	0.8	0.9	1.1	0.5
Lower Zambezi (VFS)	78.1	10.4	2.3	0.7	2.1	2.3	2.6	0.6	0.11	0.04	0.7	69	200	616	6	15	6	153	4	41	9	68	<20	51	2.1	1.4	1.2	0.9	1.0	1.2	0.6
MUD (<32 µm)																															
Uppermost Zambezi	55.4	15.0	7.0	0.7	1.1	0.2	1.0	0.9	0.13	0.08	18	53	54	301	17	34	11	246	8	134	15	89	34	83	2.9	3.7	21.4	3.3	1.9	6.4	1.8
Kasaya	53.5	16.1	5.8	0.8	1.8	0.3	1.7	1.0	0.41	0.04	n.d.	147	84	459	16	37	22	372	9	122	19	109	43	78	3.0	2.5	14.2	2.1	0.7	4.4	1.3
Ngwezi	51.1	18.6	8.5	1.5	1.6	0.6	2.1	1.1	0.08	0.12	15	163	101	555	24	41	18	232	6	157	17	144	55	76	1.8	3.3	8.2	1.9	0.8	4.2	1.2
Kwando	43.3	5.9	3.1	3.3	10.6	0.1	0.5	0.4	0.08	0.21	30	44	339	707	6	14	6	170	5	82	8	55	34	23	0.3	0.2	21.7	2.9	0.9	0.4	0.3
Sinde	45.5	14.6	14.2	2.0	3.0	1.0	0.9	3.5	0.22	0.18	15	26	194	362	32	40	4	321	10	348	17	123	81	66	1.1	1.4	3.7	3.4	3.8	1.7	1.5
Zambezi up. V. Falls	54.0	10.6	7.3	1.4	2.7	0.6	0.8	1.8	0.13	0.08	20	37	125	251	18	32	10	623	19	171	19	96	45	62	1.1	1.1	4.6	3.1	1.9	2.0	1.5
Matetsi	44.4	14.2	12.2	3.7	6.2	1.7	0.9	2.0	0.39	0.17	14	22	291	332	31	33	3	201	6	259	11	109	74	50	0.6	0.6	2.2	3.3	4.4	1.1	1.5
Zambezi up. Kariba	50.7	12.7	10.1	2.1	3.1	0.7	0.9	1.5	0.17	0.22	18	51	137	374	21	33	9	274	8	211	15	103	55	63	0.9	1.1	4.6	3.1	1.7	2.1	1.2
Zambezi up. Kariba	51.4	10.4	10.3	2.6	3.8	0.8	0.8	2.5	0.18	0.16	17	39	134	262	23	39	12	627	18	258	21	130	64	55	0.6	0.8	3.3	2.8	1.8	1.8	1.4
Umguza	51.0	15.0	8.8	2.0	3.0	0.6	1.2	1.4	0.21	0.10	16	55	147	303	22	25	6	175	4	196	10	137	77	67	1.1	1.4	6.4	2.8	1.9	2.4	1.8
Upper Gwai	48.6	16.3	8.9	1.7	2.3	0.4	1.5	1.2	0.20	0.22	18	75	125	410	22	30	10	200	6	174	13	137	70								

Classic multi-element chemical indices used to estimate weathering and calculated using molecular proportions of mobile alkali and alkaline-earth metals include the CIA (Chemical Index of Alteration; Nesbitt and Young, 1982) and the WIP (Weathering Index; Parker, 1970), although the latter merely measures the amount of a set of mobile elements that decreases rapidly wherever quartz is added to the sediment, making it an index of quartz recycling more than an index of weathering. Weathering intensity and other controls on geochemical composition are best detangled and separately assessed if mobile elements (e.g. Mg, Ca, Na, K, Sr, and Ba) are considered one by one. This can be done by using $\alpha^{Al}E$ values, defined as $(Al/E)_{\text{sample}}/(Al/E)_{\text{standard}}$ (Garzanti *et al.*, 2013a, 2013b), which compare the concentration of any mobile element E with reference to non-mobile Al in our samples versus an appropriately selected standard composition (e.g. the UCC, Upper Continental Crust standard of Taylor and McLennan, 1995; Rudnick and Gao, 2003). Aluminium, hosted in a wide range of rock-forming minerals with diverse densities, shapes, and sizes including feldspars (concentrated in sand) and phyllosilicates (concentrated in mud), is used as a reference for all elements rather than Ti, Nd, Sm, or Th (Gaillard *et al.*, 1999), which are hosted preferentially in ultradense minerals and thus may reach strongly anomalous concentrations because of hydrodynamic processes. Geochemical data are summarized in Table 3.2.

3.3.3 Isotope Geochemistry

Sixteen samples from the middle and lower Zambezi catchment were treated using a sequential leaching procedure for removal of Fe-oxide phases and organic matter (Bayon *et al.*, 2002). Before digestion by alkaline fusion, (fourteen 63-2000 μm fractions), or HNO_3 -HF mixture (seven < 32 μm fractions, nine 32-63 μm fractions, and two bulk samples) the resulting residual fraction was cleaned from fine silt and clay particles (<15 μm) by low-speed centrifugation (200 rpm). Following Bayon *et al.* (2009), the concentrations of Ba, Y, Zr, Hf, and light and heavy rare earth elements (LREE and HREE) were determined at the Pôle Spectrométrie Océan (PSO) with a Thermo Scientific Element XR sector field ICP-MS, yielding uncertainties better than 10%.

Neodymium isotopes were measured at PSO using a Thermo Scientific Neptune multi-collector ICP-MS, after Nd purification by conventional ion chromatography. Repeated analyses of a JNdi-1 standard solution gave $^{143}\text{Nd}/^{144}\text{Nd}$ of 0.512114 ± 0.000005 (2σ , $n=10$), in full agreement with the recommended value of 0.512115 (Tanaka *et al.*, 2000) and corresponding to an external reproducibility of ca. $\pm 0.10 \text{ } \epsilon$ (2σ). Epsilon $\epsilon_{\text{Nd}(0)}$ values were calculated using $^{143}\text{Nd}/^{144}\text{Nd} = 0.512630$ (Bouvier *et al.*, 2008). Neodymium depleted mantle model ages (TNd,DM) were calculated following the approach described in DePaolo (1981), using measured Sm and Nd concentrations ($^{147}\text{Sm}/^{144}\text{Nd} = \text{Sm}/\text{Nd} \cdot 0.6049$) and present-day $^{143}\text{Nd}/^{144}\text{Nd}$ (0.512630) and $^{147}\text{Sm}/^{144}\text{Nd}$ (0.1960) chondritic values (Bouvier *et al.*, 2008). Isotope data, including results previously obtained on the upper Zambezi catchment (Garzanti *et al.*, 2014a), are summarized in Table 3.3.

Table 3.3: Neodymium isotope values and Sm-Nd model ages for cohesive mud (> 32 μm), frictional silt (32-63 μm), and sand (63-2000 μm) fractions of Zambezi sediments (FS= fine sand; VFS = very fine sand)

River	ϵ_{Nd}			t_{DM} (Ma)		
	<32 μm	32-63 μm	63-2000 μm	<32 μm	32-63 μm	63-2000 μm
Uppermost Zambezi	-15.5	n.d.	n.d.	2162	n.d.	n.d.
Kasaya	-14.0	n.d.	n.d.	2006	n.d.	n.d.
Ngwezi	-15.6	n.d.	n.d.	2128	n.d.	n.d.
Kwando	-17.3	n.d.	n.d.	2320	n.d.	n.d.
Sinde	-5.3	n.d.	n.d.	1608	n.d.	n.d.
Zambezi@Vic.Falls	-12.5	n.d.	n.d.	2056	n.d.	n.d.
Matetsi	-4.1	n.d.	n.d.	1454	n.d.	n.d.
Upper Zambezi	-12.0	n.d.	n.d.	2010	n.d.	n.d.
Upper Zambezi	-12.5	n.d.	n.d.	2092	n.d.	n.d.
Unguza	-14.7	n.d.	n.d.	2177	n.d.	n.d.
Upper Gwai	-11.6	n.d.	n.d.	1872	n.d.	n.d.
Tinde	-14.4	n.d.	n.d.	1953	n.d.	n.d.
Gwai	n.d.	n.d.	-24.6	n.d.	n.d.	2690
Kafue (FS)	n.d.	-16.5	-17.7	n.d.	2029	2107
Kafue (VFS)	-14.8	-16.4	-15.0	1935	1976	1762
Middle Zambezi	-13.8	-16.2	-14.5	1925	2084	2106
Luangwa	n.d.	-20.1	-16.5	n.d.	2244	2155
Mufa	n.d.	n.d.	-8.8	n.d.	n.d.	2195
L.Zambezi @Tete	-7.8	-7.7	-10.0	1552	1864	1735
Morrunguze	n.d.	n.d.	-1.9	n.d.	n.d.	1162
Mazowe	n.d.	n.d.	-18.2	n.d.	n.d.	2781
Luenha	n.d.	n.d.	-19.4	n.d.	n.d.	2504
Sangadze	-15.3	-21.1	-19.5	1887	2028	2094
Shire	-7.3	-8.0	-7.7	1279	1333	1455
Lower Zambezi (FS)	-16.0	-19.3	-14.8	1995	2221	2188
Lower Zambezi (VFS)	-14.3	-17.4	-14.5	1990	2242	2242
Quelimane (estuary)	n.d.	n.d.	-18.3	n.d.	n.d.	2319
Quelimane (beach)	n.d.	n.d.	-12.7	n.d.	n.d.	1968

*Data for Uppermost and Upper Zambezi muds after Garzanti et al. (2014a)

3.3.4 Detrital-Zircon Geochronology

Detrital zircons were identified by Automated Phase Mapping (Vermeesch *et al.*, 2017) with a Renishaw inViaTM Raman microscope on the heavy-mineral separates of 18 samples, concentrated with standard magnetic techniques and directly mounted in epoxy resin without any operator selection by hand picking. U-Pb zircon ages were determined at the London Geochronology Centre using an Agilent 7700x LA-ICP-MS (laser ablation-inductively

coupled plasma-mass spectrometry) system, employing a NewWave NWR193 Excimer Laser operated at 10 Hz with a 25 μm spot size and $\sim 2.5 \text{ J/cm}^2$ fluence. No cathodo-luminescence imaging was done, and the laser spot was always placed “blindly” in the middle of zircon grains in order to treat all samples equally and avoid bias in intersample comparison (“blind-dating approach” as discussed in Garzanti *et al.*, 2018). No common Pb correction was applied. The mass spectrometer data were converted to isotopic ratios using GLITTER 4.4.2 software (Griffin *et al.*, 2008), employing Plešovice zircon (Sláma *et al.*, 2008) as a primary age standard and GJ-1 (Jackson *et al.*, 2004) as a secondary age standard. A NIST SRM612 glass was used as a compositional standard for the U and Th concentrations. GLITTER files were post-processed in R using IsoplotR 2.5 (Vermeesch, 2018). We used $^{206}\text{Pb}/^{238}\text{U}$ and $^{207}\text{Pb}/^{206}\text{Pb}$ ages for zircons younger and older than 1100 Ma, respectively; ages with $> +5/-15\%$ discordance was discarded. The complete geochronological dataset, comprising 1913 concordant ages (> 100 ages on 10 samples) – calculated as the maximum likelihood intersection between the concordia line and the error ellipse of $^{207}\text{Pb}/^{235}\text{U}$ and $^{206}\text{Pb}/^{238}\text{U}$ ages (Ludwig, 1998).

3.4 Results and discussion

This section briefly summarizes petrographic and heavy-mineral data, and illustrates original data on clay mineralogy (Figure 3.3), elemental geochemistry for sand and mud samples (Figure 3.4), REE geochemistry (Figure 3.5), isotope geochemistry (Figure 3.6), and detrital-zircon geochronology data (Figure 3.7) from the whole Zambezi sedimentary system.

Five main zircon-age ranges recur among the analysed samples, corresponding to main thermal events of crustal growth across southern Africa (Hanson, 2003; Dirks *et al.*, 2009; Andersen *et al.*, 2016, 2018): A) Triassic-Permian (“Karoo”; 0.2-0.3 Ga); B) Ordovician-Cryogenian (“Pan-African”; 0.45-0.65 Ga); C) Stenian (“Irumide”; 1.0-1.1 Ga); D) Ectasian (“Kibaran”; 1.2-1.4 Ga); E) Orosirian (“Eburnean”; 1.8-2.05 Ga); and, F) Neoproterozoic (“Limpopo”; 2.5-2.8 Ga). The youngest ages were obtained from single zircon grains in Gwai (138 Ma), Shire (126 Ma), and lowermost Zambezi (116 Ma) sands.

3.4.1 The Uppermost Zambezi

Uppermost Zambezi and Kwando River sands are pure quartzose. Sand of left Zambian tributaries range from quartz-rich feldspatho-quartzose with K-feldspar $>$ plagioclase and muscovite (Kabombo, Ngwezi) to pure quartzose with K-feldspar \gg plagioclase (Kasaya). Smectite prevails over kaolinite and mica/illite in mud of the Zambezi mainstem and occurs in even higher proportions in Ngwezi and Kwando muds (Figure 3.3). Chlorite or vermiculite were not detected (Table 3.1).

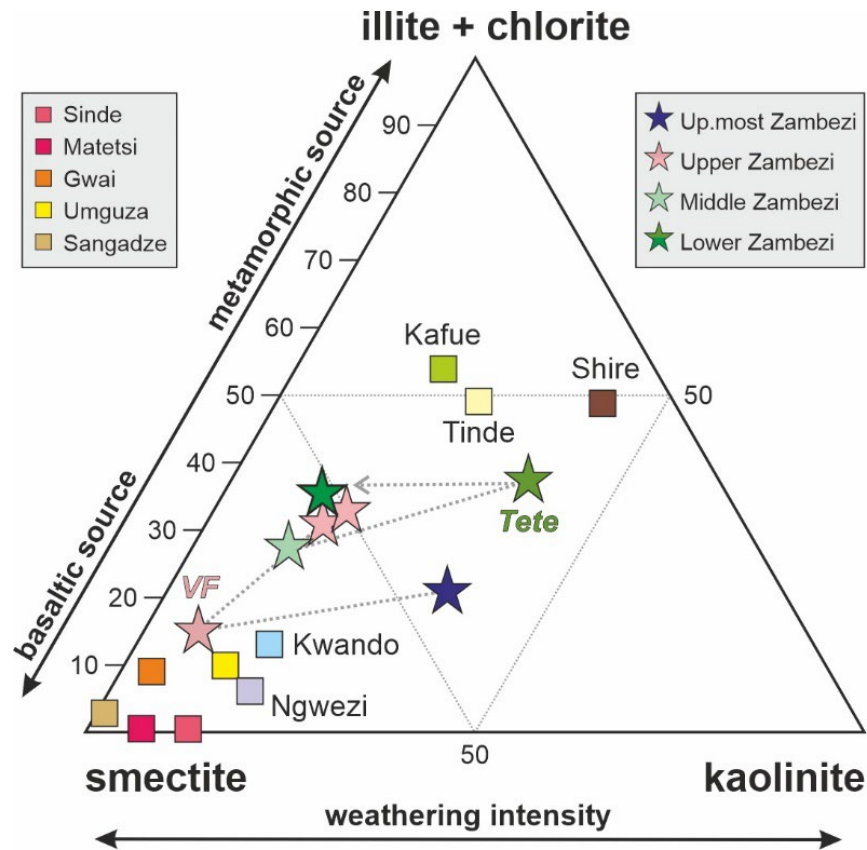


Figure 3.3: Composition of the Zambezi river sands

Clay mineralogy depends not only on present and past weathering intensity but also on source-rock lithology. Compositional trends downstream the Zambezi are thus erratic (grey dotted arrow). Kaolinite is common in both Uppermost and Lower Zambezi catchments (Tete sample and Shire mud, where it is largely reworked from Cretaceous to Cenozoic peneplains). Smectite is derived from Karoo basalts both upstream (Sinde) and downstream (Matetsi) of Victoria Falls (VF), but also produced in low-relief landscapes of the Kalahari Plateau drained by the Kwando, Ngwezi, and Gwai Rivers and of Mozambican lowlands drained by the Sangadze River. Illite is most common in the Kafue and Tinde muds derived from metasedimentary and siliciclastic rocks of the Irumide and Pan-African belts.

SiO₂ is overwhelming (> 98%) in Zambezi and Kwando sands (Figure 3.4A). The concentration of all other elements is consequently very low, including Zr (62-114 ppm) and REE (Figure 3.5). The CIA is ≥ 77 , the WIP < 1, $\alpha^{Al}Ca \geq 3$, and $\alpha^{Al}Na \sim 4$. Ngwezi sand is less SiO₂-rich, with consequently higher Al, Ca, Na, K, Rb, Sr, and Ba but very low Mg (Figure 3.4B). Kasaya sand has intermediate composition. Chemical indices are CIA 83, $\alpha^{Al}Ca$ 4, $\alpha^{Al}Na$ 21 for Zambezi mud and CIA 77 ± 1 , $\alpha^{Al}Ca$ 2.9 ± 0.5 , and $\alpha^{Al}Na$ 11 ± 4 for Kasaya and Ngwezi muds. Kwando mud has anomalously low $\alpha^{Al}Ca$, $\alpha^{Al}Mg$, $\alpha^{Al}Sr$, and $\alpha^{Al}Ba$ (Table 3.2). The

general observed order of element mobility is $Na \approx Ca > Sr$ for sand and $Na \gg Sr > Ca > Mg \approx K$ for mud.

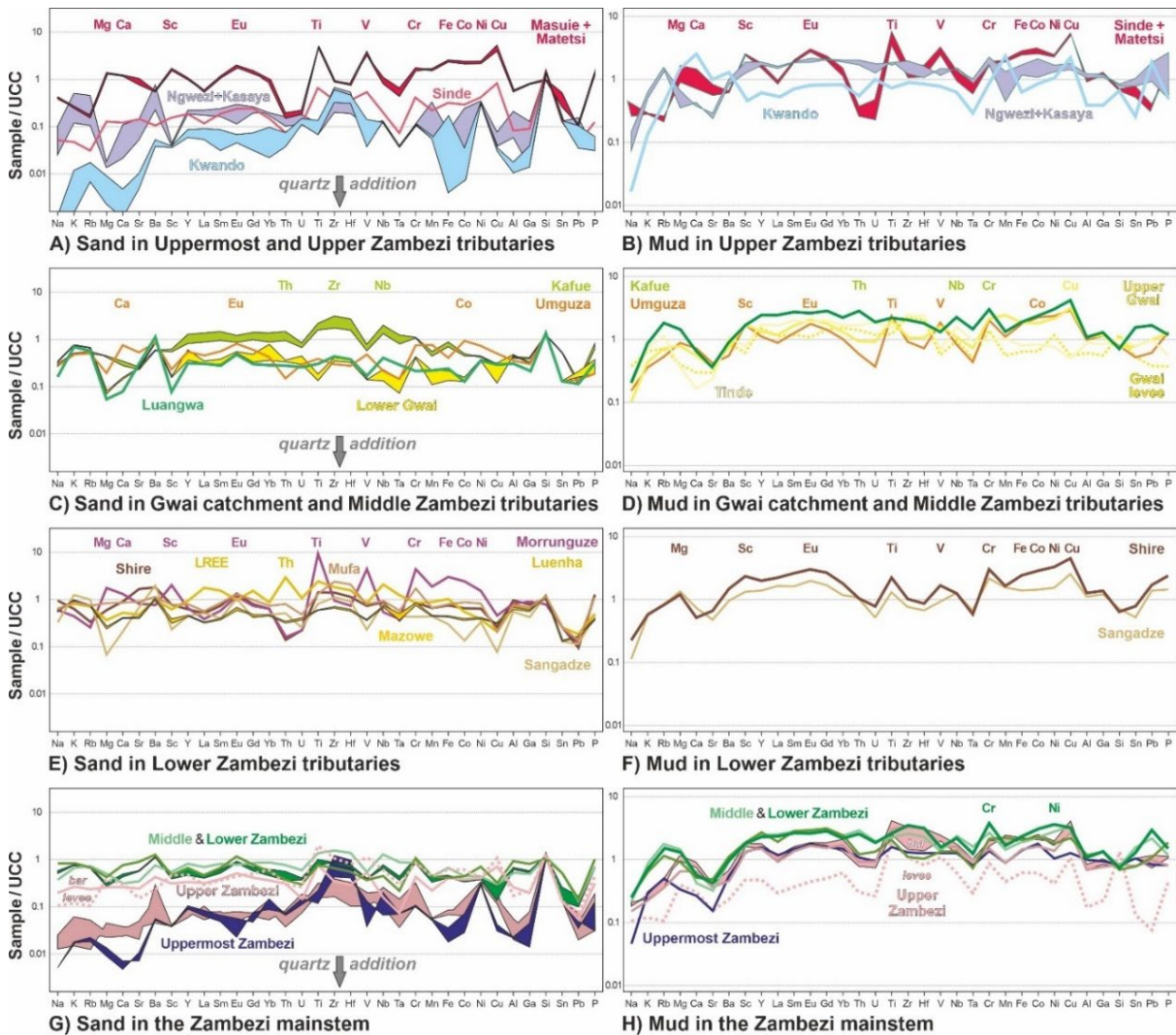


Figure 3.4: Sand and mud geochemistry (in UCC-normalized diagrams elements are arranged following the periodic table group by group)

Where: A & B = In Zambezi headwaters, extensive quartz addition by recycling is reflected by low concentration of elements other than Si in sand. Supply from Karoo basalts leads to marked increase in ferromagnesian metals and lack of Eu anomaly. High Ca, Sr, Mg, and Ba in Kwando mud reflect reworking of calcrete soils. C & D = Kafue samples are slightly enriched in elements hosted in ultra-dense minerals. Umguza and Upper Gwai sediments include minor detritus from Karoo basalts. Luangwa sand is partly recycled from Karoo sediments. E & F = Most Lower Zambezi tributaries carry sediments undepleted relative to the UCC. In Morrunguze sediments, high ferromagnesian metals and lack of Eu anomaly reflect supply from the Tete gabbro-anorthosite complex. High LREE and Th in Luenha sand suggests presence of monazite. G & H = Quartz addition by recycling decreases downstream the

Zambezi mainstem. Lower Zambezi sand is only moderately depleted, and mud is undepleted relative to the UCC.

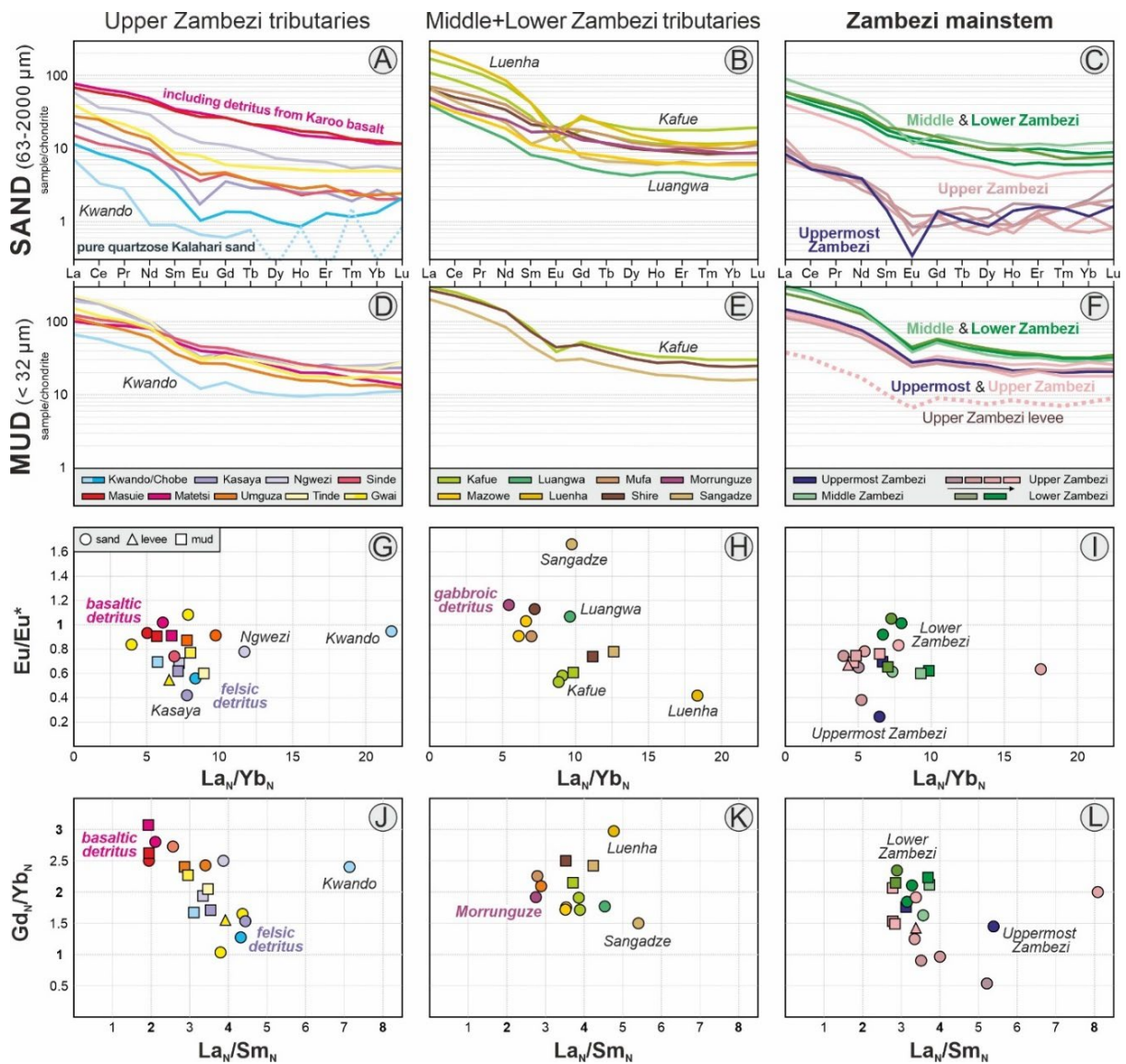


Figure 3.5: Rare earth elemental geochemistry

Where: A, B, & C = Chondrite-normalized REE patterns for sand. D, E, & F = Chondrite-normalized REE patterns for mud. G, H, & I = Steepness of REE pattern versus europium anomaly. J, K, & L = LREE versus HREE fractionation.

Mafic detritus, conspicuous in Matetsi, Masuie and Morrunguze sediments and present in Sinde, Umguza, and Uppert Zambezi sediments, is characterized by higher REE concentration, less inclined REE patterns, null Eu anomaly, low LREE fractionation, and high HREE fractionation. Pure quartzose sand of the Kwando River has poorly defined HREE pattern because of very low REE concentration. Increasing basaltic detritus along the Upper Zambezi

is reflected in increasing REE concentration and decreasing LREE fractionation and Eu anomaly. Absence of Eu anomaly in most Lower Zambezi sands largely reflect feldspar abundance. Steepest REE patterns with strongly negative Eu anomaly in Luenha sand indicates presence of monazite (as confirmed by high Th; Table 3.2), whereas strongly positive Eu anomaly in Sangadze sand reflects abundant feldspar with fewer heavy minerals.

In mud samples, REE patterns normalized to CI carbonaceous chondrites (Barrat *et al.*, 2012) display classical shapes with higher LREE than HREE fractionation and moderately negative Eu anomaly. Pure quartzose sands display slightly stronger LREE enrichment, negative Ce anomaly, more strongly negative Eu anomaly, and low but poorly defined HREE fractionation because of very low concentration too close to analytical detection limit for REE with odd atomic numbers (i.e. Tb, Ho, Tm, and Lu). The ϵ_{Nd} values vary between -14 for Kasaya mud and -17 for Kwando mud (-15.5 for Uppermost Zambezi mud; Table 3.3).

Zircon grains in Uppermost Zambezi, Kwando, and Kasaya sands display polymodal spectra, with mostly Cambrian to Stenian ages including a main Irumide (~1050 Ma) and subordinate Pan-African (500-630 Ma) peaks (Figure 3.7). Orosirian ages are common in Uppermost Zambezi and Kwando sands and minor in Kasaya sand. Kwando sand is distinguished by a Neoproterozoic age cluster, whereas Kasaya sand yielded several zircon grains with Devonian to Triassic ages.

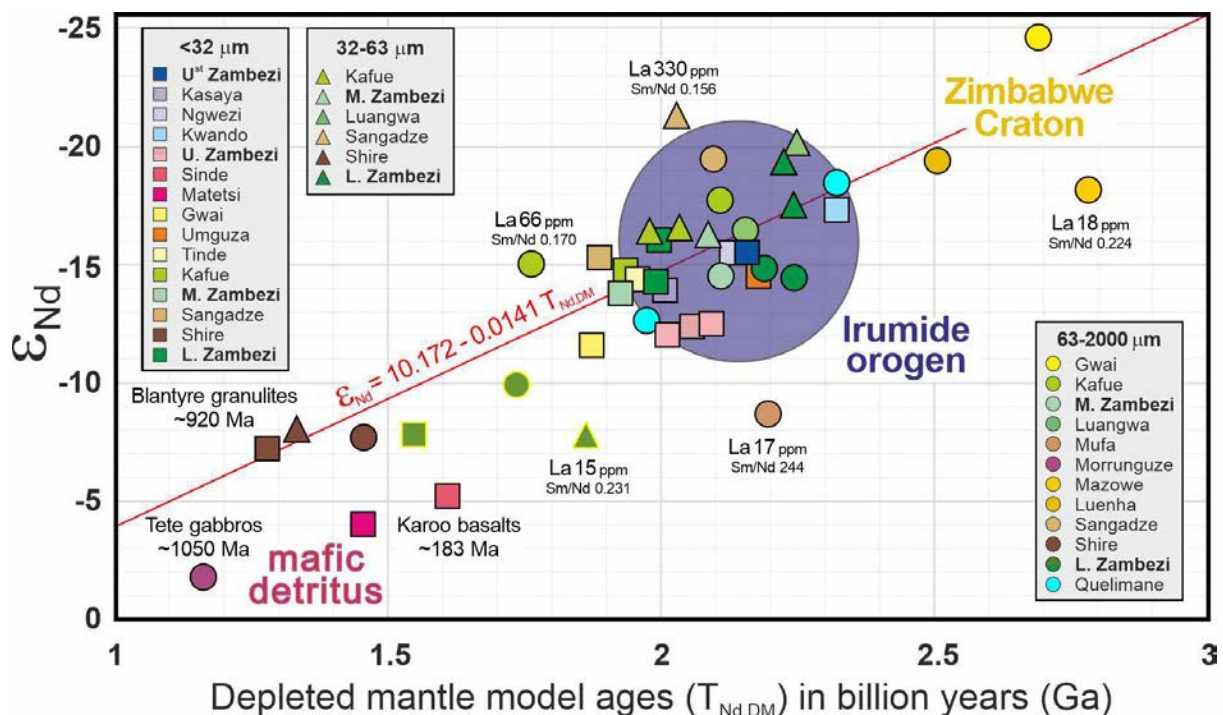


Figure 3.6: Relationship between $\epsilon_{Nd(0)}$ values and depleted mantle model ages ($T_{Nd,DM}$) for the Zambezi mainstem and tributaries

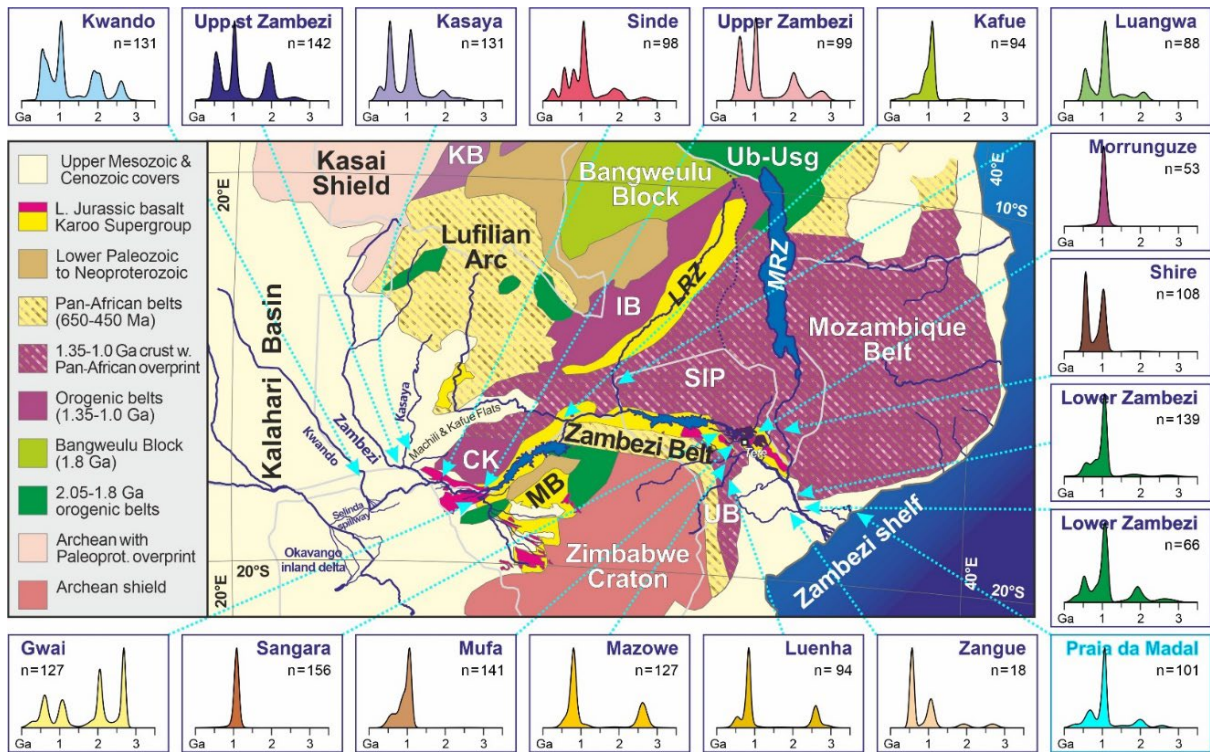


Figure 3.7: U-Pb age spectra of detrital zircons (age vs. frequencies plotted as Kernel Density Estimates using the provenance package of Vermeesch et al., 2016)

Archean ages are most common in sand of the Gwai, Mazowe and Luenha Rivers sourced in the Zimbabwe Craton. Orosirian ages are most common in sand of the Kwando and Uppermost Zambezi Rivers recycling Kalahari dunes and of the Gwai River draining the Paleoproterozoic Magondi Belt. Irumide ages are widespread, overwhelming in Sangara and Morrunguze sands and dominant in Lower Zambezi sands. Pan-African zircons are also widespread, and locally prevalent (Shire and Zangue sands). Geological domains after Hanson, 2003 and Thiéblemont et al., 2016). CK = Choma-Kalomo block; IB = Irumide Belt; KB = Kibaran Belt; LRZ = Luangwa Rift Zone, activated in the Permian and reactivated in the Neogene; MB = Magondi Belt; MRZ = Malawi Rift Zone; SIP = South Irumide Province; UB = Umkondo Belt; Ub-Usg = Ubendian-Usagaran Belts.

3.4.2 The Upper Zambezi

Zambezi sand becomes progressively enriched in basaltic detritus downstream of the Kwando confluence and more rapidly across the gorges downstream of Victoria Falls. Bedload sand and levee silty sand upstream of Lake Kariba are, respectively, quartzose with plagioclase \approx K-feldspar and litho-feldspatho-quartzose with plagioclase \gg K-feldspar, mafic volcanic rock fragments, and green augite. Basaltic detritus increases from west to east also in Zambezi tributaries, being minor in quartzose Sinde sand and roughly as abundant as quartz in lithic-rich litho-quartzose and quartzo-lithic Masuie and Matetsi sands containing common augite.

Smectite predominates over mica/illite and kaolinite in Zambezi mud and is overwhelming in muds of the Sinde and Matetsi tributaries, which contain kaolinite but no detected mica/illite or chlorite/vermiculite (Figure 3.3).

SiO₂ decreases progressively along the Upper Zambezi, with corresponding increase in most other elements, including Fe, Mg, Ca, Na, Sr (Figure 3.4G, 4H) and REE (Figure 3.5C) but not Zr, Hf, and Nb. Chemical indices upstream of Lake Kariba are CIA 49, $\alpha^{Al}Ca$ 0.9, $\alpha^{Al}Na$ 1.2 for sand, CIA 45, $\alpha^{Al}Ca$ 0.5, $\alpha^{Al}Na$ 1.5 for silty sand, and CIA 59±6, $\alpha^{Al}Ca$ 0.9±0.3, $\alpha^{Al}Na$ 3.9±0.9 for mud. Tributaries draining progressively larger portions of Karoo basalts display an even sharper trend from west to east. Masuie and Matetsi sands have much lower SiO₂ than Sinde sand and consequently higher concentration of all other elements (Figure 3.4A). In these rivers, both sand and mud are markedly enriched in Mg, Ca, Sc, Ti, V, Cr, Fe, Mn, Co, Ni, Cu (Figure 3.4B), and display regular chondrite normalized REE patterns with lack of Eu anomaly (Figure 3.5G). The ϵ_{Nd} value ranges between -12 and -12.5 in mud of the Zambezi mainstem between Victoria Falls and Lake Kariba and is much less radiogenic for Matetsi (-4) and Sinde (-5) muds.

Sinde sand yielded a zircon-age spectrum with dominant Irumide peak, common Neoproterozoic ages, and minor Permian-Triassic, Eburnean, and Neoproterozoic ages. Upper Zambezi sand upstream of Lake Kariba yielded a polymodal spectrum with main Pan-African and Irumide peaks (24% of ages between 497 and 634 Ma and 26% of ages between 943 and 1069 Ma) and minor Orosirian-Rhyacian and Neoproterozoic clusters (Figure 3.7).

Lower Gwai sand is feldspatho-quartzose with plagioclase > K-feldspar, biotite, and amphibole. Smectite predominates largely over kaolinite, chlorite/vermiculite, and mica/illite in muds of the upper Gwai and its Umguza tributary, whereas mica/illite prevails over kaolinite, smectite, and chlorite/vermiculite in mud of the lower-course Tinde tributary (Figure 3.3).

Chemical indices are CIA 54, $\alpha^{Al}Ca$ 2.9, $\alpha^{Al}Na$ 1.4 for lower Gwai sand and CIA 73, $\alpha^{Al}Ca$ 1.9, $\alpha^{Al}Na$ 10 for upper Gwai mud. Umguza sand is much richer in Fe, Mg, Ca, Ti, Mn, Sr, V, Co, Ni, and Cu than lower Gwai sand, whereas Umguza mud is similar to upper Gwai mud (Figure 3.4C, 4D). Tinde mud is richer in Si, Na, K, Rb, Ba, YREE, Th, U, Zr, Hf, Nb, Ta, and poorer in Fe, Mg, Ca, P, Mn, Sc, V, Cr, Co, Ni, and Cu (Table 3.2).

The ϵ_{Nd} value ranges between -12 and -15 in upper Gwai, Umguza and Tinde muds, but is strongly radiogenic in Gwai sand upstream of lake Kariba (-25), which yielded a polymodal zircon-age spectrum with major Neoproterozoic and Eburnean peaks and minor Irumide and Pan-African peaks (Figure 3.7).

3.4.3 The Middle Zambezi

Between Lakes Kariba and Cahora Bassa, Zambezi sand has the same feldspar-rich feldspatho-quartzose composition as Kafue sand, with K-feldspar \gg plagioclase, metamorphic rock fragments, mica, and amphibole. The Luangwa River carries feldspatho-quartzose sand with K-feldspar \gg plagioclase, granitoid to gneissic rock fragments, and amphibole. Smectite predominates over mica/illite and kaolinite in mud of the Zambezi mainstem, whereas mica/illite predominates over smectite and kaolinite in Kafue mud (Figure 3.3).

Chemical indices are CIA 51 ± 3 , $\alpha^{\text{Al}}\text{Ca}$ 2.1 ± 1.3 , $\alpha^{\text{Al}}\text{Na}$ 1.6 ± 0.2 for sand and CIA 67 ± 3 , $\alpha^{\text{Al}}\text{Ca}$ 2.1 ± 0.6 , $\alpha^{\text{Al}}\text{Na}$ 5.2 ± 0.2 for mud. The observed order of element mobility is $\text{Ca} > \text{Na} > \text{Sr}$ for sand and $\text{Na} > \text{Sr} > \text{Ca} > \text{K} > \text{Ba}$ for mud. Luangwa sand is higher in SiO_2 , K, Ba, and low in most other elements (especially Mg, Ti, and Sc; Figure 3.4C). The finer grained of the two Kafue sand samples are notably enriched in Zr, Hf, REE, Th, U, Nb, Ta (Table 3.2). Kafue and Middle Zambezi muds have virtually identical chemical composition (Figure 3.4D, 4H). All ϵ_{Nd} values range between -14 and -18, reaching -20 only in the 32-63 class of Luangwa sand.

The zircon-age spectrum of Kafue sand displays a single dominant Irumide zircon-age peak with minor Pan-African, and a few Triassic and Paleoproterozoic to Neoproterozoic ages. Luangwa sand is characterized by a major Irumide and minor Pan-African zircon-age peaks, with several Calymmian to Rhyacian ages (Figure 3.7).

3.4.4 The Lower Zambezi

In Mozambique, Zambezi sand ranges from quartzo-feldspathic to feldspar-rich feldspatho-quartzose with K-feldspar \geq plagioclase, locally common biotite, amphibole, and garnet. Most tributaries carry quartzo-feldspathic sand with K-feldspar \geq plagioclase, amphibole, garnet, clinopyroxene, epidote, and hypersthene. Feldspar (mostly plagioclase) is twice as abundant as quartz in Shire sand from Malawi. Metabasite grains are common in Morrunguze sand. Kaolinite, mica/illite, and smectite occur in subequal amount in Zambezi silt collected at Tete, whereas smectite predominates over mica/illite and kaolinite is subordinate upstream of the delta (Figure 3.3). Sangadze mud consists almost exclusively of smectite, whereas Shire mud contains mica/illite and kaolinite in subequal proportions. Chlorite/vermiculite was not detected (Table 3.1).

Chemical indices are remarkably constant in sediments of the Zambezi mainstem and most of its main tributaries (CIA 50.4 ± 0.5 , $\alpha^{\text{Al}}\text{Ca}$ 1.6 ± 0.5 , $\alpha^{\text{Al}}\text{Na}$ 1.2 ± 0.2 for sand and CIA 70 ± 3 , $\alpha^{\text{Al}}\text{Ca}$ 2.0 ± 0.4 , $\alpha^{\text{Al}}\text{Na}$ 6.0 ± 2.6 for mud) (Table 3.2). Common lack of Eu anomaly reflects feldspar abundance (Figure 3. 5H, 5I). The observed order of element mobility is $\text{Ca} > \text{Na} > \text{Sr}$ for sand and $\text{Na} > \text{Sr} > \text{Ca} > \text{K} > \text{Rb}$ for mud. In all grain-size fractions of Lower Zambezi sediments, ϵ_{Nd} values become much more radiogenic from Tete to upstream of the delta, where the very-fine-sand sample yielded fewer negative values than the fine-sand sample (Table 3.3).

Sand of the Morrunguze River draining gabbroic rocks of the Tete complex is low in SiO₂ (52%), K, and Rb, notably rich in Fe, Mg, Ca, Ti, Mn, Sc, V, Cr, Co, Ni and Cu (Figure 3.4 E), and yielded the least negative ϵ_{Nd} value (Figure 3. 6). Mufa sand, enriched in the same elements but to a much lesser extent, yielded high Zr and Hf concentrations (Table 3.2) and a more radiogenic ϵ_{Nd} value. Luenha sand is relatively rich in Zr and Hf, U, Nb, Ta and REE, is the richest in Th (Figure 3.4E), displays the steepest REE patterns with most negative Eu anomaly (Figure 3.5H, 5K), and is the only sample with negative loss on ignition (LOI -0.3). Mazowe and Luenha sands have radiogenic ϵ_{Nd} values of -18 and -19. Shire sand is highest in Al, Na, Sr, and P, and shows much less radiogenic ϵ_{Nd} values (Figure 3.7). Sangadze sand is the richest in K, Rb, and Ba, and displays a strongly positive Eu anomaly (Figure 3.5H) – reflecting abundant feldspars and fewer heavy minerals – and radiogenic ϵ_{Nd} values. Among mud samples, Shire mud is low in SiO₂ (42%) and highest in Al, Fe, Sr, Ba, P, Sc, V, and Cu (Figure 3.4F). Zambezi mud upstream of the delta is high in Zr and Hf, REE, Th, U, Nb, Ta, Cr, Mo, W, Co, and Ni (Figure 3.4H), and displays a negative Eu anomaly (Figure 3.5I).

The U-Pb age spectrum of zircons grains supplied by the Zambezi River to its delta displays a dominant Irumide peak, with common Neoproterozoic, some Orosirian, and a few Neoproterozoic and late Paleozoic ages (Figure 3.7). Sangara and Morrunguze zircons display a simple unimodal Irumide age peak. The Irumide age peak is dominant also in Mufa sand, which yielded more Neoproterozoic ages. Instead, Luenha and Mazowe sands yielded bimodal zircon-age spectra with Neoproterozoic (Cryogenian) and Neoproterozoic peaks. The spectrum of Shire sand is bimodal with Irumide (Stenian) and Pan-African (Ediacaran) peaks. The Pan-African peak prevails over the Irumide peak in Zangue sand.

3.4.5 The Northern Zambezi Delta

Estuary and beach sand ~100 km north of the Zambezi mouth is feldspatho-quartzose with plagioclase \geq K-feldspar and a rich transparent-heavy-mineral suite including amphibole, epidote, and clinopyroxene. The ϵ_{Nd} value of bulk sand ranges between -13 and -18. The U-Pb zircon-age spectrum displays a dominant Irumide peak with common Neoproterozoic, some Orosirian and a few Neoproterozoic and Permian ages, similarly to Lower Zambezi sand (Figure 3.7).

3.4.6 Provenance Insights from Clay Mineralogy and Sediment Geochemistry

Clay mineralogy and sediment geochemistry are largely controlled by factors other than provenance. If weathering is intense, then they reflect the lithology of source rocks only poorly, which explains why they have long been used to evaluate weathering intensity (e.g. Nesbitt and Young, 1982; Velde and Meunier, 2008) rather than provenance. However, despite the complexities associated with multiple controls on sediment composition (Johnsson, 1993), clay minerals and elemental and especially isotope geochemistry do offer complementary

information useful to augment the completeness and robustness of provenance analysis for several reasons (McLennan *et al.*, 1993). First, most other provenance techniques are best suited to tackle sand and, in case of detrital geochronology, only a millesimal fraction of total sand. Geochemistry, instead, can be applied to bulk-sediment samples of any size fraction from clay to granule. This allows us to investigate almost the entirety of the sediment flux, including silt and clay that account for most of the detrital mass transported in river systems as suspended load (e.g. Hay, 1998; Milliman and Farnsworth, 2011). The aim of this subsection is thus to complement previous considerations based only on sand with inferences derived independently from the mineralogy and geochemistry of mud.

a. Clay Minerals

Clay mineralogy is largely dependent on weathering processes in soils (e.g. kaolinite formation) but reflects provenance as well, especially in semiarid climates where illite and chlorite are largely derived from phyllosilicate-rich metamorphic bedrocks whereas smectite is shed by mafic lavas (e.g. Chamley, 1989). Among the studied samples, smectite is the dominant clay mineral (> 85%) in mud transported by the Sinde and Matetsi tributaries of the Upper Zambezi and by the Umguza tributary of the Gwai River, all partly draining Karoo basalts between southern Zambia and western Zimbabwe. Smectite, however, is produced in abundance also in dry regions lacking significant exposures of mafic lavas (e.g. Kwando catchment) and represents the virtually exclusive clay mineral in mud of the Sangadze River flowing across Mozambican lowlands, indicating incomplete flushing of mobile ions in poorly drained low-relief regions (Wilson, 1999). Illite is the most abundant clay mineral in mud of the Kafue and Shire Rivers chiefly draining Proterozoic crystalline basement, and in mud of the Tinde River draining Neoproterozoic molasse.

b. Sand Geochemistry

The piece of provenance information most readily obtained from geochemical data is the supply from mafic source rocks, revealed by high concentrations of ferromagnesian metals including Mg, Sc, Ti, V, Cr, Mn, Fe, Co, and Ni (Figure 3.8; McLennan *et al.*, 1993; von Eynatten *et al.*, 2003). Among the analysed samples, these elements reach the highest values in Masuie and Matetsi sands draining Karoo basalts and in Morrunguze sand draining the Tete gabbro-anorthosite complex (Figure 3. 4). Intermediate values for these elements are obtained for the Sinde and Umgutza tributaries draining Karoo basalts more marginally, and for the Middle Zambezi upstream of Lake Kariba (Table 3.2). Other samples in the Upper Zambezi catchment have $\text{SiO}_2 > 90\%$, revealing extensive recycling of pure quartzose Kalahari sand.

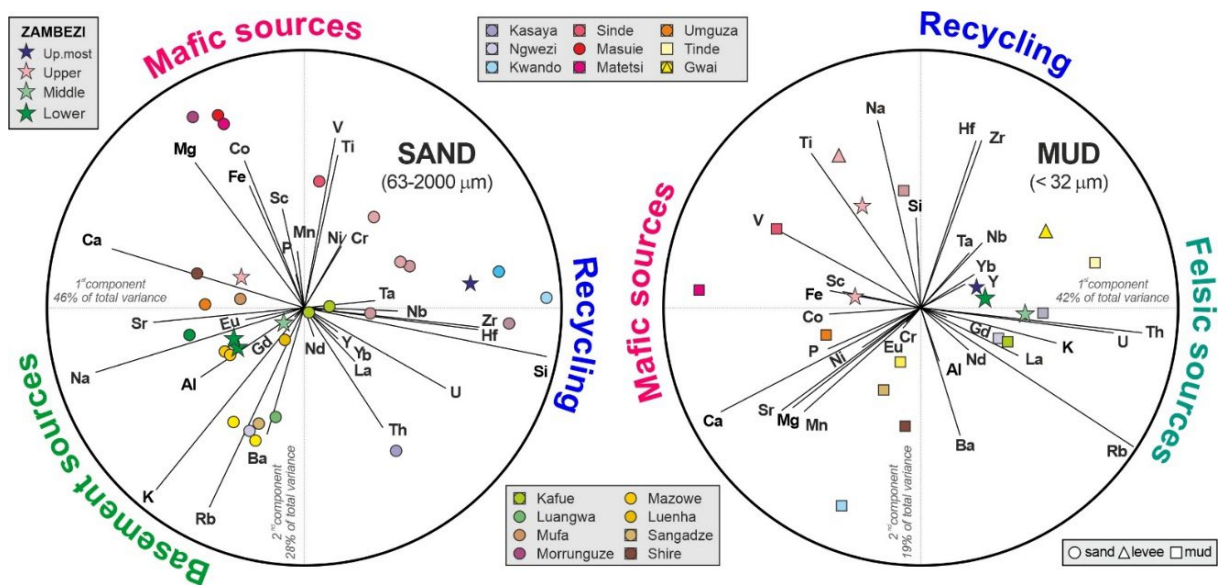


Figure 3.8: Relationships among chemical elements in Zambezi sand and cohesive mud

Provenance control is evident especially for sand: ferromagnesian metals are enriched in basaltic or gabbroic detritus, Al, Na, Ca, K, Rb, and Ba largely hosted in feldspars are enriched in detritus derived first-cycle from mid-crustal basements, and Si, Zr, Hf are enriched in pure-quartzose, zircon-bearing sediment recycled from Kalahari dunes. Both multivariate observations (points) and variables (rays) are displayed in the compositional biplot (Gabriel, 1971). The length of each ray is proportional to the variance of the corresponding element in the data set. If the angle between two rays is close to 0° , 90° , or 180° , then the corresponding elements are directly correlated, uncorrelated, or inversely correlated, respectively.

The virtually identical chemical composition of Kafue and Middle Zambezi muds confirms that the Kafue is by far the most important source of sediment to the Middle Zambezi between Lake Kariba and the Luangwa confluence. Slightly above 80% in Kafue and Middle Zambezi sand, SiO_2 raises to nearly 90% in Luangwa sand that contains a greater proportion of detritus recycled from Karoo siliciclastic strata. In sand of Lower Zambezi tributaries, SiO_2 mostly ranges between 70 and 80%. Composition is closest to the UCC for sand carried by the Lower Zambezi to the Indian Ocean, confirming its dominantly first-cycle provenance from mid-crustal basement rocks (Garzanti et al., 2021a).

Chemical indices provide further clues. Because the addition of quartz grains directly affects the WIP, but not the CIA, the CIA/WIP ratio can be considered as an index of recycling. This ratio reaches ≥ 100 in Uppermost Zambezi and Kwando sands that consist almost entirely of recycled Kalahari dune sand, decreases to 30 ± 9 in Upper Zambezi sand below and above Victoria Falls, and next drastically to 3.1 ± 0.7 in Upper Zambezi sand and silty sand upstream of Lake Kariba. The CIA/WIP ratio decreases further to 1.7 ± 0.3 in sands of Middle Zambezi

tributaries and mainstem and is lowest (0.9 ± 0.1) in sands of Lower Zambezi tributaries and mainstem, confirming their largely first-cycle provenance.

c. Mud Geochemistry

The geochemical composition of mud samples is more homogeneous. SiO_2 varies between 42% and 54%, being notably higher (68%) only for Tinde mud reflecting recycling of siliciclastic Pan-African molasse. Kwando mud is markedly enriched in Ca, Sr, Mg, and Ba (Figure 3.4B), revealing contribution from calcrete and dolocrete soils (Shaw, 2009; McFarlane *et al.*, 2010). Fe, Ti, Sc, V, Co, and Cu are highest in Sinde mud and Mg in Matetsi mud (Figure 3.4A, 4B) largely derived from Karoo basalts. Lower Zambezi mud upstream of the delta is richest in Cr and Ni (Figure 3.4H), suggesting significant supply from mafic Proterozoic rocks including the Tete gabbro-anorthosite complex.

d. Isotope geochemistry

The $^{143}\text{Nd}/^{144}\text{Nd}$ ratio is controlled by multiple factors, including lithology and age of source rocks, grain size, and hydraulic-sorting effects (Garzanti *et al.*, 2021b). Nevertheless, the provenance signal emerges clearly from data obtained from all analysed size fractions – cohesive mud ($< 32 \mu\text{m}$), frictional silt ($32\text{-}63 \mu\text{m}$), and sand ($63\text{-}2000 \mu\text{m}$), which clearly discriminate between sediments derived from mafic igneous rocks versus old granitoid basements (Figure 3.9).

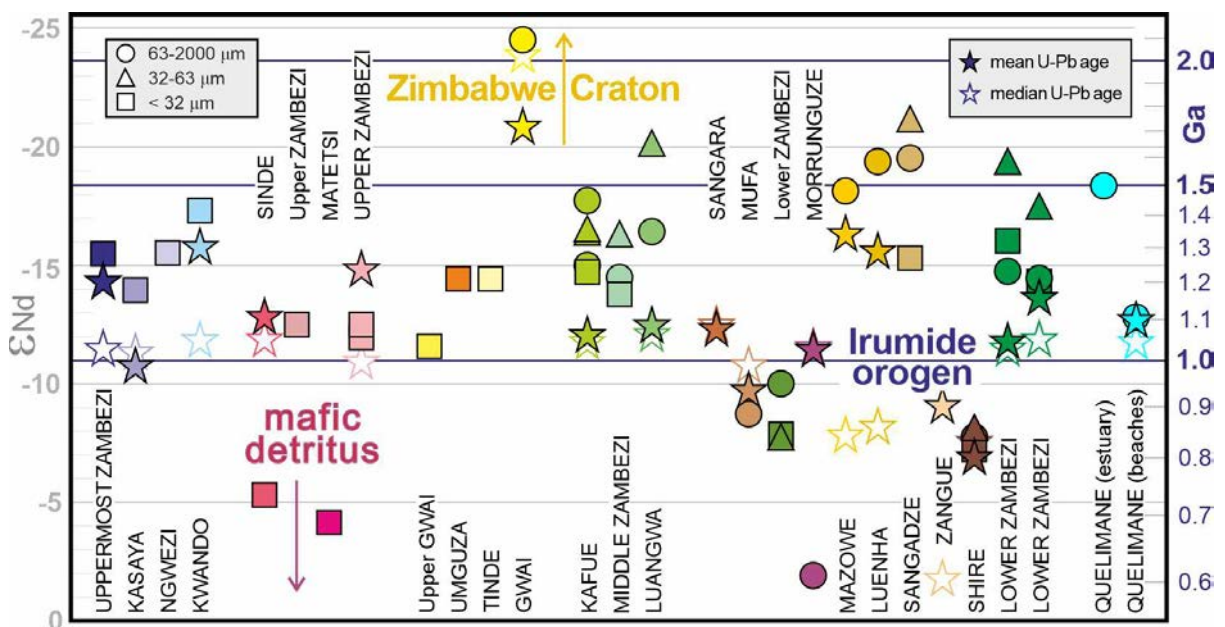


Figure 3.9: Multiple controls on $^{143}/^{144}\text{Nd}$ isotope values

NB: Most prominent are the effects of lithology (mafic detritus being least radiogenic) and average age of source rocks (as highlighted by generally good correlation with average detrital-zircon U-Pb ages). Grain-size-controlled intrasample variability is limited.

The least radiogenic values characterize Morrunguze sand, largely derived from the upper Stenian Tete gabbro-anorthosite complex, and Sinda and Matetsi muds, partly derived from Lower Jurassic Karoo basalts (Figure 3.6). Only slightly more radiogenic values were obtained from Mufa sand, partly derived from mafic rocks of the Tete complex, from all size fractions of Shire sand largely derived from mafic granulites of the Blantyre domain, and from all size fractions of Lower Zambezi silt collected at Tete upstream of the Luenha confluence and mostly derived from the Southern Irumide Province (Table 3.3).

At the other extreme, highly radiogenic values characterize Gwai, Mazowe, and Luenha sands partly derived from Archean gneisses of the Zimbabwe Craton. Intermediate values characterize muds in the upper catchments of the Zambezi and Gwai Rivers. The ϵ_{Nd} value becomes less radiogenic as the Upper Zambezi traverses basaltic gorges downstream of Victoria Falls but more radiogenic as the Lower Gwai steeply cuts across granitoid gneisses of the Dete-Kamativi Inlier. Similarly, or slightly more radiogenic values characterize Kafue and Luangwa sediments in the middle catchment, Sangadze sediments in the lowermost catchment, and Lower Zambezi sediments upstream of the delta.

The grain-size controlled intrasample variability of ϵ_{Nd} values is limited (average standard deviation 1.6 ± 0.9). The sand fraction (63-2000 μm) generally contains more radiogenic heavy minerals than the cohesive mud fraction ($< 32 \mu\text{m}$) and thus may yield more negative ϵ_{Nd} values. Most negative ϵ_{Nd} values are typically obtained from the 32-63 μm class of sand samples, representing the fine tail of the size distribution where ultradense minerals including monazite concentrate because of the settling-equivalence principle (Rubey, 1933; Garzanti *et al.*, 2008). The opposite holds for the Lower Zambezi silt collected at Tete, where the 32-63 μm class is part of the coarse tail of the size distribution depleted in denser minerals and consequently yields a less negative ϵ_{Nd} value than both $< 32 \mu\text{m}$ and 63-2000 μm fractions (Table 3.3).

Depleted mantle model ages ($t_{Nd,DM}$) for the Zambezi mainstem and tributaries mainly range between 2.0 and 2.3 Ga. Matetsi and Sinda muds partly derived from Karoo basalts yielded notably lower values around 1.5 Ga, and Morrunguze sand largely derived from gabbroic rocks of the Tete domain the lowest value (1.16 Ga). Values between 2.5 and 2.8 Ga characterize the three rivers sourced in the Archean Zimbabwe Craton (Gwai, Mazowe, and Luenha).

Sm-Nd model ages depend on REE fractionation, being lower in samples containing LREE-rich minerals such as monazite or allanite and higher in samples containing MREE-rich minerals such as xenotime, titanite or apatite (fig. 7 in Garzanti *et al.*, 2021b). LREE-rich ultradense minerals such as monazite are concentrated in the fine tail of the size distribution, which explains why the 32-63 μm class of the Zambezi silt collected at Tete is much lower in LREE, has a higher Sm/Nd ratio, and thus yielded a notably higher Sm-Nd model age than the $< 32 \mu\text{m}$ fraction despite its slightly lower ϵ_{Nd} value (Figure 3.6). In Lower Zambezi samples, the 63-2000 μm fraction has lower LREE fractionation (higher Sm/Nd) than both 32-63 μm and $< 32 \mu\text{m}$ fractions, and thus yielded older Sm-Nd model ages than the $< 32 \mu\text{m}$ fraction

even though ϵ_{Nd} values are very similar, and almost the same Sm-Nd model ages than the 32-63 μm class despite the latter yielded notably more negative ϵ_{Nd} values (Figure 3.6).

e. Provenance Insights from Detrital Geochronology

Age spectra of detrital zircons enrich provenance information by providing insight into events of crustal growth in diverse source-rock domains (Figure 3.10). In the general case, these can only be considered as “protosources” (Andersen *et al.*, 2016, 2018), because they represent the true sediment source only in the specific case of first-cycle detritus supplied directly from igneous or metamorphic basement. Most sedimentary basins, however, are fed with a mixture of first cycle and recycled sediment in a proportion that can be only roughly evaluated from independent compositional data (Garzanti *et al.*, 2019).

Petrographic, mineralogical, and geochemical information concurs to reveal that Uppermost Zambezi sand is dominantly recycled from Kalahari dune fields (Garzanti *et al.*, 2014a, 2014b, 2022). The Kwando River in particular drains entirely within the Kalahari Erg, whereas some first-cycle detritus is supplied by Zambian tributaries sourced in the Lufilian arc or Choma-Kalomo Block and carrying a little more feldspar, epidote, garnet, and amphibole (e.g. Ngwezi River). In sharp contrast, Lower Zambezi sand is mostly derived first-cycle from igneous and metamorphic Precambrian basements rejuvenated during Neogene southward propagation of the East African Rift (Garzanti *et al.*, 2021a).

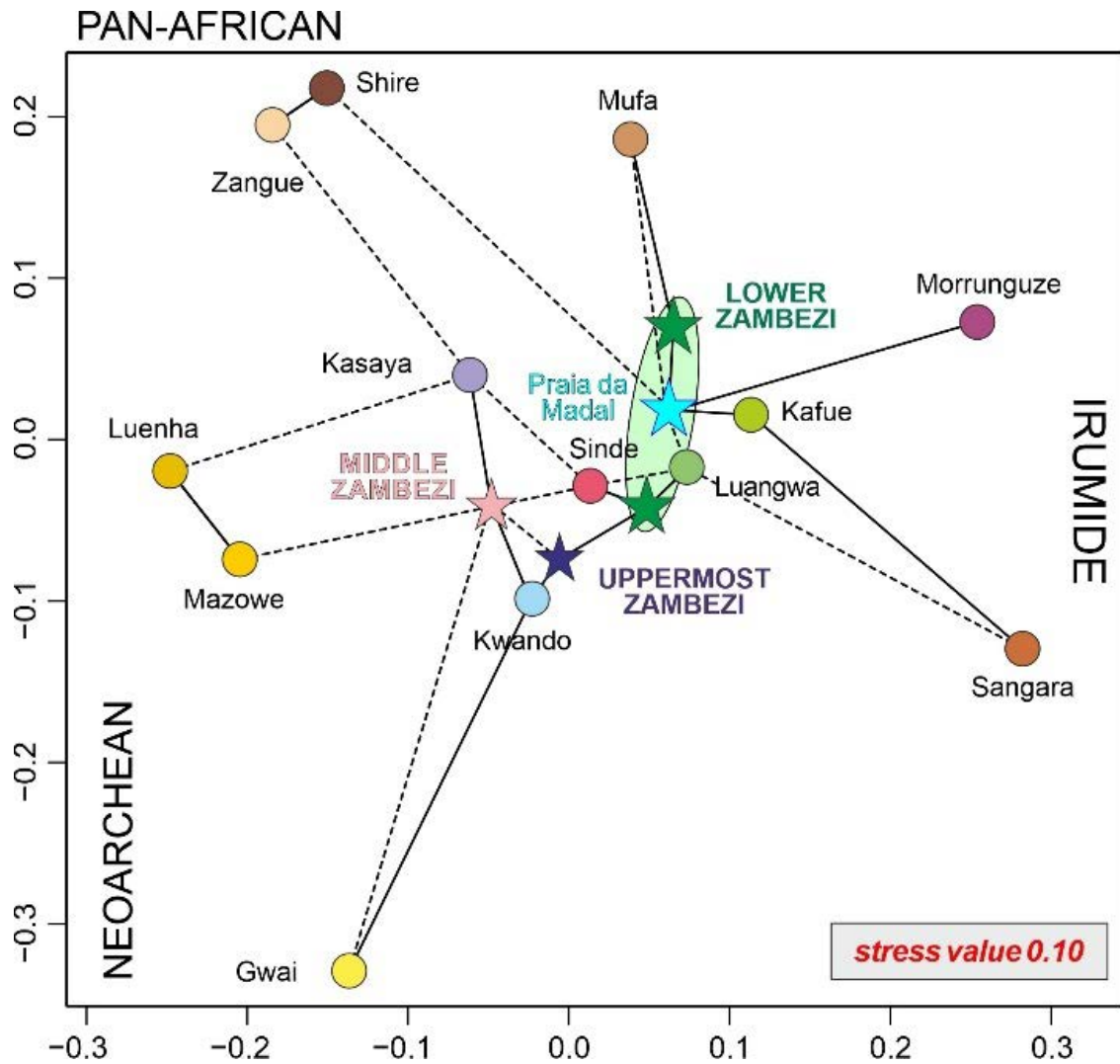


Figure 3.10: Multidimensional scaling map based on U-Pb zircon-age spectra

NB: Lower Zambezi zircons are mostly derived from Irumide (exclusive for Sangara and Morrunguze sands and dominant for Mufa, Kafue, and Luangwa sands), Pan-African (prevalent in Shire and Zangue sands), and Neorchean protosources (Gwai, Luenha, and Mazowe sands partly derived from the Zimbabwe Craton). In the map, samples with similar age-spectrum plot close together and dissimilar samples far apart. Closest and second closest neighbours are linked by solid and dashed lines, respectively. Axes units are normalised values based on Kolmogorov-Smirnov distance. Goodness of fit is evaluated using the “stress” value of the configuration (0.2 = poor; 0.1 = fair; 0.05 = good; table 3.1 in Vermeesch, 2013).

- Zircon Ages

Geochronological analysis indicates the Irumide and Pan-African crustal domains as the main protosources of zircon grains in rivers draining the northern Kalahari (Figure 3.7). Neoproterozoic ages ultimately derived from the Kasai Shield are common only for Kwando sand in the west. Paleoproterozoic grains ultimately derived from the Angola Block, common in both Kwando and Uppermost Zambezi sand, are few in eastern Zambian tributaries (Kasaya and Sinde). Paleoproterozoic zircons are more common in sand of the Sinde River sourced in the Choma-Kalomo Block, whereas Neoproterozoic zircons are much more abundant in Kasaya sand largely derived from the Lufilian Arc. The Irumide peak is invariably prominent.

Zircon grains yielding Permian to Triassic Karoo ages constitute a minor population in Sinde sand but are lacking in Zambezi sand downstream of the basaltic gorges. Jurassic Karoo basalts do not contain significant amounts of zircons.

Despite extensive remobilization during the Pan-African orogeny (Figure 3.7 in Goscombe *et al.*, 2020), zircon grains in sand of northern (Kafue, Luangwa, Morrunguze) and western (Sangara, Mufa) tributaries to the Middle and upper Lower Zambezi yielded mostly or even exclusively Irumide ages. The dominant Irumide zircon-age peak displayed by Kafue sand suggests that Neoproterozoic zircons sourced in the Lufilian Arc are retained in the Itezhi-Tezhi Reservoir and/or in the Kafue Flats and do not reach the lower gorge, where Irumide-aged zircons are derived mostly from the Mpande gneiss (~1.1. Ga; Hanson *et al.*, 1994; fig. 6 in Goscombe *et al.*, 2020).

Pan-African ages are lacking in sand of the Morrunguze River draining entirely within the Southern Irumide Province but more abundant than Irumide ages in sands of the Shire and Zangue tributaries joining the Zambezi mainstem upstream of the delta (Figure 3.7). Archean zircons are common (27-30%) in the Gwai, Mazowe, and Luenha Rivers sourced in the Zimbabwe Craton. Gwai sand also carries ~20% of zircons derived from the Paleoproterozoic Dete-Kamativi Inlier cut across in the lower course.

The multimodal age-spectrum of Zambezi zircons eventually supplied to the delta and dragged by littoral currents to the northern Quelimane region indicates predominance of zircon grains derived directly or indirectly from the Irumide belt, with subordinate late Neoproterozoic zircons mainly supplied by domains of the Irumide belt most severely remobilized during the Pan-African event. Neoproterozoic zircon grains derived from the Zimbabwe craton via the Mazowe and Luenha Rivers are minor (Figure 3.7).

A few Permian-Triassic zircons generated from Karoo tuffs on the Kalahari Plateau are identified in Kasaya, Sinde, and Gwai sands and a few Triassic zircons were recorded from Kafue sand, but Permian-Triassic zircons were never recorded from any other tributary downstream. Yet, a few Permian and rarer Triassic zircons occur in Lower Zambezi sand upstream of the delta, suggesting supply from Karoo volcanic rocks exposed in the Moatize-

Minjova basin. Single Jurassic or Cretaceous ages are sporadically recorded, among which most significant is one zircon dated as 116 Ma in the terminal tract of the Lower Zambezi, pointing at provenance from igneous rocks emplaced during the incipient opening of the Mozambique Channel (König and Jokat, 2010; Resentini *et al.*, 2020).

- Zircon Fertility

The joint consideration of petrographic, mineralogical, and geochemical datasets does not only offer a panorama of compositional signatures but also useful information to evaluate the zircon fertility of sediment sources (e.g. diverse tributary catchments in Zambezi drainage system), which is required for a correct use of zircon-age data in the calculation of provenance budgets (Malusà *et al.*, 2016). As a very-high-density mineral, zircon is invariably segregated in the fine tail of the size distribution of each sample deposited by a tractive current and may be even strongly concentrated locally by selective-entrainment processes in lag deposits (Garzanti *et al.*, 2008, 2009). These issues generally hamper the accuracy of fertility determinations based on mineralogical or geochemical data from sediment samples that cannot be proved to be truly representative of the weighted average of their source-rock lithologies (Vezzoli *et al.*, 2016).

In our sample set, sands from the upper part of the Zambezi catchment have a notably lower concentration of zirconium (Zr 232 ppm in one trunk-river sample, but otherwise invariably below the UCC standard and mostly in the 30-80 ppm range) than in the Middle and Lower Zambezi catchment (between 330 and 600 in Kafue and Mufa samples, and above the UCC also for the Middle Zambezi, Luenha, and Shire samples). Mineralogical data confirm that zircon concentration is markedly lower in the Uppermost to Upper Zambezi catchment (maximum 0.2%, median 0.02% of bulk sand), than in Middle to Lower Zambezi catchment (median 0.16%, with maximum values obtained from Shire sand).

A most useful parameter to detect hydraulically controlled concentration of denser minerals is the weighted average density of terrigenous grains (SRD index of Garzanti and Andò, 2007), which for each sample should be equal to the weighted average density of source rocks in the ideal absence of environmental bias. The SRD index of most sands in rivers on the Kalahari Plateau ranges between 2.65 and 2.68 g/cm³ (just a little higher than quartz density), increasing to 2.79 and 2.90 for Masuie and Matetsi sands containing 50% and 70% of detritus from dense basaltic rocks. In the Middle to Lower Zambezi catchment, SRD mostly ranges between 2.7 and 2.8 g/cm³, which is the expected density range for upper to middle crustal basements (Garzanti *et al.*, 2006). The finer-grained Kafue (SRD 2.79) and Luenha (SRD 2.78) sands are those richest in elements preferentially hosted in ultradense minerals (Figure 3.4). Luenha sand has high LREE and Th, negative LOI, but only moderately high Zr values, indicating concentration of ultradense monazite and magnetite but only moderately high zircon content (0.16% of bulk sand). The high SRD values observed for Shire (2.82) and Morrunguze sands (2.87) reflects contributions from high-grade and largely mafic basement rocks of the Blantyre and Tete domains (figs. 2 and 7 in Goscombe *et al.*, 2020). Ultradense garnet, zircon, monazite, and opaque Fe-Ti-Cr oxides have been markedly concentrated by selective entrainment

processes only in Lower Zambezi sample S5778 (SRD 3.34), a garnet placer lag that was not analysed for either geochemistry or zircon geochronology.

Petrographic, heavy-mineral, and geochemical data converge to indicate that the zircon concentration in our samples provide an imprecise but broadly reliable indication of zircon fertility in the corresponding catchments. Zircon fertilities are estimated to range from 0.02% for Kalahari dune sands to 0.2% for mid-crustal basement rocks exposed in the Middle to Lower Zambezi catchment.

f. Provenance Budgets and Erosion Patterns

- Provenance Budgets

The relative contribution from each tributary or geological domain to the sediment flux of a trunk river can be quantified mathematically with forward mixing models, provided that the compositional signatures of sediment in each potential source are distinct and accurately determined (Weltje, 1997; Garzanti *et al.*, 2012). Fortunate conditions, however, are rarely met in natural environments, because compositional signals are influenced by several factors including grain size. Robust results are obtained only by analysing a sufficient number of replicate samples in various parts of the catchment and by integrating information from multiple datasets.

In this paragraph, calculations based on independent elemental-geochemistry, isotope-geochemistry, and geochronological data are used to better constrain the rough provenance budget based on detrital modes presented in Garzanti *et al.* (2021a). Integrated compositional data indicate that Upper Zambezi sand and silty sand delivered to Lake Kariba consists of $\geq 80\%$ of quartz-rich detritus recycled from Kalahari dunes, $16\pm 4\%$ of largely basaltic volcanic detritus, and the remaining $\leq 5\%$ from Precambrian basements exposed in Zambia and Zimbabwe. The age spectrum of zircon grains supplied by the Upper Zambezi to Lake Kariba is intermediate between those of Uppermost Zambezi and Kwando sands. These two river branches are thus revealed as the most prominent zircon sources, in a relative proportion that cannot be accurately determined because of the similarly very low zircon fertility indicated by both geochemical and mineralogical data.

Because sand generated in the Upper and Middle Zambezi catchments is all stored in Lakes Kariba and Cahora Bassa, all sand carried to the delta (zircon grains included) is generated in the Lower Zambezi catchment. Petrographic and heavy-mineral data indicated major sand contribution from the Southern Irumide Province drained upstream of the Luenha confluence (30-40%) and from the Mazowe-Luenha River system sourced in the Zimbabwe Craton (30-40%). The Umkondo Belt and the Karoo, Cretaceous, and Cenozoic extensional basins drained by the Minjova, Sangadze, and Zangue tributaries were held to contribute much of the rest (~20%), whereas supply from the Tete and Blantyre domains drained respectively by the

Morrunguze and Shire tributaries appeared to be subordinate (~10% each; Garzanti *et al.*, 2021a).

New complementary information obtained from elemental geochemistry suggests that as much as 70% of Lower Zambezi sand may be supplied by the Mazowe-Luenha River system, with subordinate contribution from the mainstem upstream of the Zambezi-Luenha confluence (20-25%), and minor supply from the Morrunguze and Shire Rivers (< 5% each) and other lowermost-course tributaries (~5%). Calculations based on ϵ_{Nd} values of sand (63-2000 μm fraction) confirm that most of the sediment in the Lower Zambezi catchment is generated in the Mazowe-Luenha catchment (50-65%), with subordinate contribution from the mainstem upstream of the Zambezi-Luenha confluence and other sources. The ϵ_{Nd} values of cohesive mud (<32 μm fraction) in the Lower Zambezi upstream of the delta are similar or more radiogenic than for sand, indicating that mud contributions from the Mazowe-Luenha River system are not lower, and possibly higher, than for sand.

Calculations based on zircon-age data suggest that at least half of zircon grains are derived from the Irumide domain, a quarter at most is generated in the Mazowe-Luenha catchment, and a fifth at most in the final part of the catchment, with very minor contribution from the Shire River. Because heavy-mineral data indicate a relatively high zircon fertility for the Shire catchment, all compositional information converges to indicate that the Shire River supplies only a very small part (< 5%) of sediment to the Zambezi Delta. This holds true also for mud, because the smectite/kaolinite ratio increases sharply downstream of the Lower Zambezi, whereas the Shire clay-mineral assemblage contains abundant kaolinite and minor smectite. Minor sediment supply from the Shire River is explained by sequestration in Lake Malawi of all sediment generated in the upper catchment and by further sediment trapping in wetlands and artificial reservoirs downstream (Nzuza *et al.*, 2017). This inference contrasts with Just *et al.* (2014 p.191), where the Shire River was considered to contribute ~28% of total Zambezi sediment load at present (~21% before construction of the Cahora Bassa Dam).

Provenance budgets based on independent datasets and on diverse size fractions are not entirely consistent. Age spectra of detrital zircons point at predominant zircon supply from the Irumide domain exposed in the upper part of the Lower Zambezi catchment, with minor zircon contribution from the Zimbabwe Craton drained by the Mazowe and Luenha Rivers. Instead, elemental-geochemistry and Nd-isotope data consistently suggest that most Lower Zambezi sediment is generated in the Mazowe-Luenha catchment. Although the robustness of diverse sets of calculations is not easily evaluated, it notably increases if end-member signatures are well distinct, precisely determined, and have little variability dependent on grain size, weathering, or hydraulic sorting. Conversely, estimates obtained on a narrow grain-size window or, worse, on a rare mineral within a narrow grain-size window, are least likely to be representative and accurately extrapolated to the entire sediment flux (Vezzoli *et al.*, 2016).

In the case of Lower Zambezi tributaries draining medium/high grade mid-crustal crystalline basements, sand petrography, heavy minerals, and elemental geochemistry show significant

overlap, and considerable hydrodynamically-controlled variability. Least robust are calculations based on zircon-age spectra because of the uncertainties involved in zircon-fertility determinations. Nd-isotope geochemistry suffers from a limited number of analysed samples, but the end members are well distinct and precisely defined, variability is limited, and all grain-sizes have been considered. The major change towards more radiogenic ϵ_{Nd} values documented in Lower Zambezi sediments for all size fractions from upstream to downstream of the Luenha confluence cannot be ascribed to Shire sediments – which yielded less radiogenic ϵ_{Nd} values for all size fractions (Figure 3.6) – and thus clearly indicates major sediment supply from the Mazowe-Luenha River. Weighing all obtained information, we conclude that between half and two-thirds of the sediment presently reaching the Zambezi Delta is generated in the Mazowe-Luenha catchment, between a quarter and a third is produced between Lake Cahora Bassa and the Zambezi-Luenha confluence, and the rest downstream, with very limited supply ($\leq 5\%$) from the Shire River.

- Erosion Patterns

Because of a general lack of gauged sediment loads, Zambezi sediment fluxes are evaluated with uncertainties of a full order of magnitude. Erosion patterns across the catchment can thus be only grossly determined. Based on the available sediment-concentration data and sediment-transport models, two end-member domains can be distinguished by their contrasting geomorphological conditions and sediment-generation modality: the low-relief Kalahari Plateau largely covered by aeolian sand in headwater regions versus rugged igneous and metamorphic terranes extensively exposed between Victoria Falls and Mozambican lowlands.

On the plateau, rivers with low channel steepness sluggishly flow for large tracts through wetlands, where sediment is sequestered rather than produced, as in the Barotse floodplain and Chobe marshes on the mainstem or in the Machili and Kafue Flats traversed by the Kasaya, Ngwezi, and Kafue tributaries. Because data on Kwando sediment load are to the best of our knowledge unavailable, information from the Okavango River similarly draining entirely within the Kalahari Basin in Angola (Shaw and Thomas, 1992; McCarthy *et al.*, 2012) allows us to broadly constrain the annual sediment yield and erosion rate in the Kalahari Basin as ≤ 2 tons/Km² and ≤ 0.001 mm. Sediment yield is estimated to increase by more than an order of magnitude where channel steepness reaches very high values, as in basaltic gorges downstream of Victoria Falls (40-90 tons/Km²; fig. 3 and p.14 in Garzanti *et al.*, 2021a).

A similar sediment-generation pattern characterizes other rivers flowing on the Kalahari Plateau in the headwaters and plunging into bedrock gorges downstream. For the Gwai River, a provenance budget based on petrographic, heavy-mineral, and geochemical data on fluvial-bar sand and levee silty sand indicates that sediment yield and erosion rate are between 20 and 50 times higher in the lower course cutting steeply across the Dete-Kamativi Inlier of the Magondi Belt than in the upper course, sourced in the Zimbabwe Craton and draining the Kalahari Basin. The same may hold true for the Kafue River, where much of the sediment is however trapped in the Kafue Flats and behind the Itezhi-Tezhi and Kafue Gorge Dams.

Annual values between 100 and 200 (150 ± 50) tons/Km² (Bolton, 1984; Ronco *et al.*, 2010), corresponding to erosion rates of 0.06 ± 0.02 mm, were estimated for Middle and Lower Zambezi tributaries flowing steeply across mid-crustal basement rocks exposed in the Archean Zimbabwe Craton or in the Proterozoic Irumide, Umkondo and Zambezi Belts in southern Zambia, northeastern Zimbabwe, and western Mozambique.

Considering that the Lower Zambezi upstream of the Luenha confluence and the Mazowe-Luenha River system have similar catchments areas, our provenance budgets imply sediment yields and erosion rates between 1.5 and 2.5 times higher in the latter. Extensive sediment trapping in Lake Malawi upstream and across wetlands or behind dams downstream (Mzuza *et al.*, 2019) prevents us to make considerations concerning erosion rates in the Shire catchment.

g. Weathering versus Paleoweathering

- Insights from Clay Minerals

Clay mineralogy is quite sensitive to weathering conditions. It has long been observed that kaolinite is abundant in hot humid regions where feldspar hydrolysis is intense, whereas smectite is common in warm regions with a dry season characterized by intense evaporation, and illite and chlorite dominate where chemical decomposition is minor (Chamley, 1989; Velde, 1995). In modern sediments, the ratio between kaolinite and illite+chlorite [Kao/(Ill+Chl)] may thus be used as a proxy for weathering intensity (He *et al.*, 2020).

Within our sample set, kaolinite is significant in all catchments and represents ~40% of the clay-mineral assemblage in Uppermost Zambezi, Lower Zambezi (Tete sample), and Shire mud (Figure 3.4). The Kao/(Ill+Chl) ratio is > 1 in Uppermost Zambezi, Kwando, Ngwezi, and upper Gwai muds generated on the Kalahari Plateau, but < 1 in Middle and Lower Zambezi tributaries downstream (Table 3.1).

- Insights from Mud and Sand Geochemistry

Geochemical indices have long been used as proxies for weathering intensity (e.g. Nesbitt and Young, 1982; Price and Velbel, 2003), although they may be even predominantly controlled by grain size (von Eynatten *et al.*, 2012, 2016), provenance (Garzanti and Resentini, 2016; Dinis *et al.*, 2017), hydraulic sorting, or quartz addition by recycling (Figure 3.11). This is especially true for sand, and weathering conditions are thus better reflected in the geochemistry of mud (Dinis *et al.*, 2020).

The most reliable indicator of weathering intensity is $\alpha^{Al}Na$, which chiefly measures the progressive leaching of Na⁺ from the plagioclase lattice. The $\alpha^{Al}Na$ value decreases quite regularly from the Uppermost Zambezi and Kwando Rivers (≥ 4 for sand, 21-22 for mud), to Victoria Falls (2.1 ± 0.1 for sand, 4.6 for mud), and to the Middle and Lower Zambezi downstream (1.3 ± 0.2 for sand, 5 ± 2 for mud).

Other α^{Al} values, and consequently the CIA and its several derivative indices, are more significantly affected by the mineralogy of sediment sources. Most evident is the anomaly of Kwando mud, which is peculiarly rich in Ca, Sr, Mg, and Ba derived from calcrete soils (Figure 3.11; McFarlane *et al.*, 2010) and consequently yielded corresponding α^{Al} indices ≤ 0.4 . Masuie, Matetsi, and Morrunguze sediments largely derived from basaltic or gabbroic rocks have high Mg and Ca and consequently low $\alpha^{Al}Mg$ and $\alpha^{Al}Ca$ (0.4-0.6). Conversely, sediments derived from gneissic basements are enriched in K and Rb largely hosted in K-feldspar and mica, which explains why $\alpha^{Al}K$ and $\alpha^{Al}Rb$ are < 1 in several tributaries (e.g. Kasaya, Ngwezi, Gwai, Kafue, Luangwa, Mazowe, Luenha, and Sangadze). Sangadze sediments have the lowest plagioclase/K-feldspar ratio of all analysed sands from the Lower Zambezi catchment, and consequently yielded the highest $\alpha^{Al}Na$ in both sand and mud, and the lowest $\alpha^{Al}K$ and $\alpha^{Al}Rb$ in sand.

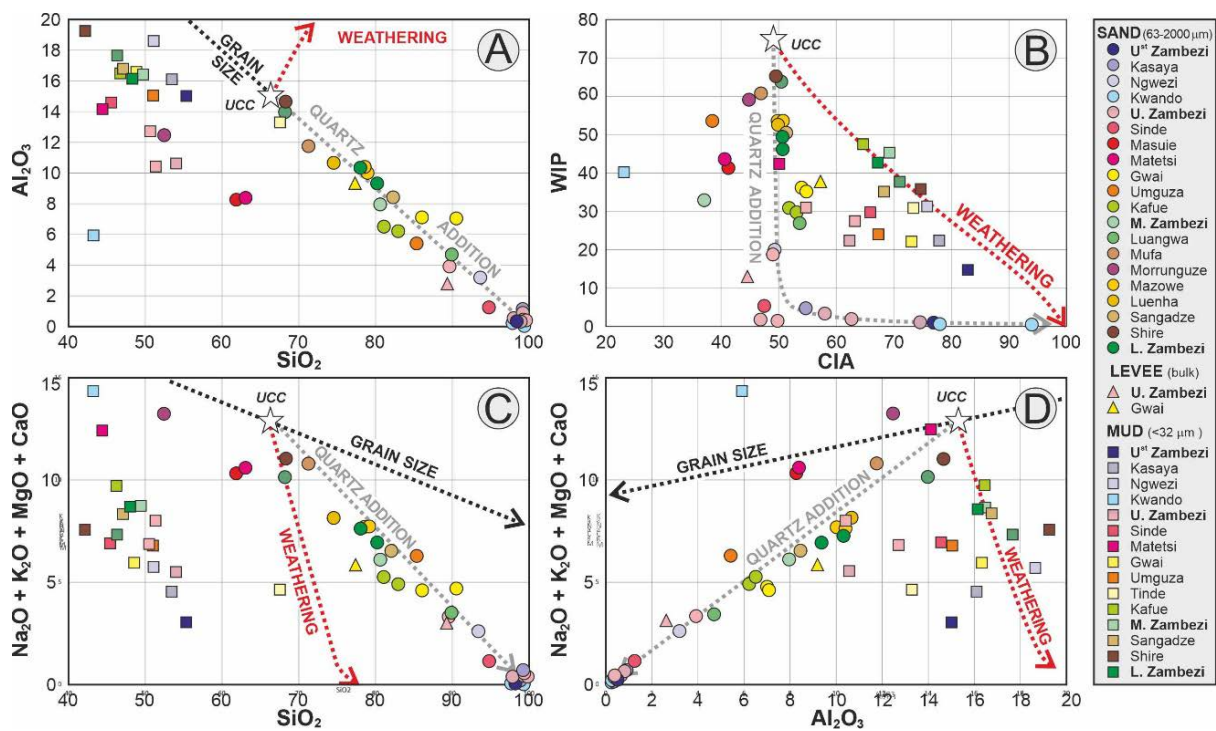


Figure 3.11: Discriminating the effects of weathering, recycling, and grain size from geochemical data of Zambezi sands, levee silty sands, and muds

NB: Theoretical trends are calculated starting from the Upper Continental Crust standard (UCC): the quartz-addition trend by progressively adding SiO_2 and the weathering trend by progressively subtracting mobile metals while assuming Si and Al as immobile. The grain-size trend is drawn parallel to empirical trends based on data from Alpine and Himalayan sediments (Garzanti *et al.*, 2010b, 2011, 2012). In all four panels, sand samples follow the quartz addition trend, indicating varying degrees of mixing with detritus recycled from quartz-rich Kalahari sands (Uppermost to Upper Zambezi catchment) or Karoo and older sandstones and metasandstones (Middle to Lower Zambezi catchment). Instead, mud samples follow the weathering trend. A) Samples plotting far below the regression line ($Al_2O_3 = -0.45 SiO_2 + 45$)

include Fe-rich Masuie and Matetsi sands derived from Karoo basalts, and Kwando mud enriched in Ca, Sr, Mg, and Ba derived from calcrete soils. B) Uppermost and Upper Zambezi muds plot below the weathering trend (low WIP), suggesting recycling and inherited weathering. In present conditions, weathering intensity slightly increasing from the Middle to the Lower Zambezi catchment may be indicated. Anomalously low CIA* (corrected for CaO in apatite but not for CaO in carbonate) in Kwando mud reflects supply from calcrete soils. C, D) Cohesive muds collected upstream of Lake Kariba reflect quartz addition from Kalahari sands (Uppermost Zambezi) and Neoproterozoic sandstones (Tinde mud).

- *Insights from Detrital Minerals*

The different stability of detrital minerals in different geomorphological conditions may be used to obtain indications on weathering intensity, although this path is fraught with problems and uncertainties. An example is the unfortunate proposal of the so-called “Mineralogical Index of Alteration” [$MIA = Q/(Q+F) * 100$; Rieu *et al.*, 2007], a parameter not only long demonstrated to markedly increase with grain size (Odom *et al.*, 1976; Garzanti, 1986) but also reaching maximum values equally in hyper-humid equatorial and hyper-arid desert conditions (Garzanti *et al.*, 2019; Pastore *et al.*, 2021).

The different stability of heavy minerals in different weathering regimes is more reliably indicative (Bateman and Catt, 2007). The ratio between garnet (G) and other nesosilicates typical of amphibole-facies metapelites (SKA = staurolite + kyanite + andalusite + sillimanite) resulted to be particularly useful to investigate the origin of weathering in diverse parts of the Zambezi catchment. Ratios characterizing Lower Zambezi mainstem and tributary sands [$G/(G+SKA) = 72 \pm 21$] are well in line with those observed and expected for modern sands derived from metamorphic basements [$G/(G+SKA) = 70 \pm 20\%$; Garzanti *et al.*, 2006, 2010a]. In contrast, markedly anomalous low ratios [$G/(G+SKA) < 5\%$] invariably characterize river and aeolian-dune sands on the Kalahari Plateau, where common kyanite and staurolite contrasts with the rarity of garnet grains. This indicates almost complete selective chemical breakdown of garnet, a mineral that proves to be extremely vulnerable in equatorial soils (figs. 9C and 9D in Garzanti *et al.*, 2013a) but very durable in dry tropical climate (Garzanti *et al.*, 2015). Even zircon results to be selectively weathered out relative to quartz in recycled sands generated on the Kalahari Plateau, as indicated by their zircon concentration lower by an order of magnitude relative to first-cycle sands generated from mid-crustal basement rocks in the Middle to Lower Zambezi catchment.

Another potentially fruitful approach is offered by surficial dissolution textures on labile ferromagnesian minerals, which provide direct evidence of chemical attack (e.g. Velbel, 2007). This approach, however, has drawbacks: i) surficial features tell us the state of what is preserved but nothing about how much was destroyed; ii) fresh and strongly weathered grains of the same detrital mineral commonly occur jointly (Van Loon and Mange, 2007); iii) slight

degrees of corrosion may not be evaluated consistently by different operators. Only semiquantitative hints on the intensity of weathering can thus be obtained.

In this study, the percentage of surficial etched grains and the degree of corrosion was recorded for over 4000 identified transparent heavy minerals following the classification of Andò *et al.* (2012). In Uppermost Zambezi mainstem and tributaries, pyroxene, amphibole, epidote, staurolite, kyanite, and andalusite are all mainly unweathered, a minority of grains are corroded but only a few pyroxene grains are deeply etched. In the Upper Zambezi mainstem and tributaries, most grains are still unweathered, but the percentage of corroded grains increases and both pyroxene and amphibole may be deeply etched. In the Middle Zambezi mainstem and tributaries, the percentage of corroded heavy minerals increases further, a larger percentage of pyroxene and amphibole grains are deeply etched, and epidote, garnet and kyanite may show deep etching. Similar features characterize Lower Zambezi mainstem and tributary sands, with epidote and garnet even more extensively corroded.

- *Present versus Inherited weathering*

Overwhelming abundance of quartz and durable heavy minerals, abundance of kaolinite, very low G/(G+SKA) ratio, CIA values > 75 in sand and > 80 in mud with $\alpha^{Al}Na$ values > 20, all testify to very high weathering intensity on the Kalahari Plateau drained by the Uppermost Zambezi and Kwando Rivers. These compositional features, typical of sediment generated in hot-humid equatorial climate, are at odds with the semiarid conditions that reign on the plateau today. The weathering effects testified in polycyclic Kalahari sand are thus inherited from much wetter conditions in the past, implying that most of these sediments were originally generated in the subequatorial climatic zone (Garzanti *et al.*, 2022).

Clay-mineral assemblages in river muds across southern Africa are never kaolinite-dominated, reflecting the limited efficiency of soil-forming processes and incomplete feldspar leaching under presently dry climates (Garzanti *et al.*, 2014a). Kaolinite must thus be largely detrital and recycled from widespread Cretaceous to Cenozoic lateritic paleosols and duricrusts (Partridge and Maud, 1987; Moore *et al.*, 2009; Dill, 2007). Even in southern Malawi – where annual rainfall increases westwards from ~0.8 m to 1.6 m at the foot of Mount Mulanje and up to 2.8 m at high elevation (peak 3002 m asl) – the abundance of kaolinite in Shire mud may be largely explained by fluvial incision of relic peneplains of Cretaceous to Cenozoic age triggered by base-level lowering of the Shire River (Dill *et al.*, 2005). This is corroborated by the great abundance of fresh feldspars in Shire sand (fig. 5G in Garzanti *et al.*, 2021a), where very limited plagioclase hydrolysis is testified by undepleted Na and Ca ($\alpha^{Al}Na = \alpha^{Al}Ca = 1.0$).

All mineralogical and geochemical parameters considered to be weathering indicators [e.g. Kao/(Ill+Chl), CIA, $\alpha^{Al}Na$] decrease downstream the Zambezi. Even when depurated from the physical effect of recycling (i.e. quartz addition), mud generated in the Uppermost Zambezi catchment appears to be more weathered than Middle and Lower Zambezi mud (Figure 3.11). Such consistent evidence, however, is not considered to be indicative of presently lower

weathering intensity in the Middle to Lower Zambezi catchment. Rather, it reflects progressive mixing of distilled polycyclic detritus generated on the Kalahari Plateau with detritus from Karoo basalts along the Upper Zambezi, followed by abrupt replacement – downstream of Lake Kariba first and of Lake Cahora Bassa next – by largely first-cycle detritus derived from Precambrian crystalline basements.

Because most sediment of the Lower Zambezi is derived first-cycle from basement rocks (Garzanti *et al.*, 2021a), surficial corrosion of detrital minerals can be interpreted as mostly reflecting present conditions of weathering. Together with weathering trends displayed by cohesive mud (Fig. 12B), these are the only features that suggest a slight increase in weathering intensity from the dry Kalahari to the middle and lower parts of the Zambezi catchment.

3.5 Conclusions

Any compositional parameter is invariably controlled by multiple physical and chemical processes that must be carefully evaluated before provenance and environmental information could be correctly detangled and understood. Diverse datasets obtained by a range of independent methods are thus integrated to constrain the many unknowns, reduce the number of potential alternative solutions, and increase the plausibility of our inferences. Following this rationale, we applied a spectrum of mineralogical, geochemical, and geochronological techniques to shed light on sedimentary processes active in the complex Zambezi big-river system. In this study, such an approach allowed us to: 1) characterize the composition of mud and sand generated in, and transported across, the Zambezi drainage basin; 2) monitor the evolution of compositional signals across a routing system rigidly segmented by both natural (tectonic depressions, lakes, wetlands) and anthropic factors (large reservoirs trapping all sediment generated upstream); 3) make inferences on sediment yields and erosion rates even in the lack of gauged sediment fluxes; 4) assess the intensity of weathering and its origin (i.e. present vs. inherited) in diverse parts of the vast catchment. The age spectra of detrital zircons reflect the four major episodes of crustal growth in Precambrian southern Africa. Irumide ages are dominant in the Lower Zambezi and in most of its tributaries, excepting the Shire and the Zangue Rivers where Pan-African ages prevail. Neoarchean ages characterize the Gwai, Mazowe and Luenha Rivers sourced in the Zimbabwe Craton. Eburnean ages are widely distributed but never prevail. Smectite is the most widespread clay mineral, dominant in muds from Karoo basalts as in the warm and poorly drained Mozambican lowlands characterized by equatorial/winter-dry climate. Illite is prevalent locally (e.g. Kafue mud) and kaolinite is ubiquitous, reaching maximum abundance in both uppermost and lower parts of the Zambezi catchment. Elemental geochemistry reflects overwhelming quartz addition by recycling of Kalahari dune sand in the Uppermost Zambezi, local supply from Lower Jurassic Karoo basalt in the Upper Zambezi, and chiefly first-cycle provenance from Precambrian basements in the Lower Zambezi. The ϵNd values range from only mildly negative for sediments derived from Stenian gabbros, Tonian mafic granulites and Jurassic basalts to strongly negative for sands derived from Neoarchean cratonic gneisses. The concentration of an ultradense Nd-rich mineral (i.e. monazite) in the fine tail of the size distribution owing to the settling-equivalence

effect controls the intrasample ϵNd variability among cohesive mud ($< 32 \mu\text{m}$), frictional silt ($32\text{-}63 \mu\text{m}$), and sand ($63\text{-}2000 \mu\text{m}$) fractions as well as deviations from the theoretical relationships between ϵNd and TNd,DM model ages, suggesting that LREE-rich monazite carries a more negative ϵNd signal than titanite, amphibole, epidote, or apatite characterized by less steep REE patterns. Elemental and isotope geochemistry reveal that 55-65% of mud and sand reaching the Zambezi Delta today, after the river course has been rigidly segmented by the closure of the major Kariba and Cahora Bassa Dams, is supplied by the Mazowe-Luenha River system. Supply from Irumide terranes exposed upstream of the Luenha confluence is subordinate and the role played by the Shire River – the outlet of Lake Malawi – is limited. Although an accurate assessment of sediment yields and erosion rates is hampered by the lack of gauged sediment fluxes, annual estimates are an-order-of magnitude less on the Kalahari Plateau ($10\text{-}20 \text{ tons/Km}^2$ and $\sim 0.005 \text{ mm}$) than in rugged terranes exposing Precambrian basements downstream ($100\text{-}200 \text{ tons/Km}^2$ and $\sim 0.05 \text{ mm}$). All mineralogical [garnet/(staurolite+kyanite+andalusite+sillimanite); kaolinite/(illite+chlorite)] and geochemical parameters (CIA^* , αAlNa) consistently point to an extreme intensity of chemical weathering on the Kalahari Plateau that cannot be referred to the dry climate of today. Selective chemical breakdown of virtually all minerals relative to quartz – including feldspars, garnet that is very labile in lateritic soils, and even zircon especially if strongly metamict – and kaolinite formation do not occur in the dry climate that reigns today on the plateau. 951 Kaolinite is chiefly detrital and produced by fluvial incision of relic Cretaceous-Cenozoic paleosoils even in the Shire catchment closer to the wetter Mozambican coast, where inefficient plagioclase hydrolysis is testified by the dominance of fresh feldspars and undepleted Ca and Na. Indications of slightly increasing weathering conditions in the Middle to Lower Zambezi catchment at present times are provided by mud geochemistry and surficial corrosion of pyroxene, amphibole, epidote, kyanite, and garnet.

CHAPTER 4

MODELLED FUTURE CLIMATIC CONDITIONS AND THE IMPLICATION ON WATER SECURITY: ORANGE & ZAMBEZI RIVER BASINS

4.1 Introduction

This report on deliverable 1.0, modelled future climatic conditions and the implication on water security, is written in the framework of the ‘effects of pliocene-pleistocene climatic changes on evolution of river systems in Southern Africa’ research project, focusing on the Zambezi and Orange River basins. The report is divided in three sections, the hydrological characterisation, future climate modelling and impacts on water security. Figure 4.1 shows the location of the Zambezi and Orange River Basin.

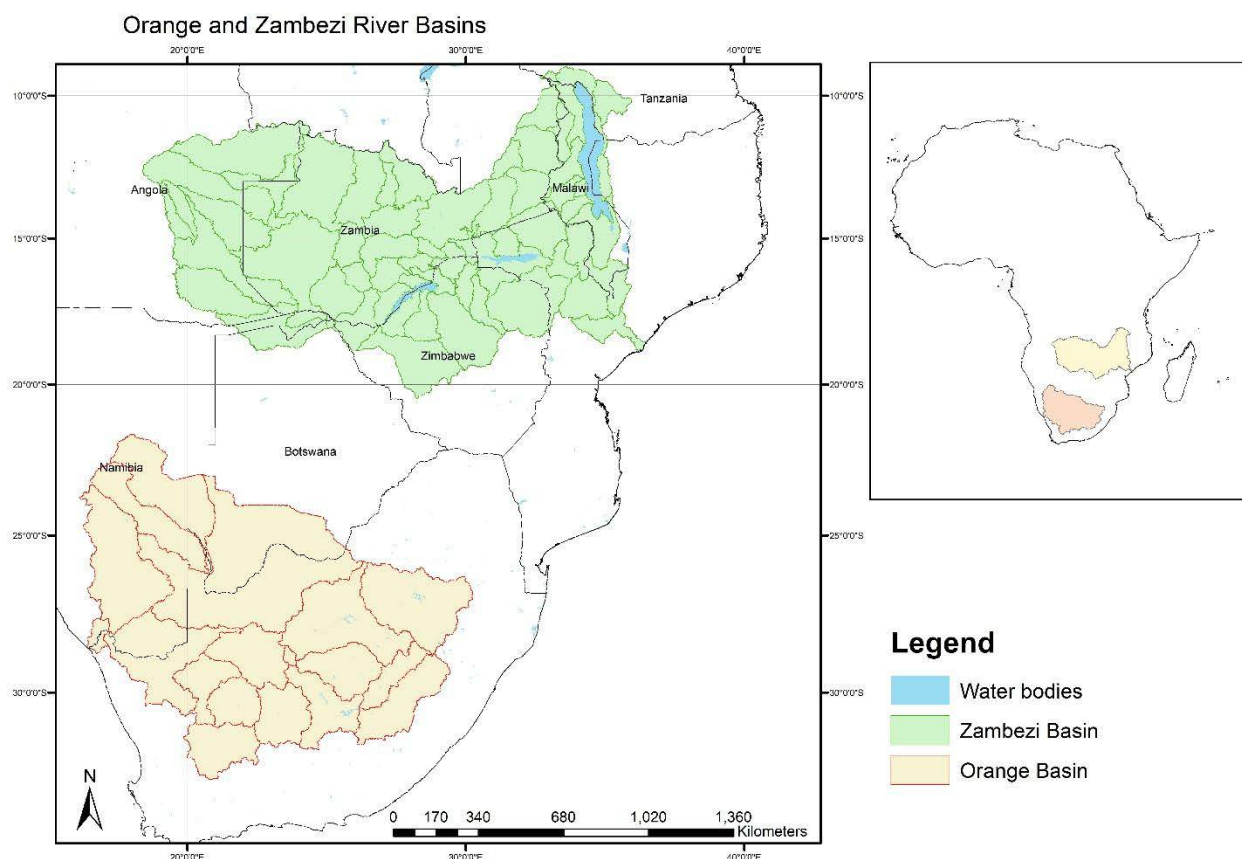


Figure 4.1: The Orange and Zambezi River Basins

4.1.1 Background

The Zambezi River Basin (ZRB), the largest African river systems flowing into the Indian Ocean (Balek, 1977), straddles across eight Southern African countries. The basin is home to about 40 million people predominantly living in Malawi, Zimbabwe, and Zambia (Wirkus and Boge, 2006). The larger part of the basin is occupied by the Central African Plateau which lies more than 900 m above sea level, rising in places near the rim to over 2 500 m (Leenaers, 1991).

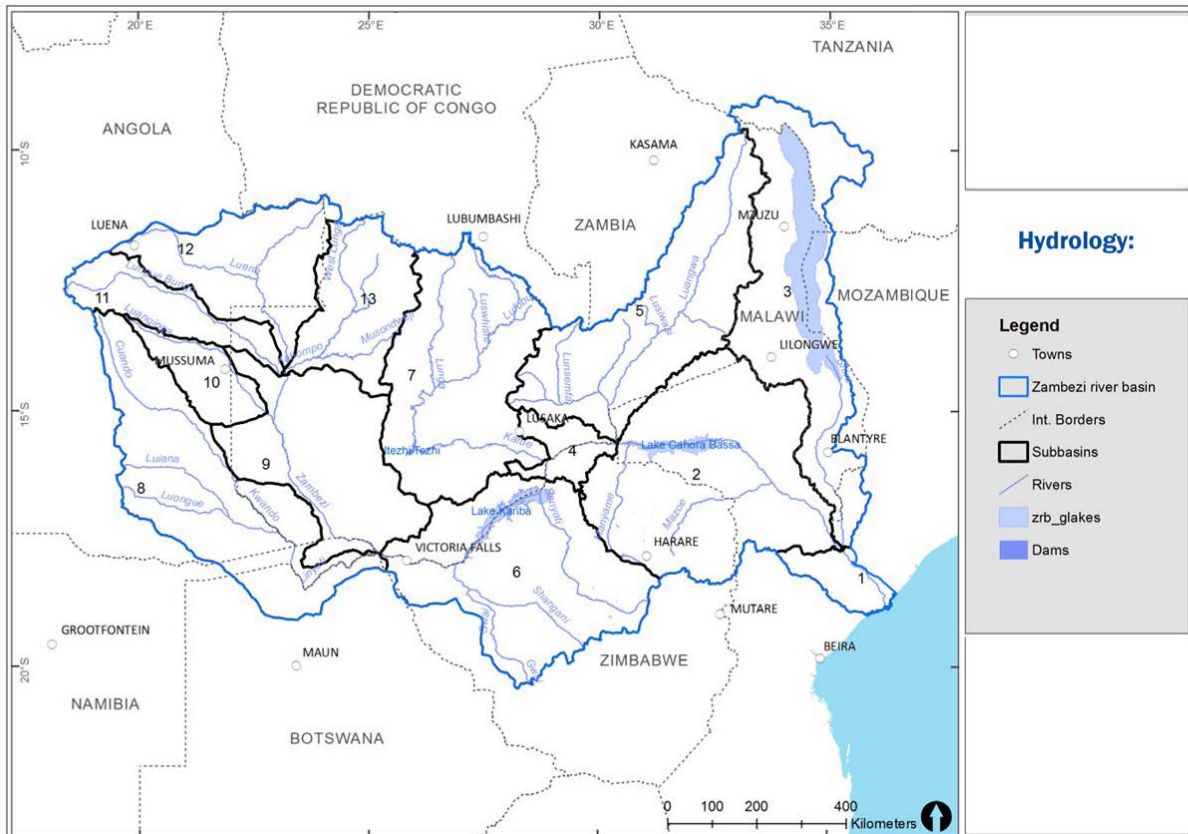


Figure 4.2: The Zambezi River Basin and its 13 subbasins

Based on hydrology and geophysical characteristics the basin can be divided into the upper, middle, and lower ZRB (Chandiwana and Snellen, 1994):

- The Upper Zambezi reach defined as the area above the Victoria Falls. The source of the Zambezi River is a marshy bog near Kalene Hills in Zambia at 1585 m above sea level. The river flows north for about 30 km, then west and southwards through Angola for about 280 km and re-enters Zambia just north of the Chavuma Falls. After the falls the river begins to meander through broad and marshy plains. The last of these plains is the Barotse floodplain. At an altitude of 1000 m the river enters a 100 km stretch of rapids. After the Katima rapids, the Zambezi flows through a sandy plain where it meanders widely and its floodwaters join with those of the Chobe River from Angola, thereby creating another permanent swamp. When the river approaches Victoria Falls it has a mean width of

1350 m.

- The Middle Zambezi reach which stretches between Victoria Falls and Cahora Bassa dam. After the Zambezi River plunges some 100 m down the Victoria Falls, the river flows eastwards for almost 1000 km through gorges and the man-made lakes Kariba and Cahora Bassa. In the middle Basin, the river is joined by its two largest tributary the Kafue and the Luangwa.
- The Lower Zambezi reach, from downstream Cahora Bassa dams until the outfall to the Indian Ocean. At Cahora Bassa, the Zambezi River begins its descent from the Central African Plateau to the coastal plain. The Shire River, which drains Lake Malawi, joins the Zambezi River near Caia. On the Mozambique plain, the river occupies a broad valley with a width up to 7 km. The river may flow in several channels in the dry season, which merge again into a single river in the wet season. The delta of the Zambezi is wide, marshy and obstructed by sandbars.

The riparian countries of the Zambezi basin have different levels of wealth, population, literacy, and access to clean water and sanitation. Furthermore, they are all plague with by the lack of information about available water resources and their uses. The increasing demand for water is a concern because of population growth, exceedingly rapid urban and increasing irrigation to increase food production, climate variability and change.

The Orange Basin, located in Southern Africa, covers almost 3% of the continent and spreads over four countries (Figure 4.1 and Table 4.1). It encompasses nearly all of Lesotho, half of South Africa, a quarter of Namibia, and part of Botswana. The source of the Orange River is in Lesotho. The river receives water from the Makhaleng tributary just before entering South Africa. The Caledon tributary flows on the border between South Africa and the north of Lesotho and flows into the Orange River further downstream in South Africa. The average annual runoff from Lesotho to South Africa is estimated at 4.73 km³/year, which is far in excess of the country's water requirements. As the Orange River passes the Lesotho Highlands at about 3300 m above sea level, it is called the Senqu River, and is the country's primary water source. In spite of only 3% of the Orange River basin being in Lesotho, Lesotho provides much of the water filling the Orange River because of its high mean annual rainfall. Almost the entire plateau of South Africa, representing over 48% of the area of the country, is drained by the Orange River and its tributaries, though they contribute only about 22% of the total runoff of South Africa. Further, the 64% of the Orange River Basin area located in South Africa also provides that country's main water supply.

Table 4.1: Orange basin: areas and rainfall by country

Country	Total area of the country (km ²)	Area of the country within the basin (km ²)	As % Of total area of basin (%)	As % of total area of country (%)	Average annual rainfall in the basin area (mm)		
					min.	max.	mean
Botswana	581730	71000	7.9	12.2	165	520	295
Namibia	824900	219249	24.5	26.6	35	415	185
Lesotho	30350	30350	3.4	100.0	575	1040	755
South Africa	1221040	575769	64.2	47.2	35	1035	365
For Orange basin		896368	100.0		35	1040	325

Sources: (FAO, 1997)

The Orange River is a part of the South Africa-Namibia boundary and several seasonal rivers in Namibia form tributaries of the Orange River. These include; the Fish, Auob, and Nossob Rivers. The most important tributary entering from Namibia is the Fish River, on which the Hardap dam was constructed in 1972. Botswana has the smallest part of the Orange River, and with its low rainfall, the country contributes the least water to the river. The Orange River itself does not flow in Botswana. A small part of southwestern Botswana is drained by the Molopo River, which is part of the Orange River Basin. The Molopo, which forms the border between Botswana and South Africa, is a fossil river, which once flowed into the Orange River. Now it receives most of its very occasional flows from its tributaries in the northern Cape province of South Africa. It is a seasonal river in a very dry area and has not flowed into the Orange River in living memory. Infrastructure development on the Orange River is extremely high, with the river boasting of 29 dams and reservoirs to control its flow, and extensive infrastructure for inter-basin transfers of water. It is estimated that major withdrawals and high evaporation have reduced the natural flow by half (Langea *et al.*, 2006). The dams on the Orange River are mostly used to regulate flows, irrigation and to produce hydroelectric power. With the exception of the water flow along the Vaal River, very little of the Orange River water flow is used for industrial or domestic purposes. The Vaal River is said to be the most important tributary of the Orange River as it supplies water to most of South Africa's industries and its largest population center in Johannesburg. It is the major tributary of the Orange River and the average annual runoff in the Vaal basin area is about 4.27 km³, of which 2.15 km³ is exploitable. Hence, most of the river water is fully utilized and contributes less to the flow of the Orange River except during times of heavy floods. For management and planning purposes, notably in South Africa's National Water Resources Strategy (DWAF, 2004), water authorities separate the Vaal River Basin from the Orange River Basin, treating it as several independent water management areas (WMAs). The Orange River is itself divided into two WMAs at the point where the Vaal River joins it. The Upper Orange River includes the Orange-Senqu River in Lesotho and part of South Africa above the Vaal confluence. The average annual runoff of

the Orange basin, excluding the Vaal River, is estimated at 7.59 km³, of which 5.76 km³ is exploitable. The Lower Orange River includes part of South Africa below the Vaal confluence, as well as parts of Botswana and Namibia (Langea *et al.*, 2006).

4.2 Hydrological features of the basins

The Zambezi Basin has the following hydrological features: reservoirs, lakes, rapids, waterfalls, islands, rivers and wetlands.

4.2.1 Rivers

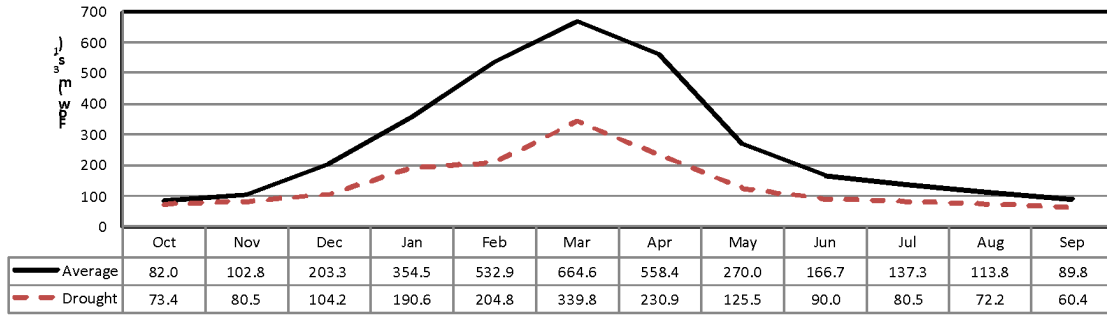
The ZRB has several rivers but in this section, we will only briefly discuss the tributaries draining the 13 subbasins. The volume of annual renewable water resources in the Zambezi River is estimated at 4 134 m³.s⁻¹ or 94 mm of equivalent rainfall, which is about 10% of the average rainfall in the basin (956 mm) with the Northern part of the basin being wetter than the south and therefore contributing more water (about 60% of the total flow). Average annual actual evapotranspiration is 870 mm; it ranges from 1 000 mm in the Luangwa, Shire and lower parts of the basin to 500 mm in the southwestern parts of the basin (Savenije and van der Zaag, 1998). The large Cuando /Linyanti/Chobe system (148 994 km², covering the Angolan Southern plateau and the Caprivi in Namibia and Botswana) in the south-west of the basin contributes less than 2 m³.s⁻¹ as most of the flow is lost through evaporation in its swamp systems (Belfius, 2001).

Table 4.2: Estimates of flow contributed by the main tributaries of the Zambezi River (World Bank, 2010)

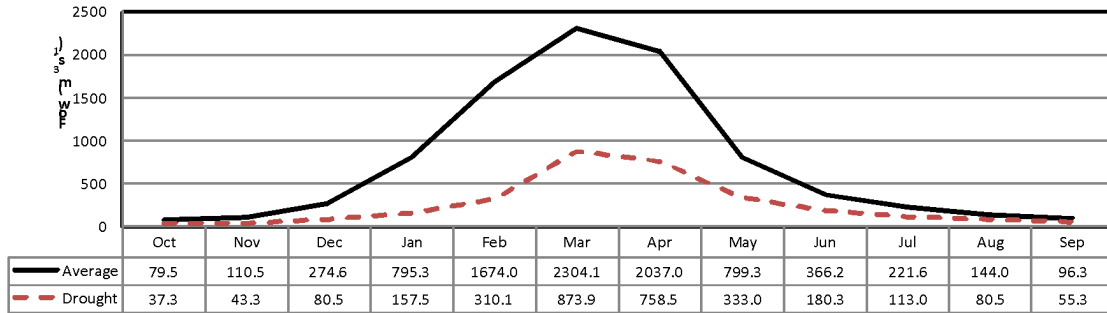
Basin no.	Subbasin	Catchment Area (km ²)	Discharge (m ³ .s ⁻¹)	Runoff depth (mm)	Cumulative Discharge (m ³ .s ⁻¹)
1	Zambezi delta	18,680	113	191.3	4,134
2	Tete	200,894	1,193	187.3	3,523
3	Shire	149,159	498	105.3	4,021
4	Mupata	23,483	54	72.5	1,812
5	Luangwa	159,615	518	102.3	2,330
6	Kariba	172,527	206	37.6	1,386
7	Kafue	155,805	372	75.3	1,758
8	Cuando/Chobe	14,8994	0	0.0	1,198
9	Barotse	115,753	-17.6	-4.8	1,180
10	Luanginga	35,893	69.4	61.0	1,198
11	Lunga	44,368	114	80.8	1,129
12	Upper Zambezi	91,317	742	256.2	1,015
13	Kabompo	78,683	273	109.4	273

The Cuando River flows through the Caprivi Strip and joins the Chobe River in Botswana. The Okavango-Chobe River system joins the Zambezi River through the Okavango-Chobe Lake. Flow analysis shows that there is an interaction of flow between the Okavango-Chobe system and the Zambezi River such that during high flows, the Zambezi River flows into the Okavango-Chobe system and vice-versa (Matondo and Mortensen, 1998). Table 2 shows estimates of the flow contributions by the main subbasins of the Zambezi River. Runoffs generated by the different tributaries over the basin vary considerably and have pronounced seasonality (Table 4.2 and Figure 4.3). As indicated in Figure 4.3, all the major tributaries are perennial.

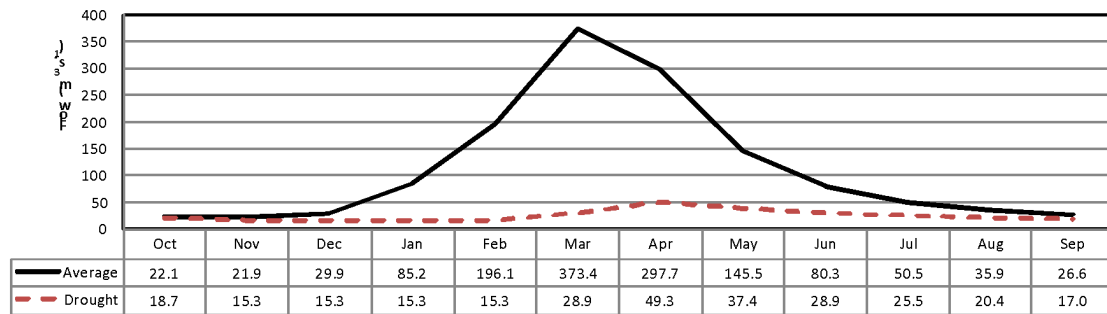
Mean monthly flow in subbasin 13: Kabompo



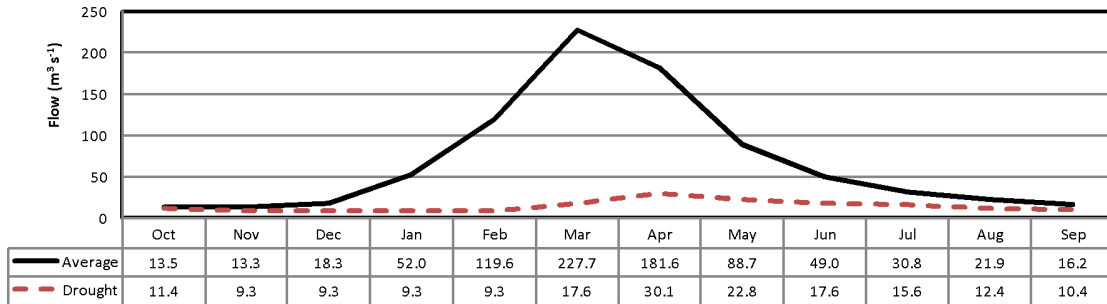
Mean monthly flow in subbasin 12: Upper Zambezi



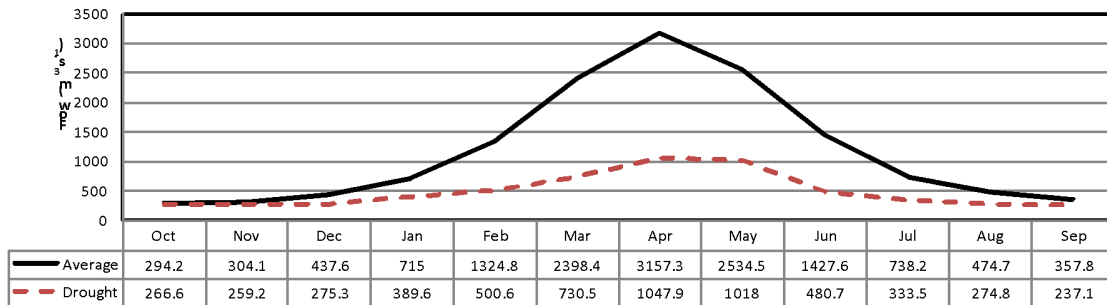
Mean monthly flow in subbasin 11: Lungúe Bungo



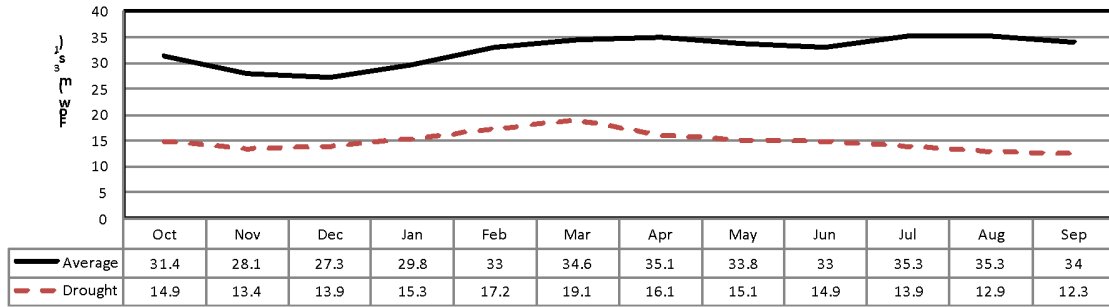
Mean monthly flow in subbasin 10: Luanganga



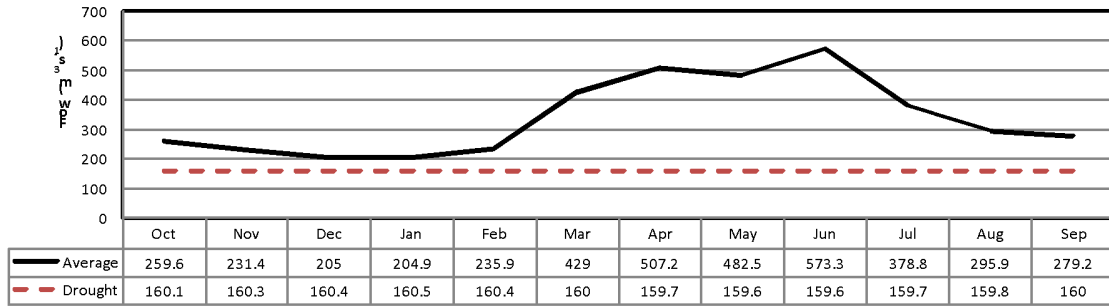
Mean monthly flow in subbasin 9: Barotse



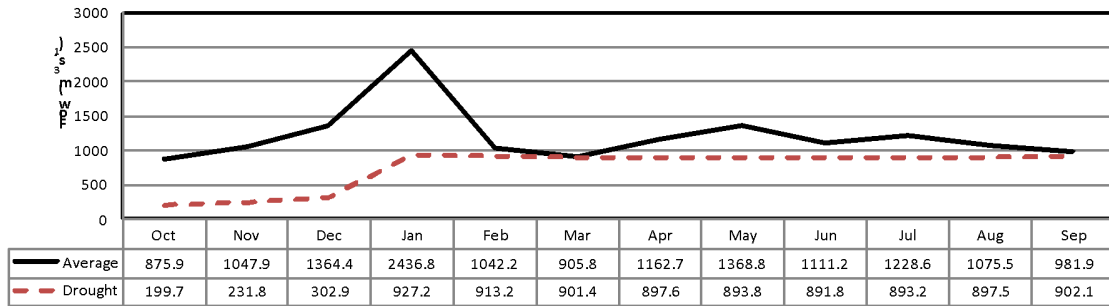
Mean monthly flow in subbasin 8: Cuando/Chobe



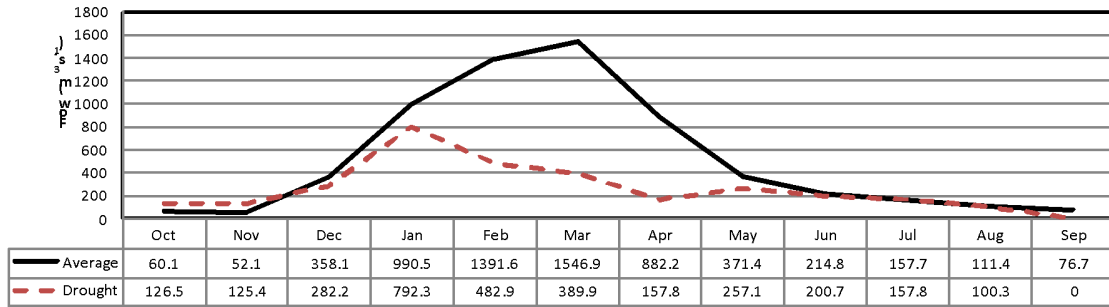
Mean monthly flow in subbasin 7: Kafue



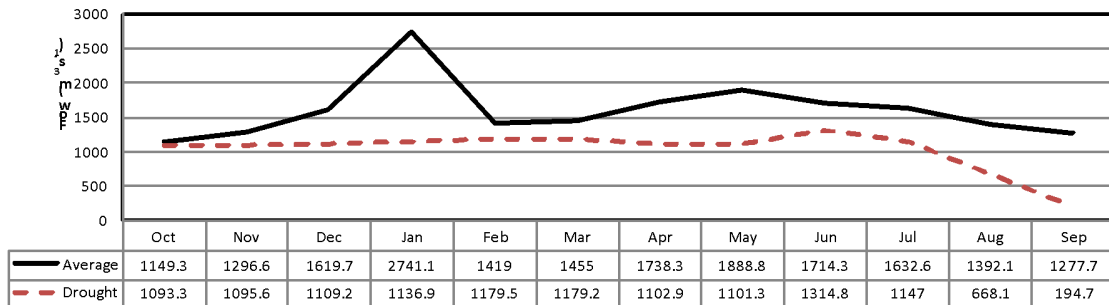
Mean monthly flow in subbasin 6: Kariba



Mean monthly flow in subbasin 5: Luangwa



Mean monthly flow in subbasin 4: Mupata



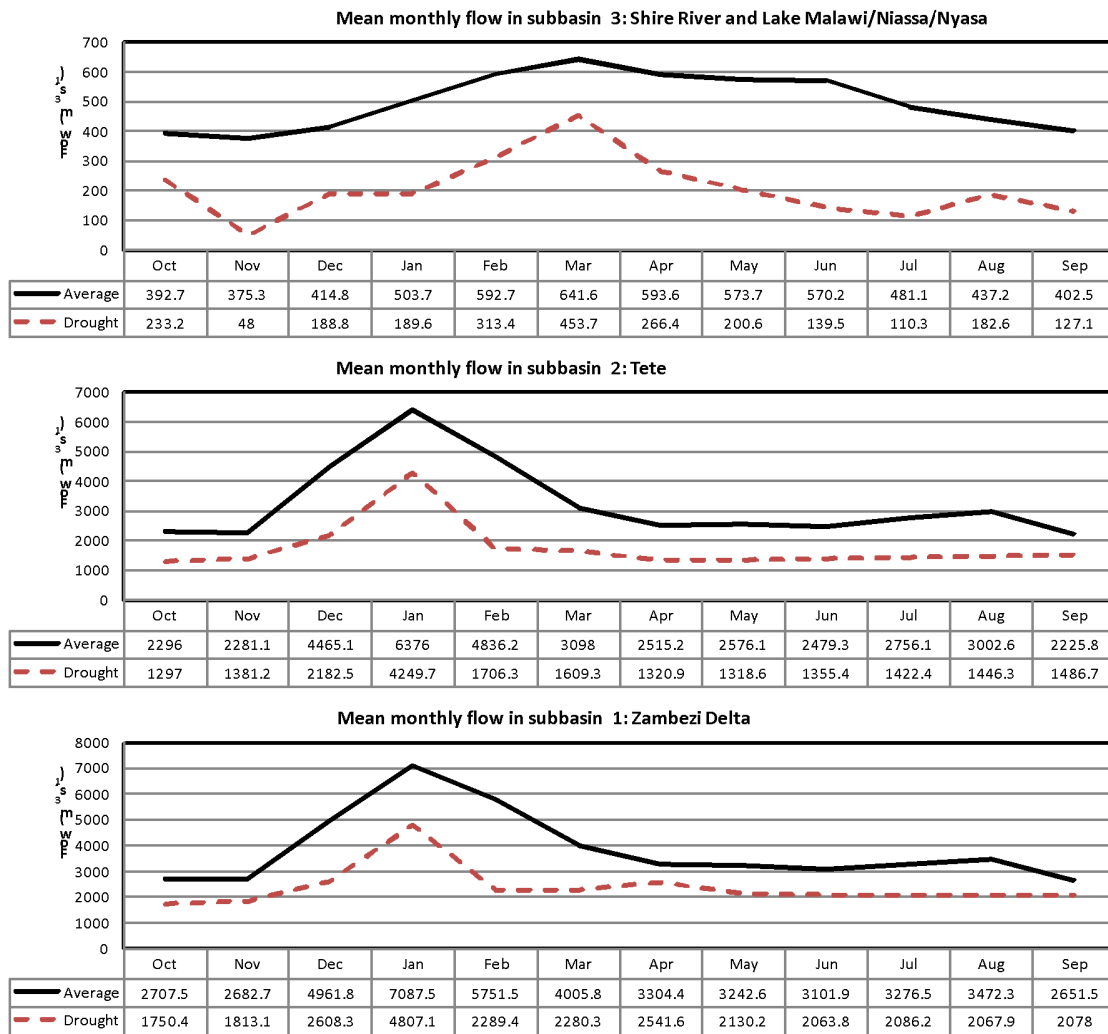


Figure 4.3: Mean monthly flow hydrograph of the 13 subbasins of the ZRB and flow hydrograph of the 1991-1992 drought (World Bank, 2010).

The Kabompo, Upper Zambezi, Lungué Bungo, Luanginga and Kafue subbasins are headwater catchment with floods occurring shortly after heavy rainfall. There is a lag time of around three months between peak rainfall and peak runoff (compared with one month in upstream subbasins). The large Barotse floodplain, located downstream of these subbasins significantly attenuates the flows and leads to high rates of evaporation thus generating a net loss for the Barotse subbasin. The Cuando/Chobe subbasin, the driest catchment of the basin, contributes only 1 percent flows. Roughly located in the middle of the basin, the Kariba subbasin has the lowest mean annual precipitation (MAP) of the basin. The Kariba dam regulates the flows and extends the lag between peak rainfall and the subsequent flood peak to four months. The Mupata subbasin has a lag time between rainfall and floods consistent with those of Lake Kariba and the upstream subbasins of Kariba, Kafue, Barotse, and Kafue Flats. The Luangwa subbasin generates considerable runoff because of a high MAP and a large surface drainage area. The Luangwa river floods from February to April. The lag between rainfall and floods is usually short, although the length of the Luangwa river can extend it. Unlike other subbasins, the Shire has high rainfall in two non-consecutive months, January and March, and thus often experiences two flood peaks. The Tete subbasin accumulates all the flow from basin except

that from the Shire subbasin. The Lake Kariba and Cahora Bassa largely control floods at the outlet. The lack of flow gauges, along with uncertainty regarding catchment boundaries, makes it difficult to determine the incremental contribution of the delta area.

4.2.2 Reservoirs

As alluded above, the Kariba and Cahora Bassa, drastically regulate the flows of the Zambezi River main stem (Figure 4.4). The Kariba dam alone has a degree of regulation exceeding 300% (Lehner *et al.*, 2011).

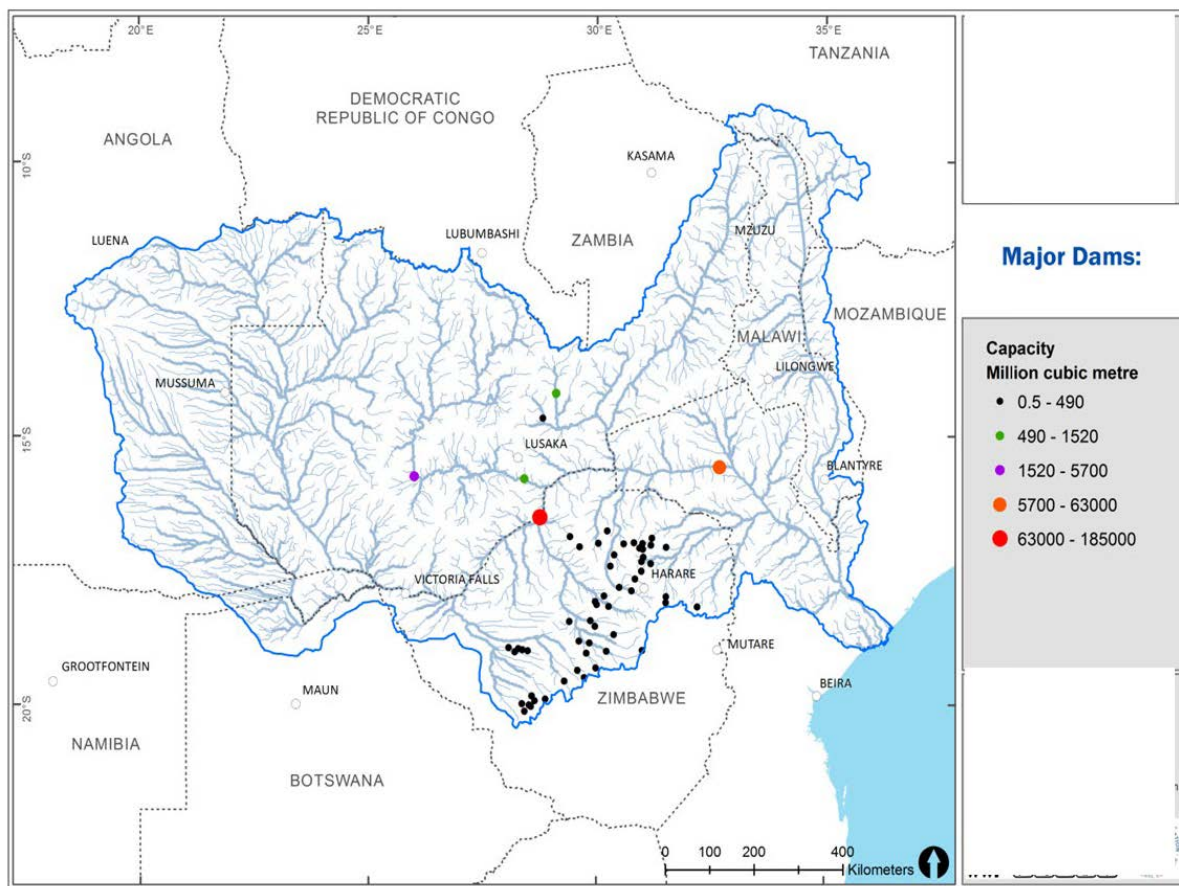


Figure 4.4: Major dams of the ZRB

NB: There are 59 major dams, mostly used for irrigation, in the ZRB: 53 in Zimbabwe, 4 in Zambia and 1 in Mozambique, with Kariba shared between Zambia and Zimbabwe.

In addition to the two big reservoirs, there are several impoundments in the Zimbabwean part of the ZRB, mostly located in the headwaters of the main tributaries (Figure 4.4). It should be noted that the numerous small farm dams built in the Zimbabwean part of the basin are not incorporated.

4.2.3 Rapids and waterfalls

The ZRB as its fair share of rapids and waterfalls (Figure 4.5). In the upper Zambezi basin, the Victoria, Sioma, Chavuma and Nyamboma falls and Katambora rapids are important falls and rapids.

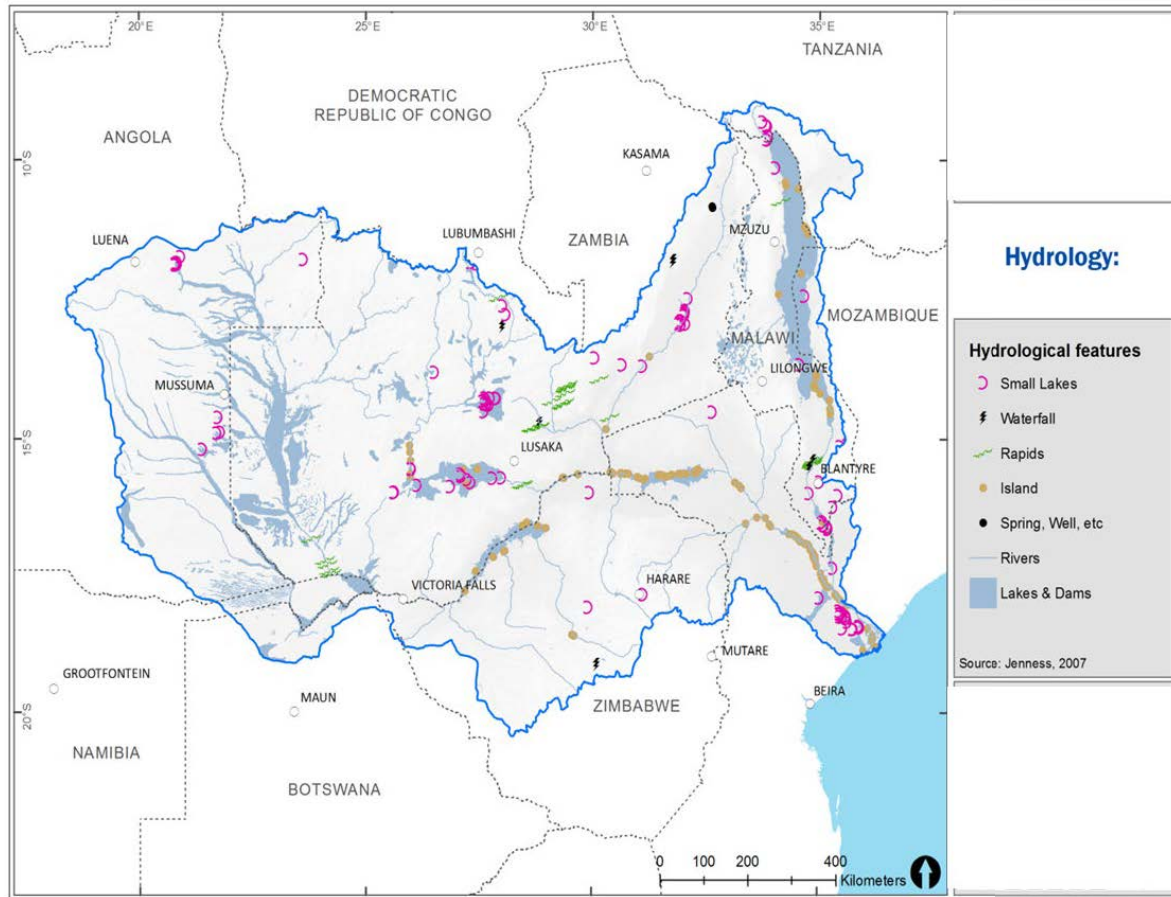


Figure 4.5: ZRB maps of hydrological features: dams, waterfalls, rapids, islands, springs, rivers, lakes (Jenness et al., 2007)

In the Lower ZRB, the Shire River leaves Lake Malawi and wanders across the upper valley before descending through the Murchison Cataracts, the Mpatamanga Gorge to the Kapichira Falls.

4.2.4 Wetlands

There are several wetland types in the Zambezi basin: floodplains, swamps, marshes, dambos and riverine wetlands. Dambos are complex shallow streamless depressions generally found at the headwaters of drainage systems (Mäckel, 1974). The riverine type is the largest by area to which most subsistence utilisation of wetlands in the Zambezi is associated with

(Seyam *et al.*, 2001). The following wetlands described in the following subsections are listed as Ramsar sites (Ramsar, 2012).

- Wetlands of the upper Zambezi

Swamps/marshes occur in the Chobe/Linyati system and Barotse plains. Notable swamps/marshes are Chobe and Linyati (51.3 km²) on the Namibia/Botswana border; Savuti (0.3 km²) in Botswana; Kabompo (18 km²), Lungué Bungo (\pm 10 km²), Luena (8.97 km²), Nyengo (7 km²), Lueti (1.4 km²) and Lui (2.35 km²) river swamps in Zambia. The Zambezi River and its tributaries seasonally inundate the Swamps/marshes. Most streams support floodplains of varying sizes, the most important being the Barotse floodplain (77 km²). The Sesheke-Maramba (15 km²) on the Zambia/Namibia border and the Cuando (4 km²) in Angola are also important floodplains.

- Wetlands in the Middle Zambezi Reach

The Kafue flows through the Lukanga (21 km²) and Busanga (6 km²) swamps. In addition to these two swamps, the Kafue River supports the Kafue flats (56.6 km²). In the Luangwa subbasin, the Luangwa River supports an extensive floodplain often known as Luangwa Valley wetlands.

- Wetlands in the Lower Zambezi Reach

Shoreline plains are associated with lakes Malawi (Karonga lakeshore plain, Limpasa dambo, Nkhotakota lowlands and Salima lakeshore plain), Chiuta, and Chilwa. The Shire River system supports the Elephant marsh (7.4 km²) and the shire wetlands downstream of the Lake Malawi in the Shire valley. Finally, the Zambezi River support the Zambezi delta (13 km²) at the river mouth in Mozambique. A conservative estimate of the total use value of the Zambezi wetlands indicates that fish production, floodplain recession agriculture, natural products and livestock grazing account for the main share in the total use value of the Zambezi wetlands.

Table 4.3: Total use values of the Zambezi wetlands (Seyam *et al.*, 2001)

Wetland service or product	(1)	(2)	(3)	(4)	(5)	(6)	(7)	
Marginal value (USD/ha/year)	128	51	0.12	9	0.66	0.11	66	Total use of the wetland
Area contribution to the service %	10%	40%	*	40%	30%	*	10%	
Wetland	Total use value of the wetland service or product (10 ⁶ \$ yr ⁻¹)							(10 ⁶ \$ yr ⁻¹)
Barotse plain	11.6	18.4	0.01	3.3	0.178	0.01	5.9	39
Kafue	8.3	13.3	0.01	2.4	0.129	0.007	4.26	29
Liuwa plain	4.5	7.2	0	1.3	0.069	0.004	2.3	15
Luangwa	3.2	5.1	0	0.9	0.05	0.003	1.64	11
Lukanga	3.2	5.1	0	0.9	0.05	0	1.64	11
Cuando	2.6	4.1	0	0.7	0.04	0.002	1.31	9
Busanga	0	0	0.02	0	0.04	0.02	1.31	1
Luena	1.4	2.3	0	0.4	0.022	0.001	0.72	5
Caprivi-chobe	0.3	0.4	0	0.1	0.004	0.002	0.13	1
Total	36	57	0.05	10	0.6	0.05	20	123

(1): Floodplain recession agriculture; (2): Fish production; (3): Wildlife services and goods; (4): Livestock grazing; (5): Eco-tourism; (6): Biodiversity; (7): Natural products and medicine. * Completely protected wetlands are assigned a fraction of 90%, partly protected areas 10% and not protected areas are assigned a fraction of 0%.

4.3 Hydrological Modelling

Given the paucity of data in the Zambezi basin, such as poor distribution of hydro-meteorological stations to perform catchment assessments, hydrological modelling is often done. Most hydrological models utilize remotely sensed data products with inherent errors. The research team have access to a hydrological model for the Zambezi River Basin based on the Pitman rainfall-runoff monthly model (Hughes *et al.*, 2006). One of the advantages of the version is the incorporation of a wetland module. This is critical considering the number of wetlands present in the ZRB. There exist large expanses of wetlands in the Kafue and Cuando parts of the basin and their hydrology is a challenge/challenging to represent. To conserve the physical integrity of the model, the parameters of the model have been quantified based on methods proposed by Kapangaziwiri and Hughes (2008). Initially, the model was set up for the rest of the Zambezi basin and was driven by CRU rainfall datasets. This global data set provided a uniform data set that covered the whole basin though the resolution is rather coarse (0.25° x 0.25°). With this dataset, the model was run for a 100-year period from January 1901 to December 2001. Where observations were available, model results were compared with these to assess the model's ability to reproduce the hydrology of the subbasin under consideration. The modelling results are shown in Table 4.3.

Table 4.4: Summary of the modelling statistics of the main subbasins of the ZRB based on CRU rainfall.

Subbasin	Precipitation (CRU) (mm)	Mean Monthly Obs Flow ($\times 10^6 \text{ m}^3$)	Mean Monthly Sim Flow ($\times 10^6 \text{ m}^3$)	Mean Annual Recharge (mm y^{-1})	Mean Mon Baseflow ($\times 10^6 \text{ m}^3$)	BFI (%)	Recharge %
Cuando	606	87.73	85.27	4.88	1.17	1.75	0.81
Gwai	662	62.19	60.60	30.77	2.12	3.50	4.49
Kabompo	1117	913.10	596.60	443.04	36.92	10.13	39.66
Kafue 1	798	726.70	750.50	36.96	21.23	2.83	4.63
Kafue 3	836	923.50	851.10	29.28	48.00	5.64	3.50
Kafue 4	963	434.30	435.20	40.62	30.25	6.95	4.22
Kasaka	778	-	27.95	30.12	4.52	16.18	3.87
Luanginga	908	155.44	139.48	3.06	2.24	1.61	0.34
Lufwanyama	1198	366.60	362.20	46.78	19.53	5.39	3.91
Lunga	1115	233.03	214.03	306.48	57.2	26.73	27.48
Luswishi	1202	50.19	53.48	15.61	8.68	16.23	1.30
Manyame	806	60.04	56.11	32.21	1.96	3.50	4.00
Mupfure	738	31.19	36.23	4.34	8.34	23.02	0.59
Namitete	1320	75.21	85.26	116.57	19.41	22.77	8.83
Zambezi 10	786	3059.32	3169.96	22.85	149.00	4.70	2.91
Zambezi 11	969	1797.98	1803.46	28.30	5.35	0.30	2.92
Zambezi 12	1087	1587.43	1488.95	36.88	11.12	0.75	3.39
Zambezi 3	1222	5760.97	6042.65	3.14	4.61	0.08	0.26
Victoria Falls	749	3185.13	3134.96	8.45	3.37	0.11	1.13

The highest baseflow contributions to surface flow were modelled in Lunga, Namitete and Mupfure subbasins, the same well-watered basins that have higher groundwater recharge values. The baseflow index (BFI), also referred to as the reliability index is a non-dimensional ratio which is defined as the volume of baseflow divided by the volume of total streamflow or alternatively, as the ratio between the average discharge under the separated baseflow hydrograph and the average discharge of the total hydrograph (Smakhtin, 2001). Catchments with high groundwater contribution to streamflow have a BFI close to 1 while, ephemeral rivers have BFI equal to zero. The BFI is shown spatially in Figure 4.6.

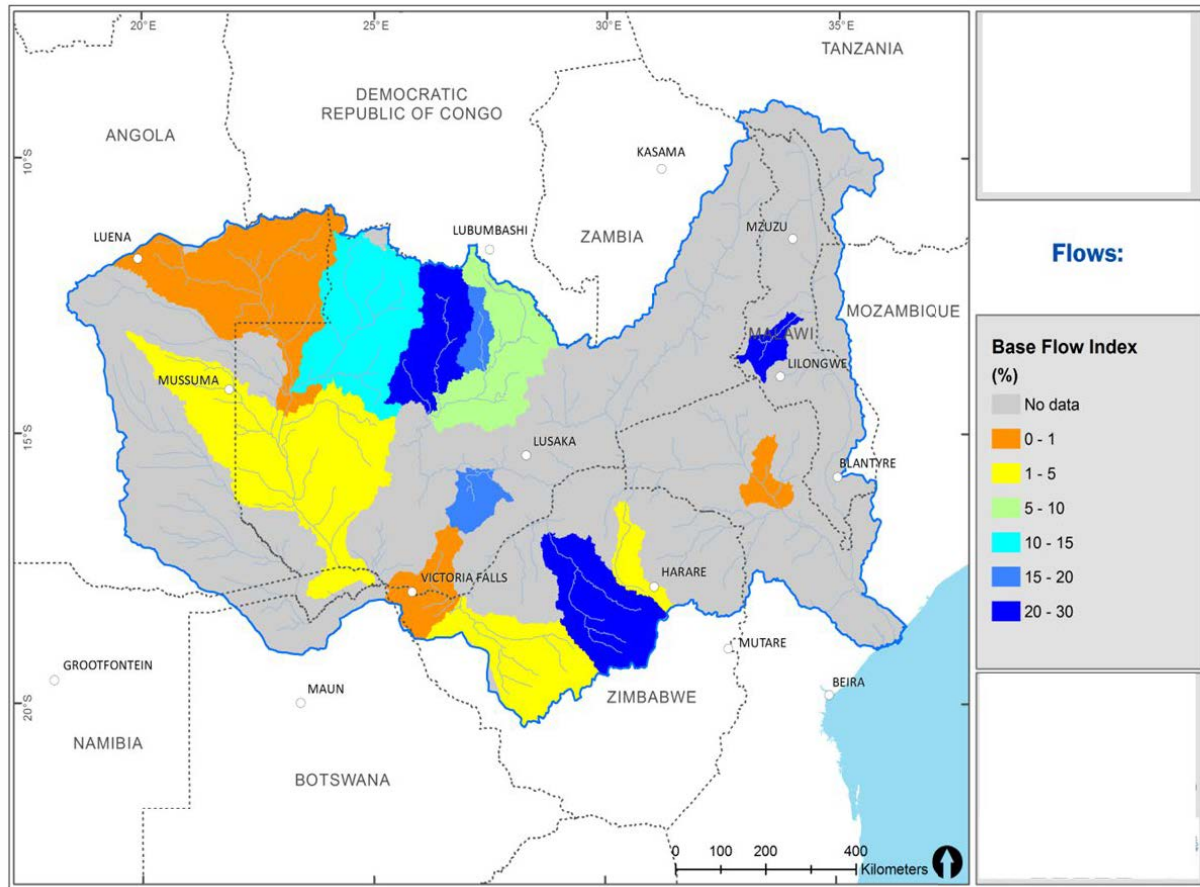


Figure 4.6: Baseflow index of tributaries of the ZRB

There are subbasins where baseflow is very low and almost zero. Arid subbasins such as the Gwai and Cuando have very low baseflows. The geology of the basin can also be used to explain the low contribution of baseflow. Precambrian and basement complex rocks predominantly underlie the basin.

4.4 Climate Modelling of the Zambezi and Orange Basin

The observed increase in greenhouse gas emissions leading to increased global warming is expected to impact on the quantity and quality of water resources and eventual water security in many parts of the world. Research has shown that the global and regional hydrological cycles have been highly affected by climate change in the past century (Brutsaert and Palange, 1998; Scanlon *et al.*, 2007; Solomon *et al.*, 2007). The created scenarios for greenhouse gas emissions by Nakicenovic *et al.* (2000) indicated increased temperatures and changes in global precipitation patterns because of climate change. Estimating changes in future precipitation patterns becomes highly uncertain the further projections are made into the future and is dependent on the nature of global or regional climate models used. When assessing the impacts of climate change on Water resources, hydrological models have been commonly used. In this study, multiple global and regional climate models were used to systematically assess the future climatic trends in the Zambezi and Orange River basins for purposes of projecting the future state of water security in the two basins.

Regional and local climates are linked to water resources through the hydrological cycle. Studies conducted have already established the vulnerability of hydrology to climatic changes (IPCC, 2007; Bates *et al.*, 2008; Kumar *et al.*, 2011). Projected changes in climate could intensify impacts observed in various water resources, and the severity of impacts may only be ascertained by modelling future impacts on local water resources. Bates *et al.* (2008) reported that with a rise in temperature, precipitation amounts will increase in high latitudes and decrease in the lower latitudes. With the increasing temperature and evaporation, the general observations are that runoff generally is reducing but not everywhere (Bates *et al.*, 2008). This runoff is the water that remains available for use after precipitation. Hence, climate change through changes in evaporation may alter the redistribution of precipitation between what returns to the atmosphere, runs in rivers and oceans or infiltrates into the ground. Studies have predicted a severe water scarcity problem impending for Africa (Falkenmark, 1986ab; 1987; 1989). In terms of these predictions, large parts of Southern Africa are expected to be severely affected (DWAF, 1997). In view of this, the study aims at modelling the impact of future climate change on water security in the Zambezi and Orange River basins by creating scenarios and generating various indices that will help understand and predict the future state of water security in the two basins.

4.4.1 Sources of data

The climate change impact on future climatic conditions and water security in the Zambezi and Orange River Basin will be studied using precipitation, minimum and maximum temperature. The sources of the meteorological parameters will be the CORDEX (Coordinated 15 Regional Climate Downscaling Experiment) African Domain (AFR-44) (Figure 4.7) and Climate Research Unit Time series version 4.03 (CRU TS v4.03). The CORDEX provides global coordination of high-resolution, historical, and future climate projections for improved regional climate change adaptation and impact assessment. It also aims to improve our understanding of climate variability and changes at regional scales by providing higher-resolution RCM simulations for 14 domains around the world (Lee *et al.*, 2018).

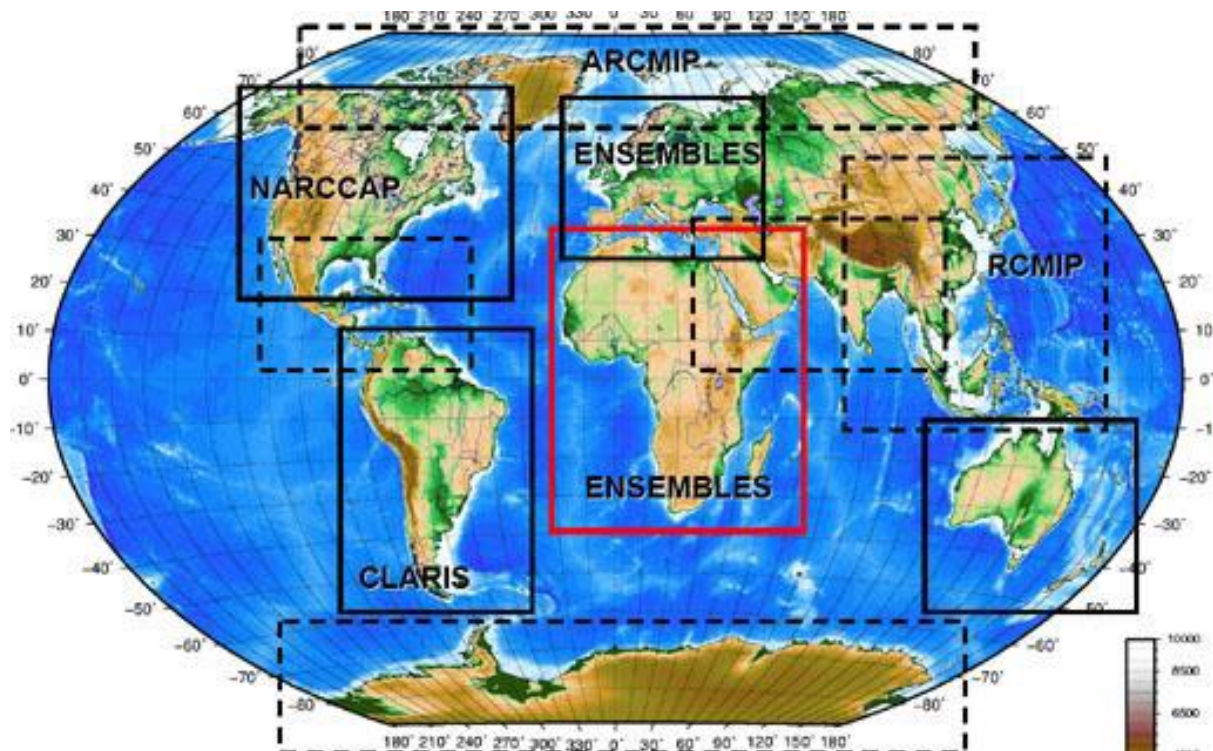


Figure 4.7: CORDEX African domain

4.4.2 Regional Climate Models Data

Most climate change projections are developed using Global Climate Models (GCMs) that generate average temperature changes that can be expected to occur over decades and far into the future at relatively coarse spatial resolution (Cooney, 2012; Lee *et al.*, 2018). Furthermore, GCMs have very coarse spatial resolution and extreme weather events may appear less powerful than those happening in real time. Downscaled Regional Climate Models (RCMs) provide scenarios for climate change adaptation planning at local and regional level. Downscaling of climate models tries to bridge the gap between global and local effects by layering local-level data over larger-scale climate models. RCMs are developed based on dynamic formulations using initial and time-dependent lateral boundary conditions of GCMs to achieve a higher spatial resolution (Chen *et al.*, 2011). Cooney (2012) reiterated that Regional Climate Models (RCMs) are being used to simulate extreme weather events such as heat waves, heat stress, heavy rains, and droughts, which occur at regional scale. Regional downscaling can simulate extreme weather events on the smaller scale because researchers input environmental processes (e.g. wind flow, rainfall) that are specific to that area. The RCM may provide baseline and future climate scenarios of the likely climate change (Buontempo *et al.*, 2015) in the Orange and Zambezi River basins.

One RCM (SMHI-RCA4) driven by seven Coupled Multi-Intercomparison Project Phase 5 (CMIP5) GCMs (CCCma-CanESM2, IPSL-IPSL-CM5A-MR, MIROC-MIROC5, MPI-M-MPI-ESM-LR, NCC-NorESM1-M, MOHC-HadGEM2-ES, NOAA-GFDL-GFDL-ESM2M)

and two scenarios (RCP4.5, RCP8.5), Table 5, used in this study was extracted from the CORDEX Africa domain (AFR-44). The RCM simulation runs at 0.5o spatial resolution of daily precipitation, minimum and maximum temperature covers 1980-2010 (baseline scenario) and 2020-2050 (future climate scenario). The 50 km resolution CORDEX African-domain RCMs was used to generate a seven-member ensemble of climate projections for the Orange and Zambezi River Basins. The Representative Concentration Pathways (RCPs) depicts greenhouse gas concentration trajectory adopted by the Intergovernmental Panel on Climate Change (IPCC) during the fifth Assessment Report (AR5) in 2014 (IPCC, 2014). The RCP4.5 represents intermediate GHG emissions (650 ppm CO2 eq) while RCP8.5 represents very high GHG emissions (1370 ppm CO2 eq).

Table 4.5: SMHI-RCA4 Africa CORDEX 50 km matrix

GCM	Historical 1950-2005	RCP8.5 2006-2100	RCP4.5 2006-2100
EC-Earth	✓	✓	✓
HadGEM	✓	✓	✓
CNRM	✓	✓	✓
MIROC5	✓	✓	✓
NorESM	✓	✓	✓
CanESM	✓	✓	✓
GFDL-ESM	✓	✓	✓
MPI-ESM	✓	✓	✓
IPSL-CM	✓	✓	✓

4.4.3 Climate Data Operators

The Climate Data Operators (CDO) were used to merge the modelled data. The CDO represents a set of statistical and arithmetic commands useful for processing atmospheric data in GRIB and NetCDF format and was developed at Max Planck Institute for Meteorology (Schulzweida *et al.*, 2010). R Programming software was used for graphing the outputs from the analysis. The CDO was used to generate and compute the multi-model ensemble and climate extreme indices, respectively

4.4.4 Observations

The Climate Research Unit (CRU) Time-series (TS) version 4.03 of high-resolution (0.5 x 0.5 degree) gridded datasets of monthly-by-month variation of precipitation, minimum, and maximum temperature (Jan 1901-Dec 2018) were extracted from [https:// crudata.uea.ac.Uk /cru/ data/ hrg/ cru_ts_4.03 /cruts. 1905011326.v4.03 /](https://crudata.uea.ac.uk/cru/data/hrg/cru_ts_4.03/cruts.1905011326.v4.03/) (Harris and Jones, 2020). The CRU

TS4.03 data have been produced using angular-distance weighting (ADW) interpolation and the data are monthly gridded fields based on monthly observational data calculated from daily or sub-daily data by National Meteorological Services and other external agents (Harris and Jones, 2020). The extracted NetCDF data files contain monthly mean values for daily mean temperature, precipitation, monthly maximum, and minimum temperature. The missing value code for 'stn' is -999.

4.4.5 Climate scenarios

The World Meteorological Organization (WMO) quantifies climate over a 30-year period (Dent, 2012; Rigal *et al.*, 2019). The observations create 30-year climate baseline, and it is against the observations upon which new observations and climatic trends are measured against. The baseline (1980-2010) and future climate (2020-2050) scenarios using RCMs for the two basins used in this study are shown in Table 5. The RCM ensemble was also used as it captures the annual cycle of temperatures and precipitation well at the regional scale. The baseline and future climate scenarios can be used as input into hydrological models. Hydrological models using RCMs data as inputs have been the primary means of assessing sectoral impacts (Ziervogel *et al.*, 2014).

4.5 Validation of the model data

The performance of the models (RCMs) and ensemble will be validated by comparing the observed (CRU TS v4.03) and simulated annual and monthly cycles of temperature and precipitation. The metrics to be used in validating the modelled data are standard deviation (SD), correlation and centered RMS difference. The Taylor Diagram (Elvidge *et al.*, 2014; IPCC, 2001; Taylor, 2001; Xu *et al.*, 2016) of spatial pattern of correlations, RSME and standard deviations with respect to the observations.

4.6 Computation of climate indices

The baseline (1980-2010) and future climate (2020-2050) scenarios for the two basins was used for the computation of selected Expert Team Sector-Specific Climate indices (ET-SCI) shown in Tables 4.6 and 4.7. The selected ET-SCI was computed using the ClimPACT2. ClimPACT2 has been developed by the World Meteorological Organization's Expert Team on Sector-Specific Climate Indices (ET-SCI) to assist researchers deliver useful and relevant climate information to sector users (Alexander and Herold, 2016). ClimPACT2 is a software package used to calculate climate indices that are relevant for the health, agriculture, and water sectors. The indices calculated by ClimPACT2 are derived from daily temperature and rainfall data. ClimPACT2 allows the calculation of the ET-SCI indices using daily weather data across an entire gridded NetCDF file (RCMs). The selected climate indices were checked for quality

and homogeneity. Homogeneity implies consistency of a series through time and is an obvious requirement for the robust analysis of climate time series (Alexander and Herold, 2016; Alexander and Arblaster, 2009; Chisanga *et al.*, 2017).

Table 4.6: Core ET-SCI indices

Name	Definition	Units	Time scale	Sector(s)
SU	Number of days when TX > 25°C	days	Mon/Ann	H
TR	Number of days when TN > 20°C	days	Mon/Ann	H, AFS
GSL	Annual number of days between the first occurrence of 6 consecutive days with TM > 5°C and the first occurrence of 6 consecutive days with TM < 5°C	days	Ann	AFS
TXx	Warmest daily TX	°C	Mon/Ann	AFS
TNn	Coldest daily TN	°C	Mon/Ann	AFS
WSDI	Annual number of days contributing to events where 6 or more consecutive days experience TX > 90th percentile	days	Ann	H, AFS, WRH
CSDI	Annual number of days contributing to events where 6 or more consecutive days experience TN < 10th percentile	days	Ann	H, AFS
TXgt50p	Percentage of days where TX > 50th percentile	%	Mon/Ann	H, AFS, WRH
TX95t	Value of 95th percentile of TX	°C	Daily	H, AFS
TXge30	Number of days when TX >= 30°C	days	Mon/Ann	H, AFS
TXge35	Number of days when TX >= 35°C	days	Mon/Ann	H, AFS
GDDgrown	Annual sum of TM-n (where n is a user-defined location-specific base temperature and TM > n)	degree-days	Ann	H, AFS
CDD	Maximum number of consecutive dry days (when PR < 1.0 mm)	days	Mon/Ann	H, AFS, WRH
R20mm	Number of days when PR >= 20 mm	days	Mon/Ann	AFS, WRH
PRCPTOT	Sum of daily PR >= 1.0 mm	mm	Mon/Ann	AFS, WRH
R95pTOT	100*r95p / PRCPTOT	%	Ann	AFS, WRH
R99pTOT	100*r99p / PRCPTOT	%	Ann	AFS, WRH
RXdday	Maximum d-day PR total	mm	Mon/Ann	H, AFS, WRH
SPI	Measure of “drought” using the Standardized Precipitation Index on time scales of 3, 6 and 12 months.	unitless	Custom	H, AFS, WRH
SPEI	Measure of “drought” using the Standardised Precipitation Evapotranspiration Index on time scales of 3, 6 and 12 months	unitless	Custom	H, AFS, WRH

Table 4.7: Non-core ET-SCI indices

Name	Definition	Units	Time scale	Sector(s)
DTR	Mean difference between daily TX and daily TN	°C	Mon/Ann	
TNx	Warmest daily TN	°C	Mon/Ann	
TXn	Coldest daily TX	°C	Mon/Ann	
TMm	Mean daily mean temperature	°C	Mon/Ann	
TXm	Mean daily maximum temperature	°C	Mon/Ann	
TNm	Mean daily minimum temperature	°C	Mon/Ann	
TX10p	Percentage of days when TX < 10th percentile	%	Ann	
TX90p	Percentage of days when TX > 90th percentile	%	Ann	
TN10p	Percentage of days when TN < 10th percentile	%	Ann	
TN90p	Percentage of days when TN > 90th percentile	%	Ann	
CWD	Maximum annual number of consecutive wet days (when PR ≥ 1.0 mm)	days	Ann	
R10mm	Number of days when PR ≥ 10 mm	days	Mon/Ann	
Rnnmm	Number of days when PR ≥ nn	days	Mon/Ann	
SDII	Annual total PR divided by the number of wet days (when total PR ≥ 1.0 mm)	mm/day	Ann	
R95p	Annual sum of daily PR > 95th percentile	mm	Ann	
R99p	Annual sum of daily PR > 99th percentile	mm	Ann	
Rx1day	Maximum 1-day PR total	mm	Mon/Ann	
Rx5day	Maximum 5-day PR total	mm	Mon/Ann	

4.7 Projected changes in temperature and precipitation

4.7.1 Zambezi River Basin

The minimum and maximum temperature would increase in the Zambezi River Basin from 2020-2050 relative to 1970-2000. Minimum temperature would range from 1.33-1.72°C (RCP4.5) and 1.34-1.85°C (RCP8.5). On the other hand, maximum temperature would range from 1.32-1.67°C and 1.36-1.86°C under RCP4.5 and RCP8.5, respectively. The projected changes in precipitation in 2020-2050/1970-2000 would range from -2.09 to 0.249 mm and -1.64 to 0.27 mm under RCP4.5 and RCP8.5 (Figure 4.8), respectively. The Zambezi River Basin has one of the most variable climates of any major river basin in the world, with an extreme range of conditions across the catchment and through time (Beilfuss and dos Santos, 2001). Average annual rainfall varies from more than 1,600 mm per year in some far northern highland areas to less than 550 mm per year in the water-stressed southern portion of the basin (You *et al.*, 2010).

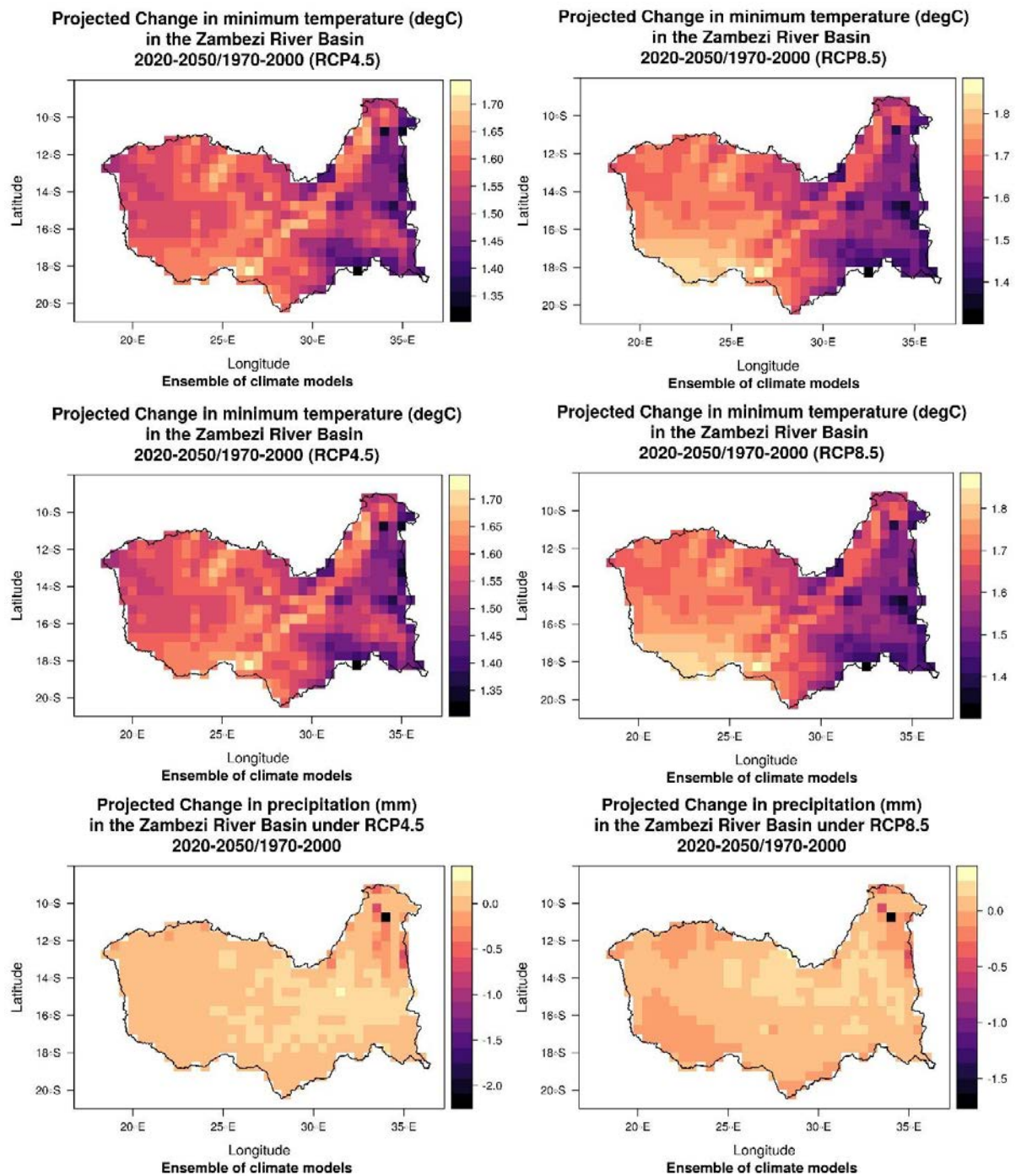


Figure 4.8: Projected changes in minimum and maximum temperature and precipitation 2020-2050/1970-2000 in the Zambezi River Basin

4.7.2 Orange River Basin

The minimum temperature within the Orange River Basin would range from 1.07-1.76°C and 1.16-1.95°C under RCP 4.5 and RCP 8.5, respectively. However, the maximum temperature would also increase within the basin relative to the baseline under RCP4.5 (0.96-1.78°C) and RCP8.5 (1.08-1.95°C). The projected changes in precipitation in 2020-2050/1970-2000 would

ranges from -1.06 to 0.27 mm and -0.33 to 0.10 mm under RCP4.5 and RCP8.5 (Figure 9), respectively.

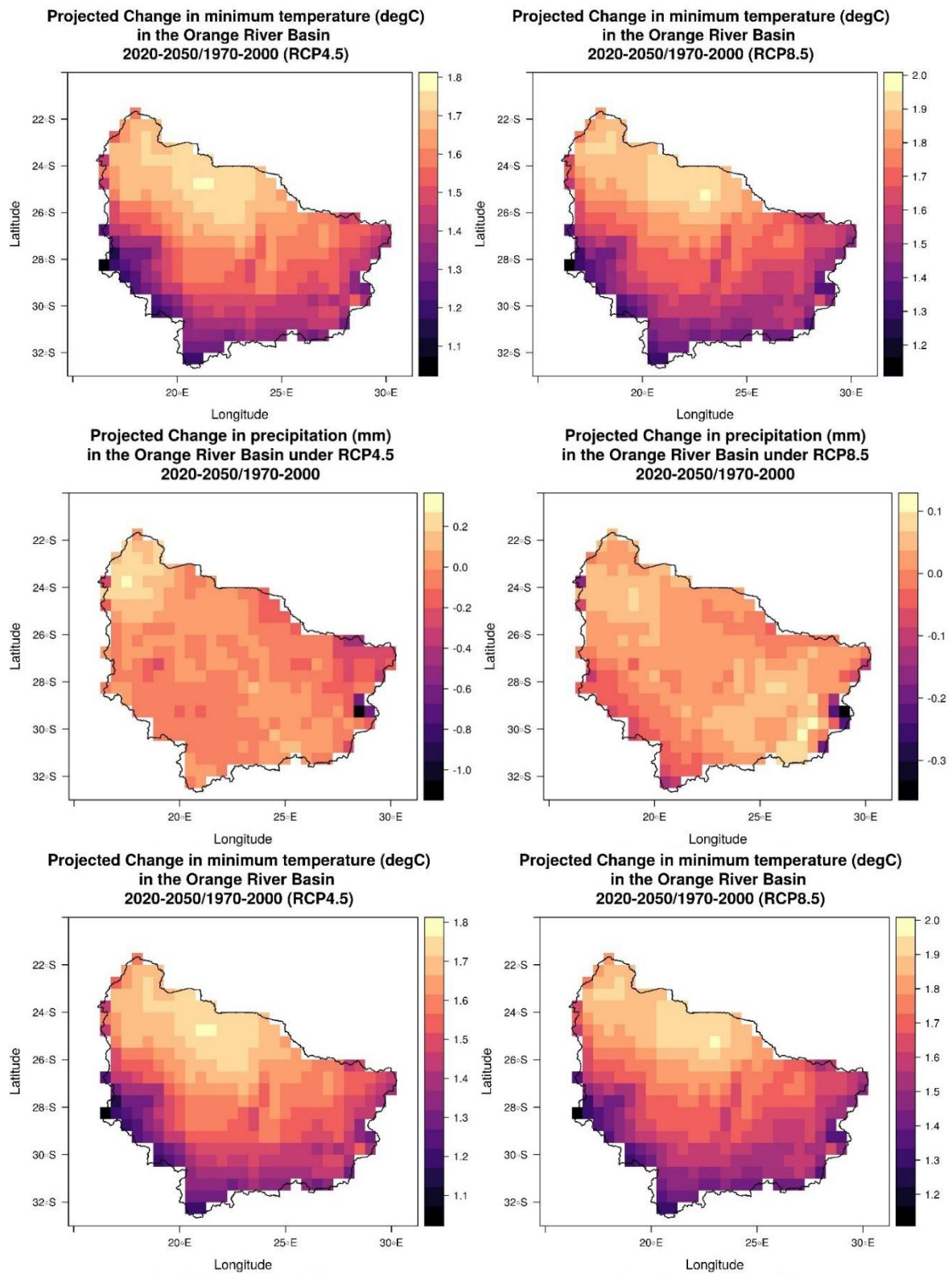


Figure 4.9: Projected changes in minimum and maximum temperature and precipitation 2020-2050/1970-2000 in the Orange River Basin.

4.8 Water Security implications

Additional work will be done on linkage between hydrological modelling water balance yields and how this will change under different climatic scenarios. Water balance yields will be compared against planned developments in the catchments. It is envisaged as a research topic for MSc studies. UNZA is currently looking for a student to perform this analysis. Several threats on freshwater in the Zambezi Basin have been mapped that include mining, hydropower and climate variability. Water security would require that appropriate water infrastructure such as dam account for this variability provided that the Zambezi Catchment will have reduced precipitation but increased temperatures. The hydrological model shows that for some catchments, this may not be a challenge as the baseflow conditions are driven by groundwater. In the Orange River, future climate projections show increased precipitation and increased temperatures. Flooding events may become more prominent and hence infrastructure should be built with the appropriate flexibility. Further work is required to account for uncertainty of climate scenarios.

CHAPTER 5

ANALYSIS OF PROJECTED IMPACTS OF SEDIMENTATION AND BATHYMETRY OF SELECTED SMALL RESERVOIRS TO WATER SCARCITY PROBLEMS ON THE PRIORITY WATER-LINKED SECTORS IN THE ZAMBEZI RIVER BASIN OF ZAMBIA

5.1 Introduction

Highly variable rainfall; observed and projected rainfall decrease; and the inability of governments to keep up with infrastructure provision for fast-growing populations and urban, agricultural, and industrial sectors; as well as a lack of sufficient information and monitoring are some of the factors that limit the ability of decision-makers to manage water resources sustainably to promote social and economic development (de Clercq, 2018, p. 54). Runoff and river channel erosion provide a continuous supply of sediment that is finally deposited into reservoirs leading to rapid sedimentation and untimely loss of reservoirs' useful life, storage capacity as well as reduced water quantity and quality (Lu *et al.*, 2013). The bathymetric approach is based on a simple comparison of reservoirs morphology at different temporal scales, which according to United States Army Corp of Engineers (USACE) (2000) and Ajith (2016) should be at least ten years to detect significant changes in sediment accumulation or bed change. Given that two-thirds of the 17 Sustainable Development Goals (SDGs) (1, 2, 3, 13, 14 and 15) are water-dependent (United Nations Development Programme (UNDP), 2018), understanding processes such as sedimentation that affect water quantity and quality is critical to a successful and domesticated implementation of SDGs in such catchments as the Orange and Zambezi River Basins by 2030. This would also ensure sustainable supply of water for economic activities thereby strengthening economies that are dependent on pastoral and crop farming. Although sedimentation in reservoir may be a natural process, in environments such as the Orange and Zambezi Basins, it is exacerbated by anthropogenic activities such as deforestation, mismanagement of riparian area, poor farming activities especially near the reservoirs (Gharehkhani, 2011). Neglect of land especially within the reservoirs and river buffer zones punctuates sedimentation and rapid loss of storage capacities, the dominant effect of damming along rivers significantly contribute to sedimentation, morphological changes and channel evolution over time (Sichingabula, 1997). Sedimentation is a major unavoidable phenomenon in all reservoirs, if uncontrolled; sediment deposition reduces storage capacities of reservoirs and eventually, water scarcities. Accumulation of sediment in a reservoir also reduces its depth, useful life and interferes with its functions. With many reservoirs rapidly losing their depths to sedimentation and reaching the end of their original design useful life, sedimentation assessment is becoming an increasingly important issue in reservoir operation and management (Doyle *et al.*, 2003; USACE, 2017).

Ronco *et al.* (2010) did earlier studies in the Zambezi Basin Kariba and Cahora Bassa Dams forecasting the future scenario of morphodynamic changes. As much these studies bring to fore profound evidence of morphological effects of climate change in large dams, there is barely any link to understanding the implication on adaptive capacity to water security because it was not the main thrust of the study. Ronco *et al.* (2010) further noted with concern the complex evolution under which the river basin was going due to anthropogenic influence such as damming that punctuate siltation. Kunz (2011) also did a study, but only focusing on the Zambezi River Basin in terms of effects of large dams on the Zambezi River Basin with specific emphasis on geospatial and temporal dynamics of sediment, carbon and nutrient fluxes. Sichingabula (2018) also did some studies in some sub-catchment of the Zambezi in the southern part of Zambia. His findings demonstrate how silt affects water quantity and quality and how these affect livestock and socio-economic development of the reservoir water-dependent communities. Being a spatially distributed problem, reservoir sedimentation transcends a singular catchment and, whilst several studies have been done in the two catchments, there remains room for continuous scientific debates with improved evidence on bathymetric assessment and sedimentation especially with regard to their implications on water-linked sectors and communities' adaptive capacities to water scarcity problem.

Based on geospatial analysis of 8 km resolution satellite imagery, Vorosmarthy *et al.* (2005) reported that 64% of Africa relies on water resources that are limited and highly variable and that, river corridor flows are critical in augmenting local runoff, reducing impacts of climate variability, and improving access to freshwater (Figure 5.1). They also observed that large river corridors, even in the driest regions, demonstrate a stabilizing effect on seasonal flows. River regulation further increases the reliability of freshwater sources throughout the year and reduces apparent levels of both annual and seasonal stress. This suggests that use of rivers and reservoirs to harness water would reduce water stress problems especially in Southern Africa most of which is under arid/ semi-arid climate. Three examples of the sensitivity in regions located in hydrologically complex transitional zones between arid/semi-arid and humid climates (Figure 5.1).

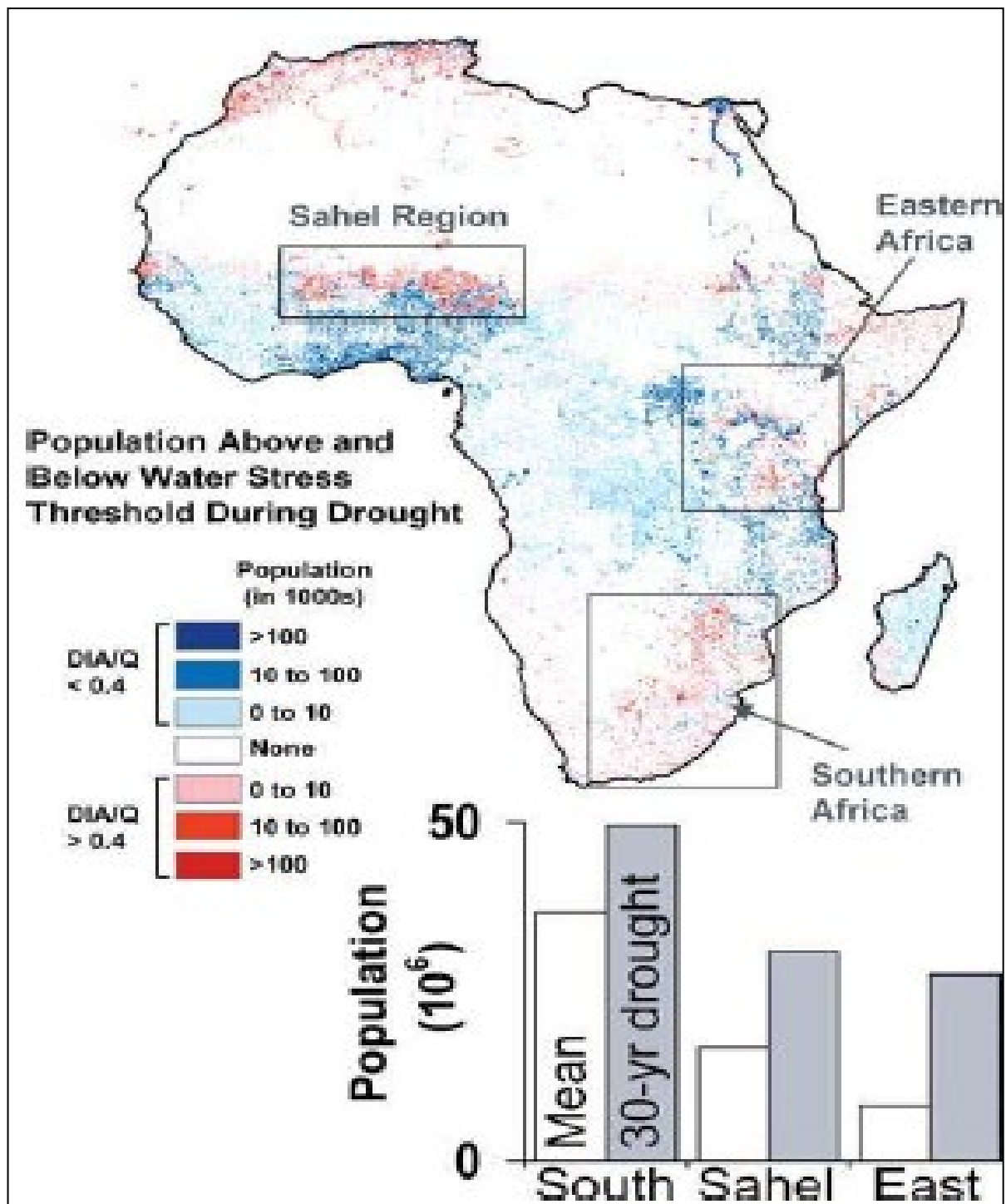


Figure 5.1: Density of human population

NB: Population living above (red) or below (blue) the relative water use threshold of 40%, presumed to indicate severe stress (34), under the 30-y recurrence drought (Source: Vorosmarthy et al., 2005).

Kusangaya et al. (2011) notes that stream flow is projected to decrease by 2050 up to 45% for the Zambezi, Limpopo, Ruvhuma and Orange Catchments with increased flooding events Mozambique, Malawi, Zambia, and Zimbabwe. Within the climate change matrix, water

resources are at the epicentre of projected climate change impacts and needs an integrated approach. If the observed changes in climate in the last century (IPCC, 2007) persist into the future, the potential impacts on water resources are likely to increase in magnitude, diversity, and severity on socio-economic activities of the local people in Kazungula (Kusangaya, 2011; Chisanga *et al.*, 2022).

According to Buffington *et al.* (2012), river systems and reservoirs can show a broad range of responses to changing inputs of water, sediment, and vegetation over human, spatial and temporal dimensions. It is worth mentioning that adjustments on reservoirs and channel morphology may range from small scale to large-scale changes of reach morphology. It is worth mentioning that when a river channel is altered under naturally dynamic hydrologic conditions, the river re-adjusts itself with respect to dimension and profile to restore its former equilibrium state (Couture, 2008). However, this process is disturbed under anthropogenic influence and eventually, all reservoirs that are linked to such systems are also destabilised leading to various water stresses and shortages especially for livestock due drop in water levels at the upstream part of the river and a rise at the downstream part which causes riverbed degradation and aggradation, respectively. River widths and bank stabilities of many rivers are disturbed due to human encroachments by damming at both river sides (Figure 5. 2).

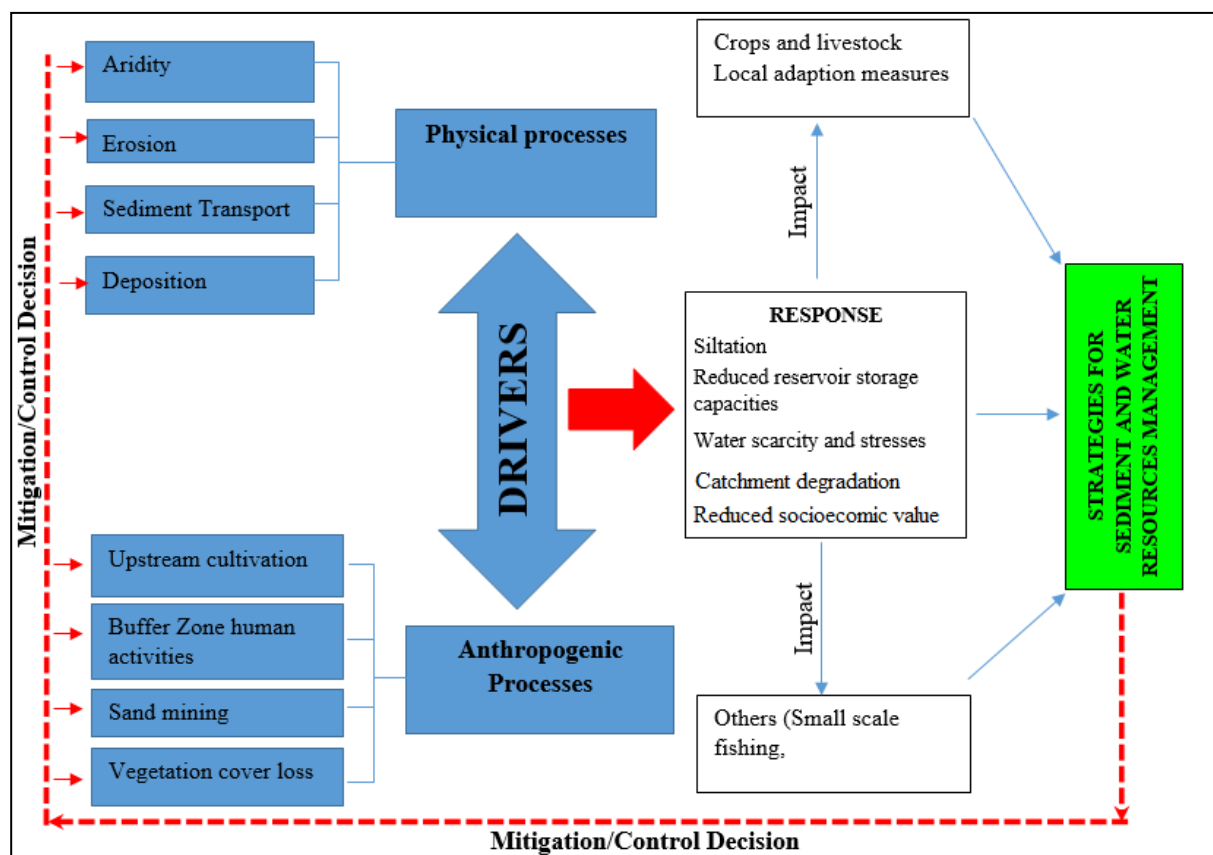


Figure 5.2: Conceptual Framework of the study

According to Huang *et al.* (2021), channel and reservoirs response may range from small scale adjustment of channel characteristics to large scale alteration of morphology, planform patterns, changes in water holding capacities as well as reduced economic value of water values. As much as these undesirable phenomena are evident in the Zambezi and Orange Basins, they could also be used as opportunities for research and scientific evidence opportunities to inform policy and strategic decisions to address drivers of riverine modifications.

To build climate change adaptive capacity and resilience to water scarcity problem, it is important to know the capacities of the reservoirs in question (Mulabalaba, Siankanga and Musokotwane dams, among others) part of whose findings and implications can be extrapolated to other contexts within the main basin to guide the broader context of decision making. The current interest in small reservoirs in Zimba-Kazungula area stems mainly from their utilization for domestic use, livestock watering, fishing, and irrigation. Rarely are small reservoirs considered important in the water resources system even though they are significant in water resource planning and management. As population is increasing in the Zambezi catchment and southern Zambia in particular, reservoirs do not serve as livelihood strategies. This implies that the owners of the dams must stop using the dams especially in dry season to maintain water supplies for other critical uses, such as livestock watering. Thus, these dams are failing to contribute significantly to ensuring whole year-round reliable water supply for domestic use such as livestock watering and irrigation farming.

5.2 Aims and objectives

The aim of the study was to determine the role and impact of sedimentation and bathymetry of small reservoirs to water scarcity problems in South Africa and Zambia.

The specific objectives of the proposed study are to:

1. Determine current storage capacities of selected reservoirs
2. Examine water scarcity risks based on the hydrological regimes of the reservoirs
3. Estimate the quantity of sediment accumulated in selected reservoirs
4. Document main drivers of sedimentation in the reservoirs
5. Assess how the status of water availability and sedimentation affect:
 - i. Livestock and crop farming
 - ii. Small scale fishing and other water-dependent socio-economic activities in the sub-catchment;
6. Conduct cost-benefit analysis of reservoir siltation on government planning process;
7. Explore community-initiated coping strategies to water stresses and scarcity; and
8. Design sediment control conceptual model and sustainable water resources management on rivers and reservoirs

5.3 Description of the study area

Zimba and Kazungula Districts are located in Southern Zambia between 15° and 18° 30” Latitudes, South as well as 25° and 27° 30” Longitudes, East (Figure 3a-b). Zimba and Kazungula Districts approximately cover total areas of 5,245.01 km² and 19,519 km², respectively.

Figure 5.5b below shows sample distribution of some dams in the target areas and their surrounding districts.

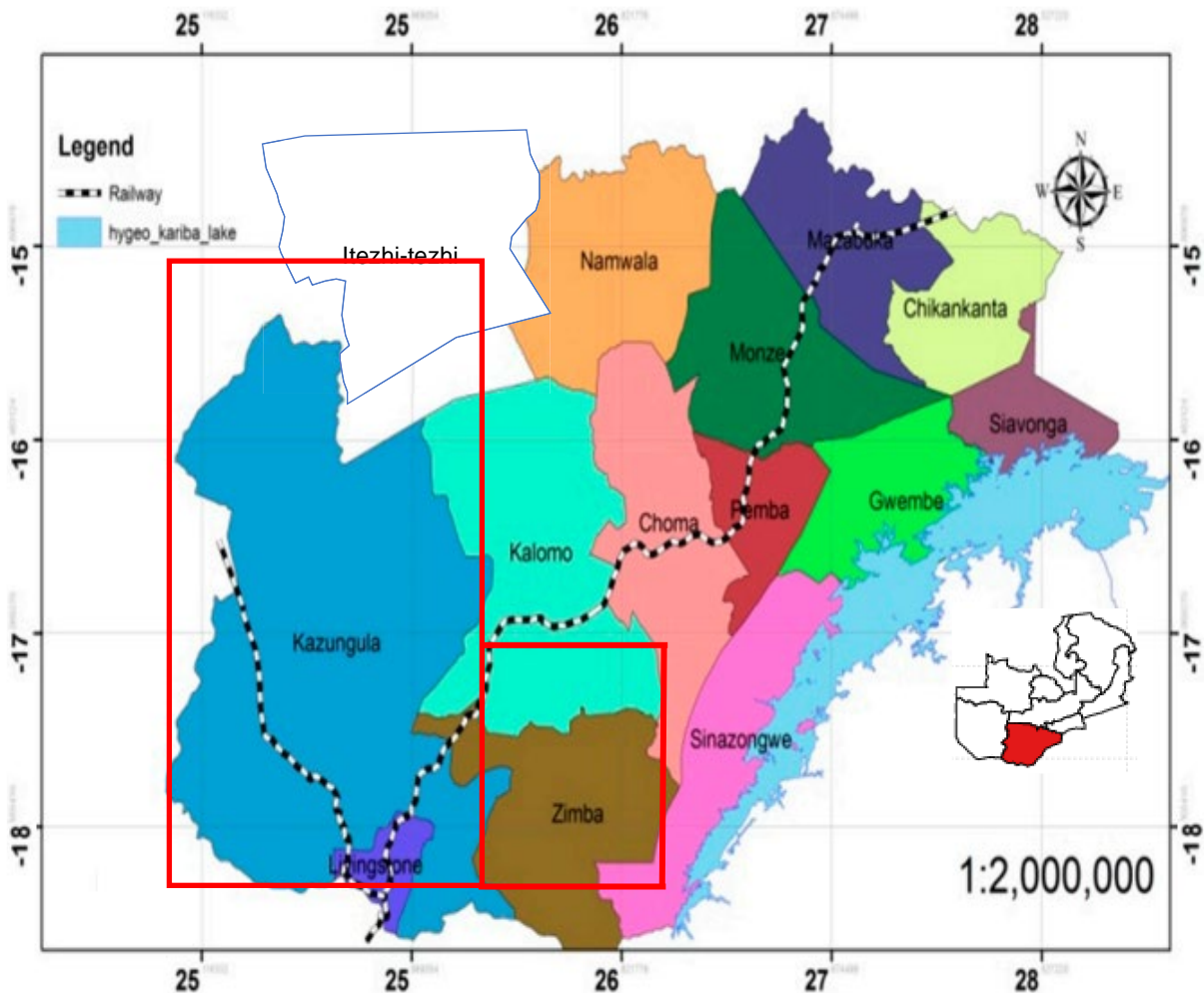


Figure 5.3a: General location of Kazungula and Zimba District in Southern Zambia (Source: Chisanga et al., 2019).

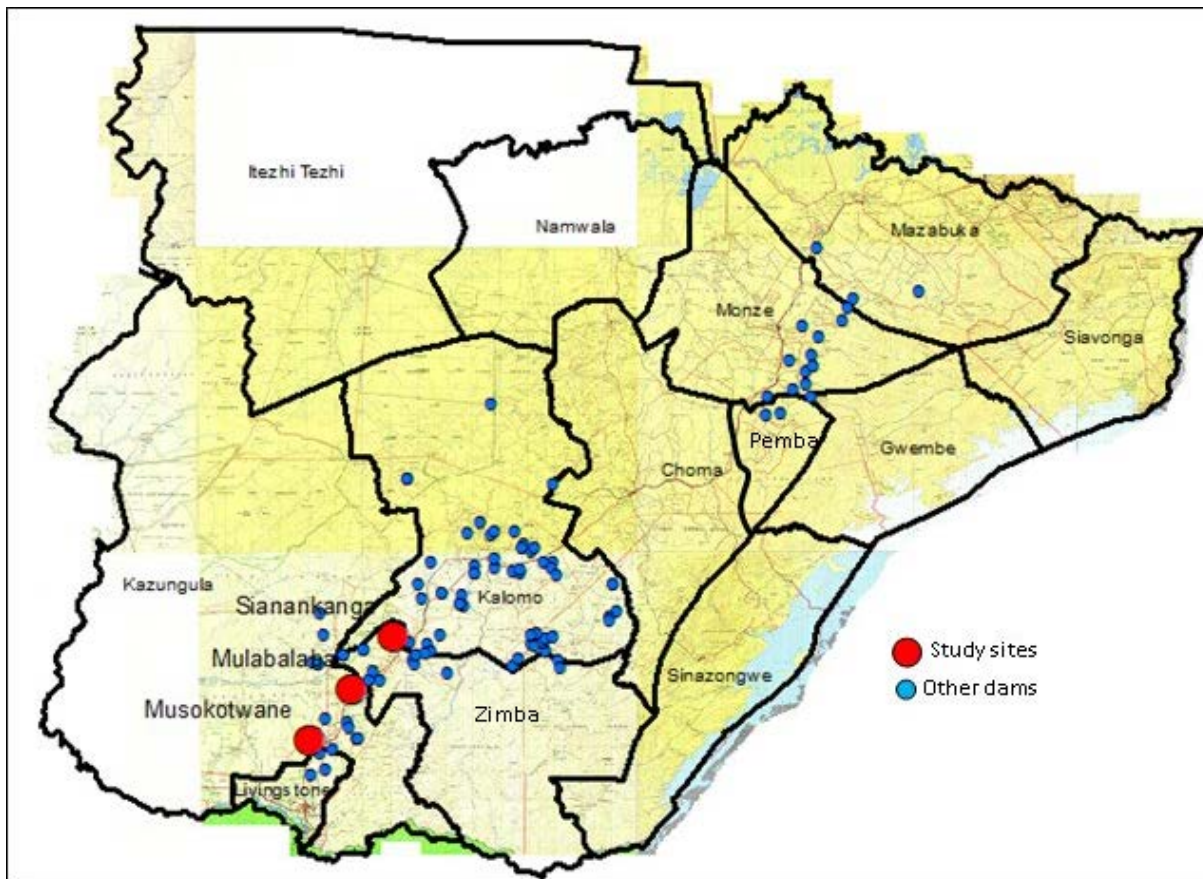


Figure 5.3b: Distribution of some dams in the Kazungula, Livingstone, Zimba and Kalomo (Source: Sichingabula, 2018).

These two districts are severely affected by a reduction in rainfall, which has impacted on farming, nutrition, surface water and groundwater (Zimba District Council, 2015). The districts have three different seasons, rainy season from November to April, Cool season from May to July and, hot season from August to October. Temperatures range from 15 to 27 °C with very low humidity. However, from October to November, the temperature can rise to over 32 °C.

The geomorphology of the study areas is explained by tectonic movement and rift valley faulting, already existing in the Proterozoic era, more than 550 years ago. The area has since experienced excessive faulting, folding and metamorphosis along with erosion and weathering, presenting large plains and the surface of the most resistant materials. Granitic and gneissic metamorphosed grounds are commonly present and tectonic movements, such as rift faulting and uplifting. Variable morphology of the area contributes to the existence of deep and shallow valleys, broad plateaus, and steep and flat river profiles (Euroconsult Mott Macdonald, 2007). The areas are underlain by Palaeozoic-Mesozoic sedimentary rocks called the Karroo Complex. The Karroo Complex is a geosyncline deposit including a glacial deposit at the initial stage and basaltic lava at the last stage. The basaltic lava is widely distributed along the middle section of the Zambezi River, forming many waterfalls and cataracts with faults such as

Victoria Falls. The basaltic lava of the Karroo Complex is covered with Tertiary-Pleistocene sedimentary rocks called the Kalahari Group. The Kalahari Group consists of calcretes, silcretes and ferricretes (laterites) which are members of the duricrust group of secondary surface deposits formed by the near-surface cementation of pre-existing soils. The large faults located in the area generally trend south westward. The vegetation in the study area is broadly classified as Zambezian biome; it covers most of the area with woodlands and grassland. Over 80% of residents in Zimba and Kazungula depend on agriculture for socio-economic livelihood. The dams play a substantial role providing environmental services to the community as well as water for food security and livestock.

5.4 Methodology

This section describes various methods, tools and analysis options which were adopted for the collection and final analysis of data.

5.5 Storage capacities of selected reservoirs

The data on this theme was collected using bathymetric surveying. A Remote-Controlled Hydrographic Survey Boat (RCHSB) Model RC-S2 mounted with Trimble Hemisphere OmniSTAR VBS for Differential Geographic Position System (DGPS) was employed to conduct bathymetric surveying on the reservoirs namely, Sianankanga, Mulabalaba and Musokotwane. The data sets collected included XY coordinates in UTM, water depths, bed profiles and wetted perimeters. The process of data collection involved multiple stages. Firstly, the RCHSB was set up using the stages presented in Figure 5.4.

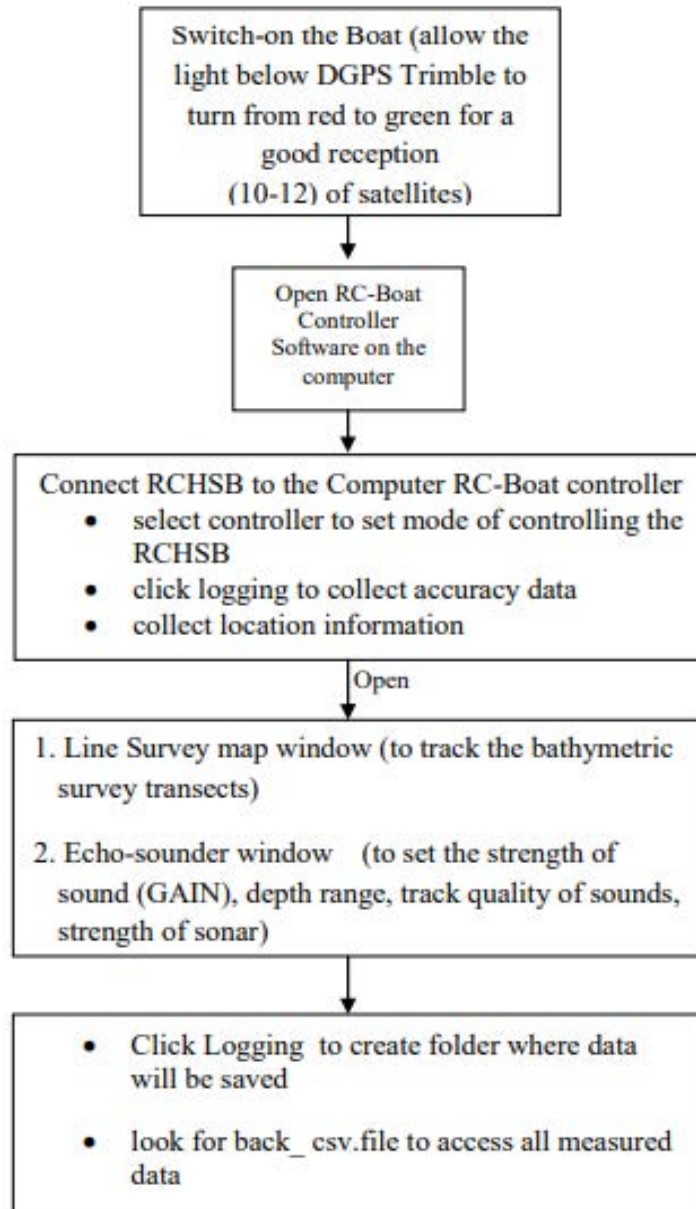


Figure 5.4: Process of setting up the equipment before deployment for bathymetric survey adapted from Muchanga (2020:59).

After setting up the RCHSB model RC-S2 boat, ground truthing of XY coordinates was done where coordinates were collected at the same point per reservoir for two minutes using boat's inbuilt DGPS. This was done to ensure that coordinate errors during bathymetric surveys were extremely minimised to as low as centimetres or millimetres accuracy. The formula used is shown in Equation 1:

$$A = \sqrt{\sum ((X_{i \dots nth} - \bar{X})^2 + (Y_{i \dots nth} - \bar{Y})^2) / N} \quad (1)$$

Where:

- A Ground accuracy;
- $X_{i \dots h}$ All individual X coordinates in UTM;
- \bar{X} Mean for X coordinates;
- $Y_{i \dots nth}$ All individual Y-coordinates in UTM
- \bar{Y} Mean for Y coordinates; and
- N Total sample of paired X and Y coordinates

Bathymetric survey was done by dragging the RCHSB-Model RC-S2 across the reservoir whilst tied to an inflatable boat driven by an outboard engine. Where the inflatable boat could not move by engine, paddling was used and where paddling was impossible because of inaccessibility, RC-S2 was connected to the boat controller software on the tough book laptop to remote control it to reach sections which were not possible to reach physically. Water depths were collected automatically through the inbuilt SONAR of the RC-S2 and were registered in the back_csv. file.

After each bathymetric survey, wetted perimeters were measured by walking around the reservoir whilst holding the DGPS on the RCHSB-Model RC-S2 which was automatically sending records of perimeter coordinates to the created folder on the laptop computer. This was useful in determining the boundary of water extent in the reservoir and was also useful in the final analysis in ArcMap and Surfer. The visual impression of measured bathymetric data was as displayed in Figure 5.4, which shows window interface impression of echo-sounding process.

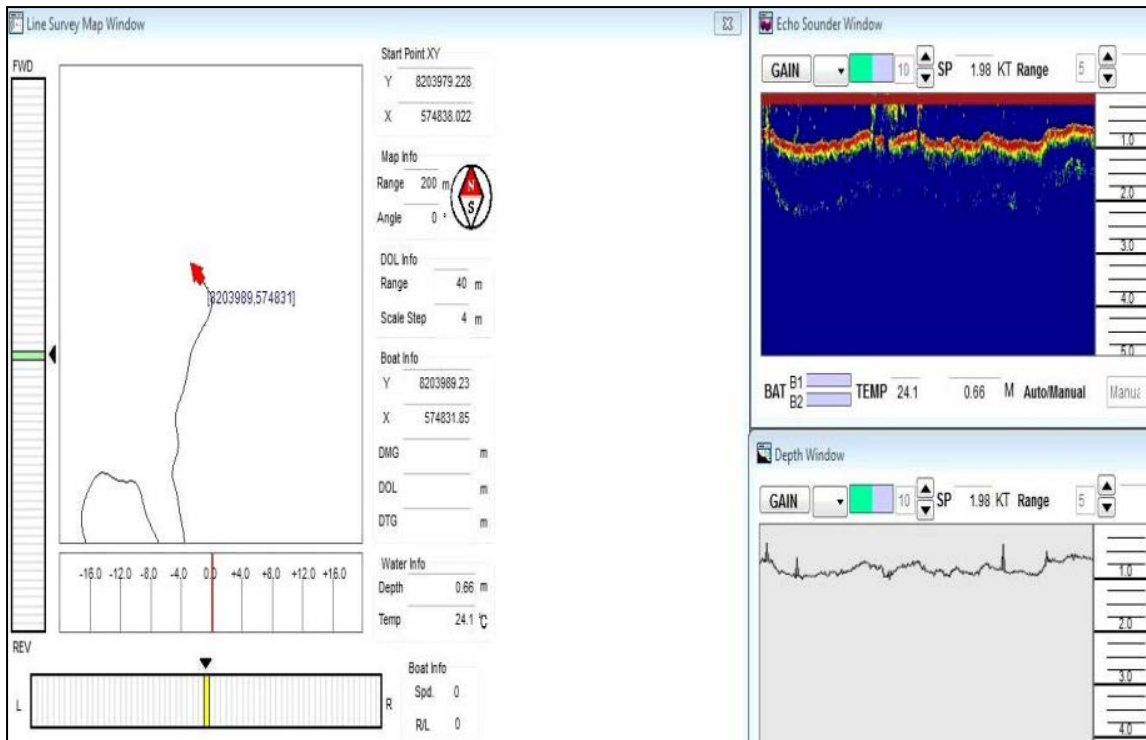


Figure 5.5: Visual impression of the window interface during Bathymetric Survey

To supplement the bathymetric data that was physically measured, the remote sensed Sentinel-2 images were accessed for 6-year period per reservoir from 2016 to 2021. These were processed in ArcMap using the image processing tool to derive the water surface area dynamics at different seasons for each selected reservoir per hydrological year. The water surface areas obtained were used to estimate the water volumes using the regressions models developed through the hydro-hypsometric rating curves. The minimal variation between physically measured data and remote sensed data was assumed to be extrapolatable to other seasons which had no physically measured data. The estimated volumes of available water were used to construct hydrological regimes for each reservoir and thereby, helping in the examining water stressful periods and potential implications for water scarcity problem amidst climate change. To ensure reliability and consistency of estimated volumes of water, more physically based bathymetric surveys were conducted in March 2022 using the ADPC for all the three reservoirs.

The reservoir water storage capacity and surface area were calculated for each reservoir using bathymetric data from the hydrographic boat for each reservoir with the application of Surfer 13 software. The point data (XY-Z (depth)) were downloaded from the boat software from back data file. Depth values were given a negative sign reason being that water surface was taken as the reference level and if minus sign was not given, the surface volume 3D analyst tool would have calculated depth values as elevations instead of depth. The XY coordinates of the reservoir shoreline were also imported with a default depth value of zero associated with each point. Thereafter, Surfer Gridding (SG) was used to produce an interpolated surface using Kriging. It is from this raster surface that the volume and surface area of the reservoir was calculated using

Volume tool in Surfer 13. Since the reservoir boundary had zero values representing the reservoir surface, the plane height was set at zero and all the reservoir depths were taken to be negative using metres as units of measurement. Hydro-hypsometric rating curves were developed to show relationships between water surface areas and depth, depth, and volume as well as volume and surface area. The data was summarised in form of table part of which was used to plot hydrological regimes for the reservoirs to visualise inter-seasonal water availability dynamics. From the data sets, bathymetric maps were developed, which visualised spatial variations in the depth across the reservoirs. This was done using Inverse Weighted Distance (IWD) tool in ArcMap 10.2 and Surfer 13.

5.6 Water scarcity risks based on the hydrological regimes of the reservoirs

Part of the data required was obtained from the bathymetric survey, particularly the hydrological regimes. Using a questionnaire, the households were asked to supply estimated volumes of water that their livestock required to be fully sustained at different seasons of the year. The specifications in Table 1 were used to determine the severity of water scarcity (Global Water Forum, 2007).

Table 5.1: Criteria for determination of Water Scarcity

SN	Description	Classification
1	<1000 m ³ / person / annum	Water scarcity
2	<500 m ³ / person / annum	Absolute water scarcity

Source: Global Water Forum (2007:2)

5.7 Estimation of quantity of sediment accumulated in selected reservoirs

The sediment quantity was determined using bathymetric surveying and Elevation Change Method (ECM). The collected data inputs were reservoir storage capacities, bed surface areas, water surface elevation, maximum water depth near crest and downstream elevation. Bathymetrically, the study compared the changes in average depth and volume of water between the initial (2016) and the current (2022) measurement to determine the levels of accumulation within the 6-year period. The difference in volumes of water at full capacity represented the sediment that had accumulated using Equation 2.

$$SV = RSC_i - RSC_{ii} \quad (2)$$

Where:

SV	Total sediment volume accumulate (m ³)
RSC _i	Initial Reservoir Storage Capacity (m ³)
RSC _{ii}	Current Reservoir Storage Capacity (m ³)

The ECM was used to estimate the long-term Total sediment that accumulates from construction date to the most recent date (2022) using Equation 3 after Muchanga (2020).

$$(3) \quad SV = A \left[\frac{[(W_e - D_{se}) - M_{wd}]}{3} \right]$$

Where:

SV	Total Sediment Volume (m ³)
A	Surface area of the Bed (m ²)
W _e	Water surface elevation of the reservoir (m)
D _{se}	Downstream elevation nearest to the Crest (m)
M _{wd}	Maximum Water depth near the crest (m)
3	Constant

The principal assumption of this formula is that the reservoir is trapezoidal in shape and that the water surface area is not significantly variable from the bed area. This formula was first tested by Muchanga *et al.* (2020) on one of the reservoirs in the Magoye Catchment with error at 6% from the physically measured volume. It was letter tested in the Mushibemba catchment by Mphande and Sichingabula (2021) with best minimal errors of 5% and worst scenario at around 15%. Ministry of Water Development and Sanitation [MWDS] (2022) also tested in on a wider sample of reservoirs with errors ranging from 3% to 25%.

5.8 Main drivers of sedimentation in the reservoirs

The data on main drivers of sedimentation were documented using field observations and interviews with selected informants within the catchments. Resulting data was analysed using thematic analysis and descriptive statistics where quantifiable data were summarised into charts and bar graphs as well as tables.

5.9 Impact of the status of water availability and sedimentation on livestock, crop farming, fishing, and other water dependent socio-economic activities

The data on how the water scarcity and sedimentation affected livestock, crop farming, fishing and other water-dependent socio-economic activities was collected using a Likert Scale where local people ranked the extent to which the water scarcity and sedimentation phenomena impacted on their livestock and crop farming. The resulting data was analysed using descriptive statistics and standard deviation of the rankings by local people. Extra data was collected through desk review and was analysed using content analysis.

5.10 Cost-benefit analysis of reservoir siltation on government planning process

Data on these thematic areas was collected using desk review of documents related to the theme. Structured interviews with key informants from the MWDS were conducted to gather extra insights on the cost of reservoir sedimentation on the local authority. Data was analysed using thematic analysis where the responses were thematised and summarised in form of graphs and tables of frequency and percentages.

5.11 Community-initiated coping strategies to water stresses and scarcity

To understand the coping strategies to water scarcity and stresses locally initiated by the people, structured interviews were conducted with local people. Here they shared their experiences on how they coped with water scarcity and how such practices could inform general sediment control measures for sustainable water resources management. Thematic analysis was used to cluster the responses into themes from which conclusions were drawn.

5.12 Sediment control conceptual model and sustainable water resources management in reservoirs

The design of sediment control conceptual model for sustainable water resource management was informed by the data gathered under the first seven objectives. Hermeneutic analysis was applied to decode the meaning of all the results to the development of the conceptual model.

5.13 Results

5.13.1 Storage capacities of selected reservoirs

As of April 2022, the total full storage capacity for Musokotwane Dam was estimated at 380,264.8 m³ with a corresponding water surface area of 103,052.79 m². These estimations were based on the physical bathymetric measurement, which was conducted when the reservoir was at full capacity. The survey transects and bathymetric map showing variations in water depths are shown in Figure 5.6a and 5.6b.

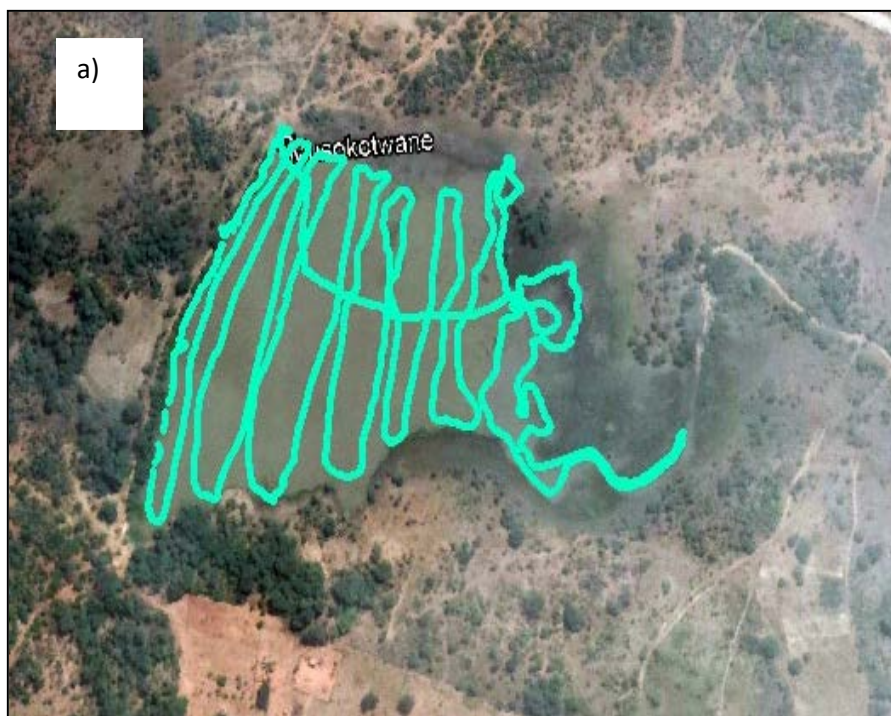


Figure 5.6a: Satellite image overlaid with survey transects

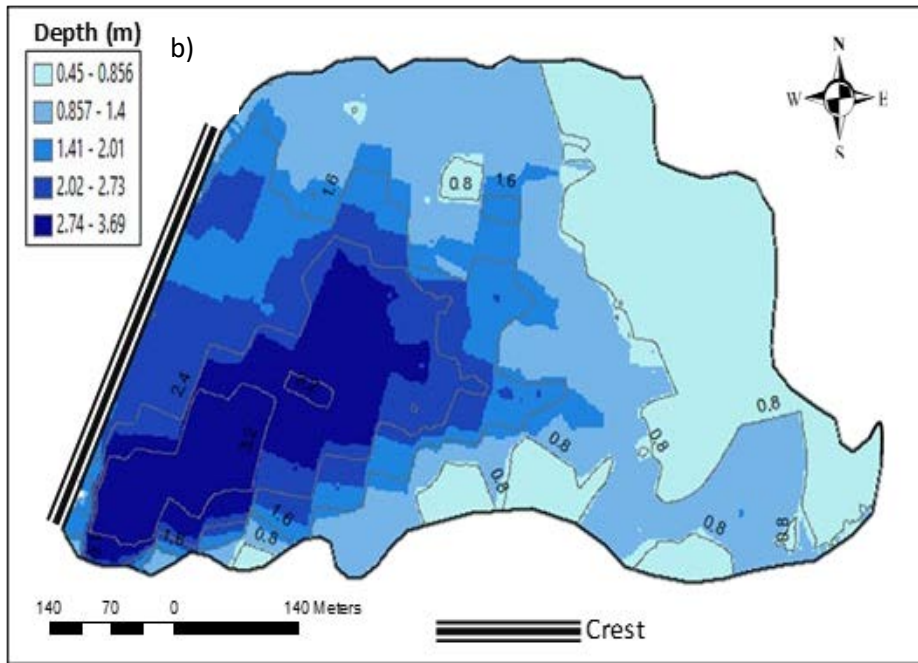


Figure 5.6b: Bathymetric Map of the Musokotwane Reservoir (Field data, April 2022).

Table 5.2: Water Depth, Surface area and Volume data for Musokotwane Reservoir

Depth (m)	Area (m²)	Volume (m³)
0	0	0
0.05	41713.14	47688.46
0.19	43852.08	52029.17
0.33	46522.64	56738.33
0.47	49082.85	61861.07
0.61	52657.22	67511.37
0.75	56055.28	73777.97
0.89	58121.62	80505.57
1.03	60636.88	87656.1
1.17	63027.6	95328.64
1.31	65796.2	103531.38
1.45	68364.87	112339.92
1.59	70782.97	121742.24
1.73	78705.2	143143.85
1.87	83503.48	155876.66
2.01	83727.74	169009.82
2.15	843345	169949.82
2.29	85233	185359.15
2.43	86872	202657.24
2.57	86504	222619.46
2.71	87330.39	244020.72
2.85	87413.34	265452.37
2.99	91323.2	286884.02
3.13	91502.23	308315.68
3.27	95233.07	329747.33
3.41	97383.18	351178.98
3.55	99142.93	372610.64
3.69	103052.79	380264.8

Details of how water volumes and water surfaces changed with changes in depth are shown in Table 2. The assessment showed a strong relationship between depth and volume as well as surface area and volume as indicated by high r^2 values of 0.96 and 97, respectively (Figure 5.7).

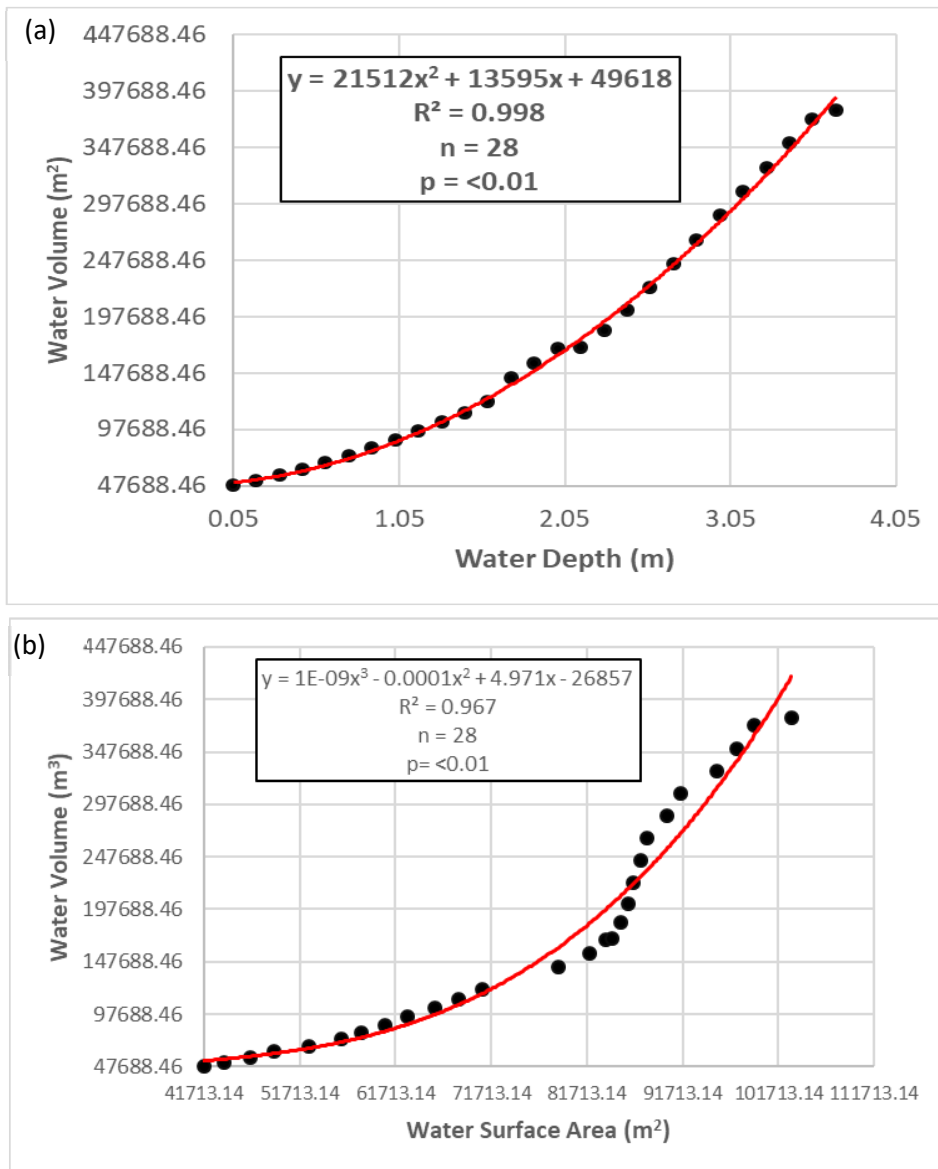


Figure 5.7: Water (a) depth-volume relationship and, (b) surface area-volume relationship for Musokotwane dam

The Musokotwane Catchment was estimated at 18 km² and was characterized mainly by human activities such as gardening, crop farming as well as human settlements. Figure 5.8 below presents delineated visual impression of the catchment.

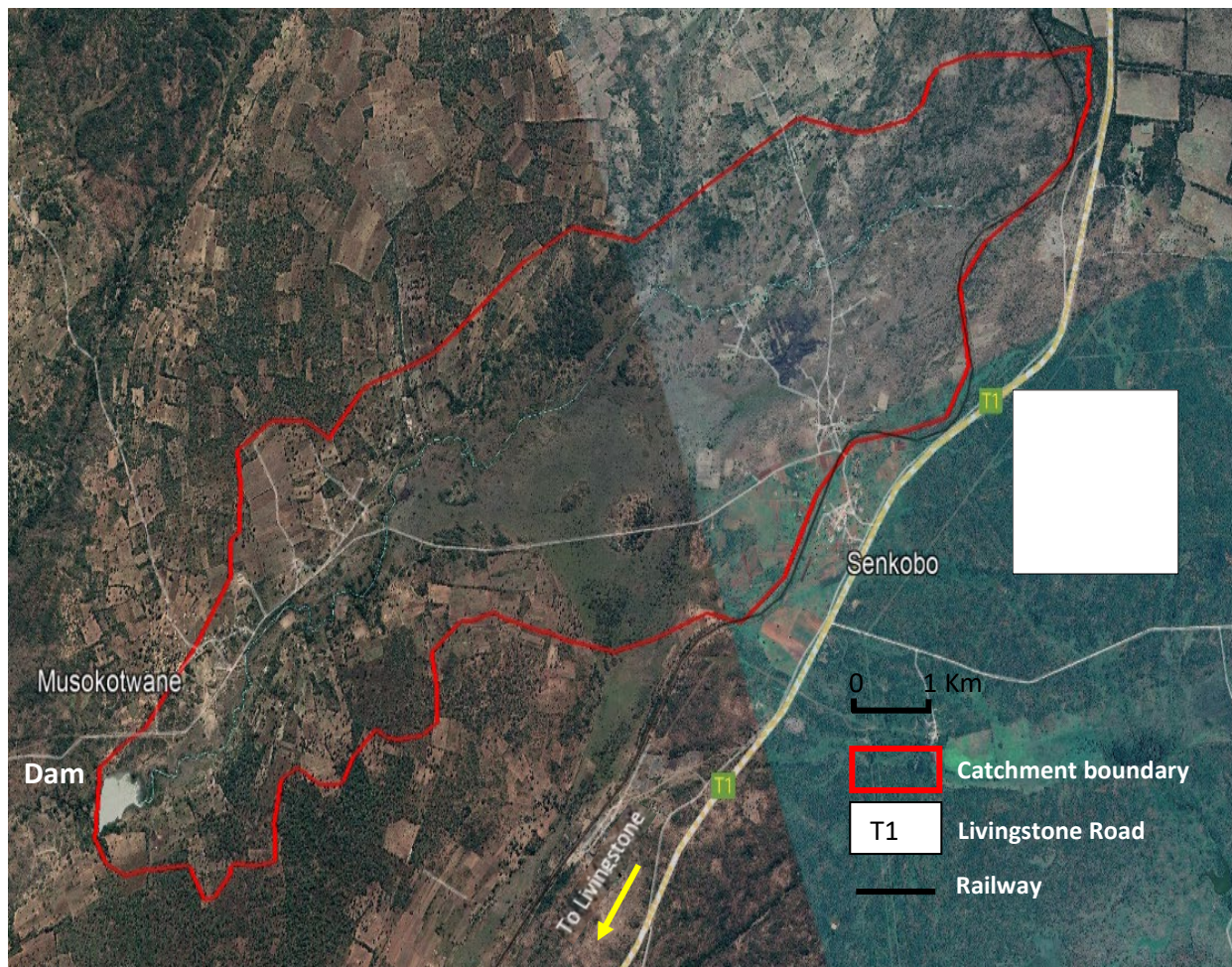


Figure 5.8: Delineated Catchment of the Musokotwane Reservoir in Kazungula District, Southern Zambia (April 2022)

Bathymetric survey for Mulabalaba reservoir was done when it was at full capacity in April, 2022. At that time, the measured volume of water was 621,737.16 m³ inundating the surface area of 117,087.98 m². Figure 9 presents the survey transects and bathymetric map of Mulabalaba Reservoir whose depth oscillated between 0.13 and 5.31 m.

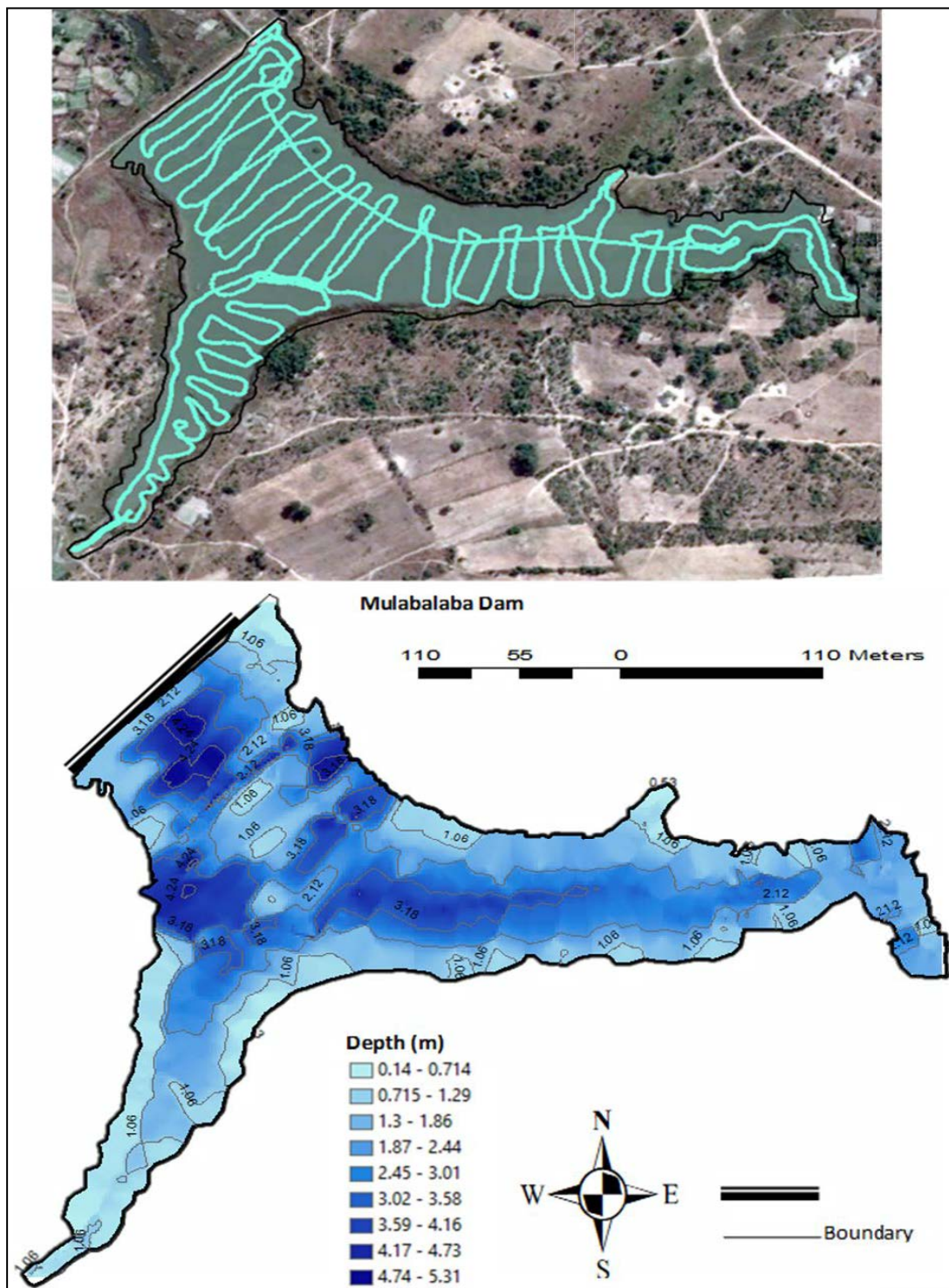


Figure 5.9: (a) Satellite image overlaid with survey transects and (b) Bathymetric Map of Mulabalaba reservoir. (Field data, April 2022).

The study found a strong relationship ($r^2 = 0.99$) between surface area of water and the corresponding volume. The same scenario was noted for the depth-volume relationship (Figure

5.10, Table 5.3). Surface areas size does not always translate into more water, it may imply silted reservoir, but whenever, it positively relates with volumes of water, it means that siltation levels could be under control.

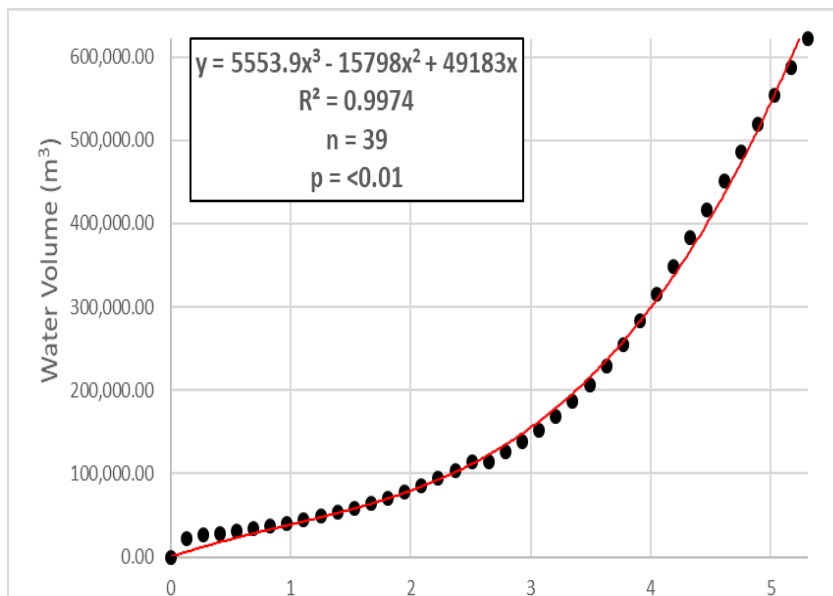
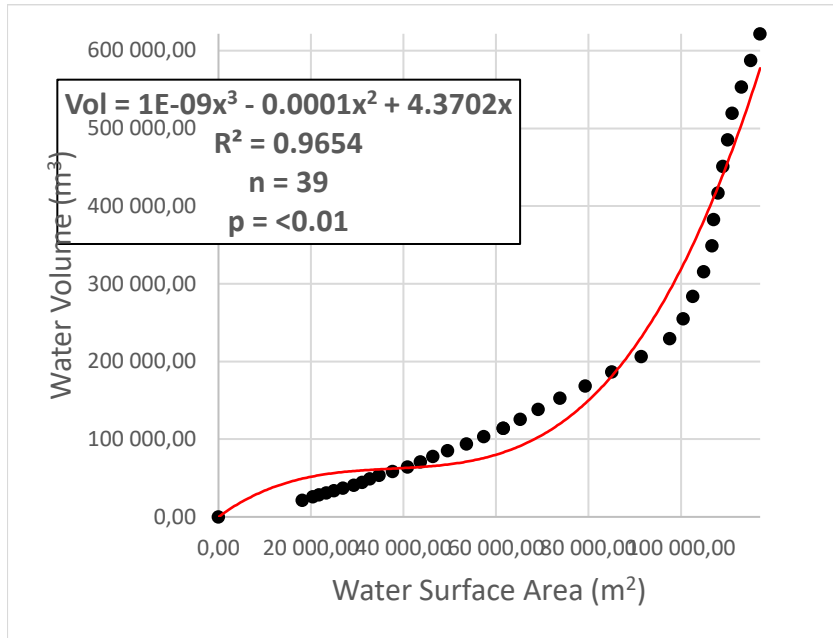


Figure 5.10: (a) Water depth-volume relationship and (b) Water surface area-volume relationship for Mulabalaba Reservoir (April 2022)

Table 5.3: Water depth, Surface, and volume relationship for Mulabalaba Reservoir

Depth (m)	AREA (m²)	Volume (m³)
5.31	117,087.98	621,737.16
5.17	115,067.98	587,630.12
5.03	113,057.97	553,523.09
4.89	111,047.96	519,416.06
4.75	110,037.96	485,309.03
4.61	109,027.94	451,201.99
4.47	108,017.93	417,094.93
4.33	107,007.91	382,987.93
4.19	106,668.89	348,968.89
4.05	104,874.85	315,531.34
3.91	102,498.66	283,894.00
3.77	100,431.30	255,097.53
3.63	97,532.81	229,393.31
3.49	91,385.40	206,664.19
3.35	85,045.76	186,519.33
3.21	79,281.17	168608.69
3.07	73,839.33	152,745.86
2.93	69,138.15	138,612.79
2.79	65,260.08	125,786.92
2.65	61,541.77	114,086.40
2.51	61,541.77	114,086.40
2.37	57,334.28	103,479.29
2.23	53,611.25	93,931.42
2.09	49,509.11	85,426.14
1.95	46,330.29	77,768.51
1.81	43,622.73	70,802.13
1.67	40,878.79	64,426.14
1.53	37,639.01	58,689.93
1.39	34,709.82	53,577.45
1.25	32,688.65	48,952.42
1.11	31,042.19	44,686.53
0.97	29,219.94	40,748.64
0.83	26,905.25	37,166.39
0.69	24,937.67	33,960.13
0.55	23,331.19	31,028.48
0.41	21,720.71	28,354.15
0.27	20,398.13	25,916.77
0.13	18,104.19	21,607.01
0	0	0

The catchment size for The Mulabalaba Catchment was estimated at 19.2 km² and was characterized mainly by human activities such as gardening, crop farming as well as human settlements. Figure 11 below presents delineated visual impression of the catchment.

The findings for Sianankanga Reservoir at its full capacity showed that 1,111,497 m³ of water was available for various uses especially municipality use and agricultural activities. This quantity of water occupied a maximum surface area of 246,999.4 m² at maximum depth of 4.5 m (Figures 5.12 and 5.13, Table 5.4). Just like in the case of Musokotwane and Mulabalaba Reservoirs, there was a very strong relationship between water volume and depth as well as water surface area as demonstrated by strong r² values of 0.99 and 98, respectively.

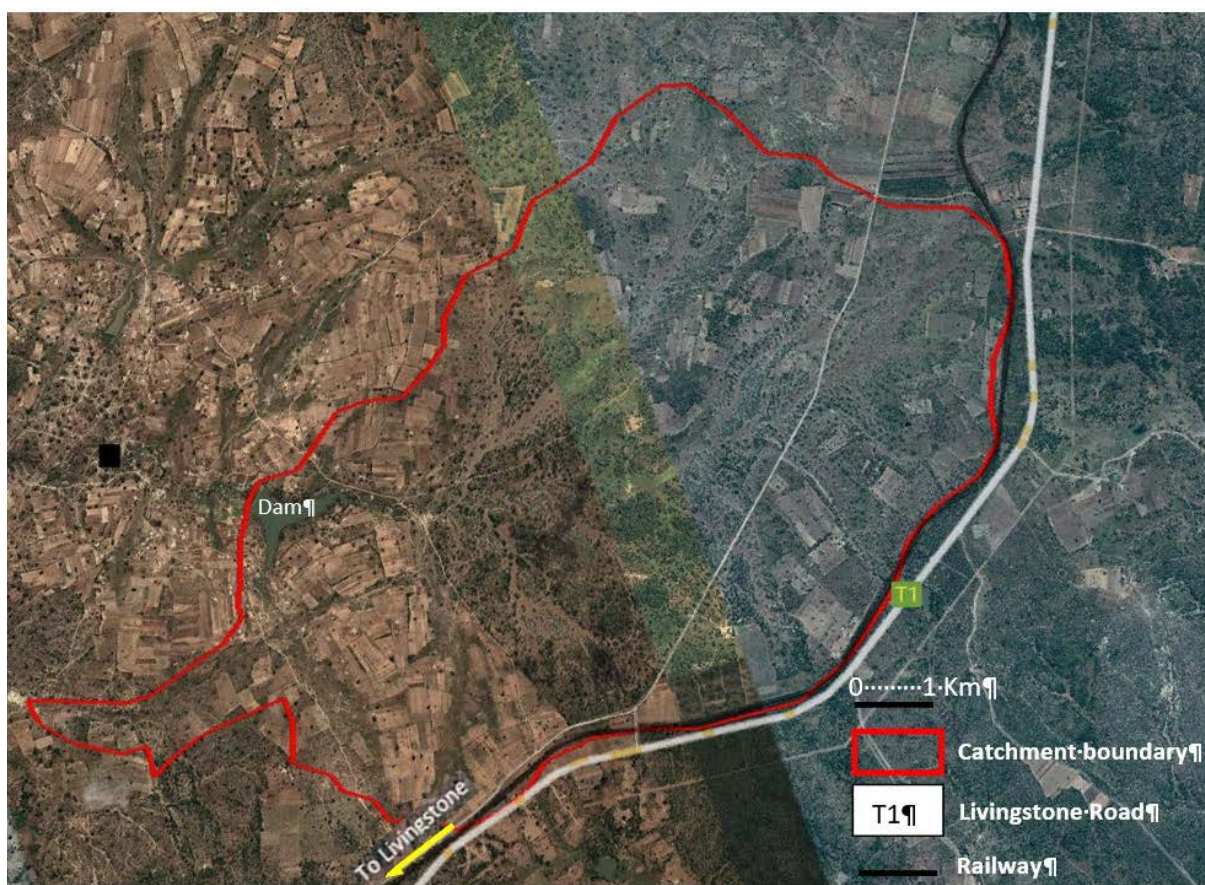
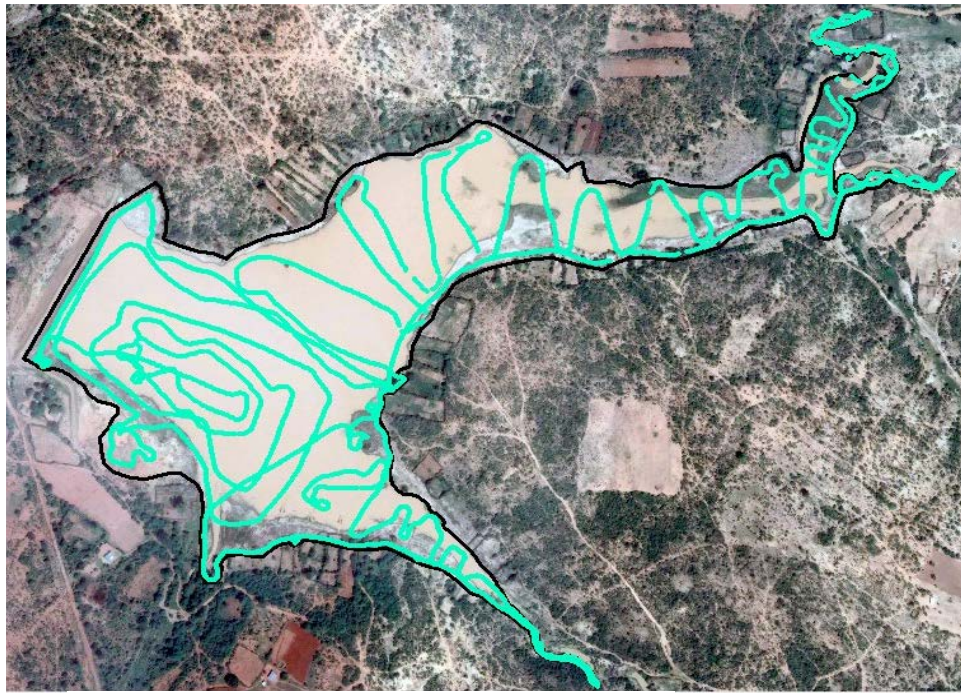


Figure 5.11: Delineated catchment of Mulabalaba Reservoir in Kazungula District, Southern Zambia (April 2022)



Siankanga Dam

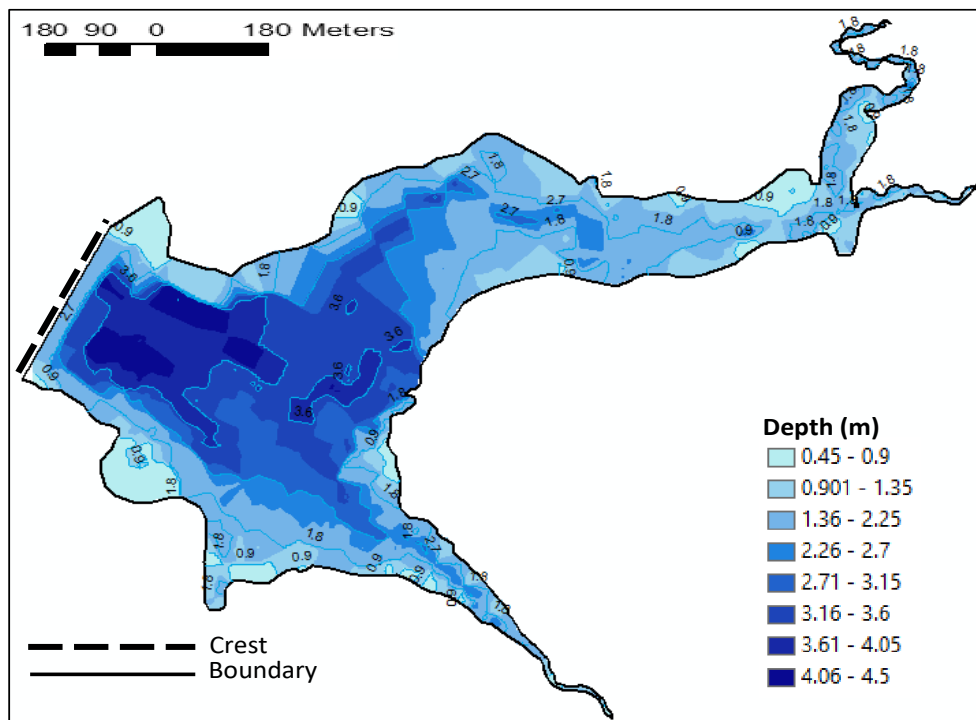


Figure 5.12: Satellite image overlaid with survey (a) pathways; and (b) Bathymetric Map of Siankanga Reservoir (Field data, 2016)

Table 5.4: Water depth, Water surface are and Volume for Sianankanga Reservoir

Depth (m)	Area (m²)	Volume (m³)
4.5	246,999.4	1,111497
4.37	246998.4	1076560
4.35	246996.4	1047446
4.3	246994.4	1012509
4.28	246990.4	977571.9
4.05	246989.4	849469.3
3.83	246979.3	715543.9
3.6	246969.3	587441.3
3.38	235587	455956.6
3.15	191820.5	354275
2.93	159773.6	280454.5
2.7	143576.7	224143.7
2.48	123865	175164.9
2.25	101471.9	139054.7
2.03	83687.96	110892.5
1.8	69742.77	90117.38
1.58	57701.26	73703.94
1.35	50205.49	61106.64
1.13	43072.79	50377.46
0.9	36804.72	41996.69
0.68	30052.44	35207.46
0.45	24882.11	30194.22
0	0	0

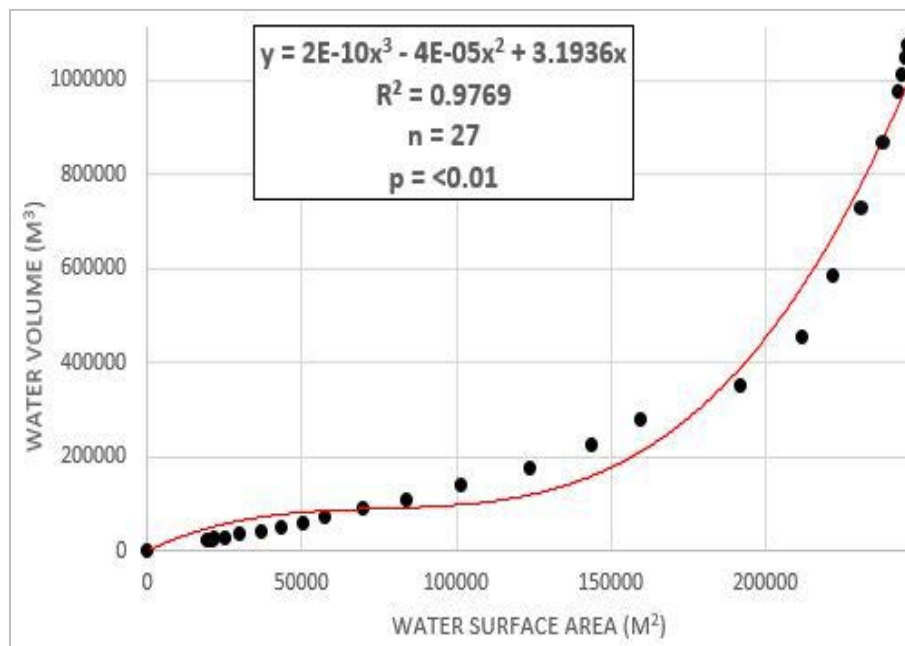
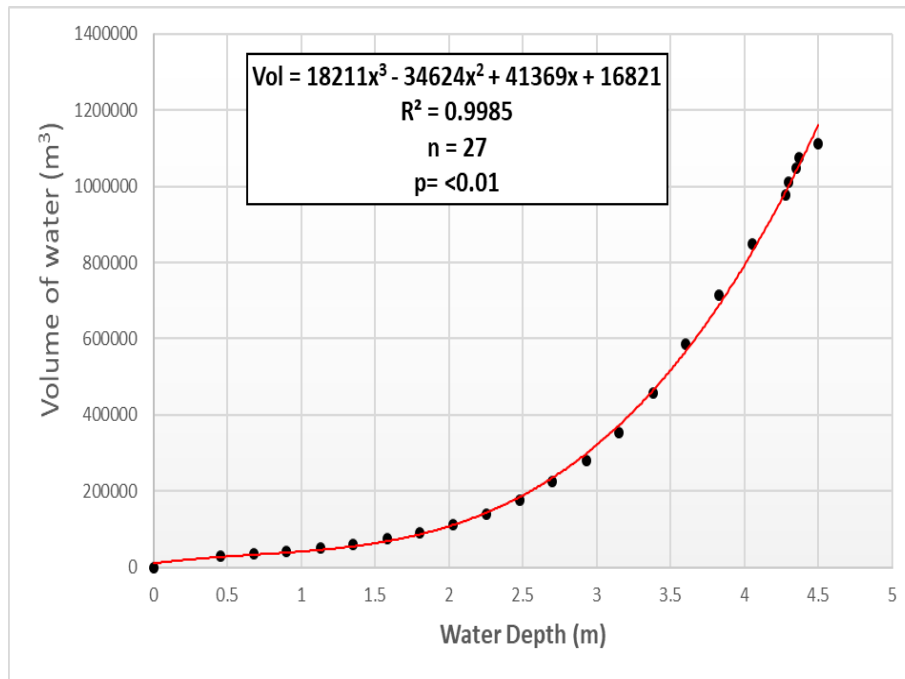


Figure 5.13: Water surface area-volume (a) and water depth-volume (b) relationships for Siankanga reservoir (Sichingabula, 2012; Field data, 2016)

Siankanga Catchment was estimated at 21.7 km² and was mainly characterized by several activities such as gardening and crop farming transcending the buffer zone of the reservoir into the waters. Figure 5.14 below presents delineated visual impression of the catchment.

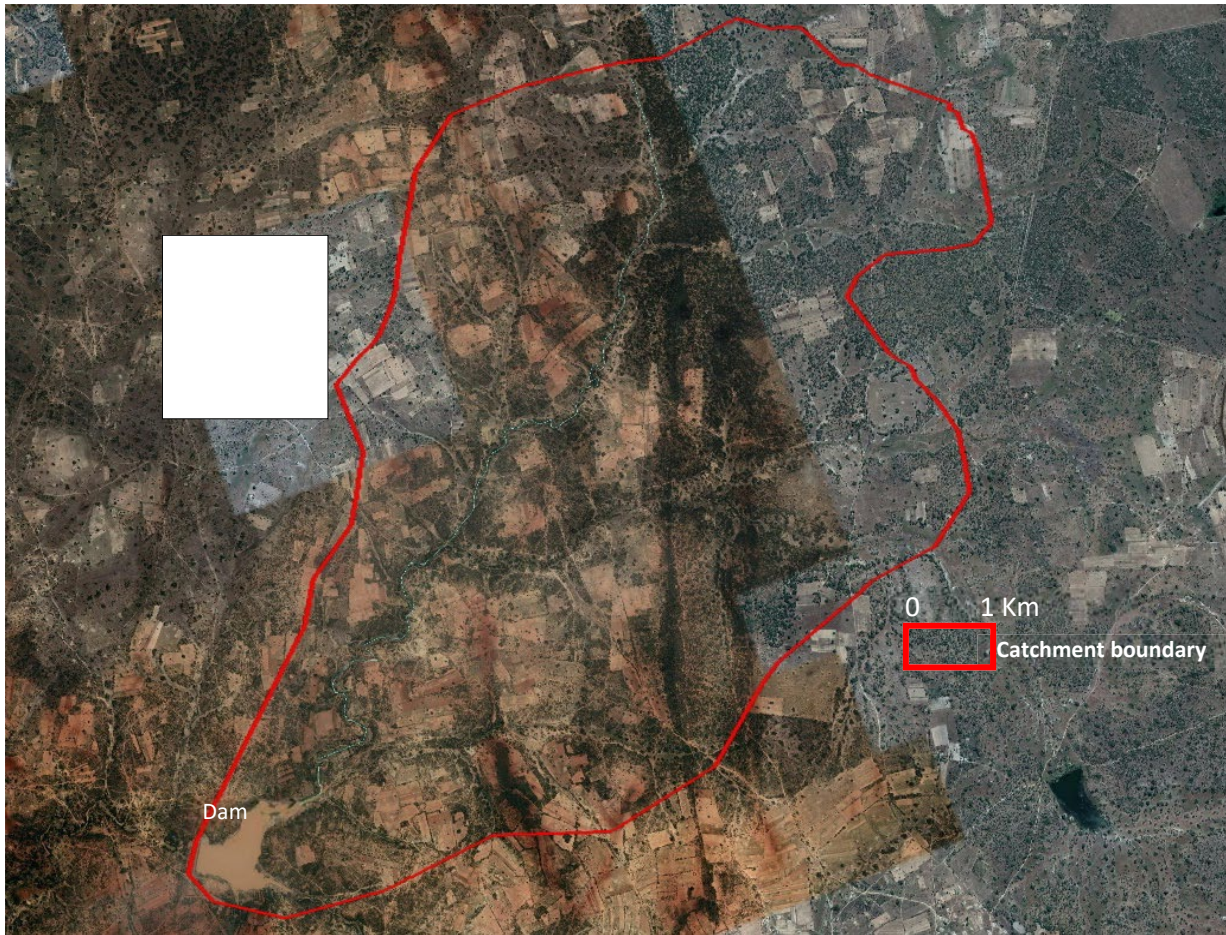


Figure 5.14: Delineated catchment of Sianankanga Reservoir in Kalomo District, Southern Zambia (April 2022)

5.13.2 Hydrological regimes of the reservoirs based on Bathymetric assessment and remote sensing.

The volumes of water in the three reservoirs were found to be volumetrically unstable with Musokotwane reservoir being the most variable due to siltation and thus, likely to experience frequent water scarcity and stresses during dry seasons. The hydrological regimes also suggest that between December 2016 and mid-2022, Mulabalaba reservoir experienced receding flows between 2018 and 2019, but between 2019 and 2022, the findings suggest stable peak flows especially during rainy seasons. On the other hand, Sianankanga Reservoir showed sharp rising and falling limbs between December 2019 and 2021 as compared to previous years (Figure 5.15).

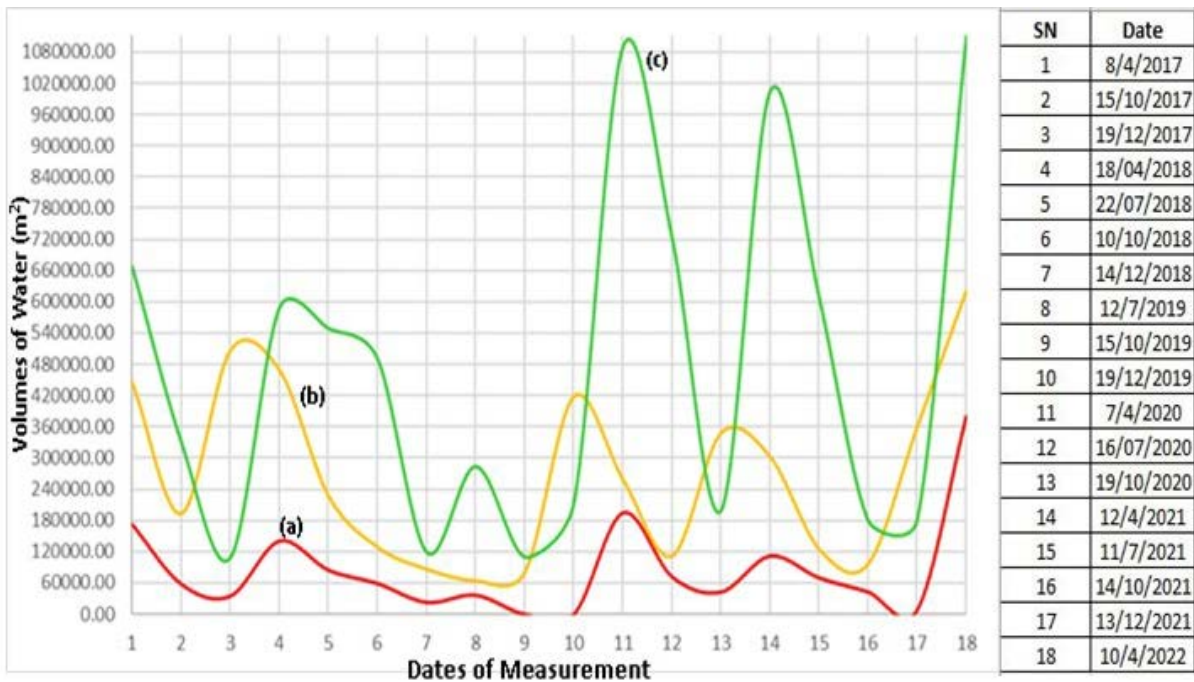


Figure 5.15: Hydrological regimes of (a) Musokotwane, (b) Mulabalaba and, (c) Siankanga Reservoirs, 2017-2022

NB: Data computed based on remote sensed water surface areas at different times from Sentinel A and B, 2022)

5.13.3 Estimation of quantity of sediment accumulated in selected reservoirs

Chihombori *et al.* (2012) used assorted mathematical algorithms to evaluate the rate of sedimentation of Marah Reservoir in Zimbabwe with a view to determine the capacity of the reservoir based on current sedimentation rate as well as the lifespan of the reservoir under the current management practices. They observed that during the first seven seasons of Marah Reservoir's life, it silted at a rate of 1.77 per cent per season, reducing its capacity from $6.67 \times 10^5 \text{ m}^3$ to $6.55 \times 10^5 \text{ m}^3$. The problem of high sediment disposition in reservoirs is quite widespread, but assessment of this phenomenon is quite a challenging task especially for reservoirs whose initial hydraulic information is not well known and if they also do not completely dry out. The ECM earlier described in methodology was developed by Muchanga (2020) to overcome the challenge. Using sediment coring and GIS approaches, the study determined siltation in the target reservoir at $87,163.14 \text{ m}^3$, but using the ECM, the volume was estimated at $79,749.38 \text{ m}^3$ with coefficient of variation (CV) at 6%. The ECM was later tested on another reservoir by Mphande and Sichingabula (2019) using bathymetric surveying method, the siltation of the GRZ Weir in the Mushibemba Catchment was estimated at $50,537 \text{ m}^3$ but using ECM it was estimated at $53,312 \text{ m}^3$. Thus, the ECM results were closely related to the hydrographic survey method at 3.8% CV. The ECM was also adopted in the rapid assessment of sedimentation in 34 reservoirs of the Magoye sub-catchment of the Kafue

Catchment within the Zambezi main catchment (Table 5.5) (Ministry of Water Development and Sanitation (MWDS, 2022)). The ECM estimated the magnitude of siltation of original storages between 8% and 57% for various reservoirs. The average siltation for 17 of the 34 reservoirs was above 91,000 m³, which signals high average siltation rate. The current study applied the ECM to estimate the quantity of sediment loaded in the three reservoirs and the findings were as presented in Table 5.5. The findings are suggesting that, siltation levels were within close magnitude as the capacity loss oscillated around 15% to 17% for all the three dams.

Table 5.5: Estimated Total Sediment Loaded in the Reservoirs

Variables	Musokotwane	Mulabalaba	Sianankanga
Water surface area (m ²)	103,052.79	117,087.98	246,999.41
Water surface elevation (m)	1061.81	1144.37	1197.54
Downstream elevation (m)	1055.83	1136.21	1190.28
Max Water Depth Near Crest (m)	3.69	5.31	4.5
Constant	3	3	3
Maximum Sediment Depth Near Crest (m)	2.29	2.85	2.76
Total Sediment Volume Loaded (m ³)	78, 663.63	111, 233.58	227, 239.46
Estimated original Storage Capacity (m ³) (Sediment Quantity + Water Quantity at current Capacity)	458, 928.43	732, 970.69	1, 338, 736.46
Estimated Storage Loss	17%	15%	17%

(Field Data, April 2022)

Apart from the earlier mentioned secondary data that employed ECM, Sichingabula (2018) also surveyed 38 reservoirs within the Zambezi basin using sediment coring method and GIS approaches where the average siltation (>98,000 m³) for 10 out of 38 reservoirs (Table 6b) was within the same magnitude as the above mentioned 34 dams. The current study used the same approach to estimate silt in the three target reservoirs. The close range of the average siltation signifies a probable spatial homogeneity of siltation magnitude in other spatial contexts within the Zambezi Basin. The study by MWDS (2022) established that, on average, the target reservoirs had lost 26% of their original storage capacities which is a significant loss given the ever-increasing demand for limited water resources (Table 5.6a).

Table 5.6a: Water availability and Sedimentation records for selected reservoirs in the Magoye sub-catchment of the Kafue Catchment in the Zambezi Basin

No	District	Name of Dam	UTM Location		Date of Measured (m)	Water Depth (m)		OSC (m ³)	Measured Water Volume (m ³)	Estimated sedimentation (m ³)	Storage Capacity Loss	CV between OSC and CSC
			X	Y		Max	Min					
1	Mazabula	Mainza A	578457.95	8212009.45	28/4/2021	3.71	0.14	330,777.02	315,134.48	15,642.54	5%	1.7%
2	Mazabuka	Nankenya Dam 1	602494.716	8214607.89	22/4/2021	4.45	0.14	264,634.05	243,039.28	21,594.77	8%	3.0%
3	Mazabula	Magoye Weir	565800.314	8230545.91	23/4/2021	6.86	0.14	372,055.73	206,513.55	165,542.18	44%	20.2%
4	Monze	Simwendengwe	547608.322	8176170.08	26/4/2021	2.8	0.14	168,276.09	151,797.58	16,478.51	10%	3.6%
5	Monze	Hachanga	560196.294	8201840.57	25/4/2021	12.16	0.26	5,387,679.37	4,689,547.25	698,132.12	13%	4.9%
6	Monze	Mainza C	576710	8208596	29/4/2021	2.56	0.1	155,254.78	131,233.00	24,021.78	15%	5.9%
7	Monze	Hanchobezyi	556940.251	8178815.09	27/4/2021	1.92	0.14	42,015.67	34,277.92	7,737.75	18%	7.2%
8	Monze	Kanyemba	561431.121	8185561.75	28/4/2021	2.14	0.13	82,331.26	66,846.30	15,484.96	19%	7.3%

No	District	Name of Dam	UTM Location		Date of Measured (m)	Water Depth (m)		OSC (m ³)	Measured Water Volume (m ³)	Estimated sedimentation (m ³)	Storage Capacity Loss	CV between OSC and CSC
			X	Y		Max	Min					
9	Monze	Lweeta	565992.52	8197852.35	25/4/2021	3.64	0.1	245,251.93	186,836.78	58,415.15	24%	9.6%
10	Monze	Singonya	561622.154	8180555.52	29/4/2021	4.73	0.14	374,049.27	277,976.63	96,072.64	26%	10.4%
11	Monze	Hambweka 1	552499	8170164	26/4/2021	1.7	0.14	33,581.25	24,313.40	9,267.86	28%	11.3%
12	Monze	Rusangu	555441.956	8189420.5	27/4/2021	4.73	0.14	229,950.38	164,885.60	65,064.78	28%	11.7%
13	Monze	Chipongwe	564295.435	8187533.61	28/4/2021	3.37	0.14	219,536.01	141,419.89	78,116.12	36%	15.3%
14	Monze	Chipembele	563871.752	8191105.29	28/4/2021	1.9	0.14	81,019.16	45,456.40	35,562.76	44%	19.9%
15	Monze	Makoye	574725.57	8204106.34	25/4/2021	1.71	0.14	167,031.15	72,650.40	94,380.75	57%	27.8%
16	Gwembe	Gwembe	563630.773	8175871.33	29/4/2021	2.29	0.45	155,472.75	76,076.58	79,396.17	51%	24.2%
17	Pemba	Hakwangala	546882.972	8169478.25	30/4/2021	4.79	0.14	308,807.41	233,688.66	75,118.75	24%	9.8%

No	District	Name of Dam	UTM Location		Date of Measured (m)	Water Depth (m)		OSC (m ³)	Measured Water Volume (m ³)	Estimated sedimentation (m ³)	Storage Capacity Loss	CV between OSC and CSC
			X	Y		Max	Min					
Source: MWDS (2022)						Mean	Mean	Total:	Total:	Total:	Mean	Mean
OSC = Original Storage Capacity CSC = Current Storage Capacity, 2021						3.85	0.16	8,617,723.28	7,061.693.7	1,556,029.59	26%	11.4%
										Mean: 91,531.15		

Table 5.6b: Sedimentation status among selected reservoirs in Kalomo, Zimba and Kazungula District in the Zambezi River Basin

No.	Date of measurement	Name of Reservoir	X	Y	District	Volume of Sediment (m ³)
1	25.07.2016	Siankanga Nabuyani	458265.19	8121420.72	Kalomo	126,303.60
2	09.09.2016	Lake Steve Mann	441367.630	8112182.009	Kalomo	111,341.00
3	13.10.2016	Maziba	435643.51	8100667.77	Kalomo	80,186.48
4	15.10.2016	Three Corner	429115.98	8104306.62	Kalomo	34,731.32
5	11.09.2016	Nangubo	416749.291	8146437.698	Kalomo	54,321.00
6	19.03.2017	Mambali	402993.78	8073062.71	Zimba	103,119.03
7	11.07.2017	Chali	400826.37	8083896.39	Zimba	36,281.47
8	11.07.2017	Masiye	393251.93	8082343.83	Zimba	188,855.35
9	24.03.2017	Simakalanga	384331.75	8078989.97	Kazungula	139,574.11
10	14.07.2017	Sikabwe	396373.85	8071517.97	Kazungula	113,416.40
Total						988,129.76
Mean						98,812.98

5.13.4 Main drivers of sedimentation in the reservoirs

Sedimentation in reservoirs is propelled by both geomorphic and anthropogenic processes. From what is already documented in previous studies by Muchanga *et al.* (2019), Sichingabula (2018), Sichingabula *et al.* (2014), Sichingabula, 2000, Sichingabula (1997) siltation in the southern part of Zambia is propelled by crop agriculture, animal grazing, natural erosion processes as well as poor siting of dams. Muchanga and Sichingabula (2021) further noted that, most reservoirs within the lower half of the Zambezi Catchment are prone to buffer zone anthropogenic activities, which include gardening, sand mining, deforestation, brick moulding among others. Table 5.7 presents factors that influence rates of reservoir sedimentation, water flows and water quality of reservoirs as found in secondary sources. The primary data from the field are presented in Figure 5.16. The findings as presented in Figure 5.16 show that most of the drivers of sedimentation were anthropogenic in nature especially agricultural activities, which loosened the soils and stimulated high sediment generation, transportation and eventually deposition into the reservoirs.

Table 5.7: Summary of factors influencing reservoir sedimentation, water flows and water quality

Factors influencing sedimentation process		Literature consulted
Physical factors	Surface runoff	Tejaswini and Sathian (2018), Leopold <i>et al.</i> , 1995.
	Groundwater hydrology: water table, flows and quantity.	Viessman and Lewis (2012)
	Soil: type, bulk density, erodibility, composition, particle sizes and chemistry.	Baishya and Sahariah (2017)

Factors influencing sedimentation process		Literature consulted
	Physical characteristics of catchment such as size, declivity angle, bank characteristics, locations, surface form, stream density, distance to the water body, vegetation cover and parent rock.	Goudie and Pye (1983) Leopold <i>et al.</i> , 1995, Walling <i>et al.</i> (2001)
	Channel characteristics: bank and channel cover, slope, erodibility factor, stream length and width.	Chiti (1987), Viessman and Lewis (2012), Leopold <i>et al.</i> , 1995, Walling <i>et al.</i> (2001)
	Climatic factors: Type of precipitation, rainy days, quantity, storm direction and rainfall distribution, antecedent rainfall events and timing,	Chiti (1987), Leopold <i>et al.</i> (1995), Sichingabula (1996), Sichingabula (2000), Viessman and Lewis (2012),
Human Factors: Land use such as riverbank agriculture, grazing, irrigation type, urbanization, and sand mining.		Leopold <i>et al.</i> , 1995, Sichingabula <i>et al.</i> (2014), Sichingabula (2018); Da Silva <i>et al.</i> (2016), Hamatuli and Muchanga (2021)

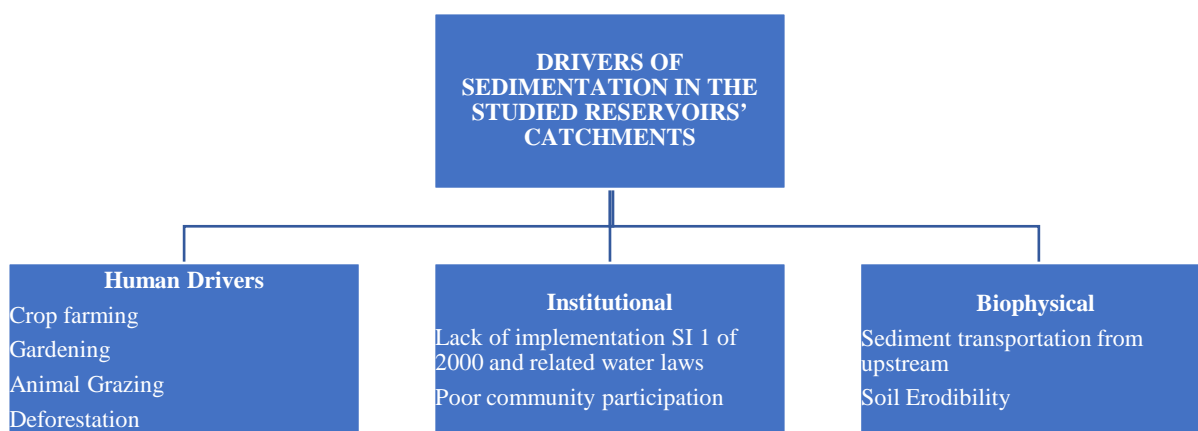


Figure 5.16: Drivers of Sedimentation in the Musokotwane, Mulabalaba and Sianankanga Catchments (Field data, 2022)

5.13.5 Community-initiated coping strategies to water stresses and scarcity

Water is becoming an increasingly scarce resource because of climate change and increased demand from a growing human population. Communities in arid and drying up environments of the Zambezi Basin are particularly vulnerable to water scarcity throughout the year (Chisanga *et al.*, 2022). Meeting the growing demand for freshwater in such locations and maintaining or repairing ecosystems so that they can replenish water sources sustainably remains one of the century's most challenging and significant issues (Hailu Shiferaw, 2021; Calow, 2006). In view of adapting to such water stressful environments, communities often devise coping strategies both sustainable and sustainable for survival purposes. Coping strategies are preventative and reformative measures taken by people and/or communities whose survival is threatened or damaged (Cull *et al.*, 2013). Cull *et al.* (2013) say that coping is a short-term solution devised by individuals and/or groups to ensure survival under stressful circumstances. The greater the degree of vulnerability, the poorer is one's capacity to deal with stressful situations, the greater one's proclivity to adopt a coping method. Mavhura *et al.* (2013) investigated diversity in the ability of households to cope and the survival strategies they employed. The study suggested that the degree to which climate change-related water insecurity affects households is a consequence of not just the magnitude of the flood and/or drought, but also of variables such as income, education, and occupation. Maystadt *et al.* (2014) suggests that loss of natural resources, particularly water resources is the primary driver of African rivalry and war. Mukhlani and Nyamupingidza (2014) study of coping methods used

by government, communities, and families under water scarcity circumstances in Bulawayo identified positive and negative coping techniques. These include 'water shedding' to maintain stable dam-water levels, water trucking, long walks to gather water, purchasing water from neighbouring towns and vendors, purchasing water containers to store water, as well as dispute, vandalism, and abuse (Hosea and Khalema, 2020). According to Mukuhlani and Nyamupingidza (2014), conflict as a negative coping technique arises because of variability in water supply, particularly during times of water scarcity and restriction. Additionally, Patrick *et al.* (2020) claimed that conflict as a coping mechanism emerges when the opportunity cost of aggression outweighs the adoption of other reaction mechanisms. Patrick (2020) asserts in his study of rural South Africa that residents are more inclined to resort to violence as a means of articulating their frustrations when resources are scarce or non-existent. Table 5.10 summarizes some of the coping strategies adopted by communities from various parts of the Zambezi Basin.

Table 5.8: *Some coping Strategies adopted by communities to water stresses induced by siltation and climate change*

Classification	Community coping strategies	Place within Zambezi Basin	References
Constructive coping Approach	Water shedding	Zimbabwe	Mukuhlani & Nyamupingidza (2014)
	Water trucking and long walks to fetch water	Zambia, Zimbabwe	Mukuhlani & Nyamupingidza (2014); Sichingabula (2018); Muchanga (2020); MWDS (2022)
	Purchasing water from neighbouring towns and vendors, water containers to store water		
	Direct rainwater harvesting and surface runoff harvesting	Botswana, Zambia, Namibia	Schlamovitz & Becker (2021), MWDS (2022),
	Adopt drought resistant crops and animals	Namibia, Zambia, Zimbabwe	Shikangalah, 2020; Muchanga, 2011;
	Alternative livelihood (honey production)	Zambia	SASSCAL, 2021
			Sichingabula, 2018, Tiffen and Mulele,

Classification	Community coping strategies	Place within Zambezi Basin	References
	Dam construction & Borehole drilling	Zambia, Zimbabwe, Malawi, Mozambique	1994, Kamtukule and Kaseke, 2012, Mavima <i>et al.</i> , 2015, Paudel, 2019.
	Soil and stone bunds	Zambia	GIZ AWARE Project
Destructive coping Approach	Dispute, vandalism, and abuse	Zimbabwe, Zambia	MWDS 2022,
	Alternative livelihood (Sand mining, Charcoal burning)	Zambia, Zimbabwe	MWDS 2022, Muchanga, 2020, Mavima <i>et al.</i> , 2015
	Digging Wells in Reservoirs and dry riverbed	Zambia	Simweene and Muchanga, 2021, Muchanga, 2020,
	Buffer zone Gardening and cultivation to access limited water resources	Zambia	MWDS (2022), Hamatuli and Muchanga (2021)
Findings from Current study	Buffer Zone Cultivation for ease of access of water Animal migration to the Kafue flats Use of borehole water when readily available Travel distance to fetch water using ox carts Cultivation on the downstream using irrigation canals so as to minimise siltation and ensure sustained water supply (Based on Fieldwork, April 2022)		

Vorosmarthy *et al.* (2005) assessed water resource exploitation by plotting water reuse index versus distance, based on basin-specific combinations of river discharge and water use progressing downstream (Figure 5.17). Each mainstem showed a unique trajectory, starting from zero at the headwaters. Rises indicate that the river encounters either significant water use (i.e. municipal or irrigation withdrawals) or a tributary with relatively large withdrawals. In contrast, reductions in the index reflect the impact of runoff and tributary inputs with less water use. Associated with increases in water reuse are, increases in competition for water, pollution, and potential public health problems.

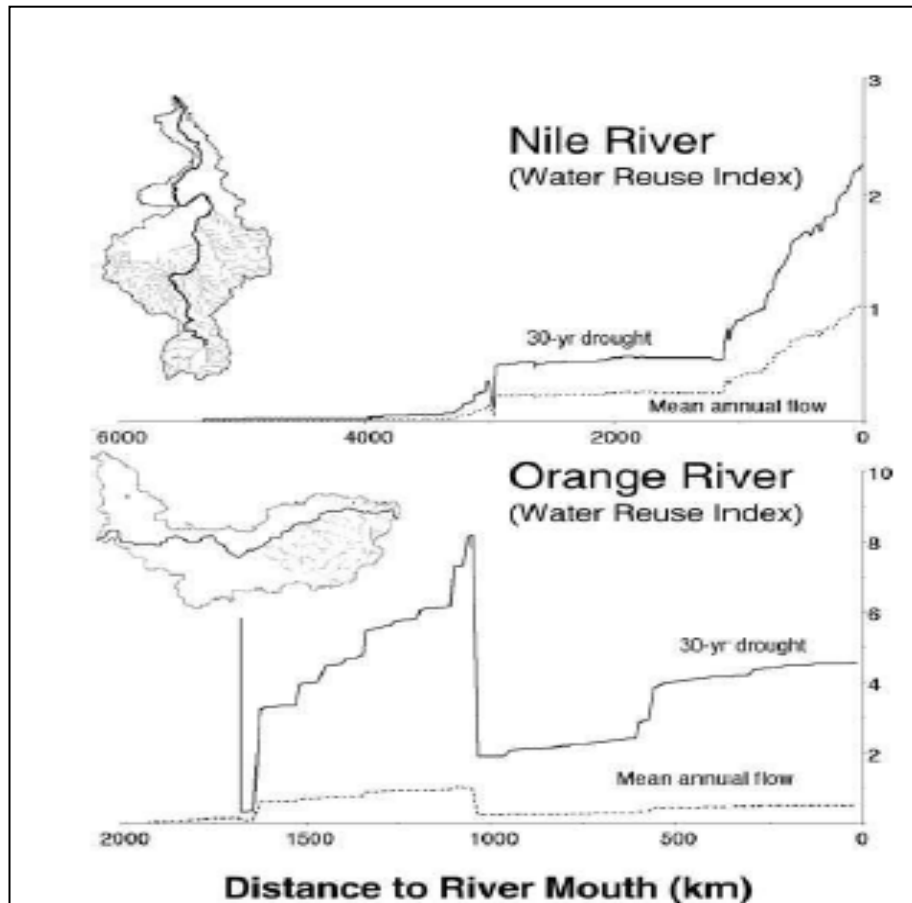


Figure 5.17: Signature of aggregate water use relative to available discharge along two major river corridors under normal and 30-year drought conditions

NB: A value of 1.0 indicates complete reuse of river water equivalent to discharge over an entire year. Source: Vorosmarthy et al. (2005, p. 235).

The figure shows that whereas for the Nile, there was progressive increase moving downstream, with initial rise associated at major irrigation schemes, followed by intensified use downstream of Aswan Dam; the Orange River was seen to react far more dramatically to climate variability. While the relative water reuse progressed downstream to a level, 50% under mean annual flow, it rose by an order of magnitude under 30-year low-flow conditions. The Orange River, since it rises from a drier region unlike the Nile; is almost completely exposed to the arid/semiarid climate making it particularly sensitive to climate variability. From the above, it would probably right to assume that the Zambezi River would also react in the manner of the Nile; on account of it originating from wet humid region in the northwest of Zambia with two major impoundments on its course. Similar detailed assessments of river water reuse are required in the Zambezi-Orange basin in the face of the current climate change being experienced.

5.13.6 Sediment control measures and sustainable water resources management in reservoirs

Several studies have documented diverse strategies to control sediment and ensure sustainable management of water resources in reservoirs. Some of these are biased towards hydraulic engineering (Jacobsen, 1997; Wang and Hu, 2009), others are hydrogeomorphological (Sichingabula, 1997; Chomba and Sichingabula, 2015, Kondolf, 2014; Mwiinde, 2017), and some are ecological (MWDS, 2022), among others. Exploring locally initiated strategies that could help reduce sedimentation and how local communities can generally manage water resource is key in developing conceptual model on how these drivers of siltation and water scarcity problem can be addressed.

5.14 Discussion

Sedimentation is an emerging challenge for some reservoirs, but for others, it is already happening and source of concern. Rapid variations in depths with a system was the first indicator of silting reservoirs whose storage capacities were so reduced to fully sustain the water demands per persons. Going by Global Water Forum (2007) and FAO (2021) standards of normal water requirements per person per annum, the total full storage for the three reservoirs could only comfortably sustain fewer people per year; yet, there were over two hundred thousand people who need water from the reservoirs. The study therefore notes that, the water which was measured could not sustain the water demand due to compromised storage capacities. Given the high-water demand (40 litres per day or 0.04 m³) for livestock such as cattle, both measured and projected storage capacities also implied an economic water scarcity for livestock business, which is the main backbone of the target catchments and, southern half of the Zambezi Basin in general.

The water scarcity and stress problem were a disturbing reality in the target catchments. The hydrological regimes suggest that small reservoirs in the Zambezi catchment are highly likely to experience prolonged water stressful periods and water scarcity that the larger ones. Water scarcity and stress were prevalent between July and November, with October as the most critical month as far as water scarcity s concerned. The worst scenario of water scarcity and stress was recorded in the Musokotwane Reservoir Catchment whose water stressful periods were according to the hydrological regimes, more prolonged than for the other two reservoirs. Hydrograph analysis revealed prolonged low flows than the peak flows for smaller reservoir than the larger ones. The findings suggests that the most water secure period of the year for all reservoirs in the Zambezi Basin was ranging from December to April, which represents about 40% of the year, that means that, during about 60% of the year, strategic water conservation measures must be employed if the already scarce water resource is to sustain the water demands. The study further noted very sharp rising and falling limbs for the Sianankanga and Mulabalaba reservoirs for the period 2019 to 2021 unlike for the period 2016 to 2019. An

earlier study by Muchanga *et al.* (2019) suggests that, whenever such a phenomenon occurs, it could be pointing to siltation problem which takes up the reservoir space such that any single storm event fills it up rapidly. On the other hand, after a storm event, the water volumes rapidly plummet due to rapid evaporation punctuated by reduced water depth, evaporation and abstraction.

Whilst other factors may affect the quantity and quality of water available in reservoirs, siltation remains the most significant driver of storage capacity loss and, under anthropogenic influence; siltation remains a very huge challenge not only for the sampled reservoirs, but for the entire Zambezi Catchment. Ministry of Water Development and Sanitation (MWDS, 2022) established reservoir siltation in the Zambezi catchment remains very high with as high as 88% of the reservoirs especially the medium to small ones being the worst affected by siltation with rapid losses in storage capacities within the magnitude of 8% to 57%. The major drivers of siltation include crop cultivation, which according to earlier studies (Sichingabula, 1997; Sichingabula, 2018, Muchanga, 2020; MWDS, 2022) could be contributing to about 36% of siltation of reservoirs and riverine environments. Mavima *et al.* (2015), Kamtukule and Kaseke, 2012 also earlier noted human activities such as crop farming as major threat to the useful economic life spans of the reservoirs in Zimbabwe and Malawi, respectively. Going beyond crop farming, animal grazing and other mixed land uses (sand mining, gardens, charcoal burning, brick moulding) in the buffer zone remain some of the major drivers of sedimentation in reservoirs and eventually, the water scarcity problem. As noted by Chisanga *et al.* (2022), water scarcity problems are likely to be frequent in the next 50 years amidst climatic changes.

The environmental problems around reservoirs in the Zambezi Basin in general and the three target areas in particular are actually social problems, many of them have been propelled by human beings, who at last, have ended up as victims. The reduction in storage capacities of reservoirs were due to human-induced siltation, this rendered the three reservoirs and others with similar characteristics within the Zambezi Basin incapable of meeting water demand. Both primary and secondary evidence show that livestock is the most affected by dwindling water resources, domestic fishing has also been affected given that, the reservoirs could no longer hold enough water during almost 60% of the year. Hence household income is affected to a point where communities may become food insecure. In a study by Muchanga *et al.* (2020) in a remote small sub-catchment of the Zambezi Basin, it was observed that, prolonged water scarcity due to dried up reservoirs costed health of livestock because there was no water to operationalise dip tanks, which resulted in animal diseases and death.

Under increasing anthropogenic activities such as irrigated farming, the governments across the Zambezi Basin have also been confronted with huge cost implications around management and control of reservoir siltation and to ensure that, water is enough to sustain socioeconomic and environmental needs (Sanchez, 2018). Findings from secondary sources (Mwiinde, 2017;

Sanchez, 2017; World Bank, 2007) reveal that, governments will have to spend a lot of funds to address dwindling water scarcity through desilting and rehabilitation of reservoirs and other water sources. For example, a case study of MWDS (2022) in the Magoye sub-catchment demonstrates that, indeed, restoring the degraded water resources infrastructure such as reservoirs and riverine environments and to filter water of sediment could be very costly not just to be the governments, but also their local and international cooperating partners. Further evidence shows that, sedimentation lowers the benefits from reservoirs' intended environmental and socio-economic use in monetary terms as manifested by Reduced Net Present Value (NPV) (Mwiinde, 2017).

Within the context of cost of sedimentation in reservoirs, Saruchera and Lautze (2019) noted that reservoirs in the Zambezi Basin produced diminishing returns due to lost storage capacities resulting from siltation. Out of the target reservoirs studied, Saruchera and Lautze (2019) noted that only Mboole (constructed in 2002) and Mulabalaba had mild sedimentation problem such that even villagers who depended on these water infrastructures failed to mention siltation as a problem. The finding for the latter reservoir resonates with the current finding, although the hydrological regimes seemed to suggest a pending siltation challenge. On the other hand, Saruchera and Lautze (2019) noted that Chuuka, Milangu and Nteme had lost over half of their storage capacity due to siltation. Generally, the study's preliminary finding show that, the reducing water storage capacities of reservoirs is a major threat to the water security and sustainable socioeconomic and cultural development of several rural communities in the Zambezi Basin and, particularly the reservoirs, which were studied. On the other hand, Mwiinde (2017) and Saruchera & Lautze (2019) noted that the same sediment which severely affects the bathymetries of almost all reservoirs within the Zambezi Basin can actually be beneficial if succinct business models are developed around them. For example, Mwiinde (2017) shows that, it would cost the government about ZMW 500,000 to dredge each small to medium reservoir, but the profits that could be realised from sale or use of dredged fertile sediment for agricultural purposes could be as higher as thrice the amounts spent on dredging.

This goes on to demonstrate that, post challenges and opportunities around water resources and siltation management must be explored to realise the benefits whilst reducing the costs. To cope with these challenges of water scarcity and siltation the local communities adopted both constructive and destructive approaches, which according to evidence in Table 6 should carefully be reconsidered in the future planning for sustainable water resources management and silt control. Evidence from the sampled studies (Sichingabula, 2018; Tiffen and Mulele, 1994; Kamtukule and Kaseke, 2012; Mavima *et al.*, 2015; MWD, 1995; Mavima *et al.*, 2015; MWDS, 2022) inherently suggests intra-basin variations in terms of how communities adapt to various challenges of water scarcity and siltation. As concluded by Vorosmarthy *et al.* (2005), there is high (25% of the population in Africa) chronic water stress (mean use: supply) and 40% experiences drought stress every 30 years. And that generally, water stress is typically low, reflecting its poor water delivery infrastructure. They contend that a well-engineered

increase in use might thus be advantageous in mitigating water-related constraints on development and pollution which also engender an array of social science and engineering issues. They argue that a more complete understanding of human-water interactions and the design of appropriate policy interventions to alleviate water stress require a broader interdisciplinary approach. This requires a physically based framework incorporating social sciences to deal with the numerous challenges faced in water resources management. Hence, the need for a proactive planning system that incapsulate strategies that are contextually useful for sustainable water resources supply for all as enshrined in the SDG 6. The study proposes a conceptual model that can arguably ensure a sustainable water resources management in reservoirs through sustainable sediment control (Figure 5.18).

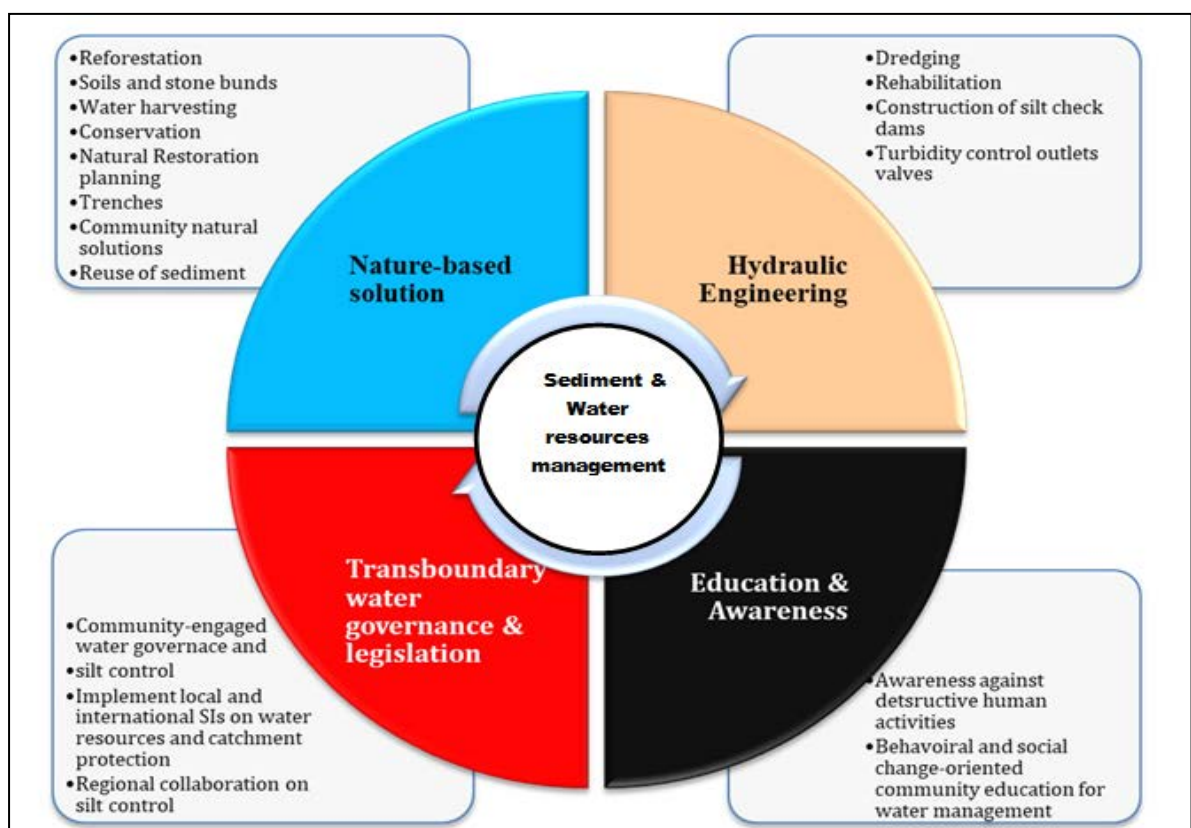


Figure 5.18: Conceptual Model for sustainable management of water resources and siltation control in reservoirs in the Zambezi River Basin

The conceptual model depicts ideas that suggest an interdisciplinary and transdisciplinary approach to addressing the challenges of water scarcity problem triggered by siltation of surface water bodies. By combining nature-based methods, hydraulic engineering techniques and implementation of effective transboundary water governance and laws would help minimise triggers or drivers of changes to water availability. In most intervention strategies, education and awareness are embraced only to a very minimal extent and, in most cases, it ends at awareness, which cannot bring about desired behavioural change for sustainable community based management of catchments. Awareness simply raises conscience, but may not

necessarily evoke desired change, which would make local communities decisively act for sustainable water resources management in view of realising long-term benefits.

5.14.1 Impact of the status of water availability and sedimentation on livestock, crop farming, fishing, and other water dependent socio-economic activities

Attaining water security is one of the major global challenges in the age of climate change, urbanization, and population increase (Pandey, 2021). With increasing population in the southern province of Zambia water demands in the study areas keep increasing as well. The situation is worsened by high rates of sedimentation that has occurred in the dams which has eventually affected livestock farming, the main livelihood strategy. With Kalomo district having a total population of 188,693, Zimba 69,877 and Kazungula 104,731 (2010 census), water availability should be priority to the rural people considering their varying demands. Water security refers to a reliable supply of safe, affordable water that is sufficient to support basic human needs, food production, livelihoods, and ecological services (Wang, 2014). Numerous factors, including population increase, agricultural development, changes in living standards, increasing water pollution, excessive groundwater extraction, and climate change, are putting a serious pressure on southern Zambia's water security (Wang *et al.*, 2012). Southern Province accounts for the highest number of Cattle (1,315,238), at 35.4 percent of the total national herd. Table 8 below shows the livestock population of the three districts.

Table 5.9: Livestock and human population in the selected districts

District	Livestock population	Human Population		
		Urban	Rural	Total
Kazungula	87,000	3,093	101,638	104,731
Kalomo ^{*1}	200,000	15,394	173,299	188,693
Zimba ^{*2}	124,000	2,385	67,492	69,877

Source: Kazungula, Kalomo and Zimba District Agriculture Offices (2022) ^{*1a}=Appendix 1a; ^{*2}=Appendix 1b

The study found that all the three reservoirs drastically lose water within short periods of time as also evidenced in the hydrological regimes. As a result, even if water may be available in rainy season, it is often not readily available during the dry season, thus increasing the water stresses for livestock.

The Kalomo District Water supplier also reported that, when dams dry up or drastically lose water, the local authority spends a lot of money to cushion the deficits. For example, when Sianankanga Reservoir, the main water supply in Kalomo significantly lost its water in 2019, the government was compelled to spend a lot of funds to fetch water through bowsers to meet the water demand. Local people also travelled long distances to fetch water for their livestock. Even boreholes could not cushion the deficit as they were also drying up as reported by Chomba *et al.* (2017).

The local authority also spends a lot of money to ensure that the quality of water meets the health standard before it is supplied to the municipality. The major expenditure was incurred on purchase of imported fine grained sand with harmonized grain size from Zimbabwe. It was also noted that the local authority incurs high cost on purchase of Aluminium Sulphate pellets that is used to filter out the finest suspended sediment from water.

Humans and livestock in Table 8 compete for already stressed water resources thus presenting water insecurities. The Ministry of Agriculture and Livestock reported that Southern Zambia and particularly Kalomo, Zimba and Kazungula Districts experience very variable and short rain days such that, water is never sufficient, leading to food insecurity risks. Water insecurity can thus have a direct and indirect effect on household output and income-generating possibilities, as well as on the quality and quantity of water consumed.

Prolonged water stresses force animals to travel long distances to fetch water and as animals from different catchments come to mix, they tend to spread diseases such as East coast fever, tick borne diseases, among others. The study noted that such a scenario leads to diversion of resources to buy medicine which should have normally been used for other purposes.

Another case from Musokotwane dam in Kazungula District showed that, siltation of the reservoir compromised the fishing activities. The weeds were growing at a faster rate such that it was difficult to control sedimentation. Generally, the impact of sedimentation and dwindling water availability was thematized as presented in Table 5.10.

Table 5.10: Summary of the Impact of sedimentation and poor water supply

Thematic area	Description
Economic Impact	Loss of animals due to diseases Low crop yields due to variable water supply High cost of purifying water of suspended sediment High cost of fetching supplementary water using bowsers during water stressful period Diversion of funds meant for other Socioeconomic activities Reduced fishing activities due to inadequate water availability
Social Impact	Reduced crop yield and food insecurity Prolonged water stress period Animal diseases on increase as animal travel long distances to fetch water to drink People travel long distances to fetch water Increase in food insecurity Poor quality of water for domestic use
Environmental	Poor water quality for aquatic biodiversity Increase risks of degradation of buffer zones and catchment

Chomba *et al.* (2017) noted that the combined water needed for livestock and garden irrigation in dry season for water points in Zimba was found to be 112,893.12 m³. This data is indicative of high the water demand for livestock is in all catchments and given that people also depend on the same water supplies, it definitely increases water scarcity and stresses. Generally, the disruption of livelihood due to water scarcity amidst climate change is evident in the whole of Zambezi Basin as also noted by Chisanga *et al.* (2022) especially on livestock. Zambezi River Basin in general experiences economic water scarcity (FAO, 2021) a finding which has been proven by other independent studies (Chisanga *et al.*, 2022; MWDS, 2022; Sichingabula *et al.*, 2018; Muchanga *et al.*, 2019).

Although the government officers could not provide exact amounts spent on water purification for security reasons, they indicated that, the cost to purify water from suspended sediment was high. Sediment accumulation has become a growing concern for governments in Sub-Saharan Africa and, Zambezi Basin. With diminished fiscal capacity, the issue of siltation in reservoirs is far from being resolved in several Sub-Saharan African countries. The study of Mwiinde

(2017) notes that, an estimated ZMW 391,759.50 to ZMW 93,363,719.00 would be required to remove and convey the sediment to areas within a 10-kilometre radius of the dams. Additionally, the investigation discovered that silt in water bodies such as reservoirs drive organizational and operational costs because of the work required to provide safe and quality water to people. Mwiinde (2017) established that a total of ZMW 846,160, or 6.42 percent of net annual revenues, was spent on paying staff to filter the water and on purchasing additional chemicals for decontaminating the water from chemical sediment. The costs of sediment and sedimentation are expected to continue for the remainder of the dams' useful lifespan, or until the dams eventually fill with sediment if no preventative measures are implemented. The cost of sediment is far reaching in the Zambezi River.

All of these variables contribute to the hydro turbine's efficiency and useful life degrading over time (Adeniyi, 2021). The study by MWDS (2022) established that, sedimentation costing the government huge sums of money as the sediment is contributing to frequent water scarcities which tend to affect government budgetary allocation to cater for those affected by crop failures, animal diseases, among others. Moreover, the damage left by uncontrolled sedimentation tends to gobble huge sums of money for strategic planning to restore damaged riverine and reservoir ecosystems and ecosystems. For example, planning restoration and protection of the Magoye sub-catchment in the Kafue Catchment of the Zambezi main basin costed the government and its cooperating partners a lot of time, energy, and resources to bring different experts to plan to address the silt problem among others. This is not the only costly venture, but also the Luangwa sub-catchment in the Zambezi catchment is calling for huge sums of money to address the challenge of siltation and its impact on water resources management. Sichingabula *et al.* (1999) earlier noted with concern how this catchment is rapidly degrading due to large scale silt generation, transportation, and deposition both onsite and offsite causing widespread impact on water resources and riverine biodiversity.

5.15 Policy implications

Many of the findings of the study speak to the SADC Water policy, which acknowledges both low urban and rural water supply leading to high incidence of water-borne diseases; rapidly growing and urbanizing populations, leading to growing water scarcity and increasing water pollution, very low water-use efficiency in irrigated agriculture; degraded watersheds and deteriorating water quality as well as high stresses within increasing importance of hydropower to the regional economy (SADC, 2005). The significant losses in storage capacities of many dams and rivers due to siltation imply that policy makers need to re-strategize both from country and basin contexts on intervention measures that can restore the dwindling water resources for the countries and basin perspectives. If that is not taken seriously with the urgency it deserves severe water scarcity problems and even water conflicts should be expected with diverse socioeconomic implications. Most water-linked sectors especially agriculture and energy are likely to be the worst affected by the water scarcity problem (Vorosmarthy *et al.*, 2005). Given the significance of these sectors among others, several ripple effects could be felt as water supply versus demand discrepancies keep on widening.

In view of addressing the problem from the root cause, the governments need to re-affirm existing national and even regional policies that are aimed at protecting water resources. For example, Zambia has specific laws on protection of buffer zones of all water bodies SI 1 of 2000, but this has been poorly implemented leading to regrettable degradation of sections of several rivers and dam buffer zones (MWDS, 2022). While this neglect may sound country bound, it has several intra and inter spatial implications as for example sediment get eroded and transported several miles and only to possibly be deposited in an area that perhaps does not generate much sediment. This scenario is extrapolatable to all countries within the Zambezi Basin and even the Orange Basin such that, policy makers in various country contexts and at basin scale should collaborate to develop and implement laws and policies that would help address pending water crises. It is no mere exaggeration that sedimentation problem and its effect on water security is predominantly anthropogenically driven and, the consequences are ending up with human beings who punctuate such problems. From policy context, it means that educational programming and policies should be factored in the processes of addressing the challenges to discourage behaviours that punctuate siltation and water scarcity as well as stresses. If that is not done, then whatever intervention policy measure shall prove futile as the behaviours that punctuate siltation remain unaddressed. This is actually also highly emphasised in the SADC Water Policy. In view of building a stronger scientific database that informs policy decisions, governments within the Zambezi and Orange Basins must consider developing new research agenda that speak to current problematic landscape as far as water security and siltation problems are concerned. Given the projected climatic changes within the two catchments (Chisanga *et al.*, 2022), augmented siltation levels and catchment degradations are highly expected such that continuous implementation of research agenda for future water security should really be integrated in every developmental narrative. Generally, a neglect of these policy issues may deter attenuation of all water-dependent SDGs and sectors.

5.16 Conclusion

Based on the preliminary findings from secondary and primary information, the study concludes that majority of reservoirs in the Zambezi Basin could be as silted up as those, which were targeted for this study such that their storage capacities may not sustain the current water demands for household and livestock use. Based on assorted bathymetrically surveyed reservoirs in selected parts of the Zambezi Basin and particularly the three surveyed in southern Zambia, the study concludes that small dams are at the highest risks of losing storage capacities. Consequently, catchments where such small reservoirs are located could also be prone to severe water scarcity and stress especially between July and early November. This inspired the conclusion that, most communities within the Zambezi basin are water insecure and are subject to high risks of economic scarcity within next 50 years amidst climatic changes. All reservoirs in the Zambezi Basin with similar characteristics as those sampled in the current study are only water-secure between December and April, a situation which affects crop and animal productivity, fishing activities, hydropower generations, among others. Agricultural activities

remain the drivers of siltation and loss of storage capacities for most reservoirs. The cost of addressing sedimentation among reservoirs bears a heavy toll on the government planning process, but at the same time, the very propellant of reservoirs' loss of storage capacities could be transformatively be utilised to build profitable business models and be reused for fertilisation of crops. This remains poorly utilised coping strategy and opportunity for most countries within the Zambezi Catchment. The coping strategies such as alternative livelihood, water harvesting, and water shedding recorded in various parts of the catchment suggests a spatially distributed nature of the problem of water scarcity due to siltation and climatic changes. Some sub-catchments within the Zambezi Basin adopted destructive approaches such as conflicts, cultivating within the legally forbidden buffer zones, digging wells right on dry beds of river channels and reservoirs, especially during water stressful period, among others as coping strategies water scarcity problem. Given the systemic and complex nature of water scarcity study proposed a conceptual model that is inherently proposing integrated and transdisciplinary approaches to address the challenges of reservoirs' storage losses and siltation challenges for sustainable water resources by 2030 and beyond.

5.17 Recommendations

- a. Based on the finding that reservoirs' storage capacities of earth dams are low and are losing storage capacities due to siltation, it is recommended that the drivers of siltation be address.
- b. The water scarcity risk within the Zambezi Basin were found to be spatially distributed across all countries that share the basin, hence, dredging more medium to large reservoirs to cushion water deficits especially during water-stressful period between July and early November.
- c. High sedimentation remains a major threat to the water security within the catchment, but the study still recommends exploration of business models around it so as to address it in a profitable way as this remains quite unexplored option.
- d. There is a need to effectively enforce both local and international laws around water protection
- e. Given the high rates of siltation and being the major threat to the sustainability of water resources amidst climatic changes, a dedicated research bathymetric surveying and siltation monitoring is recommended to determine the full extent of the problem and how it is punctuating waters scarcity
- f. Given that, the water challenges within the Zambezi are largely human induced, there is also need for deliberate educational programmes that bring about behavioural changes for sustainable small basin management.

CHAPTER 6

ANALYSIS OF PROJECTED IMPACTS OF SEDIMENTATION AND BATHYMETRY ON THE GARIEP DAM TO WATER SCARCITY PROBLEMS ON THE PRIORITY WATER-LINKED SECTORS IN THE ORANGE RIVER BASIN OF SOUTH AFRICA

6.1 Introduction

The document focuses on the approach of using remote sensing to assess dam water volumes, calibrated against existing data. Dams and reservoirs play a crucial role in providing sustainable water supply and regulating flow within catchments. Larger dams, such as those in the Zambezi and particularly the Gariep dam in the Orange River, directly impact power generation as the reservoir level is closely tied to capacity. It is important to model the effects of changes in flow and sedimentation rates to effectively plan and manage the reservoir/dam and associated hydropower plants. This includes ensuring adequate water levels for power generation and mitigating flood risks (Okumura & Sumi, 2012). Furthermore, considering the potential impact of climate change on sedimentation rates is essential in these modelling exercises (Schleiss *et al.*, 2016).

For accurate modelling, it is vital to have historical data on reservoir capacities and their levels over time. While electronic logging is prevalent for most measurements, smaller dams often still rely on stage measurements. Managing siltation is crucial as dam volumes gradually decrease over time. Some dams have expected useful lifespans and maintenance requirements, while planning for new dams should always be on the agenda.

Due to physical constraints during the COVID-19 pandemic, the study team adopted a remote evaluation methodology, with a specific focus on the Gariep dam. The available information was utilized to understand the project's objectives and generate outcomes that can inform the assessment of smaller dams in South Africa. This research aims to provide timely planning information for communities dependent on specific dams, ensuring sustainable water management.

Gariep dam, situated on the Orange River in South Africa, is one of the country's largest dams. It plays a crucial role in supplying water to various sectors, including agriculture, urban areas, and industry. With changing weather patterns and growing water demand, understanding the current water status of Gariep dam is essential for effective water resource management. Bathymetry, which involves studying underwater depth and topography, provides critical data

for assessing the dam's capacity and health. By mapping the underwater terrain and monitoring changes in water level and sediment deposition, bathymetric studies can offer valuable insights into the dam's current state and potential challenges in the future. The objective of this study is to reflect on the water status of Gariep dam by conducting a comprehensive bathymetric survey, analysing the collected data, and providing recommendations for the sustainable management of water resources.

6.2 Work planning and task description

The task has two tranches that will have to inform each other. Within each of the tranches, there are several blocks that will have to be mastered to collectively derive at the task conclusions. During the process, the two tranches will have to consult each other to discuss progress.

Tranche 1: An investigation into the current and past management of the Gariep dam based on the information gathered and utilized for planning

Tranche 2: This tranche will investigate using remotely sensed information to better the current methodology.

Below this section, a resource section is provided to be used in working with these tasks. While we provide information sources for both the Orange River and the Zambezi, the task for now will focus on the Gariep dam. Please feel free to consult all the resources provided.

The WRC Interns and their projects

Tranche 1

1. Produce maps of the topography of the dam floor. In this task, all possible resources will have to be used to produce the original dam floor topography. This approach can be published as an article.
2. Produce the perimeter maps of the dam from satellite imagery for various stages of dam fullness. Compare the results with the recorded dam water levels for the same day. Set up a correlation between water body surface area and correlate with recorded depth values.
3. Set up an automated procedure for recording dam water body surface area from satellite imagery. Present this as a product that could replace the level recordings done by the DWA.
4. Use the paleo topography of the dam floor, with the old stream pattern to reflect and argue where most sedimentation will occur.
5. In GIS do a calculation of the dam water volume, based on the mapped surface areas and the dam floor topographic map (Best done in Raster format).

6. Plan a dam survey based on your findings to prove the theory. Coordinates of the positions where no sedimentation is expected and positions where most sedimentation is expected need to be listed.
7. Write up the processes used as a manual and an article.
8. Apply the technique to the Vanderkloof Dam.

Tranche 2

1. Find all the literature about the Gariep dam with published figures around dam volume, the rate of siltation and prepare this as a publishable literature study highlighting the need for accurate dam water volume information.
2. Duplicate the proposed engineering process of dam siltation evaluation using their data. Reflect on your findings and if you think the accuracy is questionable
3. Distinguish between rain, heavy rain and storm events in terms of the sedimentation impact on dams, and especially the Gariep. Use the old climate data to categorize these events. Find news briefs or published confirmation on increase erosion because of rain events. Correlate these events with the dam water colour observed in the satellite information available.
4. Use other dams in the region as part of the study. Also look at the water colour in sections of the Orange River upstream of Gariep dam to confirm change in visible detection of increased sedimentation. Can you quantify the changes in colour? Is it possible to use smaller dams close to the Gariep dam as instruments for sedimentation measurement? Do the colour changes provide info on the intensity of sedimentation events? Reflect on the possibility and prospect of building sedimentation dams upstream of the Gariep dam to buffer sedimentation of the Gariep dam.
5. Indicate the concept of sedimentation detection and the automation of the detection.

6.3 Projects

The following section provides an overview of all the topics dealt with regarding the Orange river, with special emphasis on the Gariep dam and the Vanderkloof Dam.

6.3.1 Water management and allocation of the Gariep dam water

Background Information

Gariep dam is built on the Orange River, on the border between the Eastern Cape and Free state provinces. The wall of this reservoir is about 88 m high and 914 m long. At full capacity, the Gariep dam covers an area of about 360 km², holding about 5.5 billion m³ of water, and making it the largest reservoir in South Africa (Van Vuuren, 2010).

The dam is managed by the Department of Water Affairs and Forestry (DWAF) based on its primary purposes. The DWAF has mapped a curve on the dam's water level, allocating the water downstream for irrigation purposes and the water above the curve to produce electricity by Eskom, South Africa's power utility (Bekker, 2011). The reservoir supplies water for consumption to the cities of Port Elizabeth and Bloemfontein and water for irrigation in the region in which it is located.

Gariiep dam has four hydroelectric generators on its wall, which are owned and managed by Eskom. The four generators generate hydroelectricity that is distributed across the country. Eskom manages this body of water using the four hydro turbines, with an individual outlet capacity of 160 cubic metres per second. It uses the turbines to minimize the possibility of spillage during floods using the restrictions designated by the DWAF. Any spillage that may take place causes financial losses to Eskom (Bekker, 2011).

As it is with many other constituents of life, human-induced climate change has a potential effect on the surface water systems, their quality, and quantity. The current and predicted weather conditions will have an impact on the river flows, further affecting the mobility dilution of contaminants.

Due to increased flooding, the rate of sediment flow into the dam is expected to increase, hence it is necessary to record accurate dam water volume. If sediments accumulate on the base of the river to a certain level, the original dam water volume is reduced. Increased temperatures are predicted to accelerate the rate of erosion, which will increase the sediment load, further reducing water yields (Alexander, 2007).

Dams silt up at an annual rate of about 0.8% on a global scale and about 0.4% in South Africa. However, many dams in South Africa are already greatly affected. The Gariiep dam is about 20% silted up. Professor Gerrit Basson, the head of Hydraulic Engineering in Stellenbosch calculated it to get to 64% by 2050 if nothing is done to manage siltation (Carnie, 2021).

South Africa is a dry country, a reduction in water quantity will potentially increase water scarcity. All aspects of life that depend on this reservoir, for example, people and animals, businesses, agricultural activities, and Eskom would be affected. Due to the huge cost of constructing new dams, siltation must be arrested swiftly to prolong the capacity and the life span of existing infrastructures (Manus, 2021).

Due to the current siltation, it is important to know accurate information pertaining to dam water volume, given that the water volumes and storage are continuing to decrease due to the number of sediments finding their way into the dam. Knowing the accurate dam water volume can also be used to determine the siltation rate, and therefore allow for better strategies to deal with and manage siltation (Townshed, 2020).

Study area: Gariep dam

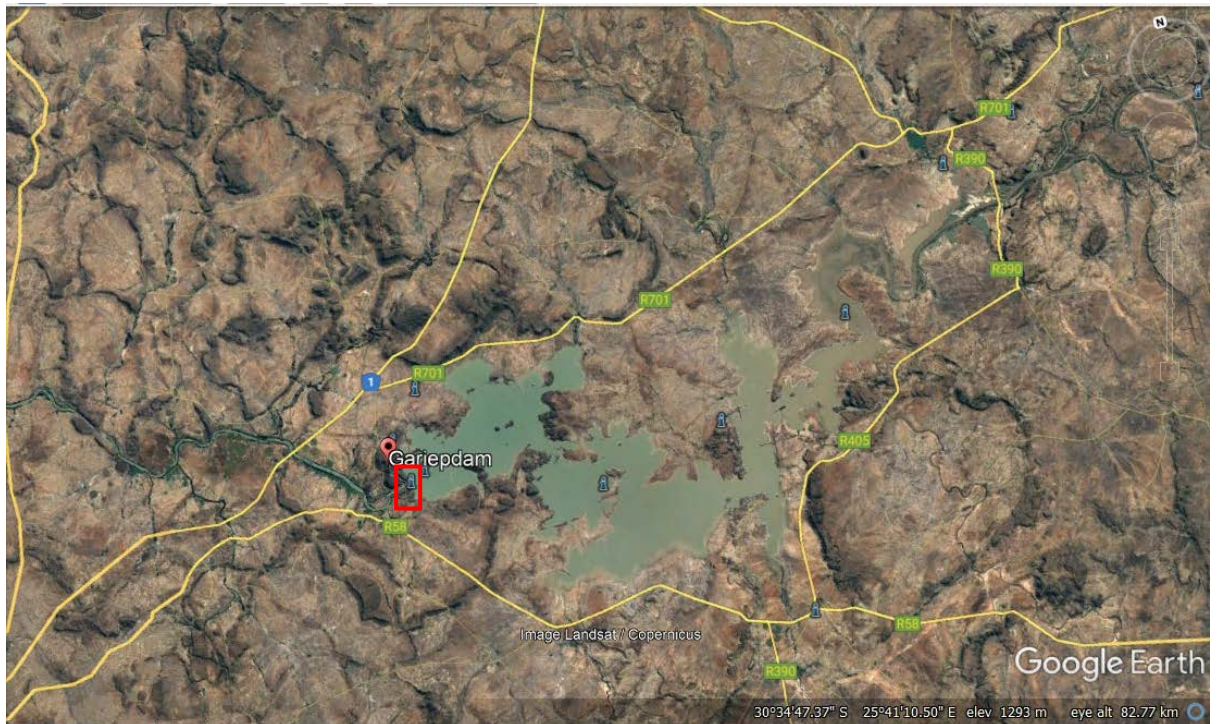


Figure 6.1: Gariep dam and the surrounding geology

NB: The picture was captured using Google Earth Pro on the 7th of March 2022. The area marked red is where the Gariep dam wall is positioned, along with the Gariep Hydro Power Station.

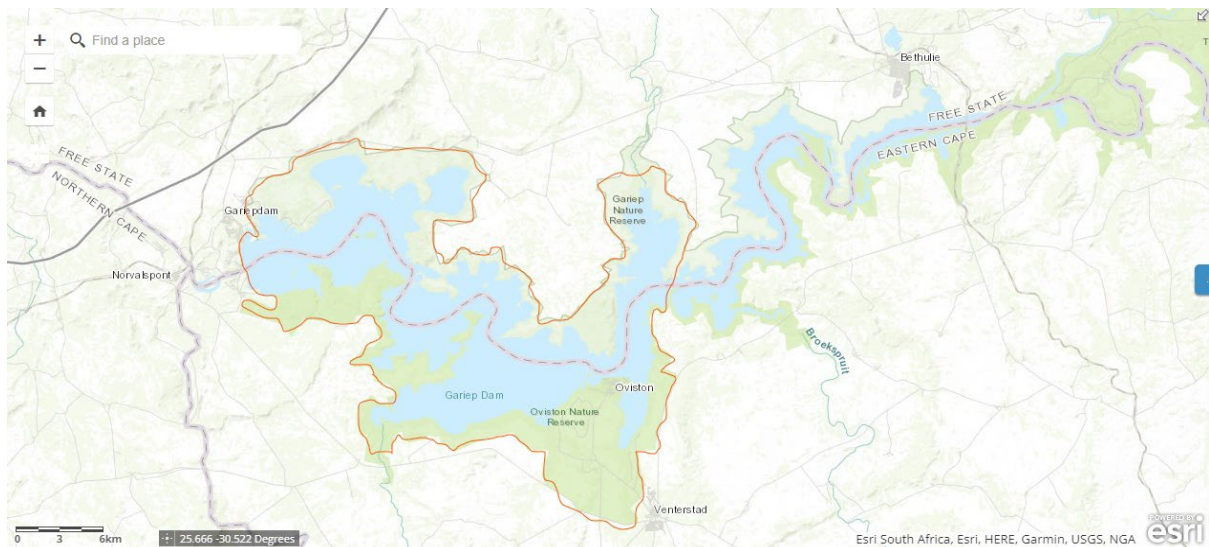


Figure 6.2: Demarcation of the Gariep dam

NB: This image was captured on the 5th of April 2022 using LANDSAT Explorer, Basemap rendering.

6.4 Research Problem Statement

Over the years, the Gariep dam has shown variations in water volume. This dam appears to be experiencing storage capacity reduction and this somehow has an impact on the Agricultural activities, businesses, and the people who are dependent on the dam for water supply. However, very little information is known regarding the dam's storage capacity reduction. In addition, the link between climate change and siltation processes and the Gariep dam's water quantity is poorly established. This project will therefore determine the effect of climate change and siltation on the Gariep dam, focusing on the changes in water storage capacities.

6.5 Aims and Objectives

Aims:

- This research aims to evaluate water management techniques in the Gariep dam while investigating how water quantity is being affected by climate change.
- To investigate the effects of siltation on dam volume, businesses, and people who are dependent on the dam.
- To also highlight the necessity for accurate dam water volume information.

Objectives:

- To investigate how Gariep dam is managed, and how water quantity is affected by climate change,
- To determine possible mitigation measures to increase the Gariep dam's life span.
- To investigate the rate of siltation in the past years
- To predict the amount of sedimentation shortly
- To determine possible ways to minimize the increased rate of siltation constituted by climate change.

6.6 Methodology

This qualitative research was conducted virtually due to restrictions in physically accessing the dam. It was accomplished using different GIS software such as QGIS and ArcGIS, an albeit like Google Earth Pro, and Department of Water and Sanitation. These were used to access the satellite imagery of the current state of the dam, which was used to study the current water volume and extent of siltation in the Gariep dam.

The software was used to view access images of how the dam used to look like to determine the changes over the years and therefore compute this data to predict the extent of siltation soon. This information would therefore be used to come up with possible mitigation strategies to reduce the possibility of the predicted siltation. The systems will be used to observe the

change in water volume in the future, study and determine whether any of the changes are a result of climate change and study the magnitude of the effects of climate change on water quantity. The different websites and software will in some instances be used for comparing the results and for validating research.

- Google Earth Pro is used to visualize the current state of the dam. Its images allow one to see the difference in water quality in the Gariep dam and across the Orange River, further allowing one to extrapolate the parts that are most silted and to determine the amount of the silt in the dam. It is also used to determine the precise coordinates of the dam and its height above sea level. Google earth is an easy tool to install and use as it does not require prior experience for information acquisition. In addition, it enables users to visualize and analyze CNRS/Airbus images of our planet while presenting a great deal of information in a geographic context.
- The Department of Water and Sanitation (DWS) website contains all the information regarding water storage, including the Gariep dam. The information on the website includes the dam volume, the height of the dam, the diameter, dam levels, dam flows, and floods. The website also possesses information regarding siltation and the amount of silt present in the dam in real time. The DWS website will be used to access the information about storage reduction throughout the years while indirectly studying the amount of silt entering the dam. The DWS website is a good resource, given that all the information presented is accurate and has been gathered by experienced professionals and most of the required information is accessible, thereby enabling researchers to do their research without having to physically go to the dam.
- LANDSAT Explorer is going to be used to travel back in time, to see what the dam was like in the past, and to study the changes to date. LANDSAT Explorer web app from Esri enables users to wield LANDSAT imagery to explore geology, vegetation, agriculture, Bathymetry, and cities anywhere in the world. This app permits individuals to better visualize the earth and understand how it has been changing over time.
- Quantum GIS is an open-source software package that benefits from the contributions of experts and users worldwide, free to use, and easily accessible. It is a significant tool for increasing the utility of spatial visualization and analysis (Friedrich, 2014). In this research, Quantum Geographical Information System will be used to visualize the Gariep dam, using different layers and to also analyze the dam and its current condition.

The Gariep dam is an important water source. Water is supplied to a large community as agricultural water, industrial water, and household water. For some, this is the only resource, to others the Gariep water complements the local water resources. All of this is managed by DWS based on availability. Table 6.1 below indicates the current water allocations, and it is quite evident that a large portion of the water is a trans basin distribution, implying that water is removed from the Orange Basin and used in other basins.

Table 6.1: Gariep dam water allocations

WATER ABSTRACTION	DISTRIBU-TIONS	AMOUNTS	REASONS
CONSUMPTION	Bloemfontein		It supplies water to the Wastewater plant owned by Bloem Water.
	Port Elizabeth		It's potable water supply comes from Gariep through the Nooitgedacht scheme, which is transported over 500 km. It receives some of its water from the Loerie dam, which receives its water from the Kouga dam canal.
	Hydropower Turbines	153 m/s carrying capacity*(4 Turbines) =612m ³ /s	The turbines were created with these carrying capacities to help generate 360 megawatts to the grid, enough to supply 7000 households.
	Irrigation	The amount spent by different farms is unknown.	Farmers receive irrigation water along the Orange River.
	Vanderkloof Dam	Dam levels:115% Inflow: 2700 m ³ /s Outflow:2900 m ³ /s	The dam level is decreasing steadily due to the outflow being greater than the inflow.
	Vaal Dam	Dam levels:107% Inflow: 750 m ³ /s Outflow:800 m ³ /s	The outflow of the Vall dam feeds into the Bloemhof dam.
GARIEP DAM'S CANALS AND RIVERS	Great fish river Sundays River Grassridge dam	Gariep dam holds about 5.5 billion cubic metres	The Orange-fish tunnel takes water from Gariep reservoir to the Great fish river and the Grassridge dam, the tunnel is 80 kms. The Fish-Sundays River canal scheme carries water from the Great Fish southwest to the

WATER ABSTRACTION	DISTRIBU-TIONS	AMOUNTS	REASONS
			Sundays River, the canal is about 13 km.
WATER LOSSES	Evaporation and Losses	1750 million m ³ /a	The rate of evaporation differs with each season, with more evaporation taking place in summer and less in winter. The driving factors are mainly temperature, surface area, humidity, and wind speed.
	Spillage	3780 million m ³ /a	Spillage occurs because of capacity loss and flooding.
	Deep Drainage	unknown	No significant resources found. Estimates were approached by this project, based on signs of long-term groundwater availability in the region of the dam.

6.7 Results and discussion

The Orange River, spanning across South Africa and Lesotho, is a significant watercourse that serves as a vital drainage system for a vast catchment area. At the heart of the Orange River Basin lies the Gariiep dam, strategically positioned in the upper-middle region. This dam holds immense importance as it forms a crucial part of the original Orange River Project (ORP).

Downstream from the Gariiep dam, numerous towns and irrigation schemes heavily rely on a consistent water supply from the dam. Additionally, the dam facilitates water transfers to support other regions in need. These transfers extend to various catchments such as the Fish River, Sundays River, and Vaal River (refer to Figure 6.1 for an overview).

To convey water from the Gariiep dam to the Great Fish River, an impressive 82 km long tunnel named the Orange-fish tunnel was constructed. This tunnel acts as a conduit, ensuring that a steady flow of water reaches the Great Fish River. Moreover, the water from the Gariiep dam is also channelled to the Grassridge dam, further enhancing water distribution in the region.

In a southwest direction, the Fish-Sundays River canal scheme plays a pivotal role in carrying water from the Great Fish River to the Sundays River. This 13 km canal effectively facilitates the transfer of water, allowing it to reach areas dependent on the Sundays River for various purposes.

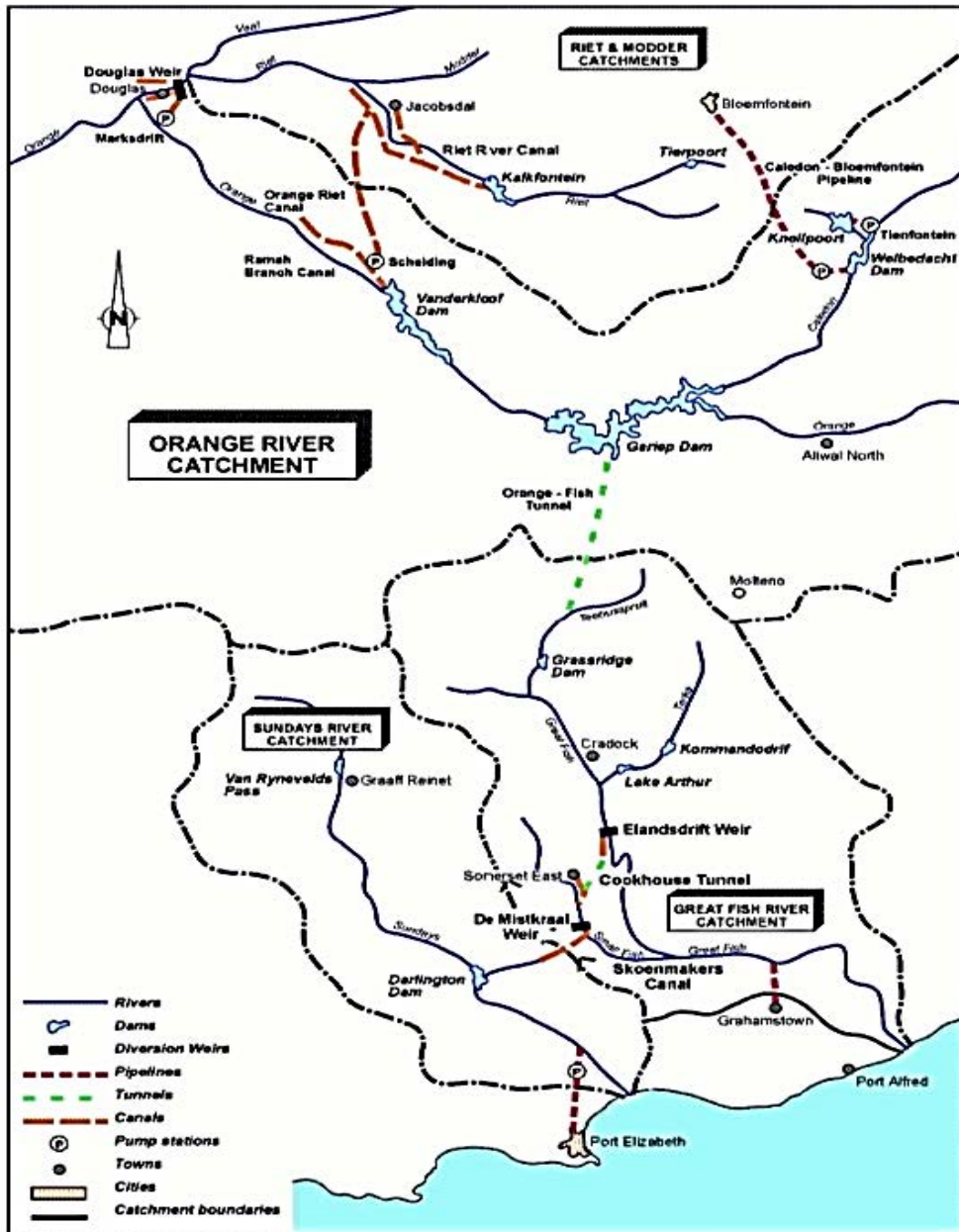


Figure 6.3: Major water transfer schemes from the Gariep and Vanderkloof dams

NB: This image was extracted from the Orange River integrated Water Resources Management Plan 2007 Report

There are several factors that contribute to spillages in Gariep dam. Some of them include flooding in the upper Orange River region, climate change and carrying capacity reduction due to siltation.

One of the primary functions of the Gariep dam is to generate hydroelectricity, making it a significant power source in the region. Eskom, the power utility company, has installed four hydro turbines along the dam wall to harness the energy potential of the water. Each turbine has a carrying capacity of 153 m³/s, and collectively they have a total capacity of 612 m³/s. At

a flow rate of approximately 200 m³/s, each turbine generates 90 MW of electricity, resulting in a combined output of 360 megawatts to the grid. This substantial power generation is achieved with a flow rate of 800 m³/s, which is sufficient to meet the energy needs of around 7,000 households.

The hydro turbines are conveniently serviced by the outlet structure located on the left flank of the dam. While the primary purpose of the outlet structure is to provide water to the hydro turbines for electricity generation, it also serves to control water releases from the dam. By regulating the water flow through the turbines, the outlet structure helps manage and mitigate the risk of water spillage.

However, despite these measures, there are instances where spillages occur in the Gariep dam. Several factors contribute to these spillages, including flooding in the upper Orange River region, climate change, and the reduction of carrying capacity due to siltation. Flooding events in the upstream areas of the Orange River can result in an increased inflow of water into the dam, exceeding its storage capacity and leading to spillages. Additionally, the impacts of climate change, such as altered rainfall patterns and increased intensity of storms, can further exacerbate the risk of flooding and subsequent spillages.

Furthermore, siltation, which refers to the deposition of sediments carried by the river, can gradually reduce the carrying capacity of the dam over time. As sediments accumulate in the reservoir, they reduce the effective storage volume and can impact the dam's ability to regulate water levels, potentially contributing to spillages during periods of high inflow.

Addressing these factors and implementing appropriate management strategies are crucial to minimize the occurrence of spillages and optimize the operation of the Gariep dam for both hydroelectricity generation and water resource management.

The Gariep dam is currently imbedded in the South African water and electricity supply systems and provides resources that support the South African economy. It is therefore imperative to deal with siltation swiftly.

a. Siltation in Gariep dam

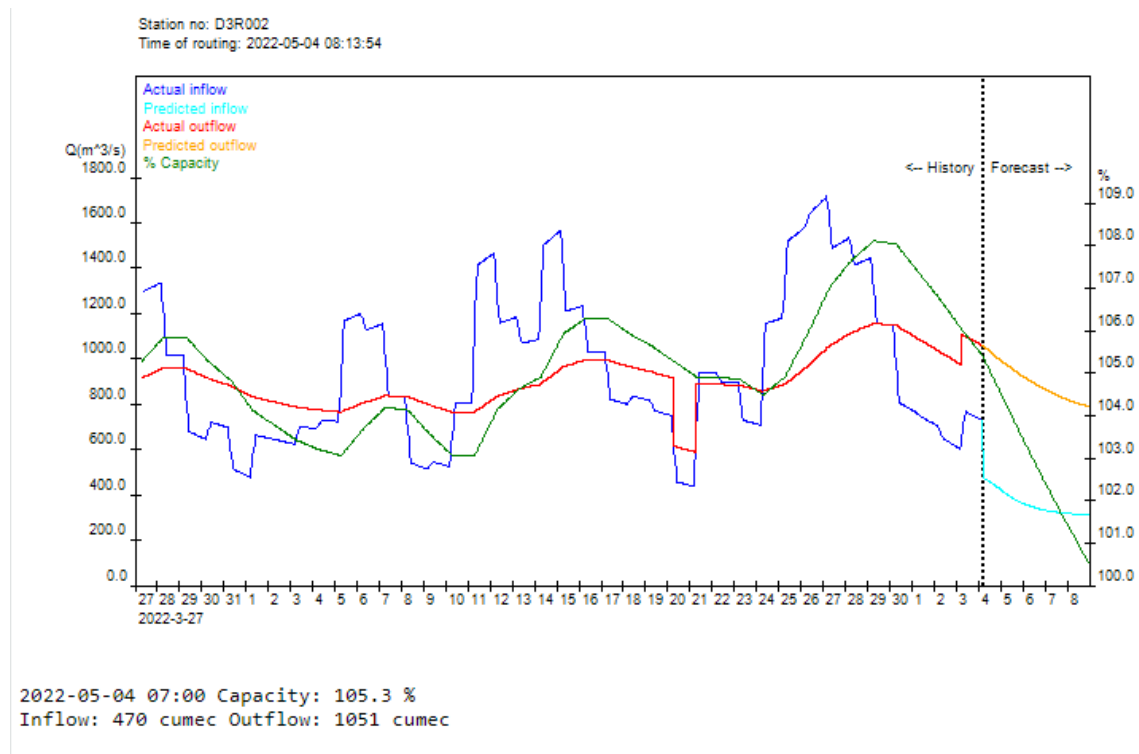


Figure 6.4: Gariep dam hydrology data

NB: The data used in this graph was captured on 4 May 2022 and the graph was downloaded from the Department of Water and Sanitation website

The graph above shows an outflow of about 21 8940 000 L/min, proposing that the dam has an overflow. Only about 282 000 000 L/min is stored in the dam. The Gariep dam storage capacity is affected by siltation. Statistics indicate that the Gariep dam is 21% silted up, entailing that about one billion one 1, 55 billion litres of the dam capacity are covered by silt (that is 21% of 5.5 billion m³). This silt is unevenly distributed in the dam. These computations show how siltation is becoming a huge problem by reducing the dam's storage capacity and threatening the lives of the people, businesses, and agricultural activities that are dependent on the dam for water.

Professor Gerrit Basson's research and calculations show that about 64% of the dam's storage capacity is covered by silt, and only about 1, 980 billion m³ of 5,5 billion m³ will be left for storage if nothing is done to reduce the amount of siltation taking place. However, the calculations above are for Gariep dam. Satellite imagery does show variations in silt distribution throughout the dam. Satellite imagery shows that the dam is heavily silted on its eastern side, i.e. from Bethulie towards the east and past the Gariep dam nature reserve, and less silted towards the dam wall.

This uneven distribution is affected by the direction and speed of the water flow. More sediments are offloaded into the dam basement as water enters the dam. The speed of the water

allows the sediments to be deposited according to grain size, with bigger grains of sand at the beginning and silt-sized sand towards the middle of the dam, and more silt deposited at the beginning of the dam, less in the middle and towards the dam wall.

b. The Significance of Correct Dam Volumes

The amount of water in the dam is calculated using the original dam's storage capacity. This is the Department of Water and Sanitation water distribution management plan's prerogative. The significance of accurate dam measurement is to know the exact amount of water that is present in the dam, and the exact dam's storage capacity, excluding silt. This enables the Department of Water and Sanitation the ability to plan, to know the number of towns that the available stored water can supply. It also allows Eskom power utility to formulate mitigation strategies against spillage. Dam spillage can potentially cause massive financial setbacks to the company.

c. The Effect of Climate Change on Water Quantity Reduction

Climate change on the other hand contributes to the changes in weather patterns, making the dry areas drier and flooding the wet areas. Gariep dam is in the Orange River. This perennial river has catchment areas that are located in wet areas and this entails that as the climate changes, the river is going to receive more water that might fill the river plains. A high volume of water from catchment areas/ highlands increases the speed of water flow, giving rise to turbulent flow. The turbulent flow carries a lot of sediments, and these sediments get deposited into the Gariep dam.

6.8 Conclusion

The available layer of silt reduces the dam's storage capacity, contributing to water spillage and causing a financial strain on Eskom. Not only does it affect Eskom, but it also threatens the lives of towns, businesses, and agricultural activities that are dependent on the Gariep dam for water supply. Climate change on the other hand contributes to the changes in weather patterns, making the dry areas to be drier and flooding the wet areas, further increasing the rate of sediment deposition into Gariep dam due to the turbulent flows associated with floods. Climate change contributes to water quantity reduction by reducing the dam's storage capacity due to increased rates of silt deposition. The best way to deal with this issue is to deal with its root cause, which means action needs to be taken to regulate and manage sediments that get deposited into the dam. This will prolong the current dam's storage capacity for people, businesses, and agricultural activities to continue receiving water. To reduce the silt that is already present in the dam, dredging process can be introduced.

6.9 Water Resources management:

Making use of the Department of Water and Sanitation's water planning information to reflect on future water needs

6.9.1 Introduction

This section included the setup of the WR 2012 Pitman model to measure and predict different scenarios.

6.9.2 Study area

Gariiep dam is located near the town of Norvalspont bordering the Free State and Eastern Cape province of South Africa. The dam has a capacity of 98,6% according to the DWS graph plotted for the year 2022. It has high inflows in summer months (October-April), i.e. during the rainy season in the catchment areas (De Waal *et al.*, 2011). It is thus significant to conduct studies in the Gariiep dam and use models such as Pitman with the purpose of simulating runoff from both gauged and ungauged catchments in South Africa. The Pitman model is extensively used in South Africa and is the catchment process module within the Water Resources Simulation Model 2000.

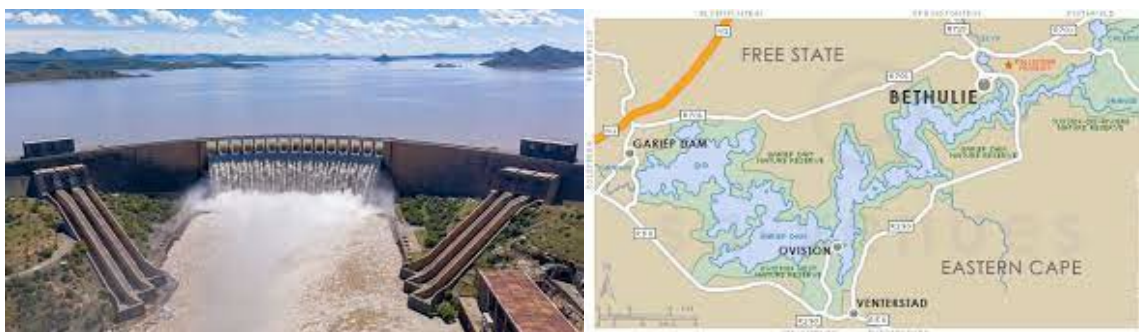


Figure 6.5: a. Picture and, b. map of Gariiep the dam (Source: google maps)

The Department of Water Affairs (DWA) is developing a framework to guide actions and decisions that will ensure water security in terms of quantity and quality to support South Africa's requirements for economic growth and social development. Sufficient supply of water is a requirement for the country to achieve its economic growth targets (DWS, 2022). The provision of potable water to every person in South Africa is also a fundamental developmental goal that needs to be facilitated by the department's framework. These two goals must be achieved without compromising the ecological sustainability of water resources (DWS, 2022).

6.9.3 Water planning and future needs

Studies are conducted in scarce water areas to reconcile the supply and demand for water with the aim to develop strategies to ensure the supply of water at adequate levels. This needs to be

achieved without affordability constraints. Appropriate levels of service to users and the protection of current and possible future water resources need to be adhered to (DWS,2022). A need to strengthen focus on water conservation and water demand management, especially since a basic cost analysis shows a better return on investment from water loss control and water use efficiency measures than from additional supply-side interventions (DWS, 2022).

Analysis shows a multi-faceted problem including the lack of managerial and technical skills, as well as funding. The DWS aims to strengthen its regulatory efforts to support this sector in a bid to ameliorate this dire situation which is further worsened by pollution of water resources due to faulty wastewater treatment works (DWS, 2022).

A balance is needed between bulk and small-scale infrastructure projects. Where a community can be serviced by existing large-scale infrastructure, this should be implemented with immediate effect. Where a community cannot be serviced by bulk infrastructure projects due to the cost of such an intervention (for example, pumping water to mountain-top communities at higher altitudes), then localised schemes must be planned and implemented. Where large-scale infrastructure could solve local water scarcity, such as the De Hoop Dam, the necessary planning and resourcing must be undertaken, and interim measures introduced to compensate for the long lead-times (DWS, 2022).

The DWS is very mindful of water use behaviour that impacts negatively on water resource quantity and quality. It is currently exploring a potential mix of mechanisms to change this behaviour that includes regulatory instruments, market-based instruments, self-regulation, and awareness and education. The Department plans to match mechanisms to offending behaviour in ways that appropriately mitigate its effects (DWS, 2022).

The Department is taking action to ensure it has reliable information to better support cross sectoral planning and development initiatives in its decisions and trade-offs. The rolling out of the Reconciliation Strategies to various parts of the country will ensure that the Department is able to anticipate and address future demand without any one aspect of water need (social, economic, or ecological) being compromised (DWS, 2022).

6.9.4 Aim and Objectives

Aim

The project aims to set up a Pitman model and run scenarios using temporal data, both measured and predicted.

Objectives

- Use both measured and predicted data from conducted studies in water scarce areas to produce the Pitman model.

- Use the downloaded data to run scenarios in the Pitman model to reflect on future water needs.

6.9.5 Methodology

Desktop work

- Download study area data from the water resources websites
- Conduct a literature search of the study area

Modelling

There are two versions of the WRSM2000/Pitman model: the most used being the monthly time step and the daily time step version (WR2012).

Monthly time step model:

Procedure to follow when using the monthly time step WRSM/Pitman model for the first time.

Click on Step1: Download the WRSM/Pitman rainfall-runoff model

- Save the Zip file to a folder, preferably: C:\WR2012\WRSM_Pitman
- In this folder right click on WRSM2000.zip and click on Extract to WRSM Pitman. This will set up a folder WRSM Pitman
- Click on this folder to run WRSM/Pitman

If the above has been done, WRSM2000 can be used to set up new systems or analyse existing systems for South Africa, Lesotho, and Swaziland. These systems have been updated for WR2012.

For existing WRSM/Pitman systems, the following steps can be implemented:

Go to Step 2: Download the network model data

- Select the preferred WMA
- If you want the entire WMA, then click on “complete folder” otherwise click on the WMA name to see what sub-systems are available
- Save the Zip file to a folder, preferably: C:\WR2012\Data\WRSM_Pitman Network Model Data
- In this folder, right click on the zip file (Olifants say) and click on Extract to 4-olifants. This will set up a folder 4-olifants
- Now run WRSM/Pitman from the folder C:\WR2012\WRSM_Pitman and under the File menu choose “Open Network”
- Follow normal procedures within the model as per the WRSM/Pitman User Guide

For the daily time step model:

Step 1: Download the daily time step WRSM2000 (Pitman) model.

Note the following:

- It is recommended that you save to a separate folder and not include with the monthly time step folder
- Read the User Manual on the daily time step version
- There are no daily data sets available for the monthly time step
- Daily rainfall and daily observed flow must be obtained from SAWS and DWS
- While this version has been tested and found to give acceptable results, it has not yet been extensively used and may contain some minor non-algorithm bugs which may affect the user friendliness. If you do encounter any problems, please report them to Allan Bailey.

An overview:

6.9.6 Results

Figure 6.6 shows the actual inflow of the Gariep dam, the predicted inflow, actual outflow, predicted outflow, and the dam capacity as represented in different colours. The model can be run for different flow regimes, but the long period of modelled information compensates for most of the possible scenarios. Extreme conditions were found to be unrealistic and as explained earlier, challenge the validity of the model. Figure 6.6 therefore represents the typical information generated by the model.

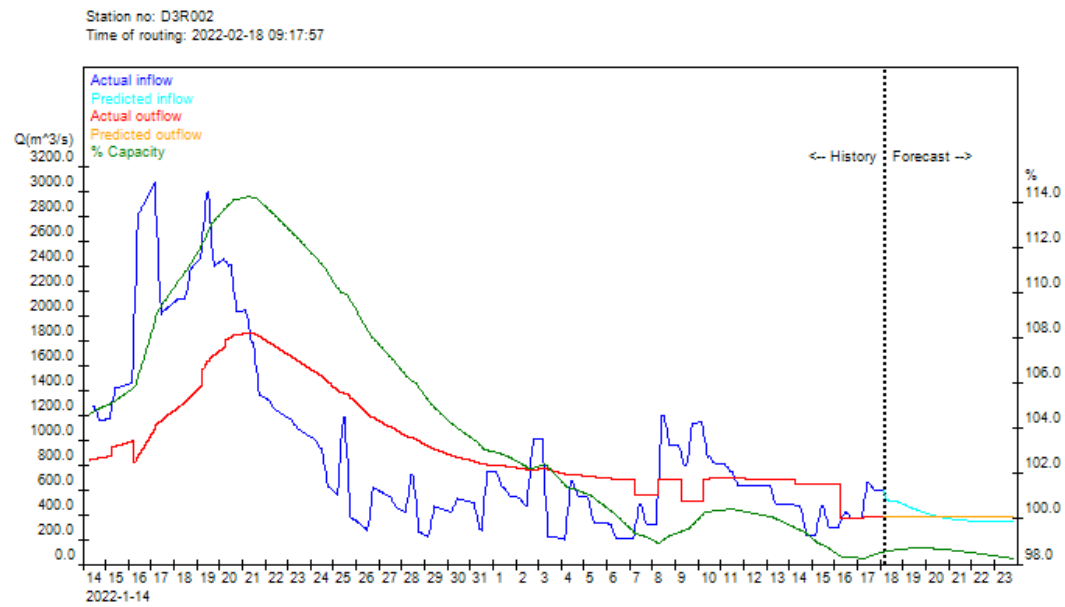


Figure 6.6: Graph showing capacity, inflow, and outflow of the Gariep dam (source: DWS 2022).

6.9.7 Conclusion

The water planning information provided by the Department of Water and Sanitation (DWS) offers a comprehensive overview of the strategies and plans implemented for water resources management. By utilizing the Pitman model to run scenarios in the study area, a better understanding can be gained to reflect on future water needs.

The WR2012 Pitman model is a widely used hydrological model in South Africa that can simulate water levels and flows in river systems. When applied to a specific case, such as the Gariep dam, it can provide valuable insights into potential water level scenarios in the immediate future. Reflecting on the use of the WR2012 Pitman model for the Gariep dam, there are a few important considerations:

Model Validity

The accuracy and reliability of any hydrological model depends on its calibration and validation using historical data. The WR2012 Pitman model should be calibrated and validated specifically for the Gariep dam catchment to ensure accurate representation of the local hydrological processes. It is possible that this was done as the WR2012 information gave good calibration information.

Input Data Quality

The quality of input data is crucial for the model's performance. Precise and up-to-date information about rainfall, evaporation rates, soil properties, and other relevant factors is necessary for accurate simulations. It is important to assess the reliability and accuracy of the input data used in the model to ensure the reliability of the results. The climate data used for the Gariep modelled information cannot be a single climate record but should rely on the best distributed input.

Assumptions and Limitations

Like any modelling approach, the WR2012 Pitman model operates based on certain assumptions and has inherent limitations. It is essential to be aware of these assumptions and limitations and understand how they may affect the model's results. For example, the model might not fully account for extreme weather events or sudden changes in dam management practices. The model may not take all the water losses and the impact of sedimentation into account.

Uncertainty Analysis

It is crucial to conduct a comprehensive uncertainty analysis when using the model for water level scenarios. This analysis helps quantify the uncertainty associated with the model's outputs, considering the inherent variability in hydrological processes and the input data. Understanding the uncertainty allows for better-informed decision-making. This relates to the previous point.

Continuous Model Evaluation

The model's performance should be continually evaluated by comparing simulated water levels with observed data. This evaluation helps identify any discrepancies or biases in the model's predictions, which can guide model refinement and improvement.

Decision Support

The water level scenarios generated by the WR2012 Pitman model can serve as valuable decision support tools for water managers and stakeholders. By exploring different scenarios, decision-makers can assess the potential impacts of various management strategies and make informed decisions to optimize water resource management.

Lastly, using the WR2012 Pitman model for the Gariiep dam to simulate water level scenarios for the immediate future can be a useful tool for water resource planning and decision-making. However, it is important to acknowledge the model's limitations, assess data quality, conduct uncertainty analysis, and continually evaluate its performance to ensure reliable results.

6.10 Using the DWS survey information to reflect on lost volume through siltation

6.10.1 Introduction

The Orange River, also referred to as the Senqu River in Lesotho, originates in the Lesotho Highlands and flows in a westerly direction 2 200 km to the west coast where the river discharges into the Atlantic Ocean (Mare, 2007). According to Mohamed (2014), the river drains an area of about 1 000 000 km² in Botswana, Lesotho, Namibia, and South Africa. Furthermore, South Africa occupies 64% of the basin area while Botswana and Namibia occupy 8 and 24.5% respectively. The Gariiep dam is the largest dam in South Africa which is situated in a gorge at the entrance to Ruigte Valley on the Orange River in quaternary catchment D35KE, upstream of Vanderkloof Dam (Mokorosi and van der Zaag, 2007). Dumpis and Lagzdinš (2020) asserted that Bathymetry is the science of measuring and displaying the depth of water bodies, its mapping provides results on waterbody dimensions.

Research has shown that every year, about 0.5-1% of the world's reservoirs lose their installed capacity owing to silt deposition (Rahmani *et al.*, 2018). If essential efforts are not implemented, the continuous loss of reservoir capacity owing to annual progressive siltation might result in a quarter of all dam and reservoir storages being lost, with a prediction of 50 years from 2000 (WCD, 2000). Bathymetric survey data is acceptable and remains one of the most dependable components of hydrographic survey and information collecting. Bathymetric survey involves sounding or impulse transmission into the water surfaces of dams and reservoirs to get xyz coordinates (Sainson, 2017).

Bathymetric surveys can be conducted using a variety of technologies, including multi-beam and single-beam surveys, ADCPs, Sub-Bottom Profilers, and the Eco-Mapper Autonomous

Underwater Vehicle (EMAUV). Bathymetric surveys allow for mapping of underwater features as well as determination of the depth of a body of water (Menna *et al.*, 2018). The emphasis on using more modern approaches for determining reservoir sediment, such as remote sensing with satellite altimetry, may not be relevant independently. This is because other approaches, aside from bathymetry, are unable to construct the baseline required to estimate reservoir catchment areas at various elevations. (Erena *et al.*, 2020). The elevation-area-capacity curve is plotted with the use of a bathymetric survey on any dam reservoir. The resulting curve is a crucial tool for determining the reservoir's capacity at any given cross-sectional area and elevation. Consequently, reservoir professional operators interpret reservoir dam characterization, flood routing, silt loading, and dam reservoir categorization using the curve's result (Rodrigues & Liebe, 2013).

Reservoirs have long been utilized for flood control, irrigation water supply, hydroelectric power generation, tourism, and ecosystem function maintenance (Ainsworth, 2005). However, silt deposition in these reservoirs could jeopardize their initial designed capabilities as well as the expected benefits. Reservoir sedimentation is essentially a continuous process that might go unnoticed for a significant amount of a reservoir's existence as silts and other earth material are moved with a reasonably high sediment transport velocity from upstream river systems to downstream of the reservoir. Decreased water velocities affect the distance of deposition. Most of the time, when more silt and/ or sediments are deposited, the reservoir capacity shrinks or decreases (Radwan, 2016).

The regular accumulation of silts and sediments in the reservoir can result in a normal distribution pattern, which can impair reservoir management during peak flood events (Sedlacek *et al.*, 2016). According to Fitzpatrick *et al.* (1987), Lake Decatur lost 9100 acre-feet of storage capacity over 61 years due to increased silt deposition, reaching a tonnage of 9,830,000 at the reservoir bed. Over the course of the study, they estimated that each acre of watershed delivered 21.4 tons of soil material to the lake. Sedimentation concerns are more evident in small to medium-sized reservoirs (Chanson and James, 2005).

In dam management, determining the degree of sedimentation and reservoir capacity has been a key difficulty. Echo sounders have become a key tool in bathymetric surveys thanks to advancements in multi-beam technology (Oke *et al.*, 2019). Acoustic multi-beam systems, which use a series of narrow beam transducers installed on a boat to pinpoint spots on or beneath the reservoir water surface, have shown to be another successful hydro survey method (Selva *et al.*, 2013).

Echo sounder bathymetry uses frequencies ranging from 12 to 500 kHz. In their bathymetry investigation of the Ruiru reservoir in Kenya, Joseph *et al.* (2017) used dual echo sounders and found distinct penetration frequencies ranging from 200 to 350 kHz. The implication is that the higher the spatial and temporal resolution of the measurements, the shorter the wavelength of the signal (Selva *et al.*, 2013).

The study seeks to duplicate the proposed engineering process of Gariep dam siltation using data collected by Department of Water and Sanitation.

6.10.2 Methodology

The main aim of this section is to present the methods and materials used in the engineering process of the Gariep dam siltation evaluation. The methodology of this study is as presented on the Department of Water and Sanitation website and is also compared with other methods employed in other African countries.

Sediment analysis is typically achieved by direct and indirect approaches. Direct approaches include hydrographic surveys that measure the volume of sediments deposited in the reservoir (Vente *et al.*, 2003). Sediment budgets, which include analysing inflow and outflow sediment samples taken at gauging stations upstream and downstream of the reservoir, and numerous models created to predict sediment yield in reservoirs, are examples of indirect approaches (Adam *et al.*, 2014).

Along range lines, hydrographic surveys measure the depth from the water surface to the settled sediments at the reservoir's bottom. Echo sounders or a tape measure with a weight attached at the bottom end are commonly used to collect measurements from a boat. Based on the bathymetry data acquired at the end of the study, a new reservoir capacity is computed. The gap between the reservoir's previously known capacity and the new capacity shows sedimentation-related reservoir capacity loss.

a) Hydrographic Survey in the context of DWS

The methodology below is as presented on the Department of Water and Sanitation (DWS) website.

The Sedimentation Surveys are meant to answer questions about new capacity, monitor available or lost water storage, flood impacts, siltation rate, and the amount of sediment deposited in reservoirs. Sedimentation Surveys rely on historical data and information as a monitoring method to determine when, where, and how much silt has been deposited in specific reservoirs.

There are two types of hydrographic surveys which are employed to determine the capacity of reservoirs, this is informed by the size of the reservoir.

- A complete contour survey of the reservoirs is performed. Total stations: RTK GPS or GNSS, or a combination of both are used to survey the areas of reservoirs that are not covered by water according to the set standards. The density of the spot shots is determined by the scale of maps required as well as the accuracy of the capacity.

The water-covered surface of the reservoir is surveyed by using various sizes of boats equipped with GPS receivers for position determination and Echo sounders for depth measurement. The density of the underwater shots is determined once again by scale and accuracy.

The reservoir's contour maps, and area capacity tables are then produced using software packages such as Hypack, Microstation, and/or Modelmaker. It is also possible to generate cross sections at various sites. Once the area capacity table is established, it can be compared to earlier surveys to evaluate sedimentation.

Only small to medium reservoirs are subjected to a comprehensive contour survey to assess their capacity. The amount of data created during such a study is enormous, and existing software application is incapable of handling massive dams.

- The second method for determining reservoir capacity is to take cross sections of the reservoir at predetermined intervals. This method is used to survey all large dams. The cross sections are repeated at regular intervals along the reservoir's length. Between two fixed beacons, the cross sections are run and Hypack software then used to collect the data. The reservoir capacity is then estimated using sediment software that is based on the end areas principle.

The results of this type of survey are substantially faster than those of a comprehensive contour survey. Cross sections are performed at a specific time interval for sedimentation determination, and the amount of sediment in the reservoir is measured by comparing the new capacity to the previous one.

Because the cross sections are run between fixed survey beacons, information such as the accumulation of silt and where it is concentrated is immediately available.

The second hydrographic survey method which involves taking cross sections of the reservoir at predetermined intervals is the one which is employed in the case of the Gariep dam. This is because the Gariep dam is the largest dam in South Africa, and the complete contour survey would not be suitable because the amount of data created in such a survey is enormous, and the existing software application is incapable of handling massive dams like the Gariep.

6.10.3 Results

When the first hydrographic survey was conducted in the Gariep dam by the Department of Water and Sanitation (DWS) in 1971, the water holding capacity was 5897.285 million m³ with 0.00 sediment percentage as shown in Figure 6.1. The area of the catchment was 70 749 km². The results obtained from the survey which was undertaken in 1979 depicts that the dam capacity was 5521.172 million m³ and the sediment percentage was 6.24 as shown in Figure 6.7. The results of the survey conducted in 1991 as demonstrated in Figure 6.7 show that the dam capacity was 5362.488 million m³ and the sediment accumulation was on 9.07%. The dam capacity was 5198.194 million m³ when the survey was carried out in 2005, whereas 11.85% was lost to sedimentation as shown in Figure 6.7. The results of the survey which was

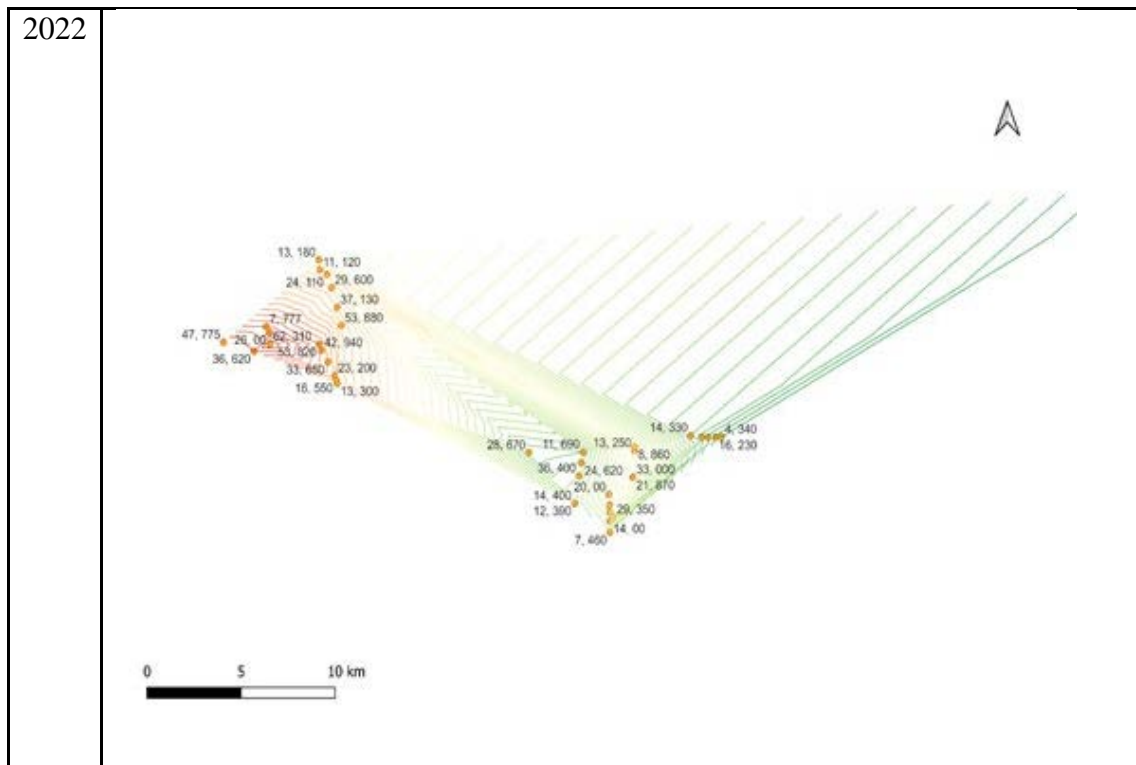
conducted in 2018 show that the dam capacity was 4904,527 million m³ while 16.83% of the dam capacity was lost to sedimentation (Figure 6.7). Results obtained from surveys that have been conducted to date, about 0.36% of dam capacity is annually lost to sediment accumulation.

Table 6.1 below shows the findings of the survey carried out in April 2022 from 39 sampling points in the Gariep dam where the deepest point is showing a depth of 62.310 m and the lowest point about 4.340 m. Using the data from Table 6.1, a contour map of the Gariep dam depth was constructed, displaying the depth as indicated by isobaths and the coordinates shown in Figure 6.7. The sections with higher values have steeper slopes showing the deepest points whereas the sections with lower values have gentle slopes displaying the shallow points.

Table 6.2: Gariep dam depths at different sampling points.

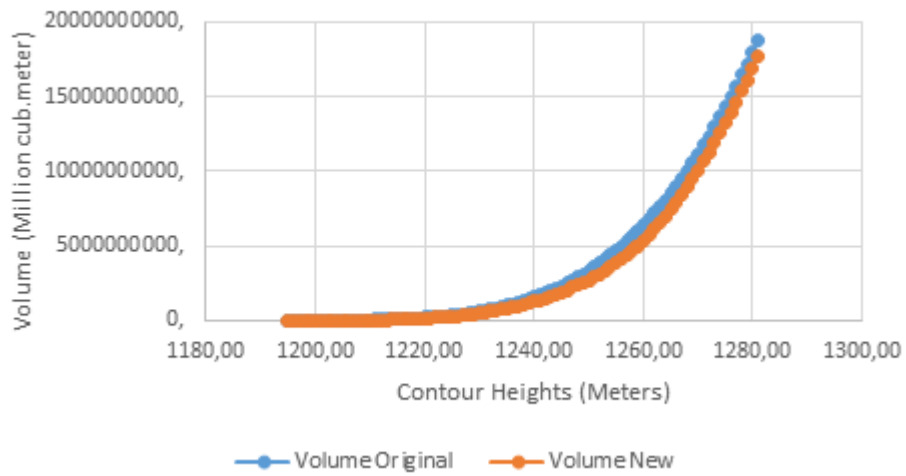
Sample point	Latitude	Longitude	Depth (m, mm)
Gariep 1	S30° 36' 47.7"	E25° 32' 23.3"	62, 310
Gariep 2	S30° 36' 44.7"	E25° 30' 50.7"	47, 775
Gariep 3	S30° 37' 00.7"	E25° 31' 51.4"	36, 620
Gariep 4	S30° 36' 25.9"	E25° 32' 22.8"	26, 00
Gariep 5	S30° 36' 16.1"	E25° 32' 16.2"	7, 777
Gariep 6	S30° 36' 48.1"	E25° 34' 02.6"	53, 820
Gariep 7	S30° 36' 59.1"	E25° 34' 06.1"	42, 940
Gariep 8	S30° 37' 20.3"	E25° 34' 19.4"	33, 650
Gariep 9	S30° 37' 45.2"	E25° 34' 33.3"	23, 200
Gariep 10	S30° 37' 53.7"	E25° 34' 36.3"	16, 550
Gariep 11	S30° 37' 59.3"	E25° 34' 38.2"	13, 300
Gariep 12	S30° 36' 13.6"	E25° 34' 46.5"	53, 880
Gariep 13	S30° 35' 40.5"	E25° 34' 37.8"	37, 130
Gariep 14	S30° 35' 04.7"	E25° 34' 27.1"	29, 600
Gariep 15	S30° 34' 40.6"	E25° 34' 17.6"	24, 110
Gariep 16	S30° 34' 32.1"	E25° 34' 03.1"	11, 120
Gariep 17	S30° 34' 14.0"	E25° 34' 01.4"	13, 180
Gariep 18	S30° 40' 50.9"	E25° 44' 30.7"	33, 000
Gariep 19	S30° 40' 50.9"	E25° 44' 30.7"	21, 870
Gariep 20	S30° 40' 02.2"	E25° 44' 33.3"	13, 250
Gariep 21	S30° 39' 55.2"	E25° 44' 34.0"	8, 860
Gariep 22	S30° 42' 03.8"	E25° 43' 51.6"	29, 350
Gariep 23	S30° 41' 22.5"	E25° 43' 42.3"	20, 00
Gariep 24	S30° 41' 41.8"	E25° 43' 43.4"	17, 800
Gariep 25	S30° 41' 54.4"	E25° 43' 43.7"	17, 400
Gariep 26	S30° 42' 10.7"	E25° 43' 44.2"	14, 00
Gariep 27	S30° 42' 31.4"	E25° 43' 44.4"	7, 460
Gariep 28	S30° 41' 38.3"	E25° 42' 34.0"	12, 390

Sample point	Latitude	Longitude	Depth (m, mm)
Gariep 29	S30° 41' 38.3"	E25° 42' 34.0"	14, 400
Gariep 30	S30° 40' 48.3"	E25° 42' 42.6"	36, 400
Gariep 31	S30° 40' 24.4"	E25° 42' 46.8"	24, 620
Gariep 32	S30° 40' 04.8"	E25° 42' 50.4"	11, 690
Gariep 33	S30° 40' 06.0"	E25° 41' 01.5"	28, 670
Gariep 34	S30° 39' 34.6"	E25° 46' 26.4"	14, 330
Gariep 35	S30° 39' 37.4"	E25° 46' 48.1"	27, 480
Gariep 36	S30° 39' 38.3"	E25° 47' 00.8"	23, 030
Gariep 37	S30° 39' 38.2"	E25° 47' 15.7"	16, 230
Gariep 38	S30° 39' 37.4"	E25° 47' 27.7"	4, 340
Gariep Hennie Steyn Bridge	S30° 32' 03.2"	E26° 01' 23.3"	16.10



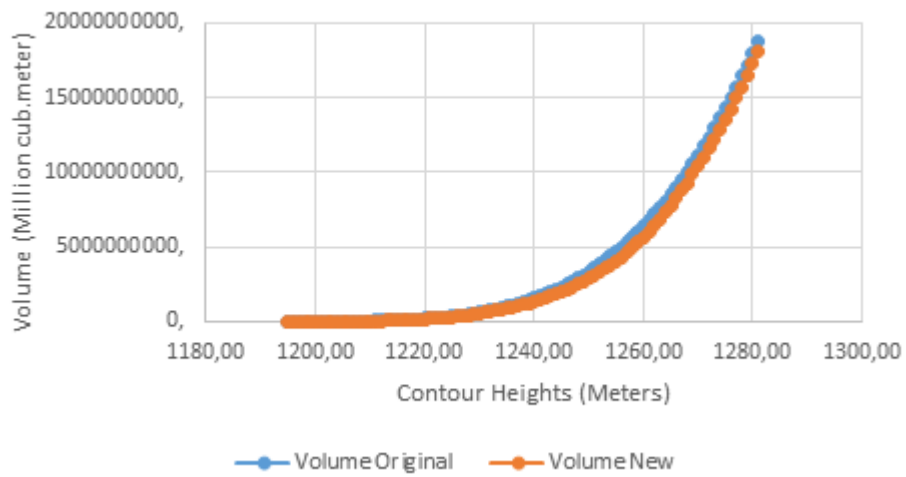
2018

Capacity Curve 2018



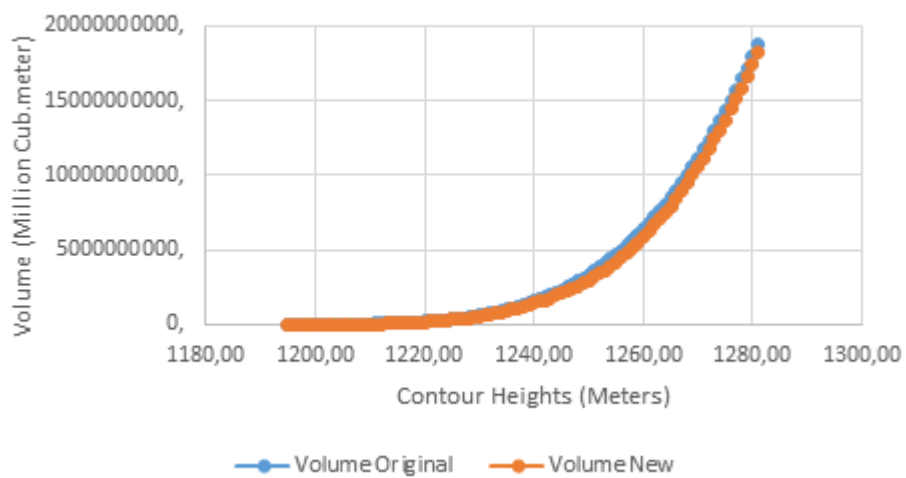
2005

Capacity Curve 2005



1991

Capacity Curve 1991



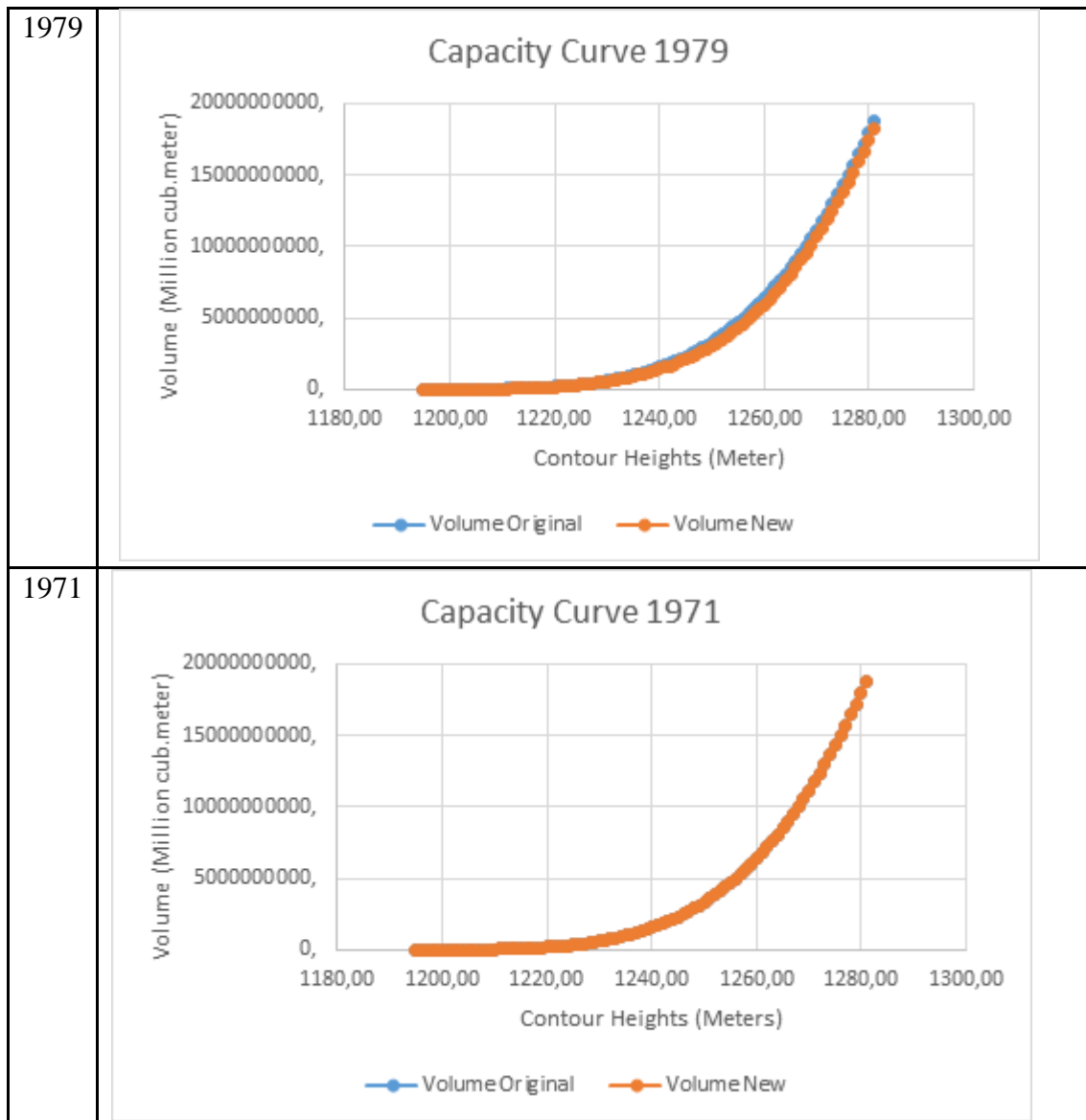


Figure 6.7: Remaining Water Capacities of Gariep dam after sedimentation

6.11 DWS planning information and water loss through evapotranspiration

6.11.1 Introduction

a) The Department of Water and Sanitation water planning

The DWS developed the Water and Sanitation Master Plan as a guide for investment planning in water resources and delivery of water and sanitation services until 2030 and beyond, with the aim of ensuring universal sanitation coverage and protecting public health (Centre for Environmental Rights, 2019). The plan prioritizes actions based on their expected impact in securing water for future uses. This is reviewed and reported annually, and an adaptive

management approach is used to restructure the plan as needed (National Water and Sanitation Master Plan, 2018)

b) Water loss through evapotranspiration

Evapotranspiration is a process by which water is lost to the atmosphere through two main processes: evaporation and transpiration. Evaporation occurs from open bodies of water, such as lakes, reservoirs, wetlands, bare soil, and snow cover, while transpiration happens from living-plant surfaces such as algae and floating water plants like hyacinth. Evapotranspiration is influenced by several factors other than the physical characteristics of water, soil, snow, and plant surface. These factors include net solar radiation, surface area of open bodies of water, wind speed, type and density of vegetative cover, availability of soil moisture, root depth, reflective land-surface characteristics, and the season of the year. All these factors have a significant impact on the evapotranspiration process.

c) Evapotranspiration prevention methods

Evapotranspiration is the simultaneous process of water transfer to the atmosphere both by soil and surface water evaporation and plant transpiration. Methods that are employed to prevent and/or reduce the rate of evapotranspiration include the following:

- Temperature regulation

Over the course of a day, an increase of air temperature causes an increase on the saturation deficit triggering a higher evaporative demand in the air and leading to high evapotranspiration rates. Therefore, a reduction in temperature decreases the evapotranspiration rate.

- Relative humidity regulation

Air relative humidity acts in conjunction with temperature. The higher the relative humidity, the lesser the evaporative demand and, therefore, the lower evapotranspiration rate.

- Monitoring wind direction

Advection represents the horizontal transportation of energy from a drier area to another more humid area, and such additional energy is utilized in the evapotranspiration process. Wind also helps remove water vapour near the plants to other regions.

- Methods used in crop production

Type of species

This factor is related to the foliar architecture (spatial distribution of the leaves), internal resistance of the plant to water transport, and other morphological aspects (number, size, and distribution of stomata, etc.), which exert a direct influence on evapotranspiration.

Reflection coefficient

Radiation reflection directly influences net radiation for the evapotranspiration process. The darker the vegetation, the lower the reflection coefficient and this consequently raises net radiation. The main task in this study is to reflect on the conditions affecting evaporation from the dam. This includes the change in sediment load causing a change in colour and an increase in water temperature. It further includes algae occurrence detected in the Gariep dam, causing transpiration losses and an impact on water temperatures that enhances evaporation. These occurrences will be shown, and an attempt will be made to quantify these water losses.

Growth stage

Such a factor is directly related to the size of transpiring foliar surface, for the larger leaf area the larger the transpiring surface, and the higher the potential for water use.

- Interrelationship atmospheric demand-soil water supply

The soil is an active reservoir that controls the rate of water use by the plants within certain limits and in conjunction with the atmospheric demand. The atmospheric demand depends on the availability of solar energy, relative humidity, and wind speed (Pereira & Pires, 2011).

6.11.2 Results

Water evaporation from large dams, such as the Gariep dam in South Africa is a complex process influenced by a variety of factors, including the surface area of the water, air temperature, humidity, wind speed, and solar radiation.

The Gariep dam is one of the largest dams in South Africa, with a surface area of approximately 374 km² and a maximum depth of 88 m. Due to its size, the dam is subject to significant evaporation losses, which can affect the availability of water for various uses, including irrigation, domestic and industrial use, and hydroelectric power generation.

The rate of evaporation from the Gariep dam and other large reservoirs is influenced by several factors. One of the most important factors is air temperature, with higher temperatures generally leading to increased evaporation rates. Wind speed is also an important factor, as it can increase the rate of evaporation by increasing the turbulence of the water surface and promoting the mixing of water molecules with the air.

Other factors that can influence evaporation rates include humidity, solar radiation, and the presence of vegetation or other obstructions that can shade the water surface and reduce the amount of solar radiation that reaches the water.

Estimating the actual amount of water lost to evaporation from the Gariep dam is a complex process that requires detailed monitoring and modelling of a variety of environmental factors. According to data from the Department of Water and Sanitation in South Africa, the estimated annual evaporation loss from the Gariep dam is approximately 3,300 million m³. This represents a significant amount of water that is lost to the atmosphere each year and highlights the importance of managing water resources effectively to ensure their sustainability for future generations.

6.12 Geology, engineering, siltation and groundwater

6.12.1 Introduction

The Gariep dam is South Africa's largest dam and is located on the Orange River, on the border between the Free State and the Eastern Cape provinces, it falls under the Kopanong Local Municipality within the Xhariep District of the Free State Province. It lies approximately between latitude 30° 37'24" S and longitude 25° 3'24" E as shown in Figure 6.8. According to van Vuuren (2010), the Gariep dam covers an area of about 360 km² and its full water holding capacity is approximately 5.5 billion m³.

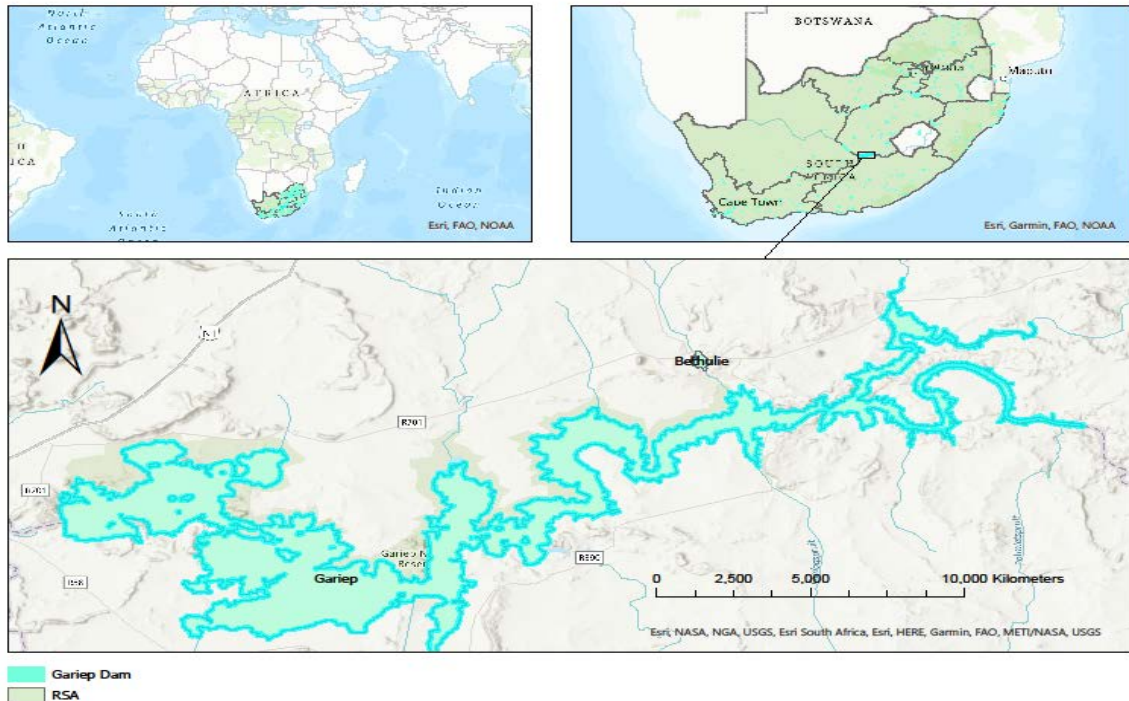


Figure 6.8: Map of the Gariep dam

The Gariep dam was built as part of the Orange River Project to serve the multi-purpose functions of river flow control, flood regulation, hydro-electric power generation, as well as the supply for irrigation, industrial, and domestic utilisation in the provinces of the Free State, Northern Cape, and Eastern Cape, through various water transfer schemes such as the Orange-Fish Transfer Scheme (DWA, 2012). This dam boasts as South Africa’s largest dam and the main water resource infrastructure of the Orange River Project (DWA, 2009), thus rendering the Gariep dam highly important in terms of addressing the water security needs of the country as well as for the provision of essential bulk water (Manus, 2021).

Aims and Objectives

Aims

This study aimed to evaluate the geology, engineering, siltation and the groundwater of the Gariep dam in the Orange River basin

Study Objectives

The specific objectives of this study were to:

- Report on the complex environmental and geological data of the Gariep dam
- Investigate the potential need for sedimentation dams upstream of the Gariep dam
- Instigate the Gariep dam contribution to groundwater through studying its geology

6.12.2 An objective summary of the DWS reports pertaining to geology and the environment in the Upper Orange River

Water and the environment as presented in the Internal Strategic Perspective (ISP): Upper Orange Water Management Area

Water resource development and management are the responsibility of the Department of Environmental Development and Management (DWAF) under the National Water Act (NWA) and other environmental regulations. The concept of environmental management has progressed from solely protecting plants and animals to managing the intricate interactions of society, economy, and ecology. As stated by the National Environmental Management Act (NEMA); ‘Environmental management is the integration of social, economic, and ecological issues into planning, execution, and decision-making so that development benefits both current and future generations.’

As required by NEMA, DWAF has created a Consolidated Environmental Implementation and Management Plan (CEIMP). This document explains the Department's functions, policies, plans, and programs, as well as how they comply with environmental regulations. NEMA and the Environment Conservation Act (ECA) are the major legislative Acts to which DWAF is required to refer. The EMF provides strategic decision-making information to DWS, and ensures environmental legal compliance, and assists in achieving environmental sustainability. Integrated Environmental Management is a collaborative governance initiative in which DWAF is a full participant. The Department has committed to creating and implementing an integrated Environmental Management Framework (EMF) through the CEIMP to ensure that its approach is consistent with the principles outlined in NEMA and the ECA.

This ISP oversees improving and maintaining the environmental awareness of DWS's water resource planners and managers. Water control has a wide range of impact, for which strategies and planning must reflect and some of those impacts include:

- The direct impact of physical constructions (for example, environmental limits to the development of weirs or dams)
- The effects of water allocation and licensing. Forestry and irrigation are two instances of users where water-based development can result in the change of large sections of ‘natural’ settings
- Water allocation for equity. Approaches to the application of *Schedule 1 Use*, i.e. general authorisations, the revitalization of irrigation schemes, among others can all be included here
- Failure to support equity or suitable development – considering the consequences of poverty
- Sanitation systems and their consequences for groundwater quality
- The Reserve's implementation

- The ability to monitor and manage compliance, thereby safeguarding the resource and the environment.

Many solutions emphasize the importance of cooperative governance and the need for increased knowledge and capacity building.

This ISP aims to address all these concerns through dialogue and a strategic approach that emphasizes the DWS's commitment to managing the environment for the benefit of the country and its people. It further expresses the department's perspective on Integrated Water Resource Management (IWRM) and the significance of biophysical factors in decision-making.

As a result, the ISP still contains an environmental strategy, whose aim is to reveal environmental issues that are at risk of being unnoticed.

The social environment

The use of water resources is for the benefit of the society, and the economy benefits society. Societal impacts are a key component of the ISP, and the danger of unexpected consequences can result in difficult decisions. The NWA's implementation necessitates keeping society at the forefront of every decision-making process. Water resource distribution and use, as well as water quality control, have significant socioeconomic implications.

The urban poor, as well as the poor in rural villages, are just as important as the rural subsistence poor in terms of water distribution and use, and this should not be overlooked in the land reform rush and the desire to create a substantial class of farmers from among the previously disadvantaged.

The goal of this ISP is to see water benefit society. This can be accomplished through the inclusion of water in livelihood strategies, small-farmer development programs, water supply and sanitation, particularly the provision of safe drinking water, and the maintenance and expansion of income-producing, job-creating, and tax-paying agricultural, commercial, and industrial strategies.

Any strategic document's social component needs to include consultation and public participation. Although strategies and plans were developed without collaboration with stakeholders, this ISP serves as DWAF's position statement on water resources management. It is an open and transparent document that reflects the department's understanding, objectives, and goals.

What is missing in these documents?

- Water loss

The information on water loss because of dams' drainage is not incorporated in these two reports. This information is crucial in determining the water that is being lost so that effective mitigation measures can be formulated and implemented.

- Bathymetric survey

Some of the essential information that is missing in the two DWS reports is the methodology that was employed to collect the data. The bathymetric survey techniques employed to gather the data are not incorporated in both DWS reports. This information is very critical because bathymetric surveys vary in accordance with the size of a dam or the reservoir where the study is being conducted.

There are two types of hydrographic surveys for determining the capacity of reservoirs as determined by the size of the reservoir (DWS-NIWIS-Water Resource Management) as follows:

- a. Using the first method, a complete contour survey of the reservoirs is performed. Total stations, RTK GPS, GNSS, or a combination of both are used to survey the areas of reservoirs that are not covered by water according to set standards. The density of the spot shots is then determined by the scale of maps required as well as the accuracy of the capacity.

The water-covered surface of the reservoir is surveyed by using various sizes of boats equipped with GPS receivers for position determination and Echo sounders for depth measurement. The density of the underwater shots is then determined by scale and accuracy.

The reservoir's contour maps, and area capacity tables are then produced using software packages such as Hypack, Microstation, and Modelmaker. It is also possible to generate cross sections at various sites. Once the area capacity table is established, it can be compared to earlier surveys to evaluate sedimentation.

Only small to medium reservoirs are subjected to a comprehensive contour survey to assess their capacity. The amount of data created during such a study is enormous, and existing software applications are incapable of handling such massive data.

- b. The second method for determining reservoir capacity involves recording cross sections of the reservoir at predetermined intervals. This method is used to survey all large dams. The cross sections are repeated at regular intervals along the reservoir's length. Between

two fixed beacons, the cross sections are run. Hypack software is used to collect the data. The reservoir capacity is then estimated using sediment software that is based on the end area' principal.

c.

The results of this type of survey are substantially faster than those of a comprehensive contour survey. Cross sections are performed at a specific time interval for sedimentation determination, and the amount of sediment in the reservoir is measured by comparing the new and previous capacity.

Because the cross sections are run between fixed survey beacons, information such as the accumulation of silt and where it is concentrated is immediately available.

6.12.3 Results

When the first hydrographic survey was conducted in the Gariep dam by the Department of Water and Sanitation in 1971, the water holding capacity was 5897.285 million m³ with 0.00 sediment percentage as shown in Figure 6.9. The area of the catchment was 70 749 km². The results obtained from the survey which was undertaken in 1979 depict that the dam capacity was 5521.172 million m³ and the sediment was 6.24% (Figure 6.8). The results of the survey which was conducted in 1991 as demonstrated in Figure 6.9 show that the dam capacity was 5362.488 million m³ and the sediment accumulation was on 9.07%. The dam capacity was 5198.194 million m³ when the survey was conducted in 2005 whereas 11.85% was lost to sedimentation as shown in Figure 6.9. The results of the survey which was conducted and completed in November 2018 show that the dam capacity was 4904,527 million m³ while 16.83% of the dam capacity was lost to sedimentation (Figure 6.9). From the results obtained on the surveys that have been conducted to date, about 0.36% of dam capacity is being lost to sediment accumulation annually.

Table 6.3 below shows the findings of a survey conducted in April 2022 on 39 sampling points in the Gariep dam. The deepest point is showing a depth of 62.310 m and the lowest point is about 4.340 m. Using data from Table 1, a contour map of the Gariep dam depth was constructed, displaying the depth as indicated by isobaths and the coordinates shown in Figure 6.9. The sections with higher values have steeper slopes showing the deepest points whereas the sections with lower values have gentle slopes displaying the shallow points.

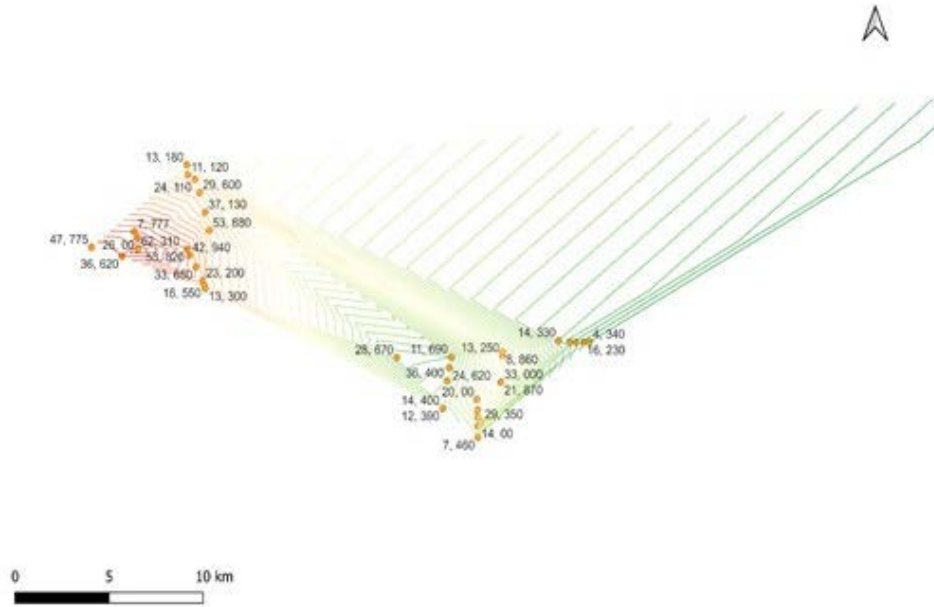
Table 6.3: Gariep dam depths at different sampling points

Sample point	Latitude	Longitude	Depth (m, mm)
Gariep 1	S30° 36' 47.7"	E25° 32' 23.3"	62, 310
Gariep 2	S30° 36' 44.7"	E25° 30' 50.7"	47, 775
Gariep 3	S30° 37' 00.7"	E25° 31' 51.4"	36, 620
Gariep 4	S30° 36' 25.9"	E25° 32' 22.8"	26, 00
Gariep 5	S30° 36' 16.1"	E25° 32' 16.2"	7, 777

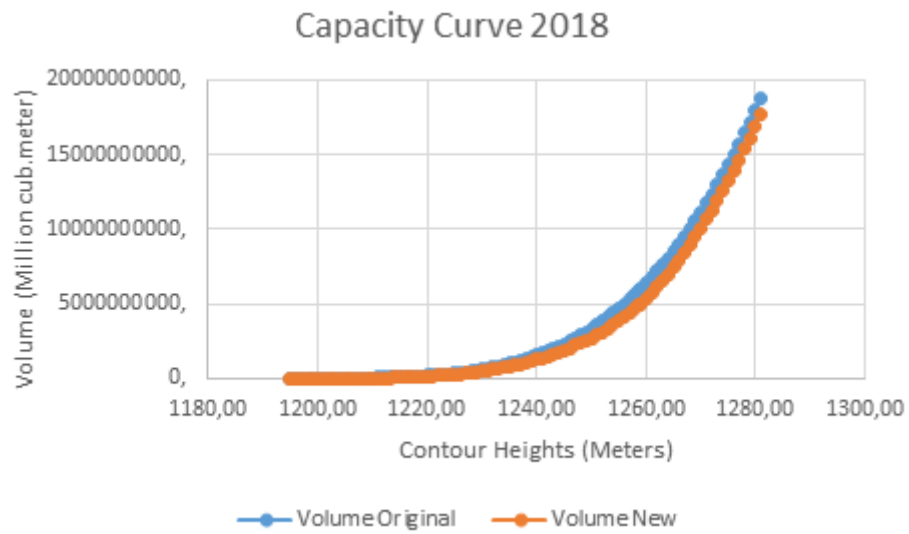
Sample point	Latitude	Longitude	Depth (m, mm)
Gariep 6	S30° 36' 48.1"	E25° 34' 02.6"	53, 820
Gariep 7	S30° 36' 59.1"	E25° 34' 06.1"	42, 940
Gariep 8	S30° 37' 20.3"	E25° 34' 19.4"	33, 650
Gariep 9	S30° 37' 45.2"	E25° 34' 33.3"	23, 200
Gariep 10	S30° 37' 53.7"	E25° 34' 36.3"	16, 550
Gariep 11	S30° 37' 59.3"	E25° 34' 38.2"	13, 300
Gariep 12	S30° 36' 13.6"	E25° 34' 46.5"	53, 880
Gariep 13	S30° 35' 40.5"	E25° 34' 37.8"	37, 130
Gariep 14	S30° 35' 04.7"	E25° 34' 27.1"	29, 600
Gariep 15	S30° 34' 40.6"	E25° 34' 17.6"	24, 110
Gariep 16	S30° 34' 32.1"	E25° 34' 03.1"	11, 120
Gariep 17	S30° 34' 14.0"	E25° 34' 01.4"	13, 180
Gariep 18	S30° 40' 50.9"	E25° 44' 30.7"	33, 000
Gariep 19	S30° 40' 50.9"	E25° 44' 30.7"	21, 870
Gariep 20	S30° 40' 02.2"	E25° 44' 33.3"	13, 250
Gariep 21	S30° 39' 55.2"	E25° 44' 34.0"	8, 860
Gariep 22	S30° 42' 03.8"	E25° 43' 51.6"	29, 350
Gariep 23	S30° 41' 22.5"	E25° 43' 42.3"	20, 00
Gariep 24	S30° 41' 41.8"	E25° 43' 43.4"	17, 800
Gariep 25	S30° 41' 54.4"	E25° 43' 43.7"	17, 400
Gariep 26	S30° 42' 10.7"	E25° 43' 44.2"	14, 00
Gariep 27	S30° 42' 31.4"	E25° 43' 44.4"	7, 460
Gariep 28	S30° 41' 38.3"	E25° 42' 34.0"	12, 390
Gariep 29	S30° 41' 38.3"	E25° 42' 34.0"	14, 400
Gariep 30	S30° 40' 48.3"	E25° 42' 42.6"	36, 400
Gariep 31	S30° 40' 24.4"	E25° 42' 46.8"	24, 620
Gariep 32	S30° 40' 04.8"	E25° 42' 50.4"	11, 690
Gariep 33	S30° 40' 06.0"	E25° 41' 01.5"	28, 670
Gariep 34	S30° 39' 34.6"	E25° 46' 26.4"	14, 330
Gariep 35	S30° 39' 37.4"	E25° 46' 48.1"	27, 480
Gariep 36	S30° 39' 38.3"	E25° 47' 00.8"	23, 030
Gariep 37	S30° 39' 38.2"	E25° 47' 15.7"	16, 230
Gariep 38	S30° 39' 37.4"	E25° 47' 27.7"	4, 340
Gariep Hennie Steyn Bridge	S30° 32' 03.2"	E26° 01' 23.3"	16.10

Figure 6.9 below indicates the results from the table above and the Gariep dam capacity over time as influenced by sedimentation.

2022

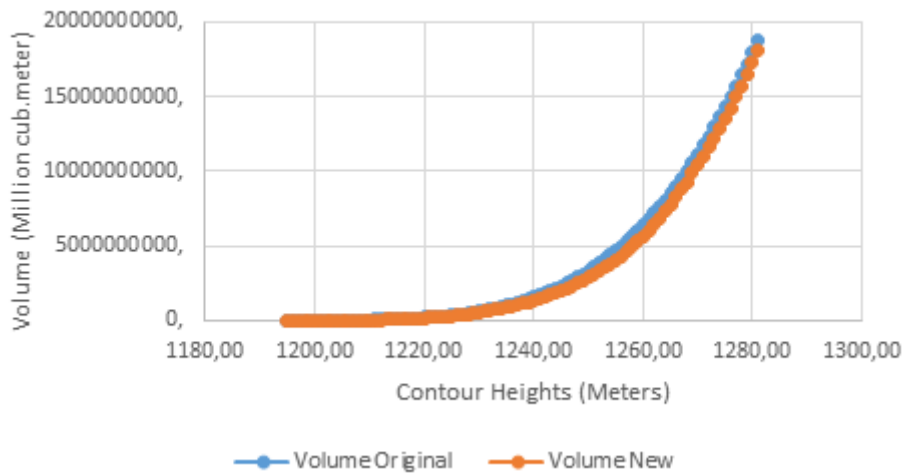


2018



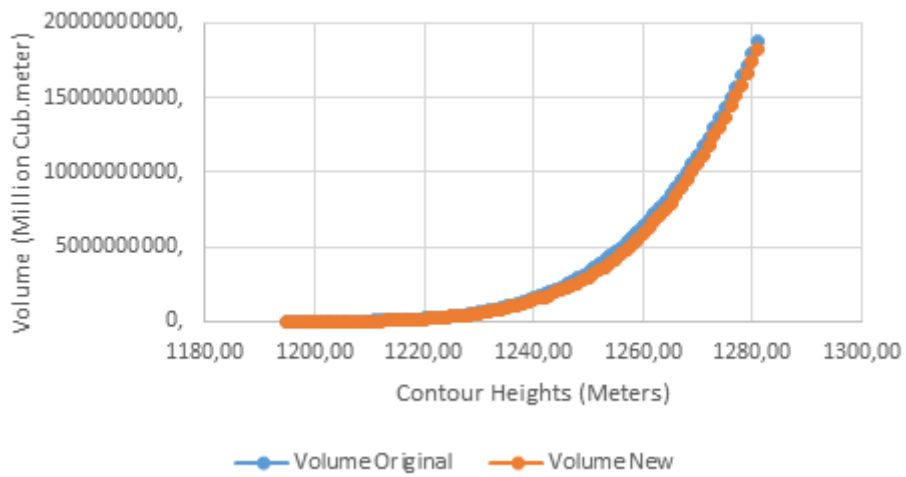
2005

Capacity Curve 2005



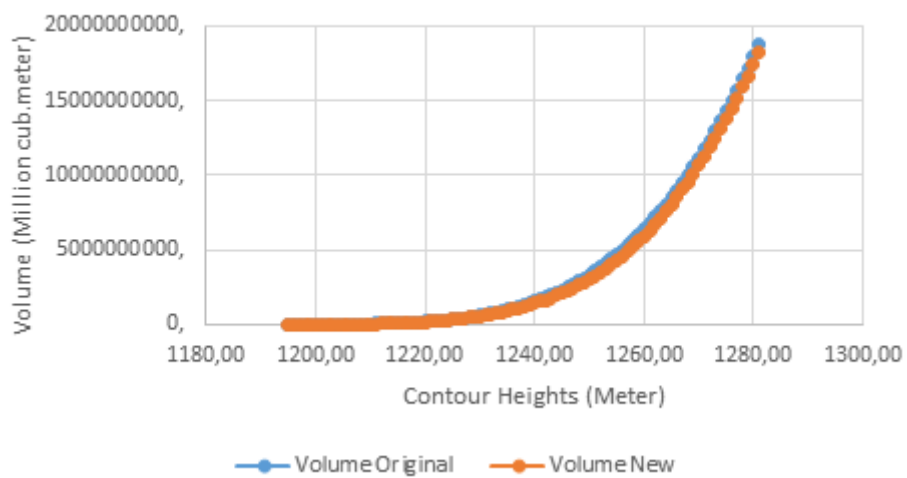
1991

Capacity Curve 1991



1979

Capacity Curve 1979



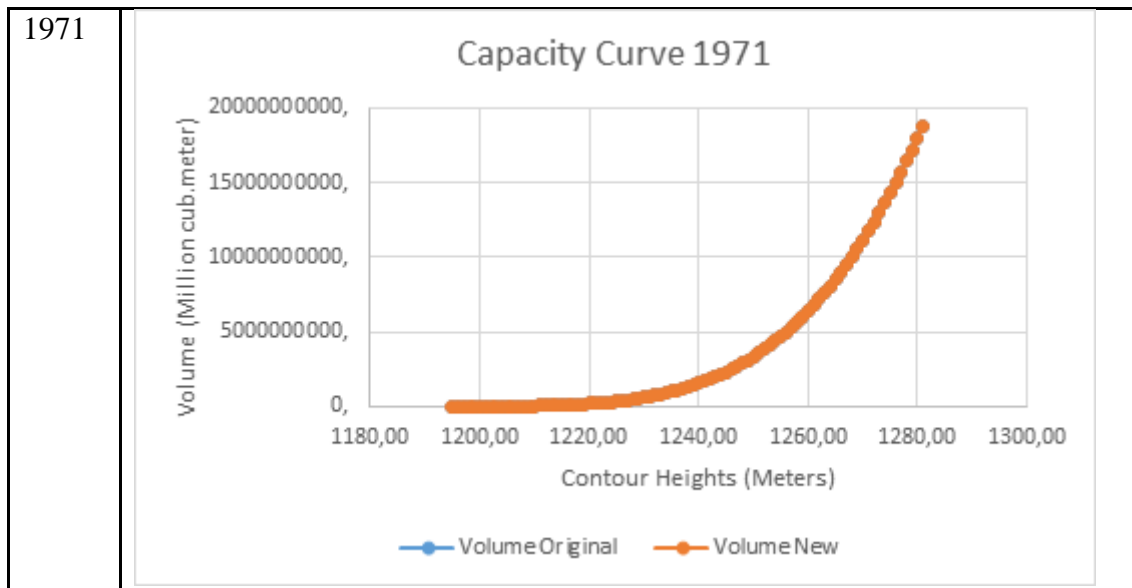


Figure 6.9: Water capacity of the Gariep dam after sedimentation from 1971 to 2022

6.12.4 Conclusion

These results indicate the complexity of dam depth measurement where sedimentation is almost out of control.

6.12.5 The Statement and Motivation of the need for sedimentation dams outside of the Gariep dam

The Gariep dam is located on the Orange River, one of the most turbid rivers in Africa and worldwide because of a high suspended sediment load (Compton & Maake, 2007). This dam is also located downstream of a catchment area that has high sediment yield and authorizations experiencing soil erosion problems (Figure 6.10B). This has been highly linked with the erosion prone soils of the Karoo Supergroup sedimentary rocks as well as poor land use practices (Compton & Maake, 2007; DWAF, 2004). As a result, the Gariep dam receives a high sediment influx from the upstream Upper Orange catchment area as shown in Figure 6.10 (Compton & Maake, 2007). Most of the eroded sediment (approximately 90%) ends up trapped and deposited in the Gariep dam reservoir, while only a small amount flows out of the dam through the spillways as well as through the lower-level river outlets and silt discharge outlets – through density current venting (Kondolf & Farahani, 2018; Kriel, 1972). Because of its size, the Gariep dam acts a large sediment trap basin (DWAF, 2009), accumulating a vast amount of sediment from the upstream catchment area (Kondolf & Farahani, 2018), in addition to having a large water storage capacity.



Figure 6.10: Sedimentation in the Gariep dam

Where: A) The pale green to brown colour on the eastern side reflects a high suspended sediment load inflow from the Orange River (Source of the imagery: Google Earth, May 2022); B) The area upstream of the Gariep dam shows the land surface mainly exposed (bare), making it susceptible to erosion (Source of the imagery: Google Earth, May 2022), and C) The Eastern side of the dam at Bethulie, downstream of the confluence of the Orange and Caledon rivers, shows the high sediment load in the dam, with channels forming because of sedimentation (Source of the imagery: Sentinel Explorer, captured on 14 May 2022).

The accumulation of sediments in a dam causes a reduction in the dam's water storage capacity which in turn compromises its useful life (Kondolf & Farahani, 2018) and its ability to perform its intended purpose. To date, the Gariep dam has lost almost 20% of its total storage capacity because of silt (Manus, 2021). This loss occurs at an annual average sedimentation rate of 0.36% (Jacobs, 2018), which is rather low compared to the global average of 0.5-1% (Schleiss *et al.*, 2016), but is still significant, more so, for a country like South Africa (Msadala & Basson, 2017) where water is considered a scarce and expensive resource (Schleiss *et al.*, 2016).

If the Gariep dam sedimentation is allowed to continue without interventions, this will ultimately threaten not only the country's water security, but also food security, ecosystems, as well as economic development (Manus, 2021). This, therefore, prompts a need to control the sedimentation of the Gariep dam to sustain its storage capacity and to prolong its useful life. This can be done by building sedimentation dams (check dams) upstream of the Gariep dam to capture and retain sediment at catchment level (Obialor *et al.*, 2019) during floods (Manus, 2021), thus, minimising the amount that reaches the dam (Obialor *et al.*, 2019).

Sedimentation dams will, therefore, extend the dam's useful life almost indefinitely (Kriel, 1972).

6.12.6 Study of the geology of the Gariep dam region and find evidence that Gariep contributes to groundwater. Estimate deep drainage losses. Motivate your estimates from literature

Recharge maintains the replenishment of groundwater naturally and when water moves downward from various sources to the subsurface and ends up reaching the water table, this is referred to as groundwater recharge (Mojid, 2019). The variability of this groundwater is due to natural factors such as climate, land cover, geology, morphology, rainfall timing and intensity, soil type, and vegetation (de Vries, 2002). Other factors which can affect recharge include topography modification, and usage of land among others. Some of the major sources for recharge include rainfall infiltration, return flow, recharge along water courses and seepage through subsurface flow by natural hydraulic gradient (Israil, 2006).

Water source availability and distribution play a massive role in total groundwater recharge. In South Africa, precipitation is the leading source of water for recharge. Hence, the analysis of rainfall patterns, frequency, number of rainy days and maximum number of rainfalls in a day along with its variation in space and time are important and influential factors for recharge (Asoka, 2018). Surface water bodies such as lakes, rivers, and canal seepage are some of the contributors of groundwater recharge (Allison, 1994).

According to Uc (2021), another factor that contributes to recharge is the geology of the area since various lithology types possess varying recharge characteristics. For example, sedimentary formations such as sand and gravel are known to be porous and permit water passing through them. The same principle occurs with fractured hard rocks, fault areas, karst topography, and the absence of barriers such as impervious formations. These are of great importance when it comes to underground seepage and recharge. Climatic factors like precipitation, evapotranspiration, soil moisture, and temperature also affect recharge rates of underground water (Hughes, 2021).

Therefore, the main purpose of this section is to investigate the groundwater recharge or deep drainage losses using the water balance concept in the Gariep dam region based on geological, hydrological, hydrogeological, and climatic data.

a. Geology of the Orange River Basin

Johnson *et al.* (2006) stated that the geology of the Orange River Basin has a widely diverse in terms of its geology. The Geology of the Orange River Basin can be described as one that is dominated by the unconsolidated sedimentary rocks of the Karoo succession which underlie the main area and have been intruded by dykes and sills, with much more pronouncement in the Beaufort Group and the volcanic extrusives of the Lesotho Highlands, dolomite successions

and Kalahari sand cover. The basin can further be comprised of three sections, namely: Karoo succession, Kalahari sand cover and basement rocks that underlie the lower Vaal, and middle to lower Gariep catchment, as well as the Fish in Namibia. Meyer (2003) described the lithology of the supergroup as indicted in Figure 6.10.

The Karoo succession comprises the foreland basin that underlies the upper and middle of the Gariep, Vaal and Senqu rivers. It is comprised of the Dwyka Group (bluish-grey, unbedded, unsorted tillite) with a thickness that varies up to 120 m, the deep to shallow marine sediments of the Permian Ecca Group (carbonaceous shale, dark bluish green to massive grey shale, olive-green micaceous shale/mudstone, light green to greenish-grey shale, mudstone, siltstone and fine-grained sandstone). This has a thickness that varies between 340-360 m, fluvials of the Permo-Triassic Beaufort Group which comprise the Adelaide Subgroup (sandstone, siltstone, grey to reddish mudstone, blue-green-grey shales and red to purple mudstone).

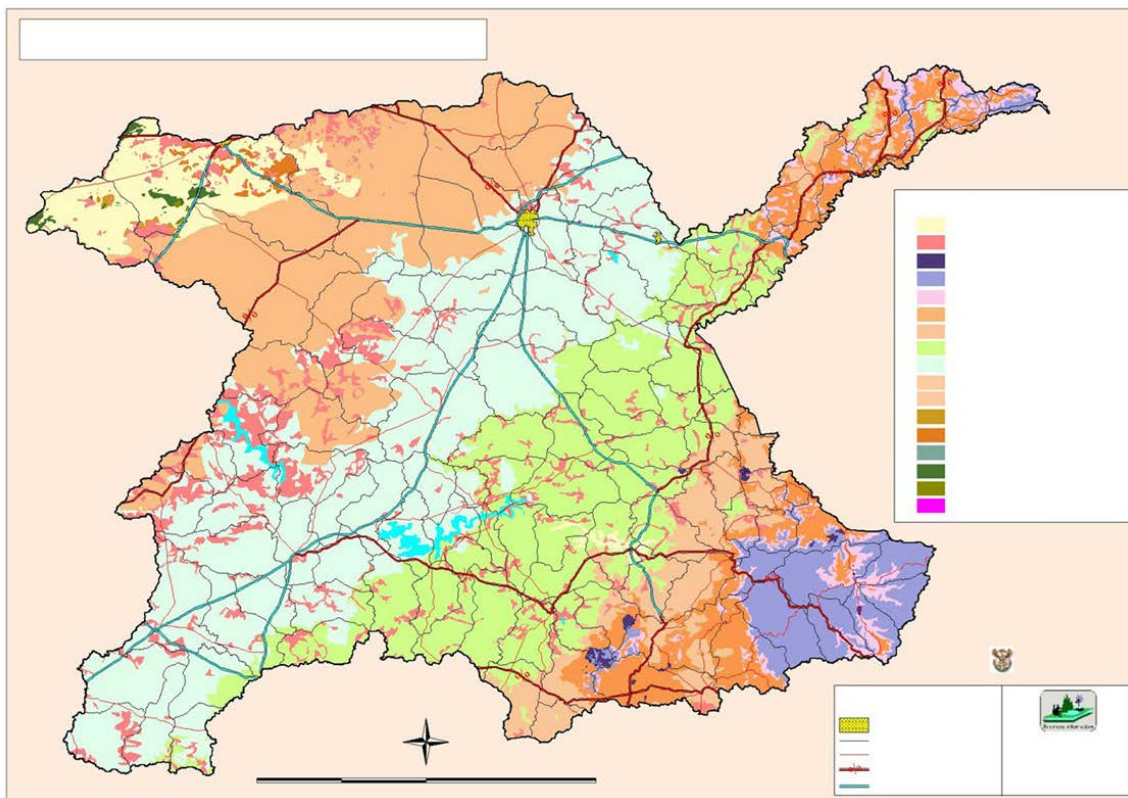


Figure 6.11: *Geology of the Upper Orange WMA*

Tarkastad Subgroup (light coloured, feldspathic sandstone, red, purple, and green mudstone) with a thickness of up to 400 m and 900 m respectively. The Molteno formation comprises of grey-green and red-purple mudstone with fine to coarse-grained sandstone bands with a thickness of about 250 m. The Elliot Formation comprises of maroon or green mudstone and medium grained feldspathic sandstone.

WMA 13 (UPPER ORANGE): GEOHYDROLOGY

The Clarens Formation is comprised of cream-colored, fine-grained, massive aeolian sandstone with a maximum thickness of about 200 m and overlain by the Drakensberg Group with sharp contacts and comprises of basaltic lava with a maximum thickness of about 900 m. A patchy occurrence of the Ventersdorp Supergroup is observed in the north-western part of the area, and it is characterized as porphyritic lava, quartzite, tuff, and volcanic breccia (Meyer, 2003). Alluvium made up of various materials such as clayey sand, sandy silt, limestone, sand pebbles and small boulders are found along streams and rivers with thickness varying from 1-15m (Meyer, 2003).

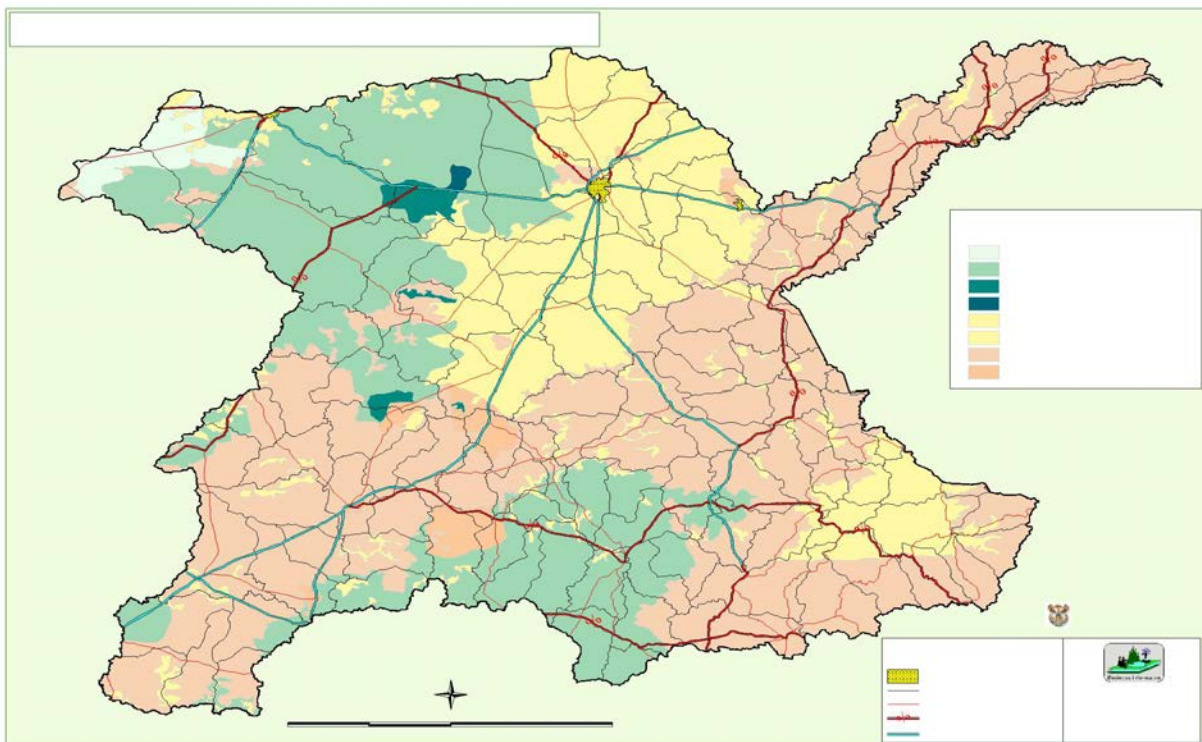


Figure 6.12: Geohydrology of the Upper Orange WMA

a. Geohydrology

The Upper Orange WMA lies mainly on the Bloemfontein 2924 1:500 000 hydrogeological map with small portions of the area on the Kimberley 2722, Kroonstad 2726, Prieska 2920, Beaufort West 3122 and Queenstown 3126 hydrogeological maps and is shown in Figure 6.12 above. Two types of aquifers are found in the area, *viz*: Dwyka, Ecca Group and portions of the Tarkastad Subgroup and fractured and intergranular (Ventersdorp Supergroup, Beaufort

Group, Molteno, Elliot and Clarens Formations) aquifers. The geohydrology of the Karoo Supergroup as described by Meyer (2003) reads as follows:

‘The total groundwater potential of the Dwyka Group rocks is 0.1-0.5 l/s but yields are associated with joints, fractures, and weathering of the rocks. The occurrence of groundwater in the Ecca Group is associated with contact zones, joints, and bedding planes. Recharge of the aquifer can be enhanced by the thick calcrete layers of a high porosity but are not found as a blanket covering the group. The average borehole yields range between 0.5-2.0 l/s yet not more than 10% of the recorded boreholes yield more than 5 l/s. The intrusion by dolerite sills along with the less extent of dolerite dykes is more prominent in the Adelaide Subgroup of the Beaufort Group. The occurrence of groundwater is mainly found in joints and fractures on the contact zones, in weathered dolerite zones, weathered and jointed sedimentary rocks and on bedding planes, thus borehole yields vary from 0.5-2.0 l/s. In the Tarkastad Subgroup of the Beaufort Group, the occurrence of groundwater occurs in dolerite contact zones, joints, and fractures and on bedding planes with Borehole yields varies from 0.5-2.0 l/s and about 17% of the recorded yields are more than 5 l/s. The Molteno, Elliot and Clarens Formations cover the eastern portion of the area as well as the Lesotho border and have been intruded by different kinds of dykes and sills. Groundwater can be established on contact zones, joints, and fractures in the sedimentary rocks and in weathered zones, but occurrence is restricted due to various factors such as high runoff and little infiltration.’

Furthermore, the scarcity of dolerite intrusions limits the possibility of borehole sites. In areas where there are joints, fractures and weathering, groundwater can occur in the dolerite dykes and sills. In the Drakensberg Group, the occurrence of groundwater is associated with weathered lava and zones of contact between lava and dolerite intrusions. Numerous low-yielding springs emerge on contacts between weathered and solid rocks; thus borehole yields are expected to be very low, with ranges between 0.1-0.5 l/s but a large proportion of boreholes with less than 0.1 l/s. In the Allanridge Formation of the Ventersdorp Supergroup, the occurrence of groundwater is associated with jointed diabase dykes and their contact zones, fractures in the occasional fault zones and weathered basins with associated joints thus making borehole yields vary from 0.5-2.0 l/s (Meyer, 2003). According to Meyer (2003) there are no meaningful intergranular (alluvial) aquifers that have been reported, although one can accept that alluvium can act as a groundwater recharge mechanism.

Vogel and van Urk (1975) stated that recharge is most likely thought to occur during heavy rain events. Due to the climate and geology of the lower portions of the catchment (Gariep dam), contribution of baseflow from the Gariep River to groundwater and vice versa has not been quantified. ORASECOM (2008) reported that the groundwater resources are somewhat limited in some areas and largely undefined within the basin.

b. Drainage

Figure 6.13 shows that the Gariep dam storage was particularly high in 2022, but not at absolute maximum. However, some potential improvement into absolute maximum storage possibly

due to improved rainfall is highly likely. Compared to the previous year, the storage is slightly higher.

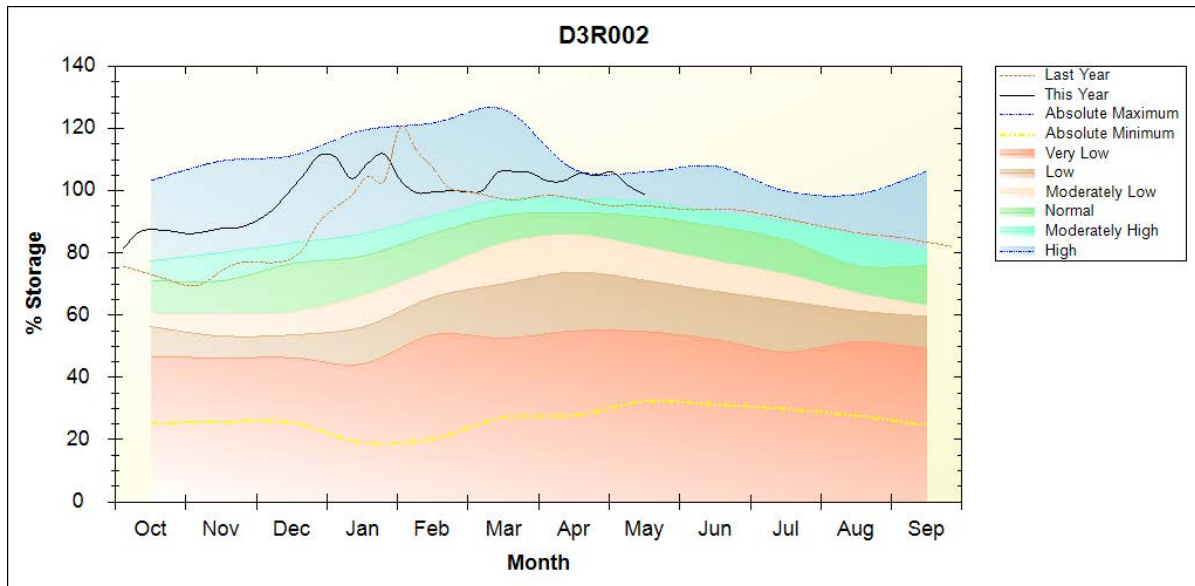


Figure 6.13: Drainage State of the Gariep dam on 16 May 2022

6.12.7 Conclusion

To make water accounting a useful tool for managing the Orange River Basin, there are several areas where substantial improvements in data are needed. First, the water accounting needs to include losses through evaporation, evapotranspiration, and spillage among others. Secondly, more reliable, and detailed information and data about water use for activities such as irrigation by crop and crop yield within the Orange River Basin is needed. In most cases, water is not metered, and farmers may switch crops annually, making it difficult to determine exactly how much water is used. Without this water usage information, it's difficult to quantify the exact amount of water seeping into the ground. Methods such as the Chloride Mass Balance model which utilize the change in chloride concentration in the soil profile over time to estimate deep drainage can be employed. Since chloride does not undergo chemical transformation in the soil, its losses or gains from the soil can be assumed to be due to movement of water containing dissolved chloride. Changes in the total amount of chloride in the soil and concentration of chloride draining from the soil profile over time are used to calculate the amount of water that has moved through the soil profile during that specified amount of time. In addition, and finally, it is important to develop a time series of water accounts for both surface and groundwater so that trends can be always monitored.

6.13 The engineering process of dam siltation evaluation in South Africa using GIS and satellite information, with a focus on the Vanderkloof dam

6.13.1 Introduction

This research project focuses on the proposed engineering process of dam siltation evaluation in South Africa using GIS and satellite information. This study includes the Gariep dam and the Vanderkloof dam and their comparison.

a. Gariep dam

The Gariep dam is South Africa's largest dam, and it was constructed during the 1970s to tame the Orange River (van Vuuren, 2010). It has a capacity of about 5 500 million m³ (de Waal, Bekker and Pretorius, 2011), and a height of 88 m (Schleiss and Boes, 2011). According to Schleiss and Boes (2011), the river section of the dam has a double curvature arch that transitions to gravity sections on the flanks. The dam's major function is to provide water for irrigation, domestic and industrial usage, as well as power generation.

b. Vanderkloof dam

The Vanderkloof dam is South Africa's second largest dam with a capacity of over 3200 million m³ and a surface area of approximately 133.43 km² at full capacity (Olofintoye, Otieno and Adeyemo, 2016). It was constructed in 1973 and put into service in 1977, and its water is supplied by the Orange River (Adeyemo and Oluwatosin Olofintoye, 2014). During times of heavy flows, the Gariep and Vanderkloof hydropower plants along the Orange River are primarily used to provide base energy (Olofintoye, Otieno and Adeyemo, 2016).

c. Dam siltation

Dam siltation occurs when the sediments are disturbed and are transported into the reservoir where they settle (Mama and Okafor, 2011). These sediments include fine silt, mud, fine particles of sand, and others. Dam siltation also affects dam storage capacity and life span (Fagorite, 2019). Dam siltation is a multifaceted process that changes depending on the amount of sediment produced in the watershed, the rate of transportation, and the mechanism of deposition (Sumi and Hirose, 2009).

6.13.2 Aims and objectives

Aim

- a. To elucidate and to investigate the proposed engineering process of the Gariep and Vanderkloof dam siltation using data from DWS.
- b. To further elucidate the findings from aim 'a' above to ensure that they make sense

- c. To conduct a field survey

Objectives

- a. To conduct a literature survey on topics related to this study
- b. To compare dam siltation of Gariep and Vanderkloof dams
- c. To access the DWS website: <https://www.dws.gov.za/Hydrology/> and Water resource: <https://waterresourceswr2012.co.za/> website for data
- d. To use Google Earth Pro demarcate the study areas

Significance of the study

To identify strategies to reduce dam siltation and boost dam storage capacity. South Africa is a semi-arid country, it is therefore important to maintain dams to ensure access to water for posterity.

6.13.3 Methodology

This chapter explains how the study was carried out using GIS and satellite imagery. The methodology is based on information obtained from different journals and information obtained from the DWS website. Software such as QGIS and Google Earth Pro were used to analyze the data.

Figure 6.15 below is a Google Earth Pro representation of the Gariep dam. The Gariep dam releases water into the Vanderkloof dam, where it is either moved to the Riet River basin through the Orange-Riet Canal or released downstream.

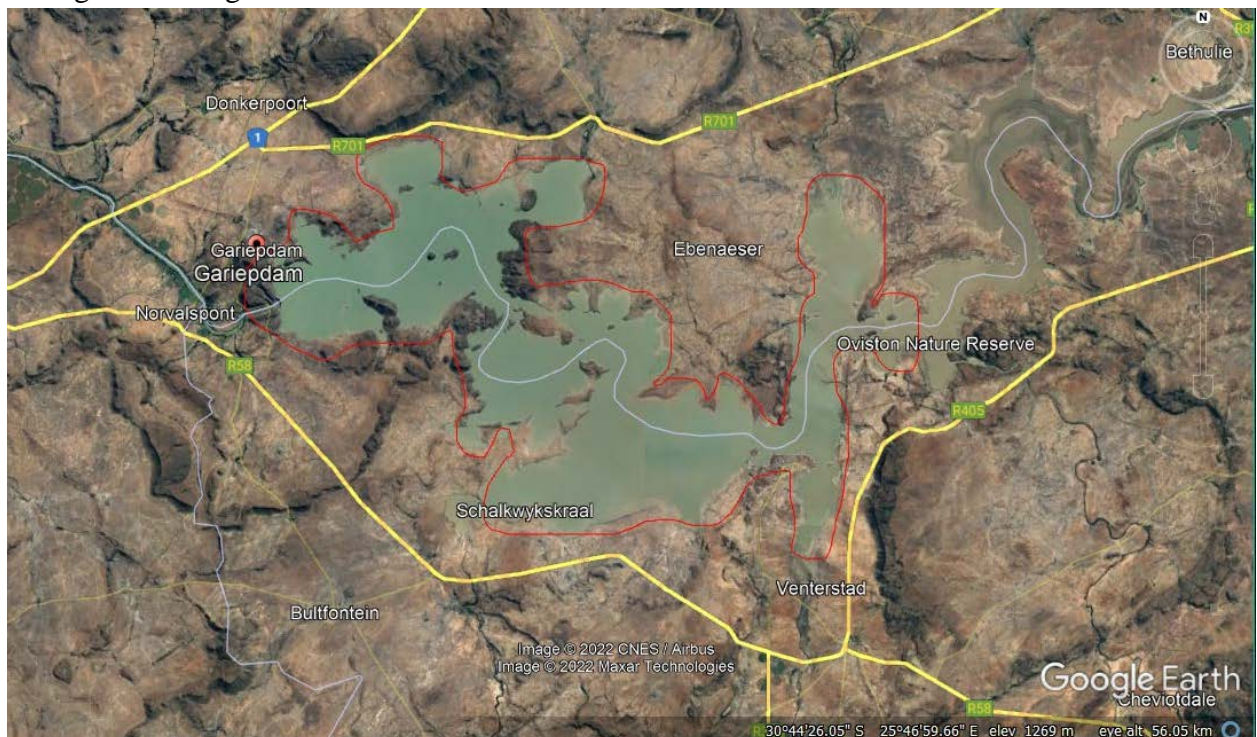


Figure 6.14: The Gariep dam



Figure 6.15: The Vanderkloof dam

6.13.4 Monitoring of the dam volume and dam siltation

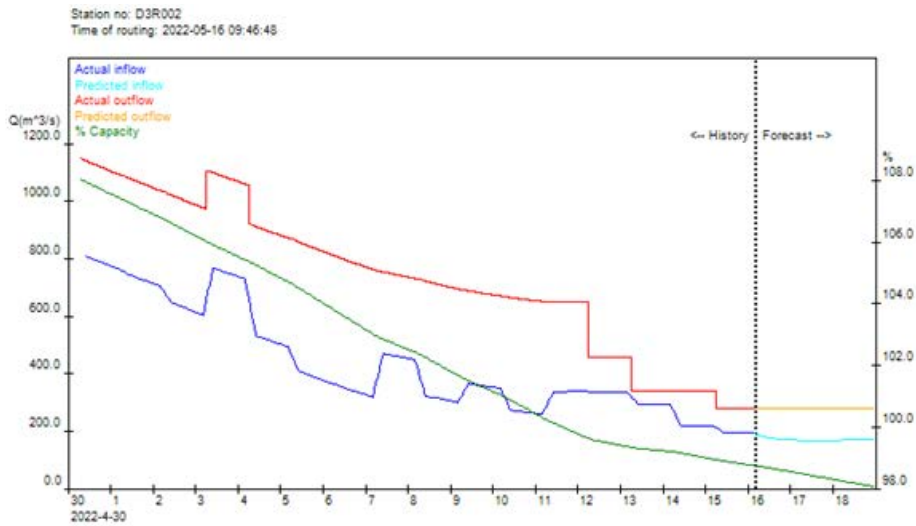
GIS and satellite remote sensing are used in this method. This can be achieved by the Digital Elevation Model (DEM) and LANDSAT TRS (Thermal Remote Sensing), where multispectral photos of the dam are produced. GIS and image processing techniques such as merging and georeferencing raw satellite data, determining the amount of water in the dam, and segmenting waterbodies using pixel level analysis are employed. Total water volume estimations are based on an empirical model constructed using previously validated data that calculates area and depth per pixel (Bhat *et al.*, 2015). This method was used in a reservoir called Krishna Raja Sagar (KRS) in the Karnataka state of India.

Sediments are transported into the dam by the river system. Estimation of sediments in running water can be achieved using traditional methods. According to the size of the region and the accuracy necessary in calculating the amount of silt with water, the sensor that is in accordance with existing objectives and facilities is selected in remote sensing data-based approaches. Photos from the past and present are then prepared, and a research team works on both the field and software fronts until the desired outcomes are obtained (Hadian and Mosaedi, 2021).

Google Earth is used to compare the level of siltation occurring in the dams, i.e. Gariep and Vanderkloof dam over time. The siltation in this study is indicated by colour change. Areas

with a significant amount of siltation have a different colour compared to low siltation areas of the dam.

6.13.5 Results and discussion



2022-05-16 07:00 Capacity: 98.7 %
Inflow: 184 cumec Outflow: 278 cumec

Figure 6.16: The hydrological state of the Gariep dam, (Source: DWS website_16 May 2022)



Figure 6.17: The Gariep dam in December 1994 captured on Google Earth

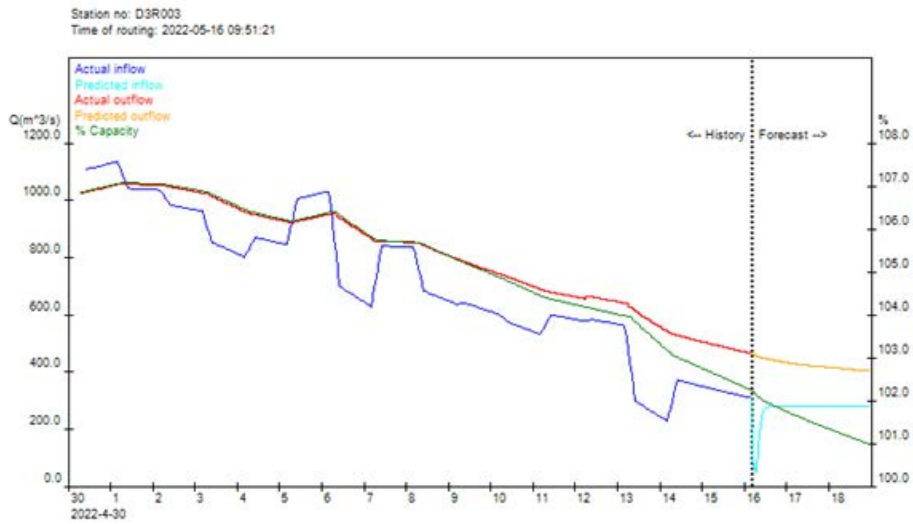


Figure 6.18: The Gariep dam in December 2012 captured on Google Earth



Figure 6.19: The Gariep dam in May 2022 captured on Google Earth

Figures 6.17-6.19 above show changes in the state of the Gariep dam over time, and corresponding siltation levels. The levels of siltation are visible on the eastern side of the dam as shown by the different colour from the rest of the dam.



2022-05-16 07:00 Capacity: 102.1 %
Inflow: 49 cumec Outflow: 457 cumec

Figure 6.20: The hydrological state of the Vanderkloof dam (Source: DWS website, 16 May 2022)



Figure 6.21: The Vanderkloof dam captured in December 1990 on Google Earth

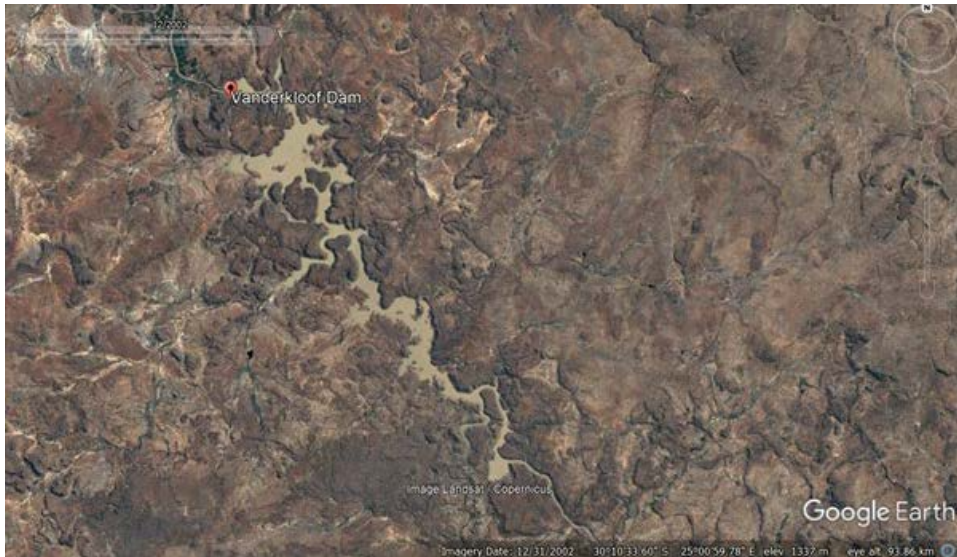


Figure 6.22: The Vanderkloof dam captured in December 2002 on Google Earth



Figure 6.23: The Vanderkloof dam captured in December 2020 on Google Earth

The up-to-date imagery of the Vanderkloof dam on Google Earth was obtained in December 2020. Figures 6. 20-6.23 above show changes that occurred in the Vanderkloof dam over time.

6.13.6 Conclusion

Dam siltation consequently leads to dam storage capacity declines. Siltation in dams is mostly experienced in periods of heavy rainfall, where sediments are swept into the dam by the turbulent Orange River flows. An increase in the number of sediments in the dam simultaneously leads to a decline in dam storage capacity.

6.14 A geological reflection on signs of water loss

6.14.1 Materials and Methods

a. Data

LANDSAT explorer web application which is used to access satellite imagery was utilized in this study along with the hydrogeological and geological data from the DWS. The satellite images were acquired through LANDSAT explorer web application which can be accessed from: <https://livingatlas2.arcgis.com/LANDSATexplorer/>

b. Method

As described by Le *et al.* (2015), satellite images allow a fast and reliable review of the land changes that occur over time through repetitive direct observation of the surface. This allows for mapping and monitoring of surface objects whilst assessing changes over time and space. The satellite system provides a main instrument which supplies regular data on land inventory and monitoring of land cover changes in a timely manner. Different sectors such as the environment, forestry, hydrology, irrigation, agriculture, geology, resource management and planning rely on such data for application purposes.

The present study presents a method of extracting changes between two periods, i.e. when the Gariep dam was overflowing and during a drought season when the dam was at its lowest. Satellite imagery was obtained from LANDSAT explorer web application from ESRI then processed using QGIS. LANDSAT explorer, as described by ArcGIS, is a web application which highlights some of the capabilities for accessing LANDSAT imagery layers powered by ArcGIS for Server, accessing LANDSAT Public Datasets running on the Amazon Web Services Cloud. The layers are updated with new LANDSAT images daily.

This application enables us to visualise the earth to understand how it changes over time. It enables LANDSAT satellites to collect data that is beyond the human visible spectrum. The App is used to draw on LANDSAT's different bands to better explore the planet's Colour Infrared, SWIR (Short Wave Infrared), Geology and Moisture Index. These band combinations and indices provided below are utilized in this method.



Figure 6.24: Colour Infrared (5, 4, 3)

This band combination is also called the near-infrared (NIR) composite. It utilizes the near-infrared (5), red (4), and green (3) spectrums. This band is useful for analysing vegetation since chlorophyll reflects near-infrared light. Healthy vegetation is bright red, water is dark areas and urban areas are white.



Figure 6.25: Short-Wave Infrared (7, 6, 4)

The short-wave infrared band combination uses SWIR-2 (7), SWIR-1 (6), and red (4) spectrums. These composite display vegetation in shades of green. Denser vegetation is indicated by darker shades of green, sparse vegetation by lighter shades, and urban areas by blue while soils have varying shades of brown.



Figure 6.26: Geology (7, 6, 2)

The geology band combination uses SWIR-2 (7), SWIR-1 (6), and blue (2) spectrums. The band is useful for highlighting geologic formations such as lithology features and faults.

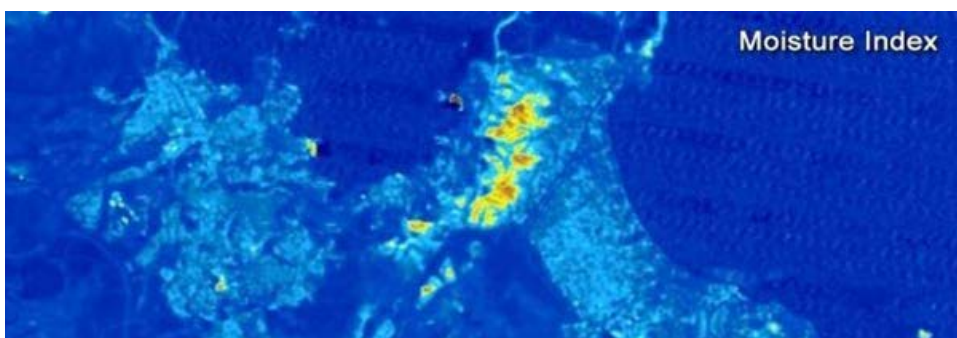


Figure 6.27: Moisture Indexes $(\text{Band } 5 - \text{Band } 6) / (\text{Band } 5 + \text{Band } 6)$

The moisture index is used to estimate the moisture content. Water appears blue along with lighter shades containing less moisture and bright orange and red showing a significantly lower moisture content.

Therefore, determining changes between the two areas using the above-mentioned indices and looking into the hydrogeology and geology of the area around the Gariep dam from the DWS report, this can be used to highlight evidence of water loss through changes in the vegetation, geology, and moisture content in the area.

6.14.2 Results

Since 2016, the Department of Water and Sanitation has been consistently urging communities and businesses to adopt water saving strategies due to reduced dam levels across the country owing to drought. In 2016, the Orange River System was between 54.4 and 55.64% full, while the Gariep dam was about 51.8 to 55.7% full. Consequently, the following data has been extracted from November 2016 as a reference to the Gariep dam's dry period. The wet period will be that of December 2021 when the dam storage was 111% full.

The following images were captured from the LANDSAT during those two periods.

a. Colour infrared

This combination of bands gives similar results to that of traditional false colour infrared photography which adds a near infrared (NIR) band and drops the visible blue band. Vegetation in the NIR has a high reflection due to chlorophyll and a NIR composite shows the vegetation in various shades of red vividly. While the urban areas are cyan blue, soils vary between dark to light brown. Coniferous trees appear darker red compared to hardwoods. In general, the deep red hues indicate healthy vegetation while lighter reds indicate sparsely vegetated areas. Water appears dark due to the absorption of energy in the visible red and NIR bands.



Figure 6.28: LANDSAT explorer rendering colour infrared image: November 2016



Figure 6.29: LANDSAT explorer rendering colour infrared image: December 2021

From Figure 6.28 and 6.29, the dry periods (November 2016) mean a lack of water in some spots while the opposite is true for the same spots in wet periods (December 2021).

Looking at LANDSAT images, some deep red lines moving towards the Bethulie dam and close to the dam wall are apparent in the November 2016 image. A similar occurrence is observed in the dry period image. This means that there is healthy vegetation around these spots and during a drought or dry period, the trees/vegetation are forced to access groundwater for survival.

In the wet period image (December 2021), reddish scattered dots in most places in colour infrared images indicate sparse vegetation due to excess water.

b. Short Wave Infrared

This combination of bands is useful for visualizing urban environments. This band combination utilizes both the SWIR bands (SWIR-2, SWIR-1), and vegetation is displayed in various shades of green. While the urban areas are cyan blue, soils vary between dark to light brown. In general, the deep green hues indicate healthy vegetation while lighter green hues indicate sparsely vegetated areas. Water appears dark due to the absorption of energy in the visible red and infrared bands.

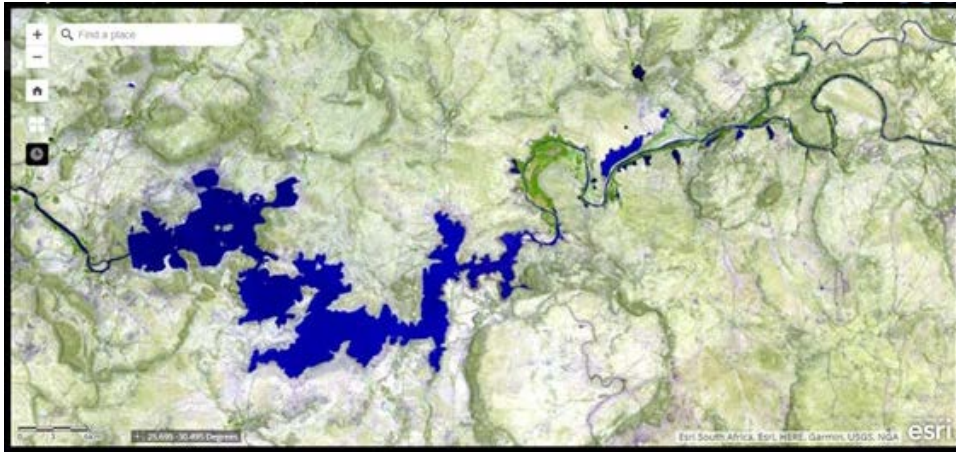


Figure 6.30: LANDSAT explorer rendering a short-wave infrared image: November 2016

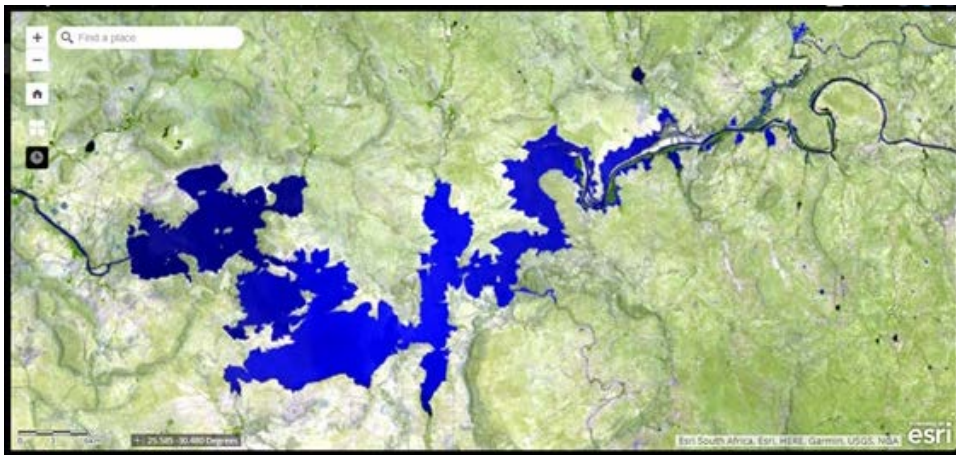


Figure 6.31: LANDSAT explorer rendering a short-wave infrared image: December 2021

From the two images (Figures 6.30 and 6.31) from different timelines and periods, it's clear that although water normally occupies some spots during the wet season (December 2021), the same spots are sometimes occupied by water in the dry season (November 2016).

The short-wave infrared LANDSAT images show a more pronounced light greenish cover in December 2021 than in November 2016. This indicates sparse vegetation, meaning that areas which normally do not have vegetation suddenly thrive due to excess water. Areas towards the Bethulie dam appear darker green, indicating denser and/or healthier vegetation. This vegetation has access to groundwater for growth during dry periods.

c. Geology

This combination of bands allows for the visualization and extraction of major structural features like thrust faults and folds, textural characteristics of igneous and sedimentary rocks, and for lithological and geological mapping such as recognizing hydrothermal altered rocks, among others.

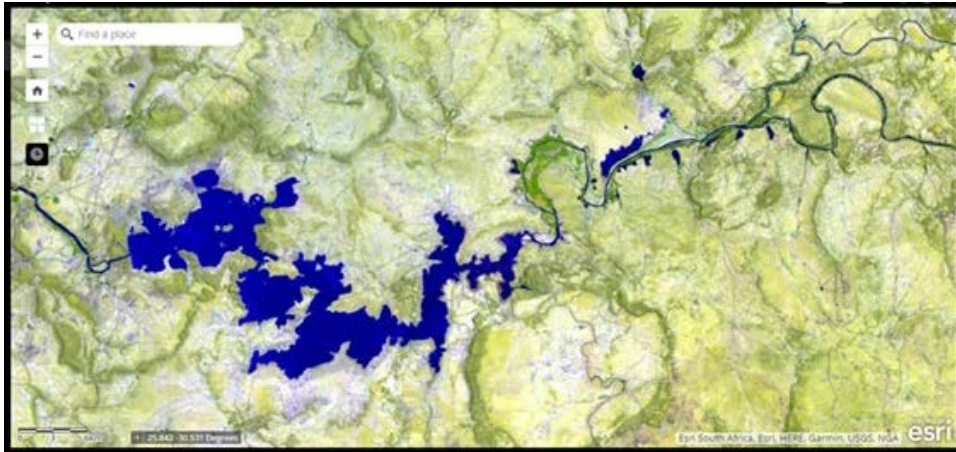


Figure 6.32: LANDSAT explorer rendering a geological image: November 2016



Figure 6.33: LANDSAT explorer rendering a geological image: December 2021

From Figure 6.32 and 6.33, rock types are not clear, but the lines on the images potentially indicate the presence of fractures or faults in the area. This band combination is visually like the short-wave infrared. The wet period image appears greenish as an indication of dense vegetation, resulting from rocks that are capable storing water and therefore sustaining plant biodiversity.

d. Moisture Index

The Normalized Difference Moisture Index estimates levels of moisture in vegetation. Wetlands and other vegetation covered areas with high levels of moisture appear blue, whereas deserts appear tan to brown.

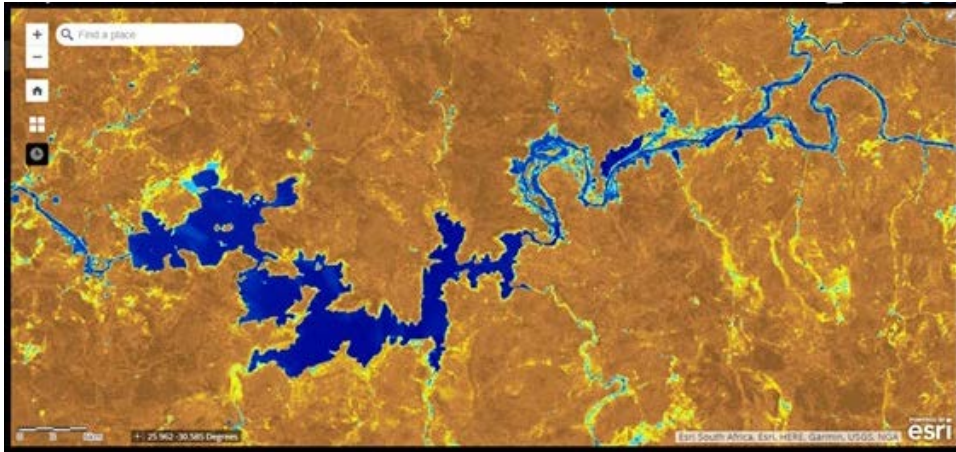


Figure 6.34: LANDSAT explorer rendering a geological image: 28 November 2016

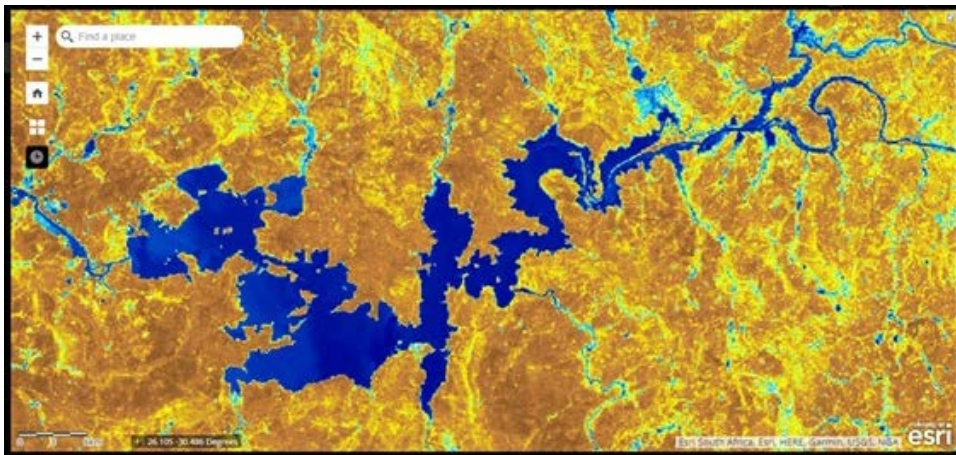


Figure 6.35: LANDSAT explorer rendering a geological image: 12 December 2021

From Figure 6.34 and 6.35, it's clear that although water normally occupies some spots during the wet season (December 2021), the same spots are sometimes occupied by water in the dry season (November 2016).

These images indicate the difference in moisture content over the two periods. The bluish colour shown on the November 2016 image indicate a drought period, in comparison with the wet period of December 2021. This can also indicate the presence of vegetation available in the area. There's more tan to brown colouring in the drought period than the wet period. This means that in the drought period, and the land was not covered with water as compared to the wet period.

6.15 Measurement of dam circumference and the dynamics of circumference change as a function of Google Earth

6.15.1 Introduction

Physiographic and climatic limitations alongside human ingenuity play a crucial role in the coherent and integrated management of hydrological resources. Hydrological resources are an integral source of water, water used to sustain several organisms within multiple cycles. Dams and reservoirs play a crucial role in (1) ensuring the supply of freshwater to end-users and (2) reducing water flow within catchments and thus necessary in the conservation of life (Conley *et al.*, 2000). South Africa is a semi-arid region and experiences hydrological extremes such as severe droughts and floods (Kirchhoff, 2008). The rainfall in the country decreases rapidly westwards from the east, thus the conservation and management of dams and reservoirs in the west critical (Andersson *et al.*, 2015). The Gariep dam is the largest dam in South Africa and located in the western part of the country. It lies along the Orange River on the border of the Free State and Eastern Cape provinces (Conley *et al.*, 2000). Water from the dam is used for irrigation, power generation, domestic supply, and industrial uses (Conley *et al.*, 2000). The dam or reservoir's volume affects its intended uses. To ensure the water in the dam/reservoir can fulfil its intended uses, it is important to always know the volume and quality of the water. This is also because the management of the dam's/reservoir's water links directly to power generation and flood prevention strategy planning. An understanding of the effect of the region's topography and an effective account of sedimentation and thus flow regimes assist in determining dam/reservoir volume. Therefore, this section demonstrates the use of Geographic Information Systems (GIS) and remote sensing techniques to produce perimeter maps of various stages of dam fullness, identifying the correlation between water body surface areas and changing water levels, finding areas for continuous measurements, and lastly setting up an automated procedure to record water body surface area from satellite imagery.

6.15.2 Aims and objectives

Aim

The aim of the study is to measure the dam volume of the Gariep dam with the use of dam floor topography, perimeter maps, and satellite imagery showing various stages of dam fullness to present a method that can replace dam level recordings done by the DWA.

Objectives

- Find maps of the topography of the dam floor.
- Produce an original dam floor topography.
- Produce the perimeter maps of the dam from satellite imagery for various stages of dam fullness.
- Compare the results with the recorded dam water levels for the same day.

- Set up a correlation between water body surface area and correlate with recorded depth values.
- Set up an automated procedure for recording dam water body surface area from satellite imagery.

6.15.3 Study Area

The Orange River basin is situated across several countries in the southern part of Africa, the region commonly known as Southern Africa. The Orange/Senqu River and associated tributaries drain most of Lesotho. After flowing across the western border of Lesotho into South Africa, the Senqu River becomes the Gariep River as shown in Figure 6.36 (Turton, 2005). The Orange River Basin varies dramatically in both climate and topography from the upper to lower catchment areas. The lower part of the Orange River Basin where the Gariep dam is located contains complex geology, with a variety of mixed mineral deposits and shallow rocky soils. By understanding the effect of the region's topography, the surface area, and thus different stages of dam fullness we can then effectively account for the dam/reservoir's volume.

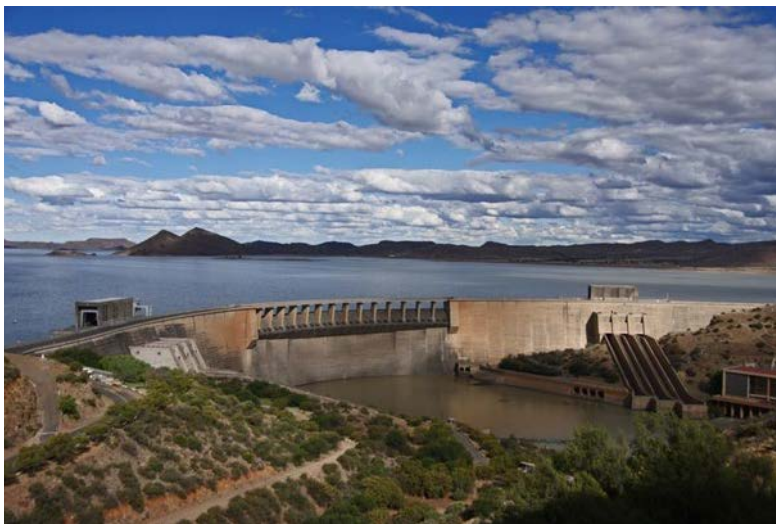


Figure 6.36: Image of the Gariep dam

6.15.4 Methodology

Creating maps of the topography of the dam floor

This study employed cutting-edge GIS/remote sensing techniques to investigate the patterns of circumference change and measurement of dam circumference. Dams have had a significant influence on the hydrology, sediment loads, and geomorphology of rivers. By utilizing remote sensing techniques, the researchers were able to observe the fluctuations in reservoir water levels and estimate the associated circumference changes in real-time.

This study was conducted in the water territory of the Gariep dam, with the aim of enhancing water provision for the western region. Observations were made using Google Earth, which provided valuable insights into the topography of the area. Based on these observations, an optimal site was selected for the dam's location and a section was designated using the command "Add Path." The chosen dam location section was saved in KML format and is presented in Fig. 6.37 below.

ESRI Earth Observation Explorer, also known as ArcGIS Earth, offers valuable capabilities for mapping the perimeter of large dams using Earth observation data. By leveraging satellite imagery, aerial photography, and other geospatial data sources, ESRI Earth Observation Explorer enables precise mapping and analysis of dam perimeters. This technology allows engineers and environmental professionals to assess the extent and condition of dam structures, monitor potential erosion or land subsidence around the perimeter, and evaluate the impact of surrounding land use on dam stability. Additionally, the software provides tools for creating accurate topographic models, generating elevation profiles, and conducting hydrological analyses, all of which contribute to a comprehensive understanding of the dam's surroundings. Ultimately, utilizing ESRI Earth Observation Explorer enhances the management, maintenance, and safety of large dams by providing essential geospatial information for decision-making and proactive maintenance strategies.

The estimation of dam circumference was carried out through various approaches, including the utilization of optical imaging from LANDSAT 5 TM and LANDSAT 7 satellites. These images were captured through different acquisition modes, with varying geometric and spectral resolutions, enabling the evaluation of multiple techniques. For each image type, a technique was tested based on visual matching with digitized contour lines to fully leverage the dataset of dam circumference, ultimately leading to the creation of a digital elevation model (DEM).

Google earth satellite images of the Gariep dam were obtained for 1984 (representing the earliest images available), 1985, (taken shortly after flow regulation began) and for 1993 (the most recent images available when dam level was very low) to 2022. All the satellite images were taken during the low flows of the dry season, so that morphological circumference change could be detected.

Mapping a dam perimeter using Google Earth involves several steps as follows:

1. Acquire imagery: In Google Earth, navigate to the location of the dam you want to map. Adjust the zoom level and tilt angle to obtain a clear view of the dam and its surroundings. Google Earth provides high-resolution satellite imagery, but keep in mind that the quality may vary depending on the location and date of the imagery.
2. Enable tools: Enable the necessary tools in Google Earth to assist with mapping. These tools include the measuring tool, polygon drawing tool, and elevation profile tool. You can find these tools in the menu bar or by right-clicking on the map.
3. Measure the dam perimeter: Use the measuring tool to trace the outline of the dam. Select the appropriate measurement unit (e.g. metres, feet) and follow the shape of the

dam's perimeter by placing points along the edges. Once you have completed the perimeter, the measuring tool will display the total length.

4. Mark key locations: Use placemarks or markers to identify key locations around the dam, such as spillways, intake structures, or monitoring stations. These markers can be added by right-clicking on the map and selecting "Add Placemark" or similar options.
5. Generate an elevation profile: Utilize the elevation profile tool to obtain a cross-sectional view of the dam and its surrounding terrain. This tool allows you to draw a line across the dam, and it will display the elevation changes along that line. This information can help assess the slope of the dam and identify any potential areas of concern.

The accuracy and level of detail of the mapping will depend on the resolution of the imagery available and the precision of measurements. It's also important to cross-reference findings with official sources. This process can however be automated, and the value reflects dam area values that can be correlated with the daily dam depth values recorded by the department of water affairs.

The Google Earth database does not present regular or daily imagery as this was not what Google Earth was designed for. The Sentinel Explorer that will be dealt with in the next section, does however provide daily imagery, at a much higher resolution.

The monitoring of dams and reservoirs is a crucial part of sustainable resource management as this information assists in the protection and preservation of a major contributor to environmental, economic, and social wellness (Gao *et al.*, 2012). The availability of regularly updated information on the level and capacity of water storage facilities is of utmost importance to the effective management of these systems. Unfortunately, for most regions around the world, this information is not readily available due to legal, financial, and political factors. Satellite remote sensing (RS) has been utilized in the calculation of water budgets and in the monitoring of watersheds. It can also be utilized to improve hydrogeologic surveys. Aside from providing useful information on the level of water storage facilities, this technology can also help in the understanding of the various factors that affect the water supply.

Topography is characteristic of the elevation or height of the land surface of an area, to adequately define the topology of an area elevation data is used to provide an image of the underlying landscape. Different forms of data can be used to determine this, for the completion of this step in the research; contour lines from the 1944 topographic map of the Gariep area map. The contour lines from this map were digitized to allow for analysis using GIS software. To start digitizing the contours, the downloaded raster imagery using 'Add Raster Layer' tool was achieved using the 1944 map. This Opens the image in the QGIS map space along with the newly created polyline shapefile. The Digitizing tools are available in the toolbar (right-clicking on the toolbar and check the 'Digitizing' is another option).

- The digitizing of raster data to create vector layers for analysis was carried out as follows:



Figure 6.38: Digitized extract of the extracted contour lines from raster data 3025DA-1994b

To open the attribute table for a vector layer, the layer was activated by clicking on it in the Layers Panel. Then, from the main Layer menu, choose Open Attribute Table. It is also possible to right-click on the layer and choose Open attribute table from the drop-down menu, or to click on the Open Attribute Table button in the Attributes toolbar.

This opens a new window that displays the feature attributes for the contour layer. The total number of features in the layer and the number of currently selected/filtered features are shown in the attribute table title. The elevation field has been created to display the label of each contour's data by manual visualization of contours from the raster data.

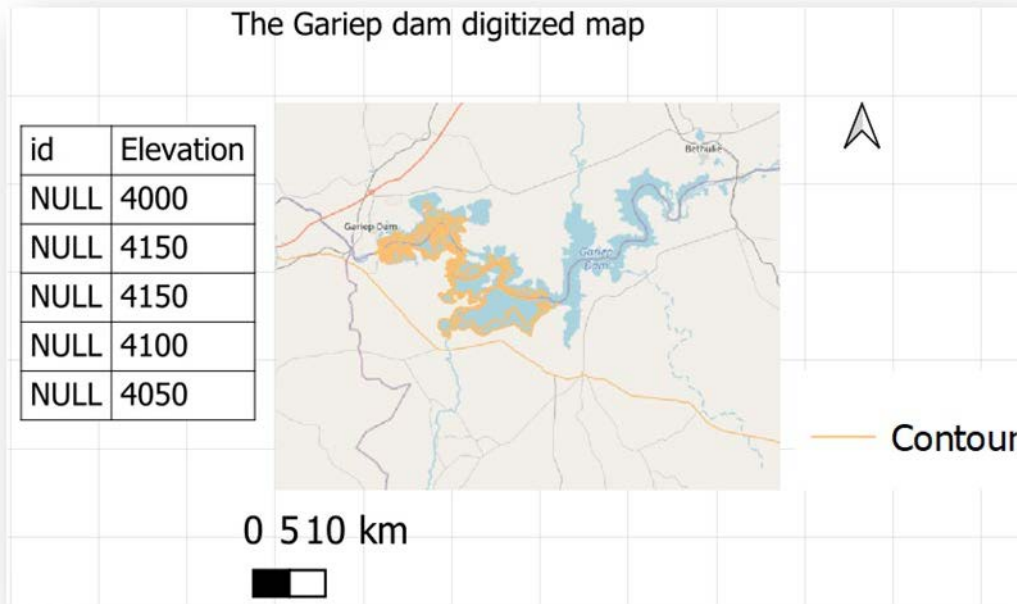


Figure 6.39: Map of digitized contours of the Gariep dam

The perimeter of the Gariep dam was measured and the surface area derived, using Google Earth Figure 6.40 demonstrates the use of Google Earth to derive a dam area and perimeter value.

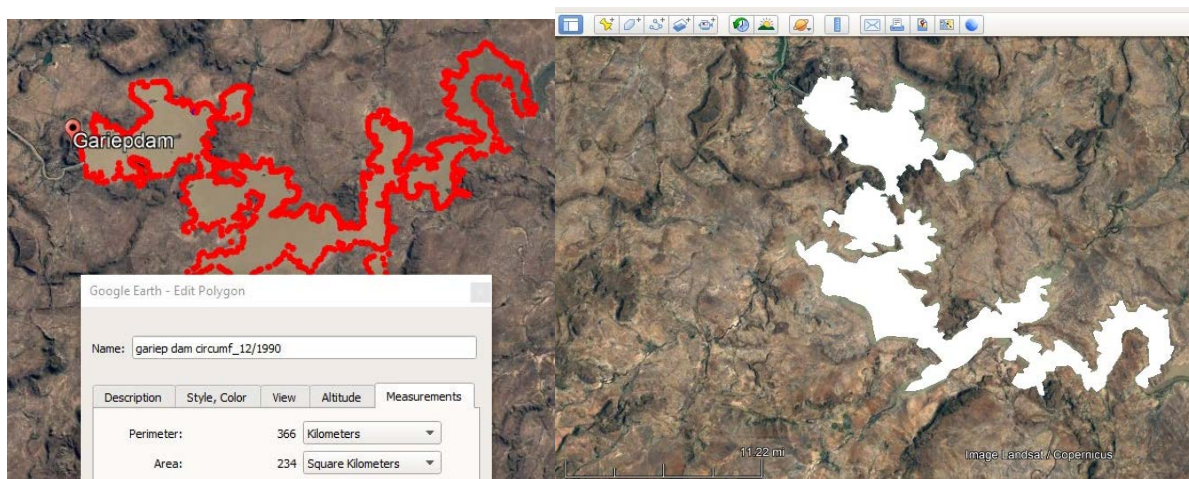


Figure 6.40: The digitized extent of the Gariep dam from the extent provided in Google Earth

6.15.5 Production of perimeter maps of the dam using satellite imagery for various stages of dam fullness

This part of the research aims to analyze the changes in the water surface area for various stages of dam fullness of the Gariep dam in South Africa in the Province of Free State using remote sensing techniques and GIS tools. In addition to this, the data will be interpreted to generate and display the digital perimeter maps of dam fullness. The data collected from satellite images taken from 1993, 1994 and 2022 were analyzed to determine the changes in the water surface area of the dam. Three LANDSAT 7 ETM+ images were used for the study.

Remote sensing is a major source of data and information and is widely used to detect changes and update existing maps. It provides a meaningful method for detecting land/water changes, for example measuring chlorophyll, watercolor and suspended sediments over large areas (Chen *et al.*, 2012; Duan *et al.*, 2012). Most researchers believe that land-use change is one of the most important factors in some of the hazards such as flood, soil erosion and sediment yield, ecological and environment dynamics, and soil property changes (Hauser *et al.*, 2012; Wijesekara *et al.*, 2012). Also change detection with RS data provides cheap and quick information about the status of the water reservoir in dams and the land use/land cover (Mustafa *et al.*, 2012; Verma A *et al.*, 2013). Moreover, GIS techniques are also used in processing multiple data that are of concern to a dam water storage assessment project. The combined use of RS with GIS has proven useful for the timely assessment of land use dynamics (Mustafa *et al.*, 2012; Wang *et al.*, 2010). Many studies have investigated land-use dynamics associated with dam construction and reservoir impoundment using RS and GIS techniques (Ouyang *et al.*, 2010; Zhao *et al.*, 2010). The purpose of this work is to determine whether the water surface area of the Gariep dam has noticeably decreased. To do this, the change of water level in the Duhok dam over time was investigated using an RS and GIS technique; temporal changes in the dam were determined by the evaluation of LANDSAT satellite images. Meteorological data for this area was examined and its relationship with water level changes was determined. To determine the temporal changes in the water surface area of the Gariep dam, three LANDSAT 7 ETM+ images acquired for 1993, 1994 and up to 2022 respectively, were used. LANDSAT satellites are the most common satellites used for the examination of natural phenomena. Although this satellite has a low spatial resolution, it has a higher spectral resolution than is obtained by other satellites.

The area determination is one of the methods to assess the goodness of the classification. Hence the deviation from area satellite to area field should be seen in relation to their size so that the deviation becomes comparable.



Figure 6.41: Gariep dam water levels in 1993

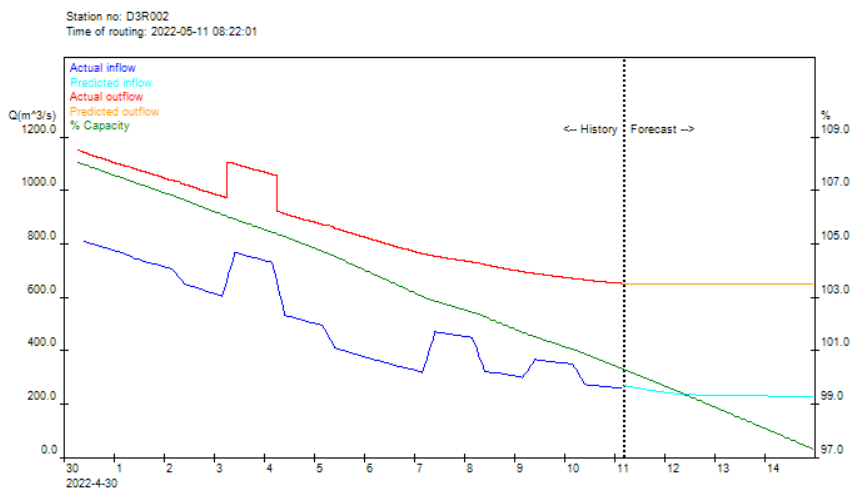


Figure 6.42: Gariep dam water levels in 1994



Figure 6.43: Image of the change in dam water levels in 2020

An increase of water level slightly more than was observed in the water surface area after 1993 period. In addition, over this time, climate conditions (rainfall, temperature, and evaporation) in the study area have been changed significantly. These changes could have affected the reservoir surface area, but so also could external human interference around the dam.



2022-05-11 07:00 Capacity: 100.2 %
 Inflow: 265 cumec Outflow: 650 cumec

Figure 6.44: Capacity comparisons of the Gariep dam (Adapted from DWA, 2022)

In this work, the changes in the water reserves in Gariep dam, which is important for ecology, tourism and historically, over the years period was investigated using RS and GIS techniques. LANDSAT images from 1993, 1994 and 2020 were assessed and the results were interpreted together with related meteorological data. The perimeter of the dam level can be digitized with the results from the time series. Continuous monitoring of such environmental regions is essential to take the necessary measures to protect water resource areas. In addition, this work showed that satellite data is useful for monitoring and estimating changes in the environment.

6.15.6 Correlation analysis between water body surface area and depth values

LANDSAT explorer was used to compare water body levels of the different years with the same date, together with the data collected by the department of water and sanitation which is illustrated in Figure 6.45. The LANDSAT extraction of the surface of the water body method is highly important for time-series analyses of extracting shorelines and water level using any number of LANDSAT image in different time intervals, and it provides an important contrast that can be used to determine water levels.

To get the different water level two satellite map was developed together with data form the department of water and sanitation, However the results show that there is a decrease in the water level in which is shown in Figure 6.46 if such decreasing tendency continues the dam will lose its maximum surface water area soon. The LANDSAT method is efficient in detecting surface water body level in Gariep dam.

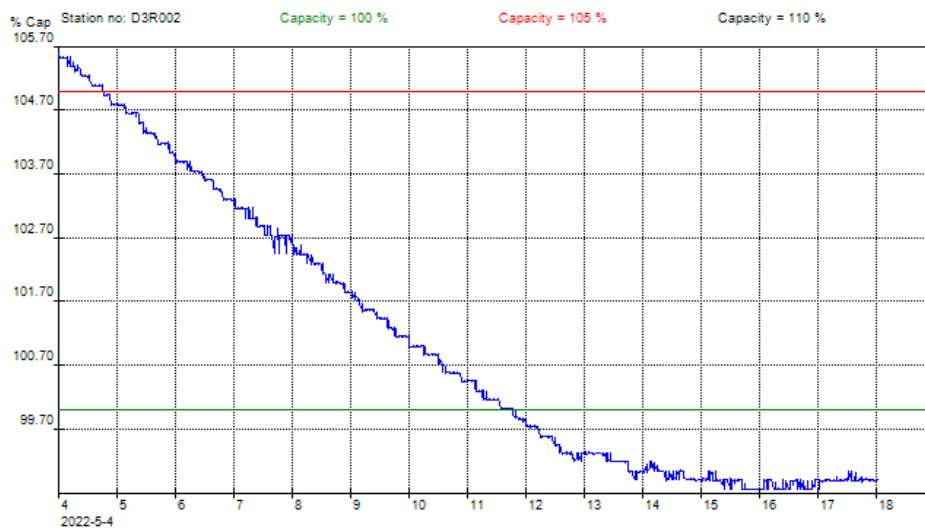


Figure 6.45: Capacity of Gariep dam (Adapted from DWA,2022)

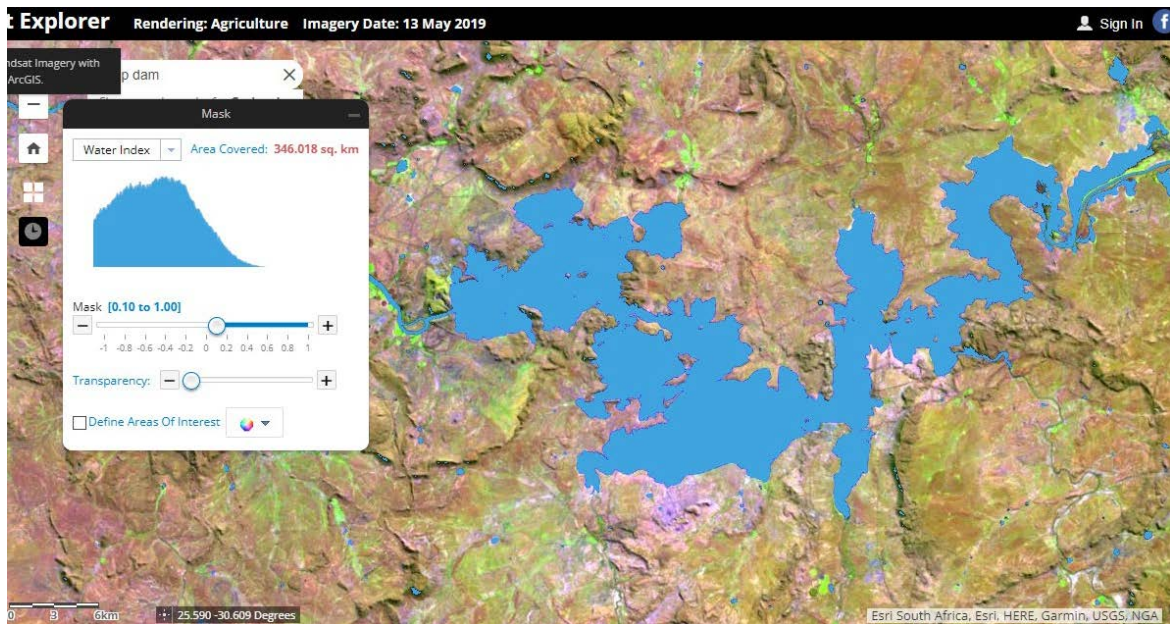


Figure 6.46: Dam water level changes in 2019

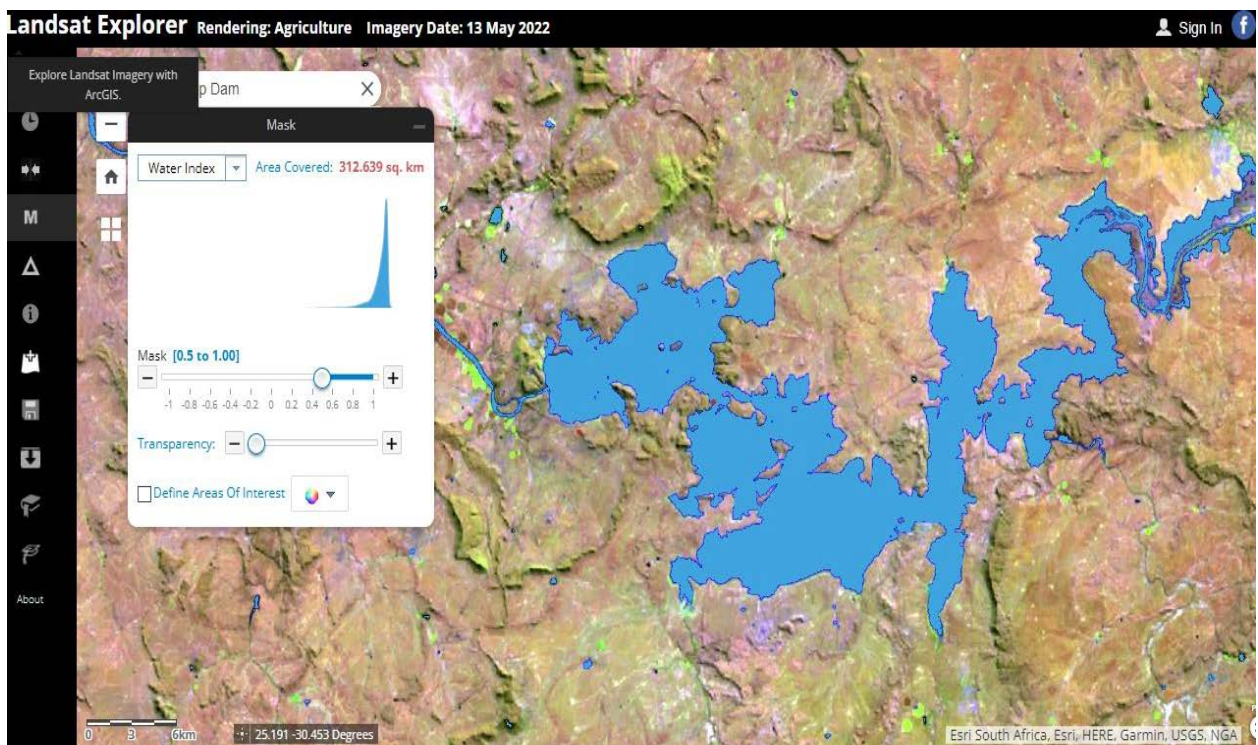


Figure 6.47: Dam water level changes in 2022

The results show that the Gariep dam level water body changed around 33,379 between 2019 to 2022.

6.15.7 Area best suited for continuous measurement whereby remote means can be focused

Remote sensing allows for the monitoring of the reservoir water level by estimating its surface extension. The surface extension can be estimated using different approaches. One is the use of unsupervised classification methods that are highly suitable to automate the process, another approach can be based on visual matching with contour lines with the aim of fully exploiting the remotely obtained datasets.

The monitoring of most reservoirs to date is done in real-time by international organizations using meteorological data; which limits the overall public and smaller organizational access (Yao *et al.*, 2019). This limitation acts as a hindrance to flow regulation planning and other management-related applications. In addition to this obstacle, there are limited amounts of gage observations in use however, remote sensing acts as a promising alternative (Berry *et al.*, 2005). Remote sensing has ensured that the automated monitoring of dam water levels is possible using surface extent. The observation of reservoir surface area is done by the (1) classification of optical satellite imagery, (2) surface elevation data from radar altimetry, and (3) ground bathymetry analysis (Berry *et al.*, 2005 & Kornienko, 2017). Remote sensing has allowed for various monitoring techniques to be used, especially space-based types, this remains an inadequate approach as there exist shortfalls in the temporal coverage of deeper water levels (Busker *et al.*, 2019).

There exists several approaches which can be used to estimate the surface extent of a water body; such as optical imagery (LANDSAT 5 TM, LANDSAT 7 ETM+ SLC-Off, LANDSAT 8 OLI-TIRS, and ASTER) and Synthetic Aperture Radar (SAR) imagery (Getirana *et al.*, 2018). The use of LANDSAT and Shuttle Radar Topography (SRTM) has made it possible to identify relationships that assist in determining water levels and reservoir fluctuations (Gao *et al.*, 2012). The collected images are characterized by different acquisition modes, geometric and spectral resolutions, allowing the evaluation of alternative and/or complementary techniques. For each kind of image, two techniques can be used. Namely, the first being based on an unsupervised classification and suitable to automate the process, the second being based on visual matching with contour lines with the aim of fully exploiting the dataset (Pipitone *et al.*, 2018). The main advantage of using as remote sensing-based techniques is that the satellites are permanently stationed and positioned relatively far from the dam, which allows the exclusion of any interaction with site deformations or any weather changes (Pipitone *et al.*, 2018).

Some sensors have high spatial resolutions, making them better suited for estimating capacities. These sensors present their own limitations such as weather specifications and repetition time disparities (Getirana *et al.*, 2018). However, there are sensors that have high temporal revisit times but present with a low spatial resolution (Getirana *et al.*, 2018). The derived information from the joint use of different remote sensing sensors, the resultant DEMs, and an

understanding of the structural and topography of the reservoir area makes it possible to determine the storage capacity of reservoirs (Gao *et al.*, 2012).

6.15.8 Automated procedure for the recording of dam water body surface area using satellite imagery; how this can replace the level recordings done by the DWA

ArcView 3.2 GIS package with Spatial Analyst, plus Surface Areas and Ratios from elevation Grid extension were used to automate surface area calculations and to provide surface area statistics of the Gariep dam (Essien *et al.*, 2019). The procedure used to estimate surface areas from satellite images follows acquisition of images (LANDSAT 5, bands 5, 4 and 2). Using Red-Green-Blue1 channel, water bodies can be depicted in colours ranging from blue to almost black.

Remote sensing and GIS techniques provide the perfect platform for a full package monitoring system. An improved understanding of how the changes in dam water levels are being related to changes in the surrounding climatic and anthropogenic factors must constantly be analysed. A previous study has shown that data for the location and area of the small dams were obtained from a dams GIS coverage produced by the Chief Directorate of Surveys and Land Information (1999).

According to the DWS, optical satellite imagery was used to map the dam surface area, a digital elevation model (DEM) was used to model underwater terrain, and in-situ data was used for validation purposes. The optical satellite Sentinel-2 is a multispectral instrument (MSI) that provides images with fine spatial resolutions of 10-, 20- and 60 m (Du *et al.*, 2016). The satellite images were carefully selected based on the available water data provided by the DWS, to ensure that the values obtained from the proposed model were comparable to the in-situ data (Duan Z and Bastiaanssen WGM (2013).

There are several procedures used to record dam water body surface area including the threshold method. Which is one of the procedures of the most widely used algorithm for the extraction of water bodies from satellite imagery. The thresholding method is considered popular for delineating water bodies because it is easy to use and less computationally time-consuming than alternative procedures (Ryu *et al.*, 2002). But this method cannot be automated, and cannot be applied to large regions. Occasionally it is complicated due to the nature of the data used. Therefore ArcView 3.2 GIS package with Spatial Analyst, plus Surface Areas and Ratios from elevation Grid extension is the enhanced automated procedures for recording the Gariep dam water body surface area from satellite imagery.

6.15.9 Novelty of research

- Investigation into current and past management of the Gariep dam
- An automated procedure for recording dam water body surface area using satellite imagery.

- Effective replacement of level recordings done by DWA
- Using Google Earth to determine dam surface areas has both pros and cons. Here are some key points to consider:

Pros:

1. Accessible and user-friendly: Google Earth is widely accessible and easy to use, making it convenient for individuals to explore and analyse satellite imagery of dams. It provides a visually intuitive interface that allows users to navigate, zoom in, and examine areas of interest easily.
2. High-resolution imagery: Google Earth offers high-resolution satellite imagery for many locations worldwide. This can provide valuable visual information about the dam, including its surface area. The clarity and quality of the imagery can help in obtaining a general estimation of the surface area. We also looked at smaller dams, and the resolution was an issue in this regard.
3. Free and readily available: Google Earth is a free application that can be accessed by anyone with an internet connection. This accessibility makes it a popular choice for individuals and organizations looking to gain insights into dam surface areas without requiring specialized software or subscriptions. We also found that the process could be automated using Google Earth from within QGIS.

Cons:

1. Limited accuracy and precision: While Google Earth provides high-resolution imagery, the accuracy and precision of measurements, including surface areas, may be limited. The resolution of the imagery may not be sufficient to accurately determine precise measurements, especially for smaller or more complex dam structures.
2. Lack of measurement tools: Google Earth does offer measuring tools, but they are more suitable for estimating distances rather than calculating precise surface areas. These tools may not account for irregular shapes or complex topography accurately, potentially leading to inaccuracies in surface area calculations. This also relates to the image resolution, which lowers the accuracy especially with smaller dams.
3. Image date and quality variation: The availability and quality of imagery on Google Earth can vary depending on the location and the date the images were captured. Outdated or low-quality imagery can affect the accuracy of surface area calculations, particularly if there have been changes to the dam since the last captured image.
4. Inability to account for elevation changes: Google Earth primarily provides two-dimensional imagery, which means it may not accurately account for changes in elevation. This is however not an issue for our quest as we aimed to correlate dam surface area at specific times with measured dam depth.

In conclusion, while Google Earth can provide a useful starting point for estimating dam surface areas, it has limitations. Since we want to persist on using remotely sensed information for dam measurements, the other products like Sentinel Explorer will also be

investigated. The most important aspect of exploring this technology, is that this could add value to dam information never acquired in the past, like farm dams, municipal dams and dams linked to the many irrigation infrastructure developments in SADC.

6.16 Mapping of the topography before the dam was built

6.16.1 Methodology

Mapped contour lines are a fundamental tool for generating accurate elevation models. Contour lines are lines that connect points of equal elevation on a map, forming a series of concentric curves. By interpreting these contour lines, it is possible to construct a three-dimensional representation of the terrain's relief and generate an elevation model. The contour lines provide valuable information about the shape and steepness of the land, allowing for the identification of ridges, valleys, and other prominent features. With the help of specialized software and precise contour data, elevation models can be created by interpolating the elevations between contour lines. These models serve numerous purposes, such as terrain analysis, hydrological modelling, urban planning, and environmental management. By utilizing mapped contour lines to generate elevation models, researchers, engineers, and planners can gain a comprehensive understanding of the landscape, aiding in decision-making processes and facilitating the design and implementation of various projects.

Two sets of storage-elevation curves were created based on the digital elevation models (DEMs) of the Gariiep dam. The first set pertains to the topography of the area in 1971, prior to the construction of the dam. The second set corresponds to the more recent bathymetric survey conducted in 2022.

6.16.2 Results and discussion

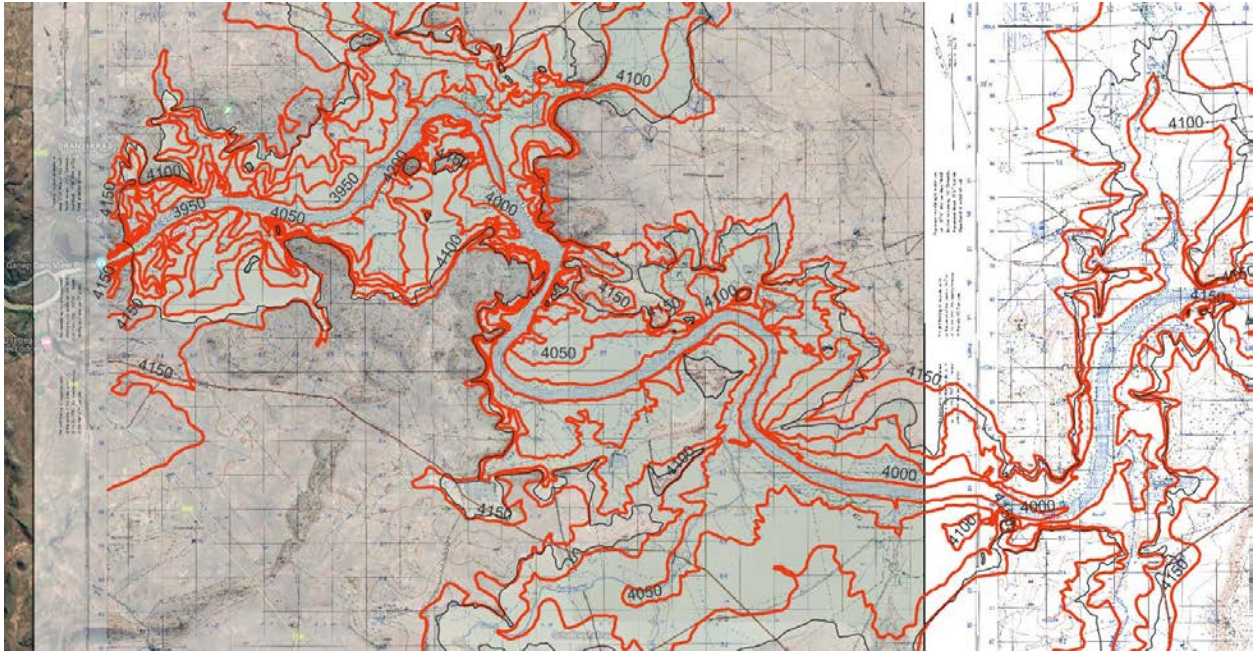


Figure 6.48: The georeferenced 1:50k maps draped over Google Earth in QGis with the digitized contours in red

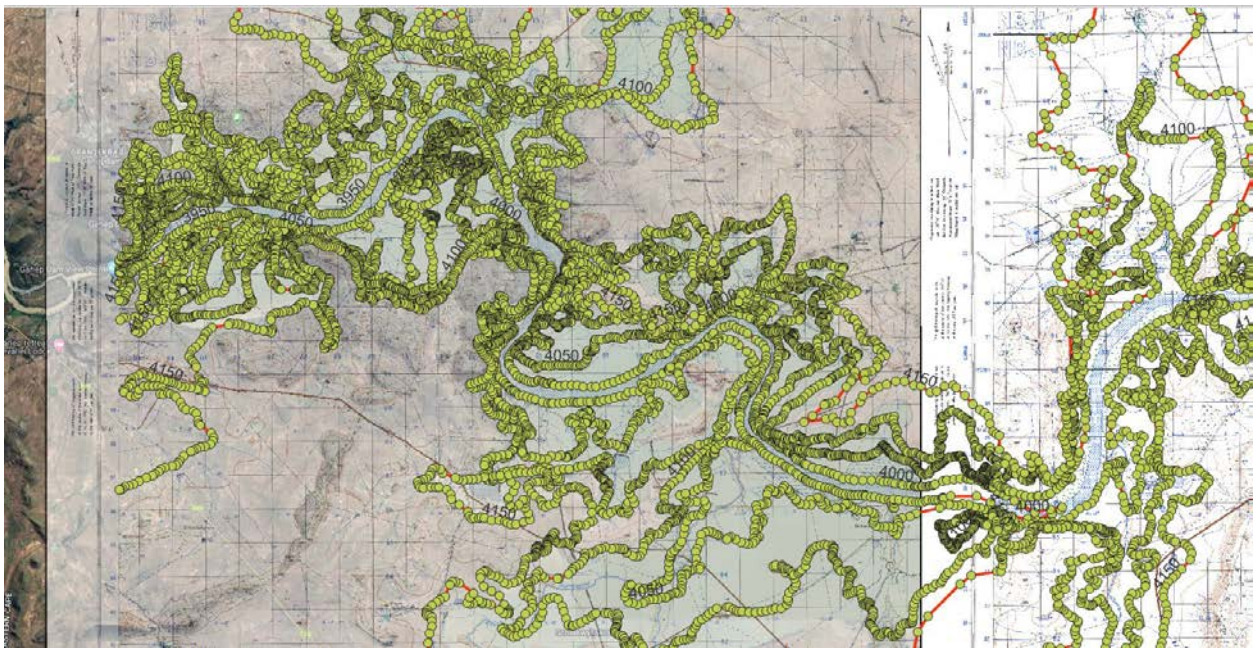


Figure 6.49: The georeferenced 1:50k maps draped over Google Earth in QGis with the digitized contours converted to points

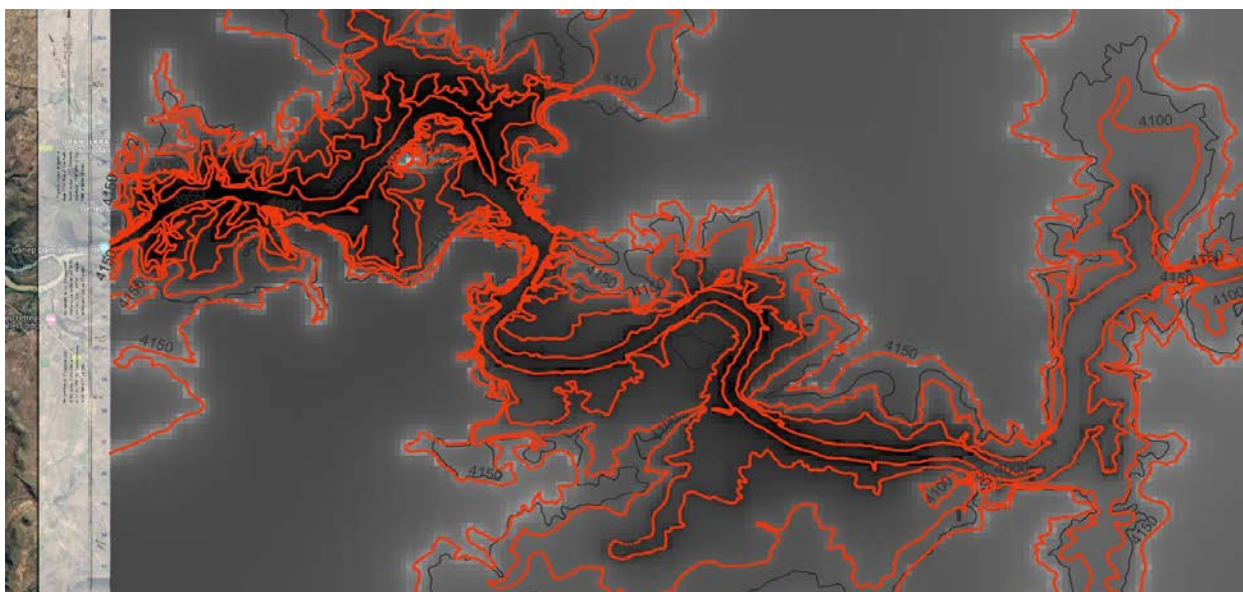


Figure 6.50: The new depth elevation model for the Gariep dam, generated from the old contour maps

6.17 Setting up a database relating dam depth and dam perimeter change

6.17.1 Introduction and methodology

The operating rules of the Gariep dam rely on hydropower generation and are designed to ensure that downstream hydropower generation requirements are met to some extent, as reported by ORASECOM (2013). These rules are determined using storage curves based on hydro-morphometric parameters such as depth and changes in perimeter, i.e. water level changes. As a result, standard values have been established to facilitate the maintenance of flow releases that align with downstream requirements. The table presented below outlines the expected area-capacity operating rules for the dam. Table 6.4: The Standard Area-Capacity relationship based on operating rules of the Gariep dam

Table 6.4: Area-capacity relationship of Gariep dam

Elevation (m)	Perimeter (km ²)	~ Storage (million m ³)
1231.6	65.69	638.09
1237.9	102.73	1163.24
1241.9	128.96	1628.18
1245.2	156.99	2092.89
1250.3	210.98	3022.55
1252.4	238.27	3488.91
1255.8	298.91	4419.49
1258.7	352.16	5348.12
1263.7	446.82	7342.93

Values from ORASECOM Report 001/2013

A well-designed database can give you access to precise and current information. To set up a database, you need to identify its purpose, which will help you gather and organize the relevant information into tables or a selected display method. This study focuses on the correlation between dam depth and perimeter change to closely monitor water level fluctuations. Hydro-morphometric parameters such as depth and perimeter change are closely linked as they provide essential characteristics needed for analysing any volume changes within a waterbody. As a standard elevation is available, it will be used as the averaged base points when analysing the relationship between the two variables. The table below shows the perimeter change of the Gariep dam, captured from the remotely sensed online LANDSAT Explorer, from March 1975 to June 2022.

Table 6.5: Table of the perimeter change of the Gariep dam from March 1975-June 2022

Perimeter (water index area in km ²)			
Date	Value in km ²	Date	Value in km ²
March 27, 1975	369.745	June 21, 2016	185,182
April 30, 1991	308.331	Jan 31, 2017	184,372
June 4, 2001	325.562	Oct 14, 2017	206,091
April 15, 2006	334.292	Feb 3, 2018	185,129
April 7, 2009	323.725	Aug 14, 2018	290,032
April 26, 2013	309.727	Feb 22, 2019	204,599
May 12, 2013	311.960	Nov 21, 2019	226,799
Nov 4, 2013	232.457	May 31, 2020	310,407
Dec 6, 2013	219.947	June 19, 2021	295,353
Mar 28, 2014	324,184	Jan 29, 2022	324,322
Sep 4, 2014	264,284	Mar 26, 2022	330, 400
June 19, 2015	260,721	May 5, 2022	326,031
Jan 29, 2016	184,259	June 6, 2022	310, 463

Data collected from remotely sensed online LANDSAT Explorer (<https://livingatlas2.arcgis.com/LANDSATexplorer/>)

6.17.2 Results

Figure 6.51 below is a graph of the results of the standard area-capacity relationship based on the operating rules of the Gariep dam. In the Graph, it is observable that there is a direct positive relationship; a rise in the perimeter also results in the rise in the elevation of the dam's water level.

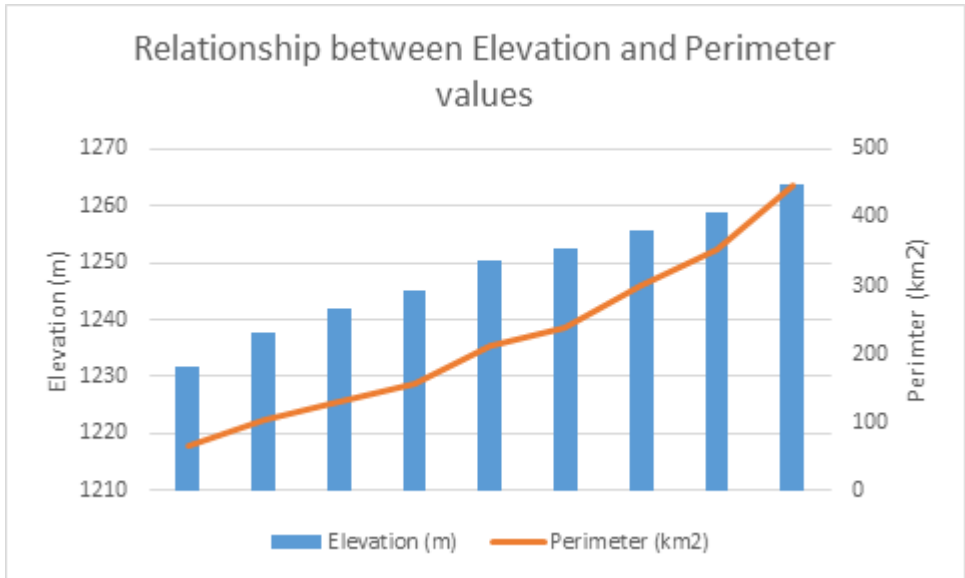


Figure 6.51: Bar graph and line graph showing the relationship between elevation and perimeter values

Below is a graphic representation of the observed perimeter values of the Gariep dam from the March 1975 to June 2022. The line graph (Figure 6.52) shows the changes in the perimeter of the dam; firstly, we can note the highest value being that of 1975 with a perimeter of ~370 km² and the lowest values being between 2016 and 2018 where the perimeter was as low as 184 km² which is Almost half of what it was in 1975. These stark changes can be attributed to the change in climate, during the years of 2015-Feb 2018 South Africa experienced drought conditions which affected overall water levels in all natural water bodies. The dam saw a rise in water levels from Aug 2018 but a drop again in 2019 followed by a steady increase leading to 2022, of which in the dam has experienced >94% FSC with values of 330 km².

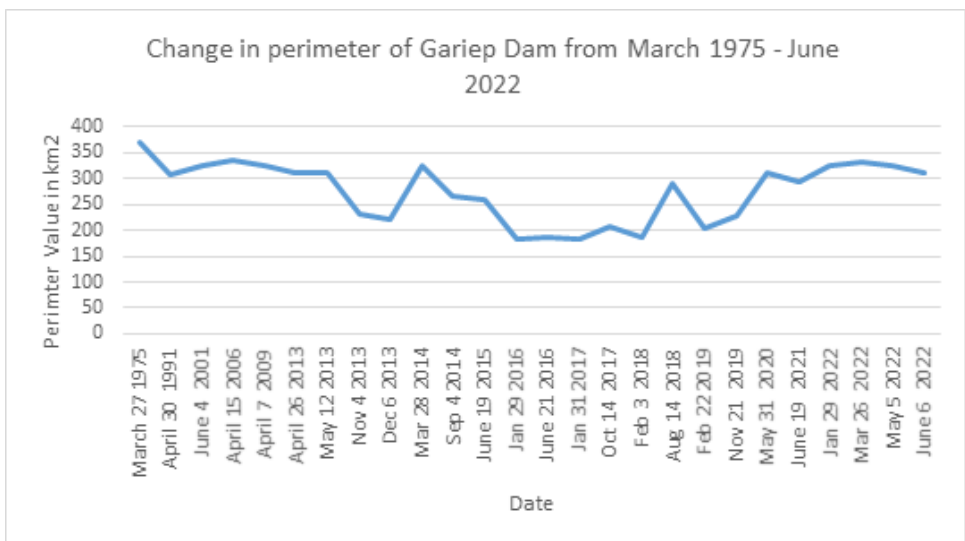


Figure 6.52: Line graph showing the change in perimeter of the Gariep dam from March 1975 to June 2022

6.18 Dam volume calculations, using GIS and the old dam floor information

6.18.1 Introduction and methodology

Using GIS and statistical methods can be a valuable tool for designing dams with a specific water volume in mind and estimating the surface area of reservoirs and dams. The Gariiep dam was designed in a suitable location on the Orange River with an 88-metre height to store a specific volume of water, and GIS has been confirmed as a robust tool for water policy makers and managers to prepare a practical approach. Reservoir volume and area can be analysed for various dam situations in a simpler way compared to traditional survey methods to find the most suitable situation for dam establishment. Digital Elevation Models (DEM) provides critical information to estimate dam volume, and a suitable computation of storage capacity may require a high-resolution DEM (5 metres or finer). To calculate stored water volume, topographic information of the dam floor and water depth is crucial, and spatial data analysis in GIS can be used to compute it. After designating the dam dimensions, such as location, height, freeboard, and designed water level H , a raster map comprising one pixel in the study area is created and used for iteration as the starting point. The storage capacity can be found by computing the storage depths by subtracting the elevation of the DEM from the designed water level H , summing up the storage depths based on the grid cell, and multiplying them by the area of the unit cell. The surface area of the dam multiplied by the depth of the dam is equivalent to the volume of the dam. QGIS software can be used for calculating the dam volume, and this study shows that various elements of dam volume assessment can be done remotely. Use the DWS survey information to reflect on volume lost through siltation.

Hydrographic surveys are essential in determining a reservoir's capacity, including large and small dams, agricultural dams, weirs, and river segments. These surveys are critical for managing available water storage, future planning, and identifying where sedimentation is occurring in the dam. To obtain bathymetric data, the Department of Water and Sanitation (DWS) runs cross sections at regular intervals along the length of the reservoir, between two fixed beacons. The survey boat used for echo sounding slowly moves along parallel lines perpendicular to the water currents while the depth finder readings are recorded. The depth finder is operated according to the manufacturer's instructions and adjusted for the estimated water depth and sensitivity to measure relative densities of the bottom.

The data collected is processed using Hypack software, and the sediment software, which runs on end areas principals, is used to calculate the dam's capacity. To determine the sedimentation, cross sections are performed at specific time intervals and the amount of sediment in the reservoir is measured by comparing the current capacity to the previous survey. Since the cross sections are run between fixed survey beacons, information such as sediment build-up and concentration are immediately available. A recent survey by this research group confirms that the Gariiep dam has lost a significant storage capacity since its construction in 1970 due to sedimentation.

6.18.2 Results

After choosing of the dam situation, reservoir volume and area was calculated for various dam crest heights at the location of the dam to specify the suitable height of the dam. Eventually, depth of water in reservoir was extracted by subtracting the height of every pixel of DEM from the designed water level H and these depths were multiplied by pixel area to obtain volume of water in each pixel. Water volume was calculated from cumulative of the pixels, which filled water. This procedure was repeated several times for different dam heights to obtain the optimum dam height.

Table 6.6: A table showing area capacity relationship of the Gariep dam

Elevation (m)	Storage (million m ³)	Surface area (km ²)
1,263.7	7,342.96	446.82
1,258.7	5,348.12	352.16
1,255.8	4,419.49	298.91
1,252.4	3,488.91	238.27
1,250.3	3,022.55	210.98
1,245.2	2,092.89	156.99
1,241.9	1,628.18	128.96
1,237.9	1,163.24	102.73
1,231.6	638.09	65.69
1,202.9	0.00	0.00

The relationships between these parameters can be summarized as follows:

Related to the Dam Surface Area and Dam Volume, as the water level in the reservoir rises, the dam surface area increases, leading to an expansion of the water body. Consequently, the dam's volume also increases, as more water is stored. Conversely, when the water level decreases, the surface area shrinks, and the dam volume decreases accordingly. Figure 6.8 indicates this relationship for the Gariep measured information. Furthermore, the dam's stage level directly influences both the surface area and the volume. A higher stage level corresponds to a larger surface area and a greater volume, indicating a higher water level in the reservoir. Conversely, a lower stage level results in a smaller surface area and reduced volume, indicating a lower water level. This is indicated by both Figures 6.8 and 6.10.

The storage in the dam and surface area seems to be directly correlated and the result is given in Figure 6.11. It is however important to note that the relationships described above assume a well-designed and properly functioning dam system.

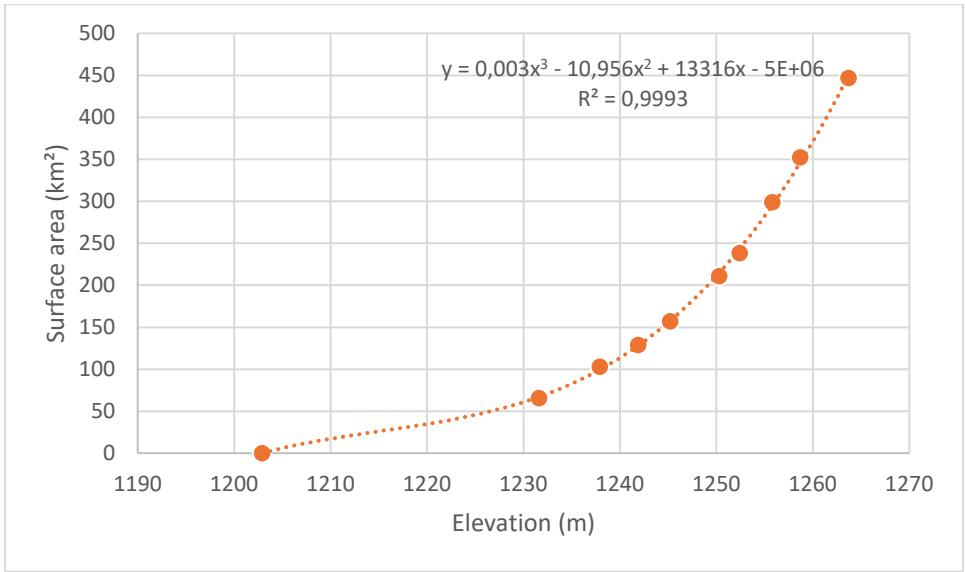


Figure 6.53: Field elevation (m) and surface area (km²) appear highly correlated

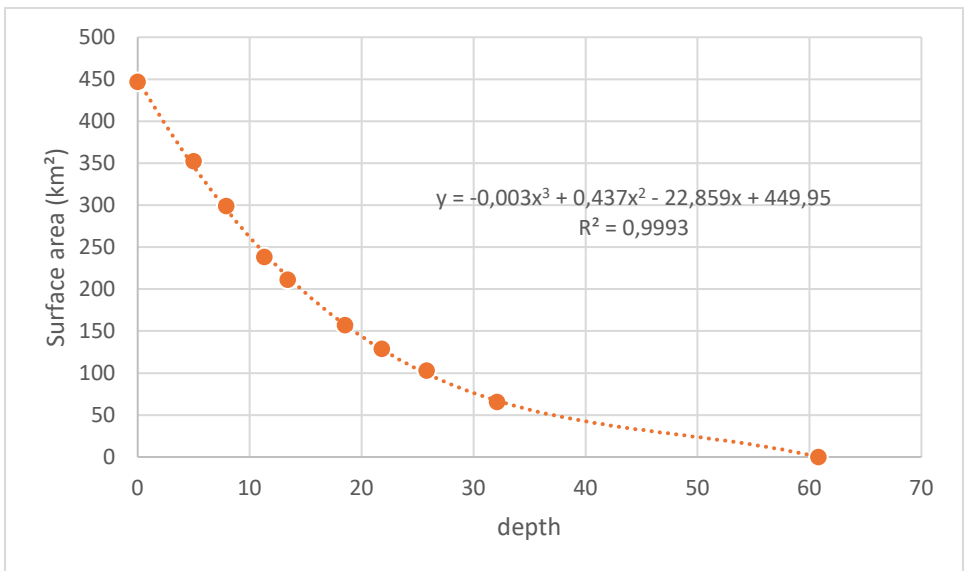


Figure 6.54: Field depth and surface area (km²) appear highly correlated

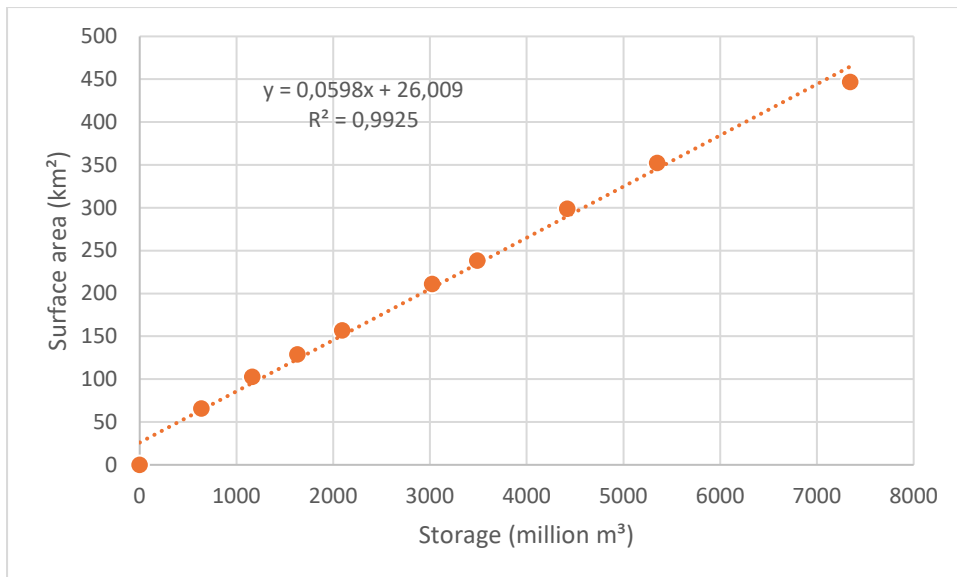


Figure 6.55: Field storage (million m³) and surface area (km²) appear highly correlated

Factors such as dam design, capacity, and environmental conditions can also impact these relationships. Additionally, sedimentation and reservoir management practices may introduce complexities in the relationships over time. Understanding these relationships is crucial for effective water resource management, flood control, and planning of water supply. Engineers and authorities responsible for dam operations closely monitor the dam stage level, surface area, and volume to ensure the safety, stability, and optimal utilization of water resources.

6.19 A reflection on sedimentation in the Gariep based on evidence found in upstream dams

6.19.1 Introduction

Reservoirs are built across rivers for purposes of irrigation, water supply, power generation, discharge regulation and flood control. A reservoir will generally be located towards the end of a large watershed and receives inflows from major rivers (Jørgensen *et al.*, 2005). On the other hand, reservoirs have a shorter residence time but a much larger watershed which can be more difficult to control (Randolph, 2004). Rainfall, runoff, snowmelt, and river channel erosion provide a continuous supply of sediment that is hydraulically transported and deposited in rivers and streams.

Reservoir sedimentation has become a worldwide problem, with the annual loss in storage capacity due to sedimentation estimated at 1% of the original storage capacity, or 50 km³ (Batuca & Jordaan, 2000). The major advantages of dams are in flood control and in transferring water to areas with deficit of water (Wang *et al.*, 2003; Mukherjee *et al.*, 2007; Goel *et al.*, 2002). There are many reservoirs that can no longer perform their design functions because much of their original active storage volume has been filled by sediment (Ijam and Al-Mahamid, 2012). The transported silt eventually gets deposited at different levels of a reservoir and reduces its storage capacity (Goel *et al.*, 2002; Jain *et al.*, 2002; Sreenivasulu and Udayabaskar, 2010).

When the river flow enters a reservoir, due to the very low velocity in reservoirs, they tend to be very efficient sediment traps. Hence transport capacity is reduced, and the sediment load is deposited in the reservoir and this deposition gradually reduces the active capacity of the reservoir and fails to provide the outputs of water with passage of time. Even though soil erosion can be caused by geomorphologic processes, accelerated soil erosion is principally favoured by human activities. Therefore, rapid population growth, deforestation, un-suitable land cultivation, uncontrolled and overgrazing have resulted in accelerated soil erosion in the world principally in developing countries like Ethiopia (Adebe and Sewnet, 2014; Tamene *et al.*, 2006).

The amount of sedimentation all through the life of the project needs to be estimated, so that suitable conservation measures can be taken. Periodical capacity surveys of the reservoir help in assessing the rate of sedimentation and reduction in storage capacity (Jeyakanthan and Sanjeevi, 2013).

A Geographical Information System (GIS) can be used to model bathymetry and the spatial distribution of sediments (Evans *et al.*, 2002). Previously, several attempts have been made to calculate the quantity of sediment using remote sensing technology (Yeo *et al.*, 2014; Narasayya *et al.*, 2013; Sri Sumantyo *et al.*, 2012). Using the Remote Sensing techniques, it

has become very efficient and convenient to quantify the sedimentation in a reservoir and to assess its distribution and deposition pattern (Narasayya *et al.*, 2013).

Remote sensing technology offers data acquisition over a long period of time and broad spectral range, can provide synoptic, repetitive, and timely information regarding the sedimentation characteristics in a reservoir. Water spread area of the reservoir for a particular elevation can be obtained very accurately from the satellite data. Reduction if any, in the water spread area for a particular elevation indicates deposition of sediment at that level. When it is integrated over a range of elevations using multi-date satellite data enables computing volume of storage lost due to sedimentation (Ninija, 2016).

Figure 6.56 shows the sedimentation of reservoirs in South Africa. In South African reservoirs, the average sedimentation rate per year was found to be 0,5%, equivalent to the loss of 150 million m³ of storage capacity each year (Jordan, 1989).

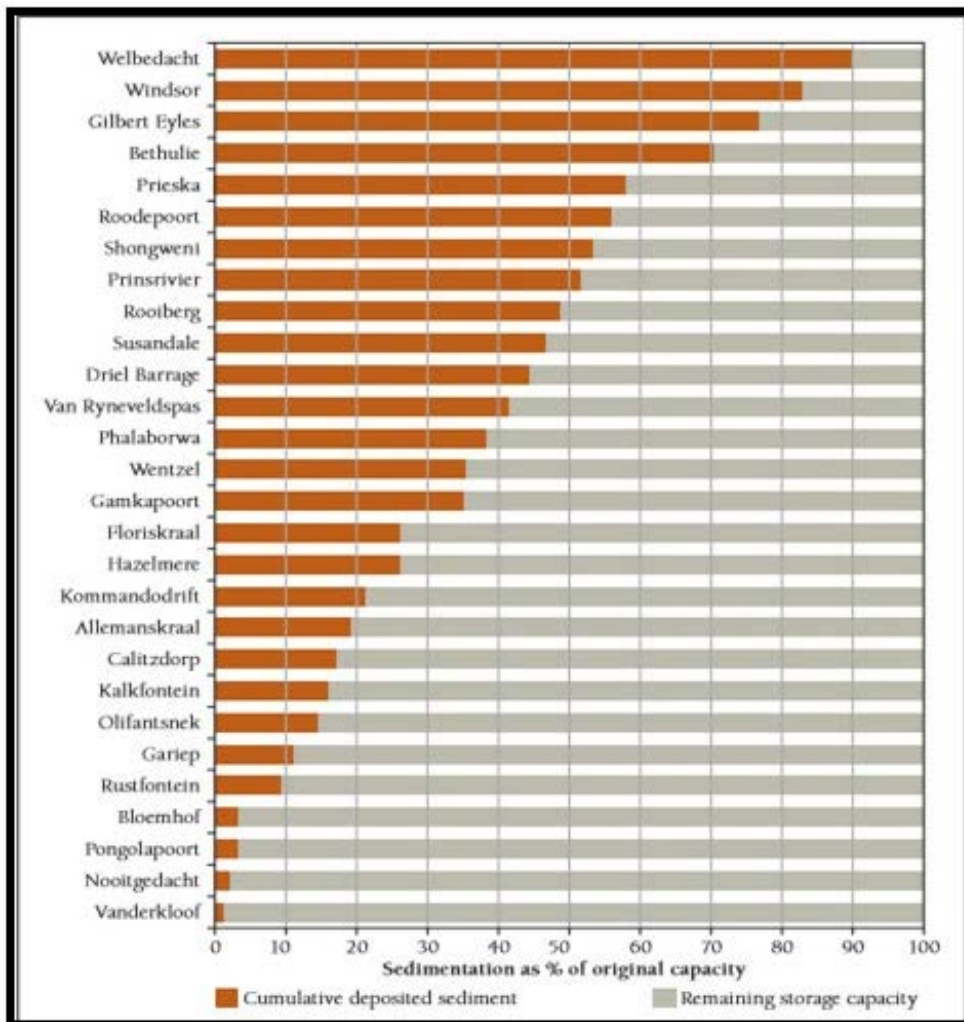


Figure 6.56: Sedimentation of reservoirs in South Africa (de Villiers, 2006)

The sedimentation rate was calculated as 0,34%, based on data from studies which were conducted recently. Worldwide there are several cases where extreme sedimentation has

reduced a reservoir's lifespan to only a few years. A well-known example of where these problems have occurred in South Africa is Welbedacht Reservoir on the Caledon River in the Free State Province (Beck and Basson, 2002).

This dam was constructed in 1973 with the purpose of supplying water to the city of Bloemfontein. By 1988, it was found that the dam had already lost 73,2% of the original storage capacity at an average annual sedimentation rate of 4,5% (Clark, 1990). By 2002 the Welbedacht Reservoir had lost 89,9% of its original storage capacity (DWAF, 2006).

6.19.2 Methodology

Remote sensing may provide a valuable tool for this study. Over the last several decades, advances in satellite remote sensing technology and data availability have provided an improved means to monitor surficial inland water properties by overcoming issues related to spatial coverage. Since the 1970s, satellite remote sensing has been used to monitor suspended sediment based on spectral reflectance data (Ritchie, 1976).

The fundamental theory is that portions of the electromagnetic spectrum, in the visible region (mainly red and near-infrared), are directly correlated to sediment concentrations (Feng, 2010; Petus, 2010). Higher levels of suspended sediment increase spectral reflectance in this region due to the associated backscattering effect caused by the elevated suspended sediment in the water column (Ritchie, 2003).

The LANDSAT 8 was chosen for this study due to the free availability of data ranging from 1982 to present and the relatively fine spatial resolution of 30 m conducive to mapping large rivers. Therefore, several data obtained from LANDSAT sensors were thoroughly interpreted to fully understand the relationship between suspended sediment, spectral reflectance, and silt movement. The LANDSAT sensors provide fine temporal resolutions with respective 16-day revisit cycles. Therefore, by utilizing LANDSAT 8 sensors, a wider temporal period can be analysed and allows for a more continuous monitoring of river systems.

The satellite imagery from the LANDSAT 8 sensor shows different colours which needs to be defined to ensure that quality interpretation of satellite imagery is conducted correctly. The colours in an image will depend on what kind of light the satellite instrument measured. True colour images use visible light red, green and blue wavelengths so the colours. However, false colour images include infrared light and may take on unexpected colours whereas water absorbs light, so it is usually black or dark blue. Sediment reflects light and colours the water. When suspended sand or mud is dense, the water looks brown. As the sediment disperses, the water's colour changes to green and then blue. Shallow waters with sandy bottoms can lead to a similar effect. In a true colour image, common features appear as shown in figure 1.2 below.



Figure 6.57: Sediment colours near the mouth of the Zambezi River as it empties into the sea

NB: The water grows darker offshore as the sediment disperses. (NASA Earth Observatory images by Robert Simmon, using LANDSAT 8 data from the USGS Earth Explorer.)

6.19.3 Results

a) Gariep dam

The Gariep dam was chosen as the main study area. The Gariep dam is situated in South Africa near the town of Novalspont in the Northern Cape Province. The wall of the Gariep dam is 88 m high and 900 m long and it is one of the largest dams in South Africa. The dam is currently utilized for several various purposes including domestic, irrigation and industrial use as well as power generation

The landscape is generally flat plains that are interrupted by low hills and river valleys. The terrain between the Orange and Caledon rivers comprises rocky ridges and ravines interspersed with areas of open plains.

The river is estimated to deliver 60 million tons of sediment each year. A high quantity of this sediment originated from soil erosion. However, the tributaries are also playing a major role in transporting sediments into the Gariep dam, and these tributaries are underlain of various geological settings.

The data that was collected from previous studies shows that the capacity of the Gariep dam has decreased over time with an increase in sediment in the dam. The Gariep dam sediment survey data is shown in Table 6.7.

Table 6.7: Sediment survey data (DWA, 2006)

Survey date	Capacity (Million m ³)	% Sediment
1971	5897.285	0.00
1979	5521.172	6.24
1991	5362.488	9.07
2005	5198.194	11.85
2018	4904.527	16.83

The average rate of sedimentation in Gariep dam per year is 0.36%. The Gariep dam has a high quantity of sediments as it receives water from various tributaries in the study area. Therefore, it was observed that extreme sedimentation has reduced the storage capacity of the reservoir over the years.

The rain records were acquired from the DWA. It was found that the rain has been increasing over the years in the Gariep dam region. The data shows that an increase in rain has an influence on silt movement and sediment loading which is supported by the sediment survey data in Table 6.7.

Table 6.8: Rain survey data (DWA, 2012)

Date	Rain (units)
2003/2004	97643
2009/2010	203060
2011/2012	1026554

b) Vanderkloof dam

Vanderkloof Dam is situated in the Free State on the Orange River (130 km downstream of Gariep dam) in quaternary catchment D31e in South Africa. The dam lies between Latitude 29° 59' 28" S Longitude 24° 43' 54" E. The dam's releases are primarily used for irrigation and hydropower generation but also supply the urban requirements of Ritchie, Jacobsdal and Koffiefontein.

The Vanderkloof Dam inflow is highly regulated due to the upstream Gariep dam, which is more dependent upon natural flows as it is far less regulated upstream. The inflow pattern for Vanderkloof is usually high in winter and low in summer. The sediment data that was acquired

proves that the storage capacity of the dam has been drastically decreasing over the years because of an increase in sedimentation.

Table 6.9: Sediment survey data (DWA, 2006)

Survey date	Capacity (Million m ³)	% Sediment
1976	3126.200	0.0
1991	3116.607	0.31
2006	3107.243	0.61

The average rate of sedimentation in Vanderkloof dam per year is 0.02%. Table 6.9: shows an upward trend regarding the quantity of rain over the years in the Vanderkloof dam. The dam has been receiving a large quantity of rain and thus may have an influence on sedimentation through soil erosion, runoff, and soil erodibility. Thereafter, it was observed that the storage capacity has been reduced due to an increase in deposited sediment over time.

Table 6.10: Showing the rain survey data (DWA, 2012)

Date	Rain
1994/1995	18718
2000/2001	42065
2009/2010	54531

c) Welbedacht dam

Welbedacht Dam, which was constructed on the Caledon River, is located in a high sediment yield region. During the first three years of operation the reservoir had lost 36 million m³ of its original 114 million m³ storage capacity due to sedimentation (De Villiers, 2007).

Figure 6.58 shows the losses in storage capacity over the years. As a result of this extreme case of sedimentation, the existing Jim Fouché Bridge experiences regular flooding. This is because the height of the bridge openings has been reduced from 13 m to only 1 m since the dam was built. The bridge is located 42,5 km upstream of the dam (De Villiers).

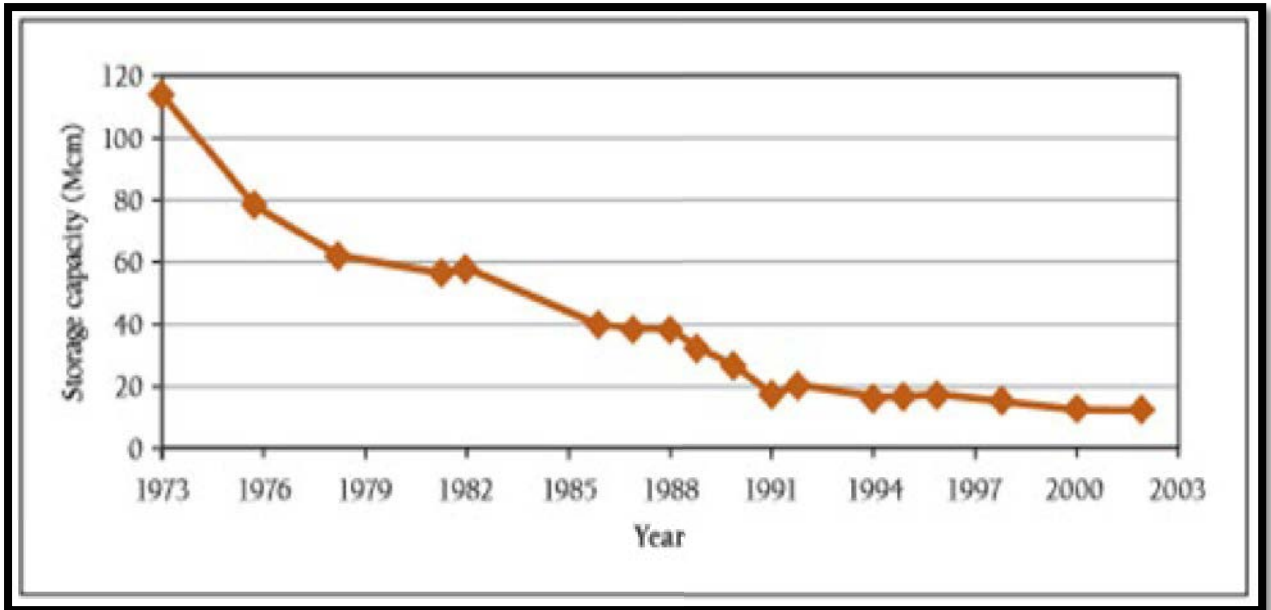


Figure 6.58: The observed loss in storage capacity due to sedimentation in Welbedacht dam (Clark, 1990).

The data collected shows that the Welbedacht dam has been receiving less rain compared to Gariep dam and Vanderkloof dam respectively. However, the Welbedacht dam has witnessed a loss in storage capacity due to extreme sedimentation caused by runoff and soil erosion. In the year 2000, the Welbedacht dam received an excessive amount of rain compared to 1994 and 2009.

Table 6.11: Showing the rain survey data (DWA, 2012)

Date	Rain
1994/1995	2812
2000/2001	5752
2009/2010	5080

d) Satellite imagery

The use of satellite images of several dams was employed for data interpretation concerning silt movement and deposited sediment in that specific dam. Satellite images can help monitor siltation/sedimentation. The satellite's frequent revisits over the same area and high spatial resolution also allow changes in inland water bodies to be closely monitored.

The satellite images were utilized for data interpretation to acquire extensive information/knowledge regarding silt movement and sediment deposition in the Gariep dam. Figure 6.59 shows the vegetation cover on the satellite image which is represented by shades of green and water bodies in black color. The water on the east side of the Gariep dam appears

in royal blue owing to a large quantity of sediments coming from the orange river, therefore appearing brighter than the water flowing out of the west side of the dam.

The satellite image shows that the water that has high content of sediment is brighter (royal blue) than the water with low quantity of sediment (navy blue). However, change in vegetation cover combined with soil erodibility can present a picture of areas which may pose a threat to water resources through high siltation rates and sediment loading.

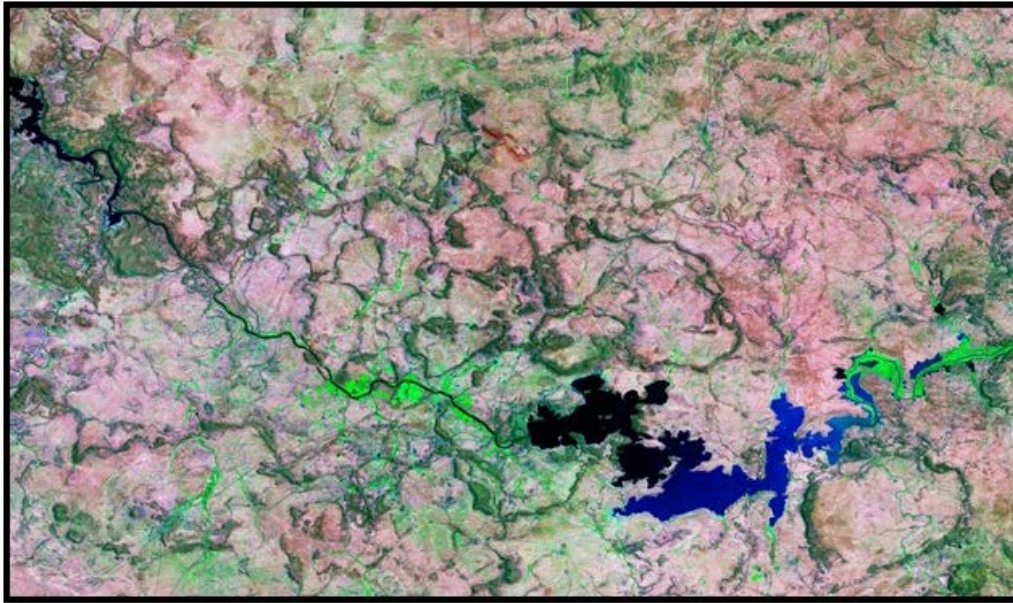


Figure 6.59: Satellite image of the Gariep dam/Orange River (ESA, 2021)



Figure 6.60: Satellite image showing the deposited sediments in Gariep dam (Google maps, 2022)

Figure 6.61 shows the satellite image which is dominated by bare soil and rocky terrain which appear in different shades of pink and red. And thus, may influence the sedimentation events or processes due to soil erosion or runoff. The high content of sediment was witnessed on the east side of the Vanderkloof dam. This is shown by the color of water which is commonly bright. Therefore, the color changes provide information on the intensity of the sedimentation events.



Figure 6.61 : Deposited sediment in the Vanderkloof dam (Google, 2022)

The satellite image shows an extreme sedimentation in the Welbedacht dam. Figure 6.62 shows the color changes in water. The presence of sediment in the dam is represented by the bright color (light green) and the absence of sediment is represented by dark color (green). There is high content of sediments transported and deposited in the Welbedacht dam/ Caledon River.



Figure 6.62: Sediments in the Welbedacht dam (Google, 2022)

6.19.4 Conclusion

The high sedimentation rate was witnessed in all the proposed study areas. However, there are several factors that play a major role in sedimentation processes including pedological, geological and climatological. It was found that the storage capacity of the selected study areas has been reduced over the years due to extreme sedimentation caused by excessive soil erosion, runoff, and high siltation rate. The relationship between the rain records and sedimentation was also observed as high rainfall regions are prone to soil erosion and high siltation rate. Also, the changes in colour provide valuable and reliable information on the intensity of sedimentation events. It was found that the water with bright colour represents the presence of sediments and the water in dark colour represents the absence or fewer amounts of sediments in the dam. It was found that satellite images can be used to monitor sedimentation in dams.

6.20 Sediment origin tracing by reflecting on evidence and sampling procedures

6.20.1 Introduction and methodology

a. Natural colour Images

Inspection of the image rendered in natural colour allows for multiple observations regarding the sedimentation process in the Gariiep dam (Figure 6.63). The first point to note is the variable colour changes in the water. The water appears to be different shades of brown/tan throughout

the dam. Secondly, the water on the eastern section of the dam is a darker brown and becomes clearer towards the western section. Thirdly, the water in the Orange River channel is a darker shade of brown than that of the water in the Caledon River.



Figure 6.63: Natural colour image of the Gariep dam as well as the Caledon River and Orange River confluence

The observation of the natural colour image provides vital information regarding the sedimentation in the Gariep dam. The colour changes can be used as a proxy to inspect the turbidity of the water and thus determine the relative sediment load. Sediment reduces the transparency and alters the colour of the water. The different shades of brown/tan indicate varying sediment concentrations. This forms the premise of the interpretations of the state of the water in the satellite images. When the river flow enters a reservoir, the velocity and energy of the sediment-laden water decrease as the reservoir gets wider and deeper. This subsequently causes deposition of the sediment carried in the water as the transport capacity is reduced (Morris & Fan, 1998). The sediment settles along the bottom of the reservoir and is sorted according to size. The distance in which the water transports the sediment depends on the decreasing water velocity. Generally, the coarse particles (gravels and sands) settle out first, and the fine material (silt) is deposited further into the reservoir (Strand *et al.*, 1982). The darker shades of brown in the eastern section of the water indicate the high sediment input from the rivers found upstream. Conversely, in the west, the water appears clearer where the sediment has settled into the dam floor.

The Gariep dam receives water mainly from the Caledon River and Orange River with most of the sediment sourced above this confluence (Bremner *et al.*, 1982). The water in the Orange River channel appears to be a darker shade of brown than the water in the Caledon River, suggesting a greater sediment content. The observation is consistent with estimates of the regional sediment load entering the Gariep dam, which reported that a higher percentage of the annual sediment load and mean runoff originate from the Orange River (Kriel, 1972).

Water Index Images

A.	
2022	
2018	
2005	-

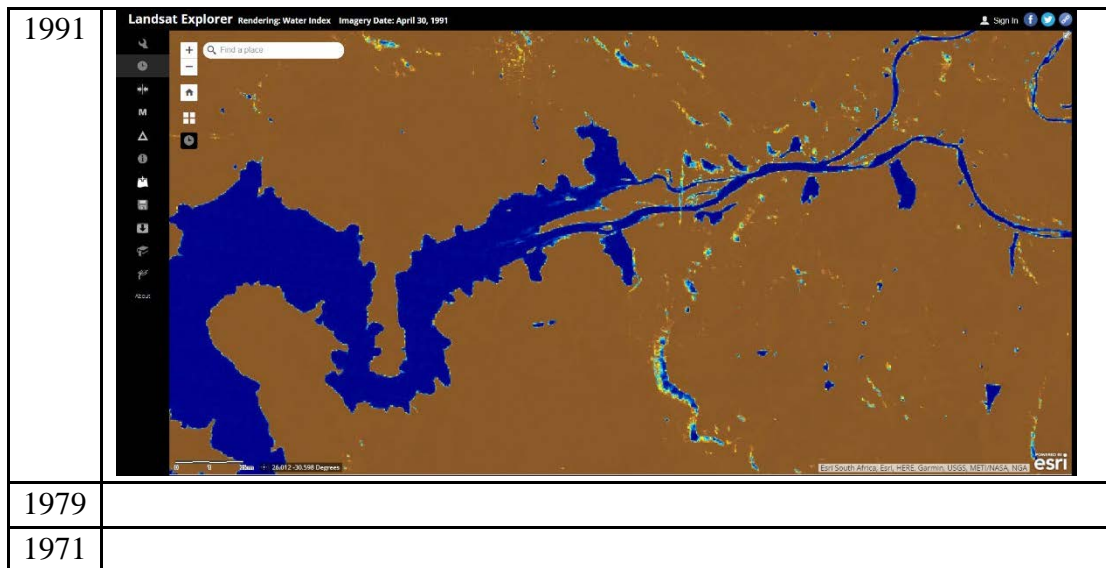


Figure 6.64: Caledon River and Orange River Confluence and the Gariep dam reservoir over time

Figure 6.64 shows images rendered for the water index over the shown period. From these images, a few observations can be made with regarding the sedimentation in the Gariep. There are ‘bars’ developing in the inlet of the Gariep reservoir, and they represent areas where there has been accumulation of sediment. The sediment bars are not only developing parallel to the flow of the water but throughout the years the bars have also extended further in the reservoir. Moving deeper into rest of the reservoir there are no notable changes that can be detected.

The areas of sedimentation accumulation could be exposed because of decreased flow in the system. The alternate reason could be a result of continuous deposition of sediment because of an increased sediment load. This has resulted in the development of a braided/anastomosing character.

b. Satellite imagery

LANDSAT imagery is used in this study because LANDSAT satellites provide high quality, multi-spectral imagery of the earth’s surface. Furthermore, the image database spans a considerable time range, from 1972 to the present day (USGS).

c. Department of Water and Sanitation

The DWS provides comprehensive hydrological data. This data is easily accessible and open to the public. The data used will be from the gauging station D3R002, a station at the Gariep dam.

Step 1: Data collection

This first step involves selecting the appropriate satellite imagery. The images are acquired through LANDSAT Explorer (<https://livingatlas2.arcgis.com/LANDSATexplorer/>).

For this study images were selected for the years 1972, 1979, 1991, 2005 and 2018. These years have been selected because they coincide with the years in which the DWS conducted sedimentation surveys of the Gariep dam. Images were also be collected for the year 2022 to assess the present-day conditions. This is important because data from the surveys can be correlated with the information determined from satellite imagery. This is followed by compiling flow records from the DWS hydrological website for the days that correspond with the satellite imagery. Images around the same time of the year are then picked to limit the interference of changes in variables such as seasonality.

Images in months in which the Orange River receives the most runoff are also picked because this is the time with the highest flows and sediment load. A cloud cover of 10% or less is used as one of the criteria for the selected images, to preserve the accuracy of the images' pixel values. The area of interest is delineated by the following co-ordinates*.

Step 2. Image processing and analysis

LANDSAT allows one to view images with different predefined band combinations and indexes to highlight various land cover features. It is also possible to create custom indexes and band combinations. To study various aspects of the sedimentation the satellite images will be rendered in natural color, Normalized Difference Vegetation Index (NDVI) and Water Index. Table 6.12 provides a summary of the properties of the rendering options as described on LANDSAT Explorer.

Table 6.12: Summary of the properties of the rendering options

Renderer	Description	Reason for use
Natural color	allows for the viewing of images close to what would be expected in real life.	Examine the turbidity of the water in the Gariep dam as well as the tributaries. (Orange River and Caledon River)
Normalized difference vegetation index	Allows for the measuring and monitoring of the vegetation cover on the land surface	For the observation of changes in patterns of land-use and land cover
Water index	Allows for the delineation of open water bodies	To observe the spatial and temporal changes in the accumulation of sediment

6.20.2 Limitations

The accuracy of image analysis is highly dependent on the resolution of the images. LANDSAT imagery obtained from more recent missions tend to have higher resolutions than those acquired in the past. However, the LANDSAT Explorer web app has gaps in its catalog of available images, which limits the amount of data that can be analyzed. Furthermore, since there is only one gauging station at the Gariep dam, flow data may not accurately represent the entire reservoir due to its size. Additionally, there is a lack of hydrological data from the DWS, which makes it difficult to correlate certain satellite imagery with hydrological data.

6.21 Reflect on the smaller dams upstream of Gariep that act as sediment traps

6.21.1 Introduction and methodology

Satellite remote sensing was utilised as the preferred methodology for this section of the study. This methodology entailed the acquisition and visualisation of satellite imagery, as well as the visual analysis/interpretation of satellite imagery, with the help of satellite imagery remote sensing techniques.

a) Satellite imagery acquisition and visualization

The imagery used in this study was acquired and visualised through the LANDSAT Explorer platform. This is an open source, web-based application that provides free access to high-resolution (30-m) multispectral satellite imagery, which is most preferred for inland water monitoring applications (Giardino *et al.*, 2019; Li & Li, 2004). Through the LANDSAT Explorer platform, both the most recent (real- to near real-time), as well as archived imagery captured since the early 1970s, are available for visualisation, thus enabling the possibility of performing a retrospective or temporal change analysis in surface water monitoring studies (Li & Li, 2004).

The satellite imagery showing the various dams were visualised in both true colour and false colour composites using the rendering tool in LANDSAT Explorer. True colour composite is generated by combining the red, green, and blue bands in the visible spectrum, and thereby, displays colours that closely resemble what the human eye perceives as "true or natural" colours of the earth's features. For example, water appears in a blue colour, while vegetation appears in green. False colour composites on the other hand, utilise the infrared spectrum and display "false" or unexpected colours of features, such as vegetation appearing in red. Thus, false colour imagery enhances certain features and makes them easily distinguishable from other features.

b) Satellite imagery interpretation

Water colour changes are linked to the presence and the concentration of optically active constituents – in this case, suspended sediments – in the water column, as they greatly control the optical properties (i.e. light absorbance and scattering/reflection processes) of water in the visible and the near-infrared (NIR) spectra (Conde *et al.*, 2019; Hellweger *et al.*, 2004).

Elevated levels of suspended sediment increase the spectral reflectance of water because of the increased associated backscattering effect caused by the high suspended sediment concentration in the water column (Peterson *et al.*, 2018). This results in water changing colour from blue (clear water) to a brownish colour because of being muddy or turbid due to the presence of suspended sediment. In a false colour infrared composite, however, clear water appears very dark blue or black, while turbid water is displayed in a cyan colour.

In this study, the satellite imagery of the dams, in both true and false colour composites, were interpreted based on the visible colour of the water in relation to the presence and the transport of suspended sediment loads in the dams and/or upstream rivers. The dams were also compared in terms of the physical, hydrological, and climatic characteristics of the dam locations. This consequently helped to understand the sedimentation process and the sediment trapping effect of the dams.

6.21.2 Results

a. Reflecting on the sedimentation of the dams using hydrological data

Pre-dam environments or small dams in river tributaries can serve as sediment and pollution traps for larger dams downstream. These upstream structures can help to reduce the amount of sediment and pollutants that reach the larger dams, which can improve water quality, prolong the lifespan of the dams, and reduce maintenance costs.

When rivers flow downstream, they carry sediment and pollutants with them. In areas with steep slopes, the velocity of the water can be high, which can cause erosion and increase sediment transport. If left unchecked, the sediment can accumulate in larger dams downstream, reducing their storage capacity and increasing the cost of maintenance.

Pre-dam environments or small dams in river tributaries can help to address this problem by slowing down the flow of water and trapping sediment and pollutants before they reach the larger dams downstream. These structures can be designed to allow water to pass through while trapping sediment and pollutants in a settling basin or similar structure. The trapped sediment can be periodically removed, reducing the amount of sediment that reaches the larger dams.

In addition to trapping sediment and pollutants, pre-dam environments or small dams in river tributaries can also provide other benefits. They can serve as a source of water for irrigation,

livestock watering, or other uses. They can also help to recharge groundwater aquifers and improve soil moisture levels, which can benefit vegetation and wildlife in the surrounding area. Overall, the use of pre-dam environments or small dams in river tributaries can be a useful tool for managing water resources, improving water quality, and reducing maintenance costs for larger dams downstream. However, their effectiveness can depend on a variety of factors, including the design of the structures, the amount of sediment and pollutants in the water, and the characteristics of the local environment.

This report from the Water Research Commission discusses the potential for small water bodies, including pre-dam environments and small dams in river tributaries, to contribute to water resource management in South Africa. The report provides case studies of successful projects and discusses the potential benefits and challenges of implementing these types of structures.

Mofokeng, M., Dlamini, D. S., & Molefe, A. (2020). Sedimentation assessment of small farm dams in the Free State Province of South Africa. *Water*, 12(3), 686. doi: 10.3390/w12030686
 This research article discusses a study of sedimentation in small farm dams in the Free State Province of South Africa. The study found that sedimentation rates varied depending on the location and size of the dams, and that sedimentation could reduce the storage capacity of the dams over time. The authors discuss the potential benefits of pre-dam environments or small dams in river tributaries to trap sediment and reduce the impact of sedimentation on larger dams downstream.

b. Bethulie dam

Bethulie dam is a medium-sized dam that was built on the Bethuliespruit river, a second order non-perennial stream that flows directly into the Gariiep dam at the town of Bethulie, in the Free State province of South Africa. The dam was built in 1921 for domestic supply to the Bethulie town. It has a free overflow/uncontrolled spillway with a capacity of 370 m³/s. It is in the 254 km² D35A quaternary catchment which has a mean annual runoff (MAR) of 4,34 million m³ (WR2012, 2022), and an annual sediment yield of 455 t/km² (WRC, 1992).

Table 6.13: *Surveyed sedimentation statistics of the Bethulie Dam (WRC, 1992)*

Survey Period	Last survey storage capacity (million m³)	Sediment Volume (million m³) of original storage capacity	% Sediment of original storage capacity
1921-1979	1,969	4,542	69,8

Information on the original and the current storage capacity of the Bethulie Dam is unavailable. However, information that is available shows that the dam lost 69,8% of its original storage capacity to sedimentation within a period of 69 years in operation (Table 6.14). The volume of the accumulated sediment that made up the 69,8% of the dam’s storage capacity was 4,542 million m³.

Table 6.14: The annual total discharge/overspill volumes at Bethulie Dam for periods when there was an overspill (DWS website, 2022).

Period (years)	Months	Spill Volume (Million m ³)
1923/1924	March	0,951
1924/1925	April-May	1,3
1929/1930	January	2,51
1933/1934	January	3,21
1936/1937	November	1,95
1945/1946	May	0,892
1947/1948	March-April	5,52
1987/1988	February-September	35,3
1988/ 1989	October-December	0,474

In a period of 69 years (1921-90), the Bethulie dam only had an overspill during 9 years of the 69 years, with much of the overspill occurring in 1988 (Table 6.13), corresponding to the Orange River flooding event that occurred during this period. This suggests that it was only during these time that a proportion of the inflowing sediment was discharged from the dam to the downstream Bethuliespruit, along with the surplus water. During the periods when there was no overspill over the Bethulie Dam spillway, such as during the period from 1948 to 1987 (Table 6.13), it can be assumed that all the inflowing sediment-laden runoff was retained in the dam, thereby allowing sediment deposition to occur within the dam. The Bethulie Dam, therefore, acts as a sediment trap for the downstream Gariep dam, trapping most of the 455 tons/km² annual sediment yield of the D35A catchment area that would otherwise flow towards the Gariep dam during high rainfall periods.

c. Gariep dam

The Gariep dam, which started operating in 1971, is South Africa's largest dam, with an original storage capacity of 5897,285 million m³ and a surface area of 35 216 ha (352,16 km²). The dam was built on one of the world's most turbid rivers, the Orange River, which drains the upper Orange, the Kraai, and the lower Caledon sub-catchments. As such, the dam drains a large catchment area of approximately 70 749 km². The Gariep dam is provided with a free (controlled) central, overspill spillway, 6 gated spillway chutes (flood gates), 8 radial river outlets, and 4 radial silt outlets, which are used for controlling inflowing flood waters and turbidity currents (Kriel, 1972) both in a controlled and uncontrolled manner.

The large size of the Gariep dam allows it to retain a most of the inflowing sediment load, while the balance gets discharged downstream through the spillways and outlets (Kriel, 1972). Figure 6.65 shows the temporal change in storage capacity and sediment accumulation of the Gariep dam. It is evident that the storage capacity of the Gariep dam has been gradually decreasing as sediment accumulates in the dam. Within a period of 45 years since the dam started operating,

its storage capacity has reduced by approximately 16,8%, from a storage capacity of 5897,285 million m³ in 1971 to a current storage capacity of 4903,5 million m³ in 2022. The storage capacity reduction of 16,8% corresponds to the percentage of sediment deposited in the dam. The mean annual rate at which sedimentation occurs in the Gariep dam is 0,36% (DWS, 2018).

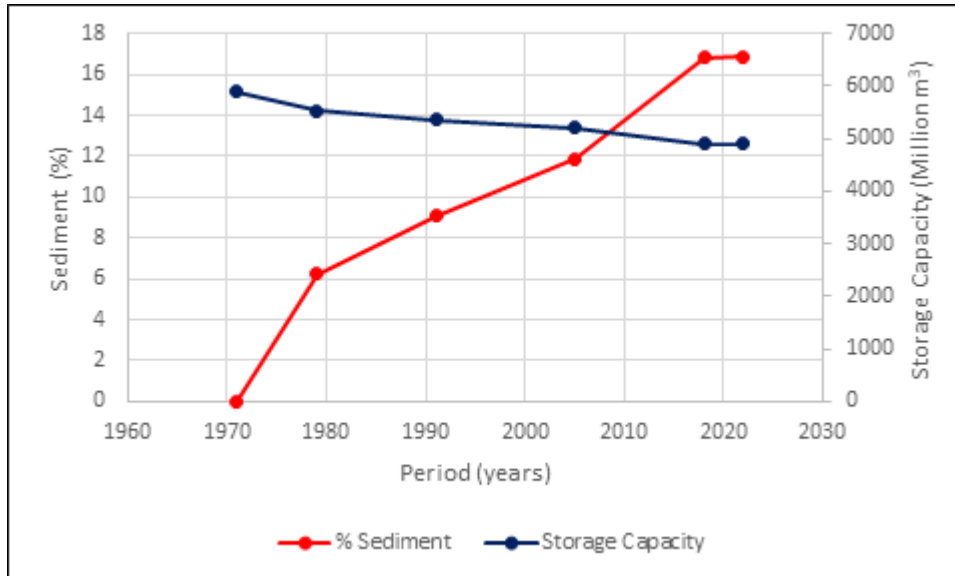


Figure 6.65: Temporal change in sedimentation and storage capacity of the Gariep dam (DWS, 2018; DWS website, 2022).

The Gariep dam, being located approximately 124 km upstream of Vanderkloof Dam, acts as a large upstream sediment trap basin for this dam, which is utilised for irrigational and hydropower generation purposes. Table 6.15 shows that the original storage capacity of the Vanderkloof Dam reduced from 3126,2 million m³ in 1976 to a current capacity of 3092,4 million m³, which is a reduction of 33,8 million m³ (or 1,08%) of the original storage capacity. The mean annual sedimentation rate of the Vanderkloof Dam is 0,02% (DWS, 2006). This is quite low, and it is due to the trapping of sediment by the Gariep dam.

Table 6.15: Sedimentation statistics of the Vanderkloof dam (DWS, 2006; DWS website, 2022).

Date	Capacity (Million m ³)	% Sediment
1976	3126,2	0
1991	3116,607	0,31
2006	3107,243	0,61
2022	3092,4	1,08

d. Reflecting on the sedimentation of the dams using satellite imagery
Gariiep dam



Figure 6.66: True colour imagery of the Gariiep dam – 5 January 2022 (LANDSAT explorer, 2022).

This is depicted by the high reflectance of the very turbid Orange River in Figure 6.66. The dark brown colour of the Orange River is due to excessive sediment transport following a high rainfall event. Figure 6.66 also shows the water in the Gariiep dam in different shades of brown, owing to the influx of sediment from the Orange River. The brown colour of the water in the dam fades or becomes lighter towards the western side because of the sediment plume from the river dispersing in the dam, leading to the deposition of the coarser sediment in the upper reaches of the dam, while the finer sediments are carried in suspension further into the dam where they will get deposited. The brown colour differences also correspond to a decrease in the flow velocity and the suspended sediment concentration from the east to the western side of the dam.

e. Comparison between the Gariiep dam and the Vanderkloof dam

Figure 6.67 shows an obvious water colour difference between the Gariiep and Vanderkloof dams. The Gariiep dam appears in a blue-green or cyan colour, indicating elevated levels of suspended sediment in the dam. The Vanderkloof dam on the other hand, shows a darker shade of blue, indicating that the water is less turbid/muddy in comparison to the Gariiep dam. The upper reaches of the Vanderkloof dam shows a presence of suspended sediment (light blue). This may be the result of erosion from the surrounding bare land, as well as the sediment-laden discharge from the upstream Gariiep dam during high flows.

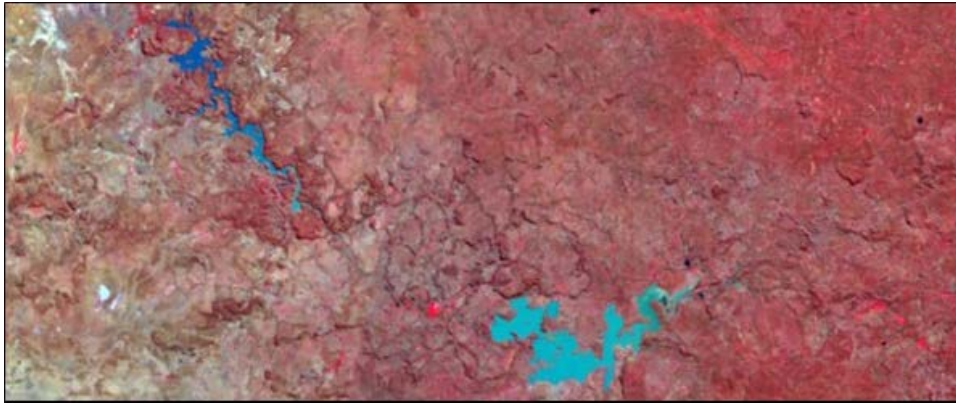


Figure 6.67: False colour (colour infrared) imagery showing the Gariep dam (bottom right) and the Vanderkloof dam (upper left) (LANDSAT Explorer, 2022).

f. Bethulie dam



Figure 6.68: Bethulie dam (top) and a portion of the Gariep dam (bottom), captured in May 2022. a) True colour, b) False colour (LANDSAT Explorer, 2022)

The Bethulie dam does not receive significant river runoff from the Bethuliespruit stream, as it is a second order, non-perennial stream. As such, it appears to be less turbid than the Gariep dam, but still shows some presence of suspended sediment in the dam (Figure 6.68). This is shown by the brownish-green colour in Figure 6.68a, and the dark blue colour with some faded blue sections in Figure 6.68b. The low turbidity may also be because most sediment have already settled in the dam, as opposed to being in suspension.

6.22 The contributions remote sensing does or don't contribute to the Gariep situation

6.22.1 Introduction

Bathymetry is the study of beds of bodies of water, including the sea, waterways, streams, and lakes (Hell *et al.*, 2012). Bathymetric data, generates data about the water depth and underwater geography of seas, oceans, and lakes, are important in many parts of the marine and lacustrine study, organization and spatial processing of sea and beach conditions and their benefits (Hell *et al.*, 2012). According to Dierssen and Theberge (2014), bathymetry was commonly

mapped using ship's sonar. A sonar sends a sound blast from a hull or foot to the seabed. The sound wave bounces back toward the ship. The time it takes for the pulse to leave and return to the ship determines the topography of the seabed. The longer it takes, the more profound the water. Although this method can produce precise depth estimations at points or along transects, it is limited by its high operational cost inefficiency, and inapplicability to shallow waters (Legleiter & Fosness, 2019). In comparison, remote sensing methods offer more flexible, efficient, and cost-effective ways to map bathymetry over large areas (Legleiter & Harrison, 2018). The remote sensing method is faster and applicable to various environments, including shallow coastal waters, clear rivers, and the relatively clean river courses in the upper parts of estuaries (Kasvi *et al.*, 2019). Measurement of bathymetry using satellite imagery is one of the basic kinds of research in the field of remote sensing (RS) of the marine environment, which has various practical applications for the coastal environment and its monitoring (Kasvi *et al.*, 2019). The aim of this research is to reflect on the contribution of remote sensing to bathymetric studies. In reaching the aim, this research will highlight the literature review on remote sensing tools to bathymetric studies by comparing non-imaging and imaging tools. The paper will further highlight research methodology.

a. Remote sensing tool to bathymetric studies

Remote sensing of bathymetry takes various forms, each with its own depth of detection, accuracy, strengths, limitations, and best application settings. These forms fall into two broad categories: non-imaging and imaging.

b. Non-imaging

The non-imaging process is illustrated by airborne LiDAR (Light Detection and Ranging) specifically designed to measure water depth. According to Zhu *et al.* (2017), bathymetry LiDAR system uses two lasers with different wavelengths. Two wavelengths are used because the sea floor needs to be measured separately from the sea surface. An infrared laser with a wavelength of 1064 nm is used to detect the water surface and a green laser with a wavelength of 532 nm to detect the seabed (Zhu *et al.*, 2017). The wavelength of the green channel is optimal for penetrating water and thus measuring water depth. The red return signal indicates the aircraft's altitude above the water. The water depth is calculated from the time difference between the two return signals. As the green laser pulse travels through the water column and reflects off the sea floor, it is absorbed, scattered, and refracted. These processes attenuate the laser's reflected energy and limit the measurable water depth. The feasibility of water depth estimation using airborne pulsed blue-green lasers was demonstrated as early as the late 1960s (Maas *et al.*, 2019). However, it did not see widespread use until the advent of the Global Positioning System (GPS) (Gao, 2009). A GPS-enabled LiDAR system enables surveying of the seabed without simultaneous measurement of water level data and avoids errors caused by highly dynamic temporal and spatial water level fluctuations (Quadros *et al.*, 2008). It can provide fast, accurate and cost-effective bathymetric surveys of fairways, coastal structures, large offshore areas, beaches and coastlines (Quadros *et al.*, 2008).

Airborne LiDAR shows promise for mapping seafloor topography in coastal waters that have low concentrations of suspended sediments or are not discoloured by organic pigments (Saylam *et al.*, 2018). A large amount of high-quality data can be efficiently recorded via variable swath widths, regardless of the water depth. LiDAR can measure water depths from 1.5 to 60 m with an accuracy of up to 15 cm (Saylam *et al.*, 2018). The maximum penetration depth ranges from 35 m to 50 m. Bathymetric LIDAR systems can also measure terrain elevation, but with typically lower accuracy and spatial resolution than the topographic equivalent (Guenther, 2004). Another limitation of all bathymetric LIDAR systems is their impotence to measure depths where the water is turbid (murky or cloudy) (Saputra *et al.*, 2021). Bathymetric LIDAR systems cannot collect reliable bathymetric data in the coastal or surf zone.

Limiting factors are identified as water clarity, weather, and sea conditions (Saputra *et al.*, 2021). To measure water depth, an Airborne LiDAR is used with the green light sensor alongside the near-infrared light sensor. However, water condition affects the ability to penetrate green light. Water clarity and vegetation are some of the limitations on green light penetration into the water, especially in inland waters. The influence of seawater parameters such as turbidity, temperature and salinity cannot be ignored when performing bathymetric LiDAR (Light Detection and Ranging) measurements. Turbidity affects the attenuation diffusion coefficient of the green laser when penetrating the air column. Turbidity causes light rays to scatter in the water column, where particle size, shape, and composition can affect their amplitude. Salinity and water temperature are considered to create the required refraction values calculated in LiDAR's bathymetry equation for each different survey location. Because the LiDAR bathymetry depth measurement capability is limited to shallow waters, calculating a single refractive index value for the entire water column is generally sufficient. The maximum depth for bathymetric LIDAR technology is affected by the interaction of ground radiation and water turbidity, as well as the angle and intensity of the incident sun. (Saputra *et al.*, 2021)

c. Imaging method

Imaging methods approximate water depth based on the pixel values or digital numbers (DN) (representing reflection or backscatter) of an image (Zhu *et al.*, 2017). Imaging methods use visible and/or near infrared (NIR) and microwave radiation (Gao, 2009). Imaging methods are implemented using either analytical modelling or empirical modelling or a mixture of both (Jawaki *et al.*, 2015). Imaging of bathymetry studies uses sensors such as optical RS, MS image sensor and video (Jawaki *et al.*, 2015). Optical RS-based bathymetry is based on the principle that the total amount of radioactive energy reflected from a water column is a function of water depth (Erena *et al.*, 2020). Optical RS uses shortwave radiation in the blue and green spectrum, which has strong penetrating capabilities (Deng *et al.*, 2008). As the incident solar radiation propagates through the water, it is scattered and absorbed by water molecules and constituents in the water, emitting variable energy and being recorded in RS images (Erena *et al.*, 2020). The energy received by the sensor is inversely proportional to water depth after removing atmospheric corrections and water column effects. Therefore, the intensity of the returned signal indicates the depth at which the solar radiation has penetrated (Cao *et al.*, 2022).

According to Flener *et al.* (2012), optical RS can be implemented for bathymetry derivation using two methods; analytical modelling and empirical modelling. Analytical modelling of bathymetry is based on the properties of light propagation in the water column. An analytical model is based on several optical properties of water, such as the attenuation coefficient and the backscatter, which are required as input parameters (Jawaki *et al.*, 2015). The model commonly used is the flow radiative transfer model, which requires input of the spectral signatures of suspended and dissolved materials and ground reflectance (Flener *et al.*, 2012). In empirical modelling, the relationship between the remotely sensed radiance of a body of water and the depth at sampled locations is determined empirically, without regard to how light is transmitted in the water (Gholamalifard *et al.*, 2013). There is a close relationship between water depth and single band radiance for water bodies with uniform optical properties and bottom reflectance. If the optical properties are not consistent, multiple tapes must be used (Jawaki *et al.*, 2015). The development of this empirical model requires a series of in situ measurements that can include water and ground reflectance, the vertically averaged diffuse attenuation coefficient, and the concentrations of suspended inorganic components, chlorophyll a, phaeopigments, and dissolved organic carbon. Spectral reflectance measured in the field over a wide range of wavelengths should reveal the most appropriate bands for capturing bathymetry. This is particularly important in the case of spatially varying turbidities. The empirical modelling procedure is valid because total water reflection is primarily related to water depth and secondarily to water turbidity.

According to Jawaki *et al.* (2015), MS/HS images provide bathymetry measurements that are not reliable enough to be used for navigation purposes. However, the image-based MS/HS method is a cost-effective option for bathymetry over large areas. These bathymetric products are suitable for a range of environmental and scientific applications (Ashphaq *et al.*, 2021). Bathymetry derived from imagery is not measured directly, it is inferred, and as such bathymetry is estimated with less accuracy than LIDAR or multibeam echosounders (Jawaki *et al.*, 2015). The depth to which the imagery is useful is limited by light attenuation. Depending on water clarity, depths derived from aerial, or satellite imagery are limited to 25-30 m due to light penetration issues. There are two accepted techniques for deriving bathymetry using MS satellite imagery: 1) radiometric approach and 2) photogrammetric approach. The radiometric approach exploits the fact that different wavelengths of light are attenuated by water to different degrees, with red light being attenuated much faster than blue light. RS technologies have surpassed the ability of existing MS satellites to detect light in the blue (450-510 nm), green (510-580 nm), and red (630-690 nm) bands to achieve superior depth estimates in water up to 15 metres deep.

Photogrammetric approach uses a digital elevation model (DEM) to derive bathymetry. In this method, stereoscopic images can be collected over the target area, a DEM, or a digital bathymetry model (DBM) of the shallow seabed can be constructed from the images (Hodul *et al.*, 2018). Early studies using both satellite imagery and digital photography appeared promising and show that this method can be used to create accurate bathymetric models of flat environments without in situ data (Jawaki *et al.*, 2015). However, the method has not been

extensively studied because of the limitations in the capabilities of current sensors. The challenge in collecting stereoscopic images of the shallow sea floor is to understand the interaction of light with the air/water interface. At high angles of incidence, the light is fully reflected off the water surface, preventing any observation of underwater features. Current multispectral satellite sensors are unable to collect enough high-resolution stereoscopic images within the narrow angle required to penetrate the sea surface (Jawaki *et al.*, 2015). Also, none of them can provide the shorter wavelength blue light needed for maximum depth penetration. Interest in this remote sensing solution has increased with the recent availability of the Sentinel-2 Multispectral Imager (MSI), which offers improved technical capabilities compared to previous optical sensors such as LANDSAT or SPOT.

6.22.2 Field methodology

To assess the relevance of remote sensing in the Gariep dam bathymetry, a 9-10 cm long white rod was inserted into the dam to check visibility. This method was chosen for this research because remote sensing uses radar pulses to measure the depth of the dam. However, sedimentation limits the accuracy of remote sensing bathymetric data. The Gariep dam was visited by the fieldwork team to check if the stake would be visible in the dam. The visibility of the stake in the dam will determine whether remote sensing will be useful for the Gariep dam. 38 stations were therefore selected for the experiment. The station data were recorded and evaluated.

6.22.3 Results

Most of the applied remote sensed methodology were found to be not successful. We could not get any depth penetration measurements using the published methodology. We expected the large sediment load, which is visible from all images used, to be the culprit. For this reason, we decided to test the light penetration in-field. Table 6.16 provides the results testing the depth that a white object could still be detected in full sunlit conditions.

Table 6.16: Gariep dam object visibility

Sample point	Position	Depth(m,mm)	Visibility(cm)
Gariep 1	S30° 36' 47.7" E25° 32' 23.3"	62, 310	18
Gariep 2	S30° 36' 44.7", E25° 30' 50.7"	47, 775	10
Gariep 3	S30° 37' 00.7", E25° 31' 51.4"	36, 620	15
Gariep 4	S30° 36' 25.9", E25° 32' 22.8"	26, 00	12
Gariep 5	S30° 36' 16.1", E25° 32' 16.2"	7, 777	11
Gariep 6	S30° 36' 48.1", E25° 34' 02.6"	53, 820	11.5
Gariep 7	S30° 36' 59.1", E25° 34' 06.1"	42, 940	10
Gariep 8	S30° 37' 20.3", E25° 34' 19.4"	33, 650	11.4
Gariep 9	S30° 37' 45.2", E25° 34' 33.3"	23, 200	9.6
Gariep 10	S30° 37' 53.7", E25° 34' 36.3"	16, 550	10.3
Gariep 11	S30° 37' 59.3", E25° 34' 38.2"	13, 300	10.1
Gariep 12	S30° 36' 13.6", E25° 34' 46.5"	53, 880	10.9
Gariep 13	S30° 35' 40.5", E25° 34' 37.8"	37, 130	9.3
Gariep 14	S30° 35' 04.7", E25° 34' 27.1"	29, 600	9.2
Gariep 15	S30° 34' 40.6", E25° 34' 17.6"	24, 110	9.9
Gariep 16	S30° 34' 32.1", E25° 34' 03.1"	11, 120	8.9
Gariep 17	S30° 34' 14.0", E25° 34' 01.4"	13, 180	10.5
Gariep 18	S30° 40' 50.9", E25° 44' 30.7"	33, 000	11
Gariep 19	S30° 40' 50.9", E25° 44' 30.7"	21, 870	8.4
Gariep 20	S30° 40' 02.2", E25° 44' 33.3"	13, 250	7.8
Gariep 21	S30° 39' 55.2", E25° 44' 34.0"	8, 860	9.3
Gariep 22	S30° 42' 03.8", E25° 43' 51.6"	29, 350	11.5
Gariep 23	S30° 41' 22.5", E25° 43' 42.3"	20, 00	9.5
Gariep 24	S30° 41' 41.8", E25° 43' 43.4"	17, 800	9.5
Gariep 25	S30° 41' 54.4", E25° 43' 43.7"	17, 400	8.1
Gariep 26	S30° 42' 10.7", E25° 43' 44.2"	14, 00	7.5
Gariep 27	S30° 42' 31.4", E25° 43' 44.4"	7, 460	9.2
Gariep 28	S30° 41' 38.3", E25° 42' 34.0"	12, 390	9.7
Gariep 29	S30° 41' 38.3", E25° 42' 34.0"	14, 400	10
Gariep 30	S30° 40' 48.3", E25° 42' 42.6"	36, 400	9.9
Gariep 31	S30° 40' 24.4", E25° 42' 46.8"	24, 620	11.3
Gariep 32	S30° 40' 04.8", E25° 42' 50.4"	11, 690	9.8
Gariep 33	S30° 40' 06.0", E25° 41' 01.5"	28, 670	9
Gariep 34	S30° 39' 34.6", E25° 46' 26.4"	14, 330	7.4
Gariep 35	S30° 39' 37.4", E25° 46' 48.1"	27, 480	8.3
Gariep 36	S30° 39' 38.3", E25° 47' 00.8"	23, 030	8.8
Gariep 37	S30° 39' 38.2", E25° 47' 15.7"	16, 230	7.4
Gariep 38	S30° 39' 37.4", E25° 47' 27.7"	4, 340	8.8

6.22.4 Conclusion

Although a lot of time was spent testing published methods for reliable outcomes, the large sediment load in this system provided a barrier for light penetration and the dam floor could not be detected. The only method that could be used was sonar depth sounding, which was used by DWS in mapping dam depth.

6.23 Discussion and conclusion

6.24 Measurement of dam circumference and the dynamics of circumference change

GIS and RS images are widely used in managing and using water resources around the world, as well as in obtaining hydrological, morphological and hydrometeorological data on the world ocean, seas, lakes, rivers, water reservoirs and other water bodies remotely and in short period of time. The Geographics Innovation Cartography Software Company's Global Mapper is one of the GIS software programs that are used. It has many capabilities such as getting into global database, opportunity to download over 300 shape files like ESRI, KML, LiDAR, MrSID, SRTM, obtain necessary data from global database and determine distance and area from these data, measure depths and height, develop contours and cross section profiles of the area, measure volumes (fill-in and cut-in), develop formation of basin channels, see simulation of water level change in the area, use Lidar Module functions, export data in more format types than other GIS software programs and others.

Within this research the software options were used to determine water surface area and volume of Gariép dam and to analyse areas and volumes by contours, to develop dynamics of circumference changes. The research work will be useful to study the site relief, measure depths and heights, determine distances and areas, water detention capability, determine water reservoir surface areas and volumes by contours within short period of time.

CHAPTER 7

PALAEO-CLIMATIC CHANGES AND DEPOSITION RATES IN SOUTHERN AFRICA: IMPACTS OF REGIONAL GROUNDWATER QUALITY

7.1 Introduction

Upon traversing the Kalahari (Figure 7.1) in the 19th Century, David Livingstone recognised a wide distribution of fossil shells, which he interpreted to have lived in a vast freshwater lake (Livingstone, 1857). He postulated that the vanishing of the lake was due to climate and tectonic events that changed the course of the Zambezi River and created an outflow at the Victoria Falls (Figure 1), which subsequently drained the lake (Livingstone, 1857). Since then, several studies have identified the existence of a large Quaternary lacustrine system with several subbasins (Passarge, 1904, Grove, 1969, Ebert and Hitchcock, 1978, Cooke, 1979, Cooke and Verstappen, 1984, Lancaster, 1989, Thomas and Shaw, 1991a, Moore, 1999, Moore and Larkin, 2001, 2002, Ringrose *et al.*, 2005, McFarlane and Eckardt, 2006, White and Eckardt, 2006, Burrough *et al.*, 2009a, Burrough *et al.*, 2009b, Moore *et al.*, 2012). This large lacustrine system was termed Lake Palaeo-Makgadikgadi by Grey and Cooke (1977), but commonly referred to as the Palaeo-Lake Makgadikgadi (PLM). PLM sustained several lake stages, the highest ~995-1,000 m above mean sea level (m asl), spanning an area in excess of 175,000 km² referred to as the Palaeo-Lake Deception – PLD (McFarlane and Eckardt, 2006, Moore *et al.*, 2012).

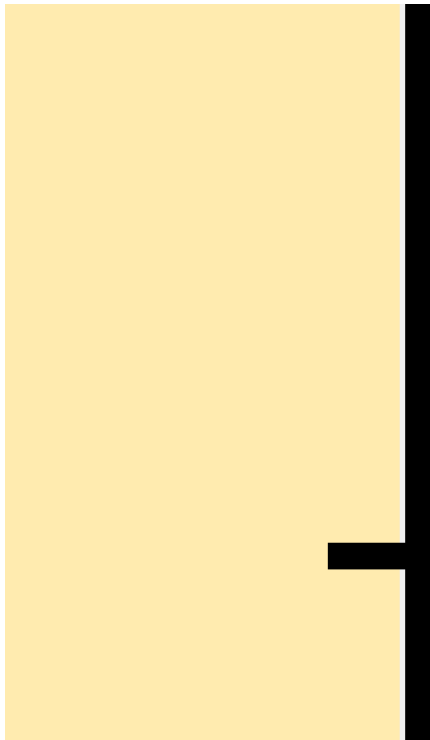


Figure 7.1: Outline of the Palaeo-Lake Deception (995 m amsl) and Palaeo-Lake Makgadikgadi (945 m amsl), extracted from the digital elevation model (Shuttle Radar Topographic Mission – SRTM) within the Kalahari Group Formation.

NB: Insert figure shows the coverage of the Kalahari Basin over Southern Africa and the tectonic axes of deposit (EGT – Etosha-Griqualand-Transvaal and OKZ – Okavango-Kalahari-Zimbabwe).

The actual age of the lake system is unknown. In-situ-sediments and palaeo-shoreline sediments (Burrough and Thomas, 2009) indicate minimum ages of c. 300 kilo-annus (ka). Early stone artefacts (McFarlane and Eckardt, 2006) and molecular dating of cichlid fish (Joyce *et al.*, 2005) found at the basin floor of PLM, suggest that by c. 500 ka the mega-lake was predominantly desiccated. More recently, Moore *et al.* (2012) speculates the lake was initiated as early as 1.4 Ma (Early Pleistocene). Geological data suggests that Neogene drainage flowing west towards the Limpopo River was disrupted between the Early to Late Pleistocene by the uplift of epirogenetic axes (Linyanti-Chobe faults, Fig 1) resulting in the creation of a huge internal drainage basin – PLM (Du Toit, 1927, Cooke, 1980, Moore and Larkin, 2001, Haddon and McCarthy, 2005).

While it can only be speculated on the events between the early to middle Pleistocene, probably due to masking or obliteration of the evidence by subsequent events (Thomas and Shaw, 1991b), geomorphological data used to explain lake evolution events in Late Pleistocene to Holocene are considered comprehensive (Riedel *et al.*, 2014). However, hydrological dynamics (forcing and feedbacks) is a contentious issue (Street and Grove, 1976, Butzer *et al.*, 1978, Heine, 1978, Street and Grove, 1979, Heine, 1982, Heine, 1992, Lancaster, 1979, Thomas and Shaw, 1991b, Burrough *et al.*, 2009b, Riedel *et al.*, 2009, Riedel *et al.*, 2012,

Riedel *et al.*, 2014) specifically, the Paleo-hydrology induced by climates of PLM before and after the Last Glacial Maximum (LGM; c. 23-18 ka (Gasse, 2000)) to indicate if surface water contributions were predominantly in high lake level at 945 m amsl of PLM or not. Heine (1982) demonstrated that results from different palaeo-climatic indicators (geomorphological, sedimentological, palaeo-botanical, palaeontological and archaeological) would have different time-stratigraphic periods for the Late Quaternary over the PLM Basin; strong winds movements are suggested to control the pluvial climatic phases [>30 -20 ka and 8-4.5 ka (De Vries *et al.*, 2000)] over southern Africa. However, lake systems from about 20-15 ka, such as Lake Victoria in East Africa (largest lake in Africa) and many others, are considered to have been completely desiccated (Johnson *et al.*, 1996, Gasse, 2000, Kafri and Yechieli, 2010). Consequently, the influence of groundwater relative to surface water inflow between humid to arid must have increased progressively to exert a controlling influence on the arid environment (Bowler, 1986). Further, this impacted geochemical, sedimentological and morphological evolution as observed in other regions such as Australia (Bowler, 1986).

The influence of Pleistocene hydrologic changes on the spatial variability, hydrological configuration and evaporite formation has been shown in other closed basins such as the Lake Chad (Edmunds *et al.*, 1999, Edmunds *et al.*, 2002), Great Artesian Lake (Bowler, 1986) and the Great Salt Lake (Spencer *et al.*, 1985a). In the light of these studies, we compile numerous studies that have focused on sedimentology, palaeontology, hydrochemistry, hydrogeophysics, stable and radiogenic isotopes in the PLM to draw insights on the influence of the Pleistocene-environmental changes and how they have shaped the groundwater environment of this mega-lake system.

7.2 Aims and objectives

The aim of this assessment was to demonstrate the paleoclimatic changes in the Southern Africa and the impact of this on the groundwater regime.

The specific objectives of the proposed study are to:

- e. O Southern Africa;
- f. Establish the effect of paleoclimatic changes effect on the groundwater quality
- g. Model water chemistry changes and explain the mechanism driving these changes; and
- h. Develop a conceptual model linking paleoclimatic changes and changes in water chemistry in this environment.

7.3 Regional setting and basin development

After the break-up of Gondwana, Southern Africa formed a passive continental margin along the Atlantic coastal margins, and a gently down warped interior basin (Ollier, 1985, Thomas and Shaw, 1991a). Offshore sedimentary data along the southern African west coast (Dingle *et*

al., 1983, Moore and Larkin, 2001, McCarthy, 2013) suggests that the Orange River in South Africa (Figure 1) drained the interior of Southern Africa to the west at the time or at least shortly after the breakup of Gondwana in the Late Jurassic-Cretaceous. Consequently, sedimentation may not have been initiated by the escarpment flexure at the time of break-up, but rather linked to the later Etosha-Griqualand-Transvaal (EGT) axis (Mid-Upper Cretaceous) and the Late Neogene Okavango-Kalahari-Zimbabwe (OKZ) axes (Moore, 1999, Moore *et al.*, 2009). These tectonic axes are shown in Figure 1. The formation of the OKZ and EGT is attributed to the propagation of the east African Rift Valley into Southern Africa (McCarthy, 2013). The formation of EGT and later OKZ created a closed basin system with active sedimentation depositing weathered sediments from the underlying Karoo Formation depositing mostly fluvio-lacustrine sediment today referred to as the Kalahari Basin (Thomas and Shaw, 1991a). The Kalahari covers seven countries of Southern Africa namely; Angola, Congo DRC, Zambia, Zimbabwe, Namibia, Botswana, and South Africa (Figure 7.1).

The restricted drainage within the OKZ formed a mega-lake system referred to as the Palaeo-Lake Deception (PLD) reaching a shoreline elevation 995-1000 m amsl. Further, this is assumed to have been in the Pliocene, 3-2.5 Ma (McFarlane and Eckardt, 2006, Moore *et al.*, 2012). Digital elevation data from SRTM showing the 995 m amsl is shown in Figure 1 above. Tectonic disruption along the Linyanti-Chobe faults formed the PLM (Figure 1) probably around 1.4 Ma (Moore *et al.*, 2012); it captured the Cubango-Cuito-Okavango, Kwando-Linyanti-Chobe and Zambezi River (Du Toit, 1927, Cooke, 1980, Nugent, 1990, Moore and Larkin, 2001, Moore *et al.*, 2012). Other prominent lake stages of the PLM are 936 m amsl (Palaeo-lake Thamalakane (PLT), 920 and 912 m amsl (Moore and Larkin, 2001, Moore *et al.*, 2012). At 936 m amsl, river contributions to the lake include, the Zambezi, Cuando and Okavango Rivers, whereas, at 920 m amsl, it was sustained by reduced inputs from the Zambezi, Cuando and Okavango. Finally at 912 m amsl, the lake was sustained by the Okavango and Cuando rivers; tectonic activities between 100 ka to present, led to formation of a full graben structure after down throw (400-700 m) bound by the Gumare and Thamalakane faults (Modisi *et al.*, 2000, Kinabo *et al.*, 2007, Kinabo *et al.*, 2008, Milzow *et al.*, 2009, Bufford *et al.*, 2012) forming the Okavango Delta and Boteti River (Figure 2). Progressive desiccation of the Makgadikgadi Pans (Sua and Ntwetwe salt pans) was the result. PLM is composed of several subbasins hosted in a fluvial-lacustrine depression (Thomas and Shaw, 1991a) known as the Makgadikgadi-Okavango-Zambezi Basin – MOZB (Ringrose *et al.*, 2005) as outlined in Figure 7.2.

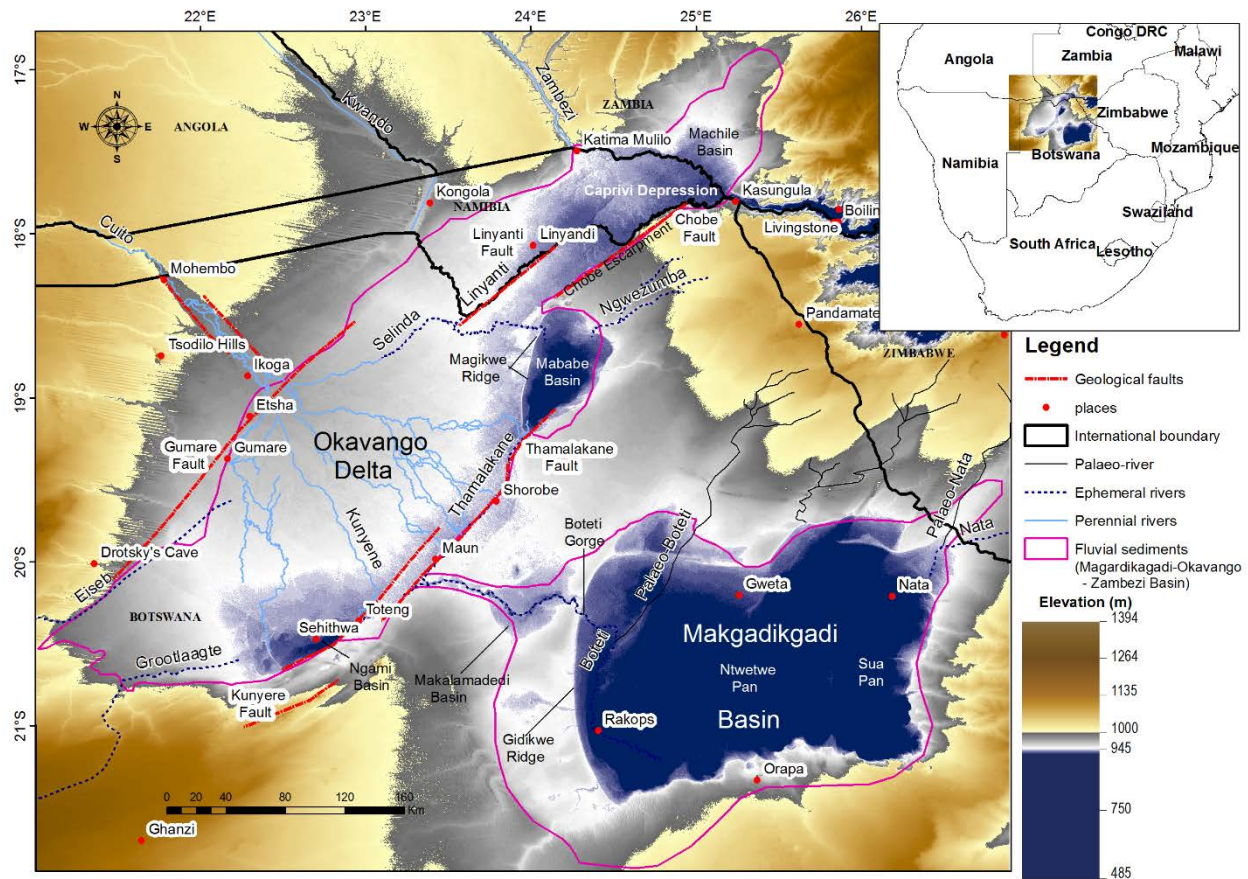


Figure 7.2: Digital elevation model (Shuttle Radar Topographic Mission – SRTM) exhibiting structural depressions of the northern and central Kalahari with geographic references

NB: Fluvial-lacustrine sediments (Pink outline) known as the Makgadikgadi-Okavango-Zambezi Basin – MOZB (Ringrose et al., 2005) host the palaeo-lakes.

7.4 Methodology

The assessment evaluated literature from peer-reviewed publications from search engines that include web of science, google scholar and Scopus. This was followed by a process of screening for eligibility and exclusion using key words reducing the number of articles of interest from over 1500 to 168. These articles were then further classified into various thematic topics to ensure adequate discussion.

7.5 Results

7.5.1 Geology and geochronology

Surficial geology within the MOZB is mainly composed of the Kalahari Group formations and outcrops of Karoo (Stromberg basalts) and Basement formations (Purdy and MacGregor, 2003) as shown in Figure 7.3. Due to the lack of exposed outcrops and consistently datable fossils or mineralogical records in the Kalahari Group formations, a lithological approach is recognised

for defining hydrogeological units (Thomas and Shaw, 1991b). Lower Kalahari Group units include; conglomerates and gravel units which sporadically occur at the base of the Lower Kalahari Group and occasionally within the units; pink to red, fine-grained, homogenous marls/clays; varicoloured, sandstones; calcretes, silcretes and other duricrusts. The Upper Kalahari Group is composed mainly of aeolian sands, colluvium, alluvial/deltaic sands, interbedded alluvium, sand, silt and clay (Thomas and Shaw, 1991b). Given that much of the Kalahari Group occurrence is less than 100 m thick within MOZB (Haddon and McCarthy, 2005), the lithological classification rather than lithostratigraphy has been widely applied to hydrogeological investigations, where the focus has largely been on recharge studies (we discuss this later in this report). Sediment ages have been measured using various materials (fluvial sediments, calcretes and fossils) with ages such as 15.4-11.5 ka BP (using shells, see Table 7.1 for references) at Caprivi Strip, fluvial sediments at Okavango Delta (146-15.5 ka BP, references in Table 7.1), and Mababe Basin with calcretes of ages 25-13 ka BP. Interpretation of sediment age has to be done with caution as the dating material including calcretes, fossils (typically shells) and speleothems represent different phases of hydrological regimes with varying palaeo-environmental conditions (Thomas and Shaw, 1991b). Stromberg Basalt and Karoo at Orapa and Serowe (further than MOZB) have ages 180-178 Ma and 305-283 Ma, respectively (Table 7.1).

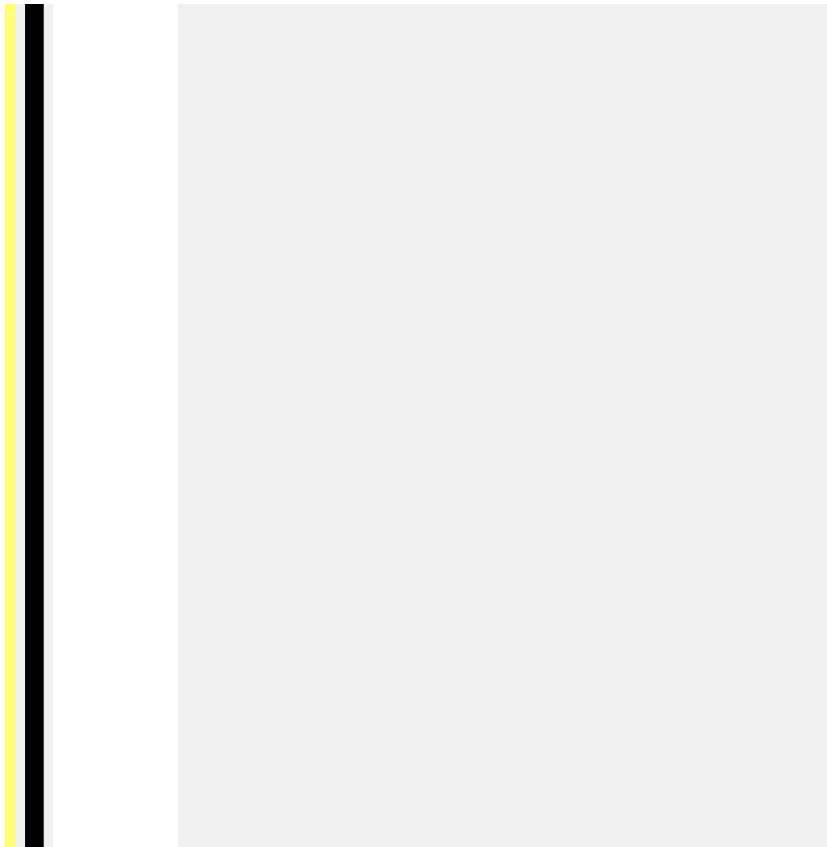


Figure 7.3: Surficial geology over the Makgadikgadi-Okavango-Zambezi Basin and the main structural fault systems

NB: Typically, the basin is covered by Pliocene Kalahari Group formations within outcrops of Stromberg basalts and undifferentiated Karoo in the fringe region (Kasane and Orapa regions) (adapted from Purdy and MacGregor, 2003). The number references are used in Table 7.1.

Geochronology in the MOZB has been determined using radiocarbon and Optically Stimulated Luminescence (OSL) dating on sediments, fossils, and sinter formations (such as speleothems). The oldest dated sediments in the basin are from the Machile Basin (up to 50 m bgl) and Palaeo-Shoreline sediments (< 2.5 m bgl) of Makgadikgadi Salt Pans (Sua Pans), using OSL, not younger than c. 300 Ka; this is the age limit of OSL method (Cordier *et al.*, 2012) and hence sediment may be much older and speculated to be 1.4 Ma (Moore *et al.*, 2012).

Table 7.1: A synthesis tabular matrix of sediment and groundwater ages within MOZB. Groundwater ages are younger (< 50 ka) compared to the sediment suggestive of groundwater infiltration after sediment deposition.

Site (location in Figure 2)	Sediment					Groundwater		References
	Material	Location Coordinates	Sampling Depth	Methods	Age	Method	Age	
Machile Basin (1)	Fluvial sediments	25.043 E -17.4899 S	~50 m	OSL	> 300 ka ⁽¹⁾	¹⁴ C	C.12-1.5 Ka ⁽²⁾	Banda (2015)
Caprivi strip (2)	Shell (spp Lymnaeae)/ Calcretes	24.4008 E -17.7393 S	~1.5 m to the surface	¹⁴ C	15.4-11.5 Ka BP ⁽¹⁾	¹⁴ C	C.15-3 Ka BP ⁽²⁾	⁽¹⁾ Shaw and Cooke (1986), Shaw and Thomas (1988), Thomas and Shaw (2002). ⁽²⁾ Margane <i>et al.</i> (2005)
Okavango Pan region (3)	Fluvial sediments	21.815 E -18.6656 S	~6 m to the surface	¹⁴ C	17-15 Ka BP ⁽¹⁾	¹⁴ C	C.15-1.7 Ka BP ⁽²⁾	⁽¹⁾ Nash <i>et al.</i> (1997) Thomas <i>et al.</i> (2003) ⁽²⁾ Vogel and Van Urk (1975)
Drotskys' Cave (4)	Stalagmites (Sinister developments)	21.917 E -20.2818 S	Cave ingrowth	¹⁴ C and Th/U	50-43 ka, 38-35 ka, 31-29 ka, 26-21 ka, 19-14 ka, 12.5-11 ka,	¹⁴ C	C.16-1.6 Ka BP ⁽²⁾	⁽¹⁾ Cooke and Verhagen (1977), Cooke (1984), Shaw and Cooke (1986), Thomas and

Site (location in Figure 2)	Sediment					Groundwater		References
	Material	Location Coordinates	Sampling Depth	Methods	Age	Method	Age	
					6.9-2.6 ka, 1.6-0.5 ka ⁽¹⁾			Shaw (2002), ⁽²⁾ Cooke (1975)
Lake Ngami Basin (5)	Calcretes ⁽¹⁾ Palaeo-shorelines ^(1b)	22.9858 E -20.4604 S	~3.5 m to the surface	¹⁴ C ⁽¹⁾ OSL ^(1b)	23.9-1.5 ka BP ⁽¹⁾ 140-3 ka BP ^(1b)			^(1a) Shaw (1985a) ^(1b) Shaw <i>et al.</i> (2003) Burrough and Thomas (2009)
Okavango Delta (6)	Fluvial sediments	23.5348 E -19.8315 S		Sedimentation Rates	146-15.5 Ka BP ⁽¹⁾	Groundwater Modelling	C.36-8.6 Ka BP ⁽²⁾	⁽¹⁾ Heine (1978) McCarthy <i>et al.</i> (2012) ⁽²⁾ McCarthy & Metcalfe (1990), Langer and Heusser (2004)
Orapa Region (7)	Stromberg basaltic minerals	25.2632 E -21.3341 S	Outcrops	⁴⁰ Ar/ ³⁹ Ar	180.9-178.3 Ma ⁽¹⁾	¹⁴ C	C.30-2 Ka BP ⁽²⁾	⁽¹⁾ Duncan <i>et al.</i> (1997), Le Gall <i>et al.</i> (2002), Jourdan <i>et al.</i> (2004), Jourdan <i>et al.</i> (2005). ⁽²⁾ Stadler (2005), Foster <i>et al.</i> (1982), Mazor <i>et al.</i> (1977)

Site (location in Figure 2)	Sediment					Groundwater		References
	Material	Location Coordinates	Sampling Depth	Methods	Age	Method	Age	
Makgadikgadi Salt Pans (Sua Pans) (8)	Calcrete and shells ⁽¹⁾ Fluvial sediments ^(1b)	25.9548 E -20.5632 S	~2.5 m to the surface	¹⁴ C ⁽¹⁾ OSL and TL ^(1b)	40.8-21.9 ka BP ⁽¹⁾ 288-8 ka BP ^(1b)			⁽¹⁾ Heine (1978), Cooke and Verstappen (1984), Riedel <i>et al.</i> (2012), Riedel <i>et al.</i> (2014) ^(1b) Ringrose <i>et al.</i> (2005), Burrough <i>et al.</i> (2009a)
Serowe region (9)	Karoo Sediments	26.6854 E -22.3734 S	~40 m	U-Pb	305-283 Ma ⁽¹⁾	¹⁴ C Argon-38	C.40-0.5 Ka BP ⁽²⁾	⁽¹⁾ Bangert <i>et al.</i> (1999) ⁽²⁾ Selaolo (1998) Kulongoski <i>et al.</i> (2004)
Mababe Basin (10)	Calcrete and shells ⁽¹⁾ Fluvial sediments ^(1b)	26.6854 E -22.3734 S	~7 m to the surface	¹⁴ C ⁽¹⁾ OSL ^(1b)	25-13 ka BP ⁽¹⁾ 35.6-5 ka BP ^(1b)			⁽¹⁾ Shaw (1985b), Shaw and Cooke (1986) Thomas and Shaw (1991b) ^(1b) Teter (2007), Burrough and Thomas (2008), Burrough and Thomas (2009)
Boteti region (11)	Calcrete and shells ⁽¹⁾	24.4286 E -20.8373 S	~6 m to the surface	¹⁴ C ⁽¹⁾ OSL ^(1b)	42-12 ka BP ⁽¹⁾ 109-8 ka BP ^(1b)	Groundwater modelling	C.12-7.5 Ka BP ⁽²⁾	⁽¹⁾ Heine (1978), Cooke and Verstappen (1984), Thomas and Shaw

Site (location in Figure 2)	Sediment					Groundwater		References
	Material	Location Coordinates	Sampling Depth	Methods	Age	Method	Age	
	Fluvial sediments ^(1b)							(1991b), Shaw <i>et al.</i> (1992), Shaw <i>et al.</i> (1997), Burrough <i>et al.</i> (2009a), Riedel <i>et al.</i> (2009), Riedel <i>et al.</i> (2014) ⁽²⁾ De Vries (1984)

7.5.2 Recharge and stable isotopes

The occurrence of groundwater recharge from rainwater (direct recharge) through the Kalahari sediments has been a controversial issue (Obakeng, 2007). Some investigators have concluded that no rainfall infiltration was occurring in the Kalahari due to seasonal moisture retention in the sands and complete loss by subsequent evapotranspiration (Van Straten, 1955, Farr *et al.*, 1981, Foster *et al.*, 1982, De Vries and Von Hoyer, 1988). Further, De Vries (1984) substantiated this view point through a numerical study of declining regional groundwater level since the last pluvial period-palaeo recharge (12 Ka) and concluded that present day discharge was at the most 1 mm/yr thus more or less a stagnant groundwater system. However, evidence of substantial rain recharge through the Kalahari sands emerged from a variety of tracer studies including: Jennings (1974), Mazor *et al.* (1974), Verhagen *et al.* (1974), Mazor *et al.* (1977), Mazor (1982), Verhagen (1990), Verhagen (1992), Beekman *et al.* (1996), Beekman *et al.* (1997), Selaolo (1998), Beekman *et al.* (1999), De Vries *et al.* (2000), and Magombedze *et al.* (2004). In addition, Osenbrück *et al.* (2009) argues higher recharge during wet climatic periods (>30-20 ka and 8-4.5 ka) in the Kalahari sands in the past based on the atmospheric contamination of noble gas isotopes ($^{20}\text{Ne}/^{22}\text{Ne}$) in the groundwater around Serowe (see Figure 2 for location). Other studies within the Kalahari Basin also support recharge during the glacial periods preserving low temperature groundwater up to 5 °C lower than current temperature (Vogel, 1982, Stute and Talma, 1998, Kulongoski *et al.*, 2004). Obakeng (2007) showed that the current substantial recharge is removed from the saturated zone through extraction by deep rooted trees as hypothesised by De Vries *et al.* (2000) and what is hosted in the aquifers is Paleo water.

Given the primary role of evapotranspiration on both surface and groundwater within MOZB, stable isotopes (^{18}O and ^2H) studies (Dincer *et al.*, 1978, Verhagen, 1995, Margane *et al.*, 2005, McCarthy *et al.*, 2012, Banda, 2015) are compiled to assess if stable isotope signature in groundwater would indicate palaeo or recent recharge and evaporation effects as shown in Figure 4. Surface water from the Okavango Delta has ^{18}O , -5 to -3 ‰, and ^2H , -30 to -20 ‰ indicative of isotopic fractional effects. It has been shown that with increasing electrical conductivity (EC) of the Okavango surface water, the range of ^{18}O becomes narrower indicative of evapotranspiration effects resulting in increased accumulation of solutes (McCarthy *et al.*, 1986, McCarthy and Metcalfe, 1990, McCarthy *et al.*, 1991, McCarthy, 1992, McCarthy *et al.*, 1993, McCarthy and Ellery, 1994, McCarthy and Ellery, 1998, McCarthy, 2006, Ramberg and Wolski, 2008, McCarthy *et al.*, 2012).

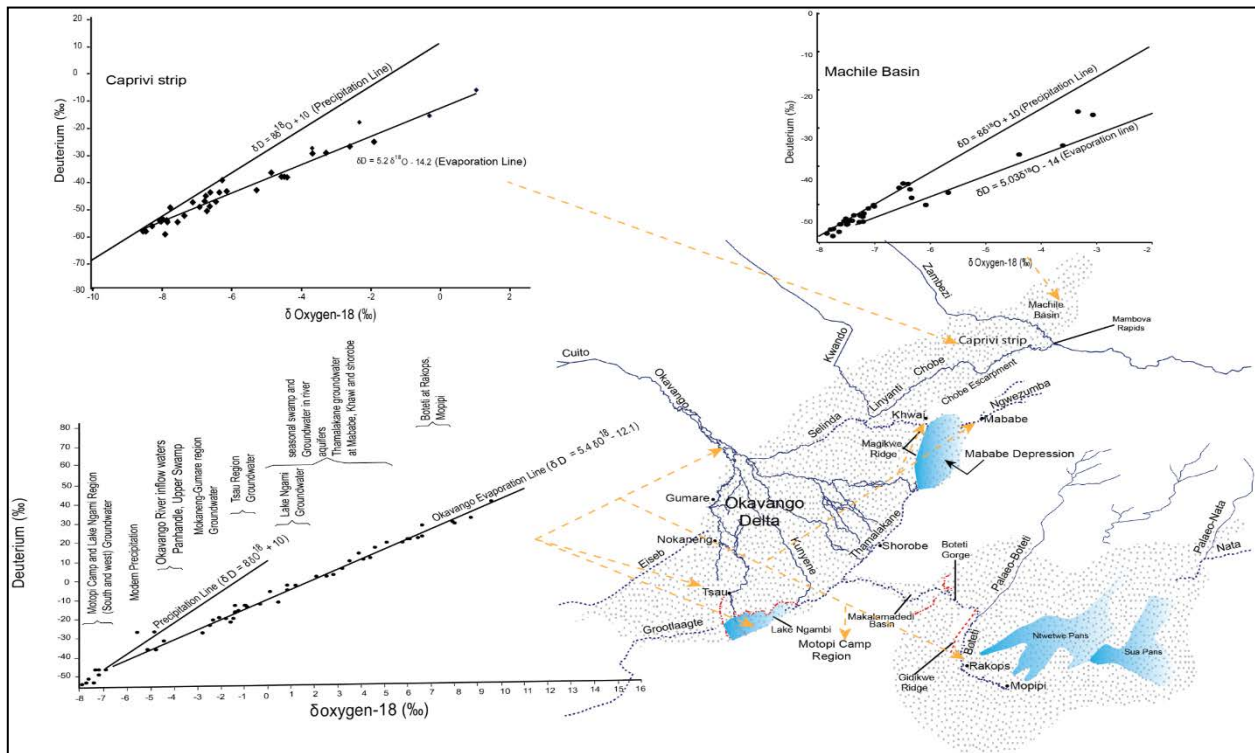


Figure 7.4: Synthesis of stable isotope of Oxygen-18 and Deuterium

The groundwater has ^{18}O , -60 to 10 ‰, and ^2H , -9 to 10 ‰ of which some of the isotopes are on the global precipitation line ($\delta\text{D} = 8\delta^{18}\text{O} + 10$) and evaporation lines (slope approximately of 5) as shown in Figure 7.4. Long-term precipitation data from the nearest global monitoring stations in Windhoek, Namibia and Harare, Zimbabwe indicate a weighted average of -5.03 ‰ and -6.14 ‰ for ^{18}O , -24.5 ‰ and -32.4 ‰, ^2H , respectively (International Atomic Energy Agency, 1992). We suggest the groundwater isotopes on the precipitation line have undergone evaporation under varied humidity conditions, which influences precipitation variability. Gonfiantini (1986) suggests a gradient of 8 in a $\delta^2\text{H}-\delta^{18}\text{O}$ plot, represents a high relative humidity (>95%), indicative of low potential evaporation effects. The evaporation slope (5) suggests a relative humidity of 75% with higher evaporation. All the groundwater isotopes have thus sustained evaporation prior to infiltration. Table 7. 1: A synthesis of stable isotope of Oxygen-18 and Deuterium (Dincer *et al.*, 1978, Margane *et al.*, 2005). Groundwater isotopes in MOZB therefore represent rapid infiltration (precipitation line) and minor evaporation loss (up to 25%) for those on the evaporation line (slope of 5). Stable isotopic variability and mineralisation processes have also been accounted for by considering EC or total dissolved solids (TDS). Consequently, high EC but low fractionation within the Okavango Region (evapotranspiration effects; Dincer *et al.*, 1978, McCarthy *et al.*, 2012), high EC and high fractionation especially in the fringe regions such as Boteti River (evaporation; Verhagen, 1995) and high EC but relatively low fractionation such as within Lake Ngami, Caprivi Strip and Machile (mineral leaching/ dissolution; Verhagen, 1995, Margane *et al.*, 2005, Banda *et al.*, submitted 2015). Stable isotopes (Figure 4) has shown that it is not possible to categorise groundwater into a palaeo and recent recharge signature within MOZB as there seems to be

some meteoric water influence that corroborate with recharge studies. Further, surface water contribution from the Okavango Delta does not interact with the regional groundwater and is predominantly lost to evapotranspiration. Several studies have demonstrated these hydrological processes in the Okavango Delta (McCarthy and Metcalfe, 1990, McCarthy *et al.*, 1991, Bauer, 2004, Bauer *et al.*, 2006a, Bauer *et al.*, 2006b, Milzow *et al.*, 2009, Kgotlhang, 2008, McCarthy *et al.*, 2012).

7.5.3 Groundwater ages

Groundwater ages are measured using ^{14}C with age ranges from 16-1.6 ka BP for Machile, Caprivi Strip, Okavango Pan Region, and Drotskys' Cave. Groundwater modelling for the Okavango Delta and Boteti Region suggest ages of 36-8.6 ka and 12-7.5 ka, respectively as shown in Table 1. The oldest groundwater ages are from Orapa and Serowe and found to be between 40-0.5 ka BP (references as per Table 1). In general, sediment ages within MOZB from the studies reviewed indicate that sediment are much older (> 300 ka) compared to groundwater ages; this includes lake sediments as well as of rock out crops outside the MOZB. Calcretes (Table 1) are interpreted to have formed under saltpan or playa conditions and are indicative of periods of low groundwater levels (Thomas and Shaw, 2002, Nash and McLaren, 2003). Drotskys' cave speleothems are inferred to have been sustained by groundwater (Cooke and Verhagen, 1977) and hence a proxy for Paleoclimatically induced recharge during humid conditions. Groundwater ages are between the Late Pleistocene to Holocene (< 50 ka) within MOZB and the rim regions including Orapa and Serowe with Karoo sediments. The age difference between the sediment (>300 ka) and groundwater (< 50 ka) suggests the occurrence of groundwater salinity (discussed later in the paper) is therefore not due to burial of Paleolake water, but other processes such as sediment leaching, evaporation, and evapotranspiration effects.

7.5.4 Groundwater chemistry

Groundwater exploration and development in the MOZB region is restricted to geophysical techniques probably owing to the thick fluvio-lacustrine sediments with little or no outcrops and widespread occurrence of high salinity groundwater (Linn *et al.*, 2003); the principal aim has been to locate fresh groundwater resources. Geophysical surveys have used ground and air-borne electrical methods to map both sediments and groundwater quality (fresh, brackish and saline); the groundwater classification ranks into three categories as fresh (Total Dissolved Solids (TDS) $< 1,000$ mg/L), brackish ($1,000 < \text{TDS} \leq 10,000$ mg/L) and saline (TDS $> 10,000$ mg/L) water (Freeze and Cherry, 1979). Table 2 summarizes the lithologies, formation resistivities and methods used within MOZB. Air-borne Electro-Magnetic (AEM) and ground-based Time Domain Electromagnetic surveying (TDEM) have essentially been used at a regional scale (references are shown in Table 2). These geo-electrical methods provide insights on aquifer variability and dimensions in the shallow and deeper levels. Geophysical resistivities within MOZB of clay is $<3 \Omega\text{m}$, clayey sands and sands, 3-10 Ωm are typically saturated with

saline and brackish water, respectively; fresh water resistivities typically occur in sands with values of 10-50 Ωm (Table 7.3 and Figure 7). Figure 7 outline the areas of geophysical mapping and cross sections from the various researchers (Sattel and Kgotlhang, 2004, Margane *et al.*, 2005, Campbell *et al.*, 2006, Podgorski *et al.*, 2013, Chongo *et al.*, 2014). Site 5, 6 and 7 shows a moderate resistivity (3-10 Ωm) occurring between a high resistivity (20-100 Ωm) below and a low resistivity ($< 3 \Omega\text{m}$) formation above, which is a signature from the underlying Karoo Formation (Sattel and Kgotlhang, 2004) as shown in Figure 7. This is probably attributed to tectonic disruptions that the basin has sustained. However, other authors specifically within site 3 – Okavango Basin (Podgorski *et al.*, 2013) interpret the high resistivity formation (20-100 Ωm) to be remnants of the proto-Okavango Megafan (Figure 7). The Proto-Okavango Megafan is suggested to have been initiated during the period of the PLD (3-2.5 Ma) (Moore *et al.*, 2012, McCarthy, 2013). The low resistivity unit ($< 3 \Omega\text{m}$) hosting saline groundwater just below the modern day Okavango Delta covers (10-50 Ωm) is interpreted as an extension of saline sediments from the PLM (Podgorski *et al.*, 2013) but mostly likely at higher level stage.

Table 7.2: Synthesis tabular matrix of regional resistivities, methods and hydrogeological interpretations in the MOZB. Resistivities are generally homogenous and have been resolved to both sediment and water quality (<3 Ωm (saline/clay), 3-10 Ωm (brackish, clayey sands), 20-100 Ωm (fresh in Basement – fresh/weathered))

Site (location number as shown in Figure4)	Lithology	Formation Resistivity (Ohm-meter: Ωm)	Method	Reference
Machile Basin (1)	Upper Kalahari (surface sands) Middle Kalahari (sand, silt, and clay) Stormberg Basalt	< 3 Ωm (Saline/clay) 3-10 Ωm (Brackish) 20-40 Ωm (Dry Kalahari sands) 20-100 Ωm (Basement rocks)	AEM TDEM	Chongo <i>et al.</i> (2011) Chongo <i>et al.</i> (2014)
Caprivi Strip (2)	Upper Kalahari (surface sands) Middle Kalahari (sand, silt, and clay)	< 3 Ωm (Saline/clay) 5-10 Ωm (Brackish) 10-50 Ωm (Fresh)	TDEM	Margane <i>et al.</i> (2005)
Okavango Delta (3)	Upper Kalahari (surface sands) Middle Kalahari (sand, silt, and clay)	<15 Ωm (Brackish-Saline), 15-40 Ωm (Fresh), >40 Ωm (Basement rocks)	AEM TDEM	Bauer (2004) Bauer <i>et al.</i> (2006c) Kgotlhang (2008) Podgorski <i>et al.</i> (2013) Meier <i>et al.</i> (2014)
Thamalakane Region (4)	Upper Kalahari (surface sands) Middle Kalahari (sand, silt, and clay)	<3 Ωm (Saline/clays) 3-8 Ωm (Brackish) 9-30 Ωm (fresh)	TDEM, AEM	Campbell <i>et al.</i> (2006)

Site (location number as shown in Figure4)	Lithology	Formation Resistivity (Ohm-meter: Ωm)	Method	Reference
South of Thamalakane Region (5)	Upper Kalahari (surface sands) Middle Kalahari (sand, silt, and clay)	< 3 Ωm (Saline/clay) 3-10 Ωm (Brackish) 20-40 Ωm (Dry Kalahari sands) 40-100 Ωm (Basement rocks)	AEM	Sattel and Kgotlhang (2004)
South of Gidikwe (6)	Karoo Group	< 3 Ωm (Saline/clay) 3-10 Ωm (Karoo mudstone) 20-40 Ωm (Dry Kalahari sands) 20-100 Ωm (Basement rocks)	AEM	Sattel & Kgotlhang (2004)
Rakops Region (7)	Middle Kalahari (sand, silt, and clay) Karoo Group	< 3 Ωm (Saline/clay) 3-10 Ωm (Karoo mudstone) 20-40 Ωm (Dry Kalahari sands) 20-100 Ωm (Basement rocks)	AEM	Sattel & Kgotlhang (2004)
Mopipi Region (8)	Upper Kalahari (surface sands) Middle Kalahari (sand, silt, and clay)	3 Ωm (Saline/clay) 3-10 Ωm (Brackish) 20-40 Ωm (Dry Kalahari sands) 20-100 Ωm (Basement rocks)	AEM	Sattel & Kgotlhang (2004)
Orapa Region (9)	Upper Kalahari (surface sands) Middle Kalahari (sand, silt, and clay)	< 3 Ωm (Saline/clay) 3-10 Ωm (Brackish) 20-40 Ωm (Dry Kalahari sands) 20-100 Ωm (Basement rocks)	AEM	Sattel & Kgotlhang (2004)

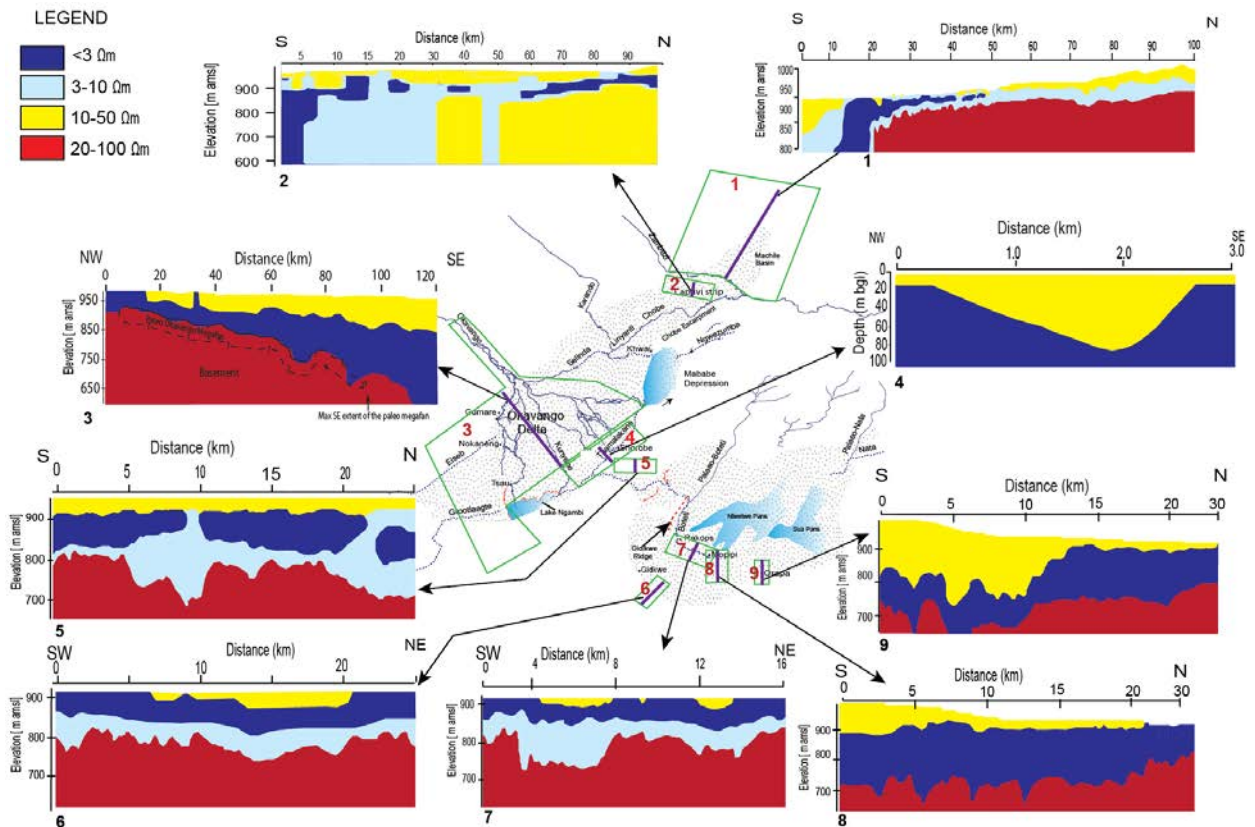


Figure 7.5: A synthesis of the regional resistivity profiles within MOZB conducted using both ground and air based geophysics (Sattel and Kgotlhang, 2004, Margane et al., 2005, Campbell et al., 2006, Podgorski et al., 2013, Chongo et al., 2014). Geo-electrical methods (AEM and TDEM) are able to constrain and resolve PLM resistivities ($<15 \Omega m$ (near surface), 3-10 Ωm (intermediate depths), 20-100 Ωm (Basement depths).

The depth to the interface from low to high resistivities (saline to fresh groundwater), although well resolved, cannot be generalised and is rather specific to which part of MOZB is mapped but ranges from 10-80 m bgl (Figure 7.5). Fresh groundwater potential exists in the near surface as perched aquifers (10-50 Ωm) linked to surficial drainages such as rivers, wetlands, alluvial deltaic features, or palaeo-drainage, whereas brackish-saline groundwater is well spread throughout the basin predominately related to the Basement geology. However, the geophysical model (site 6 and 7; Sattel and Kgotlhang, 2004), delineates resistivities of 3-10 Ωm just below an impervious saline layer ($< 3 \Omega m$), this was interpreted as a sandstone formation within the Karoo Formation (Mosolotsane Formation; (Sattel and Kgotlhang, 2004), that hosts fresh water. Conversely, high salinity formations, mapped within the Orapa Region (site 9, Figure 7.5) were interpreted as deep sediments (mudstone, shales and sandstones) of the Karoo Formation (Ecca Group; (Sattel and Kgotlhang, 2004) and suggests an extension of high salinity groundwater beyond the MOZB. Ecca Group sediments are suggested to be the origin of high salinity water in salt-pans widespread in Southern Africa (Seaman et al., 1991, Day, 1993).

7.5.5 Hydrochemistry

Groundwater chemistry was compiled from various researchers (Mazor *et al.*, 1980, McCarthy *et al.*, 1991, Klock, 2001, Vogel *et al.*, 2004, Margane *et al.*, 2005, McCarthy, 2006, Bäumle *et al.*, 2007, Eckardt *et al.*, 2008, Stadler *et al.*, 2008, Banda *et al.*, submitted 2015) with a background of PLD and PLM outlines (Figure 8a); water quality types are carbonates (Ca-Mg-HCO₃/Na-Ca-HCO₃), sulphate (Na-Cl-SO₄) and chloride (Na-SO₄-Cl). Carbonate groundwater occurs within the Okavango Delta and the fringe region with active groundwater recharge; carbonate groundwater within the Okavango Delta has concentrations from 300-6,500 mg/L precipitating trona (NaHCO₃.Na₂CO₃. 2H₂O) on the surface because of evapotranspiration losses within the salt pans/saline islands (McCarthy *et al.*, 1986, McCarthy *et al.*, 1991, McCarthy and Ellery, 1994, McCarthy and Ellery, 1998, McCarthy *et al.*, 1998). In addition, chloride concentrations range from 5 to 6,500 mg/L and sulphate 5 to 2,000 mg/L within the Okavango Delta (McCarthy *et al.*, 1986, McCarthy and Metcalfe, 1990, McCarthy *et al.*, 1991, McCarthy and Ellery, 1994, McCarthy, 2006). In the northern margin of MOZB, Machile and Caprivi Strip, groundwater concentrations include: sulphate (280-10,600 mg/L), chloride (150-5,500 mg/L) and carbonate (290-2,300 mg/L) (Margane *et al.*, 2005, Banda *et al.*, submitted 2015). In other parts, Mababe, Makalamabedi and Ngami Basin, groundwater concentrations include: sulphate (70-4,000 mg/L), carbonate (360-2,500 mg/L) and chloride (30-2,200 mg/L) (Mazor *et al.*, 1980, Aquatec, 1982). The Makgadikgadi salt pans (Sua and Ntwetwe pans) have groundwater concentrations including: chloride (46,000-5,300,000 mg/L), sulphate (4400-1,550,000 mg/L) and carbonate (6,000-1,150,000 mg/L) with mineral precipitates of mirabilite (NaSO₄.10H₂O), halite (NaCl) and trona (NaHCO₃.Na₂CO₃.2H₂O) (Vogel *et al.*, 2004, Eckardt *et al.*, 2008, Wood *et al.*, 2011).



Figure 7.6: Water quality sampled points over the MOZB with a background of lake stages at 995 and 945 m amsl, with corresponding ages of 3-2.5 and 1.4 Ma, respectively (Mazor *et al.*, 1980, Vogel *et al.*, 2004, Margane *et al.*, 2005, Bäumle *et al.*, 2007, McCarthy, 2013)

The spatial variability of groundwater types is such that the chloride water is hosted in the central regions, where the palaeo-lake sediments are thickest, and shifts from sulphate to carbonate towards the fringes and the Okavango Region (Figure 7.6). We suggest the chloride and sulphate water are a result of dissolution of evaporites, which had undergone differential levels of evapo-concentration (Eugster and Jones, 1979). The carbonate water type such as that of the Okavango Region and the fringes is from recent recharge by meteoric water (Stadler *et al.*, 2008, McCarthy, 2013). However, the presence of chloride and sulphate ions in the fringes (south of the Okavango Delta) suggests leaching to the surrounding or underlying formation (Karoo) during the pluvial climatic period given that the Kalahari Group is thinner in this region (1-50 m).

7.6 Discussion

7.6.1 River water chemistry and formation of evaporites

Palaeo-Lake Makgadikgadi (PLM) evolved through a series of five major lake stage changes (~995, 945, 936, 920 and 912 m asl) changing the drainage regime within Southern Africa driven primarily by tectonic disruptions and climatic variability (Moore and Larkin, 2001, Moore *et al.*, 2012). The water budget of the system (Moore *et al.*, 2012) with lake area change from 995 m amsl, 175,400 km² at a potential evaporation loss of ~ 1,000 mm/yr (Moore *et al.*, 2012). The evaporation losses over the different lake phases were an important mechanism for accumulation of solutes within lake water. The contributing river water chemistry (Hall *et al.*, 1977, Balon, 1978, Cronberg *et al.*, 1995, Huntsman-Mapila *et al.*, 2006) was probably not different at the time of formation compared to what we observe today; hydrochemistry is summarised in Table 3. River water interacts with rocks and minerals producing the anion alkalinity, almost exclusively HCO₃ (0.33-1.15 mmol/L), SO₄ (0.002-0.038 mmol/L) and Cl (0.011-0.0625 mmol/L) as shown in Table 3. River water chemistry of the Kafue (Table 3) has a very high sulphate concentration probably from anthropogenic activities and is not considered as potential contribution to the palaeo-lake. Other solute constituents, including Ca (0.1-0.29 mmol/L), Mg (0.037-0.18 mmol/L), Na (0.087-0.367 mmol/L), are leached from aluminosilicate minerals such as plagioclase, biotite, muscovite and hornblende. The average river water chemistry (Table 3) has Ca, 0.162 mmol/L, Na, 0.237 mmol/L, Mg, 0.108 mmol/L, alkalinity, 0.798 mmol/L, Cl, 0.030 mmol/L and SO₄, 0.036 mmol/L.

Table 7.3: The river water chemistry of major rivers (Hall *et al.*, 1977, Balon, 1978, Cronberg *et al.*, 1995, Von Der Heyden and New, 2003, Huntsman-Mapila *et al.*, 2006) that contributed to the palaeo-lake system during various stages of evaporation. The rivers are typically calcium carbonate dominated

River	Site	Ca mmol/L	Mg mmol/L	Na mmol/L	Alkalinity (as HCO ₃) mmol/L	Cl mmol/L	SO ₄ mmol/L
Okavango ^(a)	Pan-handle area	0.102	0.037	0.087	0.334	0.011	0.002
Luangwa ^(b)	Before the confluence with the Zambezi	0.294	0.181	0.293	0.778		0.094
Upper Zambezi ^(c)	Upper Zambezi before the Kariba Dam	0.129	0.151	0.367	1.15	0.063	0.108
Kwando ^(d)	James Camp	0.126	0.071	0.201	0.917	0.015	0.025
Kafue ^(e)	Before the Kafue	8.70	11.03	12.53	0.708		26.96
Average (1, 2, 3, 4)		0.162	0.108	0.237	0.798	0.030	0.036

Sources: ^(a) Huntsman-Mapila *et al.* (2006), ^(b) Hall *et al.* (1977), ^(c) Balon (1978), ^(d) Cronberg *et al.* (1995), ^(e) Von der Heyden and New (2004)

To explore the probable mineral evolution in the evaporative basin as a function of the concentration factor, the geochemical software, PHREEQC 3 (Parkhurst and Appelo, 2013), was used. We assume a situation where a finite volume of lake water evaporates (declining volume) and the sequence of minerals precipitated is calculated by assuming equilibrium for the most probable minerals based on the calculated saturation state of the water. The Pitzer database, included with PHREEQC 3, capable of handling the high ionic strength (Pitzer, 1973, Pitzer, 1975), was used in the calculation. A declining lake volume was assumed because no thick deposits of evaporites were observed within the Makgadikgadi Region. The initial model solution comprised 100 m³, rather than the default volume of 1 litre, to avoid numerical problems as the water is removed (evaporated). The initial model chemistry is the average river inflow water (Table 3). The saturation of evaporite minerals as equilibrium phases (allowed to dissolve and precipitate) is followed for calcite (CaCO₃), magnesite (MgCO₃), gypsum (CaSO₄·2H₂O), bassanite (CaSO₄·½H₂O), anhydrite (CaSO₄), mirabilite (Na₂SO₄·10H₂O), thenardite (Na₂SO₄), bischofite (MgCl₂·6H₂O), bloedite (MgSO₄·Na₂SO₄·4H₂O), burkeite (Na₂CO₃·2Na₂SO₄), carnallite (KMgCl₃·6H₂O), epsomite (MgSO₄·7H₂O), halite (NaCl), hexahydrate (MgSO₄·6H₂O), kieserite MgSO₄·H₂O, sylvite (KCl), gaylussite (Na₂CO₃·CaCO₃·5H₂O), nahcolite (NaHCO₃), thermonatrite (Na₂CO₃·H₂O), natron

($\text{NaCO}_3 \cdot 10\text{H}_2\text{O}$) and trona ($\text{NaHCO}_3 \cdot \text{Na}_2\text{CO}_3 \cdot 2\text{H}_2\text{O}$). In the geochemical modelling, the pH of lake water was buffered by equilibrium with atmospheric PCO_2 of 200 ppm corresponding to the CO_2 partial pressure in the atmosphere of about 1.4 Ma BP during formation. To calculate the concentration factor of the river water, Br was included in the inflow water with a concentration of 10^{-6} mmol/L.

The output from the PHREEQC 3 model (Figure 9a & b) shows that the river precipitates calcite and dolomite first after a 10 times concentration factor. With increased precipitation, solute accumulation increases through a gypsum saturation and precipitation halite after ~50,000 times of concentration. Simulation concentration show Ca, 1.48 mmol/L and alkalinity of 0.731 mmol/L at calcite and dolomite precipitation hence a ratio of 2 Ca:1 alkalinity. The evaporation sequence of the river water can be explained using the Hardie-Eugster Model (Hardie and Eugster, 1970). Figure 10, shows a modified version of the Hardie-Eugster (Drever, 1997) of which we infer based on the 2 Ca:1 alkalinity ratio during calcite and dolomite precipitation, that the evolution of the palaeo-lake system followed path II. The sequence of mineral salts that precipitate follow a chemical divide proposed as shown in Figure 7.8; typically, during evapo-concentration, saturation of alkali earth carbonates is reached quickly (Hardie and Eugster, 1970, Eugster and Jones, 1979, Jankowski and Jacobson, 1989). Subsequent precipitation of silicates, carbonates, sulphates, and chlorides are controlled by the relative concentration of magnesium, calcium, carbonate, sulphate and chloride (Jones *et al.*, 1977, Eugster, 1980, Spencer *et al.*, 1985b). The PHREEQC simulation results (Figure 7.7a & 7.7 b) supports a carbonate river water evolution within the PLM, that endured evaporation, under closed basin conditions, up to halite evaporites particularly in the deepest part of the lake Makgadikgadi Basin.

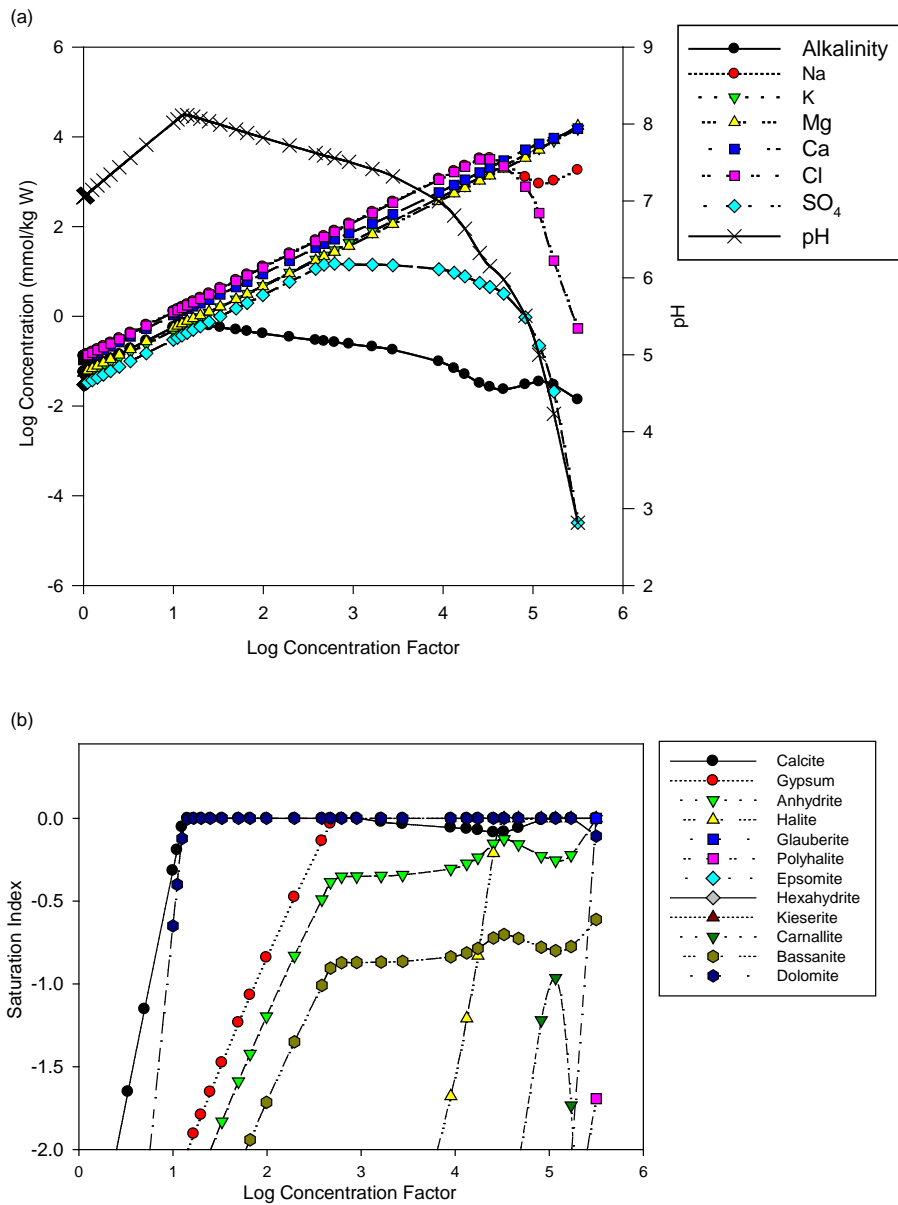


Figure 7.7: (a) PHREEQC 3 simulation of evolving lake chemistry in the closed lake filled with fresh water (Zambezi water) with evaporation and precipitation of minerals.

Concentration factor represents the degree to which the remaining water is concentrated after water is evaporated. Carbonates are precipitated first followed by sulphates in accordance with Eugster's model under closed basin conditions (Hardie and Eugster, 1970). (b) Plot showing the mineral saturation against concentration.

It is probable that the precipitates within MOZB formed during deposition (syn-depositional). The notion is supported with core samples that are intimately intermixed with the detrital fraction as seen in the Machile Basin (Banda, 2015). Similar evaporite mineralogy in the stratigraphic column has been observed in the Sambhar Salt Lake (Sinha and Raymahashay,

2004), Searles Lake (Eugster and Smith, 1965), Great Salt lakes (Bowler, 1986), Ceylone (Last, 1989) and North Ingebrigt (Shang and Last, 1999). However, the PLM endured episodic tectonic activity, periodic flooding and overtopping of shorelines that raised and lowered the drainage divide to allow possible escape of solutes. Hence, chemical differentiation and thus mineral accumulation could have resulted from selective erosion of soluble salts and/or selective precipitation in the basin (Sinha and Raymahashay, 2004); progressive evaporation (Figure 10) would thus not form some subsequent minerals. Consequently, this contributed to hydro-geochemical zoning (Figure 8b) of the mega-lake resulting in a predominately sulphate saturation stage in the fringe zones (such as Caprivi depression and the Machile) and chloride saturation in the central region (Makgadikgadi Basin). Similarly, hydro-chemical zoning has been observed in closed basin salt lakes of Australia (such as Lake George), of which Bowler (1986), postulates that in the drying stages of any flat-floored basin, rapid transfer of salts from the surface to sub-surface occurs. Furthermore, high evaporative loss results in part of the upper waters exceeding sulphate saturation hence gypsum is precipitated interstitially. Finally, evaporative loss through the capillary fringe results in efflorescence of the more soluble salts, halite, in the central zone, provided groundwater evaporation/evapotranspiration at the margins (described as stage 4 of chemical accumulation; Bowler (1986) takes place. In this regard, we suggest that the chloride probably is a result of groundwater discharge with progressive evaporation and sulphate is an imprint of evapo-centration in the initial phases of lake development desiccation.

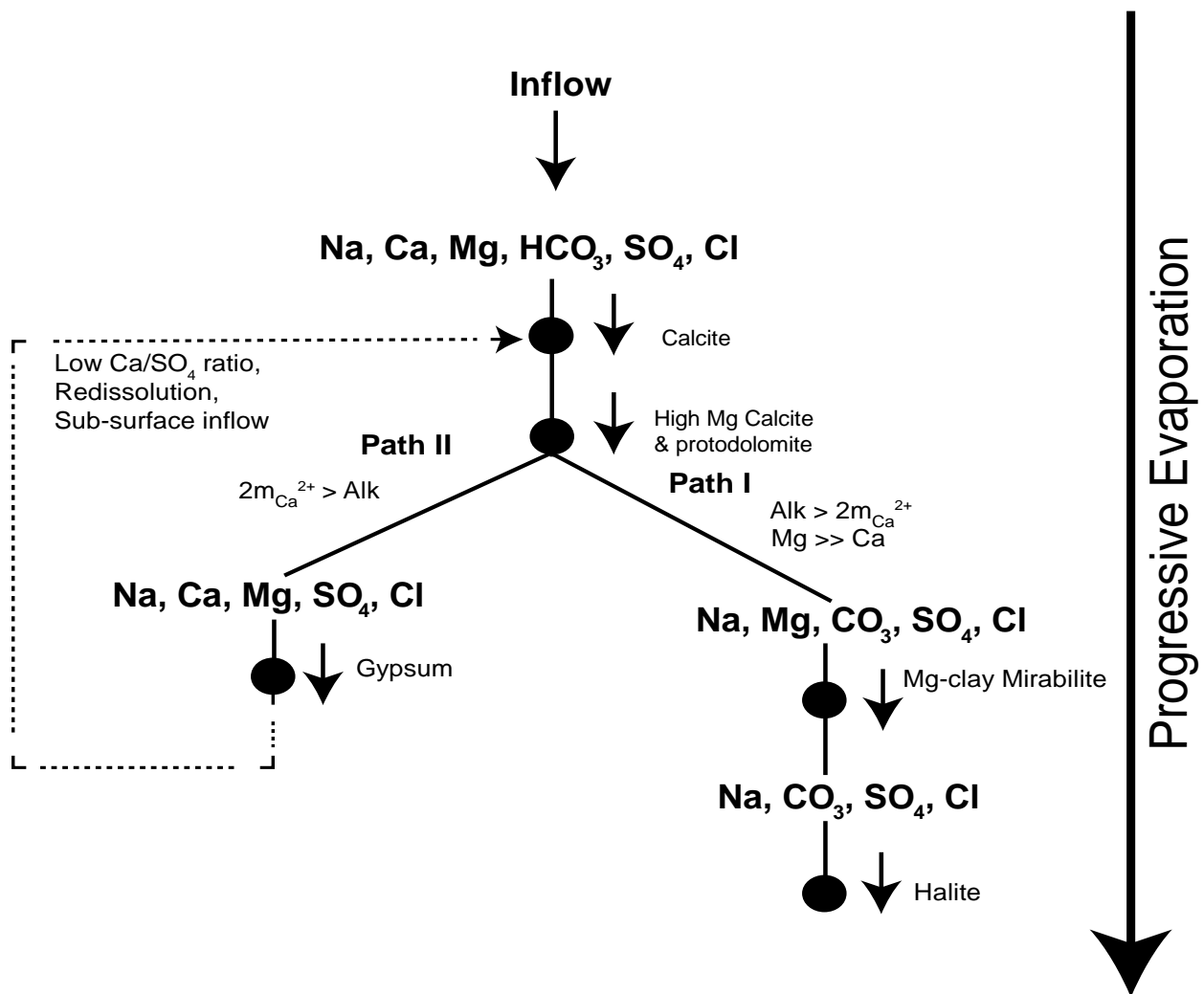


Figure 7.8: Evaporation path of closed lake system of solutes with progressive evapo-concentration (Source: Eugster and Hardie, 1978).

NB: Halite precipitation is typically at the last to form but the most soluble whereas, the least soluble, typical carbonates, will form first.

7.6.2 Conceptual lake stage development and groundwater salinity

We suggest the development of groundwater salinity based on evidence from earlier sections (geochronology, groundwater ages, Paleoclimatics and recharge) is shown in the conceptual model of Figure 11. The evolution steps indicate initially the formation of the PLD (3-2.5 Ma) within a closed basin sustained by surface water contribution, and later PLM (1.4 Ma) shown as stage 1 and 2, respectively, driven by tectonics and climate. Reduced flow from 88-66 km³/yr to the lake system after tectonic disruptions was balanced to evaporation of approximately from 946-395 mm/yr (Shahin, 2002, Moore *et al.*, 2012); the main contributing river was the Zambezi, Okavango, Kwando and Kafue rivers (Moore and Larkin, 2001, Moore *et al.*, 2007, Moore *et al.*, 2012). In stage 3, most of the PLM desiccated by 500 ka, during which groundwater influence probably was profound. Stage 4, progressive evapo-concentration led

to rapid surface water-groundwater exchange precipitating carbonates (calcite and dolomite). Increased capillary fringe evaporation losses created a density flow at the discharge zone at the fringes hence precipitating gypsum. Increased evaporation and density flow continued forming halite following Hardie-Eugster's evaporation model in the central region. Consequently, hydro-chemical zoning of chemical facies of chloride in the centre, and sulphate in the fringes was formed. We assume this process should have taken place ~ 500-100 ka before tectonic activities within the Okavango Delta Region. Formation of the Okavango Graben is estimated to be below 100 ka (Moore *et al.*, 2012). Geophysical mapping has clearly shown a low resistivity layer below the Okavango Delta sediments probably as part of the PLM system (Podgorski *et al.*, 2013). In stage 5, Pluvial climatic activities in the Pleistocene to Holocene (< 50 Ka), specifically, >30-20 ka and 8-4.5 ka, partially flushed or leached the evaporites that formed hence giving rise to younger groundwater ages than sediment ages.

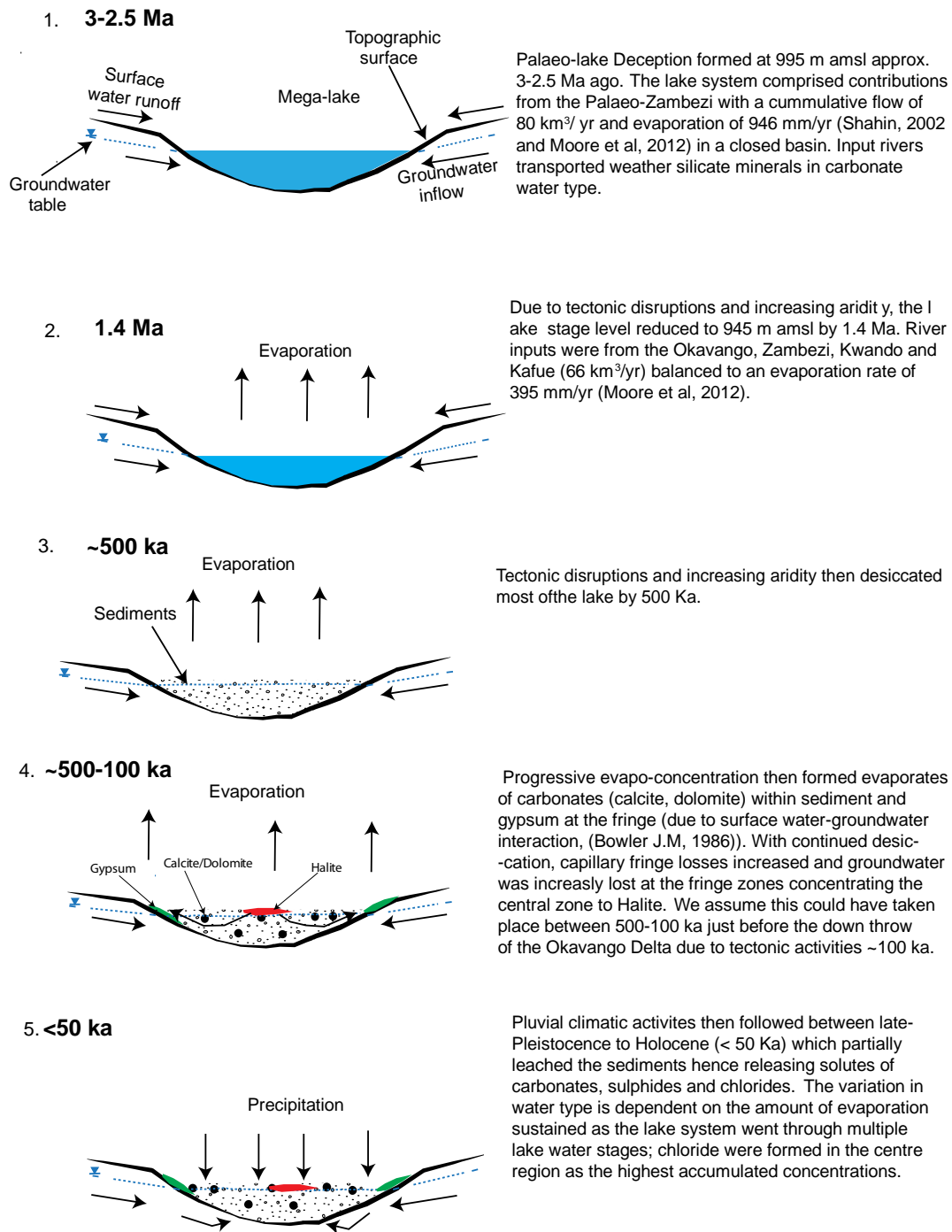


Figure 7.9: Summaried conceptual model of the evolution stages from the formation of the PLD to formation of evaporities that were partially flushed resulting in salinity

NB: The four stages represent salinity accumulation in the lake system and subsequial leaching to the groundwater.

7.7 Conclusions

The following can be deduced from this assessment:

Various studies investigated recharge mechanisms in MOZB, which suggest recharge occurs within the MOZB, but is lost to the vegetation cover; regional studies support this assertion and further confirms that isolation of palaeo and recent recharge is not possible;

Sediment ages within the MOZB are generally old (> 300 Ka) compared to groundwater ages, which are Late Pleistocene to Holocene (< 50 Ka). Saline groundwater observed today is not a result of connate lake water preserved in sediments but other processes including evapotranspiration and mineral dissolution processes;

Hydrochemical facies within MOZB are generally a result of redissolution of evaporated minerals, composed of chloride (in the central zone), sulphate (in the fringes) and carbonates typically beyond the boundaries of MOZB or within the Okavango Delta. We suggest sulphate is a result of surface water-groundwater interaction in which evaporation from the surface water formed primary evaporites rapidly exchanged solutes to the groundwater; increased solute accumulated then formed evaporites of sulphates. Precipitation of halite is a result of progressive evaporation loss from the capillary fringe and groundwater discharge at the shoreline margins of the lake system. Carbonate groundwater is due to recent recharge water within the surrounding fresh groundwater input and surface water (particularly in the Okavango Delta Region);

River chemistry water from present day river channels within the PLM (Zambezi, Okavango, Kwando/Linyanti) are carbonate dominated. We demonstrate that under progressive evaporation, the river water under chemical evolution following Hardie-Eugster's model precipitate halite after 50,000 times concentration; and

Sediments within the MOZB have been resolved using geophysics and typically are of resistivities $< 3 \Omega\text{m}$ (saline/clay), $3\text{-}10 \Omega\text{m}$ (brackish, clayey sands), $20\text{-}100 \Omega\text{m}$ (Kalahari sands and Basement rocks) using electrical based methods. Recent works within the Okavango Delta have mapped and resolved a high saline formation below the Okavango Delta probably hosting connate saline-brackish lake water from an earlier stage of the PLM.

CHAPTER 8

ARIDITY EVOLUTION IN SOUTHERN AFRICA SINCE THE PLIOCENE USING WILDFIRE HISTORY AND SAVANNA EXPANSION ACROSS SOUTHERN AFRICA SINCE THE LATE MIOCENE

8.1 Introduction

Savanna vegetation, which is characterized by a mixed community of trees with C4 grasses, supports a large proportion of the human population, livestock and wild herbivore biomass in the modern world (Scholes and Archer, 1997). The studies have shown that the savanna grassland has expanded to cover over 20% of the global terrestrial surface (Sankaran *et al.*, 2005) since 10-6 Ma (Cerling *et al.*, 1997; Edwards *et al.*, 2010; Keeley and Rundel, 2005; Polissar *et al.*, 2019; Strömberg, 2011). However, the driving force behind the savanna birth/expansion has been debated for a long time, with decreasing global CO₂ content (Cerling *et al.*, 1997; Ehleringer *et al.*, 1997; Polissar *et al.*, 2019) and increased regional fire activities (Beerling and Osborne, 2006; Bowman *et al.*, 2009; Hoetzel *et al.*, 2013; Keeley and Rundel, 2005; Osborne, 2008) considered two end-member forcing models. In addition, regional climate change (Edwards *et al.*, 2010; Sage, 2001; Strömberg, 2011) and even herbivores (Archibald and Hempson, 2016; Sankaran *et al.*, 2005) are also suggested as potential forcings. The existing records basing on the isotope, pollen, and charcoals, etc. mainly focus on savanna origination (Beerling and Osborne, 2006; Edwards *et al.*, 2010; Polissar *et al.*, 2019) or early expansion (Hoetzel *et al.*, 2013) and a lack of continuous high-resolution records covering the last several million years prevents us from understanding the dominant forcing behind further savanna development.

In this study, we obtained four microcharcoal-based fire records covering the last ~6 Ma across southern Africa, retrieved from the International Ocean Discovery Program (IODP) Expedition 361 marine sediment cores, to investigate their implications for savanna evolution (Figure 8.1a).

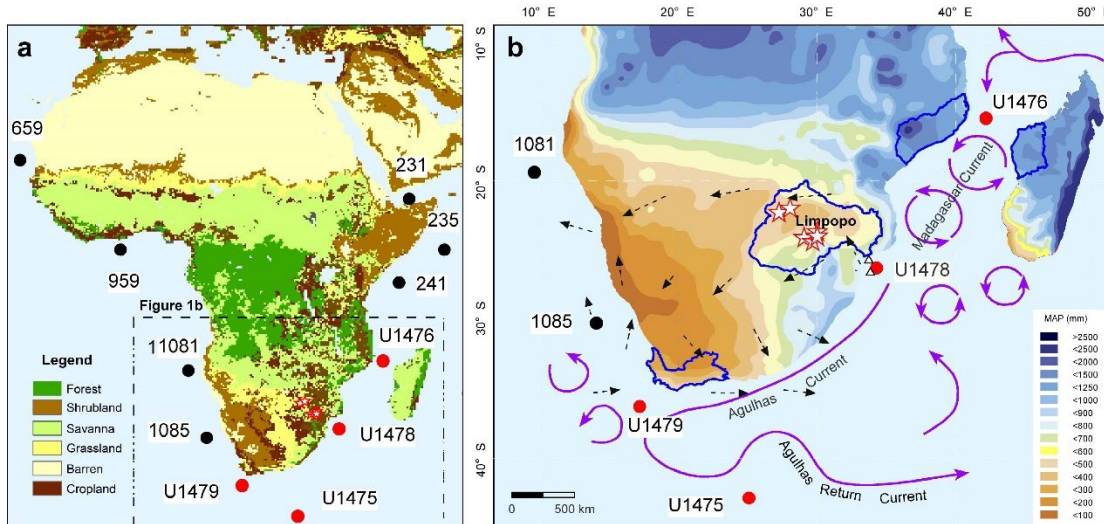


Figure 8.1: Study sites used to evaluate savanna evolution

Where: a. Sites used to study the C4 plants evolution. Black circles: DSDP Sites 235, 241 (Polissar *et al.*, 2019) and 231 (Feakins *et al.*, 2013), ODP Site 659 and 959 (Polissar *et al.*, 2019), ODP Site 1081 (Hoetzel *et al.*, 2013) and ODP Site 1085 (Dupont *et al.*, 2011). Red circles: IODP Sites U1475, U1476, U1478 and U1479 and red stars: surface samples analysed in this study. Vegetation cover adopted from (Loveland *et al.*, 2009). b. Detailed mean annual precipitation (MAP) and wind directions (black dashed arrows) across the southern Africa (Tyson and Preston-Whyte, 2000), main drainage catchments (blue thick lines) matched to the IODP sites (UNEP *et al.*, 2010) and oceanic surface current systems (purples curves with arrows) surrounding the mainland (Hall *et al.*, 2017). Two black hollow triangles near Site U1478 showing gravity cores of Geob20616-1 (north) (Hahn *et al.*, 2020) and (south) MD96-2048 (Dupont *et al.*, 2011) mentioned in this study.

8.2 Geographical and Geological Setting

The southern Africa lies at the edge of the tropics between the Indian and Atlantic Oceans and only the tip reaches into the winter rain zone touched by the circumpolar Antarctic Westerlies (Dupont *et al.*, 2011). The southwestern part of southern Africa ranges from an arid to semi-arid climate zone, whereas only a small area in the easternmost part of southern Africa is humid with seasonal rainfall characteristics (Dupont *et al.*, 2013; Tyson and Preston-Whyte, 2000). The Limpopo drainage is dominated by summer precipitation (Caley *et al.*, 2018) (Figure 8.1b).

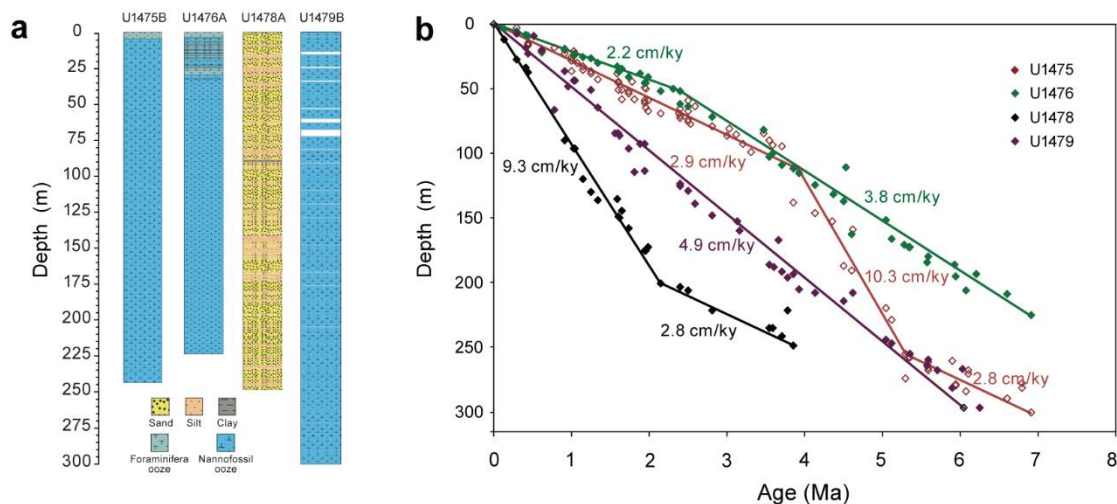


Figure 8.2: Summary of a. Major lithological characteristics of sediment cores and b. Age-depth relationships of Sites U1475, U1476, U1478, and U1479 in Expedition IODP 361. Time estimates and implied sedimentation rates based on a mixture of major planktonic foraminifer, calcareous nannoplankton, diatom, and paleomagnetic data (Hall *et al.*, 2017).

Correspondingly, the largest biome in southern Africa is a savanna composed of trees, shrubs, and herbs: including woody C3 type and herbaceous C4 type. In detail, the C4 plants in southern Africa are abundant but scattered, and the relative quantities of herbaceous and woody species are quite different – among which the proportion of C4 plants in the Limpopo drainage reaches 20%-40% (Rommerskirchen *et al.*, 2003) (Figure 8.1a).

The studied four sites were drilled along the southern African margin and in the Indian-Atlantic Ocean gateway, southwest Indian Ocean, in Expedition IODP 361 (Hall *et al.*, 2017). Sites U1476 and 1478 are near Mozambique, U1479 is near South Africa, and U1475 is located on the southwestern flank of the Agulhas Plateau, ~850 km to the south of South Africa. The lithological characteristics of these four sites are shown in Figure 8. 2a. Site U1478 is characterized by dark grey sandy sediments mainly discharged by the Limpopo River, which has a catchment area exceeding $3.85 \times 10^6 \text{ km}^2$ dominated by typical savanna grassland (White, 1983). The drainage areas of Sites U1476 and U1479 are both roughly a quarter of the Limpopo River catchment (Figure 8.1b). Deciduous forest-woodland savanna and Mediterranean evergreen forest-hard leaf scrub thrive in these two regions respectively (White, 1983). These two cores are characterized by white-grey to greenish grey pelagic sediment. Site U1475 lies under the Agulhas Return Current, as the natural extension of the Agulhas Current (Lutjeharms, 2006) (Figure 8.1b), which primarily consists of light greenish or pale grey to white-grey nannofossil ooze. The oldest age estimates for Sites U1475, U1476, U1478 and U1479 are 7.0, 6.9, 4.0 and 7.0 Ma (Figure 8.2b), respectively, according to a mixture of major planktonic foraminifer, calcareous nannoplankton, diatom and paleomagnetic dating (Hall *et al.*, 2017).

8.3 Methodology

We analysed 127 samples from Site U1475 (covering the last 5.7 Ma), 86 samples from Site U1476 (7.1 Ma), 139 samples from Site U1479 (5.9 Ma) and 119 samples from Site U1478

(3.9 Ma) (Hall *et al.*, 2017), as well as six modern terrestrial samples from the Limpopo drainage in order to understand the microcharcoal changes at Site U1478 (locations see Figure 8.1). Microcharcoals were extracted from samples using a standard pollen methodology. Samples were treated with 10% hydrochloric acid (HCl) and 70% hydrofluoric acid (HF) to remove carbonates and silica, and microcharcoals were separated using a 10- μm nylon sieve. The microcharcoals were identified and counted under a light microscope at a magnification of $\times 400$ in regularly spaced transects (Miao *et al.*, 2019).

A known number of *Lycopodium clavatum* spores were initially added to each sample, to enable calculation of the total microcharcoal influx (MI):

$$\text{MI} = \text{N}/\text{L} \times \text{T}/\text{W} \times \text{R} \times \text{V}$$

where N is the counted number of microcharcoals (grains), L is the counted number of *Lycopodium clavatum* (grains), W is the dry sample weight (g), T is the number of added *Lycopodium clavatum* spores (grains), R is sedimentation rate (cm/kyr) and V is the volume (cm^3).

Microcharcoal grain shapes were classified according to their measured length to width ratios, and described as L (sub-long) or R (sub-round) for ratios higher or lower than 2.5 respectively (Miao *et al.*, 2019). The ratios of L to R in MI are denoted as $\text{MI}_\text{L}/\text{MI}_\text{R}$.

8.4 Results

MI at all four studied sites show stable trends. For example, MI values for Site U1475 are within the range 5.4 to 7.2 (log scale, grains/ cm^2/kyr), with an average of 6.2. MI values for Site U1476 are within the range 5.5 to 6.8 (average 6.4), MI values for Site U1478 are within the range 5.2 to 6.9 (average 6.2), and MI values for Site U1479 are within the range 5.7 to 6.4 (average 6.0) (Figure 8.3a).

In contrast, the ratios of MI_L to MI_R at the four sites show two distinct patterns. The MI_L to MI_R ratio at Site U1475 varies between 0.02 and 0.53 (average 0.20), followed by a continuous increasing trend. Site U1478 shows a similar increasing pattern, with values varying between 0.07 and 0.57 (average 0.23). In contrast, MI_L to MI_R ratios at Sites U1476 and U1479 are low and there are no monotonic increasing trends (Figure 8.3b). For the surface samples, the data of MI_L to MI_R ratio range between 0.16 and 0.38 with an average 0.26, which are well matched with the youngest records of Site U1478 (Figure 8.3b).

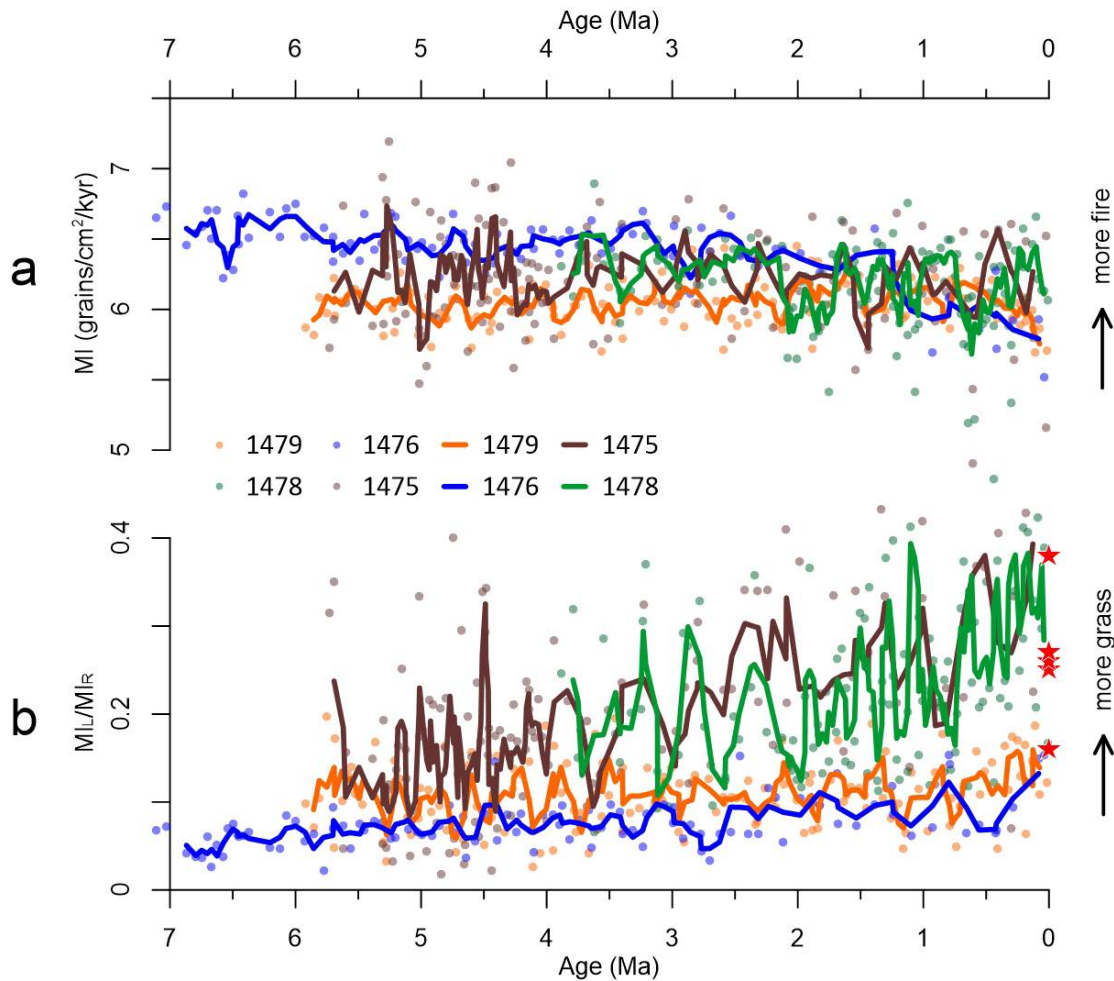


Figure 8.3: Fire evolution and savanna expansion across southern Africa

Where: a) Microcharcoal influx (MI). b) Ratios of MIL/MIR at four sites (plotted data have been smoothed using a 3-point moving average; Red stars represent the surface samples in the Limpopo drainage).

8.5 Discussion

8.5.1 Wildfire evolution and C4 plant expansion routes in southern Africa

Past studies demonstrate that higher values of MI can be related to increased wildfire activity (frequency or intensity) (Bond, 2015; Daniu *et al.*, 2013b; Herring, 1985; Hoetzel *et al.*, 2013; Miao *et al.*, 2019), similar to the principle of black carbon in explanation of the wildfire (Han *et al.*, 2020; Jia *et al.*, 2003). Therefore, the stable MI trends of the four sites in this study mainly reflect the stable wildfire across southern Africa over the last 7 Ma (Figure 8.3a), which is in contrast to the most significant increase in wildfire at 7-6 Ma found at the ODP Site 1081 in southern Africa (Hoetzel *et al.*, 2013). Unfortunately, there is no record for 2.8-0 Ma (Hoetzel *et al.*, 2013). If all the records are considered together, we can say that the wildfires across southern Africa reached their maximum during the late Miocene (7-6 Ma) and then remained stable afterwards (Figure 8.4c).

However, the microcharcoals of the grass and wood show long and round shapes respectively (Crawford and Belcher, 2014; Daniau *et al.*, 2013b; Umbanhowar Jr and McGrath, 1998), and the higher MIL/MIR ratios indicate a greater proportion of burnt grasses (Daniau *et al.*, 2013a; Miao *et al.*, 2019). Therefore, the increase trends of MIL/MIR ratios at IODP Site U1478 represent the herbaceous plants expansion. Furthermore, considering that the herbs in the African savanna are mainly C4 types (Loveland *et al.*, 2009), the result at IODP Site U1478 can represent C4 plants expansion over the last 6 Ma. The modern samples from the Limpopo drainage (Figure 3b) show such inheritance. Here, the modern data of the MIL/MIR ratios are closer to the youngest data of the IODP Site U1476 than the Sites U1476 and 1479. IODP Site U1475 (away from the land) showed high similarities to Site U1478, possibly indicating that formation of the Agulhas Current brought more microcharcoals downstream. According to the winds, perennially consistent easterly and westerly winds are dominant and blow over 22-27°N and 30-35°N of southern Africa respectively throughout the year (Daniau *et al.*, 2013b; Shannon and Nelson, 1996; Tyson and Preston-Whyte, 2000) (Figure 1b). This means that little possibility of the mirocharcoals brought by the winds into the IODP Site U1475 can be found (Figure 1b). Apart from the data from Sites U1475 and U1478, Sites U1476 and U1479 are roughly stable (with a slight increase only) (Figure 3b), which indicate almost no expansion of grasses and C4 plants at these two drainages since the late Miocene (Rommerskirchen *et al.*, 2003). In summary, the expansion of C4 plants across southern Africa had a limited region and eventually reached the current distribution area (Figure 4a).

For the age of the C4 plants onset/expansion, although debate across the world include for example the late Miocene versus Pliocene (Edwards *et al.*, 2010; Lu *et al.*, 2020; Shen *et al.*, 2018; Strömberg, 2011), more proof indicate ~10 Ma ago across Africa. For example, based on the carbon isotopic composition of leaf-wax molecules, the C4-dominated ecosystems expanded synchronously across northwestern and east Africa after 10 Ma, and subsequently continued to increase (Polissar *et al.*, 2019) (Figure 8.4b). In northeast Africa, DSDP Site 231 indicates two distinct phases of increasing C4 biomass, with the earliest period of 11-9 Ma ago (Feakins *et al.*, 2013). In southwest Africa, the ODP Sites 1085 (Dupont *et al.*, 2013) and 1081 (Hoetzel *et al.*, 2013) indicates a synchronous C4 increase around the same period.

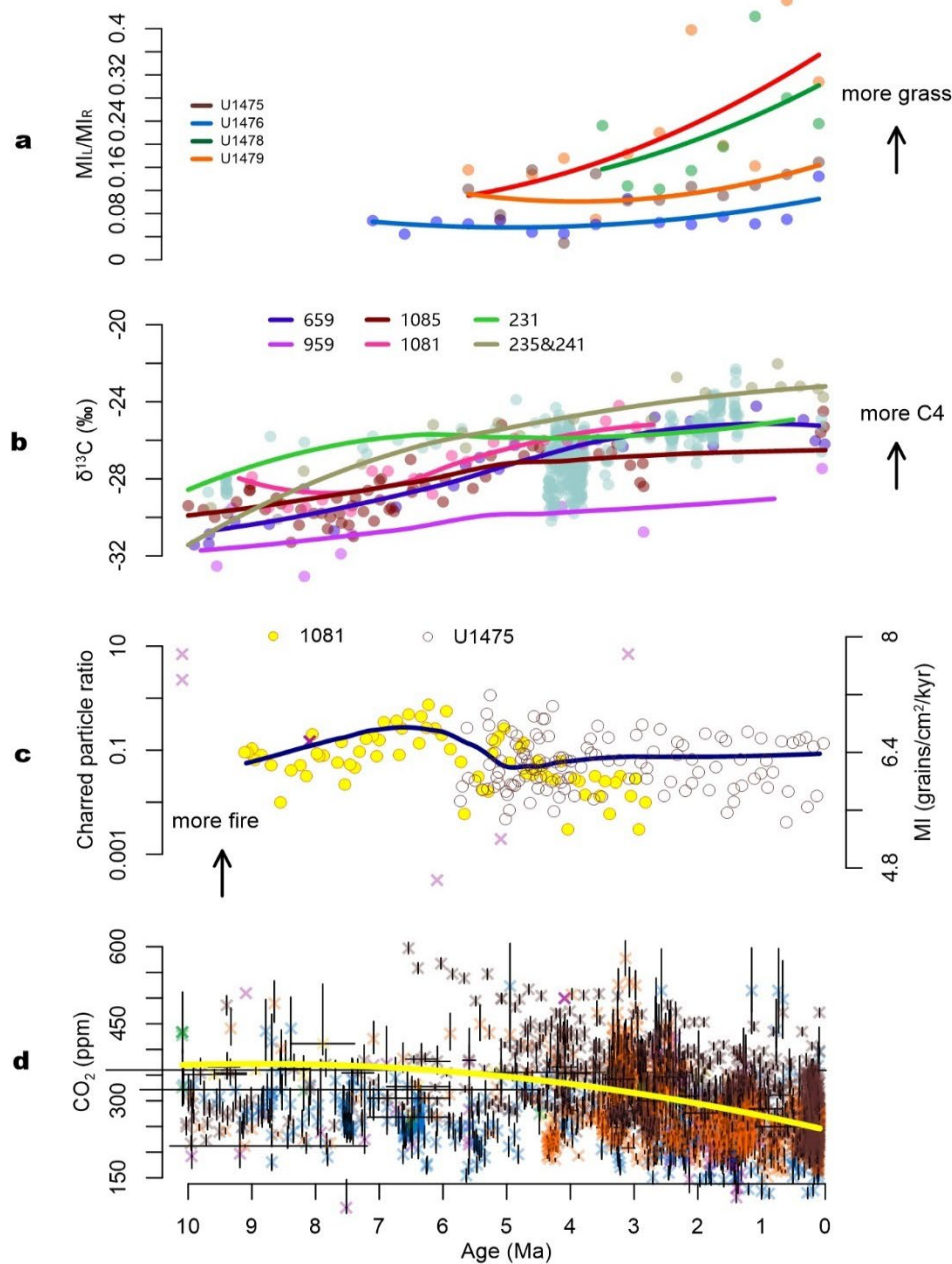


Figure 8.4: Evolution of Savanna across Africa over the last 10 Ma basing on microcharcoals, isotope records, and correlations with the wildfire and atmospheric CO₂

Where: a) Ratios of MIL/MIR-based C4 plants evolution obtained from the IODP Sites U1475, U1476, U1479 and U1478 in southern Africa $\delta^{13}C_{C31}$ -based C4 expansion at ODP 659 and 959 (Polissar et al., 2019) and DSDP Sites 235 and 241 (Uno et al., 2016) in north Africa, and $\delta^{13}C_{C30}$ -acid-based DSDP Site 231 (Feakins et al., 2013) in northeast Africa, ODP 1081 (Hoetzel et al., 2013) and 1085 (Dupont et al., 2011). c) Ratio of charred particles over the sum of charred particles, spores and pollen (Hoetzel et al., 2013) and MI (microcharcoal influx, log scale) at IODP Sites U1475 and U1478. d) Synthesis of published CO₂ proxy data (Different colours represent different indexes. The error bars are expressed as 25% of the original error. For details, see <https://www.paleo-co2.org/> and its accompanying references). All curves in a-d data are interpolated with 0.5 Ma and adopt polynomial fit method, polynomial degree=2.

In summary, if we put all the records together, the origination and expansion routes of the C4 plants across Africa are clear: the onset of C4 plants in Africa was about 10 Ma ago, which expanded south-eastward over the last 6 Ma before reaching the present region.

8.5.2 The driving mechanism of C4 expansion across Africa

The driving mechanism of C4 plants expansion has been controversial for a long time, mainly including two end-member models: driven by CO₂ or wildfire. For the CO₂, it is because C4 plants can maintain a relatively high photosynthesis efficiency even when the CO₂ concentration is lower than C3 plants, so as to be more adapted to the environment with low CO₂ concentration (Cerling *et al.*, 1997; Edwards *et al.*, 2010; Ehleringer *et al.*, 1997; Sage, 2001). Therefore, it is believed that low CO₂ concentration can be the direct cause for C4 plants expansion (Polissar *et al.*, 2019).

For the wildfire to be a potential forcing for C4 origination and expansion, there are two reasons. Firstly, the high light conditions after the fire are conducive to the growth of C4 plants and the increase in the productivity of C4 plants increases the load of highly combustible fuel, thereby further increasing the fire activity (Keeley and Rundel, 2005). Secondly, fire can directly destroy the forest to make room for the grass (Beerling and Osborne, 2006; Bond and Van Wilgen, 2012; Bowman *et al.*, 2009; Hoetzel *et al.*, 2013; Keeley and Rundel, 2005; Osborne, 2008); moreover, it can help to create hotter, drier conditions that favor grass (Beerling and Osborne, 2006). Therefore, the maximum wildfire around 7-6 Ma found in southern Africa can be attributed to the C4 plants expansion (Hoetzel *et al.*, 2013) (Figure 8.4c).

In addition, regional climate change such as warm, seasonally dry climatic conditions is important for savanna expansion (Edwards *et al.*, 2010; Sage, 2001; Strömberg, 2011). C4 plants in the savanna have an open tree canopy that grows under warm climatic conditions. That is, the C4 pathway is better adapted to warm, dry and low-CO₂ conditions because the metabolism as a whole, which includes photosynthesis and growth, is sensitive to chilling temperatures – a feature that strongly curtails the growing season in cool climates (Lawlor, 1993).

Based on the aforementioned analysis of the driving mechanism of C4 expansion, we agree that the emergence of C4 plants in Africa around 10 Ma is closely related to the lower CO₂ concentration (Polissar *et al.*, 2019) (Figure 8.4d) but the changes around 7-6 Ma, it may be mainly related to wildfire (Hoetzel *et al.*, 2013) (Figure 8.4c). However, the further expansion of C4 plants after 6 Ma along specific routes across south-eastern Africa is complex.

Firstly, the CO₂ had already dropped below the critical threshold since the early Oligocene (Cui *et al.*, 2020; Rae *et al.*, 2021). If the CO₂ was always the main driving force over the last 6 Ma, the global C4 expansion patterns should be very similar. However, across the whole Africa, the details (Figure 8.3b) and trends (Figures 8.4a and 8.4b) of the C4 plants are clearly

inconsistent. Furthermore, the research on a global scale clearly show that no highly consistent changes over either late Cenozoic (Edwards *et al.*, 2010) or the last 6 Ma (Lu *et al.*, 2020; Shen *et al.*, 2018) have been found. Secondly, although the significant peak of paleo-fire record during 7-6 Ma is thought of as the factor driving the C4 plants expansion (Hoetzel *et al.*, 2013), the stable fire trends over the last 6 Ma (Figure 8.3a) are inconsistent with the details and trends of the C4 plants expansion (Figures 8.4a and 8.4b). Similar situations also occurred at inner and eastern Asia over the late Cenozoic (Jia *et al.*, 2003; Miao *et al.*, 2016; Miao *et al.*, 2019; Shen *et al.*, 2018). Thirdly, although the modern mammal herbivores' control of vegetation type and size are observed (Archibald and Hempson, 2016), it is also unlikely that the herbivores can drive the C4 plants expansion greatly. This is because the herbivores' evolution seems to depend on the climate-determined food abundance, unrelated to either C3 or C4 herbs (Cerling *et al.*, 1997; Zhang *et al.*, 2012).

In this study, we consider that the expansion of C4 plants since 6 Ma is mainly related to regional hydrological and climate changes.

First, the drainage area where Site U1476 is located, is in a tropical semi-humid climate zone, with a mean annual precipitation (MAP) of over 900 mm. Most of the precipitation is concentrated from November to April, and the mean annual temperature (MAT) is 25°C (Ribeiro *et al.*, 2009), breeding the deciduous forest-woodland savanna and East Africa coast forest (White, 1983). The drainage area near Site U1479 is in the Mediterranean climate zone, with a MAP of 450 mm, mainly from November to March, and MAT of 18°C (Spano *et al.*, 2003). The drainage area develops Mediterranean evergreen forest-hard leaf scrub and is a semi-desert (White, 1983). In the Limpopo drainage, Site U1478 is in the transition zone between tropical and subtropical climates and the MAP ranges from 1400 mm in the mountains to 600 mm in the lowlands. Rain falls mostly in summer. The corresponding MATs are 24 and 16°C (Dupont *et al.*, 2011). The typical savanna grassland dominates this region (White, 1983). Thus, judging from the spatial distribution of the modern savanna environment, it has highly selective hydrological and climate conditions.

Secondly, on a short timescale, the hydrological and climate changes in southeast Africa are correlated to the local sea surface temperature variations (Dupont *et al.*, 2011). This means that during a cold period, lower summer precipitation into the north of southern Africa (South Africa and southern Mozambique) induces a tight coupling of C4-dominated grass dynamics, and vice versa (Hahn *et al.*, 2020) (Figure 8.5a). On a long timescale, the grass ratios in combustion from Site U1479 (this study) and drought degree (Hoetzel *et al.*, 2013) during 6.0-4.0 Ma are well correlated (Figure 8.5b) (they are both in the west of southern Africa, controlled by a similar climate) – that is, the drier climate can be inferred and vice versa. Therefore, the MC_L/MC_R at four sites indicate climate evolution along the special routes, including the continuous aridification at Site U1478 versus stabilities at Sites U1476 and U1479.

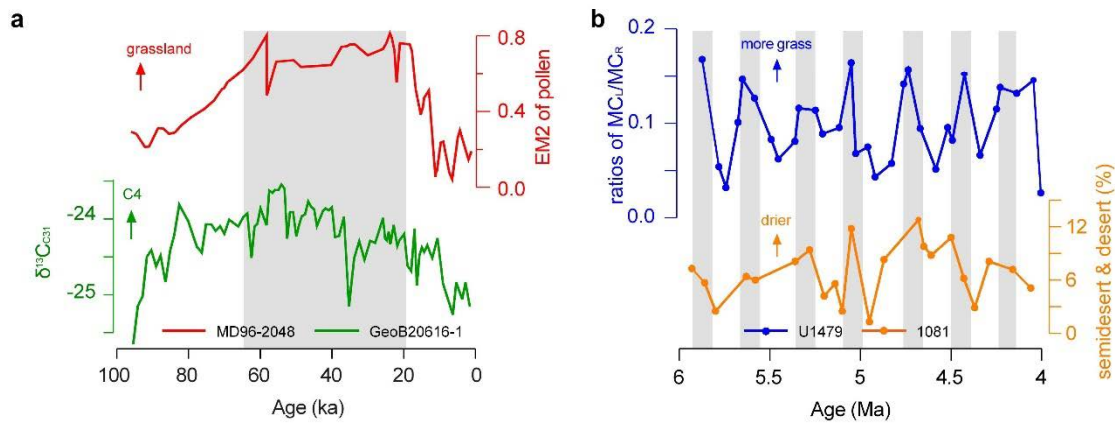


Figure 8.5: Correlations between grass-based climate and C4 plants changes during two different periods at the Limpopo drainage, south-eastern Africa

Where: a. is the C4 type according to the $\delta^{13}C_{C31}$ (green line) (Hahn et al., 2020) against pollen-based grasses development (Dupont et al., 2011) during the last 100 ka; b. the grasses obtained according to the microcharcoal assemblages in this study and pollen-based drought degree (Hoetzel et al., 2013) during 6.0-4.0 Ma.

Thirdly, we argue that the greater Agulhas Current system might have played an important role in driving the rainfall seasonality. The greater Agulhas Current system (as a fundamental part of the South Indian Ocean subtropical gyre circulation) constitutes the strongest western boundary current in the southern hemisphere oceans, transporting $\sim 70 \times 10^6 \text{ m}^3/\text{s}$ of warm, saline tropical surface waters to the tip of Africa (Lutjeharms, 2006). This transported volume fosters exchanges of heat and moisture with the atmosphere that influence the regional climate and the weather system in South Africa (Reason and Mulenga, 1999). The study shows that the warm or cool SST events in the Agulhas Current and neighbouring marine areas can significantly influence the rainfall over large parts of southern Africa (Reason, 1998). For example, based on the analysis of the atmospheric general circulation model (AGCM), when the greater Agulhas Current system is smoothed out, it appears that the rainfall will decrease $\sim 40\text{-}20 \text{ mm}$ over the Limpopo drainage in summer (January-March), and increase correspondingly in winter. That is, the greater Agulhas Current system has enhanced the rainfall seasonality correlated to the savanna region. However, in the forest region away from the greater Agulhas Current system, the influence becomes less (Reason, 2001). In fact, studies in mid-latitude Asia have shown that the expansion of C4 plants is also related to changes in regional hydrology and climate (Shen et al., 2018).

8.6 Conclusion

The savanna's origination, enlargement, and underlying forcing mechanisms have been hotly debated. In this study, we firstly presented microcharcoal-based fire activities over the last ~7 Ma from four IODP cores surrounding southern Africa. The results showed that the fire strength/frequency in both savanna and non-savanna regions were stable since 6 Ma, but the grasses in burnt biomass expanded continuously to the present savanna-dominated region since around 6 Ma. We argue that although the low CO₂ concentrations might have led the appearance of C4 plants at ~10 Ma and high frequency wildfires during 7-6 Ma further expanded C4 plants, the regional climate changes since 6 Ma began to drive the C4 plants expanding into today's savanna habitat along the special routes.

CHAPTER 9

CLIMATE CHANGE AND WATER SECURITY: DEVELOPMENTAL PERSPECTIVES FOR WATER-LINKED SECTORS IN A FUTURE CLIMATE FOR AFRICA (BI-NATIONAL ASSESSMENT)

9.1 Introduction

The Zambezi River is a primary water supply for both social and economic activities in the riparian states. The current economic activities such as crop irrigation, hydropower generation, manufacturing, commercial fishing, and mining operations depend on the Zambezi water resource. Apart from the effects of climate change, the Zambezi River Basin's water resource is further threatened by:

- a. The heavy reliance on the shared water resource between different riparian states,
- b. Prioritization of certain social and economic activities over one another (Spalding-Fletcher *et al.*, 2014),
- c. Population growth and increased size of the urban population,
- d. Lack of joint administration of the water resource in most projects leading to the country-level water resource management (Shela, 2000).

This study examines water utilization in the Zambezi River Basin with a particular focus on hydropower generation activities and the effects of climate change on the energy source. Maintaining sustainable water utilization while exploring means of mitigating climate change is a key focus. The study gives an overview of current and planned hydropower generation on the Zambezi River and the status of energy in the Southern African Development Community (SADC) region. Emphasis is given to the Zambezi water utilization, electricity demand, and supply between SADC member states. Furthermore, the study assesses the risks associated with climate change and hence the threats to the Zambezi River Water resource. The benefits of hydropower in mitigating climate change presented are also presented.

9.2 Study aims and objectives

This study forms part of deliverable 3, aimed at conducting a comparative analysis of climate change impacts on future development and economic growth for priority water-linked sectors on the African continent, with the focus on riparian states of the Zambezi River. The study focuses on the impacts of climate change on the Zambezi River Basin with a particular focus on the planned and existing hydropower generation.

The objectives of the study were to:

- a. Characterize and assess the impact of the projected future climate on energy and water security.
- b. Conduct a comparative analysis of the impact associated with the hydropower generation
- c. Provide an analysis of expected changes in extreme climate and weather events.
- d. Give an overview of individual countries' policies and strategies on energy generation and climate change to determine whether appropriate actions that will address the identified impacts are addressed.
- e. Assess risks/threats and opportunities that are likely to arise from the changing climate.
- f. Recommend appropriate short, medium- and long-term adaptation strategies to mitigate impacts of climate change on hydropower generation and the environment.

9.3 Project locality

The Zambezi River Basin is Southern Africa's largest drainage basin, estimated at 1 300 000 km² and covers about 2600 km (Shela, 2000). The river's geographic location from its source extends for about 50 km northward, towards the Democratic Republic of Congo into the Kalene Hills before the river changes its course towards the south-west, a direction that is maintained for approximately 270 km into Angola. From Angola, the river flow changes direction to the south back to Namibia and finally flows in an eastward direction towards the border of Namibia and Botswana, Zambia and Zimbabwe passing through to Mozambique and emptying into the Indian Ocean (Figure 9.1). The Zambezi River Basin (ZRB) flows across eight countries. A significant share of the watershed lies in Zambia (40.7%, followed by Angola (18.3%), Zimbabwe (15.9%), Mozambique (11.4%), and Malawi (7.7%) while Namibia, Malawi, and Tanzania constitute 6% of the catchment area (Shela, 2000). The most striking physical features are floodplains, waterfalls, lakes and constructed hydroelectric dams. The notable tributaries of the Zambezi River are Luena in Angola; Lungue Bungo flowing within Angola and Zambia; the Luangwa, Kafue and Kabompo Rivers in Zambia; the Cuando flowing through Angola and the Caprivi Strip of Namibia before it enters Botswana as Chobe River and finally the Shire River flowing through Malawi and Mozambique.

The Zambezi River basin is subdivided into three distinctive geomorphological sections from the west to east: The Upper, Middle and Lower Sections (Wellington, 1955 and Moore *et al.*, 2007).

9.3.1 Upper Zambezi Section (UZS)

The UZS covers an area of approximately 515,008 km² and it comprises the northwestern and western territories of Zambia, parts of the eastern regions of Angola and borders north of Namibia, Botswana, and Zimbabwe. The UZS section represents the highest elevation of the river, with a maximum elevation of 1500 m above sea level (m asl) in the north and a maximum elevation of 900 m asl in the south, close to the Victoria Falls.

The UZS section also hosts the headwaters from the north of Zambia, and the watercourse stretches to Angola, and then back to the Zambian territory before it ends towards the Victoria Falls of Zimbabwe. In the segment where the river re-enters Zambia, there is a drastic drop in the elevation, and this resulted in the development of the Chavuma Falls. Further, downstream, one of the largest tributaries, the Kabompo River, joins the main Zambezi River. At this juncture, the river widens into one of the most extensive wetlands in Africa, the Barotse Floodplain, measuring about 230 km in length and 35 km in width. Further, downstream, the river flows into Ngoye/Sioma Falls (1000 m asl). From this juncture, the river flows slightly in a south-east direction and briefly borders Namibia's Caprivi Strip where the course changes in an easterly direction, towards the Victoria Falls, where the elevation is about 950 m

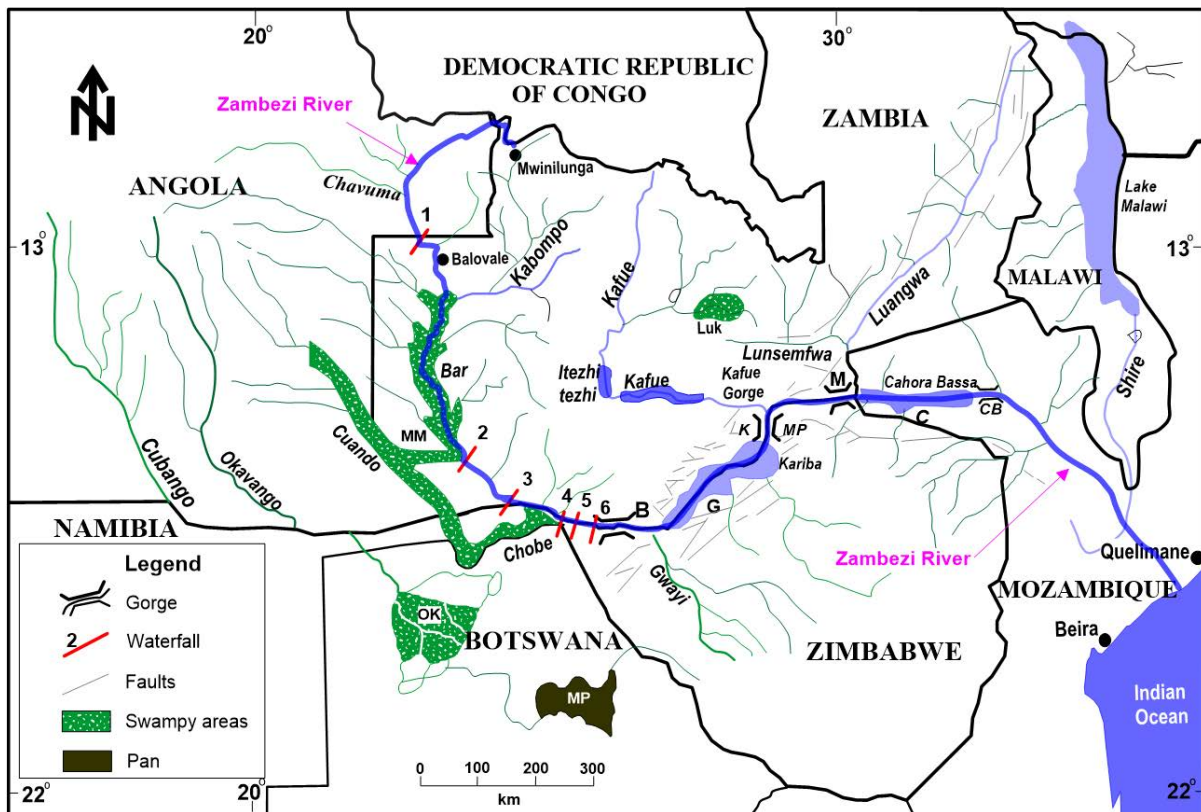
9.3.2 Middle Zambezi Section (MZS)

The MZS covers an area of approximately 511,430 km². The MZS section is mainly composed of the Copper belt, Central, Southern, and Lusaka territories together with small areas of the north-western and eastern provinces of Zambia. The section also covers Matabeleland North, the Midlands, and western Mashonaland areas of Zimbabwe. The Victoria waterfalls in Zimbabwe are considered the boundary that separates the upper and middle sections of the Zambezi River. Downstream from the Victoria Falls, the river continues to flow to the east through a deep incision, the Batoka Gorge at an elevation of 650 m asl.

Further downstream, after 100 km the river flows into Devil's Gorge, which has an elevation of approximately 600-450 m asl. Further downstream, at about 10 km from the Devil's Gorge the river drains into Lake Kariba (one of the most prominent structures measuring approximately 240 km in length and 10-20 km in width). At about 70 km downstream another tributary, the Kafue River that flows from the Copper belt region of northern Zambia is encountered. From this point, the river flows for about 100 km and is joined by the Luangwa tributary in the north. This point marks the end of the Cahora Bassa Reservoir and the international boundary between Zambia and Mozambique.

9.3.3 Lower Zambezi Section (LZS)

The LZS section covers an area of approximately 340,000 km² stretching below the eastern end of the 200 km long Cahora Bassa Dam to the Indian Ocean (Beilfuss, 2012). The drainage area covers the whole of Malawi, a small strip of southern Tanzania along the eastern coast of the Malawi River, north-eastern and central areas of Mozambique, and some areas in northeast Zimbabwe. The Shire River, which originates as an outflow from Lake Malawi/Niassa/Nyasa is the largest tributary in the LZS section, flowing through southern Tanzania, Malawi, and Mozambique north of the Zambezi.



Abbreviations and Symbols

Rift Basins: G → Gwembe Trough (mid-Zambezi Basin); MP → Mana Pools Basin; C → Cahora Bassa Basin;
Gorge: B → Batoka Gorge; B → Kariba Gorge; M → Mupata Gorge; CB → Cahora Bassa Gorge;
Rapids and Falls: 1 → Chavuma; 2 → Ngonye Falls; 3 → Katima Mulilo; 4 → Mambova; 5 → Katombora; 6 → Victoria Falls;
Floodplains: Bar → Barotse floodplain; Luk → Lukanga; MM → Mulonga-Matebele; OK → Okavango Delta
Pans: MP → Makgadikgadi Pans

Figure 9.1: Southern African map showing the Zambezi River and associated geomorphological features (After Moore et al., 2007)

9.3.4 Rainfall patterns

The average rainfall dataset information for the lower, middle, and lower sections of the ZRB as compiled by Kaseke (2016) are presented in Figure 9.2 and summarised as follows:

- a. The rainfall is variable throughout the Zambezi River Basin, with generally higher rainfall in the northern and western areas and lower rainfall in the south.
- b. In some areas of the UZS and around Lake Malawi, average rainfall reaches up 1 400 mm/year, while in the southern territories of Zimbabwe it drops to 500 mm/year.
- c. Therefore, the Northern and Western tributaries contribute significantly to the Zambezi River water pool compared to the southern tributaries. However, the existing water bodies such as reservoirs and wetlands often hold the water back, thus, only smaller quantities reach the Indian Ocean. Higher rainfall in the southern and western areas of the UZS contribute to the vegetation, which in turn contributes to higher humidity in the region.
- d. The Upper Zambezi section is well vegetated in the north, and the average rainfall ranges from 1000 to 1500 mm/year.

- e. The Middle Zambezi is characterized by lower rainfall (500 to 700 mm/year) towards the southern areas such as Zimbabwe, Botswana and Namibia and slightly higher rainfall (700 to 1100 mm/year) towards northern territories of Zambia.
- f. The Lower Zambezi region is characterized by higher rainfall (800 to 1300 mm/year) in the northern territories such as Tanzania, Malawi and north of Mozambique and lower rainfall (500 to 700 mm/year) in the central parts of Mozambique, and parts of north-eastern Zimbabwe.

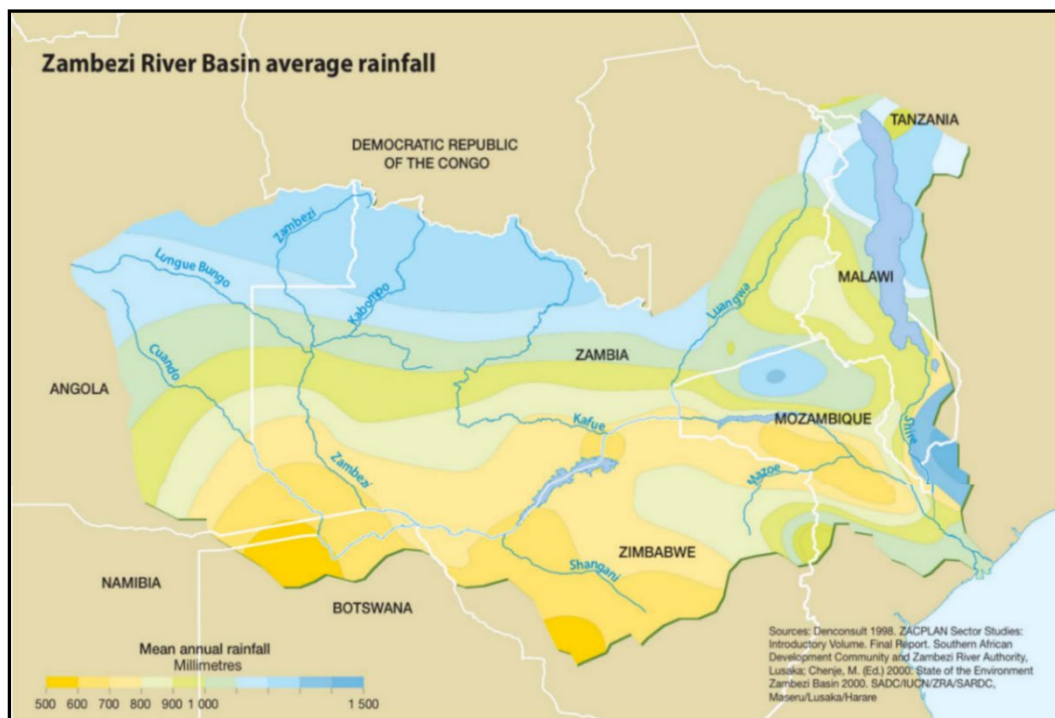


Figure 9.2: The average rainfall of the Zambezi River Basin based on various literature (Source: Kaseke, 2016)

9.4 Zambezi River Basin: hydropower resource assessment

9.4.1 Introduction

The Zambezi River and some of its main tributaries host major hydroelectric plants that are a main source of electricity for its African riparian states. The existing and proposed hydropower plants in the Zambezi River Basin influence the utilization of water resources. This study subdivides the hydropower plants into major producing plants (a generation capacity of above 100 megawatts (MW)), and minor producing plants (less than 100 MW of capacity). The planned hydropower projects and upgrades on existing hydroelectric plants are briefly discussed with consideration of water resource utilization. The extensive account of the Zambezi water resource utilization by riparian countries, the reservoir and irrigation schemes assessment and modelling based on demand and supply was discussed by in World Bank, (2010).

9.4.2 Existing Hydropower Stations

9.4.2.1 Major Hydropower Station

a. Cahora Bassa

The Cahora Bassa hydropower plant is in the lower section of the ZRB in the Mozambique territory. This is considered the largest hydroelectric plant in Southern Africa with a total installed capacity of 2075 MW. The Cahora Bassa scheme was commissioned in 1975 with the arrangement that most of the electricity generated would be imported by South Africa. Currently, South Africa imports 70% of Cahora Bassa's production while Mozambique uses 24%. The rest is distributed to other neighbouring countries through the shared interconnected electrical power lines.

b. Kariba

The Kariba Power Plant is the second largest hydroelectric plant in the Zambezi River Basin. Electricity is generated by drawing water from Kariba Reservoir, the largest artificial lake in Africa, with a surface area of 5,577 km². The electricity is generated from the two power plants, the Kariba North Power Plant (1080 MW) and Kariba South Power plant (1050 MW) contribute to the combined installed capacity of 2130 MW per year. The Kariba South Power Station plant was commissioned in 1962 to provide electricity to Zambia and Zimbabwe. The Kariba South Power Plant is owned and operated by the state-owned Zimbabwe Power Company (ZPC), the largest source of Zimbabwe's electricity supply. The Kariba North Power Plant is owned by Zambia Electricity Supply Corporation (ZESCO) and produces about 45% of Zambia's electricity. The Zambezi River Authority (ZRA), a statutory body formed by the Zimbabwean and Zambian governments, is responsible for the allocation of water used by Zimbabwe's Kariba South and Zambia's Kariba North Power Stations.

c. Kafue Gorge Upper

The Kafue Gorge power plant is located on the upper sections of the Kafue River, one of the major Zambezi tributaries. It was commissioned in 1972, and currently supplies about 41% of Zambia's electricity. The construction of this power station started in 1967. This is the third-largest producing power plant in the entire Zambezi River Basin with an installed capacity of 990 MW produced from six generators of 165 MW each (ZESCO, 2020).

d. Itezhi Tezhi Power Plant

The construction of the Itezhi-Tezhi Dam on the Kafue River in Zambia was completed in 1977. The initial purpose of the dam was to regulate water supply to the Kafue Gorge Upper power plant located downstream. During the rainy seasons, the Kafue River is prone to flooding, and with the hydropower generation requiring a constant supply of water, Itezhi-

Tezhi Dam serves to retain water in the wet season. The construction of the 120 MW hydropower station at Itzhi-Tezhi Dam started in 2016 (ZESCO, 2020).

e. Victoria falls

Victoria Falls hydropower plant is owned and operated by ZESCO. The following three power stations with a combined generation capacity of 108 MW:

- i. Plant A, commissioned in 1937, has an installed capacity of 8 MW.
- ii. Plant B, commissioned in 1968, has an installed capacity of 60 MW.
- iii. Plant C, commissioned in 1972, has an installed capacity of 40 MW.

f. Nkula

Nkula Hydropower Station is in the Shire River, one of the major distributaries of the Zambezi River. The plant comprises of Nkula A substation commissioned in 1966 with the total generation capacity of 35.1 MW produced from 3 turbines and Nkula B substation commissioned in 1966 with the total generation capacity of 100 MW produced from 5 turbines. The Nkula plant is the first major hydropower station in Malawi and currently the biggest in the country with a combined generation capacity of 135.1 MW.

g. Kapichira

The Kapichira hydroelectric power is owned by the Electricity Supply Commission of Malawi (ESCOM) and operated by Electricity Generation Company (Egenco) in Malawi. The plant is located on the Shire River, a major tributary of the main Zambezi River in Malawi. Kapitchira power was commissioned in 2017. The power plant is operated by 4 turbine engines each with a generation capacity of 32.4 MW which translates to a total installed capacity of 129, 6 MW.

h. Tedzani

The Tedzani Hydro Power Station is located on the Shire River in Malawi, about 6 km downstream of Nkula Hydro Power Plant. The Tedzani station has a total generation capacity of 102 MW produced from the following three substations (Egenco, 2020):

- Tedzani I commissioned in 1972 with a generation capacity of 20 MW.
- Tedzani II was commissioned in 1976 and with a generation capacity of 20 MW.
- Tedzani III was commissioned in 1995 with a generation capacity of 62 MW.

Minor Hydropower plants

a) Mulungushi Power and Lunsemfwa

The Mulungushi River is a tributary to the Lunsemfwa River, which in turn is a tributary of the Luangwa River, one of the major tributaries of the Zambezi River. The Mulungushi and

Lunsemfwa hydropower plants are among the oldest hydro plants in Africa, commissioned in 1925 and 1945 respectively, and have a combined generation capacity of 56 MW. The hydropower plants are operated by an independent power producer, Lunsemfwa Hydro Power Company Limited which sells its electricity to ZESCO.

b) Lusiwasi Upper hydropower

Lusiwasi Hydro Power station is in the northern provinces of Zambia. It has been upgraded to a generation capacity of 12 MW. The Lusiwasi River is a tributary of the Luangwa River, one of the major tributaries to the Zambezi River.

c) Wovwe Hydropower Station

The Wovwe Hydroelectric Power Station located on the Wovwe River in Malawi was commissioned in 1996 and has an installed capacity of 4.35 MW.

Based on this study, the current installed generation capacity in the Zambezi River is 5 862 MW with the Cahora Bassa hydropower power plant in Mozambique contributing 35.4%, followed by the Kariba North plant in Zambia at 18.42% (Table 9.1). Zambia has the largest hydropower generation capacity at 40.3% Mozambique at 35.4%.

Table 9.1: Current hydropower generation in the Zambezi River Basin

Hydropower Plant	River	Country	Generation Capacity (MW)	Total contribution by country (%)	Total capacity by country
Cahora Bassa	Zambezi	Mozambique	2075	35,40	2075 (35,4%)
Kariba South	Zambezi	Zimbabwe	1050	17,91	1050 (17,9%)
Kariba North	Zambezi	Zambia	1080	18,42	2366 (40,3%)
Kafue Gorge Upper	Kafue	Zambia	990	16,89	
Itezhi Tezhi	Kafue	Zambia	120	2,05	
Victoria	Zambezi	Zambia	108	1,84	
Mulungushi & Lunsemfwa	Mulungushi & Lunsemfwa	Zambia	56	0,96	
Lusiwasi	Lusiwasi	Zambia	12	0,20	
Nkula Hydro Power (A&B)	Shire	Malawi	135,1	2,30	371,05 (6,5%)
Kapichira	Shire	Malawi	129,6	2,21	
Tedzani	Shire	Malawi	102	1,74	
Wovwe	Wovwe	Malawi	4,35	0,07	
Total			5862,05	100	

9.5 New and planned hydropower projects

This section briefly describes the planned potential hydropower generation projects on the Zambezi River Basin to address the growing demand for electricity in the SADC region. While some of these projects have suffered setbacks, they still provide a potential for further consideration. The potential ZRB hydropower projects are based on the information available in 2020. The source information used to update progress on these details includes data obtained from ministerial statements, approved government policies, and updated information from countries' electric power utilities.

The proposed and ongoing hydropower expansion projects by country are presented and summarized below:

9.5.1 Mozambique hydropower potential

The list of potential hydropower projects on the Zambezi River is outlined in the Mozambique Integrated Master Plan (IMP) of 2018. The planned project has a total generation capacity of amounts to 5670 MW from the following projects that are still at conceptual or pre-feasibility stages:

Cahora Bassa North Bank (extension)

The project involves upgrading the northern section of the existing Cahora Bassa dam to produce an additional capacity of 1245 MW. The project is scheduled for completion by 2026 and upon completion; will supply Mozambique and neighbouring countries.

Mphanda Nkuwa Dam

The project is located downstream of Cahora Bassa, in the Province of Tete and has a planned capacity of 1500 MW. The construction works on Mphanda Nkuwa hydroelectric dam began towards the end of 2019 and the project is scheduled for completion in the next five years. Phase 2 of this project will include a further expansion by an additional 1125 MW. Another component of the project involves the CESUL Transmission Line Project that will transfer the electricity generated from the Mphanda Nkuwa hydroelectric dam throughout Mozambique and other neighbouring countries. The electricity generated from the Mphanda Nkuwa scheme is set to address the medium and long-term demand for energy and will benefit both domestic and cross-border markets.

Boroma Project

The project involves the construction of a power plant with a generation capacity of 200 MW on the Zambezi River in the Tete Province of Mozambique. In 2018, the Boroma project was in a pre-feasibility stage with no significant progress reported in the last two years. It has been reported that the project would depend on the success of the Mphanda Nkuwa project, as it will serve to provide regulation of fluctuating downstream river flows.

Lupata Dam Project

The project is located on the lower section of the Zambezi River and involves the construction of a hydroelectric power plant with a generation capacity of 650 MW. There has been no further progress update on this project since the pre-feasibility stages. This project is reportedly dependent upon the success of the CESUL Transmission Project.

Chemba Hydropower Project

The 1000 MW Chemba hydropower project on the main Zambezi River in the centre of Mozambique was announced in 2014 and subsequently, feasibility studies were undertaken. There has been no significant development on this project reported in recent years.

9.6 Zambia hydropower potential

Zambia has the potential to add a further 3750 MW of hydropower capacity from the following confirmed projects:

9.6.1 Devil's Gorge Project

The Devil's Gorge is the bilateral project between Zambia and Zimbabwe and has the proposed generation capacity of 600 MW built on either side of the riverbanks. While this project is currently on hold, it has been reserved as one of the potential sites for future development (Zambezi River Authority, 2020).

9.6.2 Batoka Gorge

The Batoka Gorge is a bilateral project in Zambia and Zimbabwe and has a proposed generation capacity of 1200 MW built on either side of the riverbank. The project is currently in the Environmental Impact Phase and should be considered a potential site for future development (Zambezi River Authority, 2020).

9.6.3 Mupata Gorge

The project is in the Zambezi River between the Kariba and Cabora Bassa Dams and has a potential generation capacity of 540 MW. The scheme is currently not being developed but has been reserved as a potential site for future development.

9.6.4 The Kafue Gorge Lower

The project is on the Kafue River, one of the major tributaries in the Zambezi River and involves an electricity generation capacity of 750 MW using five generators, each producing 150 MW. The project is located below the Kafue Gorge Upper (KGU) Power Station and will use the same water used by the KGU power station. Construction of the Hydropower plant commenced in 2016 with the first generator unit (150 MW) scheduled for completion by mid-2020 or latest quarter 4 of 2020 (ZESCO, 2020). Although the project is not complete the project is at an advanced stage.

9.7 Tanzania hydropower potential

While Tanzania currently does not generate any power from the Zambezi River, the following potential projects will contribute to the installed generation of the country. The following projects are being undertaken through the state-owned electricity utility Tanzania Electric Supply Company (TANESCO) which is regulated by the Ministry of Energy and Minerals.

9.7.1 Rumakali Hydropower Scheme

The project involves the construction of a 222 MW hydropower plant on Rumakali River, West of Njombe (Mdee *et al.*, 2018,). In 2020, a consultant was appointed to conduct feasibility studies, prepare conceptual design, and undertake environmental and social impact assessment studies.

9.7.2 Songwe hydropower scheme

The project is in the Songwe River that forms the border between Malawi and Tanzania; hence, the electricity generated will be shared equally between the countries. Three sites Songwe Bipugu (upper), Songwe Sofre (middle), Songwe Manolo (lower) each with the proposed generation capacity of 29.4 MW, 158.9 MW, and 177.9 MW respectively were identified and updated in the 2012 Power System Master Plan (PSMP) for Tanzania. In 2019, the Malawi and Tanzania governments jointly invited suitable consultants to conduct the feasibility study for the construction of the 180 MW Lower Songwe project. Based on the 2017 Integrated Resource Plan for Malawi, about 9150 MW would be developed on the Songwe Lower and scheduled for completion by 2029 or 2032 (World Bank, 2020).

9.8 Malawi hydropower potential

9.8.1 Tedzani IV

The project involves the addition of a fourth substation on Tedzani hydropower station on the Shire River. This project is under construction with a planned production capacity of 18 MW. Based on the 2019 Malawi Sustainable Energy Investment Study, the Tedzani IV project was scheduled for completion in 2020.

9.8.2 Songwe

The project is located on the Songwe River, a border between Malawi and Tanzania hence the electricity generated will be shared equally between the countries. Three sites Lower Songwe (Bipugu), middle Songwe (Manolo) and upper Songwe (Sofre), each with a proposed generation capacity of 29.4 MW, 129.9 MW and 177.9 MW respectively (Tanzania Government, 2016). In 2019, the governments of Malawi and Tanzania jointly invited suitable consultants to conduct the feasibility study for the construction of the Lower Songwe project. Based on the 2017 Integrated Resource Plan for Malawi, the lower Songwe project was prioritized and scheduled for completion by 2029 although the 2020 World Bank reports it is scheduled for completion by 2032.

9.8.3 Kholombidzo hydro

Kholombidzo Hydroelectric Power Station is located on the Shire River, about 54 km from Blantyre in Chikhwawa, Malawi. The project is planned for a generation capacity of 213 MW. The feasibility studies on the project were undertaken in 2018 and is was scheduled for completion in 2026 (Malawi Sustainable Energy Investment Study, 2019).

9.8.4 Mpatamanga Hydropower Project

The project is located about 40 km west of Blantyre, Malawi on the Shire River, between the existing Tedzani and Kapichira hydropower plants. The project has a planned generation capacity of 350 MW and developed by the government of Malawi in partnership with the World Bank. The project is scheduled for completion by 2024 and it remains the top priority financing support by the World Bank Integrated Resource Plan (World Bank, 2020).

9.8.5 Lower Fufu hydro-power project

The project involves the construction of a 261 MW hydroelectric power plant project in Rumphu, Malawi. The project is undertaken by the Malawian government in partnership with the World Bank, which provided funds to conduct the feasibility study.

9.8.6 Kapichira III

The third phase of the Kapichira hydroelectric power project will involve an additional generation capacity of 110-112 MW. Based on the 2019 Malawi Sustainable Energy Investment Study, the Kapichira project is scheduled for completion in 2024.

In summary, the above-mentioned planned hydropower expansion projects on the Zambezi River Basin will potentially produce about 13 126 MW of total hydropower potential. Mozambique is expected to contribute about 43% of the planned total generation capacity, with Zambia, Zimbabwe, and Malawi respectively contributing about 29%, 24%, and 10%. Although Tanzania is currently not producing any hydropower from the Zambezi River Basin, the country is expected to contribute about 4% of the planned output.

9.9 Southern African power generation overview

9.9.1 Establishment of the Southern African Power Pool

The installed capacity in the Zambezi River Basin also includes electricity generated from smaller hydropower plants in the Lunsemfwa River, the Lusiwasi River in Zambia and the Wovwe River in Malawi. The hydropower generated from the Zambezi River basin forms an integral part of the energy mix of the SADC. Although electricity from the Zambezi River Basin is an important resource, it is important to consider other energy sources, to focus on creating a common power grid and a competitive market, and establish power transmission lines linking the SADC region. Thus, a platform where electricity generated in the Zambezi River Basin could benefit not only the riparian states but also other SADC nations was established. In 1995 twelve member states of the SADC region (except Mauritius) represented by their respective power utilities founded cooperation of electricity power pool, the Southern African Power Pool. Subsequently, the memorandum of understanding, which endorses the establishment of the pool, was signed between member states.

The Southern African Power Pool's objective was to plan; coordinate and operate member state's electric power systems; ensure the successful expansion of the energy generation and transmission systems to the entire SADC region (notably to rural communities); and support and promote a fair and competitive market for electricity between member states. Furthermore, the Southern African Power Pool provides a platform for the development of a dominant, strong, safe, cost-effective, reliable, and stable interconnected electrical system in the SADC region. The Pool hopes to manage any negatively impacts on power generation and transmission

The SAPP is constituted by the following member states represented by respective power utilities:

1. South Africa represented by Eskom utility,
2. Malawi represented by Electricity Supply Corporation of Malawi (ESCOM) utility,

3. Mozambique represented by Electricidade de Mozambique (EDM) utility,
4. Zambia represented by ZESCO Limited,
5. Tanzania represented by Tanzania Electricity Supply Company Ltd (TANESCO)
6. Democratic Republic of Congo (DRC) represented by Societe Nationale d'Electricite (SNEL)
7. Zimbabwe is represented by Zimbabwe Electricity Supply Authority (ZESA).
8. Botswana is represented by Botswana Power Corporation
9. Namibia is represented by Nam Power
10. Angola is represented by Rede Nacional de Transporte de Electricidade (RNT)
11. Lesotho is represented by Lesotho Electricity Corporation (LEC)
12. Swaziland is represented by Eswatini Electricity Company (EEC)

Two types of membership exist between SAPP member states:

1. Operating membership for those countries with power transmission systems connected to at least one other member state, hence enabling power trading with each other. The operating members are responsible for all SAPP's activities related to the operation of the power pool, such as decision-making and signing of all SAPP's governing documents and on adherence to all policy procedures and guidelines. There are currently nine operating members in the SAPP's pool comprising of South Africa, Botswana, Mozambique, Eswatini, Lesotho, Namibia, Zimbabwe, Zambia, and DRC.
2. Non-operating membership for those members without an established grid interconnection and hence cannot trade power with any other member states. The non-operating members sign documents on the Inter-utility memorandum of understanding and participate in all activities except those related to the operation of the power pool. These countries include Malawi, Angola, and Tanzania. In 2019, SAPP signed an agreement for the establishment of a Transmission Interconnector between Mozambique and Malawi. Upon completion of the power connection, Malawi will benefit from the SAPP electricity trading and thus become an operating member.

9.9.2 The SAPP energy generation capacity

Energy is the backbone of all sectors of the economy and hence the essential component of any nation's development. The affordable and reliable supply of energy in each country ensures continuity of economic activities and improves foreign direct investment. The high demand for energy and weak and unstable power generation had adverse effect on growth and economic transformation. While SAPP strives to ensure wider coverage and consistent transmission of electricity, issues associated with power generation, such as intermittent outages are not unique in SADC member states. Based on the SAPP 2019 annual report, operating member states had a total installed generation capacity of 63 157 MW, but an operating generation capacity of 53 883 MW. With the inclusion of power generation from non-operating members, i.e. Malawi, Angola and Tanzania, the total generation capacity could be 70 455 MW. Their connection to the SAPP grid would yield significant benefits for the SADC region. In 2019, 2054.2 GWh of electricity was traded among the nine SAPP operating member states with a value of USD 107

million. South Africa accounts for 77% of the SAPP installed generation capacity from the nine operating members and such dominance will continue to the near future (Figure 9.33 and Table 9.2). Based on Table 9.2 below, SAPP planned to commission 18 509 MW from 2020 to 2023 with an almost equal share of the planned generation capacity coming from South Africa and Tanzania, each contributing 32% and 30% respectively. The committed generation capacity project is derived from various energy sources with 4 939 MW is planned to be commissioned in 2021.

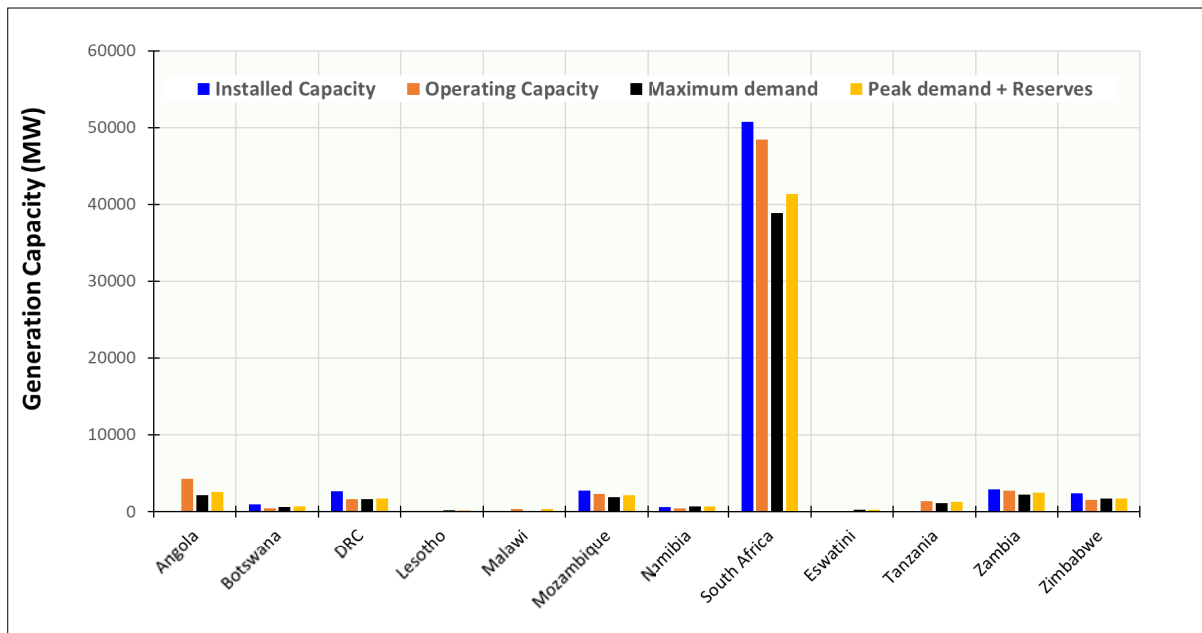


Figure 9.3: SAPP energy mix and electricity (installed vs operating vs maximum demand vs peak demand+reserves) generation capacity (Source: SAPP, 2019 annual report)

Table 9.2: Committed planned generation capacity (by country) from 2020 to 2023

Country	2020	2021	2022	2023	Total	% Share
Angola	65	-	2100	-	2165	11,7
Botswana	410	-	-	-	410	2,2
DRC	360	-			360	1,9
Lesotho	-	20	-	-	20	0,1
Malawi	60	278	-	258	596	3,2
Mozambique	30	-	550	-	580	3,1
Namibia	220	44	-	0	264	1,4
South Africa	1219	2342	1525	805	5891	31,8
Swaziland	-	10	-	5	15	0,1
Tanzania	27	1525	3430	600	5582	30,2
Zambia	765	120	200	101	1186	6,4
Zimbabwe	240	600	600	-	1440	7,8
Total	3396	4939	8405	1769	18509	100

Source: SAPP_2019 annual report

9.9.3 Energy generation mix

The SAPP's energy generation mix is dominated by coal (60%) followed by hydro (21%), open cycle gas turbine (OCGT) at 8%, wind and nuclear energy at 3.5 and 3% respectively (Figure 9.4). South Africa as the leading energy producer in the SAPP contributed 80% of wind energy, 84% of solar PV, 94% of thermal (coal) energy, 100% of solar CSP and 100% of nuclear power. Furthermore, South Africa provides all the SAPP's solar energy. Most of the hydropower generated comes from Angola (22%), DRC (17%), Zambia (16%), South Africa and Mozambique.

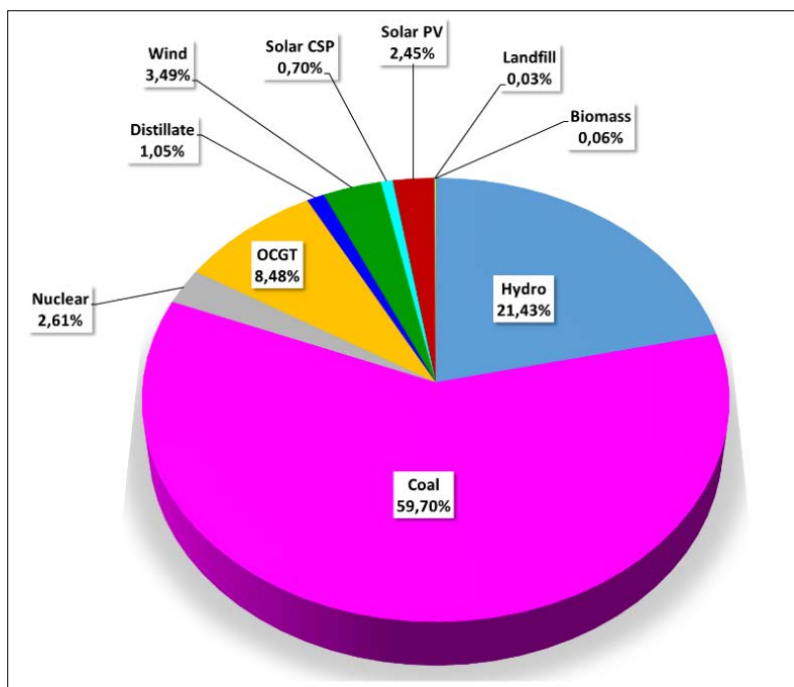


Figure 9.4: The SAPP 2019 generation energy mix from operating members

A brief overview of the SAPP member state’s energy generation with a particular focus on the contribution from the Zambezi River hydropower is now discussed.

9.9.4 The role of Zambezi River in Mozambique energy mix

According to Mozambique 2018 Integrated Master Plan (IMP), the country had an installed total electricity generation capacity of about 2 811.97 MW. Mozambique’s energy market is dominated by hydropower contributing about 81% of the total generation mix. The Mozambique power system, as of 2017, was divided into two systems: the southern system, and the central / northern systems. These two energy systems have separate grids and the power transmission from the Cahora Bassa Hydropower Plant to the south, where there is power demand, is carried by South Africa. The central and northern regions have a generation capacity of 660 MW from 11 power plants. The installed capacity comprises of 91% hydropower and 9% thermal power (Figure 9.5). The installed capacity in the southern region is about 442 MW from 9 power plants. The installed capacity comprised of 2% hydropower and 98% thermal power (Figure 9.5).

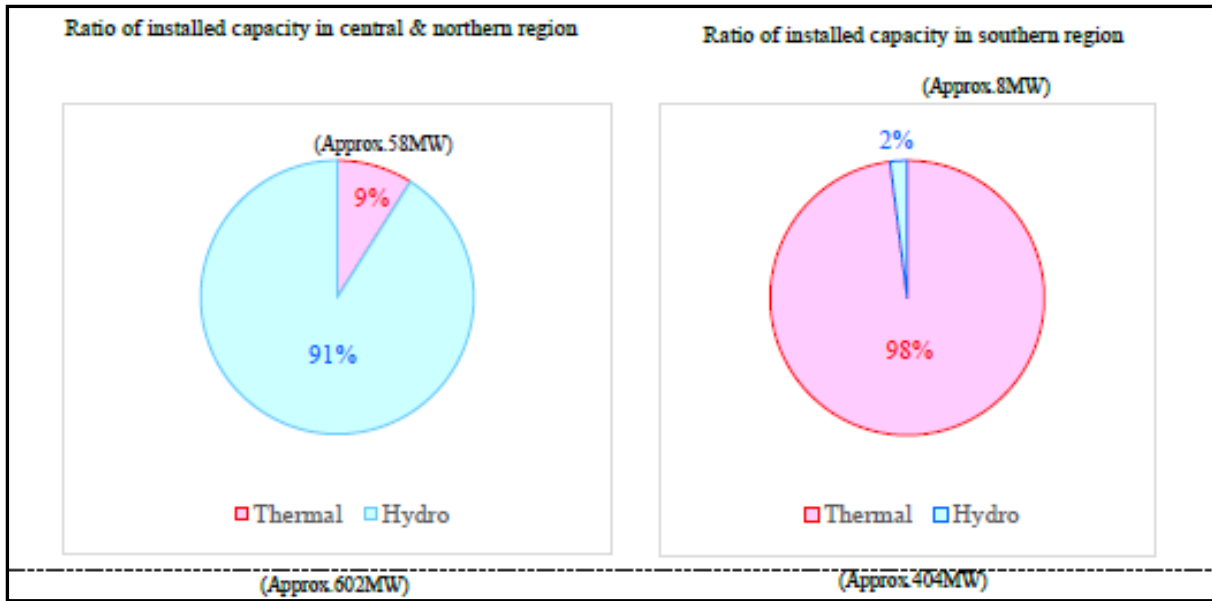


Figure 9.5: Ratio of installed capacity in the Central & Northern region, and southern area (Source: Mozambique Integrated Master Plan 2018-2043)

About 95% of Mozambique’s hydropower capacity is generated by the 2 075 MW Cahora Bassa Hydroelectric (HCB) facility located in the Zambezi Basin and is 92.5% owned by the government-owned electricity utility, Electricidade de Mozambique (EDM). According to Mozambique EDM Annual Report, 2019, 32% of the country’s population had access to electricity. South Africa exports 70% of the 2075 MW HCB electricity due to a long-term treaty. The state-owned electricity utility of EDM procures about 24% for domestic use while the rest is transmitted to Zimbabwe and Botswana via the SAPP (Mozambique IMP, 2018; Mozambique Business Plan, 2020-2024, EDM strategy 2018-2028). Mozambique has the 4th largest share (11.4%) of the Zambezi watershed; and it is the second largest producer of hydropower in the Zambezi River Basin. Furthermore, the country has the largest potential in the Zambezi River Basin with a planned generation capacity of about 5 670 MW.

9.9.5 The role of Zambezi River in Zambia energy mix

The installed electricity generation capacity in 2019 stood at 2 981 MW (Zambia Energy Regulator Annual Report, 2019). Hydropower accounts for 81% of Zambia's total installed energy mix, with about 99% of hydropower developed in the Zambezi River Basin. Of the other riparian states, Zambia has the second largest hydropower potential (3 750 MW) and the largest hydropower generation and resource, as the country occupies the largest share (41%) of the Zambezi River Basin. According to the Zambia National Energy Policy of 2019, about 31.4% of households had access to electricity, of which approximately 67.3% of households were in urban areas and 4.4% of households in rural areas. The Zambia government's rural access to electricity is expected to increase due to the Rural Electrification Act No. 20 of 2003 which provides for the Rural Electrification Authority to provide electricity infrastructure to rural areas of Zambia using appropriate technologies.

9.9.6 The role of Zambezi River in Tanzania energy mix

Tanzania has one the fastest growing economies. It has a total installed electricity generation capacity of 1 602 MW, with thermal based generation contributing the largest share of 63.36% and while hydropower contributes 36.64%. While Tanzania does not have hydropower generation on the Zambezi River Basin, and are still to connect to the SAPP grid, the country is set to benefit from about 588.2 MW planned projects. As of 2019, about 41% of the population has access to electricity. The Tanzanian government has launched several generation and transmission strategies to expand rural access to electricity such as national energy plans and studies on resource potential and technology costs of planned projects.

9.9.7 The role of the Zambezi River in the Angolan energy mix

According to the 2020 reports by the United States Agency for International Development (USAID) and International Renewable Energy Agency (IRENA), the country's generation mix of 5 236 MW is dominated by hydropower (59%). In addition, according to the 2019 SAPP annual report, hydropower contributed about 64% to the countries' total energy generation. While Angola has the second largest share (18.3%) of the Zambezi basin, none of its hydropower resource is generated from the Zambezi River Basin. Furthermore, the country is not connected to SAPP and hence derives no direct or indirect benefit from the Zambezi River basin in terms of energy generation. According to the USAID 2020 report, about 36% of the population in Angola have access to electricity, again, mainly the urban areas.

9.9.8 The role of the Zambezi River in the Namibian energy mix

By the end of 2019, Namibia had a total generation capacity of 614.5 MW, with about 56% derived from hydropower. Currently, Namibia does not have active or planned hydropower generation schemes on the Zambezi River Basin and the only benefit is through electricity imports from South Africa and other riparian states. Each year Namibia imports more than 50% of its electricity, mainly from South Africa (through a long-term contract) and to a lesser extent from Mozambique, Botswana, Zambia, Zimbabwe, and the Democratic Republic of Congo (DRC), through short-term power purchase agreements. The Namibian government has adopted several strategies aimed at reducing this heavy reliance on imported electricity, due to South Africa's ongoing domestic electricity generation crisis.

9.9.9 The role of the Zambezi River in the Zimbabwean energy mix

By the end of 2019, Zimbabwe had a total generation capacity of 2 412 MW, with hydropower contributing 44%, which is almost entirely (98%), generated from the Kariba hydropower plant in Zambezi River Basin. Of the confirmed planned project, Zimbabwe has the potential to generate 1 800 MW from the Zambezi River Basin. Zimbabwe heavily relies on electricity imports from South Africa and Mozambique, along with a few other countries. The country

plans to reduce the heavy reliance on imported energy once their coal-fired and hydropower expansion projects are completed.

9.9.10 The role of the Zambezi River in the Malawian energy mix

The country has a combined total energy generation capacity of 5 236 MW, and 75% of the total generation capacity is from hydropower. About 99% of the hydropower is generated from the Shire River with about 1% contributed by the Wovwe River. The rural access to electricity is extremely low, accounting for about 5%. Significant developments in Malawi's energy sector and recent sector reforms, including the unbundling of the national utility, ESCOM and the establishment of the Electricity Generation Company of Malawi (EGENCO), and the planned 1 318.2 MW Zambezi River hydropower potential is hoped to improve the country's electrification program. Furthermore, the Malawi energy policy of 2018 supports the diversification and restructuring of Malawi's power market to favour foreign direct investment and participation of Independent Power Producers (IPPs).

9.9.11 The role of the Zambezi River in the DRC energy mix

The DRC has a total energy generation capacity of 2 624 MW which is 99.9% from hydropower (SAPP, 2019) mainly from the Congo River. Currently, the DRC does not have hydropower plants on the Zambezi River. While the DRC has the largest energy generation potential (100 000 MW) in Africa, with hydropower accounting for 13% of the global hydro potential. The country has one of the lowest electrification access rates (9%) globally, with rural access currently at 1% (USAID, 2020).

9.9.12 The role of the Zambezi River in the Botswanan energy mix

Botswana has a total installed energy generation capacity of 892 MW, with 732 MW generated by the Morupule Power Station and the remaining 160 MW from emergency (and costly) diesel-powered plants (Botswana Power Corporation Annual Report, 2019). To meet the countries' electricity demand, Botswana imports electricity. In 2019 Botswana distributed 1 088 MW of electricity, with 52% (557 MW) generated locally and 48.8% (531 MW) imported from neighbouring countries (Botswana Statistics Department, 2019). South Africa remained the main source of imported electricity at 78% and SAPP supplied 15.9%. The remaining 4.8% and 1.4% electricity was sourced from cross-border markets and Namibia respectively. Cross-border electricity markets is an arrangement whereby towns and villages along the border are supplied with electricity directly from neighbouring countries such as Namibia and Zambia. According to Botswana Statistics Department third-quarter report of 2020, the country imported 39.1% of total electricity demand with South Africa contributing 34.2% of total electricity imports, Namibia accounted for 30.3%, while 26.5%, 5.6%, and 3.4% were sourced from the Southern African Power Pool (SAPP), cross-border electricity markets and Mozambique respectively. As of January 2018, Botswana's rural access was at 80%. The country has planned 100% rural access by 2020. While Botswana has a smaller share in the

Zambezi River water resource, hydropower does not form part of the country's installed energy capacity. Furthermore, there are no planned hydropower projects on the Zambezi River.

9.9.13 The role of the Zambezi River in the Lesotho energy mix

The country has one of the lowest rates energy accesses with a total energy generation capacity of 74.8 MW comprises entirely of hydropower generation. In 2019, peak demand reached 160 MW and Lesotho imported about 85 MW with (75%) of the imported electricity sourced from South Africa and 25% from Mozambique (World Bank, 2019; Lesotho Bureau of Statistics, 2019). The electricity demand in Lesotho has always outpaced production, and the peak demand was focused to grow to 304 MW by 2020 and 432 MW by 2030 (World Bank, 2019). Lesotho has one of the lower electricity access rates. Over 70 percent of the urban population of Lesotho has access to electricity, but only 20 percent of the rural population has.

9.9.14 The role of the Zambezi River in the South African energy mix

9.9.14.1 *Installed generation capacity*

South Africa is the leading producer of electricity in Africa accounting for about 40% of the electricity generated (South Africa Energy Sector Report, 2019). South Africa accounts for about 67% of total electricity produced in the SADC region (SAPP, 2019). The country has the highest levels of national electrification access rates and is one of only three with access levels above 60% in the SAPP countries (Eskom Integrated Report, 2020). In 2020 South Africa had an installed capacity of 50 323 MW, with 45 117 MW from Eskom-owned power stations capacity and 5 206 MW capacity from IPPs (Figure 9.6). The coal-fired thermal power dominates the installed capacity accounting for 83% of Eskom's station generation mix and 74% of the combined capacity when considering IPP (Eskom Integrated Report, 2020). Eskom's hydropower generation remains at 1.3%, which is about 600 MW of the total installed capacity. An additional boost to the South African grid is the 1 500 MW hydropower imported from Mozambique's 2 075 MW HCB under a long-term Power Purchase Agreement that ends in 2029 (EDM Strategy 2018-2028). Mozambique's electricity utility, EDM imports 950 MW from South Africa through a long-term agreement ending in 2025, at three times the price it was sold by Mozambique HCB to supply the Mozal SA aluminium smelting company in Mozambique (EDM Strategy 2018-2028).

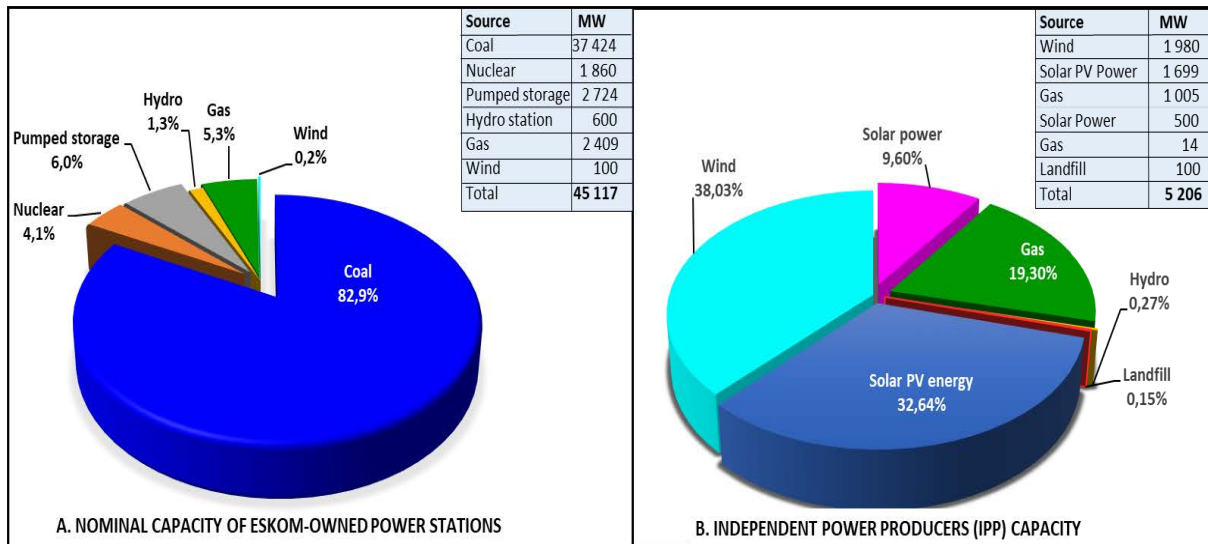


Figure 9.6: South African installed Generation capacity from Eskom-owned power stations (A) and IPPs based on operating stations (Source: Eskom Integrated report 2020)

9.9.14.2 Electricity Distribution

The South African distribution electricity in 2020 stood at 237 985 Gigawatt hours (GWh) with 90% generated by all Eskom power stations, 5% purchased from IPPs, 4% imported from Lesotho, Mozambique, Zambia, and Zimbabwe while 1% is from wheeling, i.e. electric power transmission (Eskom Integrated Report, 2020). According to Eskom’s integrated report, 2020, about 83% of the available electricity supply was consumed locally, 6% exported to Botswana, eSwatini, Lesotho, Mozambique, Namibia, Zambia, Zimbabwe, and SAPP utilities (Figure 9.7). The remaining 10% of the available electricity was lost due to technical losses, electricity theft and billing errors. The electricity imported by South Africa and from SADC countries is used to meet its high domestic demand and for other neighbouring countries connected on the South Africa grid based on their peak demand.

While South Africa is not part of the riparian states of the Zambezi River Basin, the country derives significant benefit from the long-term export contracts (since 1976) of hydropower exported from Mozambique HCB dam. The imported electricity contributes about 3% of the South African total installed capacity. South Africa is the main supplier of electricity for domestic use to approximately 70% of SADC countries. Therefore, the exported HCB hydropower forms an important component in the energy grid and assists with addressing the increasing demand.

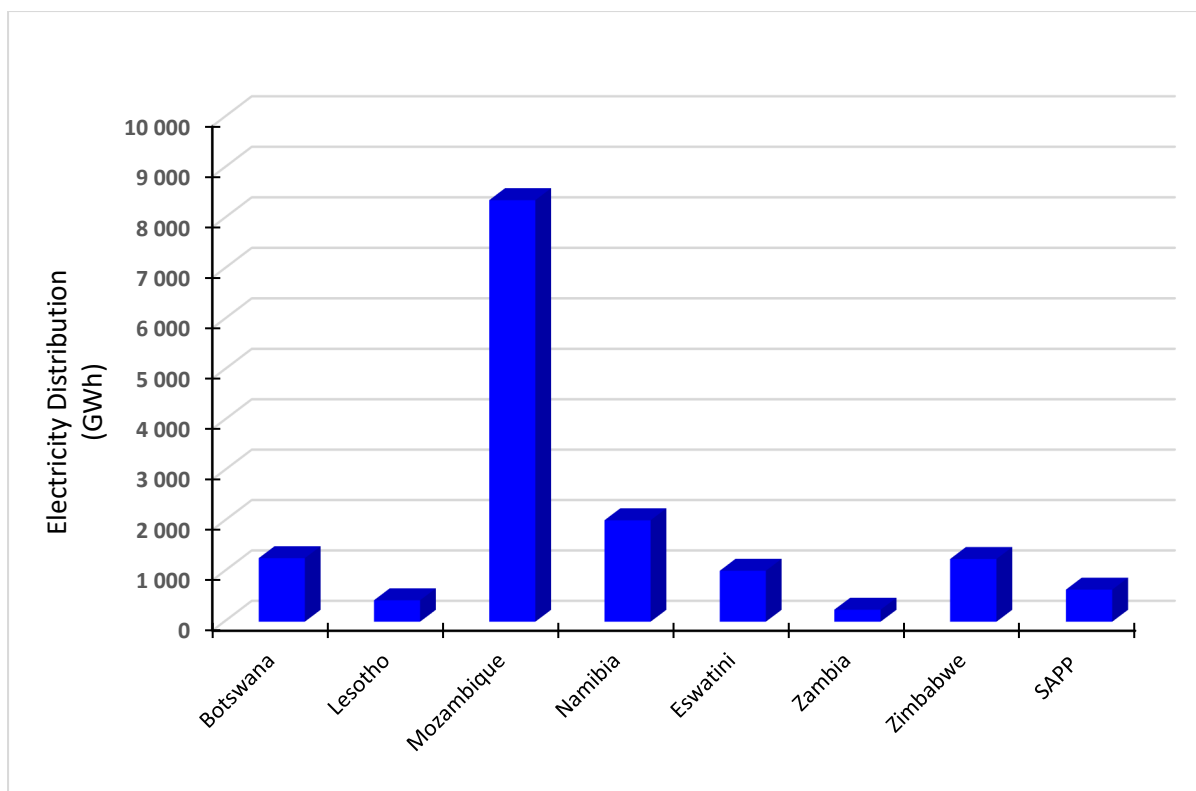


Figure 9.7: South African electricity exports to SADC countries (Source: Eskom Integrated report, 2020)

9.9.15 Advantages of hydropower

9.9.15.1 Zambezi River Hydropower

The Zambezi River is Southern Africa’s largest drainage basin and provides a primary freshwater resource to eight riparian countries. The river plays a pivotal role in ensuring the sustainable supply of energy, food, and water not only to countries constituting the watershed but also to most SADC countries. The vast water resource such as the Zambezi River Basin provides a major potential for hydropower generation, regarded as cost-effective and environmentally friendly compared to coal-fired power stations. The availability of cheap power stimulates economic growth, the development of towns, and the creation of employment. While initial investment costs for hydropower projects are relatively high, operating costs remain low and the plants have a long lifespan (Bartle, 2002). The river water resources are widely spread, often close to remote communities, and the resource remains mostly untapped. Large-scale hydropower generation also serves multiple purposes, such as irrigation, domestic water supply and recreation facilities (Bartle, 2002).

9.9.15.2 Climate Change Mitigation

The water resource of the Zambezi River is under strain due to various factors that include mining in the catchment area, sedimentation of the river, agricultural impacts, power generation, water pollution, deforestation and more recently by climate change characterised by unpredictable weather patterns, floods, droughts and heat waves. The average global temperatures continue to rise. Continued environmental degradation due to the massive destruction of forests is also a major cause for concern. Furthermore, demand for water has drastically increased over the last decade and is projected to further increase in Africa.

Studies by the World Nuclear Association (WNA) (2011) and Intergovernmental Panel on Climate Change (IPCC) (2012) show that hydropower is amongst the lowest greenhouse gas emitters throughout their lifecycle, even better than solar and biomass (Figure 9.8). Although hydropower resource is an alternative to coal and nuclear power, it is not without its challenges.

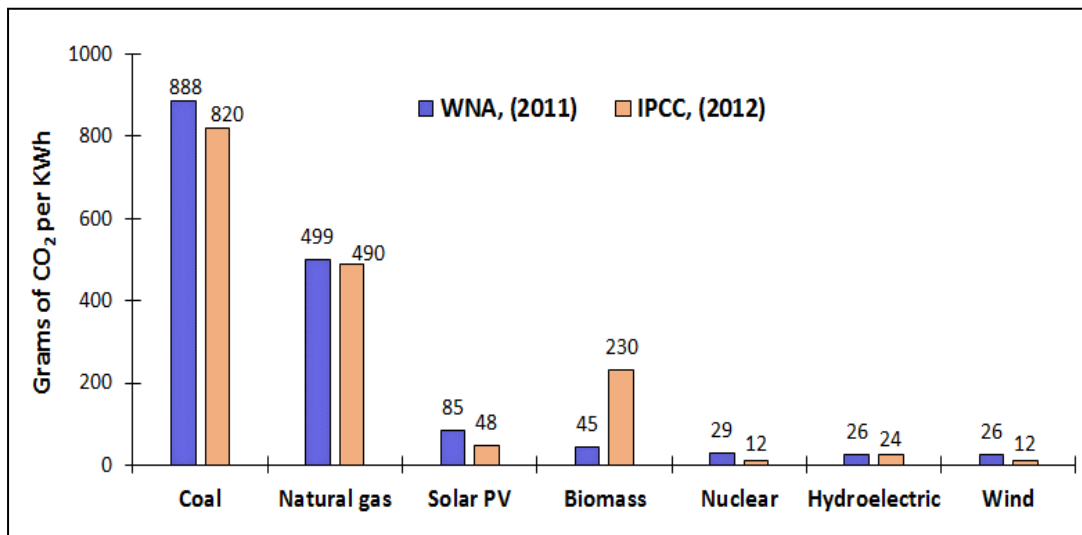


Figure 9.8: Lifecycle (median estimates) of greenhouse gas (GHG) emissions of selected energy sources (Sourced: IPCC, 2012 and WNA, 2011)

9.10 Effects of climate change on hydropower

Different sections of the Zambezi River have experienced climate variability. But it is predicted that droughts and floods will increase with climate change, adversely impacting on human lives and the economy of the SADC region.

9.10.1 Droughts

The current hydropower plants and planned hydroelectric projects (about 5 862 MW and the 13 126 MW respectively) on the Zambezi River Basin will increase water demand and hence require adequate stream flows. Apart from that, the Zambezi water resource is utilized for many social and economic activities. Prolonged drought periods adversely affect the output of current operating plants with the success of planned hydropower projects on the Zambezi River

depends on the availability of water. Climate variability from 2015 to 2020, resulted in lower water levels at the Kariba Dam. During this period, the sub-catchments in the Zambezi River drainage basin and its major tributaries experienced a water deficit. In some sections of the ZRB, less stream power and increased sediment deposition occurred, resulting in narrowing and/or shallower channel sections. Thus, reduced quantities of water reached the hydroelectric dams, thereby negatively affecting plant performance. As a result, Zimbabwe has experienced one of the worst power crises during 2019 with low water levels at the Kariba Dam compounding power outages. In 2019, the effects of low water levels in the Zambezi River led to the Zambian government imposing restrictions on water usage. The Zambian government through recommendations from Zambezi River Authority and ZESCO proposed the following restrictions on water usage and reduced generation to allow for planning and operation in the 2019/2020 season (Zambia Ministerial Statement, 2019):

1. From 1 June 2019, load shedding was implemented with an initial duration of four hours. Due to strain on the power grid, load reduction was further increased from four to eight hours to mitigate the possibility of a total blackout and damage to the national power infrastructure.
2. The generation at the 1 080 MW Kariba North Bank Plant was adjusted to 790 MW until the end of 2019, while generation at the 990 MW Kafue Gorge Power Station was revised down to 700 MW. The generation reduction led to a deficit of 600 MW during normal operating times and 700 MW during peak times.
3. The IPPs contributed to mitigating the further power crisis, however, the Lunsemfwa Hydro Power company which had operations at Mulungushi River and the Lunsemfwa River was shut down in July 2019 due to the non-availability of water for generation purposes.

Apart from load management through generation reduction Zambia further engaged South African energy utility, Eskom to import 300 MWs of power.

While the upper and middle sections of Zambezi River have experienced poor rainfall throughout 2019, torrential rainfall negatively affected transmission lines from Mozambique to South Africa.

9.10.2 Catastrophic natural disasters

The lower sections of the ZRBs have experienced persistent drought periods with occasional flooding and torrential downpours. The catastrophic effects of the Cyclones Idai and Kenneth in 2019 has not only threatened food security, resulted in people's displacement and loss of lives but also caused instability in the energy supply. The interconnections from Zambezi River's Cahora Bassa hydropower plant in Mozambique to South Africa were damaged, compounding the electricity crisis. After Cyclone Idai alone, South Africa's Eskom lost about 1 000 MW of hydroelectricity imported from the Cahora Bassa hydroelectric system in Mozambique. As the major consumer of hydropower from Cahora Bassa Dam and a leading supplier of electricity for domestic consumption and export to most SADC countries, South Africa's power supply was heavily affected. While the power lines connecting South African,

and Mozambique were undergoing repairs to restore power to the grid, South Africa and certain parts of the neighbouring countries were affected by intermitted load shedding

9.11 Electricity supply threats and challenges

9.11.1 The Role of South Africa in the SADC region

South Africa dominates the SADC regional power market as seven of the eight other countries (i.e. Botswana, Lesotho, Eswatini, Namibia, Mozambique, Zimbabwe, and Zambia) currently interconnected on the SAPP grid rely on imports from South Africa to meet their power requirements. When South Africa experiences supply shortages, there is a direct reduction in power available to sell to SAPP countries and therefore a direct reduction in regional trade. The climate variability in the years 2007/2008 and 2018/2019 led to prolonged unplanned generation outages that forced Eskom to notify Botswana, Swaziland, Lesotho, Zimbabwe, Zambia, and Mozambique that they would have to reduce their demand. Furthermore, according to Eskom's 2020 integrated report, load shedding in 2020 was implemented for 46 days/year due to aging infrastructure. The projected increase in demand for electricity and the impact of aging coal-fired power stations will negatively affect the entire SADC region's economic growth. Thus, any measures to improve supply into the Eskom system will directly contribute to supporting continued and expanded SADC regional electricity trade.

9.11.2 Impact of Load Shedding on the economy

Between February and March 2019, South Africa experienced one of the worst, unprecedented power crises since 2008, with rotational load-shedding reaching up to Stage 4 to ease about 4 000 MW from the national grid. Stage 4 load shedding involves intermittent rotational power cuts, three times per day for two hours at a time, or twice a day for four hours at a time (Eskom, 2019). The history and challenges related to the energy crisis in South Africa and its associated impacts are well documented. Chettiar *et al.* (2009) gives a detailed review of decade-long events and key indicators that led to the 2008 electricity crisis in South Africa. A study by Goldberg (2015) estimated the cost of load shedding at approximately R14 billion rand over the six months of load shedding in 2015. Therefore, South Africa is likely to have lost more than 200 billion ZAR in GDP since 2008 due to load shedding. This excludes the costs to South African households (see Nkosi and Dikgang, 2018). Thus, the planned hydropower projects in the Zambezi River are hoped to bring much-needed relief to the SADC region.

9.12 Energy policy framework, laws, and regulations

Energy supply is a key driver of economic development. The countries in the SADC regions have developed energy policies aimed at addressing the increasing demand for electricity for investment purposes and the need to improve their population's access rate to electricity. These policies, laws and regulations give an overview of countries' vision, policy principles, strategic goals, and objectives to inform the public and the international community on strategies that

are implemented in promoting energy and how to achieve them. Due to the establishment of SAPP co-operation, which aims at creating a competitive regional electricity market, the establishment of energy policy by members are to be based on SADC Protocol on Energy.

- The SADC Protocol on Energy of 1996 commits member states to develop and use energy to support economic growth and development, poverty alleviation and improvement of the standard and quality of life throughout the sub-region. The Protocol further commits member states to the main objectives, which include co-operation in the development and utilization of energy and energy pooling to ensure security and reliability of energy supply in the most efficient and cost-effective manner.
- The SADC Energy Sector Action Plan of 1997 recommends that the SADC energy program concentrates on priority activities that could be implemented efficiently on a regional basis for the benefit of the entire region.

The energy policies for some of the SAPP member states are summarised below:

9.12.1 South Africa

The South African energy mix is still dominated by coal, and this is expected to continue into the near future. While the introduction of load shedding and restrictions on the use of electricity by consumers is expected to continue. Eskom has introduced far-reaching measures to mitigate load shedding, implemented a proactive maintenance programme at existing power stations (Eskom Integrated Annual report, 2020). These measures, may, however, not provide a long-term solution. As a result, more and more commercial firms and South African households are opting to go either partially or fully off-grid, by installing gas stoves, geysers or opting for solar power. Despite this, the South African government has established the following short and long-term key energy development strategies based on countries' laws policies and legislation to diversify and strengthen the generation capacity:

9.12.1.1 *White Paper on the Energy Policy, December 1998*

This White Paper gives an overview of the South informs the public and the international community. It concludes that the sector can greatly contribute to a successful and sustainable national growth and development strategy.

9.12.1.2 *Renewable Energy White Paper (2003)*

White Paper on Renewable Energy laid a foundation for the promotion of renewable energy and affirmed the government's commitment, vision, and strategic goals aimed at increasing electrification rate and reduce reliance on fossil fuel through the integration of low-carbon emission renewable energy sources into the mainstream energy. To achieve these objectives, the Government set a target of 10 000 GWh of renewable energy increase by 2013, which was to be produced mainly from biomass, wind, solar and small-scale hydropower. This is approximately 4% (1 667 MW) of the projected electricity demand for 2013 (41 539 MW). This commitment was achieved as the current total renewable energy generation from both

Eskom and IPP is at 11% (5 560 MW) of the total generation capacity of 50 323 MW. Hydropower contributes about 11% (600 MW) of the current total renewable energy.

9.12.1.3 *Integrated Resource Plan (IRP) 2010-2030*

The integrated Resource Plan (IRP) outlines the projected energy demand in the next two decades (2010-2030) and pledged support for countries' energy diversification and requirements to achieve these targets. The plan on the electricity infrastructure development was intended to be a “living document” that would be periodically revised by the Department of Energy. The plan was promulgated in 2011 and it was updated in 2018 to include the new additional capacity of 18 000 MW since promulgation. The 2018 draft IRP was published for public comments and in 2019 was adopted.

The Draft IRP of 2019 made provision for the following new additional capacity by 2030:

- 1 500 MW of coal;
- 2 500 MW of hydro from the Inga Hydropower project
- 6 000 MW of solar PV;
- 14 400 MW of wind;
- 1 860 MW of nuclear;
- 2 088 MW for pumped storage schemes;
- 3 000 MW of gas/diesel; and
- 4 000 MW from other distributed generation, co-generation, biomass and landfill technologies.

Apart from the planned 2 500 MW Inga Hydropower project from South Africa-DRC treaty, there is a potential for run-off river hydro projects in South Africa's rivers. Apart from that, the long-term treaty between South Africa and Mozambique to import electricity from the 2075 MW Cahora Bassa dam terminates in 2029. Eskom may lose the 1 500 MW generated from Cahora Bassa as the old purchase agreement favours South Africa. According to Mozambique's EDM strategy report of 2018, the current tariff arrangement is not in Mozambique's best interests, since South Africa imports up to 1 500 MW at approximately 2.5 US cents/kWh but sells back 950 MW for the operation of Mozambique's Mazol Smelter at an average price of 9.5 US cents/kWh.

The planned generation programmes include a significant portion of renewable energy to reduce carbon emissions, and ease pressure on the continuously growing electricity demand in South Africa and SADC region, coal-fired generation will continue to dominate the energy mix soon. While the country moves towards a more environmentally friendly power sources, more emphasis should be directed effects of climatic changes as part of government strategies and project planning.

9.12.2 Mozambique

Mozambique's energy sector is dominated by hydropower and contribute about 4% of the SAPP's total generation capacity. The energy sector in Mozambique is based on the following main strategies, policies acts, and regulations as outlined by Mozambique Governmental Framework, 2020 and Mozambique Integrated Master Plan 2018.

9.12.2.1 *The Electricity Law (No. 21/97)*

- The electricity law defines a policy for the organization of the electrical energy sector and the administration of the supply of electrical energy.
- It also prescribes the general legal framework for electrical energy generation, transmission, distribution, and sale within the country; and controls the exportation and importation of energy from outside of the national territory, and the granting of concessions for such activities.
- The Electricity Law also allowed for private participation in the electricity industry.

9.12.2.1.1 *Energy Policy 1998*

It outlines the following vision for the sector: (1) a reliable supply of energy, at the lowest possible cost, in order to meet present demand and future levels based on economic development trajectories; (2) an increase in the energy options available for household consumption; (3) more efficiency in energy utilization; (4) the development of environmentally friendly conversion technologies, namely hydro, solar, wind and biomass and (5) the promotion of competitive, dynamic and more efficient entrepreneurs.

In terms of Renewables (2011-2025) the aim is to develop 125 MW of small HEP schemes and 100 MW by 2025. It also hopes to use solar PV.

9.12.2.1.2 *National Energy Strategy (2014-2023)*

Reinforces the Energy Policy of 1998, but with a specific focus on enabling better access to power by rural and peri-urban areas.

9.12.2.1.3 *Integrated Master Plan 2018-2043*

The integrated master plan encompasses all existing major laws, legislation, and policies in the power sector of Mozambique.

1. The national energy plan presents the comprehensive national power system development master plan including power generation, transmission, and distribution planning for the next 25 years (2018-2043).
2. The plan is aimed at balancing various energy sources including hydro, coal-fired thermal and gas-fired thermal.

3. The generation development plan advocates for diversification of the energy sector by meeting the following objectives:
 - Stage 1 – minimizing reliance on exported electricity.
 - Stage 2 – exporting 20% of domestic peak demand. PV and wind power will be installed to meet 10% of domestic peak demand. Gas-fired power plants will enable electricity exports to the region. The official target is to achieve universal electricity access by 2030.

For the period 2018-2027, development of generation capacity of around 4 172 MW is expected, 2 200 hydro, 792 gas, 170 solar, 60 wind (Mozambique EDM Strategy 2018-2028).

9.12.3 Zambia

Zambia's energy policy is designed to enable both public and private investors (IPP) to contribute to the renewable energy sector. The National Energy Policy 2019 (NEP 2019) builds on previous policies of 1994 and 2008 and is anchored on the Seventh National Development Plan (7NDP) and Vision 2030. The policy enables the government to purchase renewable energy at predetermined costs, reducing price volatility and attracting significant private sector investment to hydropower schemes.

9.12.4 Angola

Based on the Angola Energy Plan 2025, the country intends to increase electricity access from 30% in 2018 to 60% by 2025 with renewable energy expected to account for about 70% of this planned increase (Angola Government, 2018). The current installed generation capacity is at 5 236 MW and based on the Angola Energy Plan this capacity would be increased to 9 900 MW by 2025 with hydropower expected to contribute about 66%. Angola has many large river systems that could provide sufficient hydropower resources, and Zambezi River Basin is currently not part of their plans.

9.13 Discussion

Most SADC countries are highly dependent on hydropower. Hydropower in Mozambique and Zambia constitute 81% of their installed capacity, while Malawi's capacity is 99% hydropower. The installed generation capacity in DRC and Angola, despite not having active hydropower projects on the Zambezi River Basin, is still dominated by hydropower with 99.9% and 59% respectively. Electricity generation in such countries is at risk due to water stress associated with drought and increasing demand for water resources. Increasing temperatures lead to water deficits and affect the performance of hydropower plants while catastrophic disasters such as floods and cyclones destroy the infrastructure for all energy sources.

The demand across the SADC continues to grow due. Therefore, it is important that necessary transmission links that connect all SAPP members be developed. While hydropower in most SADC countries is the main source of energy, it is important to balance hydropower with other

economically reducing greenhouse gas emissions energy options. The effects of climate change on the Zambezi River have resulted in the cancellation or postponement of several hydropower projects or output revision in the generating capacity planned projects or operating of the hydropower plants. Thus, a better understanding of climatic change cycles and the changes in aridity trends will improve the planning and management of the Zambezi River water resource and assist in the modelling of the flood and drought patterns.

9.14 Conclusion

It can be concluded that the increasing demand for electricity throughout the SADC region can be met if these issues are addressed:

- Any planned projects on renewable energy and energy efficiency strategies should be based on extensively researched information on paleo-climate change patterns to predict future impacts.
- Studies on paleo-climate changes should be based on scientific evidence and must be aimed at modelling the changes in the river morphologies, flow and flood patterns, aridity evolution, and sediment deposit rates and frequencies.
- Despite hydropower and other renewable energy sources having the potential of providing a reliable, greenhouse gas emission-free energy source, the main barrier to HEP is the impact of climate change. The energy strategies and government policies do not acknowledge the impact of climate change, with no impacts modelled.

9.15 Recommendations

Hydropower is one of the major resources, not only to seven riparian states of the Zambezi River Basin but other major rivers in the SADC region such as Orange River in South Africa and Congo River in DRC. The total developed capacity in the main Zambezi River and along its major tributaries is currently 5 862 MW and confirmed potential projects have an additional capacity of 13 126 MW. The SADC countries that do not have a share in the Zambezi River waters derive indirect benefits through regional power exchanges managed through SAPP interconnection. It is therefore imperative that the development of hydropower within the Zambezi River Basin include both riparian states and members of SAPP. Furthermore, energy laws and policies should be developed in line with the following SADC Protocols:

- The SADC Protocol on Energy of 1996 commits member states to develop and use energy to support economic growth and development, poverty alleviation, and improvement of the standard and quality of life throughout the sub-region
- SADC Energy Sector Action Plan of 1997 recommends that the SADC energy program concentrates on priority activities that could be implemented efficiently on a regional basis for the benefit of the entire region.

For countries that solely rely on hydropower, it is recommended that alternative sources of electricity be incorporated to provide stability and free the committed flows for other uses such as irrigation and mining activities. The effects of climate change must form the basis of any

strategic plan and the issue of energy diversification be prioritized as the pressure for Zambezi water demand is mounting due to other uses that benefit the greater SADC region. The projections of future water demand need to be made against the background of future water resource availability, as the key driver of water resource availability is rainfall. Possible changes in rainfall patterns, water distribution, and utilization, and timing of hydropower will directly impact the water resources.

CHAPTER 10

CLIMATE CHANGE AND WATER SECURITY: DEVELOPMENTAL PERSPECTIVES FOR WATER-LINKED SECTORS IN A FUTURE CLIMATE FOR AFRICA (BI-NATIONAL ASSESSMENT): DIFFERENT DEVELOPMENTAL RESPONSE MODELS CONSIDERING SOCIO-ECONOMIC DRIVERS

10.1 Introduction

The effects of rising temperatures due to the greenhouse gas emissions into the earth's atmosphere and continued environmental degradation including global warming mostly due to increasing deforestation, burning of fuel is of public interest and hence requires coordinated efforts, to mitigate climate change its impacts. Determining how important climatic variables will change, quantifying their natural variability on multi-decadal or longer timescales, provides an opportunity for better risk management, reduced mitigation costs and enables the exploration of opportunities considering rising temperatures. While impacts of changing climate have been extensively discussed amongst professionals, however public education and awareness aimed at addressing negative public perception remains missing. The Water Research Commission of South Africa sees climate change adaptation as an integral component for the building of resilience and coping capacity of vulnerable communities.

The study, therefore, focuses initially and continuously on building the capacity of water-linked sectors within the two river basins, focusing on water resource utilisation and environmental issues including the impact of climate change on the water resource and possible contamination impacts. Furthermore, it is important that the vulnerability assessment of the two water resources and communities residing within these basins is investigated based on the updated information. Effective strategies aimed at managing the river water resource, mitigate and adapt to changing climate will in a long-term assist with the economic development of the region and save lives of communities residing in these communities. The outcome of the study will ensure local capacities are prioritized and utilized efficiently; the adaptative strategies are cost-effective, practical, and sustainable. Specific focus throughout is directed towards helping communities adapt to climate threats and utilize the water resource sparingly. Study outcomes must reach the intended audiences through proper channels including the dissemination of information through educational awareness campaigns to the communities relying on the two rivers for their livelihoods, industries such as mining, agriculture and fisheries. Such an approach will ensure local capacities are prioritized and utilized efficiently; strategies serve to minimize costs and promote the long-term sustainability of the initiative.

10.2 Aims and objectives

The main study objectives are:

- To conduct a vulnerability assessment of Zambezi and Orange River Basins focusing on riparian countries and communities.
- To provide adaptive response strategies to water resource vulnerability to increase the resilience of the water-linked sectors considering a changing climate that negatively impacts the Zambezi and Orange River Basins.
- To provide adaptive response strategies to extreme changing climate events such as prolonged draught periods and catastrophic. The suggested strategies provide alternative development options aimed at improving and sustaining the people's adaptive capacity due to extreme climate change events.

These objectives are to be achieved through an extensive evaluation of:

- The Zambezi and Orange River Basins' water utilisation by various sectors in the riparian states and Southern African Development Community.
- Environmental issues affecting the quality of each Basin's water resource such as contamination from mining and agricultural activities.
- Disaster management and emergency response and preparedness plans.
- Environmental threats affecting the quantities of water resource of Zambezi and Orange-Senqu Basins which negatively impacts the people. The specific focus is on climate change impacts on the basins' water resources.
- Educational Awareness programs aimed at demystifying climate change and promote responsible use of water resources and conservations. Existing policies and legislations on water management of these two basins.

10.3 Study area

10.3.1 The Orange River Basin

a. Background

The Zambezi River Basin is Southern Africa's largest drainage basin, estimated at 1,300,000 km² and covers about 2600 km (Shela, 2000). The river's geographic location from its source extends for about 50 km northward, towards the Democratic Republic of Congo before the river changes its course towards the south-west, a direction that is maintained for approximately 270 km into Angola. From Angola, the river flow changes direction to the south back to Namibia and finally flows in an eastward direction towards the border of Namibia and Botswana, Zambia and Zimbabwe passing through to Mozambique and emptying into the Indian Ocean. The Zambezi River Basin (ZRB) flows across eight countries and according to the Zambezi River Authority, the percent share of the river basin area in each country is as

follows: Zambia (40.7%), Angola (18.2%), Zimbabwe (16.0%), Mozambique (11.4%), Malawi (7.7%), Botswana (2.8%), Tanzania (2.0%) and Namibia (1.2%) The shared water resource is used for both the social and economic development of most of the riparian states. In addition, the basin plays a pivotal role in ensuring the sustainable supply of energy, food, and water securities not only to countries constituting the watershed but the Southern African Development Community (SADC). The total population of the Zambezi River Basin is about 45.3 million people with notable contributions from Malawi, Zambia, and Zimbabwe at approximately 15.2 M, 12.2M and 10.2 respectively (Ainsworth *et al.*, 2021).

Table 10.1: Percent of the River Basin in each country and population

Country	Percent of the river basin area in countries	The population of the river basin
Zambia	40.7	12 919 544
Angola	18.2	668 664
Zimbabwe	16.0	10 236 651
Mozambique	11.4	4 294 607
Malawi	7.7	15 270 979
Tanzania	2.0	1 768 732
Botswana	2.8	22 700
Namibia	1.2	105 891
Total	100	45 287 768

b. Geomorphology

The entire Zambezi River system is characterized by various geomorphologically unique features such as intensive incisions, faulting, rifting, uplifts, folding, and metamorphism attributed to the tectonic movements dating back to the breakup of Gondwanaland, about 160-140 Ma years ago (Figure 10.1). The occurrence of steep gorges and plateaus, waterfalls, valleys, vast flat floodplains, deep and shallow valleys, and meandering rivers are attributed to the tectonic movement, faulting, metamorphic activity, and folding followed by erosion and weathering processes (Moore, Larkin (2001); Timberlake, and Childes, 2004; Sanchez, 2018). Geomorphological features such as undulating terrains, variation in elevations, floodplains valleys, ravines, gorges, rapids, and waterfalls play a crucial role in controlling the flow of water (Shela, 2000; Moore *et al.*, 2007) and hence are exploited in the establishment of many hydropower plants in the region. The floodplains are associated with sideways erosion of the River and deposition of sediments, whereas the occurrence of other unique features such as gorges and falls is attributed to headwaters undercutting, erosion and incision (Timberlake and Childes, 2004) as steeper gradients characterize such areas.

The Zambezi River basin is subdivided into three distinctive geomorphological sections from the west to east: The Upper, Middle and Lower Zambezi Sections. The Upper Zambezi Section (UZS) covers an area of approximately 515,008 km² and it comprises the north-western and western territories of Zambia including the river source from the north, parts of the eastern

regions of Angola and borders north of Namibia, Botswana, and Zimbabwe. The UZS section represents the highest elevation of the river, with a maximum elevation of 1500 m above sea level (m asl) in the north and a maximum elevation of 900 m asl in the south, close to the Victoria Falls. The Middle section of the Zambezi starts below Victoria Falls covers an area of approximately 511,430 km² including the Copper belt, Central, Southern, and Lusaka territories together with small areas of the north-western and eastern provinces of Zambia, and Matabeleland North, the Midlands, and western Mashonaland areas of Zimbabwe (Beilfuss, 2012). Downstream from Victoria Falls, the river continues to flow to the east through a deep incision, the Batoka Gorge Devil's Gorge about 100 km further downstream. Lake Kariba is the most prominent structure measuring approximately 240 km in length and 10-20 km in width. Further downstream, the Kafue River one of the major tributaries is encountered. The Luangwa River is encountered about 100 km downstream. The Luangwa River marks the eastern end of the 200 km long Cahora Bassa Dam, the international boundary between Zambia and Mozambique and the lower section of the main Zambezi. The Zambezi Section (LZS) covers an area of approximately 340,000 km² and encountered stretching below the eastern end of the 200 km long Cahora Bassa Dam to the Indian Ocean (Beilfuss, 2012). The drainage area covers the whole of Malawi, a small strip of southern Tanzania along the eastern coast of the Malawi River, north-eastern and central areas of Mozambique, and some areas in northeast Zimbabwe. The Shire River, which originates as an outflow from Lake Malawi/Niassa/Nyasa is the largest tributary in the LZS section, flowing through southern Tanzania, Malawi, and Mozambique north of the Zambezi to the Indian Ocean

c. Geology

The Zambezi River has its formation dating back to the breakup of the Gondwanaland, which was followed by Karoo dolerite intrusions, coupled with the formation of the flood basalts (Elburg and Goldberg, 2000). The basement rock formations in the Upper section of the Zambezi River are mostly covered by Tertiary-age sediments belonging to the Kalahari formation (Figure 10.1). Few observable rock outcrops such as Karoo sandstones at Kalene Hills about 50 km from the source are observed. Further downstream and copper-rich sandstones, quartzites, arenites and conglomerates of the Copperbelt region further downstream which are covered by deep Kalahari cover are encountered. The termination point of the upper Zambezi River at Victoria Falls is characterized by Karoo-age basalt (Figure 10.1). The predominance of Kalahari Sands in the upper section of the Zambezi River Basin generally renders this section unsuitable for agriculture, except for small areas of subsistence agriculture along the richer soils on river terraces (Ashton *et al.*, 2001). The Middle section from the Victoria Falls and further downstream through lake Kariba and the west end of the Cahora Bassa Dam; the Lower part stretching from the west end of Cahora Bassa Dam to the Zambezi Delta are also characterised by Karoo age basalts and intrusive igneous basement rocks which are covered by Kalahari sands. The Middle section of the Zambezi River in the vicinity of the Kariba sub-catchment in Zambia is characterized by a plateau comprising of quartzites and associated rocks, underlain by Karoo Supergroup sedimentary rocks and basalt. These rock formations are deeply incised by the numerous streams flowing from the plateau to

Lake Kariba. The sub-catchment in the vicinity of the Kafue River, one of the major tributaries to the Basin drains the important minerals notable copper-rich sandstones and other rocks formations such as quartzites, arenites and conglomerates of the Copperbelt region. The Luangwa River, an important Zambezi River tributary drained variable source rocks, mostly dominated by Mesoproterozoic Irumide Belt in the north, coupled with younger Jurassic Karoo sediment within the Luangwa Valley such as composed of quartzites, sandstones, granites, and gneisses, underlain by sedimentary rocks.

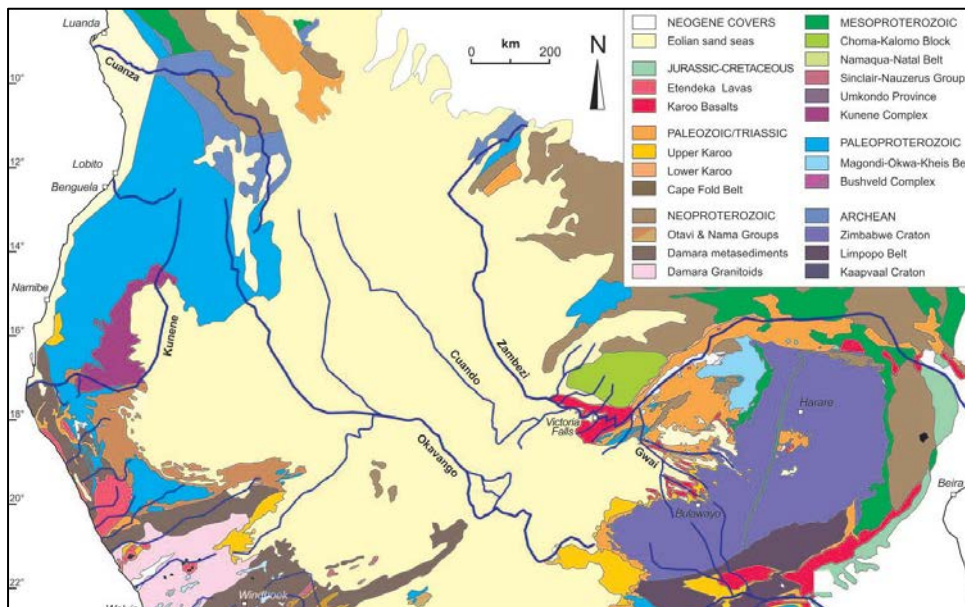


Figure 10.1: Generalised Geological map of the Zambezi River basin (Garzanti et al., 2014).

d. Climate Conditions

Temperature Patterns

The Zambezi River is characterised by variable weather patterns. According to the information published on the Zambezi River Basin Atlas, 2013 and (Chenge, 2000), the following average temperature patterns were recorded throughout the Basin (Figure 10.2):

- July is the coldest month, and the mean monthly temperatures vary from below 13°C for higher elevation areas in the south of the basin to 23°C for low elevation areas in the delta in Mozambique.
- The south-eastern part of the basin which comprises part of Zambia and the other part is in Zimbabwe is the coolest area.
- Ground frost occurs locally in some parts of the basin between July and August daily minimum temperatures in higher elevation areas in some parts of the basin can be below 0°C.
- October and November are the warmest months with the mean daily temperatures varying from around 23°C in the highest elevation areas, to 31°C for the lower parts of the Zambezi Valley (Chenje, 2000).

- The basin experiences a high daily range of temperatures, with an average range of about 10°C in the rainy season and as much as 20°C in the dry season in the southern parts of Zambia and northern Zimbabwe.

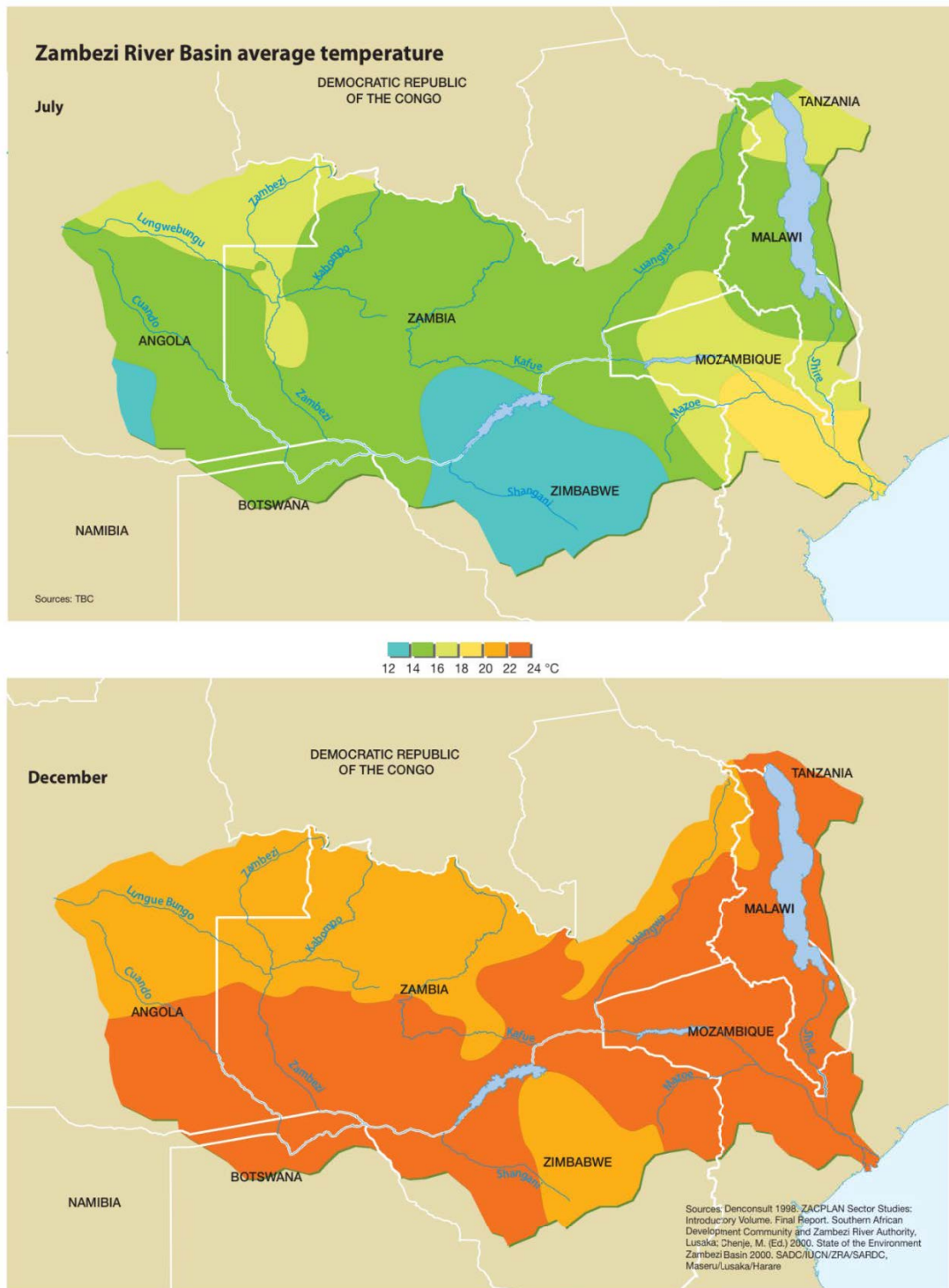


Figure 10.2: Zambezi River Basin average temperature (Source: Zambezi River Basin Atlas, 2013)

Rainfall Patterns

The average rainfall dataset information for the lower, middle, and lower sections of the ZRB are presented in Figure 10.3 and summarised as follows Kaseke (2016):

- The rainfall is variable throughout the Zambezi River Basin, with generally higher rainfall in the northern and western areas and lower rainfall in the south.
- In some areas of the UZS and around Lake Malawi, average rainfall reaches up 1,400 mm/year, while in the southern territories of Zimbabwe it drops to 500 mm/year.
- Therefore, the Northern and Western tributaries contribute significantly to the Zambezi River water pool compared to the southern tributaries. However, the existing water bodies such as reservoirs and wetlands often hold the water back, thus, only smaller quantities reach the Indian Ocean. Higher rainfall in the southern and western areas of the UZS contributes to the vegetation, which in turn contributes to higher humidity in the region.
- The Upper Zambezi section is well vegetated in the north, and the average rainfall ranges from 1000 to 1500 mm/year.
- The Middle Zambezi is characterized by lower rainfall (500 to 700 mm/year) towards the southern areas such as Zimbabwe, Botswana and Namibia and slightly higher rainfall (700 to 1100 mm/year) towards northern territories of Zambia.
- The Lower Zambezi region is characterized by higher rainfall (800 to 1300 mm/year) in the northern territories such as Tanzania, Malawi and north of Mozambique and lower rainfall (500 to 700 mm/year) in the central parts of Mozambique, and parts of north-eastern Zimbabwe.

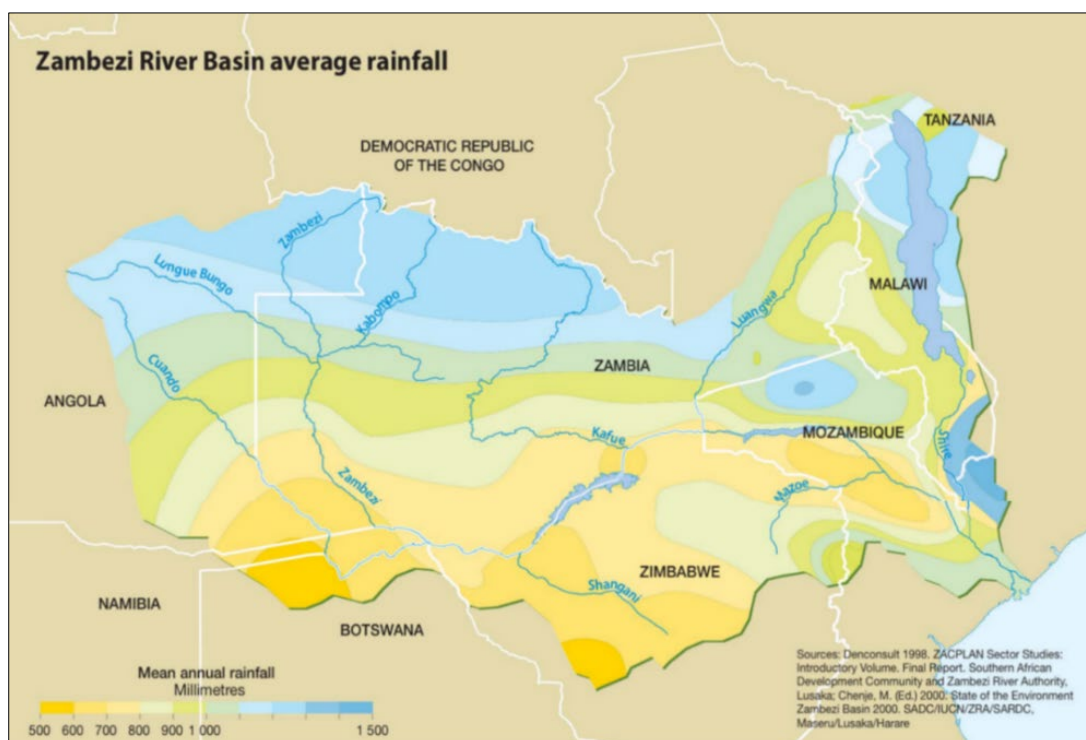


Figure 10.3: The average rainfall of the Zambezi River Basin (Source: Kaseke, 2016)

10.3.2 The Orange-Senqu River Basin

a. Location

The Orange-Senqu River Basin is one of the biggest rivers in Southern Africa flowing over four riparian states namely Lesotho, South Africa, Botswana, and Namibia before it empties to the Atlantic Ocean (Figure 10.4). The river covers the total catchment area of measuring 896,368 km² with South Africa occupying the largest share while Lesotho has the smallest share (Table 10.1) Lesotho, Namibia, and Botswana. The river has its catchment area in the Maluti Mountains (Drakensberg Mountains) of Lesotho and flows through central and western South Africa. The river receives its water inflows from several tributaries, which include Vaal, Makhalleng, Caledon, Fish, Auob and Nossob. The Orange River drainage basin is one of the five largest basins in the SADC, currently drains most of the plateau interior (nearly 1x10⁶ km²) between its source in the Drakensberg Mountains of Lesotho (maximum elevation of 3482 m asl) and the Atlantic Ocean on the west coast of the Republic of South Africa. The river flows westwards for approximately 2300 km across an arid interior plateau before emptying its waters into Atlantic Ocean (Garzanti *et al.*, 2012). The basin has a total drainage area of approximately 1,000,000 km² (Garzanti *et al.*, 2014) of which almost 600,000 km² is within the Republic of South Africa with the remainder in Lesotho, Botswana and Namibia (Table 10.2). The effective catchment area is difficult to determine since it includes many pan areas and several large ephemeral tributaries, such as the Molopo and Nossob in Botswana, that rarely contribute to flows in the main river channel The river is characterized by several physical features of economic value: waterfalls and natural and human-made dams and reservoirs.

Table 10.2: Geographic coverage of the Orange River Basin per country

Country	Orange River Basin- Geographic Coverage	Percentage of Basin Area
South Africa	528,857 Km ²	59%
Namibia	242,019 Km ²	27%
Botswana	98,600 Km ²	11%
Lesotho	26.891 Km ²	3%
Total Basin Area	896,368 Km ²	100%

Table 10.3: Summary of Basin Characteristics per country

Country	Proportion (%) of basin area	Contribution to natural runoff (%)	Proportion (%) of basin population	Water use in 2005 (Mm ³)
Botswana	7.9	0.3	0.3	negligible
Lesotho	3.4	41.5	15.4	20
Namibia	24.5	5.2	2.6	76
South Africa	64.2	53.0	81.7	5,309

Source: ORESECOM TDA, 2014

b. Geomorphology

The Orange River and its many tributaries (the Fish and the Vaal Rivers) have played a major role in shaping the landscape since the late Mesozoic (Nakashole, 2017). Periods of uplift and associated increased erosion in southern Africa include the Cretaceous, the Miocene and the Pliocene (Ibid, 2017). Jacob (2005) provided the geomorphological characterization of southern Africa dominated by several major landforms:

- The Upper Orange River section represents the eastern part of southern Africa is characterised by an uplift of the Drakensberg Mountains of Lesotho (maximum elevation 3482 m asl).
- Middle Orange River: This section is characterised by an elevated central plateau underlain by much of the Kaapvaal craton and it stands at more than 1 Km (>1000 m above mean sea level). It is separated by the Great Escarpment from the coastal margins along the Indian and Atlantic Oceans characterised by a high-relief low elevation coastal plain. The Great Escarpment is situated which occurs between 50-200 km inland from the coast (Nakashole, 2017).
- Lower Orange River: It is marked by outcrops of both Namaqua Metamorphic Complex and Gariep Belt rocks together with the Orange River making up the main geomorphic features in the area. The area between Noordoewer and the Orange River mouth is characterised by a low relief coastal plain and high relief inland area. High relief in the area is a product of the resistant lithologies that comprise the Namaqua Metamorphic Complex rocks. Ephemeral tributaries to the lower Orange River include the Gamkab River, Fish River and Boom River. From Noordoewer towards the river mouth, the palaeo-Orange River valley (early to middle Miocene) widens from 550 m to 2300 m and its gradient decreases downstream (from 0.87 m/km to 0.38 m/km) with an overall gradient of 0.69 m/km (Jacob, 2005).

c. Climate Conditions

In general, the climatic conditions are highly variable within the Orange River Basin. Not only are conditions very different spatially, but seasonality and extreme events such as droughts and floods are significant. The climate within the Orange River Basin varies widely from the source of the river in the east of the basin to the mouth in the west.

Temperature Patterns

The average daily temperature varies significantly across the basin. It ranges from approximately 12°C in the Lesotho Highlands to more than 22°C in the Richtersveld region near the river mouth. Extreme temperatures more than 50°C are often experienced along the banks of the Lower Orange River, while in the Lesotho Highlands temperatures below -10°C are common with some areas experiencing more than 200 days of frost per year.

Rainfall Patterns

Similarly, rainfall amount varies across the Orange River Basin. At the source of the Orange River, in the mountains of the Lesotho Highlands, the average annual rainfall is between 1,800 mm and 2,000 mm. On the contrary, the lower section of the Orange River, near the Atlantic Ocean, receives low rainfall in the order of 25-50 mm per annum. It explains the increasing aridity from east to west of the basin. The overall mean annual precipitation over the entire basin is estimated to be between 330- and 400-mm. Rainfall usually occurs from summer to late autumn. Interestingly, Lesotho has an average rainfall of about 760 mm per year, below the world average of 860 mm per year. Rainfall varies from less than 300 mm per year in the western lowlands to more than 1,800 mm per year in the north-eastern highlands. About 85% of the rainfall is received in the period October to April. Very intense storms occur, especially in the lowlands, and as much as 15% of annual rainfall may occur in a 24-hour period in some areas

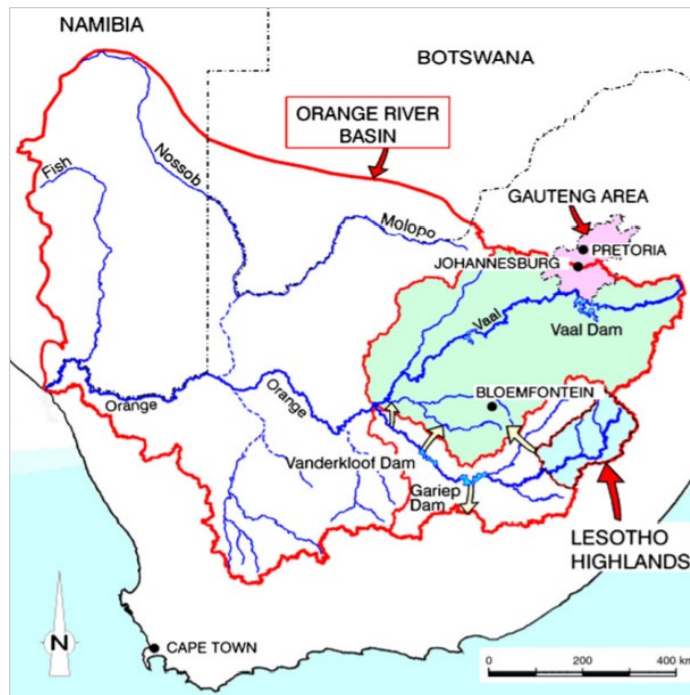


Figure 10.4: The Orange Basin (Source: Lange *et al.*, 2007)

d. Geology

The study area, the Orange River drainage basin, is characterized by all the geological formations in southern Africa, from relatively young basalts, sandstones, shales and tillites of the Karoo System to the granites, lavas, and quartzites of the Archaean complex (Jacob, 2005). The basement upon which the geological formations of South Africa have developed is the Kaapvaal Province (Craton), which occupies the central and northeastern part of the country. The Upper Orange River catchment, including Lesotho, has thick basalt block, which caps the sandstones and clay shales of the plateau at 3000 m. As the Orange River and its tributary Vaal traverse to the Atlantic Ocean, within the confines of the Kaapvaal Craton, they encounter a series of Late Archaean and Early Proterozoic basins namely: Witwatersrand, Ventersdorp and Transvaal Supergroups, all of which accumulated in response to the progressive northward migration of depocentres (Tankard *et al.*, 1982). Further to the west, the Orange River traverses through Namaqua-Natal Metamorphic Province (NMP), an arcuate belt which is converged onto the western and southern margins of the Kaapvaal Craton, where both older crystalline rocks and their supracrustal cover were affected by this orogenic activity (Tankard *et al.*, 1982; Wilson, 1998). The NMP forms most of the crystalline basement of southwestern Africa in a triangular shape, the longer sides of which are 850 and 700 km in length. Lastly, the Gariep Supergroup, its foreland basin and some outcrops of Nama Group have been incised by Orange River as it enters Atlantic Ocean. All the above geological formations could potentially provide clasts to the river basin (Jurgen, 2005).

10.4 Zambezi and Orange-Senqu river water management

In the past, Zambezi and Orange-Senqu Rivers experienced challenges due to a lack of agreement on the management of the shared water resource by the riparian countries. Multiple and competing interests from these countries have led to difficulties for them to formally agree to equitable water resources allocation. In addition, numerous issues have added difficulty to reaching an agreement, starting with lack of time, money and attention required to solve other existing issues, legal and economic constraints and poor training, data collection and communication were severely affecting the water resource. While issues on management of the resource, this situation has improved there are still riparian countries that are not part of the joint management of the shared water.

The following commissions were established to oversee management and utilisation of the shared water resource between these rivers:

10.4.1 Zambezi River Authority

The Zambezi River Authority (ZRA) was established so that Zambia and Zimbabwe form an agreement, on the management of the water resource shared by these two countries. The ZRA functions include the operation, monitoring and maintenance of the Kariba and Victoria Falls hydropower stations (Sachez, 2018). investigation and development of new dam sites on the Zambezi River and analysing and disseminating hydrological and environmental information pertaining to the Zambezi River and Lake Kariba.

10.4.2 Zambezi Watercourse Commission

As the Zambezi River Basin provides essential water resources to eight countries there was no established formal organization that brought all countries together in agreement for the management of the watershed. The Zambezi Watercourse Commission (ZAMCOM) was then formed in 2014 as an intergovernmental institution with a clear objective “to promote the equitable and reasonable utilization of the water resources of the Zambezi Watercourse as well as the efficient management and sustainable development thereof” (ZAMCOM, 2021). ZAMCOM comprises all eight riparian countries.

10.4.3 The Orange-Senqu River Commission

The Orange-Senqu River Commission (ORASECOM) was established in 2000 to advise the four State Parties of Botswana, Lesotho, Namibia, and South Africa with respect to the sustainable management and development of the water resources of the basin. The role of ORASECOM is advisory in nature and the Commission, supported by the State Parties and several International Cooperating Partners (ICPs), has played a key role in improving our common understanding of the water resources of the basin through a wide range of studies such as the development of a basin-wide Integrated Water Resource Management (IWRM) Plan. The five to 10 years, plans enable a common understanding of the resource and its status as a

driver of economic growth and by its transboundary nature requiring joint management and sustainable development. Furthermore, the plans ensure that the management of the basin's water resources is optimised and sustainable support socio-economic upliftment and eradication of poverty in the basin; to ensure that the adverse effects of catchment degradation are reduced, and the sustainability of the resource use is improved; and resilience from water-related disasters, especially flood and drought, is maximised.

10.5 Water resources utilisation

10.5.1 Non-consumptive uses

a. Hydropower

Zambezi River Basin

The hydropower generation in the Zambezi River Basin contributes a total of 5862.05 MW (Table 10.4). The hydropower plants are located at Victoria Falls, Kariba Dam and Cahora Bassa and Victoria Falls on the main Zambezi River; Itzhi Tezhi and Kafue Gorge Upper in the Kafue River; Nkula, Kapichira, Wovwe and Tedzani on Shire River; and hydropower plants at Mulungushi River (a tributary of the Lunsefwa River) and Lunsefwa River a tributary of the Luangwa River (Table 10.4). There is an estimated 13126 MW of hydropower potential, mainly on the main Zambezi River and some from the wider Zambezi River Basin. Most hydropower projects within the Basin are not being developed but have been reserved as one of the potential sites for future development. The extensive details on the impact of hydropower generation in the Zambezi River are discussed in deliverable 3 progress of the Water Research Commission.

Table 10.4: The current hydropower generation in the Zambezi River Basin

Hydropower Plant	River	Country	Capacity (MW)	Contribution by country (%)	Total generation by Country	
					MW	Total %
Cahora Bassa Dam	Zambezi	Mozambique	2075	35,40	2075	35, 4%
Kariba South	Zambezi	Zimbabwe	1050	17,91	2366	40.3%
Kariba North	Zambezi	Zambia	1080	18,42		
Kafue Gorge Upper	Kafue	Zambia	990	16,89		
Itzhi Tezhi	Kafue	Zambia	120	2,05		
Victoria	Zambezi	Zambia	108	1,84		

Hydropower Plant	River	Country	Capacity (MW)	Contribution by country (%)	Total generation by Country	
					MW	Total %
Mulungushi and Lunsemfwa	Mulungushi and Lunsemfwa	Zambia	56	0,96		
Lusiwasi	Lusiwasi	Zambia	12	0,20		
Nkula Hydro Power	Shire	Malawi	135,1	2,30	371,05	6.5%
Kapichira	Shire	Malawi	129,6	2,21		
Tedzani	Shire	Malawi	102	1,74		
Wovwe	Wovwe	Malawi	4,35	0,07		
Total			5862,05	100		100%

Orange-Senqu River Basin

There are several dams constructed across rivers within the Orange River Basin. Some of these dams predominantly provide hydropower to the local community within the basin and heavy industrial areas such as Gauteng. Below is a summary of some of the large storage reservoirs on the Orange-Senqu Rivers Basin:

- The Lesotho Highlands Water Project (LHWP) has a combined storage capacity in the Katse and Mohale dams of 2376 Mm³. The present rate of transfer, from Phase I of the project, is of the order of 780 million m³/a, or just over 7% of the overall Basin's natural annual runoff of 1300 million m³.
- The Vaal and Bloemhof dams with a combined storage of 3 843 million m³/a.
- The Gariiep dam forms the largest reservoir in South Africa with a capacity in excess of 5,000 million m³.
- Vanderkloof Dam is the second-largest reservoir with a storage capacity of over 3,200 million m³.

a. Fisheries

Zambezi River Basin

Fish is the primary source of protein for large parts of the population of the Zambezi River Basin. Therefore, fisheries play a significant in providing food security in the basin especially in Zambia, Angola, Malawi, Zimbabwe, and Mozambique. Fishing is mainly undertaken on artisanal (small-scale), medium-scale and large commercial scale in inland, lake-based, and riverine sections including floodplains during flooding. All kinds of fishing and related activities in the Zambian section of the Zambezi River Basin in mainly concentrated in seven

(7) major capture fishery areas namely: Upper Zambezi (e.g. Barotse Floodplain), Lukanga swamps, Lake Kariba (including Zimbabwe section), Lake Itzhi-tezhi and Kafue flats and Lower Zambezi. While it is very difficult to obtain the exact and updated trading and production figures of fishing within the Zambezi Basin, Ainsworth et al., 2021 provided an estimated fisheries production in the main Zambezi, its major tributaries and lakes from various literature sources ranging from 1980 to 2016. To ensure equitable utilisation of water resources, the fishing industry in the basin is strictly regulated. For example, the Zambian Ministry of Fisheries and Livestock requires that all commercial uses including commercial fish farmers are issued with aquaculture permits valid for five (5) years. On the contrary, small scale or subsistence fishing operation does not need a permit, and this benefits mostly rural communities (Zambian Ministry of Fisheries and Livestock, 2021). The study by Food and Agriculture Organization in 2000 reported annual catches averaging around 10 000 million tonnes for the Zambian sector, where over 2 000 small-scale fishers were reported to be operating with a fleet of some 1 700 canoes. In addition, the fisheries of the Zambezi drainage, excluding Lake Kariba, provide catches of about 20 000 million per annum, harvested by about 10 000 local fishers using mainly gillnets and a fleet of some 6 000 canoes. Fisheries provide income opportunities to an estimated two million people, especially in the flood plains riverain and coastal. In Zambia, about 8 430 people are estimated to be involved in processing and trade, although this is likely an underestimation (Ainsworth et al., 2021).

b. Navigation

Zambezi River Basin

Passenger and cargo navigation services are mainly practiced on Lake Malawi, having ports and boat facilities that handle more than 150,000 tonnes and 300,000 persons per annum, respectively. In fact, because of difficult terrain and inadequate road networks around Lake Malawi, Kariba and Cabora Bassa, ships or boats are the only means of transporting goods and passengers for most of the lake shore settlements. The lakes of Kariba and Cabora Bassa are also popular for tourists and sports boating. Navigation on the main river itself is, however, limited by shallow depths, rapids, and high flow velocities. The Barotse floodplains of the Zambezi River in the Western Province of Zambia are also navigable, especially during the rainy season. Navigation in the Barotse flood plains is the only transport between Mongu, the provincial capital, and the west bank of the river. Navigation is also popular in the area as it is used for the centuries-old traditional and cultural evacuation from and reoccupation of the summer and winter residences of the Barotse king, Litunga.

10.5.2 Consumptive uses

a. Water supply

Zambezi River Basin

While reliable data on domestic water and institutional water use are not readily available, a portion of the water used by domestic and urban users in the Zambezi River Basin is derived from groundwater sources. Several urban centres in the Zambezi River Basin such as Kitwe, Ndola, Lusaka, and Kafue in Zambia; and Bulawayo, Gweru, Kwekwe, Harare in Zimbabwe have significant industrial and commercial activity requiring reliable water supply from the Zambezi River (World Bank 2010). In 2000, the requirements for water supply and sanitation, estimated from the basin and hinterland population of 45.3 million, is about 3340 million cubic metres per year or 80 m³ /s (Shela, 2000). Although surface water resources are the commonest sources of water supply systems, most of the population uses groundwater sources through boreholes and wells (Shela, 2000). With increasing population growth, urbanisation, and other urban development projects such as construction, the supply is expected to surpass the demand.

10.5.2.1 Orange-Senqu Basin

Lesotho supplies water to South Africa through the Lesotho Highlands Water Project (LHWP) from the Orange-Senqu River Basin. Furthermore, Lesotho is expected to supply to South Africa through the LHWP infrastructure, Lesotho's royalty income from water delivery and electricity sales will make the water resources of the Orange River Basin an even more important factor for the national economy, even though the country does not use most of the water for itself.

a. Agriculture: Irrigation

The Zambezi River

Agriculture is the largest water consumer in the Zambezi River Basin and agricultural activities are dominant in Malawi, Mozambique, Tanzania, Zambia, and Zimbabwe. The smallholder farmers, private estates and public irrigation schemes irrigate cereals (mainly rice, wheat and maize), vegetables, sugar plantations and tea (Shela, 2000). Notable large irrigation fields with at least 10,000 hectares each are sugar plantations in Malawi and Zambia (Shela, 2000). Senzanje and Dirwai, 2020 gives give an extensive review of the current agriculture activities, future potential irrigation developments and food security to face climate variability in the Zambezi River Basin. Based on the study, more than 90% of the agricultural activity in the basin is based on flood plain cultivation and rain-dependent agriculture, and this is what sustains the bulk of the rural population in the Zambezi River Basin. While irrigation is the largest water consumer the agricultural sector covers an estimated are of 147 000 ha to 259 000 ha it remains water-use intensive, and hence greatly contributes to the water utilisation in the basin. Irrigation is estimated to consume about 3 235 million cubic metres of water currently

amounting to 1.4% of the basin's renewable water resources (Senzanje and Dirwai, 2020). There is huge irrigation development potential in the basin, and indeed there are ambitious plans to triple the area under irrigation by 2025 which will increase the water for irrigation to about 4.1% of the basins' renewable water resources (Senzanje and Dirwai, 2020). Smallholder irrigation practices are dominant in the Zambezi River Basin, consequently, basic agricultural water management coupled with sustainable agricultural intensification is a key aspect of agricultural production supporting many rural households. Typical practices in the basin include; bucket irrigation systems, gravity-fed off-river and reservoir irrigation, dambo irrigation farming, treadle pumps used in conjunction with bucket or drip kit irrigation, motorized pumping irrigation, drip irrigation including drip kits, sprinkler irrigation and centre pivot irrigation (Senzanje and Dirwai, 2020). There is evidence that water demand for irrigation has over the last 20 years. A study by Shela, 2000 estimated that some 200,000 hectares have been developed for irrigation and about 7 million hectares can be irrigated within the basin and the demand and commitments for irrigation requirements ranging between 200 and 400 m³ /s at peak abstraction times.

The Orange-Senqu River

Agricultural activities in the basin area have supported the local and national economies of South Africa and Lesotho significantly. 70% of South Africa's cereal crop is produced in the area. These agricultural activities in the South African portion of the basin support both local and national economies. Food production in the basin contributes to livelihoods, markets, raw materials, and foreign exchange. The lower section of the basin has received significant support from the government in terms of irrigation schemes. It has been more efficient, diverse, and productive. In the area from the Orange / Vaal confluence to the river mouth at Alexander Bay (lower Orange) the significance of commercial agriculture (crops such as grains and fodders) as an economic sector becomes greatest. Lower parts of the basin concentrate on high value crops such as citrus, table grapes, pistachios, and pecan nuts, with livestock being kept in the drier areas. In Lesotho, almost 50% of the population sustains their livelihoods from crop cultivation and agriculture accounts for around half the country's income. The main commercial agricultural zone is the western lowlands, but small-scale agriculture is also practiced wherever the terrain of the Maloti Mountains allows it. There is a high reliance on rainfed agriculture, with only around 3% of the total irrigable area under water management.

10.6 Inter-basin transfer

Several inter-basin water transfers from the Zambezi River to the southern regions of SADC, which include irrigation requirements, are being contemplated currently. Yet there are un-exploited irrigable tracks of land along the river, for example, the Kafue flats, Gwembe and Lusito valleys near Lake Kariba and the Lower Zambezi and Shire flood plains, that can be developed as viable irrigation schemes.

10.6.1 Mining

a. The Zambezi River

Mining in the Zambezi River Basin is one of the major water consumers of surface water during the mining operation. Major mining activities in the Zambezi River Basin include the extraction of gold, platinum, chrome, and copper and the acid mine drainage is associated with all these types of mining. In Zambia's Copperbelt Province lies the mineral-rich area, the Copperbelt, which mainly falls within the Kafue River Basin. Therefore, Kafue River drains heavy metals such as copper, manganese, and lead to the main Zambezi River.

b. The Orange-Senqu River

Mineral extraction is one of the potential important economic sectors in the area. Owing to the region's geology, the basin contains fuel deposits (coal) and mineral resources of regional and global importance. Large mining operations have been established, related to diamonds and other minerals. They contribute to economies and create employment. In recent years, mining activities in Lesotho have increased. The Letseng diamond mine, the world's highest at 3,200 metres above sea level, has started producing some of the largest diamonds in the world. These mining activities have started providing jobs to people in the Highlands area. Environmental issues related to mining activities include effluent discharges, increasing acid mine drainage (AMD), elevated sediments concentration resulting from runoff from cleared overburden mine wastes, Water turbidity downstream for a long distance resulting from diamond mining and uncontrolled river sand abstraction.

10.7 Vulnerability assessment

The vulnerability assessment in this study can be broadly categorised into basins vulnerability assessment and Community vulnerability assessment and further discussions are provided below:

10.7.1 Basin's water resource vulnerability

a. Water utilisation: Demand and Supply

The increasing demand for water by various sectors such as hydropower, agriculture, fishing and mining renders the river basin vulnerable due to supply constraints., Hydropower, agriculture and mining are the main sectors that greatly contribute to the water utilisation in Zambezi and Orange Rivers and in some cases, the increase in demand due to an increase in abstractions may exceed the supply. Zambezi water resource is utilised by different countries and according to a study by Senzanje and Dirwai, 2020 and Shela 2000, the demand for water in the basin has increased significantly over the last 20 years The increased mining activities especially in the mineral-rich Copperbelt of Northern Zambia and the chromium and nickel,

gemstones and gold found in multiple small areas in Zimbabwe, hydropower generation and agriculture sectors resulted to the intensive use of the water resource. The smallholder farmers, private estates and public irrigation schemes irrigate cereals (mainly rice, wheat and maize), vegetables, sugar plantations and tea. Notable large irrigation fields with at least 10,000 hectares each are sugar plantations in Malawi and Zambia. The utilisation of water resources for various economic activities results in reduced volumes of water reaching the mouth of the river and the situation has not improved over the last 20 years. Shela, 2000 reported that, in cases, the Zambezi River Basin has had cases where there is little or no water supply (recharge of the river) due to prolonged droughts periods some parts of the basin may have significantly low available water resources to meet the increasing demand.

b. Climate Change variability – Rainfall patterns

As the demand for water increases the hydrological regime changes. This negatively impacts the availability of water resources for various economic activities such as irrigation, mining and tourism are negatively affected. Seasonal farming and spectacular tourist attractions such as Victoria Falls are negatively affected. When the mean annual runoff is reduced due to prolonged drought periods, and current and planned production across the river is also reduced as rivers would have to rely on inadequate natural flows. Lower rainfalls may lead to diseases outbreaks as there is less water in the system to dilute increasing volumes and types of contaminants on water used for drinking. The reduced and altered patterns of flow and changes in sediment load and balance changes river morphology. Therefore, changes in river flow regimes impact not only production but the ecosystems downstream.

c. Water Resource Pollution

The major sources of pollution include contamination from domestic waste, agriculture, the mining sector, and industries. Degraded water quality has widespread economic and environmental impacts, and often poses a direct threat to human and animal health if not managed. Various activities such as both legal and illegal mining activities at close proximities to the water resource contribute to the decline in the quality of the resource. Process water and slurry spillages from the mining of different commodities containing various contaminants that disturb the water salinity of the rivers. During mining activities, water may react with other acidic rock-bearing ores to produce acid mine drainage that may contaminate the nearby streams. Ashton *et al.*, 2001 provided an extensive study of the impact of mining and mineral processing operations on water resources and water quality in the Zambezi. The study indicated that contamination in the Zambezi River is generally low to medium. Agriculture is another source of contamination in these river basins. Fertilisers such as phosphate used during farming generally contain naturally occurring radioactive materials and Irrigation return flows if not properly managed may contaminate nearby rivers. Lack of proper sanitation (toilets) on rural settlements residing on the banks of the river and poorly operated sewage treatment works from urban settlements may result in microbial (faecal matter) deposition, which contaminates the rivers. The major implications of untreated domestic sewage that end up in the water resource

risk of waterborne diseases such as cholera and typhoid. The contaminants such as radionuclides, heavy metals and persistent organic pollutants, may pose a basin-wide risk, if not properly addressed.

d. Land degradation

Inadequate land management associated mostly with agriculture and mining in parts of the river basin has led to the loss of wetland storage and aquifer recharge, increased sediment loads, deteriorating water resources quality, increased distribution and abundance of alien invasive plants, loss of biodiversity and lowered land productivity. Poverty, population pressure and poor land-use practices have led to widespread catchment degradation, water resources degradation and pollution. Consequently, there are some serious soil erosion and increased runoff problems, with rivers flooding more frequently. Efforts to deal with the land and associated water resources degradation and pollution problems are frustrated by the fact that in certain cases poor communities unknowingly degrade the environment. Their survival means does not give them any other choice than to grow food by whatever means, or indiscriminately fell trees or burn coal to sell for survival. They cannot even afford to invest in good land husbandry practices. Yet the degradation and pollution is not only an environmental loss but has an economic cost which someone has to pay directly or indirectly.

e. Proper management of shared water resources

The challenges can only be addressed through coordinated efforts between the eight riparian countries (Angola, Botswana, Malawi, Mozambique, Namibia, Tanzania, Zambia and Zimbabwe). Therefore, better basin management is a priority due to the challenges the watershed is facing and those that it will face in the future. Multiple and competing interests from these countries have led to difficulties for them to formally agree to equitable water resources allocation. In addition, numerous issues have added difficulty to reaching an agreement, starting with lack of time, money and attention required to solve other existing issues, legal and economic constraints and poor training, data collection, and communication. The intergovernmental institution, (ZAMCOM) established in 2014 brought riparian countries together to discuss issues related to the management of the watershed. Orange-Senqu River Commission (ORASECOM) was established in 2000 to advise the four State Parties of Botswana, Lesotho, Namibia, and South Africa with respect to the sustainable management and development of the water resources of the basin. However, there is still gaps that will take various intervention.

While contribution made by these organisations is commendable, there are still various issues that impact management of these water resources. This includes lack of data contribution between all eight countries. Some countries have collected hydrological data for multiple years, while others do not possess the tools to maintain them or to make use of them. Uncertainty on the data collected causes gaps of climatic information for the overall region. Data on monitoring contamination along the basin is not uniform to allow for early detection pollution

of the river. Political conflicts have also affected the functionality of these commission and some of the installed data collection systems (sensors) are not tested and serviced to ensure functionality. The lack of system testing interrupted data sets and gaps in data collection cause a lack of precision in the outcome of any research. As different countries are involved, there is generally reluctance in sharing information and hence it is a challenge to create an integrated database with information collected by all riparian states. It is important that data on changes in climatic condition and patterns be collected consistently over a long period so that changes in precipitation patterns are model for decades ahead. Huge e uncertainties on data collected provide unreliable outcomes. The above-mentioned challenges are less severe between Zambia and Zimbabwe due their proximity and the fact that Zambezi River Authority has been in existence over the past 35 years. As the Zambezi River Authority focuses its activities on the section of the Zambezi River shared by Zambia and Zimbabwe, it was easy to set up an efficient monitoring system and database. Each basin state maintains its system of meteorological and hydrological data collection, primarily for use at the national level. Whilst these systems are at very different levels of coverage in the different states, all data is fed into regional data systems such as the Drought Monitoring Centre in Harare, Zimbabwe, where the data provides important information for national and regional agricultural planning systems.

10.8 Peoples' vulnerability

Water is the most important resource and hence its vulnerability of the water resource directly impact people rendering them vulnerable. People relying on the water resource are vulnerable to the following threats related to water quality and quantity:

10.8.1 Economic vulnerability

a. Hydropower generation

The water demand for hydropower generation on the main Zambezi River is 1700 m³ /s and is likely to double soon with the planned hydropower projects that is expected to increase hydropower generation capacity. The designated operating levels of the hydropower plant in the main Zambezi River are shown in Table 10.2. By the end of July 2021, the available water levels were slightly below the designated operating levels. The maximum performance of any hydropower plant depends on maximum operating water levels and water inflows from the tributaries and rainfall discharges. Therefore, where water levels in hydropower reservoirs drop to their lowest levels than the designated capacity, the plant cannot operate at full capacity and therefore certain adjustments may have to be implemented including deactivating turbine engines resulting in low electricity generation. Due to water demand, inadequate flows, water commitments to other sectors, which are also not always met, it is quite unlikely the planned hydropower would be accommodated with challenges. While hydropower generation currently provides the main source of electricity in most riparian countries alternative environmentally friendly sources of electricity that may free the committed flows for other uses such as

irrigation and water supply. This must be considered sooner or later, particularly with the mounting pressure to use the Zambezi waters for the benefit of other riparian countries.

Table 10.5: The hydrological data from the two major hydropower plants in the Zambezi River major tributaries – 27 July 2021

Hydropower Plant	River	Designated Operating Water Levels	Current Water Level (m)	Inflow (m ³ /s)	Outflow (m ³ /s)
Cahora Bassa	Zambezi	327 .0 m	324.57	2319.0	1 734
Kariba	Zambezi	488.50 m	482.37	816	1842

b. Fisheries

One of the threats associated with fisheries especially in the Zambezi River is the water pollution that arises from water transport systems such as fishing vessels that discharge tons of human waste directly to the lakes each night (Magadza, 2006). Furthermore, big public transport ferries and small boats used for fishing and transporting people daily, present water pollution through discharges of human waste. While Zimbabwe Inland Shipping Act requires that vessels of specific size incorporate sewage containment facilities onboard, there are no harbour facilities to service such sanitation services, and the legal requirement is that sewage tanks not be discharged less than 5 km from the shore (Magadza, 2006). Most countries within the Zambezi Basin have legislation governing fishing activities across the Zambezi River Basin. In Zambia, the Department of Fisheries manages fisheries through the Fisheries Act 2011 limits the use of certain fishing such as seine nets and bans on other destructive fishing methods. The Fisheries Act also encourages community participation in fisheries management. The Namibian Inland Fisheries Resources Act, 2003 provides management for inland fisheries. The Act banned destructive fishing methods such as seine nets and restrictions on gillnet fishing are imposed, however, these are widely ignored. In Zimbabwe, fisheries management comes under the National Parks Act, 1975, which regulates the number of fishing licenses, gear, area restrictions and mesh sizes, however poaching is a major problem (Tweddle, 2010). Furthermore, Ainsworth et al., 2021 give a detailed review of the fishing sector in the world's major basins including the Zambezi River and large lakes. The study suggests that availability of fish in the Zambezi River Basin is declining. Based on the study, the general catch trends and rates throughout the basin have declined and this is attributed to a rise in the fishing effort by increasing numbers of fishers and decreases in catch/fisher. Fish catches have been declining throughout these fisheries despite a series of high flood years between 2007 and 2011 is some floodplains. The decline in catches has mainly been attributed to major increases in fishing effort, overfishing, environmental conditions and the invasion of water hyacinth in the Zambezi Delta. The further decline in fish catches resulted in a shift in fishing methods have shifted from multifilament nets to monofilament nets to compensate for the increased fishing effort (Ainsworth *et al.*, 2021). Climate change and increasing population growth contribute to the declining fisheries sector (Tweddle *et al.*, 2015).

10.8.2 Social vulnerability

a. Drought impacts

Based on the outcomes of this study, it is evident that droughts are recurrent phenomena in the Zambezi Basin and have devastating effects on the people and economies of the region, especially the poorest members of the population. The aridification of the Zambezi River due occurrence of sporadic droughts lead to the sedimentation of the river channel resulting in poor water quality, reduced stream power. The impact of prolonged drought periods means affect food production, energy generation and water supply are affected leading to famine, widespread mortality, while an estimated 15% of the population was in need of food aid.

b. Floods impacts

In 2019 the persistent drought period in the Zambezi River Basin was followed by flooding from torrential downpours. The catastrophic effects of the cyclones Idai and Kenneth in 2019 have not only threatened food security and resulted in people's displacement and loss of lives but also caused instability in the energy supply. The interconnections from Zambezi River's Cahora Bassa hydropower plant in Mozambique to South Africa were damaged and this compounded to the electricity crisis (Deliverable 3 report, 2021). Furthermore, the Zambezi River's Kariba hydropower plant, which supplies both Zambia and Zimbabwe, was unable to generate electricity at optimal capacity resulting in rotational power cuts of up to 10 hours in a day. As the leading consumer of the shared ZRB's Cahora Bassa hydroelectricity, South Africa's uninterrupted power supply both locally and to some of Southern African

c. Developing countries

Climate variability and environmental degradation due to floods and droughts also affect other sectors depending on the shared water resource such as farming (agriculture), mining and fishing. While predictions of future climate changes remain the subject to scientific uncertainty that is characterised by various socio-economics challenges including epidemics in Southern Africa, they assist in providing adaptive strategies to the vulnerability of communities across the region.

10.9 Adaptive response strategies

Considering the documented threats to the Zambezi and Orange-Senqu River Basins, and vulnerabilities posed to the water resource and people, it is important to improve regional and national drought coping mechanisms, and in countries' strategies. Water management approaches and policies, which can cope with current climatic variability and periodic droughts, will also reduce vulnerability to long-term climate change.

10.9.1 Strategies on drought vulnerabilities

The following drought coping measures are recommended:

1. Educating the poor communities on improved agricultural practices such as higher-yielding or fast-maturing crops,
2. Awareness training on a better understanding of groundwater and groundwater recharge in the Zambezi Basin and promotion of sustainable groundwater development. Groundwater is the largest storage in the basin and is resilient to temporary weather fluctuations; however, an understanding of it is still fragmented.
3. Promotion of water harvesting and catchment improvements, as particular measures to capture sporadic rainfall and conserve soil moisture to better cope with extended dry periods.
4. Educating sustenance farmers about the concept of crop adaptation, looking at crops and varieties better adjusted to higher temperatures and aridity
5. Educating communities about logistics of food supply, including storage and, the maintenance and storage of emergency supplies, to respond to local shortages. As floods and especially droughts will become more frequent and more pronounced, strategic food reserves need to be in place to prevent food shortages and famines

These strategies can be achieved through Support development of drought management plans, including local irrigation development, improved food stock logistics, crop adaptation and public education awareness programmes. For any development that requires water, drought forecasting in water resources planning and management is of importance.

10.9.2 Strategies on improve flood management

Floods are a recurrent feature in several parts of the Zambezi Basin causing often extensive damage in terms of human casualty, lives, and economic losses. For example, catastrophic damage from the Mozambique floods of 2000 impacted various sectors and industries among others, agriculture, health, education, housing and property, water and sanitation, energy, telecommunication, and transport (World Bank, 2000, Foley, 2007). In 2019 Mozambique was heavily hit by two cyclones, Idai and Kenneth, leaving a trail of destruction with close to 2.2 million people (374,000 people from Cyclone Kenneth and 1.85 million from Cyclone Idai). Apart from Mozambique, parts of Malawi and Zimbabwe were affected, and the overall damage was estimated to cost billions of rands. Climate change predictions create a further imperative for strengthening flood management in the Zambezi Basin and this requires close cooperation between riparian countries. The following three areas of improvement must be met to improve flood management throughout the Zambezi River Basin:

- a. Integration of flood management into development programmes directed to urban and rural communities. The vulnerability towards extreme weather events can be reduced flood risk is included in programmes covering land use planning, settlement development, infrastructure planning, and related policies. This should start from the preparation of flood

hazard maps – that should document areas highly exposed and local flood buffering mechanisms. Wetlands in particular can reduce flood risk, by acting as a sponge, and should be carefully protected. Further study is required to enhance knowledge on wetland vegetation, which plays an important part in the retention and delay of peak flows.

- b) The improvements of early warning systems. Though further improvement is required for instance by adding flow measuring stations having direct satellite communication.
- c) The effective flood preparedness and response systems throughout the Basin. There were important positive lessons learned on the handling of the Mozambique Floods of 2000 and 2019, for example, and the handling of these.

While these lessons are mostly applicable in the Zambezi River Basin, they can be adopted in the Orange-Senqu Basin

10.9.3 Improved water management and collaboration

The main challenge in the shared management of the two river basins is the sustainable water resources management that guarantees security in water supply and sanitation services, food and electricity supply from limited and vulnerable but considerably competed for water resources. Collaboration has the potential to increase the efficiency of water use, strengthen environmental sustainability, improve regulation of the demands made on natural resources, and enable greater mitigation of the impact of droughts and floods. The main area that needs to be considerably strengthened is the improvement in real-time forecasting. In the event of a flood emergency response, personnel are/is put in the difficult position of predicting where the flood will occur, issuing adequate and timely warnings, and developing evacuation plans with limited information to draw on. There is a consensus that Mozambique's response strategies to floods have improved with lower human casualty and overall damage, because of the experience learned from previous catastrophic events (Foley, 2007).

Mozambique is in a better position to collaborate with other riparian states and exchange knowledge on flood response strategies. Such experience includes information on clear command structure during events such as establishment of high-level committee of ministers supported by a technical committee comprising experts from the various departments and science councils. Some of the experience to be shared with other countries that have been less affected by floods includes effectiveness of collaboration between the National Institute of Meteorology and the National Disaster Management. There is a need to share knowledge on what contingency plan for responding to emergencies were implemented and how donations such as food, non-food items were handled. There is a need to exchange ideas on other flood response measures that have worked well during these floods. Lastly one of flood management responses is the systematic review of dam operational procedures. The Cahora Bassa Reservoir operation has been adjusted to enhance its flood storage function, which was previously not there.

10.9.4 Public educational awareness programme

a. Climate Change Awareness

The public knowledge on climate variability and climate change in the SADC region, and especially the impact on water resources remains low. Comprehensive assessment of the vulnerability of the Basin's water resources to climate change will form the basis for improved flood and drought management. The persistent droughts have made seasonal variation in runoff quite severe in recent years. It is widely documented that droughts and floods are cyclic and, in the future, the impact of drought and floods will become worse than experienced previously as population, industrialisation, urbanisation and the need for expanded agriculture/irrigation, water supply and sanitation services, etc., continue to rapidly grow. These persistent extreme weather patterns should, therefore, be considered in any strategic planning and management of water resources rather than being treated reactively. While issues related to climate change impacts are well documented, there is a need to educate the entire public on these issues to demystify any negative public perception.

b. Pollution Prevention Awareness

The emerging water scarcity, degradation and pollution problems are transboundary and require common basic policy, legal and institutional arrangements amongst riparian countries. Controlling water pollution from point sources, especially from urban centres and mining areas is of utmost importance. The promotion of sustainable fishery management will contribute to regional food security and minimise river pollution.

An effective public information programme that creates public awareness, builds effective public outreach, develops regional, sub-regional, and national public relations programmes, and produces necessary communication materials, is an essential basis for both Zambezi and Orange-Senqu River Basin cooperation. This should go beyond one-off events but should permeate in local media and local discussions.

Activities should be:

- Strengthen stakeholder participation through policy and legislation review and revision throughout the basin states
- Formulate and implement a public information programme to raise awareness among the broad range of stakeholders.
- Strengthen and sustain the Annual Basin Forum meetings as part of awareness and information sharing among basin stakeholders.

10.10 Discussion

Climate change is expected to result in increased frequency of extreme events such as droughts and floods affecting agricultural crop and livestock production as well as wildlife. Rising temperature is expected to affect fish production from major lakes and reservoirs, as well as cause higher evaporation from these main water bodies and reduce the yield of main agricultural crops. Wetland ecosystems will be affected as run-off patterns will change. Precise assessments of climate change are inadequate and are often limited to mean temperature and precipitation, with relatively little known about changes in extremes. Response strategies to climate changes include:

- a. Improvements on the knowledge base on climate variability and climate change and their impacts on water resources; improve on flood management and mitigation mechanisms at the national and regional scale;
- b. Improvements on regional and national drought management;
- c. Development of regional capacity to adapt to climate change and make use of the development opportunities associated with global climate change mitigation

10.11 Conclusions and recommendations

The Zambezi River Commission and Orange-Senqu River Commission respectively developed the Integrated Water Resources Management Strategies to promote equitable, sustainable, and efficient management of water resources. One of the main components of the IWRM strategy is environmental management and sustainable development through which strategies to promote sustainable fisheries and other issues on utilisation and management of the water resource such as hydropower generation and irrigation activities. The success of sustainable water management and suggested response strategies will depend to a large extent on the training of the relevant stakeholders to capacitate them in terms of knowledge, attitude, and skills. Before any training can be undertaken, typically a needs assessment has to be undertaken to determine the stakeholders who require training, the type of training required and the best way to offer that training. For agricultural water management interventions, returns to training investment are best if this training is focused on those working directly with farmers and the farmers themselves. Short courses for the training of agricultural extension staff and farmers were identified, and these included; smallholder irrigation water management and crop production, dambo irrigation farming with ecosystems goods and services in mind, drip kit irrigation, operation and management for local food security, and soil and water conservation practices and conservation agriculture under rain-fed agriculture. Public Educational awareness programmes on climate change and water pollution must be intensified and directed to communities and across other disciplines as these issues affect everyone but not only the scholars who generally discuss and provide recommendations without imparting knowledge to the affected communities.

CHAPTER 11

RECOMMENDATIONS FOR POLICY

11.1 Introduction

Water management consists of water resources management and the provision of water services, which two functions, although distinguishable, cannot be separated in practice. The objective of water resources management is to ensure that water resources are protected, used, developed, conserved, managed, and controlled to achieve optimum and environmentally sustainable social and economic benefits. Water services, on the other hand, are the services necessary to enable water users to use water resources on a sustainable basis. Various organizations provide water resources management and water services. These include regulators, water-service providers, facilitators, conflict resolvers, water users and other interested groups. The framework in which these organizations have to operate is very complex. The framework is also very dynamic due to, among other things, the political, social and economic development in riparian states. Various processes are under way to restructure and transform the existing organizations and to establish new ones. While organizations have emerged to play a role in transboundary water management, there is a need to formulate policy which governs transboundary water management.

Within each riparian states, governments are constituted into national, provincial and local spheres of government. In some riparian states, the constitution is not clear on the use of water resources. However, in South Africa, the constitution states that these spheres are distinct, interdependent, and interrelated, and sets out the functional areas for each. Water resources management is an exclusively national government function. Managing waste-generating activities and the waste generated and regulating land uses that might affect water resources could, just as the provision of water services, be either an exclusively international, regional, national, concurrently national and provincial, exclusively provincial or a local government function, depending on which sector and activities are involved.

In riparian states, the policies and activities of one sphere of government may impact on the responsibilities and functions of another. Therefore, all three spheres of government and all organs within each sphere must cooperate and consult with each other, respect the responsibilities of the others, and exercise powers and perform functions in such a way as not to encroach on the integrity of another. Furthermore, the different spheres and organs may only exercise those powers and perform those functions conferred on them.

This report is on suggestion for policy development for the management of the Zambezi and Orange River catchment and resources, The establishment of a catchment management agency for the two-river basin as well as the development of a catchment management strategy will

assist greatly in achieving these ideals relating to water resources management and the provision of water services to support life and hygiene in the river basin.

Policy development of a drainage basin includes among others:

- An analytical description of the policies that influence hydro-institutional arrangements and interactions.
- An analytical description of water-related laws, in the case of the riparian states, i.e., in South Africa – the National Water Act, 1998 (Act No. 36 of 1998) (NWA) and the Water Services Act, 1997 (Act No. 108 of 1997) (WSA).
- Identification and mapping of the entire complex hydro-institutional relationships.
- An analysis of the various organizations in the public and private sectors engaged in hydro-management of the rivers.

11.2 Aims and objectives

The objectives of water resources management policies are to ensure that water resources are protected, used, developed, conserved, managed, and controlled in such a way as to achieve optimum, long term, environmentally sustainable social and economic benefits for the society. The interactions and relationships between the following organizations and the society are of importance:

- Organizations involved in the monitoring and regulating of the activities of the society that might impact on the water resources.
- Organizations involved in the monitoring and regulating of those activities that generate waste and the waste generated that might affect water resources.
- Organizations involved in the monitoring and regulating of different land uses and the activities associated with each land use that might affect water resources.

If done correctly, such monitoring and regulation could assist in achieving the objectives of water resources management and assist in ensuring sustainable provision of water services for these activities.

11.3 Provision of water services

Water services are the services necessary to enable water users to use their water resources on a sustainable basis. Provision of water services therefore includes activities such as the abstraction, conveyance, treatment, and distribution of water-to-water users; the collection, removal, treatment, and disposal of waste generated due to the use of water; and the provision of resources, assistance and information associated with these activities. The provision of sustainable water services should be done in such a way as to ensure the achievement of the objectives of water resources management. This could be done as follows;

- Putting in place an enabling framework for sustainable provision of water services to the different sectors. These sectors could be small-scale irrigation, feedlots, supporting life and personal hygiene, power generation, mining, etc.
- Putting in place a framework for assisting and monitoring the organizations responsible for and associated with the provision of water services.
- The establishment of the necessary organizations or assigning the function to existing organizations to undertake sustainable provision of water services.

11.4 Study areas

See description of the Zambezi and Orange drainage basins in the previous chapters.

11.5 Energy policy framework

Energy supply is a key driver of economic development. The countries in the SADC regions have developed energy policies aimed at addressing the increasing demand for electricity for investment purposes and the need to improve their population's access rate to electricity. These policies, laws and regulations give an overview of countries' vision, policy principles, strategic goals, and objectives to inform the public and the international community on strategies that are implemented in promoting energy and how to achieve them. Due to the establishment of SAPP co-operation, which aims at creating a competitive regional electricity market, the establishment of energy policy by members are to be based on SADC Protocol on Energy.

- The SADC Protocol on Energy of 1996 commits member states to develop and use energy to support economic growth and development, poverty alleviation and improvement of the standard and quality of life throughout the sub-region. The Protocol further commits member states to the main objectives, which include co-operation in the development and utilization of energy and energy pooling to ensure security and reliability of energy supply in the most efficient and cost-effective manner.
- The SADC Energy Sector Action Plan of 1997 recommends that the SADC energy program concentrates on priority activities that could be implemented efficiently on a regional basis for the benefit of the entire region.

The energy policies for some of the SAPP member states are summarised below:

11.5.1 South Africa

The South African energy mix is still dominated by coal, and this is expected to continue into the near future. While the introduction of load shedding and restrictions on the use of electricity by consumers is expected to continue. Eskom has introduced far-reaching measures to mitigate load shedding, implemented a proactive maintenance programme at existing power stations (Eskom Integrated Annual report, 2020). These measures, may, however, not provide a long-term solution. As a result, more and more commercial firms and South African households are

opting to go either partially or fully off-grid, by installing gas stoves, geysers or opting for solar power. Despite this, the South African government has established the following short and long-term key energy development strategies based on countries' laws policies and legislation to diversify and strengthen the generation capacity:

1. White Paper on the Energy Policy, December 1998

This White Paper gives an overview of the South informs the public and the international community. It concludes that the sector can greatly contribute to a successful and sustainable national growth and development strategy.

2. Renewable Energy White Paper (2003)

White Paper on Renewable Energy laid a foundation for the promotion of renewable energy and affirmed the government's commitment, vision, and strategic goals aimed at increasing electrification rate and reduce reliance on fossil fuel through the integration of low-carbon emission renewable energy sources into the mainstream energy. To achieve these objectives, the Government set a target of 10 000 GWh of renewable energy increase by 2013, which was to be produced mainly from biomass, wind, solar and small-scale hydropower. This is approximately 4% (1 667 MW) of the projected electricity demand for 2013 (41 539 MW). This commitment was achieved as the current total renewable energy generation from both Eskom and IPP is at 11% (5 560 MW) of the total generation capacity of 50 323 MW. Hydropower contributes about 11% (600 MW) of the current total renewable energy.

Integrated Resource Plan (IRP) 2010-2030

The integrated Resource Plan (IRP) outlines the projected energy demand in the next two decades (2010-2030) and pledged support for countries' energy diversification and requirements to achieve these targets. The plan on the electricity infrastructure development was intended to be a "living document" that would be periodically revised by the Department of Energy. The plan was promulgated in 2011 and it was updated in 2018 to include the new additional capacity of 18 000 MW since promulgation. The 2018 draft IRP was published for public comments and in 2019 was adopted.

The Draft IRP of 2019 made provision for the following new additional capacity by 2030:

- 1 500 MW of coal;
- 2 500 MW of hydro from the Inga Hydropower project
- 6 000 MW of solar PV;
- 14 400 MW of wind;
- 1 860 MW of nuclear;
- 2 088 MW for pumped storage schemes;
- 3 000 MW of gas/diesel; and
- 4 000 MW from other distributed generation, co-generation, biomass, and landfill technologies.

Apart from the planned 2 500 MW Inga Hydropower project from South Africa-DRC treaty, there is a potential for run-off river hydro projects in South Africa's rivers. Apart from that, the long-term treaty between South Africa and Mozambique to import electricity from the 2075 MW Cahora Bassa dam terminates in 2029. Eskom may lose the 1 500 MW generated from Cahora Bassa as the old purchase agreement favours South Africa. According to Mozambique's EDM strategy report of 2018, the current tariff arrangement is not in Mozambique's best interests, since South Africa imports up to 1 500 MW at approximately 2.5 US cents/kWh but sells back 950 MW for the operation of Mozambique's Mazol Smelter at an average price of 9.5 US cents/kWh.

The planned generation programmes include a significant portion of renewable energy to reduce carbon emissions, and ease pressure on the continuously growing electricity demand in South Africa and SADC region, coal-fired generation will continue to dominate the energy mix soon. While the country moves towards a more environmentally friendly power sources, more emphasis should be directed effects of climatic changes as part of government strategies and project planning.

11.5.2 Mozambique

Mozambique's energy sector is dominated by hydropower and contribute about 4% of the SAPP's total generation capacity. The energy sector in Mozambique is based on the following main strategies, policies acts, and regulations as outlined by Mozambique Governmental Framework, 2020 and Mozambique Integrated Master Plan 2018.

The Electricity Law (No. 21/97)

- The electricity law defines a policy for the organization of the electrical energy sector and the administration of the supply of electrical energy.
- It also prescribes the general legal framework for electrical energy generation, transmission, distribution, and sale within the country; and controls the exportation and importation of energy from outside of the national territory, and the granting of concessions for such activities.
- The Electricity Law also allowed for private participation in the electricity industry.

Energy Policy 1998

It outlines the following vision for the sector: (1) a reliable supply of energy, at the lowest possible cost, in order to meet present demand and future levels based on economic development trajectories; (2) an increase in the energy options available for household consumption; (3) more efficiency in energy utilization; (4) the development of environmentally friendly conversion technologies, namely hydro, solar, wind and biomass and (5) the promotion of competitive, dynamic and more efficient entrepreneurs.

In terms of Renewables (2011-2025) the aim is to develop 125 MW of small HEP schemes and 100 MW by 2025. It also hopes to use solar PV.

National Energy Strategy (2014-2023)

Reinforces the Energy Policy of 1998, but with a specific focus on enabling better access to power by rural and peri-urban areas.

Integrated Master Plan 2018-2043

The integrated master plan encompasses all existing major laws, legislation, and policies in the power sector of Mozambique.

1. The national energy plan presents the comprehensive national power system development master plan including power generation, transmission and distribution planning for the next 25 years (2018-2043).
2. The plan is aimed at balancing various energy sources including hydro, coal-fired thermal and gas-fired thermal.
3. The generation development plan advocates for diversification of the energy sector by meeting the following objectives:
 - Stage 1 – minimizing reliance on exported electricity.
 - Stage 2 – exporting 20% of domestic peak demand. PV and wind power will be installed to meet 10% of domestic peak demand. Gas-fired power plants will enable electricity exports to the region. The official target is to achieve universal electricity access by 2030.

For the period 2018-2027, development of generation capacity of around 4 172 MW is expected, 2 200 hydro, 792 gas, 170 solar, 60 wind (Mozambique EDM Strategy 2018-2028)

11.5.3 Zambia

Zambia's energy policy is designed to enable both public and private investors (IPP) to contribute to the renewable energy sector. The National Energy Policy 2019 (NEP 2019) builds on previous policies of 1994 and 2008 and is anchored on the Seventh National Development Plan (7NDP) and Vision 2030. The policy enables the government to purchase renewable energy at predetermined costs, reducing price volatility and attracting significant private sector investment to hydropower schemes.

11.5.4 Angola

Based on the Angola Energy Plan 2025, the country intends to increase electricity access from 30% in 2018 to 60% by 2025 with renewable energy expected to account for about 70% of this planned increase (Angola Government, 2018). The current installed generation capacity is at 5 236 MW and based on the Angola Energy Plan this capacity would be increased to 9 900 MW by 2025 with hydropower expected to contribute about 66%. Angola has many large river

systems that could provide sufficient hydropower resources, and Zambezi River Basin is currently not part of their plans.

11.5.5 Discussion

Most SADC countries are highly dependent on hydropower. Hydropower in Mozambique and Zambia constitute 81% of their installed capacity, while Malawi's capacity is 99% hydropower. The installed generation capacity in DRC and Angola, despite not having active hydropower projects on the Zambezi River Basin, is still dominated by hydropower with 99.9% and 59% respectively. Electricity generation in such countries is at risk due to water stress associated with drought and increasing demand for water resources. Increasing temperatures lead to water deficits and affect the performance of hydropower plants while catastrophic disasters such as floods and cyclones destroy the infrastructure for all energy sources.

The demand across the SADC continues to grow. Therefore, it is important that necessary transmission links that connect all SAPP members be developed. While hydropower in most SADC countries is the main source of energy, it is important to balance hydropower with other economically reducing greenhouse gas emissions energy options. The effects of climate change on the Orange and Zambezi drainage basins have resulted in the cancellation or postponement of several hydropower projects or output revision in the generating capacity planned projects or operating of the hydropower plants. Thus, any policies formulated with regards to hydro power must take into consideration climatic change cycles, changes in aridity trends and modelling of flood and drought patterns.

11.6 Adaptive response strategies policy framework

Considering the documented threats to the Zambezi and Orange-Senqu River Basins, and vulnerabilities posed to the water resource and people, it is important to improve regional and national drought coping mechanisms, and in countries' strategies. Water management approaches and policies, which can cope with current climatic variability and periodic droughts, will also reduce vulnerability to long-term climate change.

11.6.1 Strategies on drought vulnerabilities

The following drought coping measures are recommended for adoption as policies:

- a. Educating the poor communities on improved agricultural practices such as higher-yielding or fast-maturing crops,
- b. Awareness training on a better understanding of groundwater and groundwater recharge in the Orange and Zambezi Basin and promotion of sustainable groundwater development. Groundwater is the largest storage in the basin and is resilient to temporary weather fluctuations; however, an understanding of it is still fragmented.

- c. Promotion of water harvesting and catchment improvements, as particular measures to capture sporadic rainfall and conserve soil moisture to better cope with extended dry periods.
- d. Educating sustenance farmers about the concept of crop adaptation, looking at crops and varieties better adjusted to higher temperatures and aridity
- e. Educating communities about logistics of food supply, including storage and, the maintenance and storage of emergency supplies, to respond to local shortages. As floods and especially droughts will become more frequent and more pronounced, strategic food reserves need to be in place to prevent food shortages and famines

These strategies can be achieved through Support development of drought management plans, including local irrigation development, improved food stock logistics, crop adaptation and public education awareness programmes. For any development that requires water, drought forecasting in water resources planning and management is of importance.

11.6.2 Strategies on improve flood management

Floods are a recurrent feature of several parts of the Orange and the Zambezi Basin – causing often extensive damage in terms of human casualty, livestock losses and economic losses. For example, the economic damage from the Mozambique floods of 2000 and 2019 where it was estimated to cost billions of rands. Climate change predictions create a further imperative for strengthening flood management in the Orange and Zambezi Basin, requiring close cooperation between riparian countries. To improve flood management, several things are required to happen. First, flood management must be integrated into development programmes directed to urban and rural communities. By including flood risk in programmes covering land use planning, settlement development, infrastructure planning, and related policies, vulnerability towards extreme weather events can be reduced. This should start from the preparation of flood hazard maps – that should document areas highly exposed and local flood buffering mechanisms. Wetlands can reduce flood risk, by acting as a sponge, and should be carefully protected. Further study is required to enhance knowledge on wetland vegetation, which plays an important part in the retention and delay of peak flows. The second area of improvement is for early warning systems to be improved. Though further improvement is required for instance by adding flow measuring stations having direct satellite communication. The third important area is that of effective flood preparedness and response systems throughout the Basin. There were important positive lessons learned on the handling of the Mozambique Floods of 2000 and 2019, for instance, and the handling of these. These lessons should be adopted throughout the Basin.

11.6.3 Improved water management and collaboration

The main challenge in the common management of the Orange and Zambezi River basin, is the sustainable water resources management that guarantees security in water supply and sanitation services, food and electricity supply from limited and vulnerable but considerably

competed for water resources. Collaboration in the form of transboundary water management has the potential to increase the efficiency of water use, strengthen environmental sustainability, improve regulation of the demands made on natural resources, and enable greater mitigation of the impact of droughts and floods. The main area that needs to be considerably strengthened is the improvement in real-time forecasting. In the event of a flood emergency response, personnel is put in the difficult position of predicting where the flood will occur, issuing adequate and timely warnings, and developing evacuation plans with limited information to draw on. Given the enormous extent of the flood in Mozambique, human casualty and overall damage was limited, because of the experience learnt from previous catastrophic events.

Mozambique is in a better position to collaborate with other riparian states and exchange knowledge on flood response strategies. Such experience includes information on clear command structure during events such as establishment of high-level committee of ministers supported by a technical committee comprising experts from the various departments and science councils. Some of the experience to be shared with other countries that have been less affected by floods includes effectiveness of collaboration between the National Institute of Meteorology and the National Disaster Management. There is a need to share knowledge on what contingency plan for responding to emergencies were implemented and how donations such as food, non-food items were handled. There is a need to exchange ideas on other flood response measures that have worked well during these floods. Lastly one of flood management responses is the systematic review of dam operational procedures. The Cahora Bassa Reservoir operation has been adjusted to enhance its flood storage function, which was previously not there.

11.6.4 Public Educational Awareness Programme Policies

Climate Change Awareness

The knowledge base on climate variability and climate change in the SADC region, and especially the effect on water resources is still very weak. It is therefore proposed to carry out a comprehensive assessment of the vulnerability of basin water resources to climate variability and climate change. This will become the basis for improved flood and drought management. The persistent droughts have made seasonal variation in runoff quite severe in recent years. It is widely documented that droughts and floods are cyclic and, in the future, the impact of drought and floods will become worse than experienced previous as population, industrialisation, urbanisation and the need for expanded agriculture/irrigation, water supply and sanitation services, etc., continue to rapidly grow. These persistent extreme weather patterns should, therefore, be considered in any strategic planning and management of water resources rather than being treated in a reactive manner. Which issue related to climate change impacts are well documented, there is a need to educate the entire public on these issues to demystify any negative public perception.

Pollution Prevention Awareness

The emerging water scarcity, degradation and pollution problems are transboundary and require common basic policy, legal and institutional arrangements. Control water pollution from point sources, especially from urban centres and mining areas; Promote sustainable fishery management as a contribution to regional food security.

An effective public information programme that creates public awareness, builds effective public outreach, develops regional, sub-regional, and national public relations programmes, and produces necessary communication materials, is an essential basis for Zambezi Basin Cooperation. This should go beyond one-off events but should permeate in local media and local discussions.

Activities should be:

- Strengthen stakeholder participation through policy and legislation review and revision throughout the basin states
- Formulate and implement a public information programme to raise awareness among a broad range of stakeholders
- Strengthen and sustain the Annual Basin Forum meetings as part of awareness and information sharing among basin stakeholders.

11.6.5 Discussion

Climate change is expected to result in increased frequency of extreme events such as droughts and floods, affecting agricultural crop and livestock production as well as wildlife. Rising temperature is expected to affect fish production from major lakes and reservoirs, as well as cause higher evaporation from these main water bodies and reduce the yield of main agricultural crops. Wetland ecosystems will be affected as run-off patterns will change. Precise assessments of climate change are inadequate and are often limited to mean temperature and precipitation, with relatively little known about changes in extremes. Response strategies to climate changes include improvements on the knowledge base on climate variability and climate change and their impacts on water resources; improve on flood management and mitigation mechanisms at national and regional scale; improvements on regional and national drought management; and development of regional capacity to adapt to climate change and make use of the development opportunities associated with global climate change mitigation.

11.7 Sedimentation policy framework

Sedimentation is an emerging challenge for some reservoirs, but for others, it is already happening and source of concern. Rapid variations in depths with a system was the first indicator of silting reservoirs whose storage capacities were so reduced to fully sustain the water demands per persons.

Based on hydrological regimes, small reservoirs in the Orange and the Zambezi catchment are highly likely to experience prolonged water stressful periods and water scarcity than the larger ones. Water scarcity and stress are prevalent between July and November, with October as the most critical month as far as water scarcity is concerned.

Whilst other factors may affect the quantity and quality of water available in reservoirs, siltation remains the most significant driver of storage capacity loss and, under anthropogenic influence, siltation remains a very huge challenge for the entire Orange and Zambezi Catchment. Ministry of Water Development and Sanitation (MWDS, 2022) established reservoir siltation in the Zambezi catchment remains very high with as high as 88% of the reservoirs especially the medium to small ones being the worst affected by siltation with rapid losses in storage capacities within the magnitude of 8% to 57%. The major drivers of siltation include crop cultivation, which according to earlier studies (Sichingabula, 1997; Sichingabula, 2018; Muchanga, 2020; MWDS, 2022) could be contributing to about 36% of siltation of reservoirs and riverine environments. Mavima *et al.* (2015), Kamtukule and Kaseke, 2012 also earlier noted human activities such as crop farming as major threat to the useful economic life spans of the reservoirs in Zimbabwe and Malawi, respectively. Going beyond crop farming, animal grazing and other mixed land uses (sand mining, gardens, charcoal burning, brick moulding) in the buffer zone remain some of the major drivers of sedimentation in reservoirs and eventually, the water scarcity problem. As noted by Chisanga *et al.* (2022), water scarcity problems are likely to be frequent in the next 50 years amidst climatic changes.

The environmental problems around reservoirs in the Orange and Zambezi Basin in general and the three target areas are social problems, many of them have been propelled by human beings, who at last, have ended up as victims. The reduction in storage capacities of reservoirs were due to human-induced siltation, this rendered the three reservoirs and others with similar characteristics within the Orange and Zambezi Basin incapable of meeting water demand.

Both primary and secondary evidence show that livestock is the most affected by dwindling water resources, domestic fishing has also been affected given that, the reservoirs could no longer hold enough water during almost 60% of the year. Hence household income is affected to a point where communities may become food insecure.

Under increasing anthropogenic activities such as irrigated farming, the governments across the Basin have also been confronted with huge cost implications around management and control of reservoir siltation and to ensure that, water is enough to sustain socioeconomic and environmental needs (Sanchez, 2018). Findings from secondary sources (Mwiinde, 2017; Sanchez, 2017; World Bank, 2007) reveal that, governments will have to spend a lot of funds to address dwindling water scarcity through desilting and rehabilitation of reservoirs and other water sources.

Therefore, post challenges and opportunities around water resources and siltation management must be explored to realise the benefits whilst reducing the costs. To cope with these

challenges of water scarcity and siltation the local communities adopted both constructive and destructive approaches.

As concluded by Vorosmarthy *et al.* (2005), there is high (25% of the population in Africa) chronic water stress (mean use: supply) and 40% experiences drought stress every 30 years. And that generally, water stress is typically low, reflecting its poor water delivery infrastructure. They contend that a well-engineered increase in use might thus be advantageous in mitigating water-related constraints on development and pollution which also engender an array of social science and engineering issues. They argue that a more complete understanding of human-water interactions and the design of appropriate policy interventions to alleviate water stress require a broader interdisciplinary approach. This requires a physically based framework incorporating social sciences to deal with the numerous challenges faced in water resources management. Hence, the need for a proactive planning system that incapsulate strategies that are contextually useful for sustainable water resources supply for all as enshrined in the SDG 6. The study proposes a conceptual model that can arguably ensure a sustainable water resources management in reservoirs through sustainable sediment control (Figure 11.1):

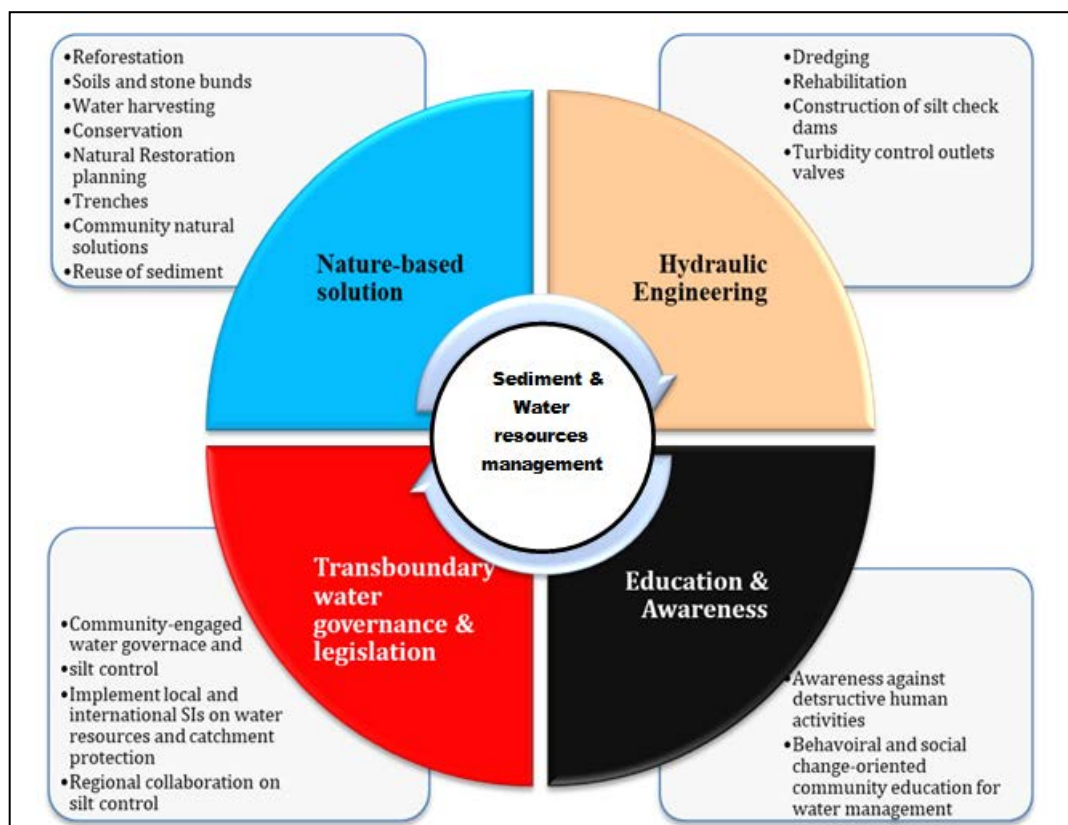


Figure 11.1: Conceptual Model for sustainable management of water resources and siltation control in reservoirs in the Orange and Zambezi River Basin.

The conceptual model depicts ideas that suggest an interdisciplinary and transdisciplinary approach to addressing the challenges of water scarcity problem triggered by siltation of surface water bodies. By combining nature-based methods, hydraulic engineering techniques

and implementation of effective transboundary water governance and laws would help minimise triggers or drivers of changes to water availability. In most intervention strategies, education and awareness are embraced only to a very minimal extent and, in most cases, it ends at awareness, which cannot bring about desired behavioural change for sustainable community-based management of catchments. Awareness simply raises conscience, but may not necessarily evoke desired change, which would make local communities decisively act for sustainable water resources management in view of realising long-term benefits.

11.7.1 Discussion

Sedimentation of reservoirs speaks to the SADC Water policy, which acknowledges both low urban and rural water supply leading to high incidence of water-borne diseases; rapidly growing and urbanizing populations, leading to growing water scarcity, and increasing water pollution, very low water-use efficiency in irrigated agriculture; degraded watersheds and deteriorating water quality as well as high stresses within increasing importance of hydropower to the regional economy (SADC, 2005).

The significant losses in storage capacities of many dams and rivers due to siltation imply that policy makers need to re-strategize both from country and basin contexts on intervention measures that can restore the dwindling water resources for the countries and basin perspectives. If that is not taken seriously with the urgency it deserves, severe water scarcity problems and even water conflicts should be expected with diverse socioeconomic implications. Most water-linked sectors especially agriculture and energy are likely to be the worst affected by the water scarcity problem (Vorosmarthy *et al.*, 2005). Given the significance of these sectors among others, several ripple effects could be felt as water supply versus demand discrepancies keep on widening.

In view of addressing the problem from the root cause, the governments need to re-affirm existing national and even regional policies that are aimed at protecting water resources. For example, Zambia has specific laws on protection of buffer zones of all water bodies SI 1 of 2000, but this has been poorly implemented leading to several regrettable degradation of several sections of Rivers and dams Buffer Zones (MWDS, 2022). While this neglect may sound country bound, it has several intra and inter spatial implications as for example sediment get eroded and transported several miles and only to possibly be deposited in an area that perhaps does not generate much sediment. This scenario is extrapolatable to all countries within the Orange and the Zambezi Basin and even the Orange Basin such that, policy makers in various country contexts and at basin scale should collaborate to develop and implement laws and policies that would help address pending water crises. It is no mere exaggeration that sedimentation problem and its effect on water security is predominantly anthropogenically driven and, the consequences are ending up with human beings who punctuate such problems. From policy context, it means that educational programming and policies should be factored in the processes of addressing the challenges to discourage behaviours that punctuate siltation and water scarcity as well as stresses. If that is not done, then whatever intervention policy

measure shall prove futile as the behaviours that punctuate siltation remain unaddressed. This is also highly emphasised in the SADC Water Policy. In view of building a stronger scientific database that informs policy decisions, governments within the Zambezi and Orange Basins must consider developing new research agenda that speak to current problematic landscape as far as water security and siltation problems are concerned. Given the projected climatic changes within the two catchments (Chisanga *et al.*, 2022), augmented siltation levels and catchment degradations are highly expected such that continuous implementation of research agenda for future water security should really be integrated in every developmental narrative. Generally, a neglect of these policy issues may deter attenuation of all water-dependent SDGs and sectors.

11.8 Conclusion and recommendations

11.8.1 Conclusion

It can be concluded that the increasing demand for electricity throughout the Orange and Zambezi riparian states (SADC) region can be met if these issues are addressed:

- Any planned projects on renewable energy and energy efficiency strategies should be based on extensively researched information on paleo-climate change patterns to predict future impacts.
- Studies on paleo-climate changes should be based on scientific evidence and must be aimed at modelling the changes in the river morphologies, flow and flood patterns, aridity evolution, and sediment deposit rates and frequencies.
- Despite hydropower and other renewable energy sources having the potential of providing a reliable, greenhouse gas emission-free energy source, the main barrier to HEP is the impact of climate change. The energy strategies and government policies do not acknowledge the impact of climate change, with no impacts modelled.

The Zambezi River Commission developed the Integrated Water Resources Management strategy to promote equitable, sustainable, and efficient management of water resources. One of the main components of the IWRM strategy is environmental management and sustainable development through which strategies to promote sustainable fisheries and other issues on utilization and management of the water resource such as hydropower generation and irrigation activities. The success of sustainable water management and suggested response strategies and policies will depend to a large extent on the training of the relevant stakeholders so as to capacitate them in terms of knowledge, attitude and skills. Before any training can be undertaken, typically a needs assessment must be undertaken to determine the stakeholders who require training, the type of training required and the best way to offer that training. For agricultural water management interventions, returns to training investment are best if this training is focused on those working directly with farmers and the farmers themselves. Short courses for the training of agricultural extension staff and farmers were identified, and these included; smallholder irrigation water management and crop production, dambo irrigation farming with ecosystems goods and services in mind, drip kit irrigation, operation and management for local food security, and soil and water conservation practices and conservation

agriculture under rainfed agriculture. Public Educational awareness programmes on climate change and water pollution must be intensified and directed to communities and across other disciplines as these issues affects everyone but not only the scholars.

11.8.2 Recommendations

Hydropower is one of the major resources, not only to riparian states of the Orange and Zambezi River Basin but other major rivers in the SADC region such as the Congo River in DRC. The total developed capacity in the main Zambezi River and along its major tributaries is currently 5 862 MW and confirmed potential projects have an additional capacity of 13 126 MW. The SADC countries that do not have a share in the Orange and the Zambezi River waters derive indirect benefits through regional power exchanges managed through various organisations interconnection. It is therefore imperative that the development of hydropower within the Orange and the Zambezi River Basin include both riparian states and members of the organisations. Furthermore, energy laws and policies should be developed in line with the following SADC Protocols:

- The SADC Protocol on Energy of 1996 commits member states to develop and use energy to support economic growth and development, poverty alleviation, and improvement of the standard and quality of life throughout the sub-region

Policy: All riparian states should develop and use energy to support economic growth and development, poverty alleviation, and improvement of the standard and quality of life for their communities

- SADC Energy Sector Action Plan of 1997 recommends that the SADC energy program concentrates on priority activities that could be implemented efficiently on a regional basis for the benefit of the entire region.

Policy: All riparian states should concentrate on priority activities that could be implemented efficiently on a regional basis for the benefits of the entire region.

For countries that solely rely on hydropower, future policies should advocate for alternative sources of electricity be incorporated to provide stability and free the committed flows for other uses such as irrigation and mining activities. The effects of climate change , forms the basis of any strategic plan and the issue of energy diversification be prioritized as the pressure for Orange and Zambezi water demand is mounting due to other uses that benefit the greater SADC region. The projections of future water demand need to be made against the background of future water resource availability, as the key driver of water resource availability is rainfall. Possible changes in rainfall patterns, water distribution, and utilization, and timing of hydropower will directly impact the water resources.

REFERENCES

- Adebe, Z. D., Sewnet, M. A. (2014): Adoption of soil conservation practices in North Achefer District, Northwest Ethiopia – *Chinese Journal of Population Resources and Environment* 12(3): 261-268., <http://dx.doi.org/10.1080/10042857.2014.934953>.
- Adeogun, A.G., Sule, B.F. and Salami, A.W. 2018. Cost effectiveness of sediment management strategies for mitigation of sedimentation at Jebba Hydropower reservoir, Nigeria. *Journal of King Saud University-Engineering Sciences*, 30(2), pp.141-149. <https://www.sciencedirect.com/science/article/pii/S1018363916000076>
- Adeyemo, J. and Oluwatosin Olofintoye, O. (2014) “Optimized fourier approximation models for estimating monthly streamflow in the Vanderkloof dam, South Africa,” *Advances in Intelligent Systems and Computing*, 288. doi:10.1007/978-3-319-07494-8_20.
- Ainsworth, R., Cowx, I.G. and Funge-Smith, S.J. 2021. A review of major river basins and large lakes relevant to inland fisheries.
- Ajith, A.V. 2016. Bathymetric Survey to Study the Sediment Deposit in Reservoir of Peechi Dam. *Journal of Mechanical and Civil Engineering (IOSR-JMCE)*. p. 34-38.
- Alessio, B.L.; Collins, A.S.; Clark, C.; Glorie, S.; Siegfried, P.R.; and Taylor, R. 2019. Age, origin and palaeogeography of the Southern Irumide Belt, Zambia. *Journal of the Geological Society* 176(3):505-516.
- Alexander, L. V., Arblaster, J.M., 2009. Assessing trends in observed and modelled climate extremes over Australia in relation to future projections. *Int. J. Climatol.* 29, 417-435. <https://doi.org/10.1002/joc.1730>
- Alexander, L., Herold, N., 2016. ClimPACT2. Indices and software. A document prepared on behalf of The Commission for Climatology (CCI) Expert Team on Sector-Specific Climate Indices (ET-SCI).
- Alexander, L., Herold, N., 2016. ClimPACT2. Indices and software. A document prepared on behalf of The Commission for Climatology (CCI) Expert Team on Sector-Specific Climate Indices (ET-SCI).
- Alexander, W., 2007. Water resources and climate change. *Sabinet African Journals*, Issue 7, pp. 34-36.
- Allison, G.B.; Gee, G.W.; Tyler, S.W. (1994)., *Vadose-Zone Techniques for Estimating Groundwater Recharge in Arid and Semiarid Regions*. *Soil Sci. Soc. Am. J.* 1994, 58, 6-14.
- Andersen, T.; Elburg, M.A.; van Niekerk, H.S.; and Ueckermann, H. 2018. Successive sedimentary recycling regimes in southwestern Gondwana: Evidence from detrital zircons in Neoproterozoic to Cambrian sedimentary rocks in southern Africa. *Earth-Science Reviews* 181:43-60.
- Andersen, T.; Kristoffersen, M.; Elburg, M.A. 2016. How far can we trust provenance and crustal evolution information from detrital zircons? A South African case study. *Gondwana Research* 34:129-148.
- Andersson, J.C.M., Pechlivanidis, I.G., Gustafsson, D., Donnelly, C. & Arheimer, B. 2015. Key factors for improving large-scale hydrological model performance. *European Water*, 49: 77-88.

- Andò S, Morton A and Garzanti, E (2014). Metamorphic grade of source rocks revealed by chemical fingerprints of detrital amphibole and garnet. Geological Society, London, Special Publications 386:351-371.
- Anon., n.d. [Online].
- Aquatec 1982. Aquatec, 1982. Watering point survey: Ngamiland cattle trek route, Aqua Tec Groundwater consultants 1982. 132 pp.
- Archibald, S., Hempson, G.P., 2016. Competing consumers: Contrasting the patterns and impacts of fire and mammalian herbivory in Africa. *Philosophical Transactions of the Royal Society B: Biological Sciences* 371, 20150309.
- Ashphaq, M., Srivatsava, P. K. & Mitra, D. 2021. Review of near-shore satellite derived bathymetry: Classification and account of five decades of coastal bathymetry research. *Journal of Ocean Engineering and Science*, 6(4): 340-359.
- Ashton, P.J., D. Love, H. Mahachi, P.H.G.M. Dirks (2001). An Overview of the Impact of Mining and Mineral Processing Operations on Water Resources and Water Quality in the Zambezi, Limpopo and Olifants Catchments in Southern Africa.
- Asoka, A.; Wada, Y.; Fishman, R.; Mishra, V. (2018). Strong Linkage Between Precipitation Intensity and Monsoon Season Groundwater Recharge in India. *Geophys. Res. Lett.*, 45, 5536-5544.
- Assessable Software:
- Bailey, A. (2013). The Orange – Senqu river basin Infrastructure catalogue. Retrieved from http://wis.orasecom.org/content/study/UNDP-GEF/general/Documents/Techincal Reports/TR21_InfrastructureCatalogue_lowres_Dec2013.pdf
- Baishya, S.J. and Sahariah, D., 2017. Application of Remote Sensing and GIS for Flood Hazard Mapping: A Case Study at Baralia-Nona River Basin, Assam, India. *Int. J. Humanit. Soc. Sci. Invent*, 5, pp.58-70.
- Balek, J., 1977. *Hydrology and Water Resources in Tropical Africa*, Elsevier, Amsterdam. 208 p.
- Balon, E. K. 1978. Reproductive guilds and the ultimate structure of fish taxocenes: amended contribution to the discussion presented at the mini-symposium. *Environmental Biology of Fishes*, 3, 149-152.
- Banda, K. 2015. Sedimentology, hydrogeology and hydrogeochemistry of Machile Basin, Zambia. PhD Thesis, Technical University of Denmark.
- Banda, K., Jakobsen, R., Bauer-Gottwein, P., Nyambe, I., Troels, L. & Larsen, F. submitted 2015. Identification and evaluation of hydro-geochemical processes in the groundwater environment of Machile Basin, western Zambia. Submitted to *Applied Geochemistry*.
- Bangert, B., Stollhofen, H., Lorenz, V. & Armstrong, R. 1999. The geochronology and significance of ash-fall tuffs in the glaciogenic Carboniferous-Permian Dwyka Group of Namibia and South Africa. *Journal of African Earth Sciences*, 29, 33-49.
- Banks NL, Bardwell KA, and Musiwa S (1995). Karoo Rift basins of the Luangwa Valley, Zambia. In: Lambiase, JJ. (ed.), *Hydrocarbon Habitat in Rift Basins*. Geological Society London, Special Publication 80:285-295.

- Barrat, J.A.; Zanda, B.; Moynier, F.; Bollinger, C.; Liorzou, C.; and Bayon, G. 2012. Geochemistry of CI chondrites: major and trace elements, and Cu and Zn isotopes: *Geochimica et Cosmochimica Acta* 83:79-92.
- Basson, G R and De Villiers, J W L. (2005). New bridge across Caledon River: Welbedacht Reservoir Sedimentation and Flood Level Study. DWAF.
- Bateman, R.M., and Catt, J.A. 2007. Provenance and palaeoenvironmental interpretation of superficial deposits, with particular reference to post-depositional modification of heavy mineral assemblages. In Mange, M.A., and Wright, D.T., eds. Heavy minerals in use. Elsevier, Amsterdam, *Developments in Sedimentology* 58:151-188.
- Bates, B C, Kundzewicz, Z W, Wu, S., and Palutikof, J.P. 2008. Climate Change and Water. Technical report, Intergovernmental Panel on Climate Change, Geneva.
- Bates, B C, Kundzewicz, Z W, Wu, S., and Palutikof, J.P. 2008. Climate Change and Water. Technical report, Intergovernmental Panel on Climate Change, Geneva.
- Batuca, D G and Jordaan, J M (Jr). (2000). Silting and desilting of reservoirs. Rotterdam: Balkema.
- Bauer, P. 2004. Flooding and salt transport in the Okavango Delta, Botswana: key issues for sustainable wetland management. PhD thesis, Swiss Federal Institute of Technology, Zurich.
- Bauer, P., Gumbrecht, T. & Kinzelbach, W. 2006a. A regional coupled surface water/groundwater model of the Okavango Delta, Botswana. *Water Resources Research*, 42, W04403.
- Bauer, P., Held, R. J., Zimmermann, S., Linn, F. & Kinzelbach, W. 2006b. Coupled flow and salinity transport modelling in semi-arid environments: The Shashi River Valley, Botswana. *Journal of Hydrology*, 316, 163-183.
- Bauer, P., Supper, R., Zimmermann, S. & Kinzelbach, W. 2006c. Geoelectrical imaging of groundwater salinization in the Okavango Delta, Botswana. *Journal of Applied Geophysics*, 60, 126-141.
- Bauer, S. and Schulz, I., 2010. Adaptation to climate change in Southern Africa: New boundaries for sustainable development. <https://www.tandfonline.com/doi/abs/10.3763/cdev.2010.0040>
- Bäumle, R., Neukum, C., Nkhoma, J. & Silembo, O. 2007. The Groundwater Resources of Southern Province, Zambia (Phase 1). Vol 1, Technical Report. Ministry of Energy and Water Development, Department of Water Affairs, Zambia, and Federal Institute for Geosciences and Natural Resources (BGR: Bundesanstalt für Geowissenschaften und Rohstoffe, Hannover).
- Beck, J S and Basson, G R. (2002). Morphological impacts and mitigation measures: control of reservoir sedimentation and environmental flood releases. Short course, Department of Civil Engineering, University of Stellenbosch.
- Beekman, H., Gieske, A. & Selaolo, E. 1996. GRES: Groundwater recharge studies in Botswana 1987-1996. *Botswana J. Earth Sci*, 3, 1-17.
- Beekman, H., Selaolo, E. T. & De Vries, J. 1999. Groundwater Recharge and Resources Assessment in the Botswana Kalahari: Executive Summary GRES II, Geological Survey Department.

- Beekman, H., Selaolo, E., Van Elswijk, R., Lenderink, N. & Obakeng, O. 1997. Groundwater recharge and resources assessment in the Botswana Kalahari-chloride and isotope profiling studies in the Letlhakeng-Botlhapatlou area and the Central Kalahari: GRES 11 Technical Report. Gaborone.
- Beerling, D.J., Osborne, C.P., 2006. The origin of the savanna biome. *Global Change Biology* 12, 2023-2031.
- Beiersdorf H, Kudrass HR, and von Stackelberg U (1980). Placer deposits of ilmenite and zircon on the Zambezi Shelf. *Geologisches Geol. Jahrbuch* D36:5-85.
- Beilfuss, R. and dos Santos, D., 2001. Patterns of Hydrological Change in the Zambezi Delta, Monogram for the Sustainable Management of Cahora Bassa Dam and The Lower Zambezi Valley.
- Beilfuss, R., 2012. A Risky Climate for Southern African Hydro: assessing hydrological risks and consequences for Zambezi River Basin Dams, *International Rivers*.
- Beilfuss, R., and dos Santos, D. 2001. Patterns of Hydrological Change in the Zambezi Delta, Mozambique. Working Paper#2. Program for the Sustainable Management of the Cahora Bassa Dam and the Lower Zambezi Valley. Baraboo, Wisconsin: International Crane Foundation, 159 p.
- Bekker, S. D. W. D. P. J., 2011. Modeling inflows into the Gariep dam: case study. *Sabinet African Journals*, 45(1), pp. 135-147.
- Berry, P., Garlick, J., Freeman, J., & Mathers, E. (2005). Global inland water monitoring from multi-mission altimetry. *Geophysical Research Letters*, 32(16).
- Bhat, N., Gouda, K.C., Varunvenkat, M and Bhat, R. (2015) Monitoring and Estimation of Reservoir Water Volume using Remote Sensing and GIS, *Geophysical Research Abstracts*.
- Bicca MM, Philipp RP, Jelinek AR, Ketzer JMM, dos Santos Scherer CM, Jamal DL. And dos Reis AD (2017). Permian-Early Triassic tectonics and stratigraphy of the Karoo Supergroup in northwestern Mozambique. *Journal of African Earth Sciences* 130:8-27.
- Blöschl, G. & Sivapalan, M. 1995. Scale issues in hydrological modelling: a review. *Hydrological Processes*, 9:251-290.
- Bolton, P. 1984. Sediment deposition in major reservoirs in the Zambezi Basin. *Challenges in African Hydrology and Water Resources*, IAHS Publ. 144:559-567.
- Bond, W.J., 2015. Fires in the Cenozoic: A late flowering of flammable ecosystems. *Frontiers in Plant Science* 5, 749.
- Bond, W.J., Van Wilgen, B.W., 2012. *Fire and plants*. Springer Science & Business Media.
- Boniface N and Appel P (2018). Neoproterozoic reworking of the Ubendian Belt crust: Implication for an orogenic cycle between the Tanzania Craton and Bangweulu Block during the assembly of Gondwana. *Precambrian Research* 305:358-385.
- Boroughs, C.B. & Zagona, E.B. 2002. Daily Flow Routing with the Muskingum-Cunge Method in the Pecos River RiverWare Model. *Proceedings of the Second Federal Interagency Hydrologic Modeling Conference*, Las Vegas, NV.
- Bowler, J. M. 1986. Spatial variability and hydrologic evolution of Australian lake basins – analogue for pleistocene hydrologic change and evaporite formation. *Palaeogeography Palaeoclimatology Palaeoecology*, 54, 21-41.

- Bowman, D.M., Balch, J.K., Artaxo, P., Bond, W.J., Carlson, J.M., Cochrane, M.A., D'Antonio, C.M., DeFries, R.S., Doyle, J.C., Harrison, S.P., 2009. Fire in the Earth system. *Science* 324, 481-484.
- Bronstert *et al.* (2014), who developed modelling techniques for erosion, sediment transport and reservoir siltation in semi-arid catchments.
- Brutsaert, W. and Parlange, M. B. 1998. Hydrologic cycle explains the evaporation paradox, *Nature*, 396, 30, doi:10.1038/23845.
- Buffington, A., Zwink, J., Fink, R., DeVine, D. and Sanders, C., 2012. Factors affecting nurse retention at an academic Magnet® hospital. *JONA: The Journal of Nursing Administration*, 42(5), pp.273-281.
- Bufford, K. M., Atekwana, E. A., Abdelsalam, M. G., Shemang, E., Mickus, K., Moidaki, M., Modisi, M. P. & Molwalefhe, L. 2012. Geometry and faults tectonic activity of the Okavango Rift Zone, Botswana: Evidence from magnetotelluric and electrical resistivity tomography imaging. *Journal of African Earth Sciences*, 65, 61-71.
- Bulambo, M.; De Waele, B.; Kokonyangi, J.; Johnson, S.P.; Kampunzu, A.B; and Tembo, F. 2006. Shrimp zircon U-Pb geochronology and geochemistry of the Choma-Kalomo Block granitoids (Zambia): Geological implications. 21st Colloquium of African Geology, Maputo, Mozambique, Abstracts volume.
- Buontempo, C., Mathison, C., Jones, R., Williams, K., Wang, C., McSweeney, C., 2015. An ensemble climate projection for Africa. *Clim. Dyn.* 44, 2097-2118. <https://doi.org/10.1007/s00382-014-2286-2>
- Burrough, S. L. & Thomas, D. S. G. 2008. Late quaternary lake-level fluctuations in the Mababe Depression: Middle Kalahari palaeolakes and the role of Zambezi inflows. *Quaternary Research*, 69, 388-403.
- Burrough, S. L. & Thomas, D. S. G. 2009. Geomorphological contributions to palaeolimnology on the African continent. *Geomorphology*, 103, 285-298.
- Burrough, S. L., Thomas, D. S. G. & Bailey, R. M. 2009a. Mega-lake in the Kalahari: A late pleistocene record of the Palaeolake Makgadikgadi system. *Quaternary Science Reviews*, 28, 1392-1411.
- Burrough, S. L., Thomas, D. S. G. & Singarayer, J. S. 2009b. Late Quaternary hydrological dynamics in the Middle Kalahari: Forcing and feedbacks. *Earth-Science Reviews*, 96, 313-326.
- Burrough, S.L; Thomas, D.S.G.; and Barham, L.S. 2019. Implications of a new chronology for the interpretation of the Middle and Later Stone Age of the upper Zambezi Valley. *Journal of Archaeological Science: Reports* 23:376-389.
- Busker, T., de Roo, A., Gelati, E., Schwatke, C., Adamovic, M., Bisselink, B., Pekel, J.-F., & Cottam, A. (2019). A global lake and reservoir volume analysis using a surface water dataset and satellite altimetry. *Hydrology and Earth System Sciences*, 23(2), 669-690.
- Butt, A.J., and Gould, K. 2018. 3D source-rock modelling in frontier basins: a case study from the Zambezi Delta Depression. *Petroleum Geoscience* 24(3):277-286.
- Butzer, K. W., Stuckenrath, R., Bruzewicz, A. J. & Helgren, D. M. 1978. Late Cenozoic paleoclimates of the Gaap Escarpment, Kalahari margin, South-Africa. *Quaternary Research*, 10, 310-339.

- Calamita, E.; Schmid, M.; Kunz, M.; Ndebele-Murisa, M.R.; Magadza, C.H.; Nyambe, I.; and Wehrli, B. 2019. Sixty years since the creation of Lake Kariba: Thermal and oxygen dynamics in the riverine and lacustrine sub-basins. *PloS One* 14(11):e0224679.
- Caley, T., Extier, T., Collins, J.A., Schefuß, E., Dupont, L., Malaizé, B., Rossignol, L., Souron, A., McClymont, E.L., Jimenez-Espejo, F.J., 2018. A two-million-year-long hydroclimatic context for hominin evolution in southeastern Africa. *Nature* 560, 76-79.
- Calow, R.C., MacDonald, A.M., Nicol, A.L., Robins, N.S. and Kebede, S. 2006. The struggle for water: drought, water security and rural livelihoods. <http://nora.nerc.ac.uk/id/eprint/501048/>
- Campbell, G., Johnson, S., Bakaya, T., Kumar, H. & Nsatsi, J. 2006. Airborne geophysical mapping of aquifer water quality and structural controls in the Lower Okavango Delta, Botswana. *South African Journal of Geology*, 109, 475-494.
- Cao, B., Deng, R., Xu, Y., Cao, B., Liu, B. & Zhu, S. 2022. Practical differences between photogrammetric bathymetry and physics-based bathymetry. *IEEE Geoscience and Remote Sensing Letters*, 19: 1-5.
- Carnie, T., 2021. What's to be done about the dam silt. *Sabinet African Journals*, 20(4), pp. 16-19.
- Catuneanu O, Wopfner H, Eriksson PG, Cairncross B, Rubidge BS, Smith RMH, and Hancox PJ (2005). The Karoo basins of south-central Africa. *Journal of African Earth Sciences* 43(1-3):211-253.
- Cerling, T.E., Harris, J.M., Macfadden, B.J., Leakey, M.G., Quade, J., Eisenmann, V., Ehleringer, J.R., 1997. Global vegetation change through the Miocene/Pliocene boundary. *Nature* 389, p.153-158.
- CGMW-BRGM (2016). In: Thiéblemont, D. (Ed.), *Geological Map of Africa, 1:10 Million Scale*, www.brgm.fr.
- Chamley, H. 1989. *Clay Mineralogy*. Springer, Berlin, 623 p.
- Chandiwana, S.K. and Snellen, W.B., 1994. Incorporating a human health component into the integrated development and management of the Zambezi river basin. Report of a Panel of Experts on Environmental Management for Vector Control mission to Zimbabwe, Zambia and Mozambique. World Health Organization, Geneva, Switzerland.
- Changes, challenges, and solutions (ed. by Revermann, R., Krewenka, K.M., Schmiedel, U., Olwoch, J.M., Helmschrot, J. & Jürgens, N.), pp. 54-65, *Biodiversity & Ecology*, 6, Klaus Hess
- Chen G, Hay GJ, Carvalho LMT, Wulder MA (2012). Object-based change detection. *Int. J. Rem. Sens.* 33(14):4434-4457.
- Chen, J., Brissette, F.P., Leconte, R., 2011. Uncertainty of downscaling method in quantifying the impact of climate change on hydrology. *J. Hydrol.* 401, 190-202. <https://doi.org/10.1016/j.jhydrol.2011.02.020>
- Chen, S.A., Micaelides, K., Grieve, S. W. D. & Singer, M. B., 2019. Aridity is expressed in river topography globally. *Nature*, Volume 573: 573-577.
- Chenje M., (Editor), (2000). *State of the Environment Zambezi Basin 2000*, SADC/IUCN/ZRA/SARDC/Sida, Maseru/Lusaka/Harare, ISBN1-77910-009-4.

- Chief directorate of surveys and land information (1999) dams and Lakes of South Africa from 1:50 000 Topographical Map Blue Plates. Polygon coverage generated by Mike Silberbauer, The Institute for Water Quality Studies, Pretoria, South Africa.
- Chihombori, J., Nyoni, K. and Gamira, D., 2012. Causes and Rate of Reservoir Sedimentation Due to Changes in Catchment Management. A Case of Marah Reservoir in Masvingo Province of Zimbabwe. *Greener Journal of Physical Sciences*. Vol. 3.p. 241-246.
- Chihombori, R.A., 2012. The mediating role of mobile technology in the linkage between customer satisfaction and customer loyalty (Doctoral dissertation, University of Fort Hare).
- Chisanga, C.B. Mubanga, K.H., Sichingabula, M. H., Banda, K.; Muchanga, M., Ncube, L.; van Niekerk, Helena, J., Zhao, B., Mkonde, A. Amanda, R. & Sonwabile, K., 2022. Modelling climatic trends for the Zambezi and Orange River Basins: implications on water security. *Journal of Water and Climate Change*, p.1-18.
- Chisanga, C.B., Mubanga, K.H., Sichingabula, H., Banda, K., Muchanga, M., Ncube, L., van Niekerk, H.J., Zhao, B., Mkonde, A.A. and Rasmeni, S.K., 2022. Modelling climatic trends for the Zambezi and Orange River Basins: implications on water security. *Journal of Water and Climate Change* (2022) 13 (3): 1275-1296. <https://doi.org/10.2166/wcc.2022.308>.
- Chisanga, C.B., Phiri, E., Chinene, V.R.N., 2017. Trends of Extreme Events in Precipitation and Temperature during the 1963-2012 Period at Mt Makulu. *J. Sci. Res. Reports* 15, 1-19. <https://doi.org/10.9734/JSRR/2017/34815>
- Chitata, T., Mugabe, F. T., & Kashaigili, J. J., 2014. Estimation of Small Reservoir Sedimentation in Semi-Arid Southern Zimbabwe. *Journal of Water Resource and Protection*, 06(11), 1017-1028. <http://suaire.sua.ac.tz/handle/123456789/1402>
- Chiti, R.M., 1987. Erosion Hazard Mapping: Zambia. Lusaka: Ministry of Agriculture.
- Chomba, I. 2017. An Assessment of Available Water for Livestock and Garden Irrigation in Dry Season for Subsistence Farmers in Zimba District. *International Journal of Research Studies in Agricultural Sciences (IJRSAS)*. 3. 14-19. 10.20431/2454-6224.0309003.
- Chomba, I.C. and Sichingabula, H.M., 2015. Sedimentation and its effects on selected small Dams East of Lusaka, Zambia. *Modern Environmental Science and Engineering*, 1(6), pp.325-340. <http://41.63.1.5/handle/123456789/7198>
- Chongo, M., Christiansen, A. V., Tembo, A., Nyambe, I., Larsen, F. & Bauer-Gottwein, P. 2014. Airborne and Ground based Transient Electromagnetic Mapping of Groundwater Salinity in the Machile-Zambezi Basin, South-western Zambia. . submitted to *Hydrogeology Journal*.
- Chongo, M., Wibroe, J., Staal-Thomsen, K., Moses, M., Nyambe, I., Larsen, F. & Bauer-Gottwein, P. 2011. The use of Time Domain Electromagnetic method and Continuous Vertical Electrical Sounding to map groundwater salinity in the Barotse sub-basin, Zambia. *Physics and Chemistry of the Earth, Parts A/B/C*, 36, 798-805.
- Clark, J. (1990). Welbedacht Dam capacity determination. Department of Water Affairs Report D200-01.

Climate data sets are available as modelled data and are publicly available from the following, for example:

Area covered and the Source

Africa:

<https://climate.copernicus.eu/data-evaluation-climate-models>

World, Africa, local:

<http://apps.ecmwf.int/datasets/>

Local and Africa:

<http://cip.csag.uct.ac.za/webclient2/datasets/africa-merged-cmip5/>

Africa:

http://sdwebx.worldbank.org/climateportal/index.cfm?page=country_historical_climate&ThisCCCode=ZAF

World:

<https://www.ecad.eu/>

Africa:

https://www.dwd.de/EN/climate_environment/cdc/cdc_node.html

Local:

<https://www.csir.co.za/developing-african-based-earth-system-model>

World:

<https://globalweather.tamu.edu/>

World, Africa and local:

<https://gisgeography.com/category/data-sources/>

World:

<http://www.worldclim.org/>

World:

<http://www.ipcc-data.org/>,

World:

<http://www.climatus.com/index.php>

World and local:

<http://www.ncdc.noaa.gov/sotc/global/2012/10>

World and local:

http://ipcc.ch/publications_and_data/publications_and_data_reports.shtml#.US9h5Dfoixk

World and local:

www.lapig.iesa.ufg.br

World:

<http://ageconsearch.umn.edu/>

World and local:

<http://glovis.usgs.gov/>

Africa:

<http://www.fao.org/climatechange/climatesmart/en/>

Africa:

ftp://ftp-anon.dwd.de/pub/data/gpcc/html/download_gate.html

Africa and local:

<http://www.climatic-maps.org/daily-data>

World and local:

<http://www.ipcc-nggip.iges.or.jp/software/index.html>

- Cohen Liechti, Théodora, *et al.* "Comparison and evaluation of satellite derived precipitation products for hydrological modelling of the Zambezi River Basin." *Hydrology and Earth System Sciences* 16.EPFL-ARTICLE-175211 (2012): 489-500.
- Collins AS, Reddy SM, Buchan C and Mruma A (2004). Temporal constraints on Paleoproterozoic eclogite formation and exhumation (Usagaran Orogen, Tanzania). *Earth and Planetary Science Letters* 224(1-2):175-192.
- Comas-Cufí, M and Thió-Henestrosa, FS (2011). CoDaPack 2.0: A Stand-Alone, Multi-Platform Compositional Software.
- Compton, J. S., & Maake, L. (2007). Source of the suspended load of the upper Orange River, South Africa. *South African Journal of Geology*, 110(2-3), 339-348.
- Condé, R. D. C., Martinez, J. M., Pessotto, M. A., Villar, R., Cochonneau, G., Henry, R., ... & Nogueira, M. 2019. Indirect assessment of sedimentation in hydropower dams using MODIS remote sensing images. *Remote Sensing*, 11(3), 314.
- Conley, A. & Van Niekerk, P. 2000. Sustainable management of international waters: The Orange River case. *Water Policy*, 2(1-2).
- Cooke, H. & Verhagen, B. T. The dating of cave development – an example from Botswana. *Proceedings of the Seventh International Speleological Congress, Sheffield, 1977.* 122-124.
- Cooke, H. & Verstappen, H. T. 1984. The landforms of the western Makgadikgadi basin in northern Botswana, with a consideration of the chronology of the evolution of Lake Palaeo-Makgadikgadi. *Zeitschrift fur Geomorphologie*, 1, 1-19.
- Cooke, H. 1975. The palaeoclimatic significance of caves and adjacent landforms in western Ngamiland, Botswana. *Geographical Journal*, 430-444.
- Cooke, H. 1979. The origin of the Makgadikgadi Pans.
- Cooke, H. 1980. Landform evolution in the context of climatic change and neo-tectonism in the Middle Kalahari of north-central Botswana. *Transactions of the Institute of British Geographers*, 80-99.
- Cooke, H. J. 1984. The evidence from northern Botswana of Late Quaternary climatic change. In: VOGEL, J. C. (ed.) *Late Cainozoic Palaeoclimates of the Southern Hemisphere.* Balkema, Rotterdam.
- Cooney, C.M., 2012. Downscaling Climate Models: Sharpening the Focus on Local-Level Changes (No. 1), *Environmental Health Perspectives.* Washington, DC.
- Cordier, S., Harman, D., Lauer, T., Voinchet, P., Bahain, J.-J. & Frechen, M. 2012. Geochronological reconstruction of the Pleistocene evolution of the Sarre valley (France and Germany) using OSL and ESR dating techniques. *Geomorphology*, 165, 91-106.

- Couture, P., Busby, P., Gauthier, C., Rajotte, J.W. and Pyle, G.G., 2008. Seasonal and regional variations of metal contamination and condition indicators in yellow perch (*Perca flavescens*) along two polymetallic gradients. I. Factors influencing tissue metal concentrations. *Human and Ecological Risk Assessment*, 14(1), pp.97-125.
- Cox K G (1989). The role of mantle plumes in the development of continental drainage patterns. *Nature* 342:873-877.
- Crawford, A.J., Belcher, C.M., 2014. Charcoal morphometry for paleoecological analysis: The effects of fuel type and transportation on morphological parameters. *Applications in plant sciences* 2, 1400004.
- Cronberg, G., Gieske, A., Martins, E., Nengu, J. P. & Stenström, I. M. 1995. Hydrobiological Studies of the Okavango Delta and Kwando/Linyanti/Chobe River, Botswana; Surface Water Quality Analysis.
- CRU data – it's an observational, gridded data product that includes monthly rainfall and temperature, but also calculated PET.
- CSIR (Council for Scientific and Industrial Research), Environmentek, 2001. Water resource accounts for South Africa, 1991-1998. Final Report to the Natural Resource Accounting Programme of Southern Africa. University of Pretoria.
- CSIR, Climate data
<https://www.csir.co.za/developing-african-based-earth-system-model>
- CSIR. 2016. CSIR climate modellers take on enormous task of modelling the future of climate change through an African lens. <https://www.csir.co.za/csir-climate-modellers-take-enormous-task-modelling-future-climate-change-through-african-lens>.
- CSIR. 2016. CSIR climate modellers take on enormous task of modelling the future of climate change through an African lens. <https://www.csir.co.za/csir-climate-modellers-take-enormous-task-modelling-future-climate-change-through-african-lens>.
- CSO (Central Statistics Office) 2010. Census of population and housing. Preliminary report. <http://www.zamstats.gov.zm>
- Cui, Y., Schubert, B.A., Jahren, A.H., 2020. A 23 my record of low atmospheric CO₂. *Geology* 48, 888-892.
- Curtarelli, M., Leao, J., Ogashawara, I., Lorenzetti, J. and Stech, J. (2015). Assessment of Spatial Interpolation Methods to Map the Bathymetry of an Amazonian Hydroelectric Reservoir to Aid in Decision Making for Water Management. *Journal of Geoinformatics*. Vol. 4. p. 220-235.
- Da Silva, A.C., Hladil, J., Chadimova, L., Slavík, L., Hilgen, F.J., Bábek, O. and Dekkers, M.J., 2016. Refining the Early Devonian time scale using Milankovitch cyclicity in Lochkovian-Pragian sediments (Prague Synform, Czech Republic). *Earth and Planetary Science Letters*, 455, pp.125-139.
- Daly, M.C.; Green, P.; Watts, A.B.; Davies, O.; Chibesakunda, F ; and Walker, R. 2020. Tectonics and landscape of the Central African Plateau and their implications for a propagating Southwestern Rift in Africa. *Geochemistry, Geophysics, Geosystems* 21(6): e2019GC008746.

- Daniau, A.-L., Goñi, M.F.S., Martinez, P., Urrego, D.H., Bout-Roumazelles, V., Desprat, S., Marlon, J.R., 2013a. Orbital-scale climate forcing of grassland burning in southern Africa. *Proceedings of the National Academy of Sciences* 110, 5069-5073.
- Data resources for South Africa
- Dauteuil, O., Bessin, P., & Guillocheau, F. (2015). Topographic growth around the Orange River valley, southern Africa: A Cenozoic record of crustal deformation and climatic change. *Geomorphology*, 233, 5-19. <https://doi.org/10.1016/j.geomorph.2014.11.017>
- Davies, B.R.; Beilfuss, R.D.; and Thoms, M.C. 2000. Cahora Bassa retrospective, 1974-1997: effects of flow regulation on the Lower Zambezi River. *Internationale Vereinigung für theoretische und angewandte Limnologie: Verhandlungen* 27(4): 2149-2157.
- Day, J. 1993. The major ion chemistry of some southern African saline systems. *Hydrobiologia*, 267, 37-59.
- De Carvalho, H.; Tassinari, C.; Alves, P.H.; Guimarães, F.; and Simões, M.C. 2000. Geochronological review of the Precambrian in western Angola: links with Brazil. *Journal of African Earth Sciences* 31(2):383-402.
- De Clercq, W., Helmschrot, J., de Witt, M., Himmelsbach, T., Kenabatho, P., Kralisch, S., Liehr, S., Ferreira Baptista, L., Mogobe, O., Mufeti, P., Müller, I., Nyambe, I., Sichingabula, H.M., Teixeira-Pinto, A., Teixeira Pires, G.J.P., Hipondoka, M. & Wanke, H. (2018) Water research in southern Africa: Data collection and innovative approaches towards climate change adaptation in the water sector. In: *Climate change and adaptive land management in southern Africa – assessments*, Publishers, Göttingen & Windhoek. doi:10.7809/b-e.00305.
- De Noyelles, F. and Jakubauskas, M., 2008. Current state, trend, and spatial variability of sediment in Kansas reservoirs. *Sedimentation in our reservoirs: causes and solutions*, 500. https://www.ksre.kstate.edu/historicpublications/pubs/kwri_book.pdf#page=10
- De Villiers, J W L. (2006). 2D mathematical modelling of turbulent transport of cohesive sediments in shallow reservoirs. Master's degree thesis, University of Stellenbosch.
- De Villiers, J.W.L. and Basson, G.R., 2007. Modelling of long-term sedimentation at Welbedacht Reservoir, South Africa. *Journal of the South African Institution of Civil Engineering= Joernaal van die Suid-Afrikaanse Instituut van Siviele Ingenieurswese*, 49(4), pp.10-18.
- De Villiers, S. 2005. "The hydrochemistry of rivers in KwaZulu-Natal." *Water SA* 31(2): 193-197.
- De Vries, J. J. & Von Hoyer, M. 1988. Groundwater Recharge Studies in Semi-Arid Botswana- A Review. In: SIMMERS, I. (ed.) *Estimation of Natural Groundwater Recharge*. Springer, Netherlands.
- De Vries, J. J. 1984. Holocene depletion and active recharge of the Kalahari groundwaters – A review and an indicative model. *Journal of Hydrology*, 70, 221-232.
- De Vries, J. J., Selaolo, E. T. & Beekman, H. E. 2000. Groundwater recharge in the Kalahari, with reference to paleo-hydrologic conditions. *Journal of Hydrology*, 238, 110-123.
- De Waal, D.J., Bekker, S.J. and Pretorius, J.H. (2011) "Modelling inflows into the Gariep dam," *South African Statistical Journal*,

- De Waal, D.J., Bekker, S.J. and Pretorius, J.H., 2011. Modelling inflows into the Gariep dam: case study. *South African Statistical Journal*, 45(1), pp.135-147.
- De Waele B, Fitzsimons ICW, Wingate MTD, Tembo 851 F, Mapani B, and Belousova EA (2009). The geochronological framework of the Irumide Belt: a prolonged crustal history along the margin of the Bangweulu Craton. *American Journal of Science* 309(2):132-187.
- De Waele B, Kampunzu AB, Mapani BSE, and Tembo F (2006). The Mesoproterozoic Irumide belt of Zambia. *Journal of African Earth Sciences* 46(1-2):36-70.
- Debruyne D, Hulsbosch N, Van Wilderode J, Balcaen L, Vanhaecke F, and Muchez P (2015) Regional geodynamic context for the Mesoproterozoic Kibara Belt (KIB) and the Karagwe-Ankole Belt: Evidence from geochemistry and isotopes in the KIB. *Precambrian Research* 264: 82-97.
- Delft University, SWAT model
<https://www.tudelft.nl/en/ceg/research/stories-of-science/a-better-understanding-of-the-zambesi-river/>
- Deltares 2011: Dam synchronisation and flood releases in the Zambezi River Basin.
<https://www.deltares.nl/en/projects/dam-synchronisation-flood-releases-zambezi-river-basin>
- Deng, Z., Ji, M. & Zhang, Z. 2008. Mapping bathymetry from multi-source remote sensing images: a case study in the Beilun estuary, Guangxi, China. *The International Archives of the Photogrammetry, Remote Sensing and Spatial Information Sciences*, 37(8): 1321-1326.
- Dent, J.E., 2012. Climate and meteorological information requirements for water management: A review of issues.
- Denys, F., Lodenkemper L. K., & Phillips, M. 2022. National Siltation Management Strategy for Dams in South Africa: Dam Engineering and Socio-ecological Systems Technology Transfer Report. WRC Report No. 3010/1/21.
- Department of Water Affairs (DWA). (2012). Development of Reconciliation Strategies for Large Bulk Water Supply Systems: Orange River: Literature Review Report. Report No. P RSA D000/00/18312/2.
- Department of Water Affairs and Forestry (DWAf). (2004). Internal Strategic Perspective: Upper Orange Water Management Area. Prepared by PDNA, WRP Consulting Engineers (Pty) Ltd, WMB and Kwezi-V3 on behalf of the Directorate: National Water Resource Planning. DWAf Report No P WMA.
- Department of Water Affairs and Forestry (DWAf). (2009). Department of Water Affairs and Forestry Water Resource Planning Systems Orange River: Assessment of Water Quality Data
- Department of Water Affairs and Forestry, (2004a). National Water Resources Strategy, 1st ed. DWAf, Pretoria.
- Department of Water Affairs and Forestry, 1997. White Paper on Water Policy. South Africa. Department of Water Affairs and Forestry: Pretoria.
- Department of Water Affairs and Forestry, 2004a. National Water Resources Strategy, 1st ed. DWAf, Pretoria.

- Department of Water Affairs and Forestry, 2004b. Water Situation Assessment Model, DWAF, Pretoria: unpublished database.
- Department of Water Affairs and Forestry, South Africa. (2004). Internal Strategic Perspective: Upper Orange Water Management Area. Prepared by PDNA, WRP Consulting Engineers (Pty) Ltd, WMB and Kwezi-V3 on behalf of the Directorate: National Water Resource Planning. DWAF Report No P WMA
- Department of Water Affairs and Forestry, South Africa. 2004. Internal Strategic Perspective: Upper Orange Water Management Area. Prepared by PDNA, WRP Consulting Engineers (Pty) Ltd, WMB and Kwezi-V3 on behalf of the Directorate: National Water Resource Planning. DWAF Report No P WMA
- Department of Water Affairs and Forestry. 1997. White Paper on Water Policy. South Africa. Department of Water Affairs and Forestry: Pretoria.
- Department of Water Affairs and Forestry. 2004a. National Water Resources Strategy, 1st ed. DWAF, Pretoria.
- Department of Water Affairs and Forestry. 2004b. Water Situation Assessment Model, DWAF, Pretoria: unpublished database.
- Department of Water and Sanitation. 2006. Capacity determination of Vanderkloof Dam 2018. Compiled by J. Jacobs on behalf of the Directorate: Spatial and Land Information Management. Report No D310-01, Hydro No D3R003.
- Department of Water and Sanitation. 2018. Capacity determination of Gariep dam 2018. Compiled by J. Jacobs on behalf of the Directorate: Spatial and Land Information Management. Report No D350-02, Hydro No D3R002.
- Derricourt RM (1976) Regression rate of the Victoria Falls and the Batoka Gorge. *Nature* 264:23-25.
- Dickinson WR (1985) Interpreting provenance relations from detrital modes of sandstones. In: Zuffa GG(Ed), *Provenance of Arenites*. Reidel, Dordrecht, NATO ASI Series 148:333-361.
- Dierssen, H.M. & Theberge, A.E. 2014. Bathymetry: History of seafloor mapping. *Encyclopedia of Natural Resources*, 2: 1-6. doi: 10.1081/E-ENRW-120047531
- Dill, H.G. 2007. A review of mineral resources in Malawi: with special reference to aluminium variation in mineral deposits. *Journal of African Earth Sciences* 47(3):153-173.
- Dill, H.G., Ludwig, R.R., Kathewera, A., Mwenelupembe, J. 2005. A lithofacies terrain model for the Blantyre Region: implications for the interpretation of palaeosavanna depositional systems and for environmental geology and economic geology in southern Malawi. *Journal of African Earth Sciences* 41(5): 341-393.
- Dincer, T., Hutton, L. & Kupee, B. 1978. Study, using stable isotopes, of flow distribution, surface-groundwater relations and evapotranspiration in the Okavango Swamp, Botswana. International Atomic Energy Agency, Proc. Ser. SM-228/52.
- Dingle, R., Siesser, W. G. & Newton, A. 1983. Mesozoic and Tertiary geology of southern Africa, A.A. Balkema, Rotterdam.
- Dinis, P.; Garzanti, E.; Vermeesch, P.; and Huvi, J. 2017. Climatic zonation and weathering control on sediment composition (Angola). *Chemical Geology* 467:110-121.

- Dinis, P.A.; Garzanti, E.; Hahn, A.; Vermeesch, P.; Cabral-Pinto, M. 2020. Weathering indices as climate proxies. A step forward based on Congo and SW African river muds. *Earth-Science Reviews* 201:103039.
- Dirks, P.H.G.M.; Blenkinsop, T.G.; Jelsma, H.A. 2009. The Geological Evolution of Africa. In De Vito, B.; Grasemann, B.; and Stuwe, K., eds. *Geology. Encyclopedia of Life Support Systems*, vol. IV., EOLSS Publishers, Paris, 978-1-84826-457-1, pp. 230-251.
- Doyle LJ, Cleary WJ, and Pilkey OH (1968). Mica: its use in determining shelf-depositional regimes. *Marine Geology* 6:381-389.
- Doyle MW, Harbor JM, Stanley EH. 2003. Toward policies and decisionmaking for dam removal. *Environmental Management* 31(4): 453-465. <https://link.springer.com/article/10.1007/s00267-002-2819-z>
- Drever, J. I. 1997. The geochemistry of natural waters: surface and groundwater environments.
- Droz L and Mougnot D (1987) Mozambique upper fan: Origin of depositional units. *American Association of Petroleum Geologists Bulletin* 71(11):1355-1365.
- Du Toit, A. 1927. The Kalahari and some of its problems. *South African Journal of Science*, 24, 88-101.
- Du Y, Zhang Y, Ling F, Wang Q, Li W and Li X (2016) Water bodies' mapping from Sentinel-2 imagery with modified normalized difference water index at 10-m spatial resolution produced by sharpening the SWIR band. *Remote Sens.* 8 (4) 354.
- Duan H, Ma R, Hu C (2012). Evaluation of remote sensing algorithms for cyanobacterial pigment retrievals during spring bloom formation in several lakes of East China. *Rem. Sens. Environ.* 126:126-135. Gao B-C (1996). NDWI – A normalized difference water index for remote sensing of vegetation liquid water from space. *Rem. Sens. Environ.* 58(3):257-266.
- Duan Z and Bastiaanssen WGM (2013) Estimating water volume variations in lakes and reservoirs from four operational satellite altimetry databases and satellite imagery data. *Remote Sens. Environ.* 134 403-416
- Duncan, R. A., Hooper, P., Rehacek, J., Marsh, J. & Duncan, A. 1997. The timing and duration of the Karoo igneous event, southern Gondwana. *Journal of Geophysical Research: Solid Earth* (1978-2012), 102, 18127-18138.
- Dupont, L.M., Caley, T., Kim, J.H., Castaneda, I., Malaize, B., Giraudeau, J., 2011. Glacial-interglacial vegetation dynamics in South Eastern Africa coupled to sea surface temperature variations in the Western Indian Ocean. *Climate of the Past*, 7, 4(2011-11-09) 7, 2261-2296.
- Dupont, L.M., Rommerskirchen, F., Mollenhauer, G., Schefuß, E., 2013. Miocene to Pliocene changes in South African hydrology and vegetation in relation to the expansion of C4 plants. *Earth and Planetary Science Letters* 375, 408-417.
- DWAF. (2006). Home page of the Department of Water Affairs and Forestry (www.dwaf.gov.za).
- DWS NIWIS Water Resource Management. (n.d.). [Www.dws.gov.za](http://www.dws.gov.za). Retrieved March 24, 2022, from <https://www.dws.gov.za/niwis2/WaterResourceManagement/SurfaceWaterStorage>
- DWS Website. Available at: <https://www.dws.gov.za/Hydrology/>. (Accessed on 16 May 2022)

- DWS Website. Available at: <https://www.dws.gov.za/Hydrology/>. (Accessed on 16 May 2022)
- Earle, A., Malzbender, D., Turton, A., & Manzungu, E. (2005). A Preliminary Basin Profile of the Orange / Senqu River. Retrieved from http://www.anthonyturton.com/assets/my_documents/my_files/Orange_Profile_4_Apl_2.pdf
- Ebert, J. I. & Hitchcock, R. K. 1978. Ancient Lake Makgadikgadi, Botswana: mapping, measurement and palaeoclimatic significance. *Palaeoecology of Africa*, 10, 47-56.
- Ebinger CE and Scholz CA (2012) Continental rift basins: The East African perspective. In: Busby, C., Azor, A. (eds.), *Tectonics of sedimentary basins: recent advances*. Oxford, Wiley-Blackwell, pp.185-208.
- Eckardt, F. D., Bryant, R. G., McCulloch, G., Spiro, B. & Wood, W. W. 2008. The hydrochemistry of a semi-arid pan basin case study: Sua Pan, Makgadikgadi, Botswana. *Applied Geochemistry*, 23, 1563-1580.
- Economic Commission for Africa. 2010. Cost-Benefit Analysis for Regional Infrastructure in Water and Power Sectors in Southern Africa. ECA/SA/TPUB/CBA/2010/1. https://www.uneca.org/sites/default/files/PublicationFiles/cost-benefit-analysis-for-regional-infrastructure-in-water-and-power-sectors_0.pdf
- Edmunds, W., Fellman, E. & Goni, I. 1999. Lakes, groundwater and palaeohydrology in the Sahel of NE Nigeria: evidence from hydrogeochemistry. *Journal of the Geological Society*, 156, 345-355.
- Edmunds, W., Fellman, E., Goni, I. & Prudhomme, C. 2002. Spatial and temporal distribution of groundwater recharge in northern Nigeria. *Hydrogeology Journal*, 10, 205-215.
- Edwards, E.J., Osborne, C.P., Strömberg, C.A., Smith, S.A., Consortium, C.G., 2010. The origins of C4 grasslands: Integrating evolutionary and ecosystem science. *Science* 328, 587-591.
- Edwards, T.K.; Glysson, G.D. *Field Methods for Measurement of Fluvial Sediment*. Available online: <https://pubs.er.usgs.gov/publication/ofr86531>.
- Eglinger A, Vanderhaeghe O, André-Mayer AS, Goncalves P, Zeh A, Durand C, and Deloule E (2016). Tectono-metamorphic evolution of the internal zone of the Pan-African Lufilian orogenic belt (Zambia): Implications for crustal reworking and syn-orogenic uranium mineralizations. *Lithos* 240:67-188.
- Ehleringer, J.R., Cerling, T.E., Helliker, B.R., 1997. C 4 photosynthesis, atmospheric CO 2, and climate. *Oecologia* 112, 285-299.
- Elvidge, S., Angling, M.J., Nava, B., 2014. On the use of modified Taylor diagrams to compare ionospheric assimilation models. *Radio Sci.* 49, 737-745. <https://doi.org/10.1002/2014RS005435>
- Erena, M., Domínguez, J.A., Atenza, J.F., Galiano, S.G., Soria, J. & Ruzafa, A.P. 2020. Bathymetry time series using high spatial resolution satellite images. *Water*, 12: 1-28.
- ESA – Earth from Space: Gariep dam, South Africa (no date). Available at: https://www.esa.int/Applications/Observing_the_Earth/Earth_from_Space_Gariep_Dam_South_Africa (Accessed: March 8, 2022).
- ESIA, 2011. Riversdale's Zambezi River Barging Project, Zambezi River, Mozambique. Final Environmental and Social Impact Assessment Report, 335 p.

- Essien, E., Jesse, E. and Igbokwe, J., 2019. Assessment of water level in Dadin Kowa Dam reservoir in Gombe State Nigeria using geospatial techniques. *International Journal of Environment and Geoinformatics*, 6(1), pp.115-130.
- Eugster, H. P. & Hardie, L. A. 1978. *Saline Lakes*. In: LERMAN, A. (ed.) *Lakes*. New York: Springer.
- Eugster, H. P. & Jones, B. F. 1979. Behavior of major solutes during closed-basin brine evolution. *American journal of science*, 279, 609-631.
- Eugster, H. P. & Smith, G. I. 1965. Mineral equilibria in the Searles Lake evaporites, California. *Journal of Petrology*, 6, 473-522.
- Eugster, H. P. 1980. Geochemistry of evaporitic lacustrine deposits. *Annual Review of Earth and Planetary Sciences*, 8, 35-63.
- Fagorite, V. (2019) **RESERVOIR SEDIMENTATION: CAUSES, EFFECTS AND MITIGATION**. Available at: <https://www.researchgate.net/publication/337254018>.
- Falkenmark, M. 1986(a). Fresh Waters as a Factor in Strategic Policy and Action, in Westing, A.A. (ed.) *Global Resources and International Conflict: Environmental Factors in Strategic Policy and Action*. Oxford University Press: New York
- Falkenmark, M. 1986(b). Fresh Water – Time for a Modified Approach, in *Ambio*, Vol. 15, No. 4; 194-200.
- Falkenmark, M. 1987. Water Related Limitations to Local Development, in *Ambio*, Vol. 16, No. 4; 191-200
- Falkenmark, M. 1989. The Massive Water Scarcity now Threatening Africa: Why isn't it Being Addressed, in *Ambio*, Vol. 18, No. 2; 112-118.
- Falkenmark, M., 1986(a). Fresh Waters as a Factor in Strategic Policy and Action, in Westing, A.A. (ed.) *Global Resources and International Conflict: Environmental Factors in Strategic Policy and Action*. Oxford University Press: New York
- FAO, 1997. Irrigation potential in Africa: A basin approach (No. 4), *FAO LAND AND WATER BULLETIN 4*. Rome, Italy.
- FAO, 1997. Irrigation potential in Africa: A basin approach (No. 4), *FAO LAND AND WATER BULLETIN 4*. Rome, Italy.
- FAO, 2000. <http://www.fao.org/fi/oldsite/FCP/en/zmb/body.htm>).
- FAO. Fisheries and Aquaculture Circular No. 1170. Rome,
- Farr, J., Cheney, C., Baron, J. & Peart, R. 1981. GS 10 Project: Evaluation of Underground Water Resources. In: *FINAL REPORT*, B. G. S. D. (ed.).
- Feakins, S.J., Levin, N.E., Liddy, H.M., Sieracki, A., Eglinton, T.I., Bonnefille, R., 2013. Northeast African vegetation change over 12 my. *Geology* 41, 295-298.
- Fearnside, P.M., 2013. Decision making on amazon dams: politics trumps uncertainty in the Madeira River sediments controversy. *Water Alternatives*, 6(2). <https://www.water-alternatives.org/index.php/allabs/218-a6-2-15/file>
- Fecher, R. (1998). Real cost of conserving energy. EDRC report series.
- Feng, L.; Hu, C.; Chen, X.; Tian, L.; Chen, L. Human induced turbidity changes in Poyang Lake between 2000 and 2010: Observations from MODIS. *J. Geophys. Res.* 2012, 117, 1-19.

- Fernandes P, Cogné N, Chew DM, Rodrigues B, Jorge RCS, Marques J, Jamal D, and Vasconcelos L (2015) The thermal history of the Karoo Moatize-Minjova Basin, Tete Province, Mozambique: An integrated vitrinite reflectance and apatite fission track thermochronology study. *Journal of African Earth Sciences* 112:55-72.
- Fey, M. 2010. *Soils of South Africa*, Cape Town: Cambridge University Press.
- FFEM (Fonds Français pour l'Environnement Mondial) 2005. Pollution monitoring and management on the Zambezi River. French Fund for Global Environment. Lusaka, Zambia, Final Report.
- Fierens R, Droz L, Toucanne S, Raison F, Jouet G and Babonneau N (2019) Late Quaternary geomorphology and sedimentary processes in the Zambezi turbidite system (Mozambique Channel). *Geomorphology* 334:1-28.
- Fierens R, Toucanne T, Droz L, Jouet G, Raison F, Jorissen EL, Bayon G, Giraudeau J and Jorry SJ (2020) Quaternary sediment dispersal in the Zambezi turbidite system (SW Indian Ocean). *Marine Geology* 428:106276, doi: 10.1016/j.margeo.2020.106276.
- Flener, C., Lotsari, E., Alho, E. & Käyhkö, J. 2012. Comparison of empirical and theoretical remote sensing based bathymetry models in river environments. *River Research and Applications*, 28(1):118-133.
- Flint JJ (1974) Stream gradient as a function of order, magnitude, and discharge. *Water Resources Research* 10:969-973.
- Flügel TJ, Eckardt FD and Cotterill WPD (2018) The geomorphology and river longitudinal profiles of the Congo-Kalahari Watershed. In Runge, J. (ed.), *the African Neogene-Climates, Environments and People: Palaeoecology of Africa*. CRC Press, Leiden, the Netherlands 34:31-52.
- Folk R.L (1980). *Petrology of Sedimentary Rocks*. Hemphill Publishing Co., Austin (USA), pp. 184.
- Frimmel, H.E., Basei, M.S., and Gaucher, C. 2011, Neoproterozoic geodynamic evolution of SW Gondwana: a southern African perspective. *Int. J. Earth Sci.* 100:323-354.
- Folk RL (1951) Stages of textural maturity in sedimentary rocks. *Journal of Sedimentary Petrology* 21:127-130.
- For South Africa, the Department Surveys and Mapping: <http://www.ngi.gov.za/index.php/contact-ngi>
- Foster, S. S. D., Bath, A. H., Farr, J. L. & Lewis, W. J. 1982. The likelihood of active groundwater recharge in the Botswana Kalahari. *Journal of Hydrology*, 55, 113-136.
- Foteh, R., Garg, V., Nikam, B. R., Khadatare, M. Y., Aggarwal, S. P., & Kumar, A. S., 2018. Reservoir Sedimentation Assessment Through Remote Sensing and Hydrological Modelling. *Journal of the Indian Society of Remote Sensing*, 46(11), 1893-1905. <https://link.springer.com/article/10.1007/s12524-018-0843-6>
- Freeze, R. A. & Cherry, J. 1979. *Groundwater*, Prentice-Hall, Englewood Cliffs, NJ.
- Frimmel, H.E.; Basei, M.S.; and Gaucher, C. 2011. Neoproterozoic geodynamic evolution of SW-Gondwana: a southern African perspective. *Int. J. Earth Sci.* 100:323-354.

- Fritz H, Abdelsalam M, Ali KA, Bingen B, Collins AS, Fowler AR, Ghebream W, Hauzenberger CA, Johnson PR, Kusky TM and Macey P (2013) Orogen styles in the East African Orogen: a review of the Neoproterozoic to Cambrian tectonic evolution. *Journal of African Earth Sciences* 86:65-106.
- Froehlich, D. C. 2018. Estimating reservoir sedimentation at large dams in India. In *E3S Web of Conferences* (Vol. 40, p. 03042). EDP Sciences.
- From DWS: Stage levels for SA dams (<https://www.dws.gov.za/Hydrology/default.aspx>) and (<https://sawx.co.za/state-of-dams/>)
- From Esri:
- From the USGS:
[ftp://rfdata:forceDATA@ftp.iiasa.ac.at/](ftp://rfddata:forceDATA@ftp.iiasa.ac.at/)
- Gabriel KR (1971) The biplot graphic display of matrices with application to principal component analysis. *Biometrika* 58:453-467
- Gaillardet J, Dupré B and Allègre CJ (1999). Geochemistry of large river suspended sediments: silicate weathering or recycling tracer? *Geochimica et Cosmochimica Acta* 63:4037-4051.
- Gao, H., Birkett, C., & Lettenmaier, D. P. (2012). Global monitoring of large reservoir storage from satellite remote sensing. *Water Resources Research*, 48, W09504.
- Gao, J. 2009. Bathymetric mapping by means of remote sensing: methods, accuracy and limitations. *Progress in Physical Geography*, 33:103-116.
- Garzanti E (2016) From static to dynamic provenance analysis – Sedimentary petrology upgraded. *Sedimentary Geology* 336:3-13.
- Garzanti E (2017) The maturity myth in sedimentology and provenance analysis: *Journal of Sedimentary Research* 87:353-365.
- Garzanti E (2019) Petrographic classification of sand and sandstone. *Earth-Science Reviews* 192:545-563.
- Garzanti E and Andò S (2007) Plate tectonics and heavy-mineral suites of modern sands. In: Mange, M.A., Wright, D.T. (eds.), *Heavy minerals in use*. Elsevier, Amsterdam, *Developments in Sedimentology* 58:741-763.
- Garzanti E and Andò S (2019) Heavy Minerals for Junior Woodchucks: *Minerals* 9(3):148, 39 doi:10.3390/min9030148.
- Garzanti E and Resentini A (2016) Provenance control on chemical indices of weathering (Taiwan river sands). *Sedimentary Geology* 336:81-95.
- Garzanti E, Andò S and Vezzoli G (2006) The continental crust as a source of sand (Southern Alps cross-section, Northern Italy). *The Journal of Geology* 114:533-554.
- Garzanti E, Andò S and Vezzoli G (2009) Grain-size dependence of sediment composition and environmental bias in provenance studies. *Earth Planet. Sci. Lett.* 277:422-432.
- Garzanti E, Andò S, France-Lanord C, Limonta M, Borromeo L and Vezzoli G (2019b) Provenance of Bengal Shelf Sediments. 2. Petrology of sand. *Minerals* 9:642, doi: 10.3390/min9100642.
- Garzanti E, Andò S, Limonta M, Fielding L and Najman Y (2018b) Diagenetic control on mineralogical suites in sand, silt, and mud (Cenozoic Nile Delta): implications for provenance reconstructions. *Earth Sci. Rev.* 185:122-139.

- Garzanti E, Bayon G, Dennielou B, Barbarano M, Limonta M and Vezzoli G (2021c) Mineralogical and Nd-isotope variability in quartzose deep-sea sand: the Congo Fan. *Journal of Sedimentary Research*, in press.
- Garzanti E, Dinis P, Vermeesch P, Andò S, Hahn A, Huvi J, Limonta M, Padoan M, Resentini A, Rittner M and Vezzoli G (2018a) Dynamic uplift, recycling, and climate control on the petrology of passive-margin sand (Angola). *Sedimentary Geology* 375:86-104.
- Garzanti E, Dinis P, Vezzoli G and Borromeo L (2021b) Sand and mud generation from Paraná-Etendeka continental flood basalts in contrasting climatic conditions (Uruguay vs. Namibia). *Sedimentology*, in review.
- Garzanti E, He J, Barbarano M, Resentini A, Li C, Yang L, Yang S and Wang H (2021a) Provenance versus weathering control on sediment composition in tropical monsoonal climate (South China) – 2. Sand petrology and heavy minerals. *Chemical Geology*, 119997 doi.org/10.1016/j.chemgeo.2020.119997.
- Garzanti E, Limonta M, Vezzoli G, An W, Wang J and Hu X (2019a) Petrology and multimineral fingerprinting of modern sand generated from a dissected magmatic arc (Lhasa River, Tibet), in Ingersoll, R.V., Lawton, T.F., and Graham, S.A., eds., *Tectonics, Sedimentary Basins, and Provenance: A Celebration of William R. Dickinson's Career: Geological Society of America Special Paper 540:197-221*, [https://doi.org/10.1130/2018.2540\(09\)](https://doi.org/10.1130/2018.2540(09)).
- Garzanti E, Padoan M, Andò S, Resentini A, Vezzoli G and Lustrino M (2013b) Weathering and relative durability of detrital minerals in equatorial climate: sand petrology and geochemistry in the East African Rift. *The Journal of Geology* 121:547-580.
- Garzanti E, Padoan M, Setti M, López-Galindo A and Villa IM (2014b). Provenance versus weathering control on the composition of tropical river mud (southern Africa). *Chemical Geology* 366:61-74.
- Garzanti E, Resentini A, Andò S, Vezzoli G and Vermeesch P (2015) Physical controls on sand composition and relative durability of detrital minerals during long-distance littoral and aeolian transport (coastal Namibia). *Sedimentology* 62:971-996, doi:10.1111/sed.12169.
- Garzanti E, Resentini A, Vezzoli G, Andò S, Malusà M and Padoan M (2012) forward compositional modelling of Alpine orogenic sediments. *Sedimentary Geology* 280:149-164.
- Garzanti E, Resentini A, Vezzoli G, Andò S, Malusà MG, Padoan M and Paparella P (2010) Detrital fingerprints of fossil continental-subduction zones (axial belt provenance, European Alps). *The Journal of Geology* 118:341-362.
- Garzanti E, Vermeesch P, Andò S, Botti E, Limonta M, Vezzoli G, Dinis P, Hahn A, Baudet D, De Grave J and Kitambala Yaya N (2019c) Congo river sand and the equatorial quartz factory. *Earth-Science Reviews* 197:102918, doi.org/10.1016/j.earscirev.2019.102918
- Garzanti E, Vermeesch P, Andò S, Vezzoli G, Valagussa M, Allen K, Khadi KA and Al-Juboury IA (2013a). Provenance and recycling of Arabian desert sand. *Earth Science Reviews* 120:1-19.

- Garzanti E, Vermeesch P, Padoan M, Resentini A, Vezzoli G and Andò S (2014a) Provenance of passive-margin sand (southern Africa). *The Journal of Geology* 122:17-42.
- Garzanti E, Vezzoli G, Andò S and Castiglioni G (2001). Petrology of rifted-margin sand (Red Sea and Gulf of Aden, Yemen). *The Journal of Geology* 109:277-297.
- Garzanti, E. 1986. Source rock versus sedimentary control on the mineralogy of deltaic volcanic arenites (Upper Triassic, northern Italy). *Journal of Sedimentary Petrology* 56(2):267-275.
- Garzanti, E., and Andò, S. 2007. Heavy-mineral concentration in modern sands: implications for provenance interpretation. In Mange, M.A., and Wright, D.T., eds. *Heavy minerals in use*. Elsevier, Amsterdam, *Developments in Sedimentology* 58:517-545.
- Garzanti, E., and Resentini, A. 2016. Provenance control on chemical indices of weathering (Taiwan river sands). *Sedimentary Geology* 336:81-95.
- Garzanti, E., and Sternai, P., 2020. Against steady state: A quixotic plea for science. *Earth ArXiv*, <https://eartharxiv.org/p9xq7/>, doi:10.31223/osf.io/p9xq7
- Garzanti, E., Vermeesch, P., Padoan, M., Resentini, A., Vezzoli, G., and Ando, S (2014). Provenance of Passive-Margin Sand (Southern Africa). *The Journal of Geology*, 2014, Vol 122, p17-432.
- Garzanti, E.; Andò, S.; and Vezzoli, G. 2006. The continental crust as a source of sand (Southern Alps crosssection, Northern Italy). *J. Geol.* 114:533-554.
- Garzanti, E.; Andò, S.; and Vezzoli, G. 2008. Settling equivalence of detrital minerals and grain-size dependence of sediment composition. *Earth and Planetary Science Letters* 273(1-2):138-151.
- Garzanti, E.; Andò, S.; and Vezzoli, G. 2009. Grain-size dependence of sediment composition and environmental bias in provenance studies. *Earth Planet. Sci. Lett.* 277:422-432.
- Garzanti, E.; Andó, S.; France-Lanord, C.; Censi, P.; Vignola, P.; Galy, V.; and Lupker, M. 2011. Mineralogical and chemical variability of fluvial sediments: 2. Suspended-load silt (Ganga-Brahmaputra, Bangladesh). *Earth and Planetary Science Letters* 302(1-2):107-120.
- Garzanti, E.; Andò, S.; France-Lanord, C.; Vezzoli, G.; Censi, P.; Galy, V.; and Najman, Y. 2010b. Mineralogical and chemical variability of fluvial sediments: 1. Bedload sand (Ganga-Brahmaputra, Bangladesh). *Earth and Planetary Science Letters* 299(3-4):368-381.
- Garzanti, E.; Bayon, G.; Dennielou, B.; Barbarano, M.; Limonta, M.; and Vezzoli, G. 2021b. The Congo deep-sea fan: Mineralogical, REE, and Nd-isotope variability in quartzose passive-margin sand. *Journal of Sedimentary Research* 91(5):433-450.
- Garzanti, E.; Padoan, M.; Andò, S.; Resentini, A.; Vezzoli, G.; and Lustrino, M. 2013a. Weathering and relative durability of detrital minerals in equatorial climate: sand petrology and geochemistry in the East African Rift. *The Journal of Geology* 121:547-580.
- Garzanti, E.; Padoan, M.; Setti, M.; López-Galindo, A.; and Villa, I.M. 2014a. Provenance versus weathering control on the composition of tropical river mud (southern Africa). *Chemical Geology* 366:61-74.

- Garzanti, E.; Padoan, M.; Setti, M.; Peruta, L.; Najman, Y.; and Villa, I.M. 2013b. Weathering geochemistry and Sr-Nd fingerprints of equatorial upper Nile and Congo muds. *Geochemistry, Geophysics, Geosystems* 14:292-316.
- Garzanti, E.; Pastore, G.; Resentini, A.; Vezzoli, G.; Vermeesch, P.; Ncube, L.; Van Niekerk, H-G.; Jouet, G.; and Dall'Asta, M. 2021a. The Segmented Zambezi Sedimentary System from Source to Sink 1. Sand Petrology and Heavy Minerals. *The Journal of Geology* 129(4): <https://doi.org/10.1086/715792>.
- Garzanti, E.; Pastore, G.; Stone, A.; Vainer, S.; Vermeesch, P.; Resentini, A. 2022. Provenance of Kalahari sand: paleoweathering and recycling in a linked fluvial-eolian system. *Earth-Science Reviews*, Submitted August 2021
- Garzanti, E.; Resentini, A.; Andò, S.; Vezzoli, G.; Pereira, A.; and Vermeesch, P. 2015. Physical controls on sand composition and relative durability of detrital minerals during ultra-long distance littoral and aeolian transport (Namibia and southern Angola). *Sedimentology* 62(4):971-996.
- Garzanti, E.; Resentini, A.; Vezzoli, G.; Andò, S.; Malusà, M. G.; Padoan, M.; and Paparella, P. 2010a. Detrital fingerprints of fossil continental-subduction zones (axial belt provenance, European Alps). *J. Geol.* 118:341-362.
- Garzanti, E.; Resentini, A.; Vezzoli, G.; Andò, S.; Malusà, M.; and Padoan, M. 2012. Forward compositional modelling of Alpine orogenic sediments. *Sedimentary Geology* 280:149-164.
- Garzanti, E.; Vermeesch, P.; Andò, S.; Botti, E.; Limonta, M.; Vezzoli, G.; Dinis, P.; Hahn, A.; Baudet, D.; De Grave, J.; and Kitambala Yaya, N. 2019. Congo river sand and the equatorial quartz factory. *Earth-Science Reviews* 197:102918, <https://doi.org/10.1016/j.earscirev.2019.102918>.
- Garzanti, E.; Vermeesch, P.; Padoan, M.; Resentini, A.; Vezzoli, G.; and Andò, S. 2014b. Provenance of passive-margin sand (southern Africa). *The Journal of Geology* 122:17-42.
- Garzanti, E.; Vermeesch, P.; Rittner, M.; and Simmons, M. 2018. The zircon story of the Nile: time-structure maps of source rocks and discontinuous propagation of detrital signals. *Basin Research* 30:1098-1117.
- Gasse, F. 2000. Hydrological changes in the African tropics since the Last Glacial Maximum. *Quaternary Science Reviews*, 19, 189-211.
- Gaudard, G & Romerio, F. 2014. The future of hydropower in Europe: Interconnecting climate, markets and policies. *Environmental Science and Policy*, 37:172-181.
- Gebreselassie, H. G., Melesse, A. M., Bishop, K., & Gebremariam, A. G. (2019). Linear spectral unmixing algorithm for modelling suspended sediment concentration of flash floods, upper Tekeze River, Ethiopia. *International Journal of Sediment Research*.
- General resources that pertain to Zambezi and SA
- Getirana, A., Jung, H. C., & Tseng, K.-H. (2018). Deriving three dimensional reservoir bathymetry from multi-satellite datasets. *Remote Sensing of Environment*, 217, 366-374.

- Gharehkhani, R., 2011. Issues Problems of Sedimentation in Reservoir Siazakh Reservoir Case Study. World Academy of Science, Engineering and Technology Vol. 60. p. 1100-1102.
- Gholamalifard, M., Kutser, T. Sari, A.E. & Abkar, A.A. 2013. Remotely sensed empirical modelling of bathymetry in the southeastern Caspian Sea. Remote Sensing, 5(6):2746-2762.
- Gholizadeh, M. H., Melesse, A. M., & Reddi, L. (2016). A comprehensive review on water quality parameters estimation using remote sensing techniques. Sensors, 16(8), 1298.
- Giardino, C., Kõks, K.L., Bolpagni, R., Luciani, G., Candiani, G., Lehmann, M.K., Van der Woerd, H.J. and Bresciani, M., 2019. The colour of water from space: A case study for Italian lakes from Sentinel-2. In Geospatial analyses of Earth Observation (EO) data. IntechOpen.
- GISGeography, Maps, software, data, especially bathymetry
<https://gisgeography.com/category/data-sources/>
- GISGeography. 2022. LANDSAT 8 Bands and Band Combinations. [online] Available at: <<https://gisgeography.com/LANDSAT-8-bands-combinations/>> [Accessed 1 July 2022].
- Global Water Partnership, 2007. In: Bodík I, Ridderstolpe P (Eds) Sustainable sanitation in central and eastern Europe – addressing the needs of small and medium-size settlements. GWP CEE, Bratislava
- Global Water Partnership, Reports case studies
https://www.gwp.org/en/learn/KNOWLEDGE_RESOURCES/Case_Studies/Africa/Zambia-Integrated-Water-Resources-Management-and-Water-Efficiency-planning-process-332/
- Glynn SM, Master S, Wiedenbeck M, Davis DW, Kramers JD, Belyanin GA, Frei D and Oberthür T (2017) The Proterozoic Choma-Kalomo Block, SE Zambia: Exotic terrane or a reworked segment of the Zimbabwe Craton? Precambrian Research 298:421-438.
- Goel, M.K., Jain, S.K., Agarwal, P.K. (2002): Assessment of sediment deposition rate in Bargi Reservoir using digital image processing – Hydrological sciences journal 47(S1): S81-S92.
- Gonfiantini, E. 1986. Environmental isotopes in lake studies. In: P.FRITZ & J.-CH.FONTES (eds.) Handbook of environmental isotope geochemistry. Amsterdam, The Netherlands: Elsevier.
- Google Earth Help Center. (n.d.). Add placemarks, lines, and shapes on Google Earth. Retrieved from <https://support.google.com/earth/answer/148118?hl=en>
- Google Earth Help Center. (n.d.). Measure distances and areas on Google Earth. Retrieved from <https://support.google.com/earth/answer/148095?hl=en>
- Google Earth Pro. <https://www.google.com/earth/download/gep/agree.html?hl=en-GB>
- Goscombe B, Foster DA, Gray D and Wade B, (2020) Assembly 972 of central Gondwana along the Zambezi Belt: Metamorphic response and basement reactivation during the Kuunga Orogeny. Gondwana Research 80:410-465.
- Goudie, A.S. and Pye, K. (eds.) (1983). Chemical Sediments and Geomorphology: Precipitates and Residual in the Near-surface Environment. New York: Academic Press.

- Goudie, A.S., 1983. Dust storms in space and time. *Progress in Physical Geography*, 7(4), pp.502-530.
- Goudie, AS (2005) "The drainage of Africa since the Cretaceous". *Geomorphology*. 67: 437-456.
- Grantham GH, Marques J, Wilson M, Manhiça V and Hartzler F (2011) Explanation of the Geological Map of Mozambique, 1: 1 000 000. Direcção Nacional de Geologia, Maputo, 383 p.
- Grayson, R. & Blöschl, G. 2000. Spatial modelling of catchment dynamics. *Spatial Patterns in Catchment Hydrology: Observations and Modelling*. 51-81.
- Greber, N.D.; Davies, J.H.; Gaynor, S.P.; Jourdan, F.; Bertrand, H.; and Schaltegger, U. 2020. New high precision U-Pb ages and Hf isotope data from the Karoo large igneous province; implications for pulsed magmatism and early Toarcian environmental perturbations. *Results in Geochemistry* 1:100005.
- Grey, D. & Cooke, H. 1977. Some problems in the Quaternary evolution of the landforms of northern Botswana. *Catena*, 4, 123-133.
- GRID-Arendal, UNEP, Catchment information
<http://www.grida.no/publications/189>
- Griffin WL, Powell WJ, Pearson NJ and O'Reilly SY (2008) GLITTER: Data reduction software for laser ablation ICP-MS. In: Sylvester, P. (ed.), *Laser Ablation-ICP-MS in the Earth Sciences: Current Practices and Outstanding Issues*. Mineralogical Association of Canada, Short Course, Series 40:204-207.
- Grove, A. T. 1969. Landforms and climatic change in the Kalahari and Ngamiland. *Geographical Journal*, 191-212.
- Guenther, G. 2004. Airborne lidar bathymetry. *Environmental sciences*, 34-50.
- Guillocheau F, Chelalou R, Linol B, Dauteuil O, Robin C, Mvondo F, Callec Y and Colin JP (2015) Cenozoic landscape evolution in and around the Congo Basin: constraints from sediments and planation surfaces. In: de Wit, M.J., Guillocheau, F., de Wit, M.J.C. (Eds.), *Geology and Resource Potential of the Congo Basin, Regional Geology Reviews*. Springer-Verlag, Berlin Heidelberg, pp. 271-313.
- Guillocheau F, Simon B, Baby G, Bessin P, Robin C and Dauteuil O (2018) Planation surfaces as a record of mantle dynamics: the case example of Africa. *Gondwana Research* 53:82-98.
- Gumbrecht T, McCarthy TS and Merry CL (2001). The topography of the Okavango Delta, Botswana and its sedimentological and tectonic implications. *South African Journal of Geology* 990 104:243-264.
- Gumbrecht, T.; McCarthy, T.S.; and Merry, C.L. 2001. The topography of the Okavango Delta, Botswana, and its tectonic and sedimentological implications. *South African Journal of Geology* 104(3):243-264.
- Haddon IG and McCarthy TS (2005) The Mesozoic-Cenozoic interior sag basins of Central Africa: The Late-Cretaceous-Cenozoic Kalahari and Okavango basins. *J. Afr. Earth Sci.* 43:316-333.

- Hadian, M. and Mosaedi, A. (2021) "Application of Remote Sensing Technology in Sediment Estimating Entering the Dam Reservoirs due to Floods," *Shock and Vibration*, 2021. doi:10.1155/2021/4469744.
- Hahn, A., Schefuß, E., Groeneveld, J., Miller, C., Zabel, M., 2020. Glacial to interglacial climate variability in the southeastern African subtropics (25-20°S). *Climate of the Past Discussions*, 1-32.
- Hall, A., Valente, I. M. C. B. S. & Davies, B. R. 1977. The Zambezi River in Moçambique. *Freshwater Biology*, 7, 187-206.
- Hall, I., Hemming, S., LeVay, L., Barker, S., Berke, M., Brentegani, L., Caley, T., Cartagena-Sierra, A., Charles, C., Coenen, J., 2017. Expedition 361 summary, *Proceedings of the International Ocean Discovery Program*, 361. International Ocean Discovery Program.
- Han, Y., An, Z., Marlon, J.R., Bradley, R.S., Zhan, C., Arimoto, R., Sun, Y., Zhou, W., Wu, F., Wang, Q., 2020. Asian inland wildfires driven by glacial-interglacial climate change. *Proceedings of the National Academy of Sciences* 117, 5184-5189.
- Hanson RE, Harmer RE, Blenkinsop TG, Bullen DS, Dalziel IWD, Gose WA, Hall RP, Kampunzu AB, Key RM, Mukwakwami J, Munyanyiwa H, Pancake JA, Seidel EK and Ward SE (2006) Mesoproterozoic intraplate magmatism in the Kalahari Craton: a review. *J. Afr. Earth Sci.* 46:141-167.
- Hanson, R.E. 2003. Proterozoic geochronology and tectonic evolution of southern Africa. In: Yoshida, M., Windley, B.F., Dasgupta, S. (eds.), *Proterozoic East Gondwana: supercontinent assembly and breakup*. *Geol. Soc. London, Spec. Publ.* 206:427-463.
- Hanson, R.E.; Wilson, T.J.; and Munyanyiwa, H. 1994. Geologic evolution of the Neoproterozoic Zambezi orogenic belt in Zambia. *Journal of African Earth Sciences* 18(2):135-150.
- Hardie, L. A. & Eugster, H. P. 1970. The evolution of closed-basin brines. *Mineral. Soc. Amer. Spec. Pap.* 3, 273-290.
- Hargrove US, Hanson RE, Martin MW, Blenkinsop TG, Bowring SA, Walker N, and Munyanyiwa H (2003) Tectonic evolution of the Zambezi orogenic belt: geochronological, structural, and petrological constraints from northern Zimbabwe. *Precambrian Research* 123(2-4):159-186.
- Harris, I.C., Jones, P.D., 2020. CRU TS4.03: Climatic Research Unit (CRU) Time-Series (TS) version 4.03 of high-resolution gridded data of month-by-month variation in climate (Jan. 1901-Dec. 2018). <https://doi.org/10.5285/10d3e3640f004c578403419aac167d82>
- Hauser S, Norgrove L, Asawalam D, Schulz S (2012). Effect of land use change, cropping systems and soil type on earthworm cast production in West and Central Africa. *Eur. J. Soil Biol.* 49:47-54.
- Hay WW (1998) Detrital sediment fluxes from continents to oceans. *Chemical Geology* 145:287-323.
- He, J.; Garzanti, E.; Dinis, P.; Yang, S.; and Wang, H. 2020. Provenance versus weathering control on sediment composition in tropical monsoonal climate (South China) – 1. *Geochemistry and clay mineralogy*. *Chemical Geology* 558:119860.
- Heine, K. 1978. Radiocarbon chronology of late Quaternary lakes in the Kalahari, southern Africa. *Catena*, 5, 145-149.

- Heine, K. 1982. The main stages of the late Quaternary evolution of the Kalahari region, southern Africa. *Palaeoecology of Africa and the surrounding islands*, 15, 53-76.
- Heine, K. 1992. On the ages of humid Late Quaternary phases in southern African arid areas (Namibia, Botswana). In: HEINE, K. (ed.) *Palaeoecology of Africa and the surrounding islands*. Balkema A.A., Netherlands.
- Hell, B., Broman, B., Jakobsson, L. & Jakobsson, M. 2012. The use of bathymetric data in society and science: A review from the Baltic sea. *A Journal of the Human Environment*, 41(2):138-50.
- Hellweger, F. L., Schlosser, P., Lall, U., & Weissel, J. K. 2004. Use of satellite imagery for water quality studies in New York Harbor. *Estuarine, Coastal and Shelf Science*, 61(3), 437-448.
- Herring, J.R., 1985. Charcoal fluxes into sediments of the North Pacific Ocean: The Cenozoic record of burning. In: *The carbon cycle and atmospheric CO₂: Natural variations Archean to present* (ed. E.T. Sundquist and W.S. Broecker); *Geophys. Monogr.* 32, 419-442.
- Hobo, N., Makaske, B., Middelkoop, H. and Wallinga, J., 2010. Reconstruction of floodplain sedimentation rates: a combination of methods to optimize estimates. *Earth Surface Processes and Landforms*, 35(13), pp.1499-1515. <https://onlinelibrary.wiley.com/doi/abs/10.1002/esp.1986>.
- Hodul, M., Bird, S., Knudby, A. & Chenier, R. 2018. Satellite derived photogrammetric bathymetry. *Journal of Photogrammetry and Remote Sensing*, 142: 268-277.
- Hoetzel, S., Dupont, L., Schefu?, E., Rommerskirchen, F., Wefer, G., 2013. The role of fire in Miocene to Pliocene C4 grassland and ecosystem evolution. *Nature Geoscience* 6, 1027-1030.
- Hopper E, Gaherty JB, Shillington DJ, Accardo NJ, Nyblade AA, Holtzman BK, Havlin C, Scholz CA, Chindandali PR, Ferdinand RW and Mulibo GD (2020) Preferential localized thinning of lithospheric mantle in the melt-poor Malawi Rift. *Nature Geoscience* 13(8): 584-589.
- Hosea, P. and Khalema, E., 2020. Scoping the nexus between climate change and water-security realities in rural South Africa. *Town and Regional Planning*, 77, pp.18-30.
- Howard, E., and Washington, R. 2019. Drylines in Southern Africa: Rediscovering the Congo Air Boundary. *American Meteorological Society* 32:8223-8242.
- <http://www.cru.uea.ac.uk/data>
- http://www.waterbase.org/download_data.html
- <https://aquaknow.jrc.ec.europa.eu/nepad-sanwatce>
- <https://archive.conscientiabeam.com/index.php/10/article/view/2000>
- <https://ccafs.cgiar.org/marksimgcm-weather-generating-tool>
- <https://climexp.knmi.nl>
- https://crudata.uea.ac.uk/cru/projects/betwixt/cruwg_hourly/
- <https://earthexplorer.usgs.gov/>
- <https://github.com/metno/wxgen>
- <https://hydrosheds.cr.usgs.gov/dataavail.php>
- <https://link.springer.com/article/10.1007/s10584-007-9261-4>

<https://livingatlas2.arcgis.com/LANDSATexplorer/>
<https://sentinel2explorer.esri.com/>
<https://www.ars.usda.gov/midwest-area/west-lafayette-in/national-soil-erosion-research/docs/wepp/cligen/>
<https://www.dws.gov.za/WFGD/documents/WfGDexecutivesummary.pdf> [Accessed 02/02/2022] <https://www.dws.gov.za/Hydrology/> [Accessed 07/02/2022]
<https://www.ncl.ac.uk/ceser/research/software/weather-generator/>
<https://www.tandfonline.com/doi/abs/10.1080/02571862.2003.10634936>
<https://www.usgs.gov/search?keywords=bathymetry>
<https://www.usgs.gov/search?keywords=bathymetry>
 Huang, C.C., Chang, M.J., Lin, G.F., Wu, M.C. and Wang, P.H., 2021. Real-time forecasting of suspended sediment concentrations reservoirs by the optimal integration of multiple machine learning techniques. *Journal of Hydrology: Regional Studies*, 34, p.100804.
 Hubert JF (1962) A zircon-tourmaline-rutile maturity index and the interdependence of the composition of heavy mineral assemblages with the gross composition and texture of sandstones: *Journal of Sedimentary Petrology* 32:440-450.
 Hughes, A.; Mansour, M.; Ward, R.; Kieboom, N.; Allen, S.; Seccombe, D.; Charlton, M.; Prudhomme, C. (2021). The impact of climate change on groundwater recharge: National-scale assessment for the British mainland. *J. Hydrol.*, 598, 126336.
 Hughes, DA. 2014. Incorporating groundwater recharge and discharge functions into an existing monthly rainfall-runoff model. *Hydrological Sciences*, 49(2) April 2004.
 Hughes, DA. 2014. Incorporating groundwater recharge and discharge functions into an existing monthly rainfall-runoff model. *Hydrological Sciences*, 49(2) April 2004.
 Huntsman-Mapila, P., Ringrose, S., Mackay, A. W., Downey, W. S., Modisi, M., Coetzee, S. H., Tiercelin, J. J., Kampunzu, A. B. & Vanderpost, C. 2006. Use of the geochemical and biological sedimentary record in establishing palaeo-environments and climate change in the Lake Ngami basin, NW Botswana. *Quaternary International*, 148, 51-64.
 IAEA 1992. IAEA – International Atomic Energy Agency, 1992. Statistical treatment of data on environmental isotopes in precipitation. Technical Report No. 331. Vienna. 793 pp.
 IFC 99392. 2015. Hydroelectric power: a guide for developers and investors. Fichtner, Stuttgart, Germany (www.fichtner.de).
 IHA. 2017. The 2017 Hydropower Status Report: an insight into recent hydropower development and sector trends around the world. International Hydropower Association.
 Ijam, A. Z., Al-Mahamid, M. H. (2012): Predicting Sedimentation at Mujib Dam Reservoir in Jordan – *Jordan Journal of Civil Engineering* 6(4): 448-463.
 Imbrie J, Berger A, Boyle EA, Clemens SC, Duffy A , Howard WR, Kukla G, Kutzbach J, Martinson DG, McIntyre A, Mix AC, Molfino B, Morley JJ, Peterson LC, Pisias NG, Prell WL, Raymo ME, Shackleton NJ, Toggweiler JR (1993) On the structure and origin of major glaciation cycles 2. The 100,000-year cycle', *Palaeoceanography*, vol. 8, no. 6, pp. 699-735. <https://doi.org/10.1029/93PA02751>
 InfoSA. (2020). Info SA. Retrieved August 7, 2020, from <https://www.infosa.co.za/land-and-people/orange-river/>

- Ingersoll RV, Bullard TF, Ford RL, Grimm JP, Pickle JD and Sares SW (1984) The effect of grain size on detrital modes: A test of the Gazzi-Dickinson point-counting method: *Journal of Sedimentary Petrology* 54:103-116.
- International Journal of River Basin Management, 1-D hydro-morphodynamic model
<https://www.scopus.com/record/display.uri?eid=2-s2.0-84882243902&origin=resultslist&sort=plf-f&src=s&sid=c3144c513b00cb8f20721d5d4546a0db&sot=autdocs&sdt=autdocs&sl=18&s=AU-ID%2826031638500%29&relpos=7&citeCnt=8&searchTerm=>
- International Journal on Hydropower & Dams, Water storage and Hydropower development for Africa, African Dams Project online water resources database
<https://infoscience.epfl.ch/record/209347>
<https://infoscience.epfl.ch/record/209347>
<https://lch.epfl.ch/page-7708-en.html>
- IPCC, 2001. *Climate Change 2001: The Scientific Basis, Contribution of Working Group I to the Third Assessment Report of the Intergovernmental Panel on Climate Change*. Cambridge University Press, Cambridge, United Kingdom and New York, NY, USA, Cambridge University Press, Cambridge, United Kingdom.
- IPCC, 2014. *Climate Change 2014: Impacts, Adaptation, and Vulnerability. Part A: Global and Sectoral Aspects. Contribution of Working Group II to the Fifth Assessment Report of the Intergovernmental Panel on Climate Change*. Cambridge University Press, Cambridge, United Kingdom and New York, NY, USA.
- Israil, M.; Al-Hadithi, M.; Singhal, D.C.; Kumar, B. (2006). Groundwater-recharge estimation using a surface electrical resistivity method in the Himalayan foothill region, India. *Hydrogeol. J.* 2006, 14, 44-50.
- Jackson, S.E.; Pearson, N.J.; Griffin, W.L.; and Belousova, E.A., 2004. The application of laser ablation-inductively coupled plasma-mass spectrometry to in situ U-Pb zircon geochronology. *Chem. Geol.* 211:47-69.
- Jacob, R. J., 2005. *The erosional and cenozoic depositional history of the lower Orange river, southwestern Africa*, Glasgow: University of Glasgow.
- Jacob, R.J. (2005). *The Erosional and Cainozoic Depositional History of the Lower Orange River. Southwestern Africa. Vol 1*. University of Glasgow, Division of Earth Sciences.
- Jacobs J, Pisarevsky S, Thomas RJ and Becker T (2008) The Kalahari Craton during the assembly and dispersal of Rodinia. *Precambrian Res.* 160:142-158.
- Jacobs, J. (2018). Directorate: Spatial and Land Information Management: Capacity determination of Gariep dam 2018. Report No. D350-02; Hydro No. D3R002.
- Jacobs, J.; Pisarevsky, S.; Thomas, R.J.; and Becker, T. 2008. The Kalahari Craton during the assembly and dispersal of Rodinia. *Precambrian Res.* 160:142-158.
- Jacobsen, M.P. and Winzor, D.J., 1997. Studies of ligand-mediated conformational changes in enzymes by difference sedimentation velocity in the Optima XL-A ultracentrifuge. In *Analytical Ultracentrifugation IV* (pp. 82-87). Steinkopff.
- Jankowski, J. & Jacobson, G. 1989. Hydrochemical evolution of regional groundwaters to playa brines in central Australia. *Journal of Hydrology*, 108, 123-173.

- Jawak, S., Vadlamani, S.S.M., Luis, A.J. 2015. A synoptic review on deriving bathymetry information using remote sensing technologies: Models, methods and comparisons. *Advances in Remote Sensing*, 4:147-162.
- Jelsma HA and Dirks PHGM (2002). Neoproterozoic tectonic evolution of the Zimbabwe Craton. In Fowler, C.M.R.; Ebinger, C.J.; and Hawkesworth, C.J. (eds.), *The early Earth: physical, chemical, and biological development*. Geol. Soc. London, Spec. Publ. 199:183-211.
- Jelsma, H.A.; McCourt, S.; Perritt, S.H.; and Armstrong R.A. 2018. The Geology and Evolution of the Angolan Shield, Congo Craton. In Siegesmund, S.; Basei, M.; Oyhantçal, P.; and Oriolo, S. eds. *Geology of Southwest Gondwana. Regional Geology Reviews*. Springer, Cham, pp. 217-239. https://doi.org/10.1007/978-3-319-68920-3_9.
- Jena, JAMS model
<http://jams.uni-jena.de/>
- Jennings, C. M. H. 1974. The hydrogeology of Botswana. PhD Thesis, University of Natal, Pietermaritzburg.
- Jeyakanthan, V.S., Sanjeevi, S. (2013): Capacity survey of Nagarjuna Sagar reservoir, India using Linear Mixture Model (LMM) approach – *International Journal of Geomatics and Geosciences* 4(1): 186-194.
- Jia, G., Peng, P.A., Zhao, Q., Jian, Z., 2003. Changes in terrestrial ecosystem since 30 Ma in East Asia: Stable isotope evidence from black carbon in the South China Sea. *Geology* 31, 1093-1096.
- John T, Schenk V, Haase K, Scherer E and Tembo F (2003) Evidence for a Neoproterozoic Ocean in south-central Africa from mid-ocean-ridge-type geochemical signatures and pressure temperature estimates of Zambian eclogites. *Geology* 31:243-246.
- John T, Schenk V, Mezger K and Tembo F (2004). Timing and PT evolution of white schist metamorphism in the Lufilian Arc-Zambezi Belt orogen (Zambia): Implications for the assembly of Gondwana. *The Journal of Geology* 112(1):71-90.
- John, T.; Schenk, V.; Mezger, K.; and Tembo, F. 2004. Timing and PT evolution of white schist metamorphism in the Lufilian Arc-Zambezi Belt orogen (Zambia): implications for the assembly of Gondwana. *J. Geol.* 112(1):71-90.
- Johnson MR, Van Vuuren CJ, Hegenberger WF, Key R and Show U (1996) Stratigraphy of the Karoo Supergroup in southern Africa: an overview. *Journal of African Earth Sciences* 23(1):3-15.
- Johnson, M.R. 1991. Sandstone petrography, provenance and plate tectonic setting in Gondwana context of the southeastern Cape-Karoo Basin. *South African Journal of Geology* 94:137-154.
- Johnson, M.R.; Van Vuuren, C J.; Hegenberger, W.F.; Key, R.; and Show, U. 1996. Stratigraphy of the Karoo Supergroup in southern Africa: an overview. *J. Afr. Earth Sci.* 23(1):3-15.
- Johnson, T. C., Scholz, C. A., Talbot, M. R., Kelts, K., Ricketts, R., Ngobi, G., Beuning, K., Semmanda, I. & McGill, J. 1996. Late Pleistocene desiccation of Lake Victoria and rapid evolution of cichlid fishes. *Science*, 273, 1091-1093.

- Johnsson, M.J. 1993. The system controlling the composition of clastic sediments. In Johnsson, M.J., and Basu, A. eds. *Processes Controlling the Composition of Clastic Sediments*. Geological Society of America, Special Paper 284:1-19.
- Johnston, R. & Smakhtin, V. 2014. Hydrological Modeling of Large river Basins: How Much is Enough? *Water Resources Management*, 28:2695-2730.
- Jones, B. F., Eugster, H. P. & Rettig, S. L. 1977. Hydrochemistry of the Lake Magadi basin, Kenya. *Geochimica et Cosmochimica Acta*, 41, 53-72.
- Jordaan, J M. (1989). The sediment problem in South African reservoirs. *Proceedings of the International Symposium on Sediment Transport Modelling, USA*.
- Jørgenson, S.E., Löffler, H., Rast, W., Straskraba, M. (2005): *Lake and reservoir management* (1st ed.) – Boston, MA: Elsevier Science.
- Jothiprakash, V. and Garg, V., 2009. Reservoir sedimentation estimation using artificial neural network. *Journal of Hydrologic Engineering*, 14(9), pp.1035-1040. [https://ascelibrary.org/doi/abs/10.1061/\(ASCE\)HE.1943-5584.0000075](https://ascelibrary.org/doi/abs/10.1061/(ASCE)HE.1943-5584.0000075)
- Jouet G and Deville E (2015) PAMELA-MOZ04 Cruise, RV Pourquoi pas, doi.org/10.17600/15000700.
- Jourdan F, Féraud G, Bertrand H, Kampunzu AB, Tshoso G, Watkeys MK and Le Gall B (2005). Karoo large igneous province: Brevity, 1033 origin, and relation to mass extinction questioned by new $40\text{Ar}/39\text{Ar}$ age data. *Geology* 33(9):745-748.
- Jourdan, F., Féraud, G., Bertrand, H., Kampunzu, A. B., Tshoso, G., Le Gall, B., Tiercelin, J. J. & Capiez, P. 2004. The Karoo triple junction questioned: evidence from Jurassic and Proterozoic $40\text{Ar}/39\text{Ar}$ ages and geochemistry of the giant Okavango dyke swarm (Botswana). *Earth and Planetary Science Letters*, 222, 989-1006.
- Joyce, D. A., Lunt, D. H., Bills, R., Turner, G. F., Katongo, C., Duftner, N., Sturmbauer, C. & Seehausen, O. 2005. An extant cichlid fish radiation emerged in an extinct Pleistocene lake. *Nature*, 435, 90-95.
- Juízo, D. & Lidén, R. 2010. Modeling for transboundary water resources planning and allocation: the case of Southern Africa. *Hydrological Earth Systems Science*, 14:2343-2354.
- Jury, M. 2010. Climate and weather factors modulating river flows in southern Angola. *Int. J. Climatol.* 30:901-908.
- Just, J.; Schefuß, E.; Kuhlmann, H.; Stuut, J.B.W.; and Pätzold, J. 2014. Climate induced sub-basin source-area shifts of Zambezi River sediments over the past 17 ka. *Palaeogeography, Palaeoclimatology, Palaeoecology* 410:190-199.
- Kafri, U. & Yechieli, Y. 2010. Salinity, Salination and Freshening of the Different Base-Levels and Their Adjoining Groundwater Systems. *Groundwater Base Level Changes and Adjoining Hydrological Systems*. Springer Berlin Heidelberg.
- Kahle, M.; Kleber, M.; and Jahn, R. 2002. Review of XRD-based quantitative analyses of clay minerals in soils: the suitability of mineral intensity factors. *Geoderma* 109:191-205.
- Kampunzu AB and Cailteux J (1999) Tectonic evolution of the Lufilian Arc (Central Africa Copper Belt) during Neoproterozoic Pan African orogenesis. *Gondwana Research* 2(3):401-421.

- Kamtukule, S.L. and Kaseke, E., 2012. The Challenge of Small Reservoir Sedimentation to Water Resources Development: The Case of Multi-Purpose Chamakala II Small Earth Reservoir in Malawi. p. 19-50.
- Kariba Reservoir: Experience and lessons learned. December 2006.
- Kaseke, E (2016). Zambezi basin strategic planning in the context of a changing climate overview. Accessed online on 24 January 2019. https://unfccc.int/sites/default/files/20160525_evans_kaseke.pdf.
- Kasvi, E.S., Salmela, J., Kumpula, T. & Lane, S.N. 2019. Comparison of remote sensing based approaches for mapping bathymetry of shallow, clear water rivers. *Geomorphology*, 333: 180-197.
- Katharine Vincent, K. Vincent, Tracy Cull, T. Cull, Diana Chanika, D. Chanika, Petan Hamazakaza, P. Hamazakaza, Alec Joubert, A. Joubert, Eulalia Macome, E. Macome, & Charity Mutonhodza-Davies, C. Mutonhodza-Davies., 2013. Farmers' responses to climate variability and change in southern Africa – is it coping or adaptation? *Climate and development*, 5, 194-205. <https://www.tandfonline.com/doi/abs/10.1080/17565529.2013.821052>
- Keeley, J.E., Rundel, P.W., 2005. Fire and the Miocene expansion of C4 grasslands. *Ecology Letters* 8, 683-690.
- Kendall JM and Lithgow-Bertelloni C (2016) why is Africa rifting? In: Wright, T.J., Ayele, A., Ferguson, D.J., Kidane, T., Vye-Brown, C. (eds.), *Magmatic Rifting and Active Volcanism Geological Society, London, Special Publications 420:11-30*, doi.org/10.1144/SP420.17.
- Key RM, Cotterill FPD and Moore AE (2015). The Zambezi River: An archive of tectonic events linked to the amalgamation and disruption of Gondwana and subsequent evolution of the African Plate. *South African Journal of Geology* 118(4):425-438.
- Kgotlhang, L. 2008. Application of airborne geophysics in large scale integrated hydrological modelling. Case study: Okavango delta, Botswana. PhD thesis, ETH ZURICH.
- Kinabo BD, Atakwana EA, Hogan JP, Modisi MP, Wheaton DD and Kampunzu AB (2007) Early structural development of the Okavango rift zone, NW Botswana. *Journal of African Earth Sciences* 48:125-136.
- Kinabo, B., Hogan, J., Atekwana, E., Abdelsalam, M. & Modisi, M. 2008. Fault growth and propagation during incipient continental rifting: Insights from a combined aeromagnetic and Shuttle Radar Topography Mission digital elevation model investigation of the Okavango Rift Zone, northwest Botswana. *Tectonics*, 27.
- Kirchhoff, J.W.C. 2008. Sustainable Water Management in the Zambezi River Basin. The Journal of the international institute,
- Klimke J, Franke D, Gaedicke C, Schreckenberger B, Schnabel M, Stollhofen H, Rose J and Chaheire M (2016) How to identify oceanic crust – Evidence for a complex break-up in the Mozambique Channel, off East Africa *Tectonophysics* 693:436-452.
- Kling, Harald, Philipp Stanzel, and Martin Preishuber, 2014. "Impact modelling of water resources development and climate scenarios on Zambezi River discharge." *Journal of Hydrology: Regional Studies* 1 (2014): 17-43.

- Klinger, J., Goldscheider, N. and Hoetzi, H. eds., 2015. SMART-IWRM-Sustainable Management of Available Water Resources with Innovative Technologies-Integrated Water Resources Management in the Lower Jordan Rift Valley: Final Report Phase II (Vol. 7698). KIT Scientific Publishing.
- Klock, H. 2001. Hydrogeology of the Kalahari in North-eastern Namibia: With Special Emphasis on Groundwater Recharge, Flow Modelling and Hydrochemistry. Selbstverlag Lehr-und Forschungsbereich Hydrogeologie.
- Knight J and Grab SW (2018) The geomorphic evolution of southern Africa during the Cenozoic. In: Holmes, P.J., Boardman, J. (eds.), Southern African Landscapes and Environmental Change. Routledge, ch.2, pp. 6-28.
- Kokonyangi JW, Kampunzu AB, Armstrong R, Yoshida M, Okudaira T, Arima M and Ngulube DA (2006) The Mesoproterozoic Kibariide belt (Katanga, SE DR Congo). *Journal of African Earth Sciences* 46(1-2):1-35.
- Kolla V, Kostecki JA, Henderson L and Hess L (1980) Morphology and Quaternary sedimentation of the Mozambique Fan and environs, southwestern Indian Oceans. *Sedimentology* 27:357-378.
- Kondolf, G. M., & Farahani, A. (2018). Sustainably managing reservoir storage: Ancient roots of a modern challenge. *Water*, 10(2), 117.
- Kondolf, G.M., 1997. Hungry Water: Effects of Reservoirs and Gravel Mining on River Channels. *Environmental Management* Vol. 21. p. 533-551.
- Kondolf, G.M., Gao, Y., Annandale, G.W., Morris, G.L., Jiang, E., Zhang, J., Cao, Y., Carling, P., Fu, K., Guo, Q. and Hotchkiss, R., 2014. Sustainable sediment management in reservoirs and regulated rivers: Experiences from five continents. *Earth's Future*, 2(5), pp.256-280.
- König M and Jokat W (2010) Advanced insights into magmatism and volcanism of the Mozambique Ridge and Mozambique Basin in the view of new potential field data. *Geophysical Journal International* 180(1):158-180.
- Kornienko, S. G. (2017). Analysis of errors in estimating changes in water body areas by satellite data: Case study of thermokarst lakes in Yamal Peninsula. *Water Resources*, 44(2), 180-192.
- Kottek M, Grieser J, Beck C, Rudolf B and Rubel F (2006) World map of the Köppen-Geiger climate classification updated. *Meteorologische Zeitschrift* 15:259-263.
- Kriel, J. P. (1972). The role of the Hendrik Verwoerd Dam in the Orange River Project. *Civil Engineering= Siviele Ingenieurswese*, 1972(2), 51-61.
- Krynine PD (1948) The megascopic study and field classification 1063 of sedimentary rocks. *The Journal of Geology* 56:130-165.
- Kulongoski, J. T., Hilton, D. R. & Selaolo, E. T. 2004. Climate variability in the Botswana Kalahari from the late Pleistocene to the present day. *Geophysical Research Letters*, 31.
- Kumar, A, Schei, T., Ahenkorah, A., Caceres, C., J. and Devernay Rodriguez, M., Freitas, M., Hall, D., Killingtveit, Å., and Liu, Z. 2011. IPCC Special Report on Renewable Energy Sources and Climate Change Mitigation – Chapter 5 Hydropower 2011: Hydropower. In IPCC Special Report on Renewable Energy Sources and Climate Change Mitigation [O. Edenhofer, R. Pichs-Madruga, Y. Sokona, K. Seyboth, P. Matschoss, S. Kadner, T.

- Zwickel, P. Eickemeier, G. Hansen, S. Schlömer, C. von Stechow (eds)], Cambridge University Press, Cambridge, United Kingdom and New York, NY, USA. Technical report, Intergovernmental Panel on Climate Change, WMO, UNEP.
- Kunz, M.J.; Anselmetti, F.S.; Wüest, A.; Wehrli, B.; Vollenweider, A.; Thüring, S.; and Senn, D.B. 2011. Sediment accumulation and carbon, nitrogen, and phosphorus deposition in the large tropical reservoir Lake Kariba (Zambia/Zimbabwe). *Journal of Geophysical Research: Biogeosciences* 116(G3): G03003, doi:10.1029/2010JG001538.
- Kusangaya, S., Warburton, M.L., Van Garderen, E.A. and Jewitt, G.P., 2014. Impacts of climate change on water resources in southern Africa: A review. *Physics and Chemistry of the Earth, Parts A/B/C*, 67, pp.47-54. <https://www.sciencedirect.com/science/article/pii/S147470651300140X>
- Kusky, T.M. 1998. Tectonic setting and terrane accretion of the Archean Zimbabwe craton. *Geology* 26:163-166.
- Kusre, B.C., Baruah, D.C., Bordoloi, P.K. & Patra, S.C. 2010. Assessment of hydropower potential using GIS and hydrological modelling technique in Kopili River basin in Assam (India). *Applied Energy*, 87:298-309.
- Lancaster, I. N. 1979. Evidence for a widespread Late Pleistocene humid period in the Kalahari. *Nature*, 279, 145-146.
- Lancaster, N. 1989. Late Quaternary paleoenvironments in the southwestern Kalahari. *Palaeogeography, Palaeoclimatology, Palaeoecology*, 70, 367-376.
- Lanci, L.; Tohver, E.; Wilson, A.; and Flint, S. 2013. Upper Permian magnetic stratigraphy of the lower Beaufort group, Karoo basin. *Earth and Planetary Science Letters* 375:123-134.
- LANDSAT explorer
- Langbein, W.B. and Schumm, S.A., 1958. Yield of Sediment in Relation to Mean Annual Precipitation. *Transaction of American Geophysical Union*. Vol. 39. No. 6. p. 1076-1080.
- Lange, G. M., Mungatana, E., & Hassan, R. (2007). Water accounting for the Orange River Basin: An economic perspective on managing a transboundary resource. *Ecological Economics*, 61(4), 660-670. <https://doi.org/10.1016/j.ecolecon.2006.07.032>
- Lange, G., Hassan, R., (2006). *The Economics of Water Management in Southern Africa: An Environmental Accounting Approach*. Edward Elgar, Cheltenham, UK.
- Lange, G., Mungatana, E., and Hassan, R. 2006. Water accounting for the Orange River Basin: An economic perspective on managing a transboundary resource. *Ecological economics*, 61 (2007) 660-670.
- Langer, T. & Heusser, D. 2004. *Geochemical Groundwater Evolution and Age Estimations for Islands in the Okavango Delta*. Department of Environmental Sciences. MSc Thesis, Swiss Federal Institute of Technology (ETH), Zürich.
- Larentis, D.G., Collischonn, W., Olivera, F. & Tucci, C.E.M. 2010. Gis-based procedures for hydropower potential spotting. *Energy*, 35:4237-4243.
- Last, W. M. 1989. Sedimentology of a saline playa in the northern Great Plains, Canada. *Sedimentology*, 36, 109-123.

- Lawlor, D.W., 1993. Photosynthesis: Molecular, physiological and environmental processes. Longman Scientific & Technical.
- Le Gall, B., Tshoso, G., Jourdan, F., Féraud, G., Bertrand, H., Tiercelin, J. J., Kampunzu, A. B., Modisi, M. P., Dymont, J. & Maia, M. 2002. $^{40}\text{Ar}/^{39}\text{Ar}$ geochronology and structural data from the giant Okavango and related mafic dyke swarms, Karoo igneous province, northern Botswana. *Earth and Planetary Science Letters*, 202, 595-606.
- Le Roux, P.A.L., Ellis, F., Merryweather, F.R., Schoeman, J.L., Snyman, K., Van Deventer, P.W., Verster, E., 1999. Riglyne vir kartering en interpretasie van die gronde van Suid-Afrika. Universiteit van die Vrystaat. (<http://www.uovs.ac.za/faculties/documents/04/116/Publications/Dr%20Pieter%20Le%20Roux/Volume1.pdf> accessed on 17 July 2009).
- Le, H., Ngoc, T. and Hens, L., 2015. Assessment of the Irrigation Capacity during the Dry Season Using Remote Sensing and Geographical Information (Case Study in the Binh Thuan Province, Vietnam). *International Journal of Geosciences*, 06(11), pp.1214-1220.
- Lee, H., Goodman, A., McGibbney, L., Waliser, D.E., Kim, J., Loikith, P.C., Gibson, P.B., Massoud, E.C., 2018. Regional Climate Model Evaluation System powered by Apache Open Climate Workbench v1.3.0: an enabling tool for facilitating regional climate studies. *Geosci. Model Dev.* 11, 4435-4449. <https://doi.org/10.5194/gmd-11-4435-2018>
- Leenaers, H., 1991. Estimating the Impact of Land Use Change on Soil Erosion Hazard in the Zambezi River Basin. International Institute for Applied Systems Analysis, Working paper WP-90-024.
- Legleiter, C.J & Fosness, R.L. 2019. Defining the limits of spectrally based bathymetric mapping on a large river. *Remote Sensing*, 11(6):665.
- Legleiter, C.J. & Harrison, L.R. 2018. Remote sensing of river bathymetry: Evaluating a range of sensors, platforms, and algorithms on the upper Sacramento River, California, USA. *Water Resources Research*, 55(3): 2142-2169. doi: 10.1029/2018WR023586
- Lehner, B., Liermann, C. R., Revenga, C., Vörösmarty, C., Fekete, B., Crouzet, P., Döll, P., Endejan, M., Frenken, K., Magome, J., Nilsson, C., Robertson, J. C., Rödel, R., Sindorf, N., and Wissler, D., 2011. High-resolution mapping of the world's reservoirs and dams for sustainable river-flow management. *Frontiers in Ecology and the Environment* 9, 494-502.
- Leopold, L.B., Wolman, M.G. and Miller, J.P., 1995. *Fluvial Processes in Geomorphology*. 4th Edition. New York: Dover Publication.
- Li, R. and Li, J., 2004. Satellite remote sensing technology for lake water clarity monitoring: an overview. *Environmental Informatics Archives*, 2, pp.893-901.
- Liechti Cohen, Theodora, *et al.* "Hydrological modelling of the Zambezi River Basin taking into account floodplain behaviour by a modified reservoir approach." *International Journal of River Basin Management* 12.1 (2014): 29-41.
- Linn, F., Masie, M. & Rana, A. 2003. The impacts on groundwater development on shallow aquifers in the lower Okavango Delta, northwestern Botswana. *Environmental Geology*, 44, 112-118.

- Lisiecki, LE, and Raymo ME (2007) Plio-Pleistocene climate evolution: ... transitions in glacial cycle dynamics, *Quaternary Science Reviews*, 26, 56-69. 22.
- Lithgow-Bertelloni C and Silver PG (1998) Dynamic topography, plate driving forces and the African superswell. *Nature* 395(6699):269-272.
- Liu, X. (2008). Airborne LiDAR for DEM generation: some critical issues. *Progress in Physical Geography*, 32(1), 31-49.
- Livingstone, D. A. 1857. Livingstone, D. A., 1857. *Missionary travels and researches in South Africa*. Salzwasser Verlag, Bremen, 2010 (reprint of original).
- Long S, Fatoyinbo T, and Policelli F (2014) Flood extent mapping for Namibia using change detection and thresholding with SAR, *Environ. Res. Lett.*, 9, 035002, doi:10.1088/1748-9326/9/3/035002.
- Loveland, T., Brown, J., Ohlen, D., Reed, B., Zhu, Z., Yang, L., Howard, S., Hall, F., Collatz, G., Meeson, B., 2009. ISLSCP II IGBP DISCover and SiB land cover, 1992-1993. ORNL DAAC.
- Lu, J., Algeo, T.J., Zhuang, G., Yang, J., Xiao, G., Liu, J., Huang, J., Xie, S., 2020. The early Pliocene global expansion of C4 grasslands: A new organic carbon-isotopic dataset from the north China plain. *Palaeogeography, Palaeoclimatology, Palaeoecology* 538, 109454.
- Lu, J.Y. and Huang, Y., 2013. Comparison of Sedimentation in Three Gorges Reservoir between Calculated Prediction and Prototype Measurement. *Journal of Yangtze River Scientific Research Institute*, 30(12), p.1. <http://ckyyb.crsri.cn/EN/abstract/abstract2323.shtml>
- Lu, X.X, Ran, L. Liu, S. S. Jiang, T. Zhang, S. R. and Wang, J. J., 2013. Sediment Loads Response to Climate Change: A Preliminary Study of Eight Large Chinese Rivers. *International Journal of Sediment Research*. Vol. 28. p.1-14.
- Ludwig, K.R. 1998. On the treatment of concordant uranium-lead ages. *Geochimica et Cosmochimica Acta* 62(4):665-676.
- Lund Schlamovitz, J. and Becker, P., 2021. Differentiated vulnerabilities and capacities for adaptation to water shortage in Gaborone, Botswana. *International Journal of Water Resources Development*, 37(2), pp.278-299.
- Lustenberger, F. (2010). *The Problem of Water in Southern Africa and in Particular the Management of Water in South Africa*. Retrieved from http://www2.agroparistech.fr/IMG/pdf/Lustenberger_en_sr.pdf
- Lutjeharms, J., 2006. *The Agulhas Current*. Springer-Verlag. Berlin, Germany.
- Lyons R.P., Scholz C.A, Cohen A.S, King J.W, Brown E.T., Ivory S.J, Johnson T.C, Deino A.L, Reinthal P.N, McGlue M.M, Blome M.W. (2015). Continuous 1.3-million-year record of East African hydroclimate, and implications for patterns of evolution and biodiversity. *Proc. Natl. Acad. Sci. USA* 112:15568-15573.
- Maas, H.G., Mader, D., Richter, K. & Westfeld, 2019. Improvements in lidar bathymetry data analysis. *The International Archives of the Photogrammetry, Remote Sensing and Spatial Information Sciences*, 42:113-117.
- MacDonald, E.M., 2007. Rapid assessment – final report. SADC-WD/Zambezi River authority, SIDA, DANIDA, Norwegian Embassy Lusaka.

- Macgregor D (2018) History of the development of Permian-Cretaceous rifts in East Africa: a series of interpreted maps through time. Thematic set: Tectonics and petroleum systems of East Africa. Geological Society London, Petroleum Geoscience 24:8-20, doi/10.1144/petgeo2016-155.
- Macgregor DS (2018) Introduction to the thematic set, Tectonics and Petroleum systems of East Africa, Petroleum Geoscience, Volume 24, Issue 1, p. 8-20.
- Mäkel, R., 1974. Dambos: A study in morphodynamic activity on the plateau regions of Zambia. *Catena*, 1, 327-365.
- Magilligan, F.J.T. & Nislow, K.H. 2005. Changes in hydrologic regime by dams. *Geomorphology*, 71:61-78
- Magomedze, L. M., Frengstad, B. & Lubczynski, M. W. 2004. Spatial variation of groundwater recharge in a semi-arid environment: Serowe, Botswana. In: STEPHENSON, D., SHEMANG, E. M. & CHAOKA, T. R. (eds.) Water resources of arid areas: proceedings of the international conference on water resources of arid and semi-arid regions of Africa WRASRA, August 3-6th, 2004, Gaborone, Botswana. Rotterdam: Balkema.
- Main M (1990) Zambezi. Journey of a river. Southern Book Publishers, Halfway Housem, South Africa, 313 p.
- Majaule T, Hanson RE, Key RM, Singletary SJ, Martin MW and Bowring SA (2001) The Magondi Belt in northeast Botswana: regional relations and new geochronological data from the Sua Pan area. *Journal of African Earth Sciences* 32:257-267.
- Malusà MG, Resentini A and Garzanti E (2016) Hydraulic sorting and mineral fertility bias in detrital geochronology. *Gondwana Research* 31:1-19.
- Mama, C., & Okafor, F.O. (2011). Siltation in Reservoirs. *Nigerian Journal of Technology*, 30, 85-90.
- Mander, M., Mander, M., Haines, C., & McKenzie, M. (2005). Orange River Basin – Baseline Assessment Report. <https://doi.org/10.13140/RG.2.1.1272.2724>
- Manninen T, Eerola T, Makitie H, Vuori S, Luttinen A, Sévanno A and Manhiça V (2008) The Karoo volcanic rocks and related intrusions in southern and central Mozambique. *Geol. Surv. Finland, Special Paper* 48:211-250.
- Manus, L. (2021). Increasing dam storage capacity through the NatSilt Programme. *Water & Sanitation*, 16(4), 18-20.
- Margane, A., Baeumle, R., Schildknecht, F. & Wierenga, A. 2005. Groundwater investigation in the Eastern Caprivi Region – Main Hydrogeological Report. Department of Water Affairs (Namibia) and Federal Institute of Geosciences and Natural Resources (Hannover).
- Maselli V, Kroon D, Iacopini D, Wade BS, Pearson PN and de Haas H (2019) Impact of the East African Rift System on the routing of the deep-water drainage network offshore Tanzania, western Indian Ocean. *Basin Research*, doi: 10.1111/bre.12398.
- Master S, Bekker A and Hofmann A (2010) A review of the stratigraphy and geological setting of the Palaeoproterozoic Magondi Supergroup, Zimbabwe-Type locality for the Lomagundi carbon isotope excursion. *Precambrian Research* 182(4):254-273.

- Matondo JI and Mortensen, P. (1998) Water Resource Assessment for the Zambezi River Basin, *Water International*, 23:4, 256-262, DOI: 10.1080/02508069808686780. Published online: 22 Jan 2009.
- Mavhura, E, Manyena, SB, Collins, AE & Manatsa, D., 2013, 'Indigenous Knowledge and Resilience to floods in Muzarabani, Zimbabwe,' *International Journal of Disaster Risk Reduction*, vol. 5. <https://www.sciencedirect.com/science/article/pii/S2212420913000368>
- Mavima, G. A., Soropa, G., Makurira, H. and Dzvairo, W., 2015. Sedimentation Impacts on Reservoir as a Result of Land Use on a Selected Catchment in Zimbabwe. *International Journal of Engineering Science and Technology*. Vol. 3. p. 6599-6608.
- Maystadt, J.F., Calderone, M. and You, L., 2014. Local warming and violent conflict in North and South Sudan. *Journal of Economic Geography*, 15(3), pp.649-671.
- Mazor, E. 1982. Rain recharge in the Kalahari – A note on some approaches to the problem. *Journal of Hydrology*, 55, 137-144.
- Mazor, E., Bielsky, M., Verhagen, B. T., Sellschop, J. P. F., Hutton, L. & Jones, M. T. 1980. Chemical composition of groundwaters in the vast Kalahari flatland. *Journal of Hydrology*, 48, 147-165.
- Mazor, E., Verhagen, B. T. & Sellschop, J. P. F. 1974. Kalahari groundwaters: Their hydrogen, carbon and oxygen isotopes. *Isotope techniques in groundwater hydrology*, IAEA, Vienna.
- Mazor, E., Verhagen, B. T., Sellschop, J. P. F., Jones, M. T., Robins, N. E., Hutton, L. & Jennings, C. M. H. 1977. Northern Kalahari groundwaters – hydrologic, isotopic and chemical studies at Orapa, Botswana. *Journal of Hydrology*, 34, 203-234.
- McCarthy, T. & Ellery, W. 1998. The Okavango Delta. *Transactions of the Royal Society of South Africa*, 53, 157-182.
- McCarthy, T. 2006. Groundwater in the wetlands of the Okavango Delta, Botswana, and its contribution to the structure and function of the ecosystem. *Journal of Hydrology*, 320, 264-282.
- McCarthy, T. 2013. The Okavango Delta and its place in the geomorphological evolution of southern Africa. *South African Journal of Geology*, 116, 1-54.
- McCarthy, T. S. & Ellery, W. N. 1994. The effect of vegetation on soil and ground-water chemistry and hydrology of islands in the seasonal swamps of the Okavango-fan, Botswana. *Journal of Hydrology*, 154, 169-193.
- McCarthy, T. S. & Metcalfe, J. 1990. Chemical sedimentation in the semi-arid environment of the Okavango Delta, Botswana. *Chemical Geology*, 89, 157-178.
- McCarthy, T. S. 1992. Physical and biological processes controlling the Okavango Delta : a review of recent research. *Botswana Notes and Records* 24, 57-86.
- McCarthy, T. S., Humphries, M. S., Mahomed, I., Le Roux, P. & Verhagen, B. T. 2012. Island forming processes in the Okavango Delta, Botswana. *Geomorphology*, 179, 249-257.
- McCarthy, T. S., McIver, J. R. & Cairncross, B. 1986. Carbonate accumulation on islands in the Okavango Delta, Botswana. *South African Journal of Science*, 82, 588-591.

- McCarthy, T. S., McIver, J. R. & Verhagen, B. T. 1991. Groundwater evolution, chemical sedimentation and carbonate brine formation on an island in the Okavango Delta swamp, Botswana. *Applied Geochemistry*, 6, 577-595.
- McCarthy, T., Bloem, A. & Larkin, P. 1998. Observations on the hydrology and geohydrology of the Okavango Delta. *South African Journal of Geology*, 101, 101-117.
- McCarthy, T., Ellery, W. & Ellery, K. 1993. Vegetation-induced, subsurface precipitation of carbonate as an aggradational process in the permanent swamps of the Okavango (delta) fan, Botswana. *Chemical Geology*, 107, 111-131.
- McCarthy, T.S.; Humphries, M.S.; Mahomed, I.; Le Roux, P.; and Verhagen, B.T. 2012. Island forming processes in the Okavango Delta, Botswana. *Geomorphology* 179:249-257.
- McCarthy, T.S.; Smith, N.D.; Ellery, W.N.; and Gumbricht, T. 2002. The Okavango Delta-semiarid alluvial-fan sedimentation related to incipient rifting. In Renaut, R.E.; and Ashley, G.M., eds. *Sedimentation in Continental Rifts*. SEPM Society for Sedimentary Geology, Special Publication 73:179-194.
- McCourt, S.; Armstrong, R.A.; Jelsma, H.; and Mapeo, R.B.M. 2013. New U-Pb SHRIMP ages from the Lubango region, SW Angola: insights into the Palaeoproterozoic evolution of the Angolan Shield, southern Congo Craton, Africa. *Journal of the Geological Society* 170(2):353-363.
- McFarlane, M. & Eckardt, F. 2006. Lake Deception: a new Makgadikgadi palaeolake. *Botswana notes and records*, 195-201.
- McFarlane, M.J.; Eckardt, F.D.; Coetzee, S.H.; and Ringrose, S. 2010. An African surface weathering profile in the Kalahari of North West Ngamiland, Botswana: processes and products. *Zeitschrift für Geomorphologie* 54(3):273-303.
- McKay, M.P.; Coble, M.A.; Hessler, A.M.; Weislogel, A.L.; and Fildani, A. 2016. Petrogenesis and provenance of distal volcanic tuffs from the Permian-Triassic Karoo Basin, South Africa: A window into a dissected magmatic province. *Geosphere* 12(1):1-14.
- McLennan, S.M.; Hemming, S.; McDaniel, D.K.; and Hanson, G.N. 1993. Geochemical approaches to sedimentation, provenance, and tectonics. In Johnsson, M.J., and Basu, A. eds. *Processes Controlling the Composition of Clastic Sediments*. Geological Society of America, Special Paper 284:21-21.
- McQueen, A. D., & Suedel, B. C. (2018). Estimating turbidity near a dredge operation using a weather balloon-mounted camera. *Western Dredging Association Dredging Summit & Expo '18*.
- Meade, R.H. *Setting: Geology, Hydrology, Sediments, and Engineering of the Mississippi River*. Available online: <https://pubs.usgs.gov/circ/circ1133/geosetting.html>
- Meier, P., Kalscheuer, T., Podgorski, J. E., Kgotlhang, L., Green, A. G., Greenhalgh, S., Rabenstein, L., Doetsch, J., Kinzelbach, W. & Auken, E. 2014. Hydrogeophysical investigations in the western and north-central Okavango Delta (Botswana) based on helicopter and ground-based transient electromagnetic data and electrical resistance tomography. *Geophysics*, 79, B201-B211.
- Meier, Philipp, Andreas Frömelt, and Wolfgang Kinzelbach. "Hydrological real-time modelling in the Zambezi river basin using satellite-based soil moisture and rainfall data." *Hydrology and Earth System Sciences* 15.3 (2011): 999-1008.

- Merritt *et al.* (2003), providing a detailed overview of erosion and sediment transport models, many of which are relevant to reservoirs.
- Merritt, W.S., Letcher, R.A. & Jakeman, A.J. 2003. A review of erosion and sediment transport models. *Environmental Modelling and Software*, 18:761-799.
- Meyer, P.S., 2003. An Explanation of the 1: 500 000 General Hydrogeological Map: Bloemfontein 2924. Directorate Geohydrology, Department of Water Affairs and Forestry.
- Miao, Y., Fang, X., Song, C., Yan, X., Zhang, P., Meng, Q., Li, F., Wu, F., Yang, S., Kang, S., 2016. Late Cenozoic fire enhancement response to aridification in mid-latitude Asia: Evidence from microcharcoal records. *Quaternary Science Reviews* 139, 53-66.
- Miao, Y., Wu, F., Warny, S., Fang, X., Shi, P., 2019. Miocene fire intensification linked to continuous aridification on the Tibetan Plateau. *Geology* 47.
- Miller, R. L., & McKee, B. A. (2004). Using MODIS Terra 250 m imagery to map concentrations of total suspended matter in coastal waters. *Remote sensing of Environment*, 93(1-2), 259-266.
- Milliman, J.D., and Farnsworth, K.L. 2011. River discharge to the coastal ocean: a global synthesis. Cambridge University Press, Cambridge (UK), 384 p.
- Milliman, J.D., and Meade, R.H. 1983. World-wide delivery of river sediment to the oceans. *The Journal of Geology* 91(1):1-21.
- Milzow, C., Kgotlhang, L., Bauer-Gottwein, P., Meier, P. & Kinzelbach, W. 2009. Regional review: the hydrology of the Okavango Delta, Botswana – processes, data and modelling. *Hydrogeology Journal*, 17, 1297-1328.
- Ministry of Water Development and Sanitation, 2022. Rapid Assessment Report for the Magoye River. Lusaka: MWDS.
- Miramontes E, Jouet G, Thereau E, Bruno M, Penven P, Guerin C, Le Roy P, Droz L and Jorry SJ, Hernández-Molina FJ, Thiéblemont A, Silva Jacinto R, Cattaneo A (2020) The impact of internal waves on upper continental slopes: Insights from the Mozambican margin (southwest Indian Ocean). *Earth Surface Processes and Landforms*, 10.1002/esp.4818.
- Modisi MP, Atekwana EA, Kampunzu AB and Ngwisanyi TH (2000) Rift kinematics during the incipient stages of continental extension: Evidence 1093 from the nascent Okavango rift basin, northwest Botswana. *Geology* 28:939-942.
- Mojid, M.A.; Parvez, M.F.; Mainuddin, M.; Hodgson, G. (2019). Water Table Trend – A Sustainability Status of Groundwater Development in North-West Bangladesh. *Water* 2019, 11, 1182.
- Monde H. & Muchanga, M. " Social Perspectives on the Effects of Buffer Zone Anthropogenic Activities on Mashili Reservoir of Shibuyunji District, Central Province, Zambia” *International Journal of Humanities Social Sciences and Education (IJHSSE)*, vol 8, no. 11, 2021, pp. 102-109. doi: <https://doi.org/10.20431/2349-0381.0811002>.
- Moore A, Blenkinsop T and Cotterill FPD (2009b). Southern African topography and erosion history: plumes or plate tectonics? *Terra Nova* 21:310-315.

- Moore AE and Blenkinsop T (2002) The role of mantle plumes in the development of continental scale drainage patterns: The southern African example revisited. *South African Journal of Geology* 105:353-360.
- Moore AE and Dingle RV (1998) Evidence for fluvial sediment transport of Kalahari sands in central Botswana. *S. Afr. J. Geol.* 101:143-153.
- Moore AE and Larkin PA (2001) Drainage evolution in south-central Africa since the breakup of Gondwana. *South African Journal of Geology* 104:47-68.
- Moore AE, Cotterill FPD, Broderick TG and Plowes D (2009a) Landscape evolution in Zimbabwe from the Permian to present, with implications for kimberlite prospecting. *South African Journal of Geology* 112:65-86.
- Moore AE, Cotterill FPD, Main MPL and Williams HB (2007) The Zambezi River. In: Gupta, A. (ed.), *Large Rivers: Geomorphology and Management*. Wiley, Chichester, pp. 311-332.
- Moore, A. 1999. A reappraisal of epeirogenic flexure axes in southern Africa. *South African Journal of Geology*, 102, 363-376.
- Moore, A. E., Cotterill, F. P. D. & Eckardt, F. D. 2012. The evolution and ages of Makgadikgadi palaeo-lakes: consilient evidence from Kalahari drainage evolution. *South African Journal of Geology*.
- Moore, A.E.; Cotterill, F.P.D.; and Eckardt, F.D. 2012. The evolution and ages of Makgadikgadi palaeo-lakes: consilient evidence from Kalahari drainage evolution south-central Africa. *South African Journal of Geology* 115(3):385-413.
- Moore, D.M., and Reynolds, R.C. 1997. *X-ray Diffraction and the Identification and Analysis of Clay Minerals*. Oxford University Press, Oxford.
- Morant, P. D. (2017). ORANGE RIVER COMPONENT OF MARINE DIAMOND MINING LICENCE 554 MRC ENVIRONMENTAL DESCRIPTION AND ESTUARINE REHABILITATION MEASURES. Retrieved from https://sahris.sahra.org.za/sites/default/files/additionaldocs/Appendix2_3_Estuarine_Assessment_0.pdf
- Morris, G., Fan, J., 1998. *Reservoirs Sedimentation Handbook: Design and Management of Dams, Reservoirs and Watershed for Sustainable Use*. McGraw-Hill Book Company, New York.
- Mpelele, E. B., 2018. Statistical projections of climate change for Zambia based on simulations of regional climate models. MSc dissertation in Statistics, Mathematics and Statistics Department, University of Zambia, Lusaka, 107 pp.
- Mphande, G. and Sichingabula, M.H., 2019. Effects of Sedimentation on Small Reservoirs in the Mushibemba Catchment, Mkushi Farm Block, Central Zambia. *Journal of Geography and Geology*; Vol. 11, No. 1. p. 55-69.
- Msadala, V. C., & Basson, G. R. (2017). Revised regional sediment yield prediction methodology for ungauged catchments in South Africa. *Journal of the South African Institution of Civil Engineering*, 59(2), 28-36.

- Muchanga, M., 2020. Determination of Sediment, Water Quantity and Quality for SWAT Modelling of Sedimentation in the Makoye Reservoir, Southern Province, Zambia. PhD Thesis, Department of Geography and Environmental Studies, University of Zambia, Lusaka, Zambia, pp. 1-357.
- Muchanga, M., Sichingabula, H.M., Obando, J., Chomba, I., Sikazwe, H. and Chisola, M., 2019. Bathymetry of the Makoye Reservoir and its Implications on Water Security for Livestock within the Catchment. *International Journal of Geography and Geology*, 8(3), pp.93-109. <https://archive.conscientiabeam.com/index.php/10/article/view/2000>
- Mukherjee, S., Veer, V., Tyagi, S.K., Sharma, V. (2007): Sedimentation Study of Hirakud Reservoir through Remote Sensing Techniques – *J. Spat. Hydrol.* 7: 122-130.
- Mukuhlani, T. and Nyamupingidza, M.T., 2014. Water scarcity in communities, coping strategies and mitigation measures: The case of Bulawayo. *Journal of Sustainable Development*, 7(1).<https://search.proquest.com/openview/6e6c039947af32bb8cfb7d87ffe5eb78/1.pdf?pq-origsite=gscholar&cbl=307060>
- Mustafa YT, Ali RT, Saleh RM (2012). Monitoring and evaluating land cover change in the Duhok city, Kurdistan region-Iraq, by using remote sensing and GIS. *Int. J. Eng. Inv.* 1(11):28-33.
- Musumali, M.M., Heck, S., Husken, S.M.C. & Wishart, M. 2009. Fisheries in Zambia: an undervalued contributor to poverty reduction. Working Paper 26. Penang, WorldFish Centre. *Lakes & Reservoirs Research & Management* 11(4):271-286.
- Mwiinde, D. 2017. Cost-benefit analysis of sediment and sedimentation in selected small dams in Lusaka and Southern provinces, Zambia. MSc dissertation, Department of Geography and Environmental Studies, University of Zambia, Lusaka, Zambia. Pp. 1-116.
- Mzuza, M.K.; Zhang, W.; Kapute, F.; and Wei, X. 2019. The Impact of Land Use and Land Cover Changes on the Nkula Dam in the Middle Shire River Catchment, Malawi. In Pepe A., and Zhao Q. eds. *Geospatial Analyses of Earth Observation (EO) data*. IntechOpen, London (UK), ch. 3, pp.37-66.
- Naidoo, R. (2019). Sustainable Use of Small Water Bodies in South Africa. Water Research Commission. Retrieved from <https://www.wrc.org.za/wp-content/uploads/mdocs/TT-746-19.pdf>
- Nakashole, A. N. (2017). Heavy Minerals in the palaeo and modern Orange River and Offshore southern Namibia. Thesis. School of Earth and Environment. The University of Leeds. London.
- Nakicenovic, N., Alcamo, J., Davis, G., de Vries, B., Fenhann, J., Gaffin, S., Gregory, K., Grübler, A., Jung, T. Y., Kram, T., La Rovere, E. L., Michaelis, L., Mori, S., Morita, T., Pepper, W., Pitcher, H., Price, L., Raihi, K., Roehrl, A., Rogner, H.-H., Sankovski, A., Schlesinger, M., Shukla, P., Smith, S., Swart, R., van Rooijen, S., Victor, N., and Dadi, Z. 2000. *IPCC Special Report on Emissions Scenarios*, Cambridge University Press, Cambridge, UK and New York, NY, USA
- Narasayya, K., Roman, U.C., Sreekanth, S., Jatwa, S. (2013): Assessment of Reservoir Sedimentation Using Remote Sensing Satellite Imageries – *Asian J. Geoinformatics*.

- Nash, D. J. & McLaren, S. J. 2003. Kalahari valley calcretes: their nature, origins, and environmental significance. *Quaternary International*, 111, 3-22.
- Nash, D. J., Meadows, M. E., Shaw, P. A., Baxter, A. J. & Gieske, A. 1997. Late holocene sedimentation rates and geomorphological significance of the Ncamasere Valley, Okavango Delta, Botswana. *South African Geographical Journal*, 79, 93-100.
- Nechaev VP and Isphording WC (1993). Heavy mineral assemblages of continental margins as indicators of plate-tectonic environments. *Journal of Sedimentary Petrology* 63:1110-1117.
- Nesbitt HW and Young GM (1982) Early Proterozoic climates and plate motions inferred from major element chemistry of lutites. *Nature* 299:715-717.
- Nugent, C. 1990. The Zambezi River – Tectonism, climatic-change and drainage evolution. *Palaeogeography Palaeoclimatology Palaeoecology*, 78, 55-69.
- Nyambe IA and Utting J (1997) Stratigraphy and palynostratigraphy, Karoo Supergroup (Permian and Triassic), mid-Zambezi Valley, southern Zambia. *South African Journal of Geology* 24:563-583.
- Nyambe, I.A. 1999. Tectonic and climatic controls on sedimentation during deposition of the Sinakumbe Group and Karoo Supergroup, in the mid-Zambezi Valley Basin, southern Zambia. *Journal of African Earth Sciences* 28(2):443-463.
- Obakeng, O. T. 2007. Soil moisture dynamics and evapotranspiration at the fringe of the Botswana Kalahari, with emphasis on deep rooting vegetation. MSc, ITC International Institute for Geo-Information science and earth observation.
- Obialor, C. A., Okeke, O. C., Onunkwo, A. A., Fagorite, V. I., & Ehujuo, N. N. (2019). Reservoir sedimentation: Causes, effects and mitigation. *International Journal of Advanced Academic Research| Sciences, Technology and Engineering| ISSN, 2488-9849.*
- O'Connor PW and Thomas DSG (1999) The timing and environmental significance of Late Quaternary linear dune development in western Zambia. *Quaternary Research* 52:44-55.
- Odom, I.E.; Doe, T.W.; and Dott, R.H. 1976. Nature of feldspar-grain size relations in some quartz-rich sandstones. *Journal of Sedimentary Petrology* 46(4):862-870.
- Okumura & Sumi (2012), proposed management measures for reservoir sedimentation
- Okumura, H. & Sumi, T. 2012. Reservoir sedimentation management in hydropower plant regarding flood risk and loss of power generation. *International Symposium on Dams for a Changing World*. Kyoto, Japan, 5 June 2012.
- Ollier, C. D. 1985. Morphotectonics of continental margins with great escarpments. In: MORISAWA, M. & HACK, J. T. (eds.) *Tectonic geomorphology*. London: George Allen & Unwin.
- Olofintoye, O., Otieno, F. and Adeyemo, J. (2016) “Real-time optimal water allocation for daily hydropower generation from the Vanderkloof dam, South Africa,” *Applied Soft Computing Journal*, 47, pp. 119-129. doi: 10.1016/j.asoc.2016.05.018.

- Opperman, J., Hartmann, J., Raepple, J., Angarita, H., Beames, P., Chapin, E., Geressu, R., Grill, G., Harou, J., Hurford, A., Kammen, D., Kelman, R., Martin, E. Martins, T., Peters, R. Rogéliz, C. & Shirley, R. 2017. *The Power of Rivers: A Business Case*. The Nature Conservancy: Washington, D.C.
- ORASECOM & Lesotho Department of Water Affairs. (2018). Protecting the source of Lesotho's 'white gold.' Retrieved from https://www.sadc.int/files/6215/3805/7503/EN_ORASECOM_Khubelu_Wetlands_Protection_Case_Study-web.pdf
- ORASECOM-Orange-Senqu River Commission (2008). Preliminary Transboundary Diagnostic Analysis
- Osbahr, H., Twyman, C., Adger, W.N. and Thomas, D.S., 2010. Evaluating successful livelihood adaptation to climate variability and change in southern Africa. *Ecology and Society*, 15(2). <https://www.jstor.org/stable/26268141>.
- Osborne, C.P., 2008. Atmosphere, ecology and evolution: What drove the Miocene expansion of C4 grasslands? *Journal of Ecology* 96, 35-45.
- Osenbrück, K., Stadler, S., Sültenfuß, J., Suckow, A. O. & Weise, S. M. 2009. Impact of recharge variations on water quality as indicated by excess air in groundwater of the Kalahari, Botswana. *Geochimica Et Cosmochimica Acta*, 73, 911-922.
- Other similar data sources
- Ouyang W, Hao FH, Zhao C, Lin C (2010). Vegetation response to 30 years hydropower cascade exploitation in upper stream of Yellow River. *Commun. Nonlin. Sci. Numer. Simul.* 15(7):1928-1941.
- Pacca, S., 2007. Impacts from decommissioning of hydroelectric dams: a life cycle perspective. *Climatic Change*, 84(3), pp.281-294.
- Pandey, C.L., 2021. Managing urban water security: challenges and prospects in Nepal. *Environment, Development and Sustainability*, 23(1), pp.241-257.
- Park, E., & Latrubesse, E. M. (2014). Modeling suspended sediment distribution patterns of the Amazon River using MODIS data. *Remote Sensing of Environment*, 147, 232-242.
- Parker, A. 1970. An index of weathering for silicate rocks. *Geological Magazine* 107:501-504.
- Parkhurst, D. L. & Appelo, C. 2013. Description of input and examples for PHREEQC version 3: a computer program for speciation, batch-reaction, one-dimensional transport, and inverse geochemical calculations. US Geological Survey.
- Particularly relevant to SWAT modelling:
- Partridge TC and Maud RR (1987) Geomorphic evolution of southern Africa since the Mesozoic. *South African Journal of Geology* 90(2):179-208.
- Partridge, T. C., Dollar, E. S. J., Dollar, L. H., & Moolman, J. (2010). The geomorphic provinces of South Africa, Lesotho and Swaziland: A physiographic subdivision for earth and environmental scientists. *Transactions of the Royal Society of South Africa*, 65(1), 1-47. <https://doi.org/10.1080/00359191003652033>
- Passarge, S. 1904. *Die Kalahari*, Dietrich Reimer (Ernst Vohsen), Berlin.
- Pastore, G.; Baird, T.; Vermeesch, P.; Resentini, A.; and Garzanti, E. 2021. Provenance and recycling of Sahara Desert sand. *Earth-Science Reviews* 2016:103606.

- Pathak, H., Pramanik, P., Khanna, M. and Kumar, A., 2014. Climate change and water availability in Indian agriculture: impacts and adaptation. *Indian J Agr Sci*, 84, pp.671-679.
https://www.researchgate.net/profile/Manoj_Khanna/publication/304659816_Climate_change_and_water_availability_in_Indian_agriculture_Impacts_and_adaptation/links/57765b0e08ae1b18a7e1a4c0/Climate-change-and-water-availability-in-Indian-agriculture-Impacts-and-adaptation.pdf
- Patrick, H.O., 2020. Climate change, water security, and conflict potentials in South Africa: Assessing conflict and coping strategies in rural South Africa. *Handbook of climate change management: Research, leadership, transformation*, pp.1-18.
- Pechlivanidis, I.G., Jackson, B.M., McIntyre, N.R. & Wheater, H.S. 2011. Catchment scale hydrological modelling: a review of model types, calibration approaches and uncertainty analysis methods in the context of recent developments in technology and applications. *Global NEST Journal*, 13 (3):193-214.
- Pereira, A. & Pires, L., 2011. Evapotranspiration and Water Management for Crop
- Pereira, L.S.F.; Andes, L.C.; Cox, A.L.; Ghulam, A. Measuring suspended-sediment concentration and turbidity in the middle Mississippi and lower Missouri Rivers using LANDSAT data. *J. Am. Water Resour. Assoc.* 2018, 54, 440-450.
- Peterson, K. T., Sagan, V., Sidike, P., Cox, A. L., & Martinez, M. 2018. Suspended sediment concentration estimation from LANDSAT imagery along the lower Missouri and middle Mississippi Rivers using an extreme learning machine. *Remote Sensing*, 10(10), 1503.
- Petus, C.; Chust, G.; Gohin, F.; Doxaran, D.; Froidefond, J.M.; Sagarminaga, Y. Estimating turbidity and total suspended matter in the Adour riverplume (south bay of Biscay) using MODIS 250-m imagery. *Cont. Shelf Res.* 2010, 30, 379-392.
- Phethean JJJ, Kalnins LM, van Hunen J, Biffi PG, Davies R.1123 J and McCaffrey KJW (2016) Madagascar's escape from Africa: A high-resolution plate reconstruction for the Western Somali Basin and implications for supercontinent dispersal, *Geochemistry Geophysics Geosystems* 17: 5036-5055.
- Phiri, J.S., Moonga, E., Mwangase, O. and Chipeta, G., 2013. Adaptation of Zambian agriculture to climate change-a comprehensive review of the utilisation of the Agro-ecological regions. A Review for the Policy Makers. *Zambia Academy of Sciences (ZaAS)*, pp.1-41.
- Pipitone, C. M., Antonino, Dardanelli, G., & Lo Brutto, M. & la Loggia, G. 2018. Monitoring Water Surface and Level of a Reservoir Using Different Remote Sensing Approaches and Comparison with Dam Displacements Evaluated via GNSS. *Remote Sensing*. DOI: 10.3390/rs10010071.
- Pitzer, K. S. 1973. Thermodynamics of electrolytes. I. Theoretical basis and general equations. *The Journal of Physical Chemistry*, 77, 268-277.
- Pitzer, K. S. 1975. Thermodynamics of electrolytes. V. Effects of higher-order electrostatic terms. *Journal of Solution Chemistry*, 4, 249-265.
- Podgorski, J. E., Green, A. G., Kgotlhang, L., Kinzelbach, W. K., Kalscheuer, T., Auken, E. & Ngwisanyi, T. 2013. Paleo-megalake and paleo-megafan in southern Africa. *Geology*, 41, 1155-1158.

- Polissar, P.J., Rose, C., Uno, K.T., Phelps, S.R., Demenocal, P., 2019. Synchronous rise of African C 4 ecosystems 10 million years ago in the absence of aridification. *Nature Geoscience* 12, 1.
- Ponte, J.P.; Robin, C.; Guillocheau, F.; Popescu, S.; Suc, J.P.; Dall'Asta, M.; Melinte-Dobrinescu, M.C.; Bubik, M.; Dupont, G.; and Gaillot, J. 2019. The Zambezi delta (Mozambique Channel, East Africa): High resolution dating combining bio-orbital and seismic stratigraphies to determine climate (palaeoprecipitation) and tectonic controls on a passive margin. *Marine and Petroleum Geology* 105:293-312.
- Potter PE (1978) Petrology and chemistry of modern big river sands. *The Journal of Geology* 86: 423-449.
- Price, J.R., and Velbel, M.A. 2003. Chemical weathering indices applied to weathering profiles developed on heterogeneous felsic metamorphic parent rocks. *Chemical Geology* 202(3-4):397-416.
- Production.
https://www.researchgate.net/publication/221919364_Evapotranspiration_and_Water_Mana
- Purdy, E. & MacGregor, D. 2003. Map compilations and synthesis of Africa's petroleum basins and systems. Geological Society, London, Special Publications, 207, 1-8.
- QGIS: <https://qgis.org/en/site/forusers/download.html>
- Quadros, N.D., Collier, P.A. & Fraser, C.S. 2008. Integration of bathymetric and topographic LIDAR: A preliminary investigation. *The International Archives of the Photogrammetry, Remote Sensing and Spatial Information Sciences*, 37(8):1299-1304.
- Rae, J.W., Zhang, Y.G., Liu, X., Foster, G.L., Stoll, H.M., Whiteford, R.D., 2021. Atmospheric CO₂ over the past 66 million years from marine archives. *Annual Review of Earth and Planetary Sciences* 49.
- Ramberg, L. & Wolski, P. 2008. Growing islands and sinking solutes: processes maintaining the endorheic Okavango Delta as a freshwater system. *Plant Ecology*, 196, 215-231.
- Randolph, J. (2004): *Environmental land use planning and management – Washington D.C.:* Island Press.
- Reason, C., Mulenga, H., 1999. Relationships between South African rainfall and SST anomalies in the southwest Indian Ocean. *International Journal of Climatology: A Journal of the Royal Meteorological Society* 19, 1651-1673.
- Reason, C.J.C., 1998. Warm and cold events in the southeast Atlantic/southwest Indian Ocean region and potential impacts on circulation and rainfall over southern Africa. *Meteorology & Atmospheric Physics* 69, 49-65.
- Reason, C.J.C., 2001. Evidence for the Influence of the Agulhas Current on regional atmospheric circulation patterns. *Journal of Climate* 14, 2769-2778.
- Reason, C.J.C.; Landman, W.; and Tennant, W. 2006. Seasonal to decadal prediction of southern African climate and its links with variability of the Atlantic Ocean. *Bulletin of the American Meteorological Society* 87(7):941-955.
- Remotely sensed online resources include:

- Republic of Mozambique, National Institute of Disaster Management, Management modelling techniques, catchment information
<https://hydro-at.poyry.com/zambezi/index.php>
- Resentini A, Goren L, Castelltort S and Garzanti E (2017) Partitioning the sediment flux by 1130 provenance and tracing erosion patterns in Taiwan. *Journal Geophysical Research – Earth Surface* 122(7):1430-1454, doi:10.1002/2016JF004026.
- Resentini, A.; Andò, S.; Garzanti, E.; Malusà, M.G.; Pastore, G.; Vermeesch, P.; Chanvry, E.; and Dall'Asta, M. 2020. Zircon as a provenance tracer: Coupling Raman spectroscopy and UPb geochronology in source-to-sink studies. *Chemical Geology* 555:119828.
- Rhodes University SPATSIM
<https://www.ru.ac.za/iwr/research/software/>
- Ribeiro, N.S., Okin, G.S., Shugart, H.H., Swap, R.J., 2009. The influence of rainfall, vegetation, elephants and people on fire frequency of miombo woodlands, northern Mozambique, 2009 IEEE International Geoscience and Remote Sensing Symposium. IEEE, pp. IV-322-IV-325.
- Riedel, F., Erhardt, S., Chauke, C., Kossler, A., Shemang, E. & Tarasov, P. 2012. Evidence for a permanent lake in Sua Pan (Kalahari, Botswana) during the early centuries of the last millennium indicated by distribution of Baobab trees (*Adansonia digitata*) on “Kubu Island”. *Quaternary International*, 253, 67-73.
- Riedel, F., Henderson, A. C., Heußner, K.-U., Kaufmann, G., Kossler, A., Leipe, C., Shemang, E. & Taft, L. 2014. Dynamics of a Kalahari long-lived mega-lake system: hydromorphological and limnological changes in the Makgadikgadi Basin (Botswana) during the terminal 50 ka. *Hydrobiologia*, 1-29.
- Riedel, F., von Rintelen, T., Erhardt, S. & Kossler, A. 2009. A fossil *Potadoma* (Gastropoda: Pachychilidae) from Pleistocene central Kalahari fluvio-lacustrine sediments. *Hydrobiologia*, 636, 493-498.
- Rieu R, Allen PA, Plötze M and Pettke T (2007) Compositional and mineralogical variations in a Neoproterozoic glacially influenced succession, Mirbat area, South Oman: Implications for paleoweathering conditions. *Precambrian Research* 154:248-265.
- Rieu, R.; Allen, P.A.; Plötze, M.; and Pettke, T. 2007. Climatic cycles during a Neoproterozoic “snowball” glacial epoch. *Geology* 35(4):299-302.
- Rigal, A., Azaïs, J.-M., Ribes, A., 2019. Estimating daily climatological normals in a changing climate. *Clim. Dyn.* 24. <https://doi.org/10.1007/s00382-018-4584-6>
- Rigal, A., Azaïs, J.-M., Ribes, A., 2019. Estimating daily climatological normals in a changing climate. *Clim. Dyn.* 24. <https://doi.org/10.1007/s00382-018-4584-6>
- Ringrose, S., Huntsman-Mapila, P., Kampunzu, A. B., Downey, W., Coetzee, S., Vink, B., Matheson, W. & Vanderpost, C. 2005. Sedimentological and geochemical evidence for palaeo-environmental change in the Makgadikgadi subbasin, in relation to the MOZ rift depression, Botswana. *Palaeogeography Palaeoclimatology Palaeoecology*, 217, 265-287.
- Ritchie, J.C.; Schiebe, F.R.; McHenry, J.R. Remote sensing of suspended sediment in surface water. *Photogramm. Eng. Remote Sens.* 1976, 42, 1539-1545.

- Ritchie, J.C.; Zimba, P.V.; Everitt, J.H. Remote sensing techniques to assess water quality. *Photogramm. Eng. Remote Sens.* 2003, 69, 695-704.
- Roberts EM, Stevens NJ, O'Connor PM, Dirks PHGM, Gottfried MD, Clyde WC, Armstrong RA, Kemp AIS and Hemming S (2012). Initiation of the western branch of the East African Rift coeval with the eastern branch. *Nature Geoscience* 5(4):289-294.
- Rommerskirchen, F., Eglinton, G., Dupont, L., Güntner, U., Wenzel, C., Rullkötter, J., 2003. A north to south transect of Holocene southeast Atlantic continental margin sediments: Relationship between aerosol transport and compound-specific $\delta^{13}\text{C}$ land plant biomarker and pollen records. *Geochemistry, Geophysics, Geosystems* 4.
- Ronco *et al.* (2010), providing a robust 1D model at river basin scale on sediment/erosion morphodynamics accounting for the changes on discharges pattern due to large reservoirs of the Lower Zambezi;
- Ronco, P., Fasolato, G., Nones, M. & Di Silvio, G. 2010. Morphological effects of damming on lower Zambezi River. *Geomorphology*, 115:43-55.
- Ronco, P.; Fasolato, G.; Nones, M.; and Di Silvio, G. 2010. Morphological effects of damming on lower Zambezi River. *Geomorphology* 115(1-2):43-55.
- Ronco, Paolo & Fasolato, Giacomo & Nones, Michael & Di Silvio, Giampaolo, 2010. Morphological Effect of Damming on Lower Zambezi River. *Geomorphology*. 115. 43. 10.1016/j.geomorph.2009.09.029.
- Rooseboom, A. 1992. Sediment transport in rivers and reservoirs – A Southern African perspective. WRC Report No. 297/1/92.
- Rubey, W.W. 1933. The size distribution of heavy minerals within a water-laid sandstone. *Journal of Sedimentary Research* 3(1):3-29.
- Rudnick, R.L., and Gao, S., 2003. Composition of the continental crust. In Rudnick, R.L., Holland, H.D., and Turekian, K.K. eds. *Treatise on Geochemistry. The Crust*, vol. 3. Elsevier Pergamon, Oxford, pp. 1-64.
- Russell RD (1937) Mineral composition of Mississippi River sands. *Geological Society of America, Bulletin* 48:1307-1348.
- Ryu, J-H., J-S Won, and K. D. Min. 2002. Waterline extraction from LANDSAT TM data in a tidal flat. A case study in Gomso Bay, Korea. *Remote Sens. Environ.* 83:442-456
- SADC, 2005. Regional Strategic Action Plan for Integrated Water Resource Management.
- Sadler, P.M., 1981. Sediment accumulation rates and the completeness of stratigraphic sections. *The Journal of Geology*, 89(5), pp.569-584. <https://www.journals.uchicago.edu/doi/abs/10.1086/628623>
- Sage, R., 2001. Environmental and evolutionary preconditions for the origin and diversification of the C4 photosynthetic syndrome. *Plant Biology* 3, 202-213.
- Salman G and Abdula I (1995) Development of the Mozambique and Ruvuma sedimentary basins, offshore Mozambique. *Sedimentary Geology* 96:7-41.
- Sankaran, M., Hanan, N.P., Scholes, R.J., Ratnam, J., Augustine, D.J., Cade, B.S., Gignoux, J., Higgins, S.I., Le Roux, X., 2005. Determinants of woody cover in African savannas. *Nature* 438 (7069), 846-849.

- SAPP. 2016. SAPP Project Advisory Unit (“PAU”). Programme for accelerating regional transformational energy projects – “AREP”. Online presentation. Available at: http://www.energynet.co.uk/webfm_send/2008.
- Saputra, L.R., Radjawane, I.M., Park, H. & Gularso, H. 2021. Effect of turbidity, temperature and salinity of waters on depth data from airborne lidar bathymetry. doi: 10.13140/RG.2.2.16200.85761
- Saruchera, D. & Lautze, J., 2019. Small reservoirs in Africa: a review and synthesis to strengthen future investment. Colombo, Sri Lanka: International Water Management Institute (IWMI). 40p. (IWMI Working Paper 189). doi: 10.5337/2019.209
- Satellite data (Bathymetry) (https://www.usgs.gov/faqs/where-can-i-find-bathymetric-data-0?qt-news_science_products=0#qt-news_science_products) and <https://gisgeography.com/category/data-sources/>
- Satellite data (Bathymetry) (https://www.usgs.gov/faqs/where-can-i-find-bathymetric-data-0?qt-news_science_products=0#qt-news_science_products) and (http://tethys.eaprs.cse.dmu.ac.uk/RiverLake/info/zambezi_modelling) and <https://gisgeography.com/category/data-sources/>
- Sattel, D. & Kgotlhang, L. 2004. Groundwater exploration with AEM in the Boteti area, Botswana. *Exploration Geophysics*, 35, 147-156.
- Savenije, H. H. G., & van der Zaag, P., 1998. The management of Shared River Basins. Focus on Development 8. Ministry of Foreign Affairs, The Hague.
- Savenije, H.H.G., 1995. Spreadsheets: flexible tools for integrated management of water resources in river basins. In: *Modelling and Management of Sustainable Basin-scale Water Resources Systems*. IAHS Publications 231, pp. 207-215.
- Sawunyama, T., Basima Busane, L., Chinoda, C., Twikirize, D., Love, D., Senzanje, A. and Mhizha, A., 2005, November. An integrated evaluation of a small reservoir and its contribution to improved rural livelihoods: Sibasa Dam, Limpopo Basin, Zimbabwe. In Abstract volume, 6th WaterNet/WARFSA/GWP-SA Symposium, Swaziland. https://www.academia.edu/download/69336636/P02_20Sawunyama_20small_20dam.pdf
- Saylam, K., Hupp, J., Averett, A.R. & Gutelius, W.F. 2018. Airborne lidar bathymetry: assessing quality assurance and quality control methods with Leica Chiroptera examples. *International Journal of Remote Sensing*, 39(8):2518-2542. doi:10.1080/01431161.2018.1430916
- Scanlon, T. S., Caylor, K. K., Levin, S. A., and Rodriguez-Iturbe, I. (2007). Positive feedbacks promote power-law clustering of Kalahari vegetation, *Nature*, 449, 209-212
- Schleiss, A. J., Franca, M. J., Juez, C., & De Cesare, G. (2016). Reservoir sedimentation. *Journal of Hydraulic Research*, 54(6), 595-614.
- Scholes, R.J., Archer, S.R., 1997. Tree-grass interactions in savannas 1. *Annual Review of Ecology & Systematics* 28, 517-544.
- Schoorl, J.M., Temme, A.J. and Veldkamp, T., 2014. Modelling centennial sediment waves in an eroding landscape-catchment complexity. *Earth Surface Processes and Landforms*, 39(11), pp.1526-1537. <https://onlinelibrary.wiley.com/doi/full/10.1002/esp.3605>

- Schultz, B. and Uhlenbrook, S., 2007. Water security: What does it mean, what may it imply? In *Water for a Changing World-Developing Local Knowledge and Capacity* (pp. 53-68). CRC Press. <https://books.google.com/books?hl=en&lr=&id=4kUDoKRbfqcC&oi=fnd&pg=PA41&dq=Water+security:+What+does+it+mean,+what+may+it+imply%3F.+In+Water+for+a+Changing+WorldDeveloping+Local+Knowledge+and+Capacity+&ots=Gyspo6uuI5&sig=qJA42ATAiCLWqgon0EIUmSy9KoI>.
- Schulz H, Lückge A, Emeis KC and Mackensen A (2011). Variability of Holocene to LatePleistocene Zambezi riverine sedimentation at the upper continental slope off Mozambique, 15-21°S. *Marine Geology* 286:21-34.
- Schulzweida, U., Kornblueh, L., Quast, R., 2010. CDO user's guide – Climate Data Operators, Version 1.4.6.
- Schwanghart W and Scherler D (2014) TopoToolbox 2 – MATLAB-based software for topographic analysis and modelling in Earth surface sciences. *Earth Surface Dynamics* 2:1-7, doi:10.5194/esurf-2-1-2014.
- Sciunnach D and Garzanti E (1992) Subsidence history of the Tethys Himalaya. *Earth-Science Reviews* 111:179-198.
- Seaman, M. T., Ashton, P. J. & Williams, W. D. 1991. Inland salt waters of southern Africa. *Hydrobiologia*, 210, 75-91.
- Selaolo, E. D. 1998. Tracer studies and groundwater recharge assessment in the Eastern Fringe of the Botswana Kalahari. The Lethlakeng – Botlhapatlou Area. Ph.D. thesis, Vrije Universiteit te Amsterdam.
- Sentinel explorer
- Senzanje, A and Dirwai, TL, 2020. WATER AND AGRICULTURE IN THE ZAMBEZI RIVER BASIN Characterization of Current Agriculture Activities, Future Potential Irrigation Developments and Food Security to Face Climate Variability in the Zambezi River Basin.
- Setti, M.; López-Galindo, A.; Padoan, M.; and Garzanti, E. 2014. Clay mineralogy in southern Africa river muds. *Clay Minerals* 49:717-733.
- Seyam, I.M., Hoekstra, A.Y., Ngabirano, G.S. and Savenije, H.H.G., 2001. The value of freshwater wetlands in the Zambezi basin. *Value of Water Research Report Series No. 7*.
- Shahin, M. 2002. *Hydrology and water resources of Africa*, Springer Science & Business Media.
- Shang, Y. & Last, W. M. 1999. Mineralogy, lithostratigraphy, and inferred geochemical history of North Ingebrigt Lake, Saskatchewan. In: LEMMEN, D. S. & VANCE, R. E. (eds.) *Holocene climate and environmental change in the Palliser Triangle: a geoscientific context for evaluating the impacts of climate change on the Southern Canadian Prairies*. Geological Survey of Canada Bulletin No. 534.
- Shannon, L., Nelson, G., 1996. The Benguela: large scale features and processes and system variability, *The south Atlantic*. Springer, pp. 163-210.
- Shaw A and Goudie AS (2002) Geomorphological evidence for the extension of the Mega-Kalahari into south-central Angola. *S. Afr. Geogr. J.* 84:182-194.

- Shaw, A.I. 2009. The characterisation of calcrete based on its environmental settings within selected regions of the Kalahari, Southern Africa. Ph.D. Thesis, University of Oxford, 606 p.
- Shaw, P. & Thomas, D. 1988. Lake Caprivi-A Late Quaternary Link Between the Zambezi and Middle Kalahari Drainage Systems. *Zeitschrift fur Geomorphologie*, 32, 329-337.
- Shaw, P. 1985a. The desiccation of Lake Ngami – a historical-perspective. *Geographical Journal*, 151, 318-326.
- Shaw, P. 1985b. Late Quaternary landforms and environmental change in northwest Botswana: the evidence of Lake Ngami and the Mababe Depression. *Transactions of the Institute of British Geographers*, 333-346.
- Shaw, P. A. & Cooke, H. J. 1986. Geomorphic evidence for the late quaternary paleoclimates of the middle Kalahari of Northern Botswana. *Catena*, 13, 349-359.
- Shaw, P. A., Bateman, M. D., Thomas, D. S. G. & Davies, F. 2003. Holocene fluctuations of Lake Ngami, Middle Kalahari: chronology and responses to climatic change. *Quaternary International*, 111, 23-35.
- Shaw, P. A., Stokes, S., Thomas, D. S. G., Davies, F. B. M. & Holmgren, K. 1997. Palaeoecology and age of a Quaternary high lake level in the Makgadikgadi basin of the middle Kalahari, Botswana. *South African Journal of Science*, 93, 273-276.
- Shaw, P. A., Thomas, D. S. & Nash, D. J. 1992. Late Quaternary fluvial activity in the dry valleys (mekgacha) of the Middle and Southern Kalahari, southern Africa. *Journal of Quaternary Science*, 7, 273-281.
- Shaw, P., and Thomas, D.S.G. 1992. Geomorphology, sedimentation and tectonics in the Kalahari Rift. *Isr. J. Earth Sci.* 41:87-94.
- Shela, O.N., (2000). 'Management of shared river basins: The case of the Zambezi River', *Water Policy*, 2(1-2), pp. 65-81. doi: 10.1016/S1366-7017(99)00022-7.
- Shen, F.; Verhoef, W.; Zhou, Y.; Salama, M.S.; Liu, X. Satellite estimates of wide-range suspended sediment concentrations in Changjiang (Yangtze) Estuary using MERIS data. *Estuaries Coasts* 2010, 33, 1420-1429.
- Shen, X., Wan, S., Colin, C., Tada, R., Shi, X., Pei, W., Tan, Y., Jiang, X., Li, A., 2018. Increased seasonality and aridity drove the C4 plant expansion in Central Asia since the Miocene-Pliocene boundary. *Earth and Planetary Science Letters* 502, 74-83.
- Shiferaw, H., Alamirew, T., Dzikiti, S., Bewket, W., Zeleke, G. and Schaffner, U., 2021. Water use of *Prosopis juliflora* and its impacts on catchment water budget and rural livelihoods in Afar Region, Ethiopia. *Scientific reports*, 11(1), pp.1-14. <https://www.nature.com/articles/s41598-021-81776-6>
- Shukri NM (1950) The mineralogy of some Nile sediments. *Quarterly Journal of the Geological Society London* 105:511-534.
- Shvetsov MS (1934) *Petrografiya osadochnykh porod (Petrography of Sedimentary Rocks)*. Moscow-Leningrad (in Russian): Gostoptekhizdat (1948), 387 p.
- Sichingabula, H. M., 1996. Estimation of contemporary suspended sediment loads on Kafue and Luangwa Rivers, Zambia'. In: B. W. Webb (ed.) *Erosion and Sediment Yield: Global and Regional Perspectives*, Poster booklet report, (Proceedings, Exeter International Symposium, July 1996), p. 96-99.

- Sichingabula, H. M., 1997. Problems of Sedimentation in Small Reservoirs in Zambia. Human Impact on Erosion and Sedimentation (Proceedings of the Rabat Symposium, April 1997). IAHS Publ. no. 245, 1997. p. 4-8.
- Sichingabula, H. M., 1999. Analysis and results of discharge and sediment monitoring activities in the southern Lake Tanganyika Basin: Final Report. Lake Tanganyika Biodiversity Project funded by UNDP/GEF/RAF/G32. <http://www.ltbp.org/FTP/SSS4.PDF>.
- Sichingabula, H.M., 1995, June. The Climate System and Climate Change; Global Warming, Drought and Desertification in Zambia. In: Zambia's National Awareness Workshop on the Convention to Combat Desertification (pp. 22-23).
- Sichingabula, H.M., 2018. Impact of Sedimentation on Ecosystems and the National Economy. SASSCAL Task 109 Completion Report (2013-2018) submitted to SASSCAL, Namibia. Lusaka: Department of Geography and Environmental Studies, University of Zambia.
- Sichingabula, M. H., 2000. Clastic Sediment Flux into Indian and Pacific Oceans by Rivers in Central Southern Africa and Western Canada. Manaus99 – Hydrological and Geochemical Processes in Large Scale River Basins. p. 15-19. Manaus, Brazil.
- Simweene, E. and Muchanga, M., 2021. Socio-hydrological learning for Integrated Siltation Control and Water Resources Management in a Small Reservoir of Southern Zambia. American Journal of Humanities and Social Science. Vol. 29. p. 24-32.
- Sinha, R. & Raymahashay, B. C. 2004. Evaporite mineralogy and geochemical evolution of the Sambhar Salt Lake, Rajasthan, India. *Sedimentary Geology*, 166, 59-71.
- Siwale, C. 2008. Assessing upstream and downstream interactions in Chalimbana River Catchment, Zambia. MSc Thesis, Department of Civil Engineering, University of Zimbabwe. July 2008.
- Siwedza, S.; Mukonzo, S.; Ngambi, C.; and Shava, S. 2021. Impacts of Cyclones Idai and Kenneth and the 2019 Floods on the Insurance Sector in South Africa and Mozambique. In Nhamo G., and Chapungu L., eds. *The Increasing Risk of Floods and Tornadoes in Southern Africa. Sustainable Development Goals Series*. Springer, Cham, pp. 157-171. https://doi.org/10.1007/978-3-030-74192-1_9
- Sláma, J.; Košler, J.; Condon, D.J.; Crowley, J.L.; Gerdes, A.; Hanchar, J.M.; Horstwood, M.S.; Morris, G.A.; Nasdala, L.; Norberg, N.; and Schaltegger, U. 2008. Plešovice zircon – a new natural reference material for U-Pb and Hf isotopic microanalysis. *Chem. Geol.* 249:1-35.
- Söderlund U, Hofmann A, Klausen MB, Olsson JR, Ernst RE and Persson PO (2010) Towards a complete magmatic barcode for the Zimbabwe craton: Baddeleyite U-Pb dating of regional dolerite dyke swarms and sill complexes. *Precambrian Research* 183(3):388-398.
- Solomon, S., Qin, D., Manning, M., Marquis, M., Averyt, K., Tignor, M. M. B., Miller Jr., H. L., and Chen, Z. 2007. (Eds.): *Climate Change: The Physical Science Basis*, Cambridge University Press, Cambridge.
- Son, S.; Wang, M. Water properties in Chesapeake Bay from MODIS-Aqua measurements. *Remote Sens. Environ.* 2012, 123, 163-174.

- Spaliviero M, De Dapper M, and Maló S (2014) Flood analysis of the Limpopo River basin through past evolution reconstruction and a geomorphological approach, *Nat. Hazards Earth Syst. Sci.*, 14, 2027-2039, doi:10.5194/nhess-14-2027-2014, 2014.
- Spano, D., Snyder, R.L., Cesaraccio, C., 2003. Mediterranean climates, Phenology: An integrative environmental science. Springer, pp. 139-156.
- Spencer, R. J., Eugster, H. P. & Jones, B. F. 1985a. Geochemistry of great Salt Lake, Utah II: Pleistocene-Holocene evolution. *Geochimica et Cosmochimica Acta*, 49, 739-747.
- Spencer, R. J., Eugster, H. P., Jones, B. F. & Rettig, S. L. 1985b. Geochemistry of Great Salt Lake, Utah I: Hydrochemistry since 1850. *Geochimica Et Cosmochimica Acta*, 49, 727-737.
- Sri Sumantyo, J. T., Shimada, M., Mathieu, P-P., Putri, R. F. (2012): Dinsar Technique for Retrieving The Volume of Volcanic Materials Erupted by Merapi Volcano – IEEE International Geoscience and Remote Sensing Symposium (IGARSS), pp: 1302-1305.
- Stadler, S. 2005. Investigation of natural processes leading to nitrate enrichment in aquifers of semi-arid regions. PhD thesis, Karlsruhe University, Germany.
- Stadler, S., Osenbrück, K., Knöller, K., Suckow, A., Sültenfuß, J., Oster, H., Himmelsbach, T. & Hötzl, H. 2008. Understanding the origin and fate of nitrate in groundwater of semi-arid environments. *Journal of Arid Environments*, 72, 1830-1842.
- Stage levels for SA dams (<https://www.dws.gov.za/Hydrology/default.aspx>) and (<https://sawx.co.za/state-of-dams/>)
- Stage levels for Zambezi (data provided by ZAMCOM)
- Stanley, J. R. & Flowers, R. M., 2020. Mesozoic denudation history of the lower Orange River. *The geological society of America*, 12(1), pp. 74-87.
- Statistics South Africa, (2004). Natural Resource Accounts: Water Accounts for Nineteen Water Management Areas. Report No. 04-05-012000. Statistics South Africa, Pretoria. Stellenbosch University, NEPAD SANWATCHE <http://nepadwatercoe.org/centres-of-excellence/>
- Stokes S, Haynes G, Thomas DSG, Horrocks JL, Higginson M and Malifa M (1998) Punctuated aridity in southern Africa during the last glacial cycle: The chronology of linear dune construction in the northeastern Kalahari. *Palaeogeography Palaeoclimatology Palaeoecology* 137:305-322.
- Stream and dam levels in SA <https://www.dws.gov.za/Hydrology/Daily/Default.aspx>
- Stream level recorders (data provided by ZAMCOM)
- Street, F. A. & Grove, A. 1976. Environmental and climatic implications of late Quaternary lake-level fluctuations in Africa. *Nature*, 261, 385-390.
- Street, F. A. & Grove, A. 1979. Global maps of lake-level fluctuations since 30,000 yr BP. *Quaternary Research*, 12, 83-118.
- Strömberg, C.A.E., 2011. Evolution of grasses and grassland ecosystems. *Annual Review of Earth & Planetary Sciences* 39, 517-544.
- Strong, A.E., 1989. Greater global warming revealed by satellite-derived sea-surface-temperature trends. *Nature*, 338(6217), pp.642-645 <https://www.nature.com/articles/338642a0>.

- Stute, M. & Talma, A. S. 1998. Glacial temperatures and moisture transport regimes reconstructed from noble gases and O-18, Stampriet aquifer, Namibia – in: *Isotope Techniques in the Study of Environmental Change*.
- Sumi, T. and Hirose, T., 2009. Accumulation of sediment in reservoirs. *Water storage, transport and distribution*, pp.224-252.
- SURFER: <https://www.goldensoftware.com/products/surfer>
- Svensen H, Corfu F, Polteau S, Hammer Ø and Planke S (2012) Rapid magma emplacement in the Karoo Large Igneous Province. *Earth Planet. Sci. Lett.* 325/326:1-9.
- Taylor SR and McLennan SM (1995) The geochemical evolution of the continental crust. *Reviews of Geophysics* 33:241-265.
- Taylor, K.E., 2001. Summarizing multiple aspects of model performance in a single diagram. *J. Geophys. Res.* 106, 7183-7192. <https://doi.org/10.1029/2000JD900719>
- Tejaswini, V. and Sathian, K.K. 2018. Calibration and Validation of Swat Model for Kunthipuzha Basin Using SUFI-2 Algorithm. *International Journal of Current Microbiology and Applied Sciences*. Vol. 7. p. 2162-2172.
- Teter, K. L. 2007. Paleoenvironmental reconstruction of Paleolake Mababe, northwestern Botswana from sediment chemistry and biological productivity data. MSc Thesis Oklahoma State University.
- The best resource to use for elevation information is the following:
The current accessible and preferred data sources for the Zambezi regarding the WACOZA project, are indicated as follows:
The spectrum of climate measuring and recording devices used in SADC is actually very narrow. A full list of climate stations and data is provided on the CSAG website of the University of Cape Town (<http://cip.csag.uct.ac.za/webclient2/datasets/africa-merged-cmip5/>). Furthermore, SASSCAL has established Weathernet (www.sasscalweathernet.org/), which provides real-time data online.
- The SRTM 30 and 90 m, that can be downloaded using Earth-Explorer, is the preferred source for hydrology. Based on the SRTM products, the USGS also provides corrected and DEM derived products in their HYDROSHEDS online facility found at:
- Thiéblemont, D.; Liégeois, J.P.; Fernandez-Alonso, M.; Ouabadi, A.; Le Gall, B.; Maury, R.; Jalludin, M.; *et al.*, 2016. Geological map of Africa at 1:10 Million scale. Paris, CGMW-BRGM (Commission for the Geological Map of the World-Bureau de Recherches Géologiques et Minières).
- Thomas D.S.G., and Shaw, P.A. 1991. *The Kalahari Environment*. Cambridge University Press, Cambridge (UK), 287 p.
- Thomas DSG and Shaw PA (1988) Late Cainozoic drainage evolution in the Zambezi basin: evidence from the Kalahari rim. *Journal of African Earth Sciences* 7:611-618.
- Thomas DSG and Shaw PA (2002) Late Quaternary environmental change in central southern Africa: new data, synthesis, issues, and prospects. *Quaternary Sci. Rev.* 21:783-797.
- Thomas DSG, O'Connor PW, Bateman MD, Shaw PA, Stokes S, and Nash DJ (2000) Dune activity as a record of late Quaternary aridity in the northern Kalahari: new evidence from northern Namibia interpreted in the context of regional arid and humid chronologies. *Palaeogeogr. Palaeoclimatol. Palaeoecol.* 156:243-259.

- Thomas, D. & Shaw, P. 1991a. The deposition and development of the Kalahari Group sediments, central southern Africa. *Journal of African Earth Sciences (and the Middle East)*, 10, 187-197.
- Thomas, D. S. & Shaw, P. A. 1991b. *The Kalahari Environment*, Cambridge University Press.
- Thomas, D. S. G. & Shaw, P. A. 2002. Late Quaternary environmental change in central southern Africa: new data, synthesis, issues and prospects. *Quaternary Science Reviews*, 21, 783-797.
- Thomas, D. S. G., Brook, G., Shaw, P., Bateman, M., Appleton, C., Nash, D., McLaren, S. & Davies, F. 2003. Late Pleistocene wetting and drying in the NW Kalahari: an integrated study from the Tsodilo Hills, Botswana. *Quaternary International*, 104, 53-67.
- Thomas, D.S.G., and Shaw, P.A. 1988. Late Cainozoic drainage evolution in the Zambezi basin: evidence from the Kalahari rim. *J. Afr. Earth Sci.* 7:611-618.
- Tierney, J. E., Russell J.M., Huang Y., Sinninghe Damsté J. S., Hopmans E. C., and Cohen A. S. (2008), Northern Hemisphere controls on tropical southeast African climate during the past 60,000 years, *Science*, 322(5899), 252-255, doi:10.1126/science.1160485.
- Tiffen, M. & Mulele, M.R., 1994. *The Environmental Impact of the 1991-1992 Drought in Zambia*. IUCN, Gland, Switzerland and Lusaka, Zambia. X + 108p.
- Timberlake, J.R. and Childes, S.L. (2004). *Biodiversity of the Four Corners Area: Technical Reviews. Volume One (Chapters 1-4)*.
- Tirivarombo, S. I. T. H. A. B. I. L. E. Climate variability and climate change in water resources management of the Zambezi River basin. Diss. PhD Thesis, Rhodes University, 2012.
- Townshed, P., 2020. Dealing with sediment build-up in dams. *Sabinet African Journals*, 15(3), pp. 34-35.
- Tumbare MJ (2004) *The Zambezi river: its threats and opportunities: 7th river symposium*, 1-3 September 2004, Brisbane. Available online on 06 March 2015.
- Turner D.P. 1991. A procedure for describing soil profiles. ISCW report No. GWA/A/91/67. ARC-ISCW, Pretoria.
- Turton, A. R. 2005. *Hydro Hegemony in the Context of the Orange River Basin*. Workshop on Hydro Hegemony, London.
- Tweddle, D., Cowx, I.G., Peel, R.A. & Weyl, O.L.F. (2015). Challenges in fisheries management in the Zambezi, one of the great rivers of Africa. *Fisheries Management and Ecology*, 22: 99-111.
- Tweddle, D. 2010. Overview of the Zambezi River System: its history, fishfauna, fisheries and conservation. *Aquatic Ecosystem Health & Management*, 13: 224-240.
- Tyson, P.D., Preston-Whyte, R.A., 2000. *Weather and climate of southern Africa*. Oxford University Press.
- Uc, C.J.L.; Leal, J.A.R.; Cruz, D.A.M.; Martínez, A.C.; Celestino, A.E.M. (2021)., Identification of the Dominant Factors in Groundwater Recharge Process, Using Multivariate Statistical Approaches in a Semi-Arid Region. *Sustainability* 2021, 13, 11543.
- Umbanhowar Jr, C.E., McGrath, M.J., 1998. Experimental production and analysis of microscopic charcoal from wood, leaves and grasses. *The Holocene* 8, 341-346.

- UNEP, Assessment, D.o.E.W., Water, A.M.C.o., Commission, A.U., State, U.S.D.o., Union, E., 2010. Africa water atlas. UNEP/Earthprint.
- United Nations Development Programme., 2018. What are the Sustainable Development Goals? <http://www.undp.org/content/undp/en/home/sustainabledevelopment-goals.html> (Accessed: 15/02/2022)
- United States Army Corps of Engineers (USACE) (2000), U.S. Army Corps of Engineer (USACE), 2000. —National inventory of reservoirs. <http://www.usace.army.mil/Library/Maps/Pages/National> (Accessed: 2/2/2022)
- University of KwaZulu-Natal ACRU Model <http://cwrr.ukzn.ac.za/resources/acru>
- University of Zambia, Data <http://dspace.unza.zm:8080/xmlui/handle/123456789/1287>
- University of Zimbabwe, WEAP model and application, <https://www.weap21.org/>, http://www.erc.uct.ac.za/sites/default/files/image_tool/images/119/Hydro-Zambezi/HZ-Water_Supply_and_Demand_Scenarios_Report.pdf
- Uno, K.T., Polissar, P.J., Jackson, K.E., deMenocal, P.B., 2016. Neogene biomarker record of vegetation change in eastern Africa. *Proceedings of the National Academy of Sciences* 113, 6355-6363.
- UN-OCHA (United Nations Office for the Coordination of Humanitarian Affairs). 2010. Pakistan floods emergency response plan, September revision. UN-OCHA.
- USACE, 2017. U.S. Army Corps of Engineers National Inventory of Dams. [Available at http://nid.usace.army.mil/cm_apex/f?p5838:12.]
- Vainer, S.; Matmon, A.; Erel, Y.; Hidy, A.J.; Crouvi, O.; De Wit, M.; Geller, Y.; and ASTER Team 2021. Landscape responses to intraplate deformation in the Kalahari constrained by sediment provenance and chronology in the Okavango Basin. *Basin Research* 33(2):1170-1193.
- Vallier TL (1974) volcanogenic sediments and their relation to landmass volcanism and sea floor continent movements, western Indian Ocean. *Leg 25, Init. Rep. D.S.D.P. 25:515-542.*
- Van der Lubbe JJJ, Tjallingii R, Prins MA, Brummer GJA, Jung SJA, Kroon D and Schneider RR (2014) Sedimentation patterns off the Zambezi River over the last 20,000 years. *Marine Geology* 355:189-201.
- Van der Lubbe, H.J.L.; Frank, M.; Tjallingii, R.; and Schneider, R.R. 2016. Neodymium isotope constraints on provenance, dispersal, and climate-driven supply of Zambezi sediments along the Mozambique Margin during the past~ 45,000 years. *Geochemistry, Geophysics, Geosystems* 17(1):181-198.
- Van Huyssteen, C.W., Le Roux, P.A.L., Hensley, M. & Lorentz, S. 2007. The relationship between soil water regime and morphology: a proposal for continued research. WRC Report No. KV 179/07.

- Van Loon, A.T., and Mange, M.A. 2007. 'In situ' dissolution of heavy minerals through extreme weathering, and the application of the surviving assemblages and their dissolution characteristics to correlation of Dutch and German silver sands. In Mange, M.A., and Wright, D.T., eds. *Heavy minerals in use*. Elsevier, Amsterdam, *Developments in Sedimentology* 58:189-213.
- Van Straten, O. J. 1955. The geology and groundwater of Ghanzi cattle route. Bechuanaland Protectorate, Geological Survey, Annual report, pp. 28-39.
- Van Vuuren, L. (2010) "Gariiep-The dam that tamed the Great River," *Water Wheel*, 9(3).
- Van Vuuren, L., 2010. Gariiep-The dam that tamed the Great River. *Sabinet African Journals*, 9(3), pp. 19-25.
- Vanderkloof Dam (no date). Available at: <https://wis.orasecom.org/content/study/UNDP-GEF/InfrastructureCatalogue/Documents/Reservoirs/Vanderkloof%20Dam.pdf> (Accessed: 8 March 2022).
- Velde, B. 1995. *Origin and Mineralogy of Clays*. Springer, Berlin.
- Velde, B.B., and Meunier, A. 2008. *The origin of clay minerals in soils and weathered rocks*. Springer Science & Business Media, 405 p.
- Verhagen, B.T. 1990. Isotope hydrology of the Kalahari: recharge or no recharge? In: KLAUSHEINE (ed.) *Palaeoecology of Africa and the surrounding islands*. Proc. ixth biennial conference at the University of Durban (South Africa), February 1989.
- Verhagen, B.T. 1992. Detailed geohydrology with environmental isotopes. A case study at Serowe, Botswana – in: *Isotope Techniques in Water Resources Development*.
- Verhagen, B.T. 1995. Semiarid zone groundwater mineralization processes as revealed by environmental isotope studies. In: ADAR, E. M. & LEIBUNDGUT, C. (eds.) *Application of Tracers in Arid Zone Hydrology*. Wallingford: International Association Hydrological Sciences, Volume 232.
- Verhagen, B. T., Mazor, E. & Sellschop, J. P. F. 1974. Radiocarbon and tritium evidence for direct rain recharge to ground waters in the northern Kalahari. *Nature*, 249, 643-644.
- Vermeesch, P. 2018. IsoplotR: a free and open toolbox for geochronology. *Geoscience Frontiers*, 9, 1479-1493.
- Vermeesch, P.; Resentini, A.; and Garzanti, E. 2016. An R package for statistical provenance analysis. *Sedimentary Geology* 336:14-25.
- Vermeesch, P.; Rittner, M.; Petrou, E.; Omma, J.; Mattinson, C.; and Garzanti, E. 2017. High throughput petrochronology and sedimentary provenance analysis by automated phase mapping and LAICPMS. *Geochemistry, Geophysics, Geosystems* 18:4096-4109.
- Vezzoli, G.; Garzanti, E.; Limonta, M.; Andò, S.; and Yang, S. 2016. Erosion patterns in the Changjiang (Yangtze River) catchment revealed by bulk-sample versus single-mineral provenance budgets. *Geomorphology* 261:177-192.
- Vicuna S., Leonardson, R., Hanemann, M.W., Dale, L.L. & Dracup, J.A. 2008. Climate change impacts on high elevation hydropower generation in California's Sierra Nevada: a case study in the Upper American River. *Climate Change*, 87: 123-137.
- Viessman, W. and Lewis, G., 2012. *Introduction to Hydrology*. 5th Edition. Upper Saddle River: Pearson Education.

- Viessman, W., Lewis, G.L., Knapp, J.W. and Harbaugh, T.E., 2012. Introduction to Hydrology, 1989. Hydrology Handbook February.
- Vincent, K., Cull, T., Chanika, D., Hamazakaza, P., Joubert, A., Macome, E., and Mutonhodz Davies, C., 2013. Farmers' responses to climate variability and change in Southern Africa – is it 334 coping or adaptation? *Climate and Development*, 5, 194-205. <https://www.tandfonline.com/doi/abs/10.1080/17565529.2013.821052>
- Vogel, J. 1982. The age of the Kuiseb River silt terrace at Homeb. *Palaeoecology of Africa*, 15, 201-209.
- Vogel, J. C. & Van Urk, H. 1975. Isotopic composition of groundwater in semi-arid regions of southern Africa. *Journal of Hydrology*, 25, 23-36.
- Vogel, J., K, M. & T, S. 2004. Nitrate hotspots and salinity levels in groundwater in the Central District of Botswana.
- Von Der Heyden, C. J. & New, M. G. 2003. The role of a dambo in the hydrology of a catchment and the river network downstream. *Hydrology and Earth System Sciences Discussions*, 7, 339-357.
- Von der Heyden, C. J. & New, M. G. 2004. Sediment chemistry: a history of mine contaminant remediation and an assessment of processes and pollution potential. *Journal of Geochemical Exploration*, 82, 35-57.
- Von Eynatten H, Pawlowsky-Glahn V, and Egozcue JJ (2002) Understanding perturbation on the simplex: a simple method to better visualise and interpret compositional data in ternary diagrams. *Mathematical Geology* 34:249-257.
- Von Eynatten, H.; Barcelò-Vidal, C.; and Pawlowsky-Glahn, V. 2003. Composition and discrimination of sandstones: a statistical evaluation of different analytical methods. *Journal of Sedimentary Research* 73(1):47-57.
- Von Eynatten, H.; Tolosana-Delgado, R.; and Karius, V. 2012. Sediment generation in modern glacial settings: Grain-size and source-rock control on sediment composition. *Sedimentary Geology* 280:80-92.
- Von Eynatten, H.; Tolosana-Delgado, R.; Karius, V.; Bachmann, K.; and Caracciolo, L. 2016. Sediment generation in humid Mediterranean setting: Grain-size and source-rock control on sediment geochemistry and mineralogy (Sila Massif, Calabria). *Sedimentary Geology* 336:68-80.
- Vormann, Franke D, and Jokat W (2020) The crustal structure of the southern Davie Ridge offshore northern Mozambique – A wide-angle seismic and potential field study. *Tectonophysics* 778:228370.
- Vörösmarty, C.J., and Moore, B. 1991. Modeling basin-scale hydrology in support of physical climate and global biogeochemical studies: An example using the Zambezi River. *Surveys in Geophysics* 12(1-3):271-311.
- Vörösmarty, C.J., Douglas, E.M., Green, P.A. and Revenga, C., 2005. Geospatial indicators of emerging water stress: an application to Africa. *Ambio*, pp.230-236.
- Vuuren, L. v. (2010). GARIEP-The dam that tamed the Great River. *The Water Wheel* 9(3), 19-25
- WACOZA datasets, including SASSCAL hourly and daily meteorological data, daily and monthly CHIRPS precipitation datasets and global surface summary (GSOD).

- Walford, H.L.; White, N.J.; and Sydow, J.C. 2005. Solid sediment load history of the Zambezi Delta. *Earth and Planetary Science Letters* 238(1-2):49-63.
- Walling, D.E., Collins, A.L., Sickingabula, H.M. and Leeks, G.J.L., 2001. Integrated assessment of catchment suspended sediment budgets: a Zambian example. *Land degradation & development*, 12(5), pp.387-415.
- Wang, F., Zhou, B., Liu, X., Zhou, G., & Zhao, K. (2012). Remote-sensing inversion model of surface water suspended sediment concentration based on in situ measured spectrum in Hangzhou Bay, China. *Environmental Earth Sciences*, 67(6), 1669-1677.
- Wang, J., Wang, E., Yang, X., Zhang, F. and Yin, H., 2012. Increased yield potential of wheat-maize cropping system in the North China Plain by climate change adaptation. *Climatic Change*, 113(3), pp.825-840.
- Wang, J.J.; Lu, X.X.; Liew, S.C.; Zhou, Y. Retrieval of suspended sediment concentrations in large turbid rivers using LANDSAT ETM+: An example from the Yangtze River, China. *Earth Surf. Process. Land*. 2009, 34, 1082-1092.
- Wang, X., Shao, X., Li, D-X. (2003): Sediment Deposition Pattern and Flow Conditions in the Three Gorges Reservoir : A Physical Model Study – *Tsinghua Sci. Technol.* 8(6): 708-712.
- WATCH WFDEI data, which is daily at 0.5 deg. It's a reanalysis dataset, i.e. it is based on climate model simulations, but it is the only one that would have internal consistency between all variables.
- WATERBASE, World grid data, http://www.waterbase.org/download_data.html
- Weather generator software for modelling can also be found online. The software is mainly used to test models within specific scenarios and it is commonly also used for scaling data. As examples the following:
- Wellington J (1955) *Southern Africa: A geographical study. Physical geography, climate, vegetation, and soils: hydrography*, V.1. Cambridge, UK, Cambridge University Press, 528 p.
- Weltje, G.J. 1997. End-member modelling of compositional data: Numerical-statistical algorithms for solving the explicit mixing problem. *Mathematical Geology* 29(4):503-549.
- Wentz, E.A., Stefanov, W.L., Gries, C. & Hope, D. 2004. Land use and land cover mapping from diverse data sources for an arid urban environments. *Computers, Environment and Urban Systems*, 30:320-346.
- Westerhof, A.P.; Lehtonen, M.I.; Mäkitie, H.; Manninen, T.; Pekkala, Y.; Gustafsson, B.; and Tahon, A. 2008. The Tete-Chipata Belt: A new multiple terrane element from western Mozambique and southern Zambia. *Geological Survey of Finland Special Paper* 48:145-166.
- Wheeler, K., Magee, T.M., Fulp, T. & Zagana, E. 2002. Alternative policies on the Colorado River. *Proceedings of the NRLC Allocating and Managing Water for a Sustainable Future: Lessons from Around the World*, Boulder, Colorado, June 2002.
- Whipple KX, (2004) Bedrock rivers and the geomorphology of active orogens. *Annual Reviews Earth Planetary Sciences* 32:151-185.

- White, F., 1983. The vegetation of Africa. UNESCO
- White, K. & Eckardt, F. 2006. Geochemical mapping of carbonate sediments in the Makgadikgadi basin, Botswana using moderate resolution remote sensing data. *Earth Surface Processes and Landforms*, 31, 665-681.
- Wijesekara GN, Gupta A, Valeo C, Hasbani JG, Qiao Y, Delaney P, Marceau DJ (2012). Assessing the impact of future land-use changes on hydrological processes in the Elbow River watershed in southern Alberta, Canada. *J. Hydrol.* 412-413:220-232.
- Wilson, M.J. 1999. The origin and formation of clay minerals in soils: past, present and future perspectives. *Clay minerals* 34(1):7-25.
- Winsemius, H. C., *et al.* "Comparison of two model approaches in the Zambezi river basin with regard to model reliability and identifiability." *Hydrology and Earth System Sciences Discussions* 2.6 (2005): 2625-2661
- Wirkus, L. and Boge, V., 2006. Transboundary water management on Africa's international rivers and lakes: Current state and experiences. *Transboundary water management in Africa: Challenges for development and cooperation*. W. Scheumann and S. Neubert. Bonn, German Development Institute.
- Wood, W., Eckardt, F., Kraemer, T. & Eng, K. 2011. Quantitative Aeolian Transport of Evaporite Salts from the Makgadikgadi Depression (Ntwetwe and Sua Pans) in Northeastern Botswana: Implications for Regional Ground-Water Quality. In: ÖZTÜRK, M., BÖER, B., BARTH, H.-J., CLÜSENER-GODT, M., KHAN, M. A. & BRECKLE, S.-W. (eds.) *Sabkha Ecosystems*. Springer Netherlands.
- World Bank, Reports
http://siteresources.worldbank.org/INTAFRICA/Resources/Zambezi_MSIOA_-_Vol_1_-_Summary_Report.pdf
<https://openknowledge.worldbank.org/handle/10986/2958>
- Wu, G.; Cui, L.; Liu, L.; Chen, F.; Fei, T.; Liu, Y. Statistical model development and estimation of suspended particulate matter concentrations with LANDSAT 8 OLI images of Dongting Lake, China. *Int. J. Remote Sens.* 2015, 36, 343-360.
- Xiao-jun, W., Jian-yun, Z., Shahid, S., Xing-hui, X., Rui-min, H. and Man-ting, S., 2014. Catastrophe theory to assess water security and adaptation strategy in the context of environmental change. *Mitigation and adaptation strategies for global change*, 19(4), pp.463-477. <https://link.springer.com/article/10.1007/s11027-012-9443-x>
- Xie, H., You, L., Dile, Y.T., Worqlul, A.W., Bizimana, J.C., Srinivasan, R., Richardson, J.W., Gerik, T. and Clark, N., 2021. Mapping development potential of dry-season small-scale irrigation in Sub-Saharan African countries under joint biophysical and economic constraints-An agent-based modelling approach with an application to Ethiopia. *Agricultural Systems*, 186, p.102987. <https://www.sciencedirect.com/science/article/pii/S0308521X20308489>.
- Xu, Z., Hou, Z., Han, Y., Guo, W., 2016. A diagram for evaluating multiple aspects of model performance in simulating vector fields. *Geosci. Model Dev.* 9, 4365-4380. <https://doi.org/10.5194/gmd-9-4365-2016>

- Yao, F., Wang, J., Wang, C., & Crétau, J.-F. (2019). Constructing long-term high-frequency time series of global lake and reservoir areas using LANDSAT imagery. *Remote Sensing of Environment*, 232, 111210
- Yepez, S., Laraque, A., Martinez, J. M., De Sa, J., Carrera, J. M., Castellanos, B., ... & Lopez, J. L. (2018). Retrieval of suspended sediment concentrations using LANDSAT-8 OLI satellite images in the Orinoco River (Venezuela). *Comptes Rendus Geoscience*, 350(1-2), 20-30.
- You, L., Ringler, C., Nelson, G., Wood-Sichra, U., Robertson, R., Wood, S., Guo, Z., Zhu, T., Sun, Y., 2010. What Is the Irrigation Potential for Africa? A Combined Biophysical and Socioeconomic Approach (No. 00993), IFPRI Discussion Paper 00993.
- Yunus DS, Fidelia NN (2012). Reservoir storage variations from hydrological mass balance and satellite radar altimetry. *Int. J. Water Resour. Environ. Eng.* 4(6):201-207.
- ZAMCOM, 2016. IWRM Strategy and Implementation Plan. SARDC publishing (http://www.zambezicommission.org/sites/default/files/publication_downloads/ZAMSTRAT-At-A-Glance-2016.pdf)
- ZAMCOM, Data and publications
<http://www.zambezicommission.org/>
- ZAMWIS DSS
- ZAMWIS, Zambezi Hydrological data
<http://zamwis.zambezicommission.org/>
- Zhang, C., Wang, Y., Li, Q., Wang, X., Deng, T., Tseng, Z.J., Takeuchi, G.T., Xie, G., Xu, Y., 2012. Diets and environments of late Cenozoic mammals in the Qaidam Basin, Tibetan Plateau: Evidence from stable isotopes. *Earth and Planetary Science Letters* 333, 70-82.
- Zhang, M.; Dong, Q.; Cui, T.; Xue, C.; Zhang, S. Suspended sediment monitoring and assessment for Yellow River Estuary from LANDSAT TM and ETM+ imagery. *Remote Sens. Environ.* 2014, 146, 136-147.
- Zheng, Z.; Li, Y.; Guo, Y.; Xu, Y.; Liu, G.; Du, C. LANDSAT-based long-term monitoring of total suspended matter concentration pattern change in the wet season for Dongting Lake, China. *Remote Sens.* 2015, 7, 13975-13999.
- Zhu, L., Suomalainen, J., Liu, J., Hyppä, J., Kaartinen, H. & Haggren, H. 2017. A review: Remote sensing sensors. In R. B. Rustamov, S. Hasanova, M. H. Zeynalova. eds. *Multi-purposeful Application of Geospatial Data*, IntechOpen, London. 10.5772/intechopen.71049.
- Ziervogel, G., New, M., Archer van Garderen, E., Midgley, G., Taylor, A., Hamann, R., Stuart-Hill, S., Myers, J., Warburton, M., 2014. Climate change impacts and adaptation in South Africa. *Wiley Interdiscip. Rev. Clim. Chang.* 5, 605-620. <https://doi.org/10.1002/wcc.295>
- Zindorf M, Rooze J, Meille C, März C, Jouet G, Newton R, Brandily C, and Pastor L (2021) The evolution of early diagenetic processes and sediment biogeochemical signatures following the post-glacial sea-level rise at the Mozambique margin. *Geochimica et Cosmochimica Acta*, in press.